frontiers | Research Topics

The Alzheimer's disease challenge, volume II, 2nd edition

Edited by
Mohammad Amjad Kamal, Athanasios Alexiou and Asma Perveen

Published in
Frontiers in Aging Neuroscience
Frontiers in Neuroscience

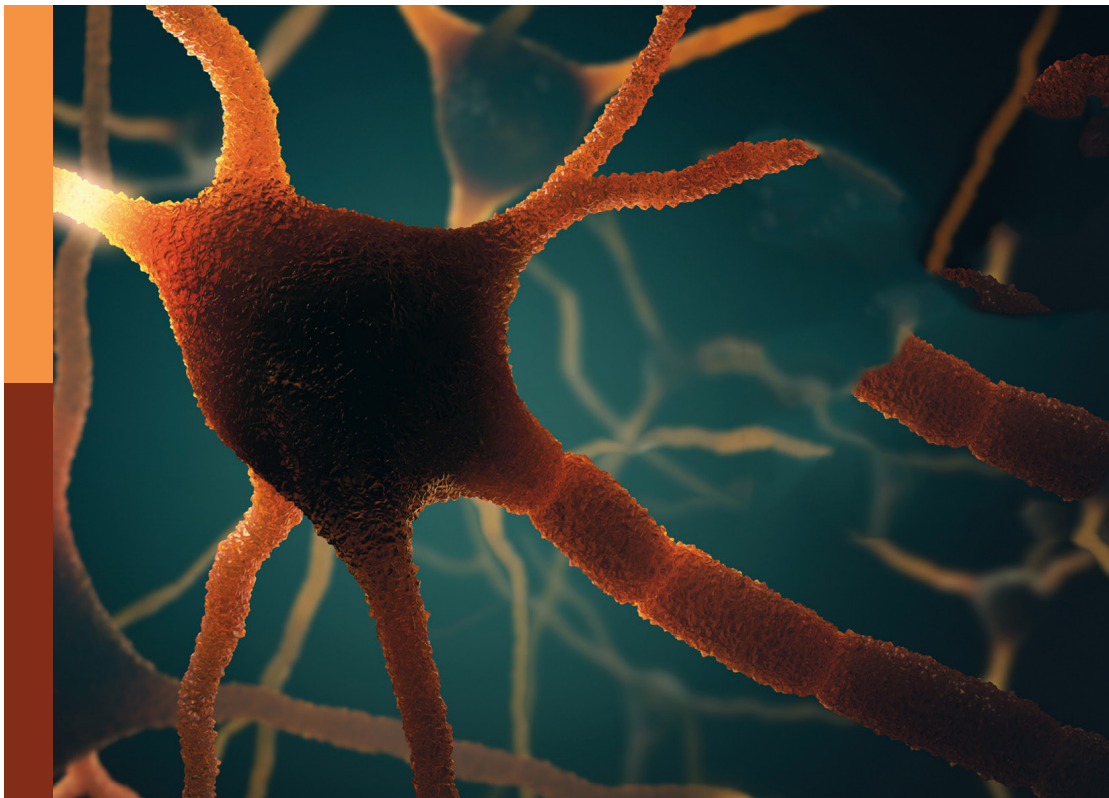

ISSN 1664-8714
ISBN 978-2-8325-4773-1
DOI 10.3389/978-2-8325-4773-1

About Frontiers

Frontiers is more than just an open access publisher of scholarly articles: it is a pioneering approach to the world of academia, radically improving the way scholarly research is managed. The grand vision of Frontiers is a world where all people have an equal opportunity to seek, share and generate knowledge. Frontiers provides immediate and permanent online open access to all its publications, but this alone is not enough to realize our grand goals.

Frontiers journal series

The Frontiers journal series is a multi-tier and interdisciplinary set of open-access, online journals, promising a paradigm shift from the current review, selection and dissemination processes in academic publishing. All Frontiers journals are driven by researchers for researchers; therefore, they constitute a service to the scholarly community. At the same time, the *Frontiers journal series* operates on a revolutionary invention, the tiered publishing system, initially addressing specific communities of scholars, and gradually climbing up to broader public understanding, thus serving the interests of the lay society, too.

Dedication to quality

Each Frontiers article is a landmark of the highest quality, thanks to genuinely collaborative interactions between authors and review editors, who include some of the world's best academicians. Research must be certified by peers before entering a stream of knowledge that may eventually reach the public - and shape society; therefore, Frontiers only applies the most rigorous and unbiased reviews. Frontiers revolutionizes research publishing by freely delivering the most outstanding research, evaluated with no bias from both the academic and social point of view. By applying the most advanced information technologies, Frontiers is catapulting scholarly publishing into a new generation.

What are Frontiers Research Topics?

Frontiers Research Topics are very popular trademarks of the *Frontiers journals series*: they are collections of at least ten articles, all centered on a particular subject. With their unique mix of varied contributions from Original Research to Review Articles, Frontiers Research Topics unify the most influential researchers, the latest key findings and historical advances in a hot research area.

Find out more on how to host your own Frontiers Research Topic or contribute to one as an author by contacting the Frontiers editorial office: frontiersin.org/about/contact

The Alzheimer's disease challenge, volume II, 2nd edition

Topic editors

Mohammad Amjad Kamal — King Abdulaziz University, Saudi Arabia

Athanasios Alexiou — Novel Global Community Educational Foundation (NGCEF), Australia

Asma Perveen — Glocal University, India

Citation

Kamal, M. A., Alexiou, A., Perveen, A., eds. (2024). *The Alzheimer's disease challenge, volume II, 2nd edition*. Lausanne: Frontiers Media SA.

doi: 10.3389/978-2-8325-4773-1

Publisher's note: This is a 2nd edition due to an article retraction.

Table of contents

frontiers | Frontiers in Neuroscience

TYPE Editorial
PUBLISHED 10 January 2023
DOI 10.3389/fnins.2022.1127189

OPEN ACCESS

EDITED AND REVIEWED BY
Mark P. Burns,
Georgetown University, United States

*CORRESPONDENCE
Mohammad Amjad Kamal
prof.ma.kamal@gmail.com

SPECIALTY SECTION
This article was submitted to Neurodegeneration, a section of the journal Frontiers in Neuroscience

RECEIVED 19 December 2022
ACCEPTED 20 December 2022
PUBLISHED 10 January 2023

CITATION
Kamal MA, Alexiou A and Perveen A (2023) Editorial: The Alzheimer's disease challenge, volume II. *Front. Neurosci.* 16:1127189. doi: 10.3389/fnins.2022.1127189

Editorial: The Alzheimer's disease challenge, volume II

Mohammad Amjad Kamal[1,2,3,4,5]*, Athanasios Alexiou[6,7] and Asma Perveen[8]

[1]Institutes for Systems Genetics, Frontiers Science Center for Disease-related Molecular Network, West China Hospital, Sichuan University, Chengdu, China, [2]King Fahd Medical Research Center, King Abdulaziz University, Jeddah, Saudi Arabia, [3]Department of Pharmacy, Faculty of Allied Health Sciences, Daffodil International University, Dhaka, Bangladesh, [4]Enzymoics, Hebersham, NSW, Australia, [5]Novel Global Community Educational Foundation, Hebersham, NSW, Australia, [6]Department of Science and Engineering, Novel Global Community Educational Foundation, Hebersham, NSW, Australia, [7]AFNP Med Austria, Wien, Austria, [8]Glocal School of Life Sciences, Glocal University, Saharanpur, Uttar Pradesh, India

KEYWORDS

Alzheimer's disease, Blood Brain Barrier, Circular RNAs, clinical decision support system, diagnosis, diverse dietary, genomics, Global Burden of Disease

Editorial on the Research Topic
The Alzheimer's disease challenge, volume II

Alzheimer's disease current status and potential biomarkers

Data analysis obtained from the 2019 Global Burden of Disease (GBD) database, the numbers and age-standardized rates (ASRs) of incidence, prevalence, death, and disability-adjusted life-years (DALYs) of AD and other dementias from 1990 to 2019 by Li X. et al. support the emerging necessity of supporting health strategies for more effective prevention and treatment measures in a rapidly increasing aging population. Li X. et al. identified a constantly increasing incidence and prevalence of AD and other dementias over these 30 years. Furthermore, the risk of developing dementia is proportional to age, with females and the elderly having a higher risk. Additionally, the researchers identified smoking as a significant risk factor for the disease burden, and the age-standardized rates (ASRs) of incidence, prevalence, and disability-adjusted life-years (DALYs) were positively correlated with the sociodemographic index (SDI) (Li X. et al.).

While China is the most populous country worldwide, Li Y. et al. performed a cross-sectional observational study to identify the current status of care given to AD patients in China and the factors that potentially influence the family burden. In a sample of 1,675 patients with probable AD from 30 Chinese provincial regions, Li Y. et al. discovered that the vast majority, over 90% of AD patients, receive family care as the primary method while the institutional care system is still underprepared in China something familiar in most of the developing countries probably due to cultural heritage.

Mumtaz et al. highlight the current trends in efficient biomarkers identification, including post-translational modifications (PTMs) of AD-related proteins like APP, Aβ, tau, and BACE1 and the forthcoming era of biomarkers based on the circadian clock genes and their dysregulations associated with AD. New AD treatment approaches against the accumulation of amyloid beta (Aβ) plaques and neurofibrillary tangles (NFTs) are presented, including siRNA/miRNA therapeutics, exosome-based drug carriers, nanoparticle-based targeted therapies, CRISPR/Cas9-based gene-editing, monoclonal antibody-based immunotherapies, and phytochemicals (Mumtaz et al.).

Qian et al.'s study on the association of plasma brain-derived neurotrophic factor (BDNF) with Alzheimer's disease (AD) among 1,615 participants (660 cognitively normal controls, 571 with mild cognitive impairment patients, and 384 AD patients) revealed fascinating results regarding the influence of AD clinical factors on the BDNF. For example, gender, age, education, and clinical variables such as AD severity, disease stage, and medication can affect blood BDNF. Therefore, the complexity of AD efficient diagnosis requires the establishment of BDNF as a biomarker along standardized detection methods and cut-off values according to the weight of each influencing factor (Qian et al.).

According to Zheng et al., a novel category of promising biomarkers for human diseases is Circular RNAs (circRNAs), which may significantly contribute to regulating gene expression and progression of AD. Therefore, the researchers performed a human microarray analysis on the differentially expressed circRNAs among subjective cognitive decline, amnestic mild cognitive impairment, and age-matched normal donors, followed by the prediction of the annotations of circRNAs-microRNA interactions, which revealed the hsa_circRNA_001481 and hsa_circRNA_000479 as differentially expressed circRNAs that could be utilized for early diagnosis of AD (Zheng et al.).

Advanced studies in Alzheimer's disease therapeutics

Even though no holistic treatments for the AD cure have been presented till now, there are several available approaches for managing symptoms, controlling cognitive and behavioral impairment, and the amyloid hypothesis effects.

Chopra et al. present in their narrative review the insights that nanotechnology offers to improve AD diagnosis and treatment and the necessity of extended pharmacokinetic and pharmacodynamic studies to establish safety rules of the emerging nanotherapeutic methods. While the failure of single-target medicine, including *ex vivo* gene therapy and immunotherapy, is apparent till now, these alternative multi-target combination nano methods offer solutions for efficient medication (chemical compounds, genes, peptides, and antibodies) delivery (Chopra et al.). Of course, before the application of nanotechnological products to the management of CNS disorders due to their successful encapsulation of highly antioxidant and anti-inflammatory bioactive substances into specified brain regions, several limitations lack solution, like the toxicity and the high cost of these products (Chopra et al.).

Even though conventional oral medicines are not a part of the general anti-AD therapeutics, Arora et al. attempt to formulate, optimize, and evaluate the efficiency of rivastigmine tartrate (RT)-loaded intranasal solid lipid nanoparticles (SLNs) employing the solvent-evaporation diffusion method for nasal delivery. Arora et al.'s *in vitro* and *ex vivo* studies revealed that the developed SLNs were safe, non-lethal, efficient, and robust for intranasal delivery with no toxicity through their histopathological and pharmacokinetic investigations on sheep mucosa.

Similarly, Zia et al. performed an *in silico* analysis to investigate the date palm (*Phoenix dactylifera*) on Aβ1–40 amyloid formation as a novel potential treatment against memory loss and cognitive dysfunction due to its potent antioxidant activity. Applying molecular docking and molecular dynamics simulation on the flavonoids Diosmetin, Luteolin, and Rutin as candidates for aggregation inhibitors, Zia et al., concluded, based on binding energies and non-bonded interactions, that Diosmetin and Luteolin may serve as better molecules for the production of more efficient inhibitors with higher affinities toward the target proteins, even though extended *in vitro* and *in vivo* tests are required.

While the latest studies confirmed the critical role of the inhibition of β-site APP cleaving enzyme-1 (BACE1) for AD management, Mukerjee et al. applied ligand-based and target-based approaches to identify the potential of naturally available food molecules to bind the BACE1's active site in a particular binding pattern. From a selection of 8,453 compounds from the food database with a high potential of showing inhibitory activity against BACE1, Mukerjee et al., *via* Combined Quantitative Structure Activity Relationship (QSARs) and molecular docking studies, identified the 4-(3,4-Dihydroxyphenyl)-2-hydroxy-1H-phenalen-1-one (PubChem ID: 4468; Food ID: FDB017657) as a suitable molecule with properties Binding Affinity = −8.9 kcal/mol, pKi = 7.97 nM, Ki = 10.715 M, which might be a potential source for more efficient BACE1 inhibitors with higher Ki values in future.

A non-invasive stimulation presented and evaluated by Stekic et al., a repetitive transcranial magnetic stimulation (rTMS) on a behavioral, neurochemical, and molecular level in a trimethyltin (TMT)-induced AD-like disease model to improve cognition and revert symptoms. The scientists specifically applied and evaluated the effect of intermittent theta burst stimulation (iTBS) in male Wistar rats with severe cognitive deficits (Stekic et al.). They identified a significant downregulation of phosphorylated forms of the PI3K/Akt/mTOR signaling pathway and concluded that the

iTBS protocol could be a potential non-invasive therapy for AD and other related disorders with cognitive lesions (Stekic et al.).

Advanced computational methods in Alzheimer's disease management

In the article of Ashraf et al., the researchers freely released a novel computational model (programmed in Python) as an assistive research tool for AD prognosis and diagnosis concerning the various dietary alterations associated with neuronal lesions in AD due to mitochondrial and dynamics dysfunction. While mitochondrial dysfunction and oxidative stress produce high levels of ROS, Ashraf et al. correlate the diverse dietary and obesity-related diseases with mitochondrial bioenergetics linked to neurodegeneration. They provided a Bayesian model to formulate the impact of diet-induced obesity with impaired mitochondrial function and altered behavior based on the probabilistic expectations of AD development or progression due to specific risk factors or biomarkers (Ashraf et al.).

Kumar et al.'s research deals with the Blood Brain Barrier (BBB) permeability methods and the importance of using computational tools to calculate their accuracy instead of using time-consuming and labor-intensive clinical experiments. The researchers, to improve the accuracy of the BBB permeability prediction, applied deep learning and machine learning algorithms to a dataset of 3,605 diverse compounds, finally developing a new (open software) deep neural network (DNN) based model that predicts the BBB permeability of compounds using their simplified molecular input line entry system (SMILES) notations (Kumar et al.). Even though extended *in vivo* studies are necessary to validate CNS-acting drug candidates, the proposed DeePred-BBB model could swiftly and accurately offer the first decision-making regarding the failures due to BBB non-permeability (Kumar et al.).

Based on the fact that many pathophysiological conditions and hypotheses could play a key role in AD development, Hausman-Cohen et al. stated that not all identified to now contributing AD key factors can be applied to each patient, and a personalized, precision medicine approach must be urgently applied. Therefore, Hausman-Cohen et al. used clinical cases of patients at AD risk due to their apolipoprotein E ε4 status to establish a curated genomics clinical decision support (CDS) platform that could benefit clinicians to identify for each patient the AD risk factors in question that must be taken into further consideration and to design a personalized treatment plan.

Conclusion

The purpose of this Research Topic, Alzheimer's Disease Challenge Volume II, is to extend and highlight in-depth the scientific inquiry in the era of an aging population, converging emerging complementary therapeutic approaches with personalized precision medicine approaches. We strongly believe that this Frontiers Research Topic, with the advanced studies and conclusions concerning the current global burden of the disease, recently established biomarkers, and open-access computational tools for early diagnosis and prognosis, will enrich the efficient management of AD.

Author contributions

All authors listed have made a substantial, direct, and intellectual contribution to the work and approved it for publication.

Acknowledgments

We sincerely acknowledge all the authors for their articles and the reviewers who have contributed to improving and clarifying these diverse contributions due to their valuable comments. Finally, we thank the Specialty Chief Editors and the Frontiers editorial team of all the Sections for their continuous support.

Conflict of interest

MK was employed by Enzymoics and Novel Global Community Educational Foundation. AA was employed by AFNP Med Austria.

The remaining author declares that the research was conducted in the absence of any commercial or financial relationships that could be construed as a potential conflict of interest.

Publisher's note

frontiers in Aging Neuroscience

ORIGINAL RESEARCH
published: 16 March 2022
doi: 10.3389/fnagi.2022.865933

Factors Associated With Alzheimer's Disease Patients' Caregiving Status and Family Caregiving Burden in China

Yuxian Li[1,2†], Fangda Leng[1†], Qi Xiong[3†], Jiong Zhou[4], Ailian Du[5], Feiqi Zhu[6], Xiaowen Kou[7], Wei Sun[1], Luzeng Chen[8], Huali Wang[9], Hengge Xie[10], Feng Gao[3], Haiqiang Jin[1*] and Yongan Sun[1*]*

[1] Department of Neurology, Peking University First Hospital, Peking University, Beijing, China, [2] Department of Neurology, Beijing Tiantan Hospital, Capital Medical University, Beijing, China, [3] Health Service Department of the Guard Bureau of the Joint Staff Department, Beijing, China, [4] Department of Neurology, The Second Affiliated Hospital, School of Medicine, Zhejiang University, Zhejiang, China, [5] Department of Neurology, Shanghai Tongren Hospital, Shanghai Jiao Tong University School of Medicine, Shanghai, China, [6] Department of Neurology, Shenzhen Luohu People's Hospital, Shenzhen, China, [7] Health Times, The People's Daily, Beijing, China, [8] Department of Ultrasonography, Peking University First Hospital, Peking University, Beijing, China, [9] Department of Psychiatry, Peking University Sixth Hospital, Peking University, Beijing, China, [10] Department of Neurology, Second Medical Center of Chinese PLA General Hospital, Beijing, China

Background: The increasing prevalence of Alzheimer's disease (AD) has emerged as a major challenge worldwide. China as the most populous country in the globe is amid rapid aging of its population, highlighting the need for appropriate social and medical policies to meet the challenge. The current multicenter cross-sectional observational study aims to provide understanding of the current status of caring given to AD patients in China and investigate the factors that influence the family burden as well as the choice of care given to AD patients.

Methods: A total of 1,675 patients with probable AD from 30 provincial regions of mainland China were enrolled in the current study from August 2019 to December 2019. We analyzed the caregiving status and its relationship with family burden and various socio-economical and medical factors.

Results: In the current study, 90.87% of the AD patients enrolled adopted family care. The choice of caregiving method was influenced by factors including age (>80 years old, OR 0.648; 95% CI, 0.427–0.983), overall family burden (high, OR 0.574; 95% CI, 0.0.373–0.884), patients' income (OR 0.511; 95% CI, 0.330–0.789) and self-care ability (OR 0.329; 95% CI, 0.183–0.588).

Conclusion: Family care is the primary method of care for AD patients in China and the institutional care system for AD patients is still underprepared in China.

Keywords: Alzheimer's disease, home care, caregiver burden, institutional care, care preference, caregiving

OPEN ACCESS

Edited by:
Athanasios Alexiou, Novel Global Community Educational Foundation (NGCEF), Australia

Reviewed by:
Mohammedamin Hajure Jarso, Mettu University, Ethiopia
Hamid Sharif Nia, Mazandaran University of Medical Sciences, Iran

***Correspondence:**
Yongan Sun
sya@bjmu.edu.cn
Feng Gao
luckygf2004@163.com
Haiqiang Jin
jhq911@bjmu.edu.cn

† These authors have contributed equally to this work

Specialty section:
This article was submitted to Alzheimer's Disease and Related Dementias, a section of the journal Frontiers in Aging Neuroscience

Received: *30 January 2022*
Accepted: *21 February 2022*
Published: *16 March 2022*

Citation:
Li Y, Leng F, Xiong Q, Zhou J, Du A, Zhu F, Kou X, Sun W, Chen L, Wang H, Xie H, Gao F, Jin H and Sun Y (2022) Factors Associated With Alzheimer's Disease Patients' Caregiving Status and Family Caregiving Burden in China. Front. Aging Neurosci. 14:865933. doi: 10.3389/fnagi.2022.865933

INTRODUCTION

China as the world's most populous country is amid the rapid aging of its population, which is accompanied by a drastic increase of dementia prevalence (Pei et al., 2014). Alzheimer's disease (AD) is the most common type of senile dementia, accounting for over 60% of all-cause dementia (Alzheimer's Association, 2018). It has been estimated that the prevalence of AD among senior citizens above 65 year old is 3.21% and increases substantially with age among Chinese population (Jia et al., 2014), which has a considerable sociological and economic impact on Mainland China. It is estimated that the average socioeconomic cost of AD per patient per year is 19,144 USD in mainland China (Jia et al., 2018). The annual total cost is predicted to reach 1.89 trillion USD in 2030 in China, rendering the care of AD patients beyond a medical issue, but also an outstanding sociological problem.

Among the issues that awaits to be addressed are how to provide AD patients with appropriate care and to reduce the burden for the families. While it has been suggested that family care might be a better method of care for patients with AD considering its emotional and psychological comfort (Luppa et al., 2010), studies from high-income countries have demonstrated that institutional care offers better functional outcome compared to family care (Afram et al., 2014; Lee et al., 2019). Further, the demands of caring responsibilities change with the stages of disease, which can be a great challenge for the family. In Europe, it has been reported that the emotional and psychological distress to family caregivers enforced by Alzheimer's disease urged families to seek professional care for the patients (Bokberg et al., 2015). However, the domestic situation with regard to care giving for AD patients remains to be investigated in China, as such socio-economical issues are highly entangled by cultural and economic factors, with huge variabilities among different nations.

As an example, in western society, the choice of home or institutional care of a patient may mainly depend on personal needs, financial situations, and the accessibility of professional care (Genet et al., 2011), while in China, sending elderlies to care homes may be seen as a betrayal to the family. To date, few studies have been conducted on the caregiving status and the relationship between caregiver burden and patient factors in China. The lack of understanding on the current status of care given to domestic AD patients, together with the short of analytical data on the underlying factors have left policymakers in dark to improve welfare for AD patients and their families. In the current study, we hypothesized that the burden of family members is a major factor that influences the decision of home or institutional care for AD patients in China. We aimed to investigate the current caregiving status and burden as well as to analyze the relationship between caregiver burden and patient factors to suggest ideas for policy and research programs on chronic diseases.

MATERIALS AND METHODS

Design and Samples

This study was approved by the Ethics Committee of Peking University First Hospital (PUFH-2019-141), the leading institution of the study, and local ethic committees in all participating centers. informed consent were obtained from all patients and family members.

This is a large-sample, multi-center, cross-sectional study performed between August 2019 and December 2019. We collected data from 30 provincial, municipal, and autonomous regions of mainland China. Among them, the eastern provinces, such as Zhejiang, Beijing, and Hebei contributed the most participants (**Figure 1**).

The recruitment of participants was based on the hierarchical healthcare structure in China, where there are 3 levels of healthcare infrastructures, with the first level being community clinics and the third level being the local health centers. The participants were referred to the local health centers by local clinics or sought consultation directly from the health centers, where the patients were diagnosed as clinical probable AD by qualified neurology specialists from the local health centers. The diagnosis of probable AD dementia was based on the diagnostic criteria established by the National Institute of Aging and Alzheimer's Association (NIA-AA) in 2011 (McKhann et al., 2011). Other inclusion criteria include: (1) capability to give written consent, (2) next of kin's consent to participate, and (3) >5 years of education. Patients with other neurological diseases that are associated with cognitive impairment and major psychiatric disorders were excluded. In particular, patients with signs and symptoms suggesting other types of dementia, such as Parkinson's disease dementia, Lewy body dementia, frontotemporal dementia, primary progressive aphasia, vascular dementia and mixed dementia.

All medical staff who conducted the study were given comprehensive training on the usage of the questionnaire used in the study. Family members and professional caregivers (for patients in nursing facilities) of the patients completed the questionnaire under the guidance of doctors. For those who had already been in care homes, the family members were instructed to answer the questionnaire according to the situation when the patients were last at home. The current study focused on the perceived care burden by family members as (1) in the vast majority of scenarios it were the family members who accompanied the patients to the health centers, and (2) the decisions of home care vs. institutional care were made by the patients and their families.

Measures and Data Collection

We designed a comprehensive questionnaire, which includes demographic characteristics, household income, medical history with regard to AD, care situation, and burden to the family. The caregiving status of the patients was divided into two categories, including family care and institutional care. Family care was defined as situations in which family members, including spouses, children, grandchildren, and other relatives, take care of

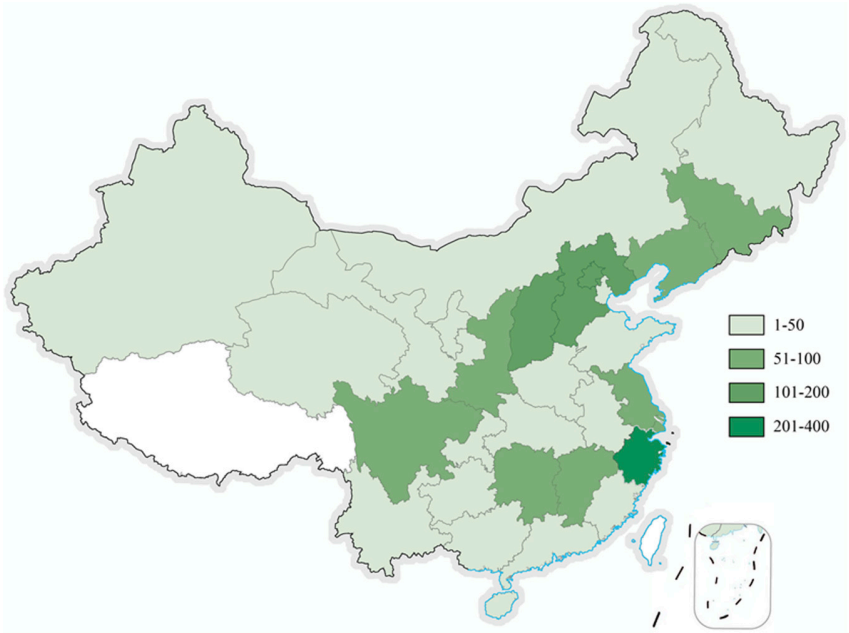

FIGURE 1 | Geographical distribution of participants in the current study.

AD patients with or without the help of a health professional. Institutional care indicates that the patients are taken care of by professionals in nursing facilities. Similarly, self-care ability was divided into two classes: basic self-care and partially or completely dependent. The type of caregiving was assessed by caregivers based on whether the patients could take care of themselves in their daily lives.

The caregiver burden inventory (CBI) (Chinese version) was used to describe the multidimensional burden of the caregivers and to distinguish related factors of different burden dimensions (Novak and Guest, 1989). The translation and validation of CBI in Chinese population was performed by Chou et al. (2002). The inventory consists of 24 questions that refer to five dimensions: time-dependence burden (questions 1–5), developmental burden (questions 6–10), physical burden (questions 11–14), social burden (questions 15–18), and emotional burden (questions 19–24). Each item was graded on a 4-point Likert scale according to the degree of each situation. A high score represented a high burden and the total score is 96. The point range from 0 to 32 was considered as a low burden, from 33 to 64 as a medium burden, and from 65 to 96 as a high burden.

The questionnaires were examined manually to ensure completeness and effectiveness immediate after the interview by staff. Incomplete questionnaire and those with obvious contradictory answers to the interview were considered invalid.

Statistical Analyses

Patients and family members' characteristics, including gender, age, housing condition, education, and annual household income were presented using descriptive statistics. Quantitative variables were examined for normal distribution and presented as the mean ± standard deviation. Independent-samples *t*-tests and one-way ANOVA were performed for group-wise comparisons of continuous variables. Chi-square tests were performed to examine cross-group differences of categorical variables. To examine the reliability performance of CBI in the settings of current study, Cronbach's alpha was calculated for all the items in the inventory and each of the five dimensions. Cronbach's alpha efficient >0.9 was considered to indicate excellent internal consistency, and >0.8 was considered to indicate good consistency. Factors with $P < 0.2$ in group-wise comparisons were then entered to binary logistic regression models to evaluate the influence of each factors in the choice of caregiving for AD patients, controlling for age and gender. All data analyses were performed using SPSS 26.0 (SPSS Inc., Chicago, IL, United States). Differences were considered statistically significant when the *P*-value was less than 0.05.

RESULTS

Patient Characteristics

A total of 1,694 people participated in the survey. After eliminating the erroneous and invalid questionnaires, 1,675 valid questionnaires were left, resulting in an effectiveness of 98.88%.

The patients characteristics are presented in **Table 1**. The 1675 AD patients were from 30 provincial, municipal, and autonomous regions of mainland China, including 650 (38.81%) men and 1,025 (61.19%) women. The participation of patients in urban areas was higher than that in rural areas (79.76 vs. 20.24%). The geographical distribution of the patients is illustrated in **Figure 1**.

TABLE 1 | Characteristics of caregivers and patients with AD (*N* = 1675).

Variable	*N*	%
Patients		
Sex		
Male	650	38.81%
Female	1025	61.19%
Age		
<70	580	34.63%
71–80	546	32.60%
>80	549	32.78%
Living area		
Urban	1336	79.76%
Rural	339	20.24%
Education level, years		
5–6	492	29.37%
7–12	776	46.33%
>12	407	24.30%
Self-care ability		
Basic self-care	424	25.31%
Partially or wholly dependent	1251	74.69%
Annual patient's income (10,000yuan)		
<3	767	45.79%
3–5	522	31.16%
>5	386	23.04%
Annual household income (10,000yuan)		
<5	611	36.48%
5–15	802	47.88%
>15	262	15.64%
Caregivers and Treatment		
Caregiving status		
Family care	1522	90.87%
Nursing facility	153	9.13%
Dementia drug application		
On medication	1278	75.30%
Used and withdrew	259	15.46%
Untreated	138	8.24%
Annual medical cost (10,000 yuan)		
<1	821	49.01%
1—2.4	585	34.93%
>2.4	269	16.06%
Annual care cost (10,000 yuan)		
<2	542	32.36%
2–6	573	34.21%
>6	266	15.88%
Unclear	294	17.55%
Caregiver burden		
Low	484	28.90%
Medium	955	57.01%
High	236	14.09%

Comparison of Characteristics Between Home-Cared and Institution-Cared Patients

Of the 1,675 AD patients sampled, 1522 (90.87%) patient chose family care and 153 (9.13%) patients lived in care homes. To identify the factors associated with the choice of care, we analyzed the characteristics of the patients' caregiving status (**Table 2**). Home cared and institution cared patients did not differ by gender or education level. Patients who were above 80 years ($P = 0.003$) and living in urban areas ($P < 0.001$) were more likely to choose institutional care compared to those who were younger and in rural regions. Concerning economic status, the choice of patient care is related to the annual income of the patient ($P < 0.001$). A greater proportion of patients living in nursing homes belong to a higher income group; however, no significant difference was found between annual household income groups ($P = 0.122$). According to self-care ability and CBI score, patients who are less capable of taking care of themselves and who impose a large burden to family caregivers tended to choose nursing facilities ($P = 0.001$).

Regression Analysis of Factors Associated With Choice of Care

We used binary logistic regression analysis to identify the relevant factors for choosing nursing facilities for patients with AD (**Table 3**). Urban patients are more likely to choose nursing

TABLE 2 | The caregiving status of the familial caregiver of patients with AD in relation to patient and caregiver characteristics (*N* = 1675).

	Family care *N* = 1522 (%)	Institutional care *N* = 153 (%)	*P*-value
Sex			0.948
Male	591 (38.83)	59 (38.56)	
Female	931 (61.17)	94 (61.44)	
Age			0.003
<70	538 (35.35)	42 (27.45)	
71–80	506 (33.25)	40 (26.14)	
>80	478 (31.41)	71 (46.41)	
Living area			<0.001
Urban	1194 (78.45)	142 (92.81)	
Rural	328 (21.55)	11 (7.19)	
Education level, years			0.052
5–6	457 (30.03)	35 (22.88)	
6–12	706 (46.39)	70 (45.75)	
>12	359 (23.59)	48 (31.37)	
Annual patient's income (1,0000 yuan)			<0.001
<3	724 (47.57)	43 (28.10)	
>3	798 (52.43)	110 (71.90)	
Annual household income (1,0000 yuan)			0.122
<5	564 (37.06)	47 (30.72)	
5–15	728 (47.83)	74 (29.25)	
>15	230 (15.11)	32 (20.92)	
Self-care ability			<0.001
Basic self-care	408 (26.81)	16 (10.46)	
Partially or wholly dependent	1114 (73.19)	137 (89.54)	
Family care burden			0.001
Low	450 (29.57)	34 (22.22)	
Medium	872 (57.29)	83 (54.25)	
High	200 (13.14)	36 (23.53)	

TABLE 3 | Logistic regression models for the caregiving status of AD patients (*N* = 1675).

	OR	(95% CI)		*P*-value
Age				
<70	Ref.			
71–80	0.744	0.489	1.131	0.167
>80	0.648	0.427	0.983	0.041
Living area				
Rural	Ref.			
Urban	2.374	1.228	4.588	0.010
Annual patient's income (10,000 yuan)				
<3	Ref.			
>3	0.511	0.330	0.789	0.003
Annual household income (10,000 yuan)				
<5	Ref.			
5–15	0.877	0.512	1.500	0.631
>15	0.726	0.462	1.141	0.165
Self-care ability				
Basic self-care	Ref.			
Partially or wholly dependent	0.329	0.183	0.588	<0.001
Family care burden				
Low	Ref.			
Medium	0.713	0.411	1.235	0.227
High	0.574	0.373	0.884	0.012

homes than rural patients (OR = 2.374; 95% CI, 1.228–4.588). Impaired self-care ability was also a predictor of choosing nursing homes over family care (OR = 0.329; 95% CI, 0.183–0.588). The family care burden is also a related factor, with families having higher perceived care burden being more inclined to seek institutional care (OR = 0.574; 95% CI,0.373–0.884).

Internal Consistency of the Chinese Version Caregiver Burden Inventory Scale

In the current study, the overall Cronbach's alpha of the CBI scale (24 items) was 0.950 (95% CI, 0.946–0.953); the time-dependence burden (5 items) dimension had a Cronbach's alpha of 0.934 (95% CI, 0.929–0.940); developmental burden (five items) dimension had Cronbach's alpha of 0.939 (95% CI, 0.933–0.944); physical burden (four items)'s Cronbach's alpha was 0.954 (95% CI, 0.950–0.959); social burden (five items) dimension's Cronbach's alpha was 0.831 (95% CI, 0.0.815–0.845); and the Cronbach's alpha of emotional burden (five items) was 0.854 (95% CI, 0.835–0.869). These coefficients indicated that the CBI scale had an excellent overall internal consistency and the sub-domains offered at least good reliability in the current study.

Burden on Caregivers of Alzheimer's Disease Patients

In this study, 25.31% of the patients could take basic care of themselves. The other 74.69% of patients were partially or wholly dependent on others for care. About 36.48% of patients were completely dependent on caregivers, indicating that a large proportion of AD patients had severe disabilities. According to the CBI scores, 28.90% of families had a relatively low level of burden, 14.09% of families had a high level of burden, and the remaining 57.01% had a medium level of burden. From the perspective of burden classification, all five dimensions of burden were separately calculated in the two different groups (**Table 4**). All aspects of family burden significantly increased when patients were not able to take care of themselves ($P < 0.001$). Caregiving status was also associated with burden grade. Families of patients who were at nursing facilities had a higher total burden of care (when the patients were last at home) compared to those home-cared ($P < 0.001$). In addition, in other aspects such as time-dependence, development limitation, health, and social contact, families bear a higher burden before the patients were sent to a nursing home than those home-cared.

The family burden was affected by both the self-care ability and caregiving status of the patients at the same time. To exclude confounding factors, we used stratified correlation analysis to determine the impact of self-care ability and caregiving status on the burden of caregivers (**Table 5**). There was no significant difference of family burden, either family care or nursing facility ($P = 0.520$), if the patients could take care of themselves. However, if the patients were incapable of self-care, the overall family burden was higher carer-dependent AD patients ($P = 0.015$), and the differences mainly manifested in the burden of time-dependence (P = 0.002) and the health of caregivers ($P = 0.008$).

DISCUSSION

Alzheimer's disease is a progressive neurodegenerative disease, which causes cognitive decline in multiple cognitive domains including language, visuospatial, executive function, complex attention, perceptual-motor, social cognition, and most commonly, memory (McKhann et al., 2011). Behavioral and psychological symptoms gradually occur in AD patients, resulting in disability and most patients are completely dependent at later stages of the disease (Atri, 2019).

In the current study, the factors associated with the choice of home or institutional care for AD patients in China. We found that age (>80 years), living in urban areas, higher patient annual income, inability of self-care and high family care burden were associated with higher probability of choosing institutional care for AD patients in China.

Our results suggest that family care is the most common choice for families of AD patients in China, which is a common phenomenon in developing countries especially in Asia (Prince and Dementia Research Group, 2004). While increasing numbers of nursing facilities is being set up, Chinese families with AD patients have a low preference for institutional care (**Table 6**). Aside from the subjective reasons (disapproval by family members or patients), our questionnaire suggested that the primary reasons against institutional care were economic burden (34.9%) and insufficient service provided by the institutions (34.5%). Many people view that nursing homes cannot provide individual care to patients. It is noteworthy that some family caregivers (4.4% of all home-cared patients and 32.6% of all patients who have experienced institutional care) mention that

TABLE 4 | CBI scores of the family of patients with AD based on the caregiving status.

Burden classification	*n*	Time-dependence (−x ± s,score)	*P*-value	Developmental (−x ± s,score)	*P*-value	Physical (−x ± s,score)	*P*-value	Social (−x ± s,score)	*P*-value	Emotional (−x ± s,score)	*P*-value	Total (−x ± s,score)	*P*-value
Self-care ability			<0.001		<0.001		<0.001		<0.001		<0.001		<0.001
Basic self-care	424	6.53 ± 4.65		7.62 ± 5.62		4.56 ± 4.16		3.30 ± 3.36		3.02 ± 3.63		25.04 ± 18.02	
Partially or wholly dependent	1251	15.45 ± 4.20		14.09 ± 4.87		9.60 ± 4.42		5.90 ± 4.07		4.82 ± 4.65		49.87 ± 16.81	
Care-giving status			<0.001		0.001		<0.001		0.008		0.510		<0.001
Family care	1522	12.98 ± 5.81		12.30 ± 5.74		8.17 ± 4.83		5.16 ± 4.02		4.34 ± 4.41		42.95 ± 20.05	
Nursing facility	153	15.29 ± 5.34		13.96 ± 6.14		9.90 ± 5.07		6.14 ± 4.41		4.62 ± 5.17		49.92 ± 21.03	

TABLE 5 | CBI scores of family members with different care status after classification according to patient self-care ability.

Self-care ability	*n*	Time-Dependence (−x ± s,score)	*P*-value	Developmental (−x ± s,score)	*P*-value	Physical (−x ± s,score)	*P*-value	Social (−x ± s,score)	*P*-value	Emotional (−x ± s,score)	*P*-value	Total (−x ± s,score)	*P*-value
Basic self-care			0.163		0.557		0.902		0.873		0.561		0.520
Family care	408	6.59 ± 4.69		7.65 ± 5.61		4.57 ± 4.14		3.30 ± 3.29		3.04 ± 3.64		25.15 ± 17.95	
Nursing facility	16	4.94 ± 3.21		6.81 ± 5.79		4.44 ± 4.84		3.50 ± 4.97		2.50 ± 3.63		22.19 ± 20.26	
Partially or wholly dependent			0.002		0.118		0.008		0.094		0.901		0.015
Family care	1114	15.32 ± 4.20		14.01 ± 4.76		9.48 ± 4.38		5.84 ± 4.05		4.81 ± 4.57		49.46 ± 16.53	
Nursing facility	137	16.50 ± 4.08		14.80 ± 5.63		10.54 ± 4.72		6.45 ± 4.26		4.87 ± 5.28		53.15 ± 18.66	

TABLE 6 | Reasons for patients not choosing to live in nursing facilities.

Item	*N*	%
Subjective factors		
Disagreement of the patient's family members.	614	36.7
Disagreement of the patient him/herself.	558	33.3
Objective factors		
No local nursing facilities.	108	6.4
Too long of the queuing time.	137	8.2
Insufficient service level of nursing facilities.	578	34.5
Too much expense of the nursing facilities.	584	34.9
Unable to move in due to physical condition (illness, disability, etc.).	199	11.9
Once lived in, but later decided against nursing facility.	74	4.4

the patients who earlier chose to live in a nursing home, for various reasons, often decide to leave the nursing home and return to family care. The striking proportion of AD patients dropping from nursing homes indicates deficiencies of Chinese institutional care system's infrastructure and proficiency, which is evidenced by a lack of care professionals' knowledge on dementia (Wang Y. et al., 2018). The low subjective preference of Chinese family for institutional care might be related to traditional cultural heritage, as Chinese people attach great importance to filial piety. In fact, during interview, some patients living nursing homes admitted feeling abandoned by their families. However, these socio-cultural factors were not quantitively analyzed in the current study and could be further investigated in following studies (Add some reference: agreement with literature, Cultural studies).

Most AD patients will deteriorate to a completely dependent state along disease trajectory, placing have care burdens to their families both economically and sociologically. An international multilateral cost-of-illness (COI) studies has summarized that the socioeconomic cost of AD includes direct medical, direct non-medical and indirect costs (Callahan, 2017). Jia et al. (2018) have predicted that the annual cost of AD patients worldwide to be US $9.12 trillion in 2050. The burden enforced by AD on families is not just financial, but also affects other aspects of life. For example, the symptoms of dementia often cause physical, emotional, and mental stress (D'Onofrio et al., 2015). Many studies have explored the influence factors of caregiver burden, indicating that the burden on caregivers is higher in families with lower income and disease severity (Montgomery et al., 2018; Kawano et al., 2020). In addition, disease related burden for family caregivers of AD patients increases drastically as disease progresses, and is influenced by the caregiver's education, and being spouse of the patient (Lou et al., 2015; Liu et al., 2017b). Most families experience mental tension due to AD and a negative psychological interactions between caregivers and patients has been reported (Andren and Elmstahl, 2008). However, there are few recent and large-scale, multicenter studies on caregiver burden of Chinese AD patients, and most studies have focused on patients receiving family care (Yu et al., 2015; Liu et al., 2017a; Zhang et al., 2018). Hence, there is a lack of research on the impact of care style on family burden inflicted by AD in Chinese population.

According to the current study, the self-care ability and the burden on family members has a significant impact on care status of AD patients. The families who choose a nursing home for their elderly who lost self-care abilities usually have suffered a higher burden before and even after the decision of institutional care is made. Underdeveloped social nursing facilities in China also bring many concerns to families of AD patients, the care of whom is different from ordinary elderlies, and providing both medically and psychologically professional care for demented patients is an imminent problem for the institutional care systems in China. On the other hand, the social insurance system also results in a higher cost of living in a nursing home for the patients' families, as reflected in by the influence of the patient's personal income on the choice of care type. Further, the general public, including the family members' lack of awareness and understanding of AD may also have negatively influence the caregiving status of AD patients and social burdens for their families (Dai et al., 2015; Zeng et al., 2015). Other aspects might also affect the choice, as studies have suggested that most families willing to send their elderly to nursing homes have a higher awareness of diseases, while less-caring families have lower perception of burden and tend to choose family care (Jia et al., 2020).

The current study has its implications for the improvement of China's social insurance system, as it reflects a lack of accessible and professional nursing assistance for patients and families impacted by AD (Samus et al., 2018). For Chinese patients with AD, there are restricted alternatives and only few choices to live their lives with financial constraints (Zeng et al., 2020). According to a study in 2015, most AD patients in China have two offspring or more (80.56%), while 19.44% of participants have only one child or no child (Jia et al., 2018). However, the consequence of the one-child policy is changing the scenario dramatically in the upcoming decades, and a foreseeable challenge to the social care system is imminent, with a simulation study in has projected the economic burden associated with AD to increase by 37-fold by 2050 compared 2011 (Keogh-Brown et al., 2016). On the other hand, a more capable social support system (aside from financial aid) needs to be established both for the patients and the family members to ease their distress (Patterson et al., 1998; Wang Z. et al., 2018). Therefore, early warns should be given to policymakers to take effective measures.

The current study has some limitations that should be noted. First, due to practical limitations, we were unable to perform multistage sampling to ensure a balanced geographical sample, and the current work was lead by local health centers which volunteered to cooperate (the top level of the hierarchical structure in China). While these centers are responsible for referred patients from community clinic and walk-in outpatient services are accessible for all citizens, they are usually located in urban areas the sampling process has a predilection for urban dwellers, who could not fully represent the AD patient population in China. Secondly, the questionnaire used here was only available to patients who were diagnosed as clinically probable AD dementia and further studies could expand their scope to possible AD, MCI and all-cause dementia. Thirdly, the severity of AD was not quantified with our study design and functional health outcomes were not evaluated due to the cross-section

nature of the study. The economic burden and mental stress of the patients' family could be investigated in more detail in retrospect, for example, the service time of a family member as care giver would an important factor. All these problems warrant further investigation in a larger and more balanced patient cohort. Nevertheless, the current study has provided a basic understanding of the caregiving status and burden on Chinese families with AD patients.

In conclusion, the economic costs of AD come from all directions. Family care is the primary method of care for AD patients in China. The method of patient care is influenced by the housing condition, patient income, and disease severity. Overall, this study reveals the present situation of AD patients and their families and provides insights to help public health policymaking.

DATA AVAILABILITY STATEMENT

The datasets presented in this article are not readily available because of institutional privacy policy. Requests to access the datasets should be directed to YS, sya@bjmu.edu.cn.

ETHICS STATEMENT

The studies involving human participants were reviewed and approved by the Ethics Committee of Peking University First Hospital. The patients/participants provided their written informed consent to participate in this study.

AUTHOR CONTRIBUTIONS

YL and FL contributed to the analysis and interpretation of the data, drafting and revision of the manuscript. QX, JZ, AD, FZ, WS, LC, HW, and HX contributed to collection of data, quality control, and establishing the database. XK contributed to advertising and coordination of the study. FG, HJ, and YS contributed to the conceptualization of the study, formulation of study protocol and intellectual revision of the manuscript. All authors contributed to the article and approved the submitted version.

FUNDING

This study was supported by the National Key R&D Program of China (2018YFC1314200), National Natural Science Foundation of China (82071306), and Group-Style Medical Aid Project for Tibet (XZ2017ZR-ZY13).

ACKNOWLEDGMENTS

We sincerely thank all members of the *Alzheimer's Disease China* for their contributions to recruiting patients and data collection, and thank *Health Times* for questionnaire design and data analysis.

REFERENCES

Afram, B., Stephan, A., Verbeek, H., Bleijlevens, M. H., Suhonen, R., Sutcliffe, C., et al. (2014). Reasons for institutionalization of people with dementia: informal caregiver reports from 8 European countries. *J. Am. Med. Dir. Assoc.* 15, 108–116. doi: 10.1016/j.jamda.2013.09.012

Alzheimer's Association (2018). 2018 Alzheimer's disease facts and figures. *Alzheimers Dement.* 14, 367–429. doi: 10.21926/obm.geriatr.1904079

Andren, S., and Elmstahl, S. (2008). The relationship between caregiver burden, caregivers' perceived health and their sense of coherence in caring for elders with dementia. *J. Clin. Nurs.* 17, 790–799. doi: 10.1111/j.1365-2702.2007.02066.x

Atri, A. (2019). The Alzheimer's Disease Clinical Spectrum: diagnosis and Management. *Med. Clin. North. Am.* 103, 263–293. doi: 10.1016/j.mcna.2018.10.009

Bokberg, C., Ahlstrom, G., Leino-Kilpi, H., Soto-Martin, M. E., Cabrera, E., Verbeek, H., et al. (2015). Care and Service at Home for Persons With Dementia in Europe. *J. Nurs. Scholarsh.* 47, 407–416. doi: 10.1111/jnu.12158

Callahan, C. M. (2017). Alzheimer's Disease: individuals, Dyads, Communities, and Costs. *J. Am. Geriatr. Soc.* 65, 892–895. doi: 10.1111/jgs.14808

Chou, K. R., Jiann-Chyun, L., and Chu, H. (2002). The reliability and validity of the Chinese version of the caregiver burden inventory. *Nurs. Res.* 51, 324–331. doi: 10.1097/00006199-200209000-00009

Dai, B., Mao, Z., Wu, B., Mei, Y. J., Levkoff, S., and Wang, H. (2015). Family Caregiver's Perception of Alzheimer's disease and caregiving in Chinese culture. *Soc. Work Public Health* 30, 185–196. doi: 10.1080/19371918.2014.969858

D'Onofrio, G., Sancarlo, D., Addante, F., Ciccone, F., Cascavilla, L., Paris, F., et al. (2015). Caregiver burden characterization in patients with Alzheimer's disease or vascular dementia. *Int. J. Geriatr. Psychiatry* 30, 891–899. doi: 10.1002/gps.4232

Genet, N., Boerma, W. G., Kringos, D. S., Bouman, A., Francke, A. L., Fagerstrom, C., et al. (2011). Home care in Europe: a systematic literature review. *BMC Health Serv. Res.* 11:207. doi: 10.1186/1472-6963-11-207

Jia, J., Wang, F., Wei, C., Zhou, A., Jia, X., Li, F., et al. (2014). The prevalence of dementia in urban and rural areas of China. *Alzheimers. Dement.* 10, 1–9. doi: 10.1016/j.jalz.2013.01.012

Jia, J., Wei, C., Chen, S., Li, F., Tang, Y., Qin, W., et al. (2018). The cost of Alzheimer's disease in China and re-estimation of costs worldwide. *Alzheimers. Dement.* 14, 483–491. doi: 10.1016/j.jalz.2017.12.006

Jia, L., Quan, M., Fu, Y., Zhao, T., Li, Y., Wei, C., et al. (2020). Dementia in China: epidemiology, clinical management, and research advances. *Lancet Neurol.* 19, 81–92. doi: 10.1016/S1474-4422(19)30290-X

Kawano, Y., Terada, S., Takenoshita, S., Hayashi, S., Oshima, Y., Miki, T., et al. (2020). Patient affect and caregiver burden in dementia. *Psychogeriatrics* 20, 189–195. doi: 10.1111/psyg.12487

Keogh-Brown, M. R., Jensen, H. T., Arrighi, H. M., and Smith, R. D. (2016). The Impact of Alzheimer's Disease on the Chinese Economy. *EBioMedicine* 4, 184–190. doi: 10.1016/j.ebiom.2015.12.019

Lee, T. W., Yim, E. S., Choi, H. S., and Chung, J. (2019). Day care vs home care: effects on functional health outcomes among long-term care beneficiaries with dementia in Korea. *Int. J. Geriatr. Psychiatry* 34, 97–105. doi: 10.1002/gps.4992

Liu, S., Jin, Y., Shi, Z., Huo, Y. R., Guan, Y., Liu, M., et al. (2017a). The effects of behavioral and psychological symptoms on caregiver burden in frontotemporal dementia, Lewy body dementia, and Alzheimer's disease: clinical experience in China. *Aging Ment. Health* 21, 651–657. doi: 10.1080/13607863.2016.1146871

Liu, S., Li, C., Shi, Z., Wang, X., Zhou, Y., Liu, S., et al. (2017b). Caregiver burden and prevalence of depression, anxiety and sleep disturbances in Alzheimer's disease caregivers in China. *J. Clin. Nurs.* 26, 1291–1300. doi: 10.1111/jocn.13601

Lou, Q., Liu, S., Huo, Y. R., Liu, M., Liu, S., and Ji, Y. (2015). Comprehensive analysis of patient and caregiver predictors for caregiver burden, anxiety and

depression in Alzheimer's disease. *J. Clin. Nurs.* 24, 2668–2678. doi: 10.1111/jocn.12870

Luppa, M., Luck, T., Weyerer, S., Konig, H. H., Brahler, E., and Riedel-Heller, S. G. (2010). Prediction of institutionalization in the elderly. A systematic review. *Age Ageing* 39, 31–38. doi: 10.1093/ageing/afp202

McKhann, G. M., Knopman, D. S., Chertkow, H., Hyman, B. T., Jack, C. R. Jr., Kawas, C. H., et al. (2011). The diagnosis of dementia due to Alzheimer's disease: recommendations from the National Institute on Aging-Alzheimer's Association workgroups on diagnostic guidelines for Alzheimer's disease. *Alzheimers. Dement.* 7, 263–269. doi: 10.1016/j.jalz.2011.03.005

Montgomery, W., Goren, A., Kahle-Wrobleski, K., Nakamura, T., and Ueda, K. (2018). Alzheimer's disease severity and its association with patient and caregiver quality of life in Japan: results of a community-based survey. *BMC Geriatr.* 18:141. doi: 10.1186/s12877-018-0831-2

Novak, M., and Guest, C. (1989). Application of a multidimensional caregiver burden inventory. *Gerontologist* 29, 798–803. doi: 10.1093/geront/29.6.798

Patterson, T. L., Semple, S. J., Shaw, W. S., Yu, E., He, Y., Zhang, M. Y., et al. (1998). The cultural context of caregiving: a comparison of Alzheimer's caregivers in Shanghai, China and San Diego, California. *Psychol. Med.* 28, 1071–1084. doi: 10.1017/s0033291798007053

Pei, J. J., Giron, M. S., Jia, J., and Wang, H. X. (2014). Dementia studies in Chinese populations. *Neurosci. Bull.* 30, 207–216. doi: 10.1007/s12264-013-1420-1

Prince, M., and Dementia Research Group (2004). Care arrangements for people with dementia in developing countries. *Int. J. Geriatr. Psychiatry* 19, 170–177. doi: 10.1002/gps.1046

Samus, Q. M., Black, B. S., Bovenkamp, D., Buckley, M., Callahan, C., Davis, K., et al. (2018). Home is where the future is: the BrightFocus Foundation consensus panel on dementia care. *Alzheimers. Dement.* 14, 104–114. doi: 10.1016/j.jalz.2017.10.006

Wang, Y., Xiao, L. D., Luo, Y., Xiao, S. Y., Whitehead, C., and Davies, O. (2018). Community health professionals' dementia knowledge, attitudes and care approach: a cross-sectional survey in Changsha, China. *BMC Geriatr.* 18:122. doi: 10.1186/s12877-018-0821-4

Wang, Z., Ma, C., Han, H., He, R., Zhou, L., Liang, R., et al. (2018). Caregiver burden in Alzheimer's disease: moderation effects of social support and mediation effects of positive aspects of caregiving. *Int. J. Geriatr. Psychiatry* Epub online ahead of print. doi: 10.1002/gps.4910

Yu, H., Wang, X., He, R., Liang, R., and Zhou, L. (2015). Measuring the Caregiver Burden of Caring for Community-Residing People with Alzheimer's Disease. *PLoS One* 10:e0132168. doi: 10.1371/journal.pone.0132168

Zeng, F., Xie, W. T., Wang, Y. J., Luo, H. B., Shi, X. Q., and Zou, H. Q. (2015). General public perceptions and attitudes toward Alzheimer's disease from five cities in China. *J. Alzheimers. Dis.* 43, 511–518. doi: 10.3233/JAD-141371

Zeng, Q., Wang, Q., Zhang, L., and Xu, X. (2020). Comparison of the Measurement of Long-Term Care Costs between China and Other Countries: a Systematic Review of the Last Decade. *Healthcare* 8:117. doi: 10.3390/healthcare8020117

Zhang, M., Chang, Y. P., Liu, Y. J., Gao, L., and Porock, D. (2018). Burden and Strain among Familial Caregivers of Patients with Dementia in China. *Issues Ment. Health Nurs.* 39, 427–432. doi: 10.1080/01612840.2017.1418034

Conflict of Interest: XK was employed by The People's Daily, China.

The remaining authors declare that the research was conducted in the absence of any commercial or financial relationships that could be construed as a potential conflict of interest.

Publisher's Note: All claims expressed in this article are solely those of the authors and do not necessarily represent those of their affiliated organizations, or those of the publisher, the editors and the reviewers. Any product that may be evaluated in this article, or claim that may be made by its manufacturer, is not guaranteed or endorsed by the publisher.

frontiers | Frontiers in Aging Neuroscience

HYPOTHESIS AND THEORY
published: 18 April 2022
doi: 10.3389/fnagi.2022.862362

Genomics as a Clinical Decision Support Tool for Identifying and Addressing Modifiable Causes of Cognitive Decline and Improving Outcomes: Proof of Concept Support for This Personalized Medicine Strategy

Sharon Hausman-Cohen[1], Carol Bilich[1], Sandeep Kapoor[2], Eduardo Maristany[3], Anne Stefani[4] and Alexandra Wilcox[1]*

[1] IntellxxDNA, Austin, TX, United States, [2] Kapoor Medical, Studio City, CA, United States, [3] Naples Center for Functional Medicine, Naples, FL, United States, [4] Resilient Health, Austin, TX, United States

OPEN ACCESS

Edited by:
Athanasios Alexiou, Novel Global Community Educational Foundation (NGCEF), Australia

Reviewed by:
Sami Ouanes, Lausanne University Hospital, Switzerland
Michael William Lutz, Duke University, United States

***Correspondence:**
Sharon Hausman-Cohen
SharonMD@intellxxdna.com

Specialty section:
This article was submitted to Alzheimer's Disease and Related Dementias, a section of the journal Frontiers in Aging Neuroscience

Received: *25 January 2022*
Accepted: *25 March 2022*
Published: *18 April 2022*

Citation:
Hausman-Cohen S, Bilich C, Kapoor S, Maristany E, Stefani A and Wilcox A (2022) Genomics as a Clinical Decision Support Tool for Identifying and Addressing Modifiable Causes of Cognitive Decline and Improving Outcomes: Proof of Concept Support for This Personalized Medicine Strategy. Front. Aging Neurosci. 14:862362. doi: 10.3389/fnagi.2022.862362

The landscape of therapeutics for mild cognitive impairment and dementia is quite limited. While many single-agent trials of pharmaceuticals have been conducted, these trials have repeatedly been unable to show improvement in cognition. It is hypothesized that because Alzheimer's, like many other chronic illnesses, is not a monogenic illness, but is instead caused by the downstream effects of an individual's genetic variants interacting with each other, the environment, and lifestyle, that improving outcomes will require a personalized, precision medicine approach. This approach requires identifying and then addressing contributing genomic and other factors specific to each individual in a simultaneous fashion. Until recently, the utility of genomics as part of clinical decision-making for Alzheimer's and cognitive decline has been limited by the lack of availability of a genomic platform designed specifically to evaluate factors contributing to cognitive decline and how to respond to these factors The clinical decision support (CDS) platform used in the cases presented focuses on common variants that relate to topics including, but not limited to brain inflammation, amyloid processing, nutrient carriers, brain ischemia, oxidative stress, and detoxification pathways. Potential interventions based on the scientific literature were included in the CDS, but the final decision on what interventions to apply were chosen by each patient's physician. Interventions included supplements with "generally regarded as safe (GRAS)" rating, along with targeted diet and lifestyle modifications. We hypothesize that a personalized genomically targeted approach can improve outcomes for individuals with mild cognitive impairment who are at high risk of Alzheimer's. The cases presented in this report represent a subset of cases

from three physicians' offices and are meant to provide initial proof of concept data demonstrating the efficacy of this method and provide support for this hypothesis. These patients were at elevated risk for Alzheimer's due to their apolipoprotein E ε4 status. While further prospective and controlled trials need to be done, initial case reports are encouraging and lend support to this hypothesis of the benefit of a genomically targeted personalized medicine approach to improve outcomes in individuals with cognitive decline who are at high risk for Alzheimer's.

Keywords: Alzheimer's, genomics, clinical decision support, APOE ε4, precision medicine, personalized medicine, natural products, MCI

INTRODUCTION

An estimated 6.2 million individuals are living with Alzheimer's in the United States alone (Alzheimer's Association, 2021). Additionally, mild cognitive impairment (MCI) prevalence has been estimated at approximately 5.9% of the adult population worldwide (Sachdev et al., 2015) and has been found in 3.7–13% of individuals aged 60–64, depending on the criteria used (Kumar et al., 2005). Individuals with MCI, progress to Alzheimer's or other forms of dementia at a high rate. In some cases, the risk of progression is over 25% per year (Kumar et al., 2005; Petersen et al., 2018).

In 2020, approximately 305 billion dollars was spent on Alzheimer's and dementia treatment in the United States alone (Wong, 2020). In addition to the direct cost of treating Alzheimer's, there are the indirect costs including the economic burden put upon family members and caregivers and lost wages for younger individuals. Thus, even preventing the progression from MCI to Alzheimer's in a portion of individuals, could represent huge cost savings to the United States and world health systems. Prevention of cognitive decline would also provide benefit for patients and their families, in both financial and emotional realms.

In the field of Alzheimer's, the common "pill for an ill" strategy has proven to be highly unsuccessful. Over 200 Alzheimer's drug trials have failed (Yiannopoulou et al., 2019). The current dogma in neurology is that Alzheimer's disease (AD) and MCI most often provide a "one-way street" toward a decline in function. In fact, the current standard used to measure a therapeutic's success in AD or MCI is a reduction of decline (Haeberlein et al., 2020). There is a need to switch the focus from slowing what is often perceived as an "inevitable decline" to the potential for improvement. Novel approaches to this global problem are needed, including looking at modifiable contributing factors.

It has been hypothesized that AD and MCI are not due to one cause, but instead multiple contributing factors and that to improve outcomes in Alzheimer's and MCI these multiple contributing factors must be addressed simultaneously (Bredesen et al., 2018). In the manuscript presented here, we take the hypothesis one step further and suggest that the lack of success in identifying a cure, or even a treatment for Alzheimer's, is because common diseases of aging such as cognitive decline, are due to a collection of genetic predispositions interacting with diet, environment, and lifestyle. Many of these predispositions can be identified using a well-curated genomics CDS. We present evidence that when root causes of cognitive decline are identified using genomics and addressed using genomically targeted interventions, improvements in cognition and the trajectory of the disease can be significantly changed.

An important point to consider in working with individuals with cognitive decline who have been labeled as "early Alzheimer's" is the potential for this diagnosis to be incorrect. The ApoE ε4 genomic variant is found in over 60% of the patients diagnosed with Alzheimer's (Riedel et al., 2016). However, even in the presence of ApoE ε4 and cognitive decline together are insufficient criteria for diagnosing Alzheimer's. The INDIA-florbetapir study showed 79% of individuals, who had been presumptively diagnosed with Alzheimer's, did not have evidence of Alzheimer's when the gold standard amyloid positron emission tomography (PET) scan was done (Boccardi et al., 2016). Although all three of the individuals presented in this manuscript had ApoE ε4 variants (and one was ApoE ε4/4), in this vein, it would be wrong to assume that this means that their cognitive decline is definitively all due to "Alzheimer's" and evidence of irreversible neurodegeneration. This brings up the question of what is causing these individuals' cognitive decline, and could there be some contributing reversible factors? In this sampling of case studies, we aim to show how the IntellxxDNA^{TM} genomics Clinical Decision Support (CDS) platform can help clinicians identify potentially modifiable factors contributing to cognitive decline. Factors evaluated included genomics contributing to specific nutrient deficiencies, decreased ability to remove toxicants, genomics that contribute to proper amyloid processing, mitochondrial function, oxidative stress, and predispositions toward brain ischemia due to clotting cascade related variants or other pathways (Armstrong, 2019). As evidenced by the last case presented, genomics can also be used to optimize function and outcomes in cases of patients with cognitive decline who are amyloid PET scan positive. Even though these patients would be considered to have presumptive early Alzheimer's, genomics can identify additional contributing factors, to help stabilize and improve cognition.

This proof-of-concept work, showing reversal of cognitive decline both in amyloid PET scan positive and other individuals is significant in that it shifts the paradigm from viewing Alzheimer's and cognitive decline as a non-reversible condition to a treatable condition. It also presents a diverging hypothesis that genomically targeted personalized treatment plans may

provide better outcomes than the standard of care options currently available.

MATERIALS AND METHODS

Patients were invited to participate through their clinician's offices. All the clinicians were trained in integrative or functional medicine and were comfortable with the concept of complex chronic illness being due to a multitude of genomic variants that can have a combinatorial effect. The specific genomic CDS platform used by all three of the physician's whose cases are reported here, was IntellxxDNA. The IntellxxDNA CDS is a scientifically rigorous genomics platform which consists of a highly cultivated collection of variants that have been shown to be clinically significant, in the form of reports categorized by specific health concerns. The CDS was developed by a team of physicians and researchers who conducted a broad review of rigorously published peer-reviewed human genomic scientific trials that looked at clinically significant genomic variants with good statistical significance related to Alzheimer's and cognitive decline.

The methodology of IntellxxDNA has been described elsewhere, in previous publications (Way et al., 2021), but central to the reports is that only genomic variants that have been shown to be highly clinically significant in the published peer reviewed scientific literature as determined by p values [$p < 0.05$ for group with variant compared to control group in disease specific studies and $<5 \times 10^{-8}$ for Genome Wide Association Studies (GWAS)] were included. Thus, the composition of the CDS reflects current evidence for genetic findings that stand up to statistical rigor related to AD and other causes of dementia.

For further rigor in our health condition specific related reports, and to keep the report a manageable size, the variants chosen for these "odds ratio reports" needed to have had evidence for them increasing or decreasing the risk of Alzheimer's or the particular disease state described by at least 20% or an odds ratio of at least 1.2. This decreased the list of candidate genes down from hundreds for each panel to just the dozen or so that are most significant. Many of the variants in the report have odds ratios of more than 2, representing a 100% increase in risk for individuals with that genetic variant. Combinations of variants that have been shown in the literature to have significant interactions are also reported. Another key factor for inclusion in the CDS is that variants displayed are determined to be potentially modifiable, not pathogenic.

All patients received the "Executive Combination Report" which is comprised of two smaller reports, the "Brain Optimization Report," and the "Medical Overview Report." The Brain Optimization report consists of over 15 different panels. The "capstone" panels in the Brain Optimization report focus on gene variants highly associated with AD, leukoaraiosis, and brain ischemia. Thus, the composition of the CDS reflects current evidence for genetic findings that stand up to statistical rigor related to AD and other causes of cognitive decline. The platform also includes variants related to hormonal factors, nutritional factors, inflammatory pathways, as well as genetic variants related to gluten intolerance, intestinal barrier function, and removal of toxicants. The Medical Overview report focuses on underlying contributing factors to other chronic medical conditions such as cardiac disease and obesity.

In an effort to learn more about the mechanisms of action of the genomic pathways and their associations with cognitive decline, the physicians underwent genomic education which was provided to them as part of the CDS support platform both in the form of live and online learning modules. They were also educated regarding the following information: combinations of gene-gene variant interactions or interactions between the genetic variants, how an individual's genomics could play into various environmental exposures including exposures to toxins and toxicants. Physicians were also educated regarding the mechanisms of supplements, vitamins, and other interventions as well as their epigenetic effects on the expression of various gene products or regulation of gene products. The clinical studies supporting the evidence for the potential interventions presented in the CDS were also covered in the supporting educational platform. Finally, the epigenetic potential of an individual's diet, nutrient intake and other lifestyle choices was recognized.

As a CDS, the purpose of the platform is to present, to physicians, information found in the published medical literature relating to these gene variants along with information regarding the numerous options for potentially responding to these variants (Potential interventions). Every sentence of the genomics CDS is thusly based on the published literature and is referenced, again conveying a high level of scientific rigor to the platform. The CDS thus allows the physician to gain better understanding of potential contributing root causes to the patient's cognitive decline and how these various root causes might be addressed.

Patient DNA was obtained via salivary collection device and then analyzed using a combination of an Affymetrix custom array and polymerase chain reaction (PCR) at RUCDR, a clinical laboratory amendments (CLIA)/College of American Pathologist (CAP) certified lab. The data was then transmitted to IntellxxDNA^{TM} and each patient's genomic information was then presented to the physician via the IntellxxDNA^{TM} CDS platform. The report format consists of the explanation of the single nucleotide polymorphism (SNP) function, how it relates to various clinically relevant conditions, along with referenced potential intervention and modification strategies.

In addition to genomic sequencing, appropriate labs were obtained by each of the patient's treating physicians, which were ordered at the physician's discretion and specific to each patient's history, physical exam, and chief complaints. These labs were addressed by each physician in their usual manner of practice.

Discussion of the Development of Potential Interventions

As a CDS platform, the genomics platform does not give patient specific treatment recommendations. Rather, it supports the clinician in better understanding the published medical literature

so s/he can make better, more targeted choices with respect to the potential interventions.

Potential intervention mechanisms for variants can take many forms. Examples include the following: (1) Supplying cofactors to pathways that are not working efficiently. An example is the glutathione peroxidase 1 variant (GPX1), where the GPX1 cofactor is selenium. Selenium is found in large amounts in Brazil nuts. Thus, adding 3–7 Brazil nuts to the diet each week or supplementing with selenium would be an included potential intervention for this variant (Stoffaneller and Morse, 2015; Cardoso et al., 2016). (2) Addressing a genomic weakness. For example, if a patient has an Interleukin 6 (IL6) SNP that has been associated with increased levels of IL6, utilizing a supplement such as curcumin that has been shown to lower IL6 and cross the blood-brain barrier would be a way to help overcome this genomic "weaknesses" (Ghandadi and Sahebkar, 2017). Another example is in raising substrate levels, such as increasing B12 levels to overcome deficiencies in transcobalamin 2 (TCN2), which is the main carrier of B12 to the central nervous system (Mitchell et al., 2014). Potential interventions listed in the cognition and memory pathway necessarily target the particular genetic variant being addressed and also have to show evidence in the literature for improving cognitive outcomes. This same genomics CDS and same method of identifying and developing a treatment plan targeted to genomic variants has been shown to be effective in individuals with autism spectrum disorder and other neurodevelopmental concerns (Way et al., 2021). While the capstone panels in the IntellxxDNA neurodevelopment report are, of course different, there is considerable overlap in the panels supporting nutrition, detoxification, oxidative stress, and inflammation.

For assessing cognitive function, three different assessment tools were utilized based on the preferences of the clinician.

1) Saint Louis University Memory Screener (SLUMS): A well-recognized and standardized screening test that efficiently and quickly identifies mild cognitive impairment as well as dementia. On the SLUMS, normal cognition is represented by a score of 27–30. Mild cognitive impairment is relayed by a score of 21–26 and dementia is correlated with a score of 20 or less (Adogwa et al., 2018).
2) The Montreal Cognitive Assessment Screener (MoCA). The MoCA is another cognitive screening tool to screen for mild cognitive impairment and provides a benefit for testing individuals with MCI over the SLUMS screening test, in that it has a wide number of versions that prevent "memorizing" the test (Lebedeva et al., 2016). For the MoCA, a score of 26 and above is considered normal, and less than 20 is consistent with dementia (Horton et al., 2015).
3) CNS vitals were also used in some of the case studies. The CNS Vital Signs tool neurocognition test is broken down into about 8–15 subsections, depending on which indices are measured, with scoring displayed graphically as well as numerically with colors of dark green (above average), green (average), yellow (low average), orange (low), and red (very low) (Littleton et al., 2015).

CASE STUDIES TO SUPPORT THIS HYPOTHESIS

Results from three case studies are presented below. The first case is presented with detail to illustrate how the platform is used and the subsequent cases are presented with more brevity, highlighting the most important findings.

Case 1: Mr. A

History and Chief Complaint

Mr. A is a 79-year-old male. He is a retired phone operator with a chief complaint of short-term memory loss and "brain fog" which he has noticed for approximately 10 months. Other complaints include low energy, fatigue, and poor sleep as well as nocturia. He presents with his partner of 35 years, and they are both worried that he is experiencing early symptoms of Alzheimer's Disease. He is a longtime patient of the physician's practice.

In particular, he has noted difficulty following conversations and is forgetting names and words. He is now feeling embarrassed in social situations. Prior to this he was social with his partner and enjoyed hosting and cooking special dinners with friends. The pandemic did decrease dinners with friends, but he also began having trouble cooking because he forgot how to make dishes that used to be his staples. He also stopped cooking for himself and his partner because he felt he could not remember the key ingredients. In lieu of cooking, they started ordering in with high frequency.

Social History

- Education: 2-year associates degree
- Smoking status: Non-smoker
- Alcohol and substance use: Occasional wine with dinner

Family History

He has a family history of Coronary Artery disease, Peripheral Artery Disease, and Alzheimer's disease.

Past Medical History

He has a past medical history of hyperlipidemia, benign prostatic hypertrophy, and mildly overweight with a body mass index (BMI) of 26.4. Body type characteristic of central obesity.

Initial Cognitive Evaluation

His initial cognitive evaluation showed him to have mild cognitive impairment with initial SLUMS score of 23/30 and MoCA score of 23/30. On both scales, a score of less than 20 is considered consistent with dementia. Baseline screening for depression was also done utilizing a Patient Health Questionnaire (PHQ9) depression screener and the score was 2 consistent with no symptoms of depression (Kroenke et al., 2001).

Initial Laboratory Results

The initial serum laboratory results are shown in **Table 1**. Previous limited genetic testing indicated that he is heterozygous for ApoE ε4 and the well-known methylenetetrahydrofolate reductase variant, (MTHFR) C677T. Most of the labs were unremarkable except for significantly low testosterone and

elevated lipoprotein a [Lp(a)]. Low-density lipoprotein (LDL) was minimally elevated, but LDL particle number was high, consistent with small particles which are more atherogenic. High sensitivity c-reactive protein (hs-CRP) and homocysteine were on the high side of ideal although still considered normal. There was no evidence of heavy metals in serum or urine.

Initial Medication and Supplements

Initial medications and supplements were limited to vitamin C, multivitamin, B12/folate, vitamin D with K2, magnesium, and zinc every other day.

Advanced Genomics Obtained

Genomics were obtained through the IntellxxDNA Clinical Decision Support platform, as described above. The Brain Optimization and Medical Overview reports were ordered and showed a wide variety of modifiable genomic factors that can contribute to cognitive decline and overall wellness. The most salient variants are discussed in detail below.

Discussion of Genomic Results

Genomic analysis was done. The specific variants which the patient had were presented in an organized fashion displaying their relationship to health issues such as cognition and memory, cardiac disease, brain ischemia, blood sugar, etc. Priority was given to addressing the variants based on their relevance to the chief complaints of the patient and the prevalence of the gene variant, with less prevalent gene variants given higher emphasis. The platform gives information on over 600 genomic variants. The variants present that were determined to be most significant to this patient are discussed below but for purposes of brevity and practicality, not all variants will be discussed.

ApoE ε4

This patient had a known "ApoE ε4," which is often thought of as an "Alzheimer's gene" variant. At least one allele of ApoE ε4 is present in over 60% of people with Alzheimer's (Riedel et al., 2016). This variant was addressed utilizing a "ketoflex" diet. A ketoflex diet is a high fat, mildly ketogenic diet that focuses primarily on highly nutritious whole foods, with many of the fat sources being plant-based. Lifestyle changes of proper sleep and exercise (swimming), brain exercises (Brain HQ), and stress reduction methods were prescribed. The importance of these interventions in ApoE ε4 individuals with early Alzheimer's or cognitive decline has been discussed and published previously by Dr. Dale Bredesen (Bredesen et al., 2016; Bredesen et al., 2018; Toups et al., 2021).

Additionally, because ApoE ε4 codes for a lipoprotein that interacts with 1,700 different gene promoters, there are many other interventions that make sense for individuals with ApoE ε4 that were referenced by the CDS, and some of these were selected and prescribed (Liao et al., 2017). ApoE ε4 conveys less ability to properly clear and cleave amyloid (Kim et al., 2009). Ashwagandha, which supports the clearance of amyloid was chosen as an intervention for this patient. Ashwagandha works in part by conveying neuroprotective effects against beta amyloid induced neuro-pathogenesis (Kurapati et al., 2013). Ashwagandha has been correlated with increased neurite outgrowth and decreased neuronal degradation and neurite retraction, as well as less programmed cell death (Kuboyama et al., 2005; Kuboyama et al., 2020). Ashwagandha has also been shown to upregulate the LDL receptor which enhances amyloid-beta clearance in animal models and has been shown to decrease neurodegeneration (Sehgal et al., 2012). It has been shown to improve memory in human subjects (Choudhary et al., 2017). It also has other mechanisms that can be particularly beneficial for ApoE ε4 individuals in that ashwagandha helps to decrease the buildup of amyloid-beta by decreasing the β-secretase (BACE) activity (Kuboyama et al., 2014). In addition to human studies supporting improvements in cognition, ashwagandha ameliorated cognitive deficits in aged transgenic mice with amyloid precursor protein (APP)/presenilin 1 (PSEN1) variants known to be associated with dementia and other animal models (Kuboyama et al., 2005; Sehgal et al., 2012).

Individuals with ApoE ε4 have also been shown to have higher levels of tumor necrosis factor-alpha (TNFα), IL-6, and interleukin 1 beta (IL-1β) (Fan et al., 2017). The patient's magnesium was switched to magnesium threonate from magnesium glycinate, as magnesium threonate has been shown to better cross the blood-brain barrier (BBB), decrease TNFα expression, and to improve cognitive outcomes in individuals with dementia (Wang et al., 2013; Wroolie et al., 2017; Yu et al., 2018).

TABLE 1 | Initial serum laboratory values for Mr. A.

Normal	Mildly elevated	Significantly elevated	Low levels
HDL: 59 mg/dL	LDL: 125 g/dL	Lp(a): 239 mg/dL	Testosterone: 290 ng/dL
Vitamin D: 53.2 ng/mL	hs-CRP: 1.7 mg/L	LDL-P: 1,984 nmol/L	Omega Index: 6.7%
Lp-PLA2: 143 nmol/min/mL	Homocysteine 8.9 μmol/L		Omega 6/3 ratio: 5.5
Hemoglobin A1C: 4.9%	Copper/Zinc Ratio: 1.4		
TSH: 1.73 μIU/mL			
Magnesium: 2.2 mg/dL			
No heavy metals detected			

HDL, high-density lipoprotein; g/dL, milligrams per deciliter; ng/mL, nanograms per milliliter; Lp-PLA2, lipoprotein-associated phospholipase-A2; nmol/min/mL, nanomoles per minute per milliliter; TSH, thyroid stimulating hormone; μIU/mL, micro-international units per milliliter; LDL, low-density lipoprotein; hs-CRP, high-sensitivity C-reactive protein; mg/L, milligrams per liter; μmol/L, micromoles per liter; Lp(a), lipoprotein(a); LDL-P, low-density lipoprotein particle number; nmol/L, nanomoles per liter; ng/dL, nanograms per deciliter.

Peroxisome Proliferative Activated Receptor Gamma Coactivator 1 Alpha

Peroxisome proliferative activated receptor gamma coactivator 1 alpha (PPARGC1A) is associated with mitochondrial biogenesis (Lehman et al., 2000). ApoE ε4 individuals have compromised mitochondrial function (Yin et al., 2019). Given that the patient was an ApoE ε4 and had two variants in a PPARGC1A SNP (Lehman et al., 2000; Cheema et al., 2015), a mitochondrial support vitamin that contained extra alpha-lipoic acid, acetyl

L-carnitine, *N*-acetylcysteine, and other mitochondrial cofactors was substituted for his usual multivitamin (Wang et al., 2010; Wright et al., 2015).

MTHFR/IL6 Combination

The patient's genomics revealed numerous vascular dementia risk factors, including two copies of an IL6 variant. This variant has been shown to increase the risk of vascular dementia by 3.7x when combined with one or more copies of MTHFR C677T, which the patient also had (Mansoori et al., 2012). The patient was already on a B vitamin with methylfolate, but IL6 had not been addressed by the initial regimen. To address this IL6 variant, omega 3s and a bioactive form of curcumin were prescribed. Both omega 3s and curcumin have been shown to lower IL6 (Blaylock and Maroon, 2012; Ramirez-Ramirez et al., 2013) and to improve measurements of cognitive decline (Sarker and Franks, 2018; Martí Del Moral and Fortique, 2019). An added benefit of curcumin is that it can help promote proper processing of APP so less amyloid beta builds up in the brain (Blaylock and Maroon, 2012). Other IL6 lowering interventions were also added such as Epigallocatechin gallate (EGCG) and dietary capsaicin (Mueller et al., 2010; Pervin et al., 2018).

Protein Kinase C Eta

Other genes were elucidated by the genomic CDS that this clinician identified to be potentially contributing factors that would not normally have been on his radar. The CDS was able to highlight genomic factors related to brain ischemia. One such factor was identified to be a variant in Protein Kinase C Eta (PRKCH), which contributes to brain ischemic risk. This PRKCH variant is only found in less than 3% of the population and has been associated with a 37% increase in stroke risk (Sherry et al., 1999; Wu et al., 2009). Protein kinase C eta is involved in tight junction integrity and variants in this gene relate to hemorrhagic and lacunar stroke risks (Willis et al., 2010; Haffner et al., 2016). Citicoline, which has been shown to improve tight junctions and decrease stroke risk, was prescribed (Fioravanti and Buckley, 2006; Martynov and Gusev, 2015). Citicoline has multiple studies showing improvement in cognition endpoints for individuals with vascular dementia risk (Gareri et al., 2015). Saffron (*Crocus Sativus*) was added to patient's regimen as another known potential intervention that both crosses and tightens the BBB (Batarseh et al., 2017). Saffron has been shown to improve cognition in human studies compared to placebo. In fact, it has outcomes data equal to donepezil or memantine in human trials of individuals with MCI/AD (Avgerinos et al., 2020). Saffron has been shown to reduce amyloid beta load in animal models (Batarseh et al., 2017).

Platelet Aggregation and Tissue Plasminogen Activator Related Variants

Other hidden genomic contributing factors that were revealed by the CDS include Glycoprotein 3 a (GP3a) and Lipoprotein A (LPA). GP3a stimulates platelet aggregation and the variant the patient had relates to more sticky platelets (Kucharska-Newton et al., 2011). The LPA gene variant which the patient had is known to lead to elevated Lp(a) levels and decrease the amount of natural tissue plasminogen activator in the blood (Ueda et al., 2018). While the LPA gene variant is most known for its ability to increase cardiac risk approximately 2-fold (Clarke et al., 2009), it has also been shown to increase stroke risk to a lesser extent (Langsted et al., 2019). Based on these cardiovascular genomic risk factors, he was started on baby aspirin which has been shown to directly lower Lp(a) levels (Ranga et al., 2007). Low dose atorvastatin was prescribed to address overall cardiovascular and vascular dementia risk factors (Geifman et al., 2017).

Glutathione and Detox Related Variants

The removal of toxins and toxicants via glutathione transferases is important for maintaining brain health and cognition. When there are variants or deletions in these pathways, heavy metals, and other toxicants such as pesticides and herbicides can build up in the brain, compromising brain heath (de Mendonça et al., 2016; Wang et al., 2016; Andreoli and Sprovieri, 2017). The patient was found to have Glutathione S-Transferase mu 1 (GSTM1) null (i.e., both copies of this gene are absent), Glutathione S-Transferase theta 1 (GSTT1) null, as well as two copies of the Glutathione S-Transferase pi 1 (GSTP1) Ile105Val variant, which is highly clinically significant. Both the GSTM1 null and GSTP1 homozygous Ile105Val have been associated with a significantly higher risk of AD (Wang et al., 2016). The cognitive effects of GSTM1 null are amplified when combined with ApoE ε4 conveying 3.07x the risk of dementia as well as 2.1x the risk of atherosclerosis (de Mendonça et al., 2016; Grubisa et al., 2018). GSTP1 Ile105Val has been shown to be associated with a 1.87x the risk of AD/MCI and greater susceptibility to the negative effects from lead exposure (Wang et al., 2016). Thus, supporting this individual's glutathione pathways became paramount. *N*-acetylcysteine (NAC) was chosen as an intervention for this patient as it has been shown to directly increase glutathione levels (Moradi et al., 2009).

Seven Months Follow Up for Mr. A

Seven months after the patient's protocol was changed to address his specific genomic findings, as identified by the CDS, the patient showed marked improvement. Given the specificity of his genomics, and the ability for his clinician to discuss these findings, the patient and his partner were motivated to incorporate recommended diet, lifestyle, and supplement regimens into their routine. He did extremely well, rapidly noticing improvement in his cognitive abilities. The physician retested the patient with MoCA (using different version) and SLUMS at this time and the patient showed notable improvement, now scoring a 26 on MoCA (previously 23) and 27 on SLUMS (previously 23). Additionally, significant improvements were seen in laboratory parameters as shown in **Table 2**.

During follow up visits, the patient noticed that he feels more energetic, empowered, and motivated to achieve further improvements in his memory and wellbeing. He is reassured and sees that he can improve his memory, not just prevent further decline. Recognizing the improvement was also reassuring and motivating to his partner.

Specific improvements noted by patient and his partner

- His mood is very improved. He feels his "glass is half full" rather than half empty-part of this he attributes to pandemic getting better, but he also feels that the improvements in his diet, exercise and supplement regimen are worthwhile for him.
- His energy is improved, and he is sleeping better.
- He has returned to previous hobbies and interests as well as cooking. He has become especially creative with his Keto-flex diet. He feels like he can remember the key ingredients for the dishes and even created a new keto-flex friendly chili-con-carne recipe. Once again, they are entertaining friends, and he is enjoying cooking for these parties. The patient has even begun teaching his friends how to eat well so they can also lose their extra abdominal fat and improve their weight. His partner notes that the patient is less fearful of social interactions, is remembering more words and names and is less embarrassed by his condition.

Case 2: Mr. B

History and Chief Complaint

Mr. B, at presentation in December of 2020, was a 70-year-old man status/post mantle cell lymphoma in 2017 treated successfully with chemotherapy and an autologous stem cell transplant. He presents complaining of worsening "brain fog" ever since chemotherapy 3 years ago. Extensive intake was done where questions were asked regarding ability to function with activities of daily living, motivation, energy, mood, and memory symptoms as well as screenings for a wide variety of physical and mental health concerns. There was no evidence of depression or underlying mood disorder so full PHQ9 was not done. Baseline labs were essentially within normal limits other than sex hormone labs which are discussed below. Thus, other labs are not reported in detail in this case.

A detailed initial cognitive assessment was done using the CNS vital signs platform, which showed his neurocognitive index to be in the 1st percentile. This patient, upon presentation, had nine areas in the red or very low category, 1 yellow (low), 2 orange (low average), 2 green (average), and 2 dark green (above average).

TABLE 2 | Comparison of pre- vs. post-intervention serum laboratory values for Mr. A.

Lab	Pre-intervention	Post-intervention
Lp-PLA2	143 nmol/min/mL	109 nmol/min/mL**
hs-CRP	1.7 mg/L	1.2 mg/L**
Total cholesterol	204 mg/dL	180 mg/dL*
LDL	125 mg/dL	104 mg/dL*
LDL-P	1,984 nmol/L	1,325 nmol/L**
SMLDL-P	605 nmol/L	375 nmol/L**
HDL	59 mg/dL	60 mg/dL*
Lp(a)	239 μmol/L	196 μmol/L*
Homocysteine	8.9 μmol/L	9.3 μmol/L
Hemoglobin A1C	4.9%	5.0%
Fasting glucose	82 mg/dL	90 mg/dL
Vitamin D	53.2 ng/mL	68.7 ng/mL**
Omega index	6.7%	8.9% **
Omega 6/3 ratio	5.5	4.5*
Testosterone	290 ng/dL	440 ng/dL**
Magnesium	2.2 mg.dL	2.2 mg/dL
Copper	100 mcg/dL	98
Zinc	72 mcg/dL	88 mcg/dL*
Copper/Zinc ratio	1.4	1.1
TSH	1.73 μIU/mL	1.07 μIU/mL**
Free T4	1.4 ng/dL	1.6 ng/dL*
Free T3	3.0 pg/mL	3.5 pg/mL*

**Denotes more than 10% improvement. **Denotes more than 20% improvement. Lp-PLA2, lipoprotein-associated phospholipase-A2; hs-CRP, hs-CRP, high-sensitivity C-reactive protein; LDL, low-density lipoprotein; LDL-P, low-density lipoprotein particle number; SMLDL-P, small low-density lipoprotein particle number; HDL, high-density lipoprotein; Lp(a), lipoprotein(a), TSH, thyroid stimulating hormone; Free T4, free thyroxine; Free T3, free triiodothyronine; nmol/min/mL, nanomoles per minute per milliliter; mg/L, milligrams per liter; mg/dL, milligrams per deciliter; nmol/L, nanomoles per liter; μmol/L, micromoles per liter; ng/mL, nanograms per milliliter; ng/dL, nanograms per deciliter; mcg/dL, micrograms per deciliter; μIU/mL, micro-international units per milliliter; pg/mL, picograms per milliliter.*

Social History

- Occupation: Firefighter chief, on the 911 response team; also has a history of working in the military on nuclear submarines.
- Smoking Status: Currently non-smoker, rarely smoked in early years but high lifetime smoke exposure as he was a firefighter.
- Alcohol and substance use: None
- The patient is one of 13 children

Family History

He had a family history of a mother with hypertension. She died of dementia at 89. His father had myocardial infarction/heart disease and colon cancer. His father died at 70. Siblings: Two of his 12 siblings had thyroid cancer, one brother with heart disease, severe atopic dermatitis, and arthritis.

Past Medical History and Initial Treatment

His past medical history was significant for Mantle Cell Lymphoma as above. From a cognitive standpoint, a magnetic resonance imaging (MRI) from June of 2021 showed no acute findings but did report mild to moderate chronic small ischemic changes and white matter disease. Volumetric interpretation using the NeuroQuant platform showed whole brain volume to be in the 32nd percentile with mild to moderate global atrophy, but hippocampal volume was in the 57.00% on left and 44.00% on the right, giving an asymmetry index of 0.26 (70.00%). The report from the radiologist concluded, "These findings are *not* strongly suggestive of neurodegenerative/Alzheimer's type dementia."

Based upon the patient's presenting symptoms and medical history, the treating physician believed that he was likely to have vascular factors contributing to his cognitive decline as well as strong components of neuronal damage and toxicity from the various chemotherapies and high lifetime environmental exposures due to his work as fire chief and on nuclear submarines. He had received combination chemotherapy which is BiCNU (Carmustine), Etoposide, Ara-C (Cytarabine), and Melphalan. The mechanisms by which chemotherapy may contribute to cognitive decline are many. Chemotherapy can contribute to oxidative stress, vascular damage, and decreased cerebrovascular perfusion. White matter abnormalities such as demyelination

and activation of microglia, alterations in neuronal signaling, as well as direct neuronal injuries from chemotherapy can contribute to neurodegeneration and immune dysregulation (Mounier et al., 2020). Thus, hyperbaric oxygen therapy (HBOT) was recommended as a first-line treatment to address some of these perfusion issues and other issues (Shapira et al., 2021). The patient consented to the risks and benefits of HBOT and started on 10 sessions of HBOT (Heyboer et al., 2017).

In 2/21, 1 month after presentation and ten sessions of HBOT, the patient's CNS vitals were repeated. The patient's Neurocognitive index increased from the first to the third percentile. However, category wise this correlated to a significant difference with only having four in the low "red zone," instead of the nine indices originally measuring in this low red range. Additionally, the patient subjectively reported noticeable improvement in the efficiency of running errands and activities of daily living. Due to seeing improvement with HBOT, the patient wanted to know if there were more specific interventions that could be recommended. Thus, "Brain Optimization" genomics were ordered to help give insight into other potential contributing factors to his cognitive decline that could be optimized.

Discussion of Genomic Results

In 5/21 the patient returned for review of genomics. The genomics findings were very informative. Many of the patient's underlying genomic "weaknesses" overlapped with mechanisms that could have been exacerbated by the neuronal effects of chemotherapy and compounding the patient's symptoms of cognitive decline.

ApoE ε4

The patient was found to be an ApoE ε3/4. As described in the published literature, ApoE ε4 individuals do not use sugar well as a brain energy source (Krikorian et al., 2012; Wu et al., 2018). They also have evidence of increased mitochondrial oxidative stress, which can lead to mitochondrial damage, and would benefit from lifestyle changes that support mitochondria (Simonovitch et al., 2019). In this case, a diet very low in sugar, as well as intermittent fasting was recommended (Zhang et al., 2017; Morrill and Gibas, 2019).

Glutathione Transferase

Like Mr. A, in the case above, Mr. B was also found to have significant issues in his glutathione transferase-related pathways with deletions of both GSTT1 and GSTM1 as well as homozygous variants in GSTP1. *N*-acetylcysteine (NAC) was started (1,200 mg a day), as well as glutathione using a combination of daily oral and weekly IV glutathione treatments to promote detoxification (Moradi et al., 2009; Hauser et al., 2009; Pizzorno, 2014; de Mendonça et al., 2016).

Endothelial Nitric Oxide Synthetase and Matrix Metalloprotease

Homozygous variants in two highly significant genomic pathways were noted: Endothelial nitric oxide synthetase (NOS3) and matrix metalloprotease (MMP13). These two pathways are known to strongly contribute to white matter changes in the brain, known as leukoaraiosis. Homozygosity for this NOS3 (endothelial NOS) variant has been shown to increase the risk of leukoaraiosis by 290%. Additionally, he was homozygous for an MMP13 variant which increased the risk of leukoaraiosis by 390% (Fernandez-Cadenas et al., 2011). Leukoaraiosis has been shown to have a significant demyelinating component and to contribute to cognitive decline (Brown et al., 2007). One study found that the presence of leukoaraiosis correlated with a lower Mini-Mental-Status Exam (MMSE) score (Schmidt et al., 2007).

Endothelial nitric oxide synthetase is hypothesized to contribute to leukoaraiosis by increasing vascular constriction and decreasing blood flow (Hassan et al., 2004). Dietary changes to incorporate more beets, leafy greens, and other high nitric oxide producing foods were recommended (Lidder and Webb, 2013). HBOT is also a direct intervention for this pathway. One animal study found that 24 h after a 60-min session of HBOT, endothelial NOS transcribed protein product was increased by 60%, and endothelial NOS messenger RNA (mRNA) content by 20–30% (Xu et al., 2009). Twenty additional sessions of HBOT were done to address this pathway at 1.8 standard atmosphere (ATM).

Matrix metalloprotease is involved in tissue remodeling and blood-brain barrier permeability (Lakhan et al., 2013). Excessive MMP13 levels lead to the degradation of important components of the extracellular matrix, resulting in blood-brain barrier leakage (Lakhan et al., 2013; Yabluchanskiy et al., 2013). Two copies of the minor allele, carried by this patient are associated with increased MMP13 expression (Shi et al., 2016). With the purpose of supporting remyelination, Nicotinamide adenine dinucleotide (NAD), and citicoline were added to the regimen. NAD has been shown to potentially improve remyelination, improve brain adenosine triphosphate (ATP) production, and improve phospholipid metabolic pathways (Wang et al., 2017; Cuenoud et al., 2020). Citicoline was added to support remyelination and leukoaraiosis pathways, but also due to variants relating to decreased ability to synthesize choline (Martynov and Gusev, 2015; Feng et al., 2017).

Brain Derived Neurotrophic Factor

This patient had a known and significant variant in the brain derived neurotropic factor (BDNF) gene, found only in 11% of the population (Sherry et al., 1999). BDNF is an important nerve growth factor, and the patient's variant has been associated with a 1.88x risk of cognitive impairment or Alzheimer's (Sherry et al., 1999; Ji et al., 2015). One of the best-studied interventions for increasing mature BDNF, the synaptogenic promoting form, is intense exercise (de Assis and de Almondes, 2017). Thus, the patient was encouraged and agreed to add exercise to his regimen 3x/week. He was to maintain his heart rate at least at 120 beats per minute for 30 min.

Other Genomic Variants and Interventions

Other variants regarding adequate conversion of folate to the methylfolate, and TNFα mediated were also addressed in a targeted fashion with methylated B vitamins and *Hericium Erinaceus*, derived from lion's mane mushroom (Li et al., 2018; Cajavilca et al., 2019).

Mr. B's sex hormone levels were checked. Both testosterone and estradiol levels were found to be low. His initial total testosterone was 249, free testosterone was 30, and estradiol was less than 15. The grouping of hormonal receptors variants carried by Mr. B have been shown to interact adversely with ApoE ε4. Even though this study was done in women, estrogen still has hormonal and brain modulation effects in men. Since estrogens are derived directly from testosterone via aromatization, men require adequate testosterone to help maintain estrogen levels in the brain-protective range (Zimmerman et al., 2011; Fernández-Martínez et al., 2013). There is evidence that men with higher estrogen levels perform better on verbal memory tests compared to men who have lower estrogen levels (Zimmerman et al., 2011). Testosterone replacement was given which corrected both the testosterone and estradiol levels and post treatment levels were brought to total testosterone levels of 400, free testosterone levels of 65, and estrogen levels 20.

Summary of Regimen

- NAC 1,200 mg/day
- Glutathione 500 mg orally a day or 3 g IV weekly
- Multivitamin, Methylated B complex
- Citicoline 250 mg/day
- Testosterone replacement
- Lion's Mane
- Checked environmental toxins/heavy metals
- 20 more HBOT sessions at 1.8 ATM × 60 min
- Exercise 3x a week, heart rate at least 120 beats per minute for at least 30 min

Three and Six Months Post-Genomic Follow-Ups for Mr. B

Three months after genomic interventions, significant improvements were noted. In 8/2021, the patient's SLUMS Score was 24, up from a previous score of 20. This transitioned the patient from having dementia into the middle of the mild cognitive impairment range. He reported feeling better overall, was able to operate more functionally, and found it easier to do errands. He also noted less forgetfulness.

Six months after interventions were introduced, the patient was contacted by phone and stated that he felt that his memory was about 70% better. In addition, he reported that his writing ability has returned to normal. The patient was able to complete his taxes with little effort, and his energy levels had improved. He no longer noted any difficulties with daily activities, and in fact, had resumed higher energy activities that he previously enjoyed such as hunting with his son. He also reported that the chronic back pain that he had for years from a firefighting injury has also improved.

Case 3: Ms. C

History and Chief Complaint

Ms. C is a 62-year-old female who presents to the office complaining of memory problems over a few years and had particularly noticed some worsening starting approximately 18 months prior to seeking help from her current physician. Her main complaint is that she has poor short-term memory; forgetting names; trouble remembering places gone the day before, as well as misplacing items that she used daily. The patient is extremely detail-oriented and quite bright. She graduated college in 3 years due to having so many credits and had a bachelor's in science. The patient had initially joined a brain research study that was being offered through a local psychiatrist's office. As part of the study, testing revealed two copies of ApoE ε4. PET brain scan indicated presence of amyloid. Amyloid PET scans have been shown to have a sensitivity of approximately 91% for AD (Marcus et al., 2014). She was aware that an amyloid positive PET scan is highly suggestive of developing Alzheimer's and upon learning that, she decided to seek more progressive care with an integrative practice. In the same study, an MRI of the brain revealed a small amount of white matter changes, which discussed above, are an independent risk factor for a decreased score on cognitive testing (Schmidt et al., 2007).

This third case is an interesting case in that patient is at extraordinarily high risk for Alzheimer's due to her being a known ApoE ε4/4. While there is some variation in risk based on other gene variants present or absent, individuals who are homozygous for ApoE ε4 have been shown to have as high as 14x the risk for Alzheimer's (Farrer et al., 1997). Additionally, at the time of presentation (4/16/19), although the patient was only 62 years old and had a college education, she had a SLUMS of 21, which put her in the category of mild cognitive impairment bordering on mild dementia (20 and below is defined as dementia) (Adogwa et al., 2018). The patient was concerned about her future, given her strong family history of neurodegenerative diseases of both Alzheimer's and Parkinson's. Her personal history of essential tremor and restless legs provided additional worry. Essential tremor has been associated with some mild defects in executive function, memory, and cognition (Bermejo-Pareja, 2011). Restless legs have been linked to cerebral microvascular disease and gliosis. Additionally, restless legs are commonly associated with Parkinson's (Bhalsing et al., 2013; Walters et al., 2021). Patient had past medical history of depression which was under control with treatment at the time of presentation to the clinic and during the course of treatment with PHQ2 and PHQ9 scores consistent with no evidence of depression or depression under full control.

Social History

- Education: She graduated college in 3 years due to having so many credits and had a bachelor's degree in science.
- Smoking status: Non-smoker
- Alcohol and substance use: No history of substance use, drinks about 1 glass of wine 5 days per week.
- Moderate exerciser.

Family History

Mother: AD (onset age 61). Parkinson's disease (onset 65). Deceased from AD age 77. Her mother also had migraines. Father with glioblastoma and hyperlipidemia. Maternal aunt with AD in her 70s and uterine cancer. Her two siblings are healthy.

Past Medical History

She has a past medical history of hyperlipidemia, subclinical hypothyroidism, essential tremor, restless legs, osteopenia, situational anxiety, depression, and eczema. Depression was under full control with PHQ 2 score of 0 when evaluated in 4/2019.

Baseline Medications and Supplements

Escitalopram 10 mg, Horizant extended release 600 mg, trazodone 50–100 mg, atorvastatin 10 mg, and Deplin (L-methylfolate) 15 mg, and NAC 600 mg.

Pertinent Initial Laboratory Results

Baseline labs were significant for elevated LDL, undetectable estradiol and testosterone, borderline low vitamin D, and elevated cortisol. See **Table 3** below for comparison of initial and post treatment labs.

Initial Interventions Prior to Genomics

Ms. C's physician was trained in the "Reversal of Cognitive Decline" (ReCODE) protocol developed by Dr. Dale Bredesen. Thus prior to obtaining results of genomics, the treating physician started her on lifestyle interventions that have been shown to be beneficial to individuals with ApoE ε4. These included a mildly ketogenic diet, exercising with intervals of intensity, and fasting 13–16 h a day (de Assis and de Almondes, 2017; Zhang et al., 2017; Morrill and Gibas, 2019). As discussed in cases above, carrying the ApoE ε4 allele has been shown to be associated with improper cleavage of APP, mitochondrial dysfunction, oxidative stress, and TNFα mediated inflammation (Kim et al., 2009; Ramirez-Ramirez et al., 2013; Fan et al., 2017; Simonovitch et al., 2019). Thus, many of the basic interventions of the ReCODE protocol were also added empirically (Bredesen et al., 2016; Bredesen et al., 2018). These included a micronized bioavailable curcumin, Omega 3s, CDP-Choline, vitamin D3-K2, sulforaphane, mitochondrial support vitamin, coenzyme q10 (CoQ10), and magnesium threonate. At the time of presentation, the patient was taking methylfolate and NAC, as started by a previous physician. She was started on Ashwagandha to lower am cortisol and for brain benefit (Chandrasekhar et al., 2012).

TABLE 3 | Comparison of pre- vs. post-intervention serum laboratory values for Ms. C.

Lab	Pre-intervention	Post-intervention
LDL	140 mg/dL	96 mg/dL*
AM cortisol	22.9 mcg/dL	21.4 mcg/dL
Vitamin D	34 ng/mL	50 ng/mL*
Zinc	105 mcg/dL	79 mcg/dL
Copper	1,050 mcg/L	882 mcg/L
TSH	2.2 μIU/mL	0.966 μIU/mL*
Free T3	2.8 pg/mL	2.8 pg/mL
Hemoglobin A1C	5.5%	5.2% *
Vitamin B12	840 pg/mL	>2,000 pg/mL
Estradiol	<17.0 pg/mL	Ranged from 38 to 98.7 pg/mL *
FSH	141.8 IU/L	Ranged from 74 to 81 IU/L*
Testosterone	<12 ng/dL	Ranged from 110 to 179 ng/dL*
Heavy metals screen	Negative	

**Denotes significant change in levels that may relate to clinical improvement. LDL, low-density lipoprotein; TSH, thyroid stimulating hormone; Free T3, free triiodothyronine; FSH, follicle-stimulating hormone; mg/dL, milligrams per deciliter; mcg/dL, micrograms per deciliter; ng/mL, nanograms per milliliter; mcg/L, micrograms per liter; μIU/mL, micro-international units per milliliter; pg/mL, picograms per milliliter; IU/L, international units per liter; ng/dL, nanograms per deciliter.*

Discussion of Initial Genomic Results

Six months later, on 10/08/19, the patient's SLUMS had improved to 24. At this point the clinician had received the patient's genomic results through the IntellxxDNA platform and accordingly adjusted her regimen.

Cyclooxygenase 1

Pyrroloquinoline Quinone (PQQ) was added to better enhance mitochondrial function and biogenesis (Chowanadisai et al., 2010) given the presence of a mitochondrial cyclooxygenase 1 (COX1) variant that has been shown to have an interactive additive effect with ApoE ε4 (Coto et al., 2011). This COX1 variant has been shown to convey reduction of cytochrome c oxidase complex IV activity. Reduced cytochrome c oxidase (complex IV) activity has been observed in post-mortem studies of AD, and particularly effects the temporal cortex and hippocampus (Wang and Brinton, 2016). While these mitochondrial variants overall increase AD by 52%, in ApoE ε4 individuals the risk of AD was shown to be increased by an astronomical 430%. This variant appears to create mitochondrial DNA replication instability (Coto et al., 2011). Mitochondrial methylation pathways were also of concern and supplement regimen was revised to include a combination of methylfolate and folinic acid.

Further Exploration of Genomics 2 Months Later

Two months later the patient was seen in a follow up. At this point, her husband was starting to notice improvement in the patient's brain function and memory in terms of her ability to organize and complete tasks successfully and she was not asking questions and repeating questions as often. Genomics was explored further at this visit. The key topic discussed was the patient's large number of glutathione-related pathways and detox pathways affected as well as her being a Human Leukocyte Antigen (HLA)-DQ2.5/2.2.

Human Leukocyte Antigen-DQ2.5/2.2

The patient also had HLA-DQ2.5/2.2. This combination put her at very high risk for gluten intolerance, with approximately 10 times the risk compared to the general population, a completely gluten-free diet was stressed (Almeida et al., 2016).

Other Pathways Addressed

For purposes of brevity, each of her detoxification-related pathways will not be discussed in detail, but detox pathways were addressed by adding intranasal glutathione in addition to optimizing her NAC and sulforaphane dosing (Moradi et al., 2009; Pizzorno, 2014; Yoshida et al., 2015).

Some of the other variants she had have been already addressed by initial supplements started. A few other genomically targeted optimizations were made, such as increasing magnesium

and increasing the dose of omega 3s and switching to one that had eicosapentaenoic acid (EPA)/docosahexaenoic acid (DHA) and docosapentaenoic acid (DPA). Hormone-related pathways were addressed with BioTe estradiol and testosterone pellets, oral micronized natural progesterone, diindolylmethane (DIM), and iodine. Thyroid hormone replacement was given for a TSH of 4.99.

Fifteen, 22, and 28-Month Post Genomic Follow-Ups for Ms. C

At 15 months, the patient returned, and SLUMS had improved to 30 (perfect score). The patient at that time was, however, losing too much weight on the ketogenic diet and thus asked if she could switch to a Mediterranean diet. She also found the intranasal glutathione irritating and difficult to travel with and stopped this.

There was then a gap in patients returning to the clinic due to Covid and travel. When she returned to the clinic at 22 months, patient and husband self-reported some mild increase in memory concerns compared to the previous visit. The clinician switched to using MoCA due to having more version options and the score was 24. She was restarted on intranasal glutathione and protocol was slightly modified. Diet was kept as Mediterranean. It is unknown what triggered her decline as there were a lot of variables including covid vaccination, extensive travel with dietary changes, etc. as well as the potential for additional neurodegeneration due to her underlying pathology and biochemistry as an ApoE ε4/4 with positive amyloid PET scan.

Twenty-eight months after starting original protocol, her MoCA was still 24 (MoCA requires quite a long delay on the memory section of the test, meaning significant delay from the time patient is asked to remember five words to the time they are asked to recall these five words), but the patient's SLUMS was back at 27 and CNS vitals showed her to be doing quite well with overall neurocognitive index of 30% and nine of the 12 indices showing her performing in the green – average category. Her verbal memory score is still significantly impaired in the red, very low range. The CNS vitals results fit with her own observations. The challenge for this patient remains with her verbal learning and verbal memory, which is often the case for individuals with ApoE ε4/4 or early Alzheimer's (Bussè et al., 2017). The patient and her husband are pleased with her progress, compared to when she presented. They realize that maintaining her previous gains as an ApoE ε4/4 will require dedication to her regimen. She has restarted her mildly ketotic diet and is working closely with a nutritionist so she can maintain her weight while on this diet. She has also begun brain plasticity training games to improve her verbal memory.

DISCUSSION OF CASE STUDIES

It is well recognized that individuals carrying the ApoE ε4 allele are at high risk for cognitive decline and AD. The three case studies above, all purposely from individuals with ApoE ε4, illustrate that it is possible to improve indices of cognitive decline and improve patient well-being and function. These case studies also support the hypothesis that the typical downward trajectory of cognitive decline can be stabilized and reversed. The third case in this series is particularly encouraging, as significant gains were achieved even though the patient is an ApoE ε4/4, had a positive amyloid PET scan and had been accepted into a study, due to meeting the criteria for early Alzheimer's.

To our knowledge, improvements in cognitive measures, especially with the magnitude of improvement seen in these patients who were optimized utilizing genomically targeted interventions, have not been previously reported in studies with any currently available pharmaceutical intervention for cognitive decline. In fact, the most recent drug approved drug for MCI or mild AD, Aducanumab, was approved based on showing no improvement in cognitive outcome measures, just less decline (Haeberlein et al., 2020).

We believe that the genomically targeted interventions provided superior outcomes for these patients because cognitive decline is due to a multitude of variables, rather than just one. This multi-pronged approach allows for many of these patient specific genomic variables to be addressed simultaneously. Alzheimer's researcher and neurologist, Dr. Dale Bredesen, pointed out in his original discussion on the topic of why Alzheimer's drugs have failed, that there are over 36 different contributing factors. This list has recently been further expanded. Identifying and treating as many of them as possible is necessary to achieve the desired outcome of improved cognition (Gustafson, 2015). These contributing factors are frequently compared to "holes in a roof." If you were to patch only one or two holes in a roof with 36 holes, the rain would still enter, and you would not see a noticeable improvement. Over 215 different genes have been implicated in Alzheimer's disease alone (Jansen et al., 2019). The advantage of a CDS for genomics is that it allows clinicians to identify and prioritize treatment recommendations to provide the best impact by identifying some of the potentially clinically significant genomic factors that are present in an individual. It is also important to note that the inclusion of diet and lifestyle changes discussed in the genomics CDS are an essential part of a "brain recovery protocol" as they are strong epigenetic modulators, as well as modulators of inflammatory and hormonal signaling (Sharma et al., 2020).

By addressing a multitude of variables identified by genomics including vascular risk factors, inflammation, brain permeability, various nutrient deficiencies, hormonal imbalances, difficulties with removing heavy metals, chemicals, and other neurotoxic substances, the above patients were able to gain significant improvements in their cognition. Each of these contributing factors has their independent effects on the brain and cognition, but they also are important to address due to their combinatorial effects. For example, elevated levels of brain inflammatory cytokines have been highly linked with cognitive decline due to the detrimental effects of inflammation on neuronal health, but also increase amyloid deposition (Wang et al., 2015). Mitochondrial deficiencies, such as those conveyed by the COX1 variant and intranuclear hormone receptors estrogen receptor (ESR) 1 and ESR2 and a multitude of other variants can interact directly with ApoE ε4, conveying an increased risk to

individuals with these variants (Coto et al., 2011; Fernández-Martínez et al., 2013). While the individuals above shared the most well-established AD genomic variant (ApoE ε4), their regimens were customized, based on their other genomics, along with their lab values, personal, and family history.

That these case reports come from three independent physician offices helps to show the reproducibility of the benefits using a genomics CDS for improvement in cognitive decline. It also provides optimism and support for further larger, controlled trials. Limitations to the data presented here include the fact that no aggregate data is given as to how many patients each clinician has treated utilizing this approach and what the average magnitude of change in cognition scores would be for a larger population of individuals. With regards to this topic of what percentage of patients might benefit from this approach, we have presented some aggregate data from one of the practices (AS) in **Table 4**.

While not done with the intention of being a prospective trial, the office of Dr. AS did collect serial data on 24 patients from their practice. SLUMS test was used in the majority of the patients for monitoring of cognition, with MoCA used as the follow-up test in three cases. Each of these tests are measured on a 30-point scale. One patient was excluded from this analysis as during the course of treatment, she was diagnosed with frontotemporal dementia.

Of the 23 patients, 43.5% improved, with an average increase in their score of 4.2 points with an average duration of follow-up being 14.7 months. 26.1% of patients' cognitive scores remained stable (between –1- and +1-point change on the 30 point scale) with a mean delta of –0.5 over 14.83 months. Finally, 30.4% of patients did not appear to benefit from this approach. In this group cognition decreased over time, consistent with what is seen classically in the Alzheimer's and MCI literature, with an average drop of 5.57 points over 16.36 months.

TABLE 4 | Changes in cognition scores for series of 23 patients from one office.

Patient and direction of change	Pre-score	Post-score	Follow up months
1 – I	26	28	9
2 – I	19	26	8.5
3 – D	18	7	17
4 – I	21	28	6.5
5 – D	20	14	10
6 – N	20	19	11.5
7 – D	17	13	8
8 – D	17	13	13
9 – D	12	6	22
10 – D	14	9	23
11 – I	22	24	9
12 – I	13	16	6
13 – I	21	29	32.5
14 – I	21	27	33
15 – D	9	6	21.5
16 – N	25	25	19.5
17 – N	21	20	14
18 – N	26	26	24
19 – I	26	29	17.5
20 – I	20	22	15.5
21 – I	20	22	9.5
22 – N	16	15	7
23 – N	19	19	13

I, improved cognitive score and function; D, decreased cognitive score and function. N, neutral (no significant change) in cognitive score or function.

Further studies with prospective analysis of variables such as the presence or absence of specific genomic variants, comorbid conditions, and patient compliance that may contribute to outcomes are needed. However, the raw data from the series of 23 patients presented, lends credence to the fact that the three cases presented are representative of an approach that can provide a reasonably high frequency of success. The ability to improve outcomes in 30–40% of a patient population with cognitive decline and to stabilize an additional 25% of cognitive decline patients would represent a very significant improvement to the available therapeutic milieu. One question the readers might ask, as they review the case reports, is whether there could be a placebo effect causing some of the gains since there was no control group. However, it is a reasonable conclusion, as these individuals were all ApoE ε4 positive, to use the published studies regarding mild cognitive impairment/early Alzheimer's as "typical controls." The natural course of AD as an illness or even MCI is continued worsening, particularly in ApoE ε4 individuals. Even using the treatment group for the Aducanumab study (as compared to their placebo group), no gains in cognitive measures were noted over an 18-month period, just 20% less loss (Haeberlein et al., 2020). Thus, the fact that these individuals showed significant improvement rather than decline, makes this method certainly worth exploring with further studies.

Another limitation of this approach is that patients in this study had the resources to afford supplements and high-quality nutritious foods as prescribed. If this approach were to be attempted in a more traditional medical practice with individuals of varying socio-economic classes this could be a barrier as supplements and interventions such as hyperbaric oxygen are not covered on Medicare, Medicaid, or commercial insurance plans. Given the tremendous cost of Alzheimer's and dementia care absorbed by both the health care system, Medicare/Medicaid and an individual and his/her family, this barrier might eventually be addressed, in part, by detailed treatment cost analysis showing the potential tremendous cost savings of this approach in the long run which would provide good evidence for Medicare and other insurance companies to consider coverage of these interventions. In the meanwhile, since changes to health policy would take time, based on cost benefit ratios many families might find it not only worthwhile but cost effective to self pay for these interventions.

While the reproducibility of this method was shown amongst clinicians trained in integrative or functional medicine in this manuscript, a third limitation to this approach is that most clinicians are not comfortable with recommending supplements or natural products, even if they are over the counter and have a GRAS (generally regarded as safe) rating. This is due to lack of knowledge of the mechanisms, efficacy and supporting research and typical dosing for vitamins and supplements. This

educational barrier can be overcome by appropriate educational platforms such as those used to educate the physicians above. Time constraints and other biases held by the physicians would need to be addressed through our continuing medical educational system before this approach could be utilized on a wide-spread scale.

Despite the barriers and potential problems with this genomically targeted approach, the potential demonstrated here for the reversal or improvement of cognitive decline is significant and should be explored further as it has tremendous societal and individual economic and emotional implications.

This approach is also ideal for addressing patients who want to focus on the prevention of cognitive decline for individuals with very mild symptoms of memory impairment that might otherwise be documented as "normal aging." The fact that that many of the interventions for addressing these root causes are nutrients, supplements, and lifestyle modifications with excellent safety profiles, makes this approach well positioned to be used for prevention. A genomically targeted approach to cognitive decline is reproducible, efficacious, and also cost-effective. Further, because the patient realizes that the genomic data being discussed is uniquely their own, they have significantly greater compliance with recommendations made.

CONCLUSION

A wide variety of hypotheses regarding Alzheimer's have been presented in the recent literature. These include hypotheses and data supporting the involvement of inflammation, small vessel disease, and hypoperfusion (Hakim, 2021), the hypothesis regarding oxidative stress and mitochondrial dysfunction (Simonovitch et al., 2019), the hypothesis regarding the potential detrimental effects of environmental exposure to toxicants (Wang et al., 2016), the role of poor amyloid processing (Armstrong, 2019), and many more. All of these hypotheses have support and are likely true. However, not all of the identified contributing factors apply to each patient. To get optimal outcomes, the treating clinician needs to be able to identify which of the plethora of AD risk factors that have been elucidated in the literature are applicable in their particular patient. Genomics is a powerful tool that can help with this step. The second half of the equation, once identified, is what can be done about each of the potential contributing factors. Taking the contributing factor back to the genomic level helps in identifying modification strategies. A curated genomic CDS that identifies the underlying genomics contributing factors provides a framework for physicians to develop a personalized treatment plan. Genomics as a part of a CDS platform (in this case, IntellxxDNA) has been shown to be beneficial for improving outcomes in other complex neurological diseases such as autism (Way et al., 2021). There is now good evidence for the hypothesis that this same genomically targeted approach can be utilized for AD and MCI.

DATA AVAILABILITY STATEMENT

The original contributions presented in the study are included in the article/supplementary material, further inquiries can be directed to the corresponding author.

ETHICS STATEMENT

Ethical review and approval was not required for the study on human participants in accordance with the local legislation and institutional requirements. The patients/participants provided their written informed consent to participate in this study. Written informed consent was obtained from the individual(s) for the publication of any potentially identifiable images or data included in this article.

AUTHOR CONTRIBUTIONS

SH-C and CB contributed to the conceptualization of this work. SH-C, SK, EM, and AS contributed to the methodology. SK, EM, and AS carried out the study investigation, as well as developed and supervised treatment plans, and collected data. SH-C, CB, and AW wrote the original draft and edited the manuscript. All authors have read and agreed to the published version of the manuscript.

ACKNOWLEDGMENTS

Thank you to all the office staff including nursing staff, dietitians, and administrative staff that helped support these patients during their brain optimization program. Additional thanks to Dale Bredesen for his foundational work in this field.

REFERENCES

Adogwa, O., Elsamadicy, A. A., Vuong, V. D., Fialkoff, J., Cheng, J., Karikari, I. O., et al. (2018). Association between baseline cognitive impairment and postoperative delirium in elderly patients undergoing surgery for adult spinal deformity. *J. Neurosur. Spine* 28, 103–108. doi: 10.3171/2017.5.SPINE161244

Almeida, L. M., Gandolfi, L., Pratesi, R., Uenishi, R. H., de Almeida, F. C., Selleski, N., et al. (2016). Presence of DQ2.2 associated with DQ2.5 increases the risk for celiac disease. *Autoimmune Dis.* 2016:5409653. doi: 10.1155/2016/5409653

Alzheimer's Association (2021). Alzheimer's disease facts and figures. *Alzheimers Dement.* 17, 327–406. doi: 10.1002/alz.12328

Andreoli, V., and Sprovieri, F. (2017). Genetic aspects of susceptibility to mercury toxicity: an overview. *Int. J. Environ. Res. Public Health* 14:93. doi: 10.3390/ijerph14010093

Armstrong, R. A. (2019). Risk factors for Alzheimer's disease. *Folia Neuropathol.* 57, 87–105. doi: 10.5114/fn.2019.85929

Avgerinos, K. I., Vrysis, C., Chaitidis, N., Kolotsiou, K., Myserlis, P. G., and Kapogiannis, D. (2020). Effects of saffron (*Crocus sativus* L.) on cognitive function. A systematic review of RCTs. *Neurol. Sci.* 41, 2747–2754. doi: 10.1007/s10072-020-04427-0

Batarseh, Y. S., Bharate, S. S., Kumar, V., Kumar, A., Vishwakarma, R. A., Bharate, S. B., et al. (2017). Crocus sativus extract tightens the blood-brain barrier,

reduces amyloid β load and related toxicity in 5XFAD Mice. *ACS Chem. Neurosci.* 8, 1756–1766. doi: 10.1021/acschemneuro.7b00101

Bermejo-Pareja, F. (2011). Essential Tremor—a neurodegenerative disorder associated with cognitive defects? *Nat. Rev. Neurol.* 7, 273–282. doi: 10.1038/nrneurol.2011.44

Bhalsing, K., Suresh, K., Muthane, U. B., and Pal, P. K. (2013). Prevalence and profile of Restless Legs Syndrome in Parkinson's disease and other neurodegenerative disorders: a case-control study. *Parkinsonism Relat. Disord.* 19, 426–430. doi: 10.1016/j.parkreldis.2012.12.00

Blaylock, R. L., and Maroon, J. (2012). Natural plant products and extracts that reduce immunoexcitotoxicity-associated neurodegeneration and promote repair within the central nervous system. *Surg. Neurol. Int.* 3:19. doi: 10.4103/2152-7806.92935

Boccardi, M., Altomare, D., Ferrari, C., Festari, C., Guerra, U. P., Paghera, B., et al. (2016). Assessment of the Incremental Diagnostic Value of Florbetapir F 18 Imaging in Patients with Cognitive Impairment: the Incremental Diagnostic Value of Amyloid PET With [18F]-Florbetapir (INDIA-FBP) Study. *JAMA Neurol.* 73, 1417–1424. doi: 10.1001/jamaneurol.2016.3751

Bredesen, D. E., Amos, E. C., Canick, J., Ackerley, M., Raji, C., Fiala, M., et al. (2016). Reversal of cognitive decline in Alzheimer's disease. *Aging* 8, 1250–1258. doi: 10.18632/aging.100981

Bredesen, D. E., Sharlin, K., Jenkins, D., Okuno, M., Youngberg, W., Cohen, S. H., et al. (2018). Reversal of Cognitive Decline: 100 Patients. *J. Alzheimers Dis. Parkinsonism* 8:450. doi: 10.4172/2161-0460.1000450

Brown, W. R., Moody, D. M., Thore, C. R., Challa, V. R., and Anstrom, J. A. (2007). Vascular dementia in leukoaraiosis may be a consequence of capillary loss not only in the lesions, but in normal-appearing white matter and cortex as well. *J. Neurol. Sci.* 257, 62–66. doi: 10.1016/j.jns.2007.01.015

Bussè, C., Anselmi, P., Pompanin, S., Zorzi, G., Fragiacomo, F., Camporese, G., et al. (2017). Specific verbal memory measures may distinguish Alzheimer's disease from dementia with lewy bodies. *J. Alzheimers Dis.* 59, 1009–1015. doi: 10.3233/JAD-170154

Cajavilca, C. E., Gadhia, R. R., and Román, G. C. (2019). *MTHFR* gene mutations correlate with white matter disease burden and predict cerebrovascular disease and dementia. *Brain Sci.* 9:211. doi: 10.3390/brainsci9090211

Cardoso, B. R., Busse, A. L., Hare, D. J., Cominetti, C., Horst, M. A., McColl, G., et al. (2016). Pro198Leu polymorphism affects the selenium status and GPx activity in response to Brazil nut intake. *Food Funct.* 7, 825–833. doi: 10.1039/c5fo01270h

Chandrasekhar, K., Kapoor, J., and Anishetty, S. (2012). A prospective, randomized double-blind, placebo-controlled study of safety and efficacy of a high-concentration full-spectrum extract of ashwagandha root in reducing stress and anxiety in adults. *Indian J. Psychol. Med.* 34, 255–262. doi: 10.4103/0253-7176.106022

Cheema, A. K., Li, T., Liuzzi, J. P., Zarini, G. G., Dorak, M. T., and Huffman, F. G. (2015). Genetic Associations of PPARGC1A with Type 2 Diabetes: differences among Populations with African Origins. *J. Diabetes Res.* 2015:921274. doi: 10.1155/2015/921274

Choudhary, D., Bhattacharyya, S., and Bose, S. (2017). Efficacy and Safety of Ashwagandha (*Withania somnifera* (L.) Dunal) Root extract in improving memory and cognitive functions. *J. Diet. Suppl.* 14, 599–612. doi: 10.1080/19390211.2017.1284970

Chowanadisai, W., Bauerly, K. A., Tchaparian, E., Wong, A., Cortopassi, G. A., and Rucker, R. B. (2010). Pyrroloquinoline quinone stimulates mitochondrial biogenesis through cAMP response element-binding protein phosphorylation and increased PGC-1alpha expression. *J. Biol. Chem.* 285, 142–152. doi: 10.1074/jbc.M109.030130

Clarke, R., Peden, J. F., Hopewell, J. C., Kyriakou, T., Goel, A., Heath, S. C., et al. (2009). Genetic variants associated with Lp(a) lipoprotein level and coronary disease. *N. Engl. J. Med.* 361, 2518–2528. doi: 10.1056/NEJMoa0902604

Coto, E., Gómez, J., Alonso, B., Corao, A. I., Díaz, M., Menéndez, M., et al. (2011). Late-onset Alzheimer's disease is associated with mitochondrial DNA 7028C/haplogroup H and D310 poly-C tract heteroplasmy. *Neurogenetics* 12, 345–346. doi: 10.1007/s10048-011-0295-4

Cuenoud, B., Ipek, Ö., Shevlyakova, M., Beaumont, M., Cunnane, S. C., Gruetter, R., et al. (2020). Brain NAD is associated with ATP energy production and membrane phospholipid turnover in humans. *Front. Aging Neurosci.* 12:609517. doi: 10.3389/fnagi.2020.609517

de Assis, G. G., and de Almondes, K. M. (2017). Exercise-dependent BDNF as a modulatory factor for the executive processing of individuals in course of cognitive decline. A Systematic Review. *Front. Psychol.* 8:584. doi: 10.3389/fpsyg.2017.00584

de Mendonça, E., Salazar Alcalá, E., and Fernández-Mestre, M. (2016). Role of genes GSTM1, GSTT1, and MnSOD in the development of late-onset Alzheimer disease and their relationship with APOE*4. *Neurologia* 31, 535–542. doi: 10.1016/j.nrl.2014.10.012

Fan, Y. Y., Cai, Q. L., Gao, Z. Y., Lin, X., Huang, Q., Tang, W., et al. (2017). APOE ε4 allele elevates the expressions of inflammatory factors and promotes Alzheimer's disease progression: a comparative study based on Han and She populations in the Wenzhou area. *Brain Res. Bull.* 132, 39–43. doi: 10.1016/j.brainresbull.2017.04.017

Farrer, L. A., Cupples, L. A., Haines, J. L., Hyman, B., Kukull, W. A., Mayeux, R., et al. (1997). Effects of age, sex, and ethnicity on the association between apolipoprotein E genotype and Alzheimer disease. A meta-analysis. APOE and Alzheimer Disease Meta Analysis Consortium. *JAMA* 278, 1349–1356. doi: 10.1001/jama.278.16.1349

Feng, L., Jiang, H., Li, Y., Teng, F., and He, Y. (2017). Effects of citicoline therapy on the network connectivity of the corpus callosum in patients with leukoaraiosis. *Medicine* 96:e5931. doi: 10.1097/MD.0000000000005931

Fernandez-Cadenas, I., Mendioroz, M., Domingues-Montanari, S., Del Rio-Espinola, A., Delgado, P., Ruiz, A., et al. (2011). Leukoaraiosis is associated with genes regulating blood-brain barrier homeostasis in ischaemic stroke patients. *Eur. J. Neurol.* 18, 826–835. doi: 10.1111/j.1468-1331.2010.03243.x

Fernández-Martínez, M., Elcoroaristizabal Martín, X., Blanco Martín, E., Galdos Alcelay, L., Ugarriza Serrano, I., Gómez Busto, F., et al. (2013). Oestrogen receptor polymorphisms are an associated risk factor for mild cognitive impairment and Alzheimer disease in women APOE {varepsilon}4 carriers: a case-control study. *BMJ Open* 3:e003200. doi: 10.1136/bmjopen-2013-003200

Fioravanti, M., and Buckley, A. E. (2006). Citicoline (Cognizin) in the treatment of cognitive impairment. *Clin. Interv. Aging* 1, 247–251. doi: 10.2147/ciia.2006.1.3.247

Gareri, P., Castagna, A., Cotroneo, A. M., Putignano, S., De Sarro, G., and Bruni, A. C. (2015). The role of citicoline in cognitive impairment: pharmacological characteristics, possible advantages, and doubts for an old drug with new perspectives. *Clin. Interv. Aging* 10, 1421–1429. doi: 10.2147/cia.s87886

Geifman, N., Brinton, R. D., Kennedy, R. E., Schneider, L. S., and Butte, A. J. (2017). Evidence for benefit of statins to modify cognitive decline and risk in Alzheimer's disease. *Alzheimers Res. Ther.* 9:10. doi: 10.1186/s13195-017-0237-y

Ghandadi, M., and Sahebkar, A. (2017). Curcumin: an Effective Inhibitor of Interleukin-6. *Curr. Pharm. Des.* 23, 921–931. doi: 10.2174/1381612822666161006151605

Grubisa, I., Otasevic, P., Vucinic, N., Milicic, B., Jozic, T., Krstic, S., et al. (2018). Combined GSTM1 and GSTT1 null genotypes are strong risk factors for atherogenesis in a Serbian population. *Genet. Mol. Biol.* 41, 35–40. doi: 10.1590/1678-4685-GMB-2017-0034

Gustafson, C. (2015). Dale E. Bredesen, md: reversing Cognitive Decline. *Integr. Med.* 14, 26–29.

Haeberlein, S. B., von Hehn, C., Tian, Y., Chalkias, S., Muralidharan, K. K., Chen, T., et al. (2020). Emerge and Engage Topline Results: phase 3 Studies of Aducanumab in Early Alzheimer's Disease: developments in clinical trials and cognitive assessment. *Alzheimers Dement.* 16:e047259. doi: 10.1002/alz.047259

Haffner, C., Malik, R., and Dichgans, M. (2016). Genetic factors in cerebral small vessel disease and their impact on stroke and dementia. *J. Cereb. Blood Flow Metab.* 36, 158–171. doi: 10.1038/jcbfm.2015.71

Hakim, A. M. (2021). A proposed hypothesis on dementia: inflammation, small vessel disease, and hypoperfusion is the sequence that links all harmful lifestyles to cognitive impairment. *Front. Aging Neurosci.* 13:679837. doi: 10.3389/fnagi.2021.679837

Hassan, A., Gormley, K., O'Sullivan, M., Knight, J., Sham, P., Vallance, P., et al. (2004). Endothelial nitric oxide gene haplotypes and risk of cerebral small-vessel disease. *Stroke* 35, 654–659. doi: 10.1161/01.STR.0000117238.75736.53

Hauser, R. A., Lyons, K. E., McClain, T., Carter, S., and Perlmutter, D. (2009). Randomized, double-blind, pilot evaluation of intravenous glutathione in Parkinson's disease. *Mov. Disord.* 24, 979–983. doi: 10.1002/mds.22401

Heyboer, M. III, Sharma, D., Santiago, W., and McCulloch, N. (2017). Hyperbaric oxygen therapy: side effects defined and quantified. *Adv. Wound Care* 6, 210–224. doi: 10.1089/wound.2016.0718

Horton, D. K., Hynan, L. S., Lacritz, L. H., Rossetti, H. C., Weiner, M. F., and Cullum, C. M. (2015). An Abbreviated Montreal Cognitive Assessment (MoCA) for dementia screening. *Clin. Neuropsychol.* 29, 413–425. doi: 10.1080/13854046.2015.1043349

Jansen, I. E., Savage, J. E., Watanabe, K., Bryois, J., Williams, D. M., Steinberg, S., et al. (2019). Genome-Wide Meta-Analysis Identifies New Loci and Functional Pathways Influencing Alzheiemer's Disease Risk. *Nat. Genet.* 51, 404–413. doi: 10.1038/s41588-018-0311-9

Ji, H., Dai, D., Wang, Y., Jiang, D., Zhou, X., Lin, P., et al. (2015). Association of *BDNF* and *BCHE* with Alzheimer's disease: meta-analysis based on 56 genetic case-control studies of 12,563 cases and 12,622 controls. *Exp. Ther. Med.* 9, 1831–1840. doi: 10.3892/etm.2015.2327

Kim, J., Basak, J. M., and Holtzman, D. M. (2009). The role of apolipoprotein E in Alzheimer's disease. *Neuron* 63, 287–303. doi: 10.1016/j.neuron.2009.06.026

Krikorian, R., Shidler, M. D., Dangelo, K., Couch, S. C., Benoit, S. C., and Clegg, D. J. (2012). Dietary ketosis enhances memory in mild cognitive impairment. *Neurobiol. Aging* 33, 555.e13–555.e14. doi: 10.1016/j.neurobiolaging.2010.10.006

Kroenke, K., Spitzer, R. L., and Williams, J. B. (2001). The PHQ-9: validity of a brief depression severity measure. *J. Gen. Intern. Med.* 16, 606–613. doi: 10.1046/j.1525-1497.2001.016009606.x

Kuboyama, T., Tohda, C., and Komatsu, K. (2005). Neuritic regeneration and synaptic reconstruction induced by withanolide A. *Br. J. Pharmacol.* 144, 961–971. doi: 10.1038/sj.bjp.0706122

Kuboyama, T., Tohda, C., and Komatsu, K. (2014). Effects of Ashwagandha (roots of *Withania somnifera*) on neurodegenerative diseases. *Biol. Pharm. Bull.* 37, 892–897. doi: 10.1248/bpb.b14-00022

Kuboyama, T., Yang, X., and Tohda, C. (2020). Natural medicines and their underlying mechanisms of prevention and recovery from amyloid B-induced axonal degeneration in Alzheimer's Disease. *Int. J. Mol. Sci.* 21:4665. doi: 10.3390/ijms21134665

Kucharska-Newton, A. M., Monda, K. L., Campbell, S., Bradshaw, P. T., Wagenknecht, L. E., Boerwinkle, E., et al. (2011). Association of the platelet GPIIb/IIIa polymorphism with atherosclerotic plaque morphology: the Atherosclerosis Risk in Communities (ARIC) Study. *Atherosclerosis* 216, 151–156. doi: 10.1016/j.atherosclerosis.2011.01.038

Kumar, R., Dear, K. B., Christensen, H., Ilschner, S., Jorm, A. F., Meslin, C., et al. (2005). Prevalence of mild cognitive impairment in 60- to 64-year-old community-dwelling individuals: the Personality and Total Health through Life 60+ Study. *Dement. Geriatr. Cogn. Disord.* 19, 67–74. doi: 10.1159/000082351

Kurapati, K. R., Atluri, V. S., Samikkannu, T., and Nair, M. P. (2013). Ashwagandha (*Withania somnifera*) reverses β-amyloid1-42 induced toxicity in human neuronal cells: implications in HIV-associated neurocognitive disorders (HAND). *PLoS One* 8:e77624. doi: 10.1371/journal.pone.0077624

Lakhan, S. E., Kirchgessner, A., Tepper, D., and Leonard, A. (2013). Matrix metalloproteinases and blood-brain barrier disruption in acute ischemic stroke. *Front. Neurol.* 4:32. doi: 10.3389/fneur.2013.00032

Langsted, A., Nordestgaard, B. G., and Kamstrup, P. R. (2019). Elevated Lipoprotein(a) and Risk of Ischemic Stroke. *J. Am. Coll. Cardiol.* 74, 54–66. doi: 10.1016/j.jacc.2019.03.524

Lebedeva, E., Huang, M., and Koski, L. (2016). Comparison of alternate and original items on the montreal cognitive assessment. *Can. Geriatr. J.* 19, 15–18. doi: 10.5770/cgj.19.216

Lehman, J. J., Barger, P. M., Kovacs, A., Saffitz, J. E., Medeiros, D. M., and Kelly, D. P. (2000). Peroxisome proliferator-activated receptor gamma coactivator-1 promotes cardiac mitochondrial biogenesis. *J. Clin. Invest.* 106, 847–856. doi: 10.1172/JCI10268

Li, I. C., Lee, L. Y., Tzeng, T. T., Chen, W. P., Chen, Y. P., Shiao, Y. J., et al. (2018). Neurohealth Properties of *Hericium erinaceus* Mycelia Enriched with Erinacines. *Behav. Neurol.* 2018:5802634. doi: 10.1155/2018/5802634

Liao, F., Yoon, H., and Kim, J. (2017). Apolipoprotein E metabolism and functions in brain and its role in Alzheimer's disease. *Curr. Opin. Lipidol.* 28, 60–67. doi: 10.1097/MOL.0000000000000383

Lidder, S., and Webb, A. J. (2013). Vascular effects of dietary nitrate (as found in green leafy vegetables and beetroot) via the nitrate-nitrite-nitric oxide pathway. *Br. J. Clin. Pharmacol.* 75, 677–696. doi: 10.1111/j.1365-2125.2012.04420.x

Littleton, A. C., Register-Mihalik, J. K., and Guskiewicz, K. M. (2015). Test-retest reliability of a computerized concussion test: CNS Vital Signs. *Sports Health* 7, 443–447. doi: 10.1177/1941738115586997

Mansoori, N., Tripathi, M., Luthra, K., Alam, R., Lakshmy, R., Sharma, S., et al. (2012). MTHFR (677 and 1298) and IL-6-174 G/C genes in pathogenesis of Alzheimer's and vascular dementia and their epistatic interaction. *Neurobiol. Aging* 33, 1003.e1–1003.e8. doi: 10.1016/j.neurobiolaging.2011.09.018

Marcus, C., Mena, E., and Subramaniam, R. M. (2014). Brain PET in the diagnosis of Alzheimer's disease. *Clin. Nucl. Med.* 39, e413–e426. doi: 10.1097/RLU.0000000000000547

Martí Del Moral, A., and Fortique, F. (2019). Omega-3 fatty acids and cognitive decline: a systematic review. *Nutr. Hospital.* 36, 939–949. doi: 10.20960/nh.02496

Martynov, M. Y., and Gusev, E. I. (2015). Current knowledge on the neuroprotective and neuroregenerative properties of citicoline in acute ischemic stroke. *J. Exp. Pharmacol.* 7, 17–28. doi: 10.2147/JEP.S63544

Mitchell, E. S., Conus, N., and Kaput, J. (2014). B vitamin polymorphisms and behavior: evidence of associations with neurodevelopment, depression, schizophrenia, bipolar disorder aerfrefnd cognitive decline. *Neurosci. Biobehav. Rev.* 47, 307–320. doi: 10.1016/j.neubiorev.2014.08.006

Moradi, M., Mojtahedzadeh, M., Mandegari, A., Soltan-Sharifi, M. S., Najafi, A., Khajavi, M. R., et al. (2009). The role of glutathione-S-transferase polymorphisms on clinical outcome of ALI/ARDS patient treated with N-acetylcysteine. *Respir. Med.* 103, 434–441. doi: 10.1016/j.rmed.2008.09.013

Morrill, S. J., and Gibas, K. J. (2019). Ketogenic diet rescues cognition in ApoE4+ patient with mild Alzheimer's disease: a case study. *Diabetes Metab. Syndr.* 13, 1187–1191. doi: 10.1016/j.dsx.2019.01.035

Mounier, N. M., Abdel-Maged, A. E., Wahdan, S. A., Gad, A. M., and Azab, S. S. (2020). Chemotherapy-induced cognitive impairment (CICI): an overview of etiology and pathogenesis. *Life Sci.* 258:118071. doi: 10.1016/j.lfs.2020.118071

Mueller, M., Hobiger, S., and Jungbauer, A. (2010). Anti-Inflammatory activity of extracts from fruits, herbs and spices. *Food Chem.* 122, 987–996. doi: 10.1016/j.foodchem.2010.03.041

Pervin, M., Unno, K., Ohishi, T., Tanabe, H., Miyoshi, N., and Nakamura, Y. (2018). Beneficial effects of green tea Catechins on neurodegenerative diseases. *Molecules* 23:1297. doi: 10.3390/molecules23061297

Petersen, R. C., Lopez, O., Armstrong, M. J., Getchius, T., Ganguli, M., Gloss, D., et al. (2018). Practice guideline update summary: mild cognitive impairment: report of the Guideline Development, Dissemination, and Implementation Subcommittee of the American Academy of Neurology. *Neurology* 90, 126–135. doi: 10.1212/WNL.0000000000004826

Pizzorno, J. (2014). Glutathione! *Integr. Med.* 13, 8–12.

Ramirez-Ramirez, V., Macias-Islas, M. A., Ortiz, G. G., Pacheco-Moises, F., Torres-Sanchez, E. D., Sorto-Gomez, T. E., et al. (2013). Efficacy of fish oil on serum of TNF α, IL-1 β, and IL-6 oxidative stress markers in multiple sclerosis treated with interferon beta-1b. *Oxid. Med. Cell. Longev.* 2013:709493. doi: 10.1155/2013/709493

Ranga, G. S., Kalra, O. P., Tandon, H., Gambhir, J. K., and Mehrotra, G. (2007). Effect of aspirin on lipoprotein(a) in patients with ischemic stroke. *J. Stroke Cerebrovasc. Dis.* 16, 220–224. doi: 10.1016/j.jstrokecerebrovasdis.2007.05.003

Riedel, B. C., Thompson, P. M., and Brinton, R. D. (2016). Age, APOE and sex: triad of risk of Alzheimer's Disease. *J. Steroid Biochem. Mol. Biol.* 160, 134–147. doi: 10.1016/j.jsbmb.2016.03.012

Sachdev, P. S., Lipnicki, D. M., Kochan, N. A., Crawford, J. D., Thalamuthu, A., Andrews, G., et al. (2015). The prevalence of mild cognitive impairment in diverse geographical and ethnocultural regions: the COSMIC Collaboration. *PLoS One* 10:e0142388. doi: 10.1371/journal.pone.0142388

Sarker, M. R., and Franks, S. F. (2018). Efficacy of curcumin for age-associated cognitive decline: a narrative review of preclinical and clinical studies. *Geroscience* 40, 73–95. doi: 10.1007/s11357-018-0017-z

Schmidt, R., Petrovic, K., Ropele, S., Enzinger, C., and Fazekas, F. (2007). Progression of leukoaraiosis and cognition. *Stroke* 38, 2619–2625. doi: 10.1161/STROKEAHA.107.489112

Sehgal, N., Gupta, A., Valli, R. K., Joshi, S. D., Mills, J. T., Hamel, E., et al. (2012). Withania somnifera reverses Alzheimer's disease pathology by enhancing low-density lipoprotein receptor-related protein in liver. *Proc. Natl. Acad. Sci. U.S.A.* 109, 3510–3515. doi: 10.1073/pnas.1112209109

Shapira, R., Gdalyahu, A., Gottfried, I., Sasson, E., Hadanny, A., Efrati, S., et al. (2021). Hyperbaric oxygen therapy alleviates vascular dysfunction and amyloid burden in an Alzheimer's disease mouse model and in elderly patients. *Aging* 13, 20935–20961. doi: 10.18632/aging.203485

Sharma, V. K., Mehta, V., and Singh, T. G. (2020). Alzheimer's disorder: epigenetic connection and associated risk factors. *Curr. Neuropharmacol.* 18, 740–753. doi: 10.2174/1570159X18666200128125641

Sherry, S. T., Ward, M., and Sirotkin, K. (1999). dbSNP-database for single nucleotide polymorphisms and other classes of minor genetic variation. *Genome Res.* 9, 677–679. doi: 10.1101/gr.9.8.677

Shi, M., Xia, J., Xing, H., Yang, W., Xiong, X., Pan, W., et al. (2016). The Sp1-mediaded allelic regulation of MMP13 expression by an ESCC susceptibility SNP rs2252070. *Scientific reports* 6, 27013. doi: 10.1038/srep27013

Simonovitch, S., Schmukler, E., Masliah, E., Pinkas-Kramarski, R., and Michaelson, D. M. (2019). The Effects of APOE4 on Mitochondrial Dynamics and Proteins *in vivo*. *J. Alzheimers Dis.* 70, 861–875. doi: 10.3233/JAD-190074

Stoffaneller, R., and Morse, N. L. (2015). A review of dietary selenium intake and selenium status in Europe and the Middle East. *Nutrients* 7, 1494–1537. doi: 10.3390/nu7031494

Toups, K., Hathaway, A., Gordon, D., Chung, H., Raji, C., Boyd, A., et al. (2021). *Precision Medicine Approach to Alzheimer's Disease: Successful Proof-of-Concept Trial [Preprint].* Available online at: https://www.medrxiv.org/content/10.1101/2021.05.10.21256982v1 (accessed January 11, 2022).

Ueda, H., Neyama, H., Sasaki, K., Miyama, C., and Iwamoto, R. (2018). Lysophosphatidic acid LPA_1 and LPA_3 receptors play roles in the maintenance of late tissue plasminogen activator-induced central poststroke pain in mice. *Neurobiol. Pain* 5:100020. doi: 10.1016/j.ynpai.2018.07.001

Walters, A. S., Paueksakon, P., Adler, C. H., Moussouttas, M., Weinstock, L. B., Spruyt, K., et al. (2021). Restless legs syndrome shows increased silent postmortem cerebral microvascular disease with gliosis. *J. Am. Heart Assoc.* 10, doi: 10.1161/JAHA.120.019627

Wang, C., Zhang, Y., Ding, J., Zhao, Z., Qian, C., Luan, Y., et al. (2017). Nicotinamide Administration Improves Remyelination after Stroke. *Neural Plast.* 2017:7019803. doi: 10.1155/2017/7019803

Wang, J., Liu, Y., Zhou, L. J., Wu, Y., Li, F., Shen, K. F., et al. (2013). Magnesium L-threonate prevents and restores memory deficits associated with neuropathic pain by inhibition of TNF-α. *Pain Phys.* 16, E563–E575.

Wang, M., Li, Y., Lin, L., Song, G., and Deng, T. (2016). GSTM1 Null Genotype and GSTP1 Ile105Val polymorphism are associated with Alzheimer's disease: a meta-analysis. *Mol. Neurobiol.* 53, 1355–1364. doi: 10.1007/s12035-015-9092-7

Wang, W. Y., Tan, M. S., Yu, J. T., and Tan, L. (2015). Role of pro-inflammatory cytokines released from microglia in Alzheimer's disease. *Ann. Transl. Med.* 3:136. doi: 10.3978/j.issn.2305-5839.2015.03.49

Wang, Y., and Brinton, R. D. (2016). Triad of risk for late onset Alzheimer's: mitochondrial haplotype, APOE genotype and chromosomal sex. *Front. Aging Neurosci.* 8:232. doi: 10.3389/fnagi.2016.00232

Wang, Y., Li, X., Guo, Y., Chan, L., and Guan, X. (2010). alpha-Lipoic acid increases energy expenditure by enhancing adenosine monophosphate-activated protein kinase-peroxisome proliferator-activated receptor-gamma coactivator-1alpha signaling in the skeletal muscle of aged mice. *Metabolism* 59, 967–976. doi: 10.1016/j.metabol.2009.10.018

Way, H., Williams, G., Hausman-Cohen, S., and Reeder, J. (2021). Genomics as a clinical decision support tool: successful proof of concept for improved ASD Outcomes. *J. Pers. Med.* 11:596. doi: 10.3390/jpm11070596

Willis, C. L., Meske, D. S., and Davis, T. P. (2010). Protein kinase C activation modulates reversible increase in cortical blood-brain barrier permeability and tight junction protein expression during hypoxia and posthypoxic reoxygenation. *J. Cereb. Blood Flow Metab.* 30, 1847–1859. doi: 10.1038/jcbfm.2010.119

Wong, W. (2020). Economic burden of Alzheimer disease and managed care considerations. *Am. J. Managed Care* 26, S177–S183. doi: 10.37765/ajmc.2020.88482

Wright, D. J., Renoir, T., Smith, Z. M., Frazier, A. E., Francis, P. S., Thorburn, D. R., et al. (2015). N-Acetylcysteine improves mitochondrial function and ameliorates behavioral deficits in the R6/1 mouse model of Huntington's disease. *Transl. Psychiatry* 5:e492. doi: 10.1038/tp.2014.131

Wroolie, T. E., Watson, K., Chen, K., Balzafiore, D., Reiman, E., and Rasgon, N. (2017). OPEN LABEL TRIAL OF MAGNESIUM L-THREONATE IN PATIENTS WITH DEMENTIA. *Innov. Aging* 1:170. doi: 10.1093/geroni/igx004.661

Wu, L., Shen, Y., Liu, X., Ma, X., Xi, B., Mi, J., et al. (2009). The 1425G/A SNP in PRKCH is associated with ischemic stroke and cerebral hemorrhage in a Chinese population. *Stroke* 40, 2973–2976. doi: 10.1161/STROKEAHA.109.551747

Wu, L., Zhang, X., and Zhao, L. (2018). Human ApoE isoforms differentially modulate brain glucose and ketone body metabolism: implications for Alzheimer's disease risk reduction and early intervention. *J. Neurosci.* 38, 6665–6681. doi: 10.1523/JNEUROSCI.2262-17.2018

Xu, X., Wang, Z., Li, Q., Xiao, X., Lian, Q., Xu, W., et al. (2009). Endothelial nitric oxide synthase expression is progressively increased in primary cerebral microvascular endothelial cells during hyperbaric oxygen exposure. *Oxid. Med. Cell. Longev.* 2, 7–13. doi: 10.4161/oxim.2.1.7697

Yabluchanskiy, A., Ma, Y., Iyer, R. P., Hall, M. E., and Lindsey, M. L. (2013). Matrix metalloproteinase 9: many shades of function in cardiovascular disease. *Physiology* 28, 391–403. doi: 10.1152/physiol.00029.2013

Yiannopoulou, K. G., Anastasiou, A. I., Zachariou, V., and Pelidou, S.-H. (2019). Reasons for failed trials of disease-modifying treatments for Alzheimer disease and their contribution in recent research. *Biomedicines* 7:97. doi: 10.3390/biomedicines7040097

Yin, J., Nielsen, M., Carcione, T., Li, S., and Shi, J. (2019). Apolipoprotein E regulates mitochondrial function through the PGC-1α-sirtuin 3 pathway. *Aging* 11, 11148–11156. doi: 10.18632/aging.102516

Yoshida, K., Ushida, Y., Ishijima, T., Suganuma, H., Inakuma, T., Yajima, N., et al. (2015). Broccoli sprout extract induces detoxification-related gene expression and attenuates acute liver injury. *World J. Gastroenterol.* 21, 10091–10103. doi: 10.3748/wjg.v21.i35.10091

Yu, X., Guan, P. P., Zhu, D., Liang, Y. Y., Wang, T., Wang, Z. Y., et al. (2018). Magnesium Ions Inhibit the Expression of Tumor Necrosis Factor α and the Activity of γ-Secretase in a β-Amyloid Protein-Dependent Mechanism in APP/PS1 Transgenic Mice. *Front. Mol. Neurosci.* 11:172. doi: 10.3389/fnmol.2018.00172

Zhang, J., Zhan, Z., Li, X., Xing, A., Jiang, C., Chen, Y., et al. (2017). Intermittent fasting protects against Alzheimer's disease possible through restoring aquaporin-4 Polarity. *Front. Mol. Neurosci.* 10:395. doi: 10.3389/fnmol.2017.00395

Zimmerman, M. E., Lipton, R. B., Santoro, N., McConnell, D. S., Derby, C. A., Katz, M. J., et al. (2011). Endogenous estradiol is associated with verbal memory in nondemented older men. *Brain Cogn.* 76, 158–165. doi: 10.1016/j.bandc.2011.01.011

Conflict of Interest: AW is an employee at IntellxxDNA^{TM}. IntellxxDNA^{TM} was the genomics clinical decision support tool used in this study but has no financial interests. SH-C is the medical director of IntellxxDNA and does have ownership interest. CB is the CEO of IntellxxDNA^{TM} and does have ownership interest.

The remaining authors declare that the research was conducted in the absence of any commercial or financial relationships that could be construed as a potential conflict of interest.

Publisher's Note: All claims expressed in this article are solely those of the authors and do not necessarily represent those of their affiliated organizations, or those of the publisher, the editors and the reviewers. Any product that may be evaluated in this article, or claim that may be made by its manufacturer, is not guaranteed or endorsed by the publisher.

frontiers | Frontiers in Neuroscience

ORIGINAL RESEARCH
published: 03 May 2022
doi: 10.3389/fnins.2022.858126

DeePred-BBB: A Blood Brain Barrier Permeability Prediction Model With Improved Accuracy

*Rajnish Kumar[1], Anju Sharma[2], Athanasios Alexiou[3,4], Anwar L. Bilgrami[5,6], Mohammad Amjad Kamal[7,8,9,10,11] and Ghulam Md Ashraf[12,13]**

[1] Amity Institute of Biotechnology, Amity University Uttar Pradesh, Lucknow, India, [2] Department of Applied Science, Indian Institute of Information Technology Allahabad, Prayagraj, India, [3] Department of Science and Engineering, Novel Global Community Educational Foundation, Hebersham, NSW, Australia, [4] AFNP Med Austria, Vienna, Austria, [5] Department of Entomology, Rutgers, The State University of New Jersey, New Brunswick, NJ, United States, [6] Deanship of Scientific Research, King Abdulaziz University, Jeddah, Saudi Arabia, [7] Institutes for Systems Genetics, Frontiers Science Center for Disease-Related Molecular Network, West China Hospital, Sichuan University, Chengdu, China, [8] King Fahd Medical Research Center, King Abdulaziz University, Jeddah, Saudi Arabia, [9] Department of Pharmacy, Faculty of Allied Health Sciences, Daffodil International University, Dhaka, Bangladesh, [10] Enzymoics, Hebersham, NSW, Australia, [11] Novel Global Community Educational Foundation, Hebersham, NSW, Australia, [12] Pre-Clinical Research Unit, King Fahd Medical Research Center, King Abdulaziz University, Jeddah, Saudi Arabia, [13] Department of Medical Laboratory Sciences, Faculty of Applied Medical Sciences, King Abdulaziz University, Jeddah, Saudi Arabia

OPEN ACCESS

Edited by:
Corinne Lasmezas, The Scripps Research Institute, United States

Reviewed by:
Sezen Vatansever, Icahn School of Medicine at Mount Sinai, United States
Mootaz M. Salman, University of Oxford, United Kingdom

***Correspondence:**
Ghulam Md Ashraf
ashraf.gm@gmail.com;
gashraf@kau.edu.sa

Specialty section:
This article was submitted to Neurodegeneration, a section of the journal Frontiers in Neuroscience

Received: *19 January 2022*
Accepted: *14 March 2022*
Published: *03 May 2022*

Citation:
Kumar R, Sharma A, Alexiou A, Bilgrami AL, Kamal MA and Ashraf GM (2022) DeePred-BBB: A Blood Brain Barrier Permeability Prediction Model With Improved Accuracy. Front. Neurosci. 16:858126. doi: 10.3389/fnins.2022.858126

The blood-brain barrier (BBB) is a selective and semipermeable boundary that maintains homeostasis inside the central nervous system (CNS). The BBB permeability of compounds is an important consideration during CNS-acting drug development and is difficult to formulate in a succinct manner. Clinical experiments are the most accurate method of measuring BBB permeability. However, they are time taking and labor-intensive. Therefore, numerous efforts have been made to predict the BBB permeability of compounds using computational methods. However, the accuracy of BBB permeability prediction models has always been an issue. To improve the accuracy of the BBB permeability prediction, we applied deep learning and machine learning algorithms to a dataset of 3,605 diverse compounds. Each compound was encoded with 1,917 features containing 1,444 physicochemical (1D and 2D) properties, 166 molecular access system fingerprints (MACCS), and 307 substructure fingerprints. The prediction performance metrics of the developed models were compared and analyzed. The prediction accuracy of the deep neural network (DNN), one-dimensional convolutional neural network, and convolutional neural network by transfer learning was found to be 98.07, 97.44, and 97.61%, respectively. The best performing DNN-based model was selected for the development of the "DeePred-BBB" model, which can predict the BBB permeability of compounds using their simplified molecular input line entry system (SMILES) notations. It could be useful in the screening of compounds based on their BBB permeability at the preliminary stages of drug development. The DeePred-BBB is made available at https://github.com/12rajnish/DeePred-BBB.

Keywords: blood-brain barrier, convolutional neural network, deep learning, machine learning, prediction, CNS-permeability

INTRODUCTION

Neurological diseases are among the most predominant health issues, with an approximately 28% prevalence in all age groups of patients (Menken et al., 2000). Despite a decrease in communicable neurological diseases, the number of deaths due to neurological diseases has increased to 39% in the last three decades (Feigin et al., 2020). This substantial increase in the absolute number of patients indicates that available therapeutics are scarce to prevent and manage neurological diseases in the current changing global demography. Therefore, it is imperative to find novel and effective therapeutics to target the central nervous system (CNS) to meet the challenges of the ever-increasing absolute number of patients with neurological diseases. An alternative method targeting the molecular and signaling mechanisms at BBB rather than the traditional approaches has become the recent trend in drug target validation (Salman et al., 2022). Drugs must cross the blood-brain barrier (BBB) to act on the CNS. There is a higher attrition rate of drug candidates failing in clinical research due to non-permeability to the BBB compared to potency issues (Dieterich et al., 2003; Pardridge, 2005; Saunders et al., 2014; Hendricks et al., 2015). The BBB is a semipermeable and selective boundary that maintains the steady state of the CNS by protecting it from external compounds (98%) (**Figure 1**; Pardridge, 2002). As drugs need to enter the CNS to impart therapeutic activity, it becomes crucial to determine BBB permeability during the initial stages of CNS-acting drug design and development (Daneman, 2015; van Tellingen et al., 2015; Saxena et al., 2019).

The BBB separates the CNS from the bloodstream, preventing contagions from invading the brain. Brain endothelial cells, astrocytes, neurons, and pericytes are four major components of the BBB. The largest constituent of the BBB is a layer containing brain endothelial cells, which serve as the first line of defense from the CNS surroundings. Endothelial cells are connected with tight junctions and adherence junctions, which create a strong barrier, restricting pinocytosis and decreasing vesicle-facilitated transcellular transport (Reese and Karnovsky, 1967; Tietz and Engelhardt, 2015). The BBB not only acts as a physical barrier but also serves as a metabolic barrier, transport interface, and secretory layer (Abbott et al., 2006; Rhea and Banks, 2019). Neurons reside very close to brain capillaries and play a vital role in maintaining ion balance in the local environment (Schlageter et al., 1999).

Clinical experiments to determine the BBB permeability of compounds are accurate; however, they are time-consuming and labor-intensive (Bickel, 2005; Massey et al., 2020; Schidlowski et al., 2020). Additionally, it is difficult to perform clinical experiments with diverse types of drug candidates (Main et al., 2018; Mi et al., 2020). Therefore, it is crucial to predict and forecast BBB permeability using computational algorithms or *in vitro* BBB mimics to elucidate the permeability of compounds across the BBB (Gupta et al., 2019). There have been numerous attempts to predict the BBB permeability of compounds since the advent of artificial intelligence (AI), primarily using machine learning (ML) algorithms such as support vector machines (SVMs), artificial neural networks (ANNs), k-nearest neighbors (kNNs), naïve Bayes (NB), and random forests (RFs) (Doniger et al., 2002; Zhang et al., 2008, 2015; Suenderhauf et al., 2012; Khan et al., 2018). In addition to above, some future directions of BBB permeability also seem promising such as application of humanized self-organized models, organoids, 3D cultures and human microvessel-on-a-chip platforms especially those which are amenable for advanced imaging such as transmission electron microscope and expansion microscopy since they enable real-time monitoring of BBB permeability (Wevers et al., 2018; Salman et al., 2020). BBB permeability prediction models developed using AI algorithms can further be assisted with the high throughput screening (Aldewachi et al., 2021), computer aided drug designing (Salman et al., 2021), and knowledge based rules, e.g., Lipinski rule of five (hydrogen bond donor $\leq$ 5, hydrogen bond acceptor $\leq$ 10, molecular weight $\leq$ 500, CLogP $\leq$ 5), Veber rule (rotatable bonds count $\leq$ 10, polar surface area $\leq$ 140), BBB rule (hydrogen bond = 8–10, molecular weight = 400–500, no acids), etc., to screen potential drug candidates with desirable end-point for prevention, mitigation and cure of neurological disorders (Veber et al., 2002; Banks, 2009; Benet et al., 2016).

In an attempt to develop the BBB permeability prediction model, Jiang et al. (2016) applied SVM with a radial basis function (RBF) kernel (Jiang et al., 2016). They used a dataset of 1,562 compounds containing 694 BBB permeable (BBB++) and 868 BBB non-permeable (BBB-) compounds. The overall accuracy, sensitivity, and specificity were reported to be more than 85%. The next year, Castillo-Garit et al. (2017) used the decision tree algorithm on 581 compounds and found that the BBB permeability prediction accuracy increased by 2.93% (Castillo-Garit et al., 2017). However, this study was performed on a much smaller dataset than Jiang et al.'s study. In another study, Yuan et al. (2018) developed SVM-based BBB prediction model using a larger dataset of 1,990 compounds with a prediction accuracy of 93.96% (Yuan et al., 2018). The sensitivity and specificity of the model were reported to be 94.3 and 91.0%, respectively. In the same year, Wang et al. (2018) applied SVM and kNN algorithms using 2,358 compounds (Wang et al., 2018). The prediction accuracy of the best-performing model was found to be 2.64% higher than that of the Yuan et al. (2018) prediction model. However, the model lagged in terms of sensitivity (0.925) and specificity (0.899). The next year, Miao et al. (2019) applied a deep learning (DL) algorithm to 462 compounds. The accuracy of the model was reported to be 97%, with decent AUC (0.98) and F1 scores (0.92). However, the dataset used for the DL study was very small compared to the earlier ML-based models for BBB prediction. Recently, Alsenan et al. (2020) proposed a recurrent neural network (RNN) algorithm-based model using 2,342 compounds for the prediction of BBB permeability (Alsenan et al., 2020). The developed model had better performance metrics with an accuracy, sensitivity, and specificity of 96.53, 94.91, and 98.09%, respectively. The Matthews correlation coefficient (MCC) (93.14) and area under the curve (AUC) (98.6) of the prediction were also found to be satisfactory. In another study, Shaker et al. (2020) applied a light gradient boosting machine algorithm to a dataset of 7,162 compounds for the prediction of BBB

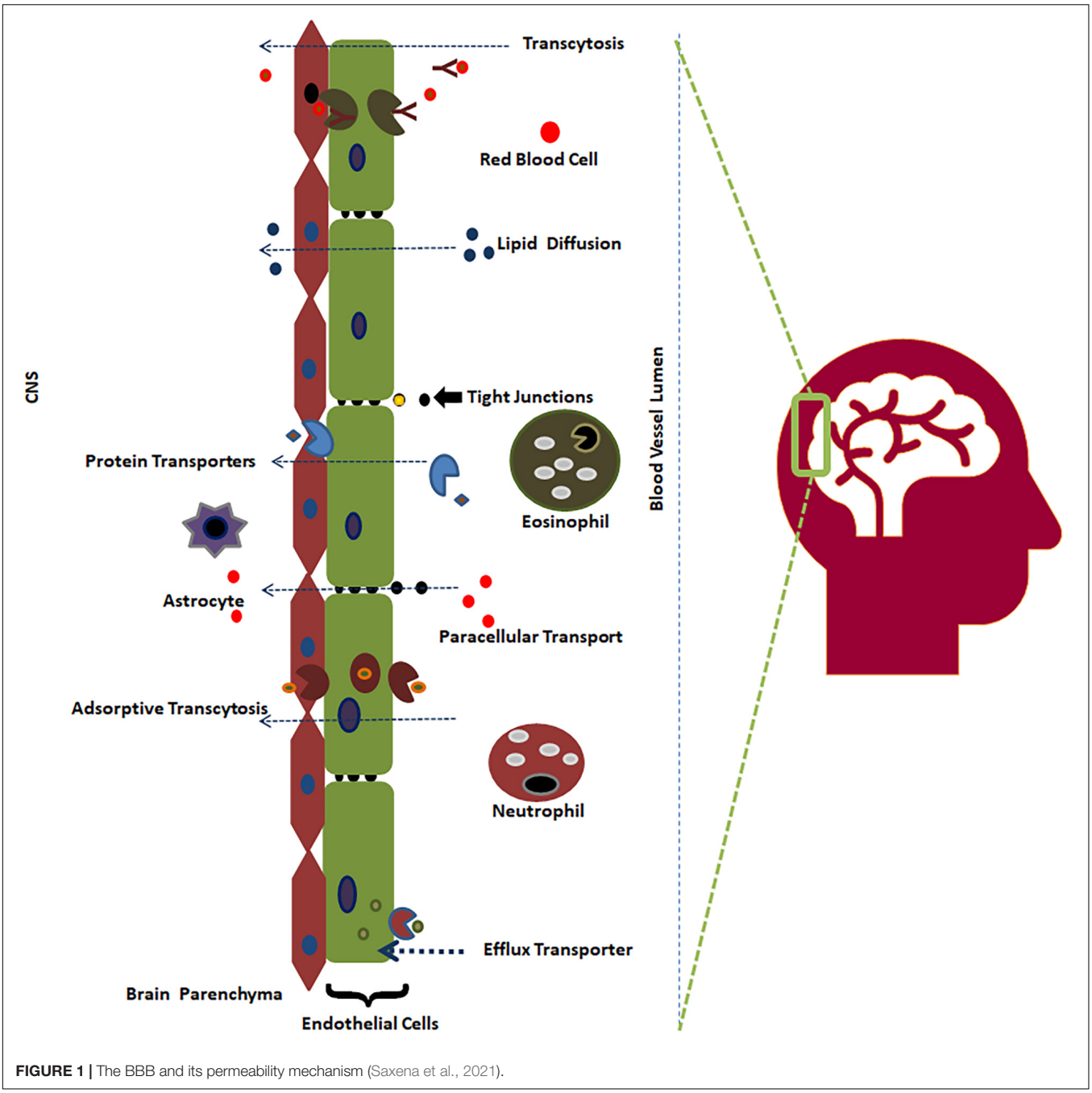

FIGURE 1 | The BBB and its permeability mechanism (Saxena et al., 2021).

permeability (Shaker et al., 2020). Although the study involved a very large dataset compared to previously reported studies, the model's accuracy was reported to be 90%, which was approximately 6.5% less than the BBB permeability prediction model proposed by Alsenan et al. (2020). In the same year, Singh et al. (2020) used random forest, multilayer perceptron, and sequential minimal optimization using 605 compounds to develop the BBB permeability prediction model (Singh et al., 2020). Upon validation of the developed model using 1,566 compounds, the prediction accuracy was found to be 86.5% only. Very recently, Saxena et al. (2021) proposed an ML-based BBB permeability prediction model using 1,978 compounds (Saxena et al., 2021). The study group found that SVM with the RBF kernel yielded an accuracy of 96.77% with AUC and F1 score values of 0.964 and 0.975, respectively, which outperformed the kNN, random forest, and naïve Bayes algorithms in the prediction of BBB permeability on the same dataset.

The major challenge while applying ML algorithms is selecting optimal features to develop predictive models based on labeled BBB permeability datasets (Hu et al., 2019; Salmanpour et al., 2020). To overcome this challenge, we applied DL algorithms and compared their performance with traditional ML algorithms.

MATERIALS AND METHODS

Data Collection

A total of 3,971 compounds with BBB permeability classes were collected from Zhao et al. (2007); Shen et al. (2010), and Roy et al. (2019). The PubChem database[1] was used to retrieve available PubChem IDs of the collected compounds. The collected datasets were checked to remove redundant compounds. After careful curation, we obtained a dataset of 3,605 non-redundant clean compounds containing 2,607 BBB permeable and 998 BBB non-permeable compounds (**Table 1** and **Supplementary File**). The class labels for BBB non-permeable and permeable compounds were kept as "0" and "1," respectively.

Feature Calculation

Three types of feature sets viz. physicochemical properties, molecular access system (MACCS) fingerprints and substructure fingerprints were used in this study. Physicochemical properties contain different types of physical and chemical information encoded in a compound, e.g., molecular weight, molecular volume, solubility, partition coefficient, etc. The molecular fingerprints are fixed-length vectors that indicate the presence/absence of an atom type or functional group in a compound. All features were calculated by open-source PaDel (Yap, 2011). Each compound was encoded with 1,917 features containing 1,444 physicochemical (1D and 2D) properties, 166 MACCS, and 307 substructure fingerprints. This feature set was used for the ML, DNN, and CNN-1D algorithms using Keras framework. For CNN-VGG16, the Python package RDKit was used to generate the structure images of the compounds using their Simplified molecular input line entry system (SMILES) notations (Lovrić et al., 2019; Bento et al., 2020). The Python package RDKit is a collection of ML and cheminformatic software and contains functions to modify chemical compounds. The RDKit package was used to generate 2D images of size 300 * 300 pixels (RGB) from SMILES notations of compounds. RDKit-generated images contain different colors to express the chemical information viz. carbon = black, oxygen = red, nitrogen = blue, sulfur = yellow, chlorine = green, and phosphorous = orange. Images generated by RDKit always fit the entire molecule, so there was no issue with different molecular sizes. The dataset was split into training and test sets at a ratio of 3:1. The test set was separated from the training set to avoid any bias (**Table 2**). To handle the data imbalance, we have already applied cost-sensitive augmentation via the class_weight argument on the fit() function when training models.

[1]https://pubchem.ncbi.nlm.nih.gov/

TABLE 1 | The final dataset and its distribution.

Dataset	BBB permeable compounds	BBB non-permeable compounds	Total
Roy et al. (2019)	819	366	1,185
Zhao et al. (2007)	1,398	393	1,791
Shen et al. (2010)	390	239	629
Total	2,607	998	3,605

TABLE 2 | Distribution of the dataset in the training and test sets.

Dataset	BBB permeable compounds	BBB non-permeable compounds	Total
Training set	1,955	749	2,704
Test set	652	249	901
Total	2,607	998	3,605

Development of Prediction Models

In this study, ML-based algorithms (SVM, kNN, RF, and NB) and DL-based algorithms DNN, CNN-1D were developed using keras framework with libraries; python, numpy, pandas, keras, and tensorflow on Anaconda 3–5.2. CNN (VGG16) was implemented using transfer learning through cloud-based computational resource of Google Colaboratory to develop prediction models for the BBB permeability of the compounds. Based on the performance of the generated prediction models, the DNN-based "DeePred-BBB" is proposed for BBB permeability prediction. DeePred-BBB performance was compared with ML algorithms viz. SVM, NB, kNN, RF, and DL algorithms CNN-1D and CNN (VGG16).

Machine Learning-Based Models

Support vector machine with four different kernels (RBF, polynomial, sigmoid, and linear), NB, kNN, and RF were applied to the training set of 2,704 compounds and tested with an independent set of 901 compounds. Principal component analysis (PCA) (Giuliani, 2017) was used for feature reduction. The component range (10, 20, 30, 40, 50, and 100) was used to find the best prediction accuracy for each applied ML algorithm. Tenfold cross-validation was applied to evaluate the efficacy of the model during training.

Support Vector Machine

Support vector machine is among the robust ML algorithms used for classification and regression (Ghandi et al., 2014; Gaudillo et al., 2019). It searches for the optimal hyperplane with maximized margins using support vectors for classification (Ben-Hur et al., 2008). This algorithm plots the data to the N-dimensional feature space and finds a hyperplane ($\Theta.x + b = 0$) to classify the data sets with minimized loss using the hinge loss function. The loss function is given in Eq. 1.

$$(\theta, b) = \arg\min_{\Theta, b} \sum_{x \in X} \left[1 - y\left(\Theta.x + b\right)\right] + \lambda| \, |\Theta| \, |_2 \qquad (1)$$

Support vector machine was applied using kernels to map the data to higher dimensions to linearly classify the data (Kumar et al., 2011). A penalty parameter "C" (Cost NAÏVE) adjusts the balance between training errors and forcing rigid margins. Another parameter, "γ," regulates the kernel function amplitude (Kumar et al., 2018). Various values of C (1, 5, 10, 50, 90) and γ (0.0001, 0.0005, 0.001, 0.005, 0.01, 0.05) were tested to find the best combination. An optimized combination of C and γ was

used for each SVM kernel (RBF, C = 10, γ = 0.005; polynomial, C = 1, γ = 0.005; sigmoid C = 90, γ = 0.0005; linear, C = 1, γ = 0.05). For the polynomial kernel, 2–6 values of degree (d) were applied and evaluated. The best performance of the polynomial kernel was found at d = 3.

Naïve Bayes

The naïve Bayes algorithm is based on the Bayes theorem. It is a probabilistic method that works on the assumption of class conditional independence (Eq. 2) (Shen et al., 2019). Each feature present in a class is independent and individually contributes to the probability with nil dependency on other features (Wang et al., 2021a). It is fast, readily manages a large dataset, and generally produces better results than other classification techniques when features existing in a class are independent.

$$P(X \mid Y) = \frac{P(Y \mid X)\, P(X)}{P(Y)} \tag{2}$$

where P(X|Y) is the posterior probability of X (class) for a given Y (feature), P(Y|X) is the likelihood, P(X) is the prior probability of class X, and P(Y) is the marginal probability of feature Y.

k-Nearest Neighbor

k-nearest neighbor is a simple and non-parametric classifier that assumes that nearby data points are similar and tend to have similar classes. Feature similarity is used to find the class label of a new data instance. It commonly uses Euclidean distance to find the closeness of the data points, and depending upon the class matching with considered k-points, the class labels are decided (Sharma et al., 2021). Here, k is the number of neighbors. The Euclidean distance between data points x (x1, x2, x3) and y (y1, y2, y3) is calculated using Eq. 3.

$$d(x,\ y)\ =\ \sqrt{\left((x_1 - y_1)^2 + (x_2 - y_2)^2 + (x_3 - y_3)^2\right)} \tag{3}$$

To determine the optimal k, a range of k-values (1–10) was evaluated. The best-performing prediction model at k = 3 was selected for further analysis.

Random Forest

Random forest uses ensemble learning to create a collection of decision trees (forest) that run concurrently and classify data instances (Yao et al., 2020). Tree construction is performed using arbitrary input vectors and node division on arbitrary feature subsets. Each tree of the RF predicts a certain class, and depending upon the highest votes, the final class label is predicted (Yang et al., 2020). In the current study, the developed prediction models were tested with variable trees in a forest (4, 8, 12, 32, 64). Each decision tree's various depths (2–5) and estimators (5, 10, 20, 30, 40) were tested to find the best performing prediction model.

Deep Learning-Based Models

Deep learning algorithms use multiple neurons and hidden layers to extract high-level functions from input data. The major advantage of DL algorithms is their inherent property of selecting the most relevant features from the training dataset. Therefore, unlike ML algorithms, separate feature selection algorithms are not required (Isensee et al., 2021). In this study, three DL algorithms, DNN, CNN-1D, and CNN-VGG16, were applied. The tenfold cross-validation method was used to assess the model's efficiency while training. The training dataset was further divided into ten subsets, iteratively training models using all subsets except one held out to test the performance.

Deep Neural Network

For DNN, 2,704 compounds, each encoded with 1,917 features (1,444 physicochemical properties, 166 MACCS, and 307 substructure fingerprints), were used to develop BBB permeability prediction models. Initial layers receive compounds encoded with feature vectors and subject them to the hidden layers. These hidden layers obtain the relevant information from the input vectors and project the freshly extracted features to the batch normalization layer. This layer increases the training process by reducing the intradata covariance. Dropout layers were applied to reduce the problem of coadaptation of neurons and overfitting (Baldi and Sadowski, 2014). These layers randomly drop the nodes as per the dropout rate. Rectified linear unit (ReLU) activation function was used, which adaptively transforms rectifier parameters. Furthermore, ReLU transforms the neuronal output by mapping it to the highest possible value or zero (if the value is negative) (Wang et al., 2021b). ReLU function is given in Eq. 4.

$$\mathrm{F(xi)}\ =\ \max(0,\ \mathrm{xi}) \tag{4}$$

where xi is input for activation function f on channel "i."

The "softmax" activation function was applied on the output layer to map the hidden layer output between 0 to 1 intervals. The Adam optimizer was used to minimize the loss value from the cross-entropy cost function.

The network performance of a DNN depends upon its depth and breadth. Therefore, it is vital to determine the optimal depth and breadth and optimize other parameters, e.g., the learning rate and dropout ratio. To achieve this, we kept other parameters fixed and evaluated the prediction accuracy by varying the hidden layers (K = 1–5) and neurons (100, 200, 300, 500, 800 neurons per layer). The DNNs were also simultaneously evaluated for five dropout ratios (0.1, 0.2, 0.3, 0.4, 0.5), and prediction accuracy was evaluated. Furthermore, various network configurations were evaluated for epochs (100, 200, 400, 500, 800) and learning rates (0.0001, 0.0002, 0.0003, 0.001, 0.002, 0.003) optimization. **Table 3** summarizes the explored values of hyperparameters for the development of the DNN-based BBB permeability prediction model.

TABLE 3 | Hyperparameter values explored for the DNN model.

Parameter	Values
Number of hidden layers	1–5
Number of neurons	100, 200, 300, 500, 800
Dropout ratio	0.1, 0.2, 0.3, 0.4, 0.5
Learning rate	0.0001, 0.0002, 0.0003, 0.001, 0.002, 0.003
Epochs	100, 200, 400, 500, 800

Convolutional Neural Network-1 Dimension (CNN-1D)

CNN is a particular type of DL that is widely used for image data classification (LeCun et al., 2015). There are three major layers in the CNN: convolutional, pooling, and fully connected layers. Cube-shaped weights and multiple filters (kernels) are applied in the convolutional layers to extract features and develop feature maps from the images (Esteva et al., 2017; Malik et al., 2021; Shan et al., 2021). The filter size may downsample the outputs; therefore, the size and number of kernels are vital (D'souza et al., 2020). To overcome the issue of downsampling, an optimized padding value is applied, which allows the filter kernels to create feature maps of the input image size.

Furthermore, other parameters of the convolutional layer also needed to be optimized, e.g., regularization type and value, activation function, and stride. Pooling layers specifically perform average or max-pooling in the filter region to lower the number of parameters and calculations by downsampling the representations. The fully connected layers flatten the output prior to the classification and are usually kept at the end. CNNs are created to process and learn from images. However, CNN-1D can be applied similarly to one-dimensional data containing physicochemical properties and fingerprints. We used three filters (15, 32, 64) to determine the local pattern in the 1,917 features, which were calculated from PaDel. After the CNN layers, dense layers (1 and 2) were tested for three dropout ratios (0.2, 0.3, 0.5). **Table 4** summarizes the explored hyperparameter values for the development of the CNN-1D model.

Convolutional Neural Network by VGG16 Transfer Learning (CNN-VGG16)

The CNN processes the input 2D images to distinguish the image objects by allocating weights and biases. CNN captures temporal and spatial relationships using the tiny squares of input images by processing them through a series of convolution layers. Filters in each convolutional layer skid on the image to find relevant and specific features, e.g., edge detection, sharpen or blur the image and produce the feature map. The feature map's size depends on filter numbers, filter slide-over pixels, and zero-padding (image borders are padded with zero). The 2D-array values of the feature map were subjected to the individual layer activation function (ReLU). Dimensionality reduction of each feature map is processed using pooling without any loss of information. The pooling layer's output is sent into fully connected layers, which classify the images. The CNN with transfer learning (VGG16) was used in this study using RDKit-generated images. The images were scaled to a pixel size of 128 * 128 to develop and validate the BBB permeability prediction model.

Furthermore, image data argumentation was performed by randomly zooming (up to 10%) and flipping the images. The CNN (VGG16) hyperparameters are given in **Table 5**. The developed model was tested with an independent test set consisting of 901 images. **Figure 2** depicts the adopted methodology to develop the DL-based prediction models.

RESULTS AND DISCUSSION

The performance metrics of the ten developed models (ML = 7, DL = 3) for BBB permeability prediction were compared to determine the best-performing model. The performance indicators used in this study were area under the curve (AUC), area under the precision-recall curve (AUPRC), average precision (AP), F1 score and accuracy, and Hamming distance (HD) of the prediction models. Among the developed ML prediction models, the SVM (RBF kernel)-based prediction model outperformed the NB, kNN, and RF algorithms for BBB permeability prediction with test set data. The accuracy of SVM (RBF) was found to be approximately 6% higher than that of NB and RF and approximately 1% higher than that of kNN. Moreover, SVM (RBF) yielded better prediction values of other performance indicators in BBB permeability prediction on the given dataset. However, the performance metrics of SVM (polynomial) at degree 3 were found to be very comparable to the SVM (RBF).

The performance metrics of the DL algorithms were found to be very close to each other. The prediction accuracies of DNN, CNN-1D, and CNN (VGG16) were 98.07, 97.44, and 97.66, respectively. However, the DNN model was superior in AUC, AUPRC, AP, F1, and HD when compared to that of CNN-1D and CNN (VGG16) (**Table 6**). The comparison of receiver operating characteristic (ROC) curves between SVM (RBF), DNN, CNN-1D, and CNN (VGG16) also indicates the superiority of DNN in BBB permeability prediction with the given dataset (**Figure 3**). Furthermore, the accuracy and loss plots of the DNN model are given in **Figure 4**. The accuracy plot shows good coherence between the training (red) and test (blue) accuracy, suggesting that the model is not overfitted. Additionally, coherence in the training (red) and validation/test (blue) loss in the loss plot (binary cross-entropy loss) is indicative of an unbiased model (**Figure 4**).

The better performance of DL algorithms compared to ML could be due to their ability to handle the large dataset and

TABLE 4 | Explored hyperparameter values for the CNN-1D model.

Parameter	Values
Number of filters	15, 32, 64
Number of dense layers	1, 2
Dropout ratio	0.2, 0.3, 0.4
Learning rate	0.0001, 0.0002, 0.0003, 0.001, 0.002, 0.003
Epochs	100, 200, 400, 500, 600

TABLE 5 | The hyperparameters for CNN (VGG16).

Parameters	VGG16
Convolutional blocks	Convolutional layers, Kernel size, Filters, Max-Pooling, Zero Padding: Predefined
Dense layers	02
Dense layers neurons	150, 104
Dropout ratio	0.5
Learning rate	0.02
Batch size	132
Epochs	800

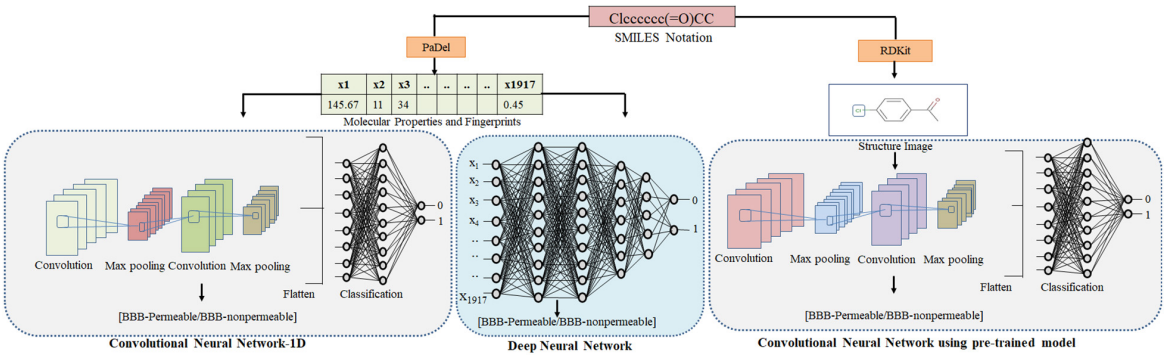

FIGURE 2 | Methodology adopted for predicting the BBB permeability of compounds using SMILES notation. The SMILES notations were used to calculate molecular properties and fingerprints using PaDel. These features were used as input to DNN and CNN-1D to generate the BBB permeability prediction models. The 2D images of compounds were generated using RDkit and fed to the CNN (VGG16) to generate the BBB permeability prediction model.

TABLE 6 | Performance metrics of ML and DL algorithms.

Algorithm	AUC	AUPRC	AP	F1	A (%)	HD	FPR (%)	FNR (%)
SVM (RBF)	0.964	0.988	0.975	0.985	96.29	0.022	6.451	0.724
SVM (Polynomial *d* = 3)	0.948	0.965	0.965	0.98	96.01	0.029	9.756	0.579
SVM (Sigmoid)	0.921	0.971	0.944	0.962	94.45	0.055	13.359	2.519
SVM (Linear)	0.916	0.969	0.938	0.963	94.56	0.054	15.242	1.497
NB	0.844	0.948	0.899	0.935	90.18	0.098	14.543	3.202
kNN (3)	0.927	0.974	0.949	0.968	95.3	0.047	12.891	1.615
RF (3, 20)	0.815	0.943	0.887	0.938	90.29	0.0971	26.666	1.471
DNN	**0.992**	**0.997**	**0.996**	**0.987**	**98.07**	**0.019**	**4.048**	**1.159**
CNN-1D	0.969	0.956	0.975	0.983	97.44	0.026	4.118	2.017
CNN (VGG16)	0.972	0.983	0.983	0.946	97.61	0.0804	4.581	2.326

AUC, area under curve; AUPRC, area under precision-recall curve; AP, average precision; F1, F1 score; A, accuracy; HD, hamming distance; FPR, false positive rate; FNR, false negative rate; SVM, support vector machine; RBF, radial basis function; d, degree; NB, naïve Bayes; kNN, k-nearest neighbor; RF, random forest; DNN, deep neural network; CNN-1D, convolution neural network-one dimension; CNN (VGG16), convolution neural network- visual geometry group16. Best performing model (highlighted in bold).

extract the most relevant features of their own. The performance metrics of DNN, CNN-1D, and CNN (VGG16) were very comparable. To our surprise, DNN was found to be slightly better in overall performance based on accuracy and other performance indicators compared to the CNN models. DNN appears to be a better option to handle the compounds encoded with physicochemical and fingerprint features for classifications and predictions. Based on the overall performance, we selected the DNN model for the development of "DeePred-BBB." DeePred-BBB can predict BBB permeability based on chemical SMILES notation. It uses PaDel to calculate the features from the SMILES notation and sends them as input to the DNN model. The output is either permeable or non-permeable.

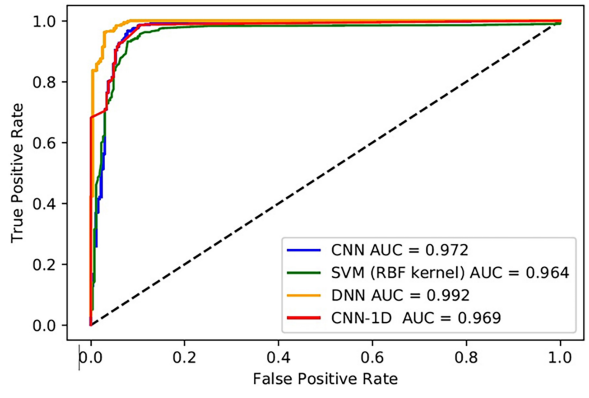

FIGURE 3 | ROCs of the best performing models (CNN, SVM, DNN, and CNN-1D) and their respective AUCs.

Compounds can penetrate the BBB using various different mechanisms, such as transmembrane diffusion, adsorptive endocytosis, saturable transporters, and extracellular pathways. Most drugs in clinical use till date are small, lipid soluble molecules that cross the BBB by transmembrane diffusion. The prediction models to determine the mechanism of BBB permeability require a mechanism-based set of compounds with their permeability class labels for each mechanism. However, the current study deals with the prediction of the BBB permeability of compounds (irrespective of how they penetrate the BBB) using their SMILES notations. The study holds limitations in identifying the mechanism by which compounds

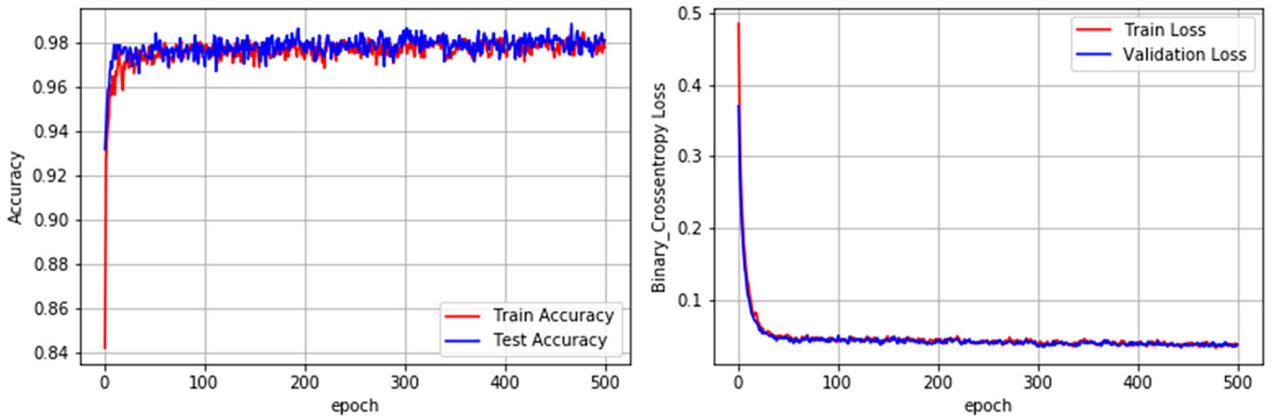

FIGURE 4 | Accuracy and loss plot of the DNN model for the prediction of BBB permeability.

TABLE 7 | Comparative analysis of DeePred-BBB with recently published BBB permeability prediction models.

Algorithm	Data set	Prediction performance	Study group
SVM (RBF)	1,562 compounds (BBB+ = 694, BBB- = 868)	>85% accuracy, sensitivity, and specificity	Jiang et al., 2016
Decision trees	581 compounds	Accuracy = 87.93%, Sensitivity = 86.67% Specificity = 89.29%	Castillo-Garit et al., 2017
SVM (RBF)	1,990 compounds (BBB permeable = 1,550, BBB non-permeable = 440)	Accuracy = 93.96%, Sensitivity = 94.3%, Specificity = 91.0%, MCC = 0.84	Yuan et al., 2018
SVM, kNN	2,358 compounds	Accuracy = 96.6%, Sensitivity = 92.5%, Specificity = 89.9%	Wang et al., 2018; Mi et al., 2020
DL	462 compounds (BBB permeable = 250, BBB non-permeable = 212)	Accuracy = 97%, AUC = 0.98, F1 = 0.92	Miao et al., 2019
RNN	2,342 compounds	Accuracy = 96.53%, Sensitivity = 94.91%, Specificity = 98.09%, MCC = 0.931, AUC = 0.986	Alsenan et al., 2020
Light Gradient Boosting Machine Algorithm	7,162 compounds (BBB permeable = 5,453 BBB non-permeable = 1,709)	Accuracy = 90%, sensitivity = 85%, specificity = 94%	Shaker et al., 2020
RF, Multilayer perceptron, Sequential minimal optimization	605 compounds (training) +1,566 compounds (validation)	Accuracy = 86.5%	Singh et al., 2020
SVM (RBF)	1,978 compounds (BBB permeable = 1,550, BBB non-permeable = 440)	Accuracy = 96.77%, AUC = 0.964, F1 = 0.975	Saxena et al., 2021
DNN	3,605 compounds (BBB permeable = 2,704 BBB non-permeable = 901)	Accuracy = 98.07%, AUC = 0.992, AP = 0.997, F1 = 0.987	Current study

AUC, area under curve; AUPRC, area under precision-recall curve; AP, average precision; BBB, blood brain barrier; DL, deep learning; F1, F1 score; kNN, k-nearest neighbor; MCC, Matthews correlation coefficient; RBF, radial basis function; RF, random forest; RNN, recurrent neural network; SVM, support vector machine.

are BBB permeable. DeePred-BBB does not take multiple SMILES notations for prediction. The user needs to input the SMILES notations of compounds one at a time for accurate prediction of BBB permeability. A comparison between DeePred-BBB and previously reported BBB permeability prediction models is given in **Table 7**.

CONCLUSION

Deep learning and machine learning algorithms were applied to a dataset of 3,605 compounds to develop a prediction model that could accurately predict the BBB permeability of compounds using their SMILES notations as input. The comparative analysis of the performance metrics of the developed models suggested that the overall performance of DNN-based BBB permeability prediction is better than that of the ML and CNN models. It was discovered that the notion of "deeper the network, better the accuracy" does not often hold true. An optimal depth of the network is required beyond which the performance of the network does not improve. A DNN model with three layers (depth) having 200, 100, and 2 nodes each was the most accurate. It was also observed that in the case of compounds, the physicochemical properties and fingerprint-based DL models yield slightly better performance than 2D-structure image-based models in BBB permeability prediction.

Based on this study, we propose the DeePred-BBB model for BBB permeability prediction of compounds using their SMILES notations as input. In DeePred-BBB, the best performing DNN model is integrated with the open-source PaDel tool to calculate

features. The calculated features are automatically fed to the DNN model as input, which predicts whether the compound will be BBB permeable or non-permeable. DeePred-BBB could assist in making quality decisions regarding which compound to carry forward in subsequent drug development stages and could potentially help in reducing the attrition rate of CNS-acting drug candidates failing due to BBB non-permeability. Inevitably, such drug candidates need further *in vivo* validation to arrive at efficacious and safe drugs at a faster rate and lower cost. DeePred-BBB could be accessed at https://github.com/12rajnish/DeePred-BBB.

DATA AVAILABILITY STATEMENT

The original contributions presented in the study are included in the article/**Supplementary Material**, further inquiries can be directed to the corresponding author/s.

AUTHOR CONTRIBUTIONS

RK and AS access to all of the data analyzed in this study, drafted the manuscript, and performed the statistical analysis. RK takes responsibility for the integrity and accuracy of the study data analysis and results. RK, AS, AA and GA involved in the study design, concept, analysis, and interpretation of data. AB, MK, AA, and GA involved in critical revision of the manuscript. All authors contributed to the article and approved the submitted version.

FUNDING

The Deanship of Scientific Research (DSR) at King Abdulaziz University, Jeddah, Saudi Arabia, has funded this project under Grant No. KEP-36-130-42. The authors therefore acknowledge with thanks DSR's technical and financial support.

SUPPLEMENTARY MATERIAL

The Supplementary Material for this article can be found online at: https://www.frontiersin.org/articles/10.3389/fnins.2022.858126/full#supplementary-material

REFERENCES

Abbott, N. J., Ronnback, L., and Hansson, E. (2006). Astrocyte-endothelial interactions at the blood-brain barrier. *Nat. Rev. Neurosci.* 7, 41–53. doi: 10.1038/nrn1824

Aldewachi, H., Al-Zidan, R. N., Conner, M. T., and Salman, M. M. (2021). High-throughput Screening Platforms in the discovery of novel drugs for neurodegenerative diseases. *Bioengineering* 8:30. doi: 10.3390/bioengineering8020030

Alsenan, S., Al-Turaiki, I., and Hafez, A. (2020). A Recurrent neural network model to predict blood-brain barrier permeability. *Comput. Biol. Chem.* 89:107377. doi: 10.1016/j.compbiolchem.2020.107377

Baldi, P., and Sadowski, P. (2014). The dropout learning algorithm. *Artif. Intell.* 210, 78–122. doi: 10.1016/j.artint.2014.02.004

Banks, W. A. (2009). Characteristics of compounds that cross the blood-brain barrier. *BMC Neurol.* 9:S3. doi: 10.1186/1471-2377-9-S1-S3

Benet, L. Z., Hosey, C. M., Ursu, O., and Oprea, T. I. (2016). BDDCS, the rule of 5 and drugability. *Adv. Drug Deliv. Rev.* 101, 89–98. doi: 10.1016/j.addr.2016.05.007

Ben-Hur, A., Ong, C. S., Sonnenburg, S., Schölkopf, B., and Rätsch, G. (2008). Support vector machines and kernels for computational biology. *PLoS Comput. Biol.* 4:e1000173. doi: 10.1371/journal.pcbi.1000173

Bento, A. P., Hersey, A., Félix, E., Landrum, G., Gaulton, A., Atkinson, F., et al. (2020). An open source chemical structure curation pipeline using rdkit. j. *Cheminform.* 12:51. doi: 10.1186/s13321-020-00456-1

Bickel, U. (2005). How to measure drug transport across the blood-brain barrier. *NeuroRx* 2, 15–26. doi: 10.1602/neurorx.2.1.15

Castillo-Garit, J. A., Casanola-Martin, G. M., Le-Thi-Thu, H., Pham-The, H., and Barigye, S. J. (2017). A Simple method to predict blood-brain barrier permeability of drug- like compounds using classification trees. *Med. Chem.* 13, 664–669. doi: 10.2174/1573406413666170209124302

Daneman, R. (2015). Prat A. the blood-brain barrier. *Cold Spring Harb. Perspect. Biol.* 7:a020412. doi: 10.1101/cshperspect.a020412

Dieterich, H. J., Reutershan, J., Felbinger, T. W., and Eltzschig, H. K. (2003). Penetration of intravenous hydroxyethyl starch into the cerebrospinal fluid in patients with impaired blood-brain barrier function. *Anesth. Analg.* 96, 1150–1154. doi: 10.1213/01.ane.0000050771.72895.66

Doniger, S., Hofmann, T., and Yeh, J. (2002). Predicting CNS permeability of drug molecules: comparison of neural network and support vector machine algorithms. *J. Comput. Biol.* 9, 849–864. doi: 10.1089/10665270260518317

D'souza, R. N., Huang, P. Y., and Yeh, F. C. (2020). Structural analysis and optimization of convolutional neural networks with a small sample size. *Sci. Rep.* 10:834. doi: 10.1038/s41598-020-57866-2

Esteva, A., Kuprel, B., Novoa, R. A., Ko, J., Swetter, S. M., Blau, H. M., et al. (2017). Dermatologist-level classification of skin cancer with deep neural networks. *Nature* 542, 115–118. doi: 10.1038/nature21056

Feigin, V. L., Vos, T., Nichols, E., Owolabi, M. O., Carroll, W. M., Dichgans, M., et al. (2020). The global burden of neurological disorders: translating evidence into policy. *Lancet Neurol.* 19, 255–265. doi: 10.1016/S1474-4422(19)30411-9

Gaudillo, J., Rodriguez, J. J. R., Nazareno, A., Baltazar, L. R., Vilela, J., Bulalacao, R., et al. (2019). Machine learning approach to single nucleotide polymorphism-based asthma prediction. *PLoS One* 14:e0225574. doi: 10.1371/journal.pone.0225574

Ghandi, M., Lee, D., Mohammad-Noori, M., and Beer, M. A. (2014). Enhanced regulatory sequence prediction using gapped k-mer features. *PLoS Comput. Biol.* 10:e1003711. doi: 10.1371/journal.pcbi.1003711

Giuliani, A. (2017). The application of principal component analysis to drug discovery and biomedical data. *Drug Discov. Today* 22, 1069–1076. doi: 10.1016/j.drudis.2017.01.005

Gupta, M., Lee, H. J., Barden, C. J., and Weaver, D. F. (2019). The blood-brain barrier (BBB) Score. *J. Med. Chem.* 62, 9824–9836. doi: 10.1021/acs.jmedchem.9b01220

Hendricks, B. K., Cohen-Gadol, A. A., and Miller, J. C. (2015). Novel delivery methods bypassing the blood-brain and blood-tumor barriers. *Neurosurg. Focus* 38:E10. doi: 10.3171/2015.1.FOCUS14767

Hu, Y., Zhao, T., Zhang, N., Zhang, Y., and Cheng, L. (2019). A Review of recent advances and research on drug target identification methods. *Curr. Drug Metab.* 20, 209–216. doi: 10.2174/1389200219666180925091851

Isensee, F., Jaeger, P. F., Kohl, S. A. A., Petersen, J., and Maier-Hein, K. H. (2021). NNU-NET: a self-configuring method for deep learning-based biomedical image segmentation. *Nat. Methods* 18, 203–211. doi: 10.1038/s41592-020-01008-z

Jiang, L., Chen, J., He, Y., Zhang, Y., and Li, G. (2016). A method to predict different mechanisms for blood-brain barrier permeability of CNS activity compounds

in Chinese herbs using support vector machine. *J. Bioinform. Comput. Biol.* 14:1650005. doi: 10.1142/S0219720016500050

Khan, A. I., Lu, Q., Du, D., Lin, Y., and Dutta, P. (2018). Quantification of kinetic rate constants for transcytosis of polymeric nanoparticle through blood-brain barrier. *Biochim. Biophys Acta Gen. Subj.* 1862, 2779–2787. doi: 10.1016/j.bbagen.2018.08.02016

Kumar, R., Sharma, A., Siddiqui, M. H., and Tiwari, R. K. (2018). Promises of machine learning approaches in prediction of absorption of compounds. *Mini. Rev. Med. Chem.* 18, 196–207. doi: 10.2174/1389557517666170315150116

Kumar, R., Sharma, A., Varadwaj, P., Ahmad, A., and Ashraf, G. M. (2011). Classification of oral bioavailability of drugs by machine learning approaches: a comparative study. *J. Comp. Interdisc. Sci.* 2, 179–196. doi: 10.6062/jcis.2011.02.03.0045

LeCun, Y., Bengio, Y., and Hinton, G. (2015). Deep learning. *Nature* 521, 436–444. doi: 10.1038/nature14539

Lovrić, M., Molero, J.M., Kern, R., Spark, P. Y., and Kit, R. D. (2019). Moving towards big data in cheminformatics. *Mol. Inform.* 38:e1800082. doi: 10.1002/minf.201800082

Main, B. S., Villapol, S., Sloley, S. S., Barton, D. J., Parsadanian, M., Agbaegbu, C., et al. (2018). Apolipoprotein E4 impairs spontaneous blood brain barrier repair following traumatic brain injury. *Mol. Neurodegener* 13:17. doi: 10.1186/s13024-018-0249-5

Malik, J., Kiranyaz, S., and Gabbouj, M. (2021). Self-organized operational neural networks for severe image restoration problems. *Neural. Netw.* 135, 201–211. doi: 10.1016/j.neunet.2020.12.014

Massey, S. C., Urcuyo, J. C., Marin, B. M., Sarkaria, J. N., and Swanson, K. R. (2020). Quantifying glioblastoma drug response dynamics incorporating treatment sensitivity and blood brain barrier penetrance from experimental data. *Front. Physiol.* 11:830. doi: 10.3389/fphys.2020.00830

Menken, M., Munsat, T. L., and Toole, J. F. (2000). The global burden of disease study: implications for neurology. *Arch. Neurol.* 57, 418–420. doi: 10.1001/archneur.57.3.418

Mi, Y., Mao, Y., Cheng, H., Ke, G., Liu, M., Fang, C., et al. (2020). Studies of blood-brain barrier permeability of gastrodigenin in vitro and in vivo. *Fitoterapia* 140, 104447. doi: 10.1016/j.fitote.2019.104447

Miao, R., Xia, L. Y., Chen, H. H., Huang, H. H., and Liang, Y. (2019). Improved classification of blood-brain-barrier drugs using deep learning. *Sci. Rep.* 9:8802. doi: 10.1038/s41598-019-44773-4

Pardridge, W. M. (2002). Why is the global CNS pharmaceutical market so under-penetrated? Drug discov. *Today* 7, 5–7. doi: 10.1016/s1359-6446(01)02082-7

Pardridge, W. M. (2005). The blood-brain barrier: bottleneck in brain drug development. *NeuroRx* 2, 3–14. doi: 10.1602/neurorx.2.1.3

Reese, T. S., and Karnovsky, M. J. (1967). Fine structural localization of a blood-brain barrier to exogenous peroxidase. *J. Cell. Biol.* 34, 207–217. doi: 10.1083/jcb.34.1.207

Rhea, E. M., and Banks, W. A. (2019). Role of the Blood-Brain Barrier in Central Nervous System Insulin Resistance. *Front. Neurosci.* 13:521. doi: 10.3389/fnins.2019.00521

Roy, D., Hinge, V. K., and Kovalenko, A. (2019). To Pass or Not To Pass: Predicting the Blood-Brain Barrier Permeability with the 3D-RISM-KH Molecular Solvation Theory. *ACS Omega.* 4, 16774–16780. doi: 10.1021/acsomega.9b01512

Salman, M. M., Al-Obaidi, Z., Kitchen, P., Loreto, A., Bill, R. M., and Wade-Martins, R. (2021). Advances in Applying Computer-Aided Drug Design for Neurodegenerative Diseases. *Int. J. Mol. Sci.* 22:4688. doi: 10.3390/ijms22094688

Salman, M. M., Kitchen, P., Yool, A. J., and Bill, R. M. (2022). Recent breakthroughs and future directions in drugging aquaporins. *Trends Pharmacol. Sci.* 43, 30–42. doi: 10.1016/j.tips.2021.10.009

Salman, M. M., Marsh, G., Kusters, I., Delincé, M., Di Caprio, G., Upadhyayula, S., et al. (2020). Design and validation of a human brain endothelial microvessel-on-a-chip open microfluidic model enabling advanced optical imaging. *Front. bioeng. biotechnol.* 8:573775. doi: 10.3389/fbioe.2020.573775

Salmanpour, M. R., Shamsaei, M., Saberi, A., Klyuzhin, I. S., Tang, J., Sossi, V., et al. (2020). Machine learning methods for optimal prediction of motor outcome in parkinson's disease. . *Phys. Med.* 69, 233–240. doi: 10.1016/j.ejmp.2019.12.022

Saunders, N. R., Dreifuss, J. J., Dziegielewska, K. M., Johansson, P. A., Habgood, M. D., Møllgård, K., et al. (2014). The rights and wrongs of blood-brain barrier permeability studies: a walk through 100 years of history. *Front. Neurosci.* 8:404. doi: 10.3389/fnins.2014.00404

Saxena, D., Sharma, A., Siddiqui, M. H., and Kumar, R. (2019). Blood brain barrier permeability prediction using machine learning techniques: an update. *Curr. Pharm. Biotechnol.* 20, 1163–1171. doi: 10.2174/1389201020666190821145346

Saxena, D., Sharma, A., Siddiqui, M. H., and Kumar, R. (2021). Development of machine Learning based blood-brain barrier permeability prediction models using physicochemical properties, maccs and substructure fingerprints. *Curr. Bioinform.* 16, 855–864. doi: 10.2174/1574893616666210203104013

Schidlowski, M., Boland, M., Rüber, T., and Stöcker, T. (2020). Blood-brain barrier permeability measurement by biexponentially modeling whole-brain arterial spin labeling data with multiple T2 -weightings. *NMR Biomed.* 33:e4374. doi: 10.1002/nbm.4374

Schlageter, K. E., Molnar, P., Lapin, G. D., and Groothuis, D. R. (1999). Microvessel organization and structure in experimental brain tumors: microvessel populations with distinctive structural and functional properties. *Microvasc. Res.* 58, 312–328. doi: 10.1006/mvre.1999.2188

Shaker, B., Yu, M. S., Song, J. S., Ahn, S., Ryu, J. Y., Oh, K. S., et al. (2020). LightBBB: Computational prediction model of blood-brain-barrier penetration based on LightGBM. *Bioinformatics* 37, 1135–1139. doi: 10.1093/bioinformatics/btaa918

Shan, W., Li, X., Yao, H., and Lin, K. (2021). Convolutional neural network-based virtual screening. *Curr. Med. Chem.* 28, 2033–2047. doi: 10.2174/0929867327666200526142958

Sharma, A., Kumar, R., Ranjta, S., and Varadwaj, P. K. (2021). SMILES to Smell: Decoding the structure-odor relationship of chemical compounds using the deep neural network approach. *J. Chem. Inf. Model* 61, 676–688. doi: 10.1021/acs.jcim.0c01288

Shen, J., Cheng, F., Xu, Y., Li, W., and Tang, Y. (2010). Estimation of ADME properties with substructure pattern recognition. *J. Chem. Inf. Model* 50, 1034–1041. doi: 10.1021/ci100104j

Shen, Y., Li, Y., Zheng, H. T., Tang, B., and Yang, M. (2019). Enhancing ontology-driven diagnostic reasoning with a symptom-dependency-aware naïve bayes classifier. *BMC Bioinform* 20:330. doi: 10.1186/s12859-019-2924-0

Singh, M., Divakaran, R., Konda, L. S. K., and Kristam, R. (2020). A classification model for blood brain barrier penetration. *J. Mol. Graph. Model.* 96:107516. doi: 10.1016/j.jmgm.2019.107516

Suenderhauf, C., Hammann, F., and Huwyler, J. (2012). Computational prediction of blood-brain barrier permeability using decision tree induction. *Molecules* 17, 10429–10445. doi: 10.3390/molecules170910429

Tietz, S., and Engelhardt, S. B. (2015). Brain barriers: crosstalk between complex tight junctions and adherens junctions. *J. Cell. Biol.* 209, 493–506. doi: 10.1083/jcb.201412147

van Tellingen, O., Yetkin-Arik, B., de Gooijer, M. C., Wesseling, P., Wurdinger, T., and de Vries, H. E. (2015). Overcoming the blood-brain tumor barrier for effective glioblastoma treatment. *Drug Resist. Updat.* 19, 1–12. doi: 10.1016/j.drup.2015.02.002

Veber, D. F., Johnson, S. R., Cheng, H. Y., Smith, B. R., Ward, K. W., and Kopple, K. D. (2002). Molecular properties that influence the oral bioavailability of drug candidates. *J.Med. Chem.* 45, 2615–2623. doi: 10.1021/jm020017n

Wang, D., Zeng, J., and Lin, S. B. (2021b). Random Sketching for neural networks with relu. *IEEE Trans Neural. Netw. Learn. Syst.* 32, 748–762. doi: 10.1109/TNNLS.2020.2979228

Wang, M. W. H., Goodman, J. M., and Allen, T. E. H. (2021a). Machine learning in predictive toxicology: recent applications and future directions for classification models. *Chem. Res. Toxicol.* 34, 217–239. doi: 10.1021/acs.chemrestox.0c00316

Wang, Z., Yang, H., Wu, Z., Wang, T., Li, W., Tang, Y., et al. (2018). In silico prediction of blood-brain barrier permeability of compounds by machine learning and resampling methods. *Chem. Med. Chem.* 13, 2189–2201. doi: 10.1002/cmdc.201800533

Wevers, N. R., Kasi, D. G., Gray, T., Wilschut, K. J., Smith, B., van Vught, R., et al. (2018). A perfused human blood-brain barrier on-a-chip for high-throughput assessment of barrier function and antibody transport. *Fluids barriers CNS* 15:23. doi: 10.1186/s12987-018-0108-3

Yang, L., Wu, H., Jin, X., Zheng, P., Hu, S., Xu, X., et al. (2020). Study of cardiovascular disease prediction model based on random forest in eastern China. *Sci. Rep.* 10:5245. doi: 10.1038/s41598-020-62133-5

Yao, D., Zhan, X., Zhan, X., Kwoh, C. K., Li, P., and Wang, J. (2020). A random forest based computational model for predicting novel lncrna-disease associations. *BMC Bioinform* 21:126. doi: 10.1186/s12859-020-3458-1

Yap, C. W. (2011). PADEL-descriptor: an open source software to calculate molecular descriptors and fingerprints. *J. Comput. Chem.* 32, 1466–1474. doi: 10.1002/jcc.21707

Yuan, Y., Zheng, F., and Zhan, C. G. (2018). Improved prediction of blood-brain barrier permeability through machine learning with combined use of molecular property-based descriptors and fingerprints. *AAPS J.* 20:54. doi: 10.1208/s12248-018-0215-8

Zhang, D., Xiao, J., Zhou, N., Zheng, M., Luo, X., Jiang, H., et al. (2015). A genetic algorithm based support vector machine model for blood-brain barrier penetration prediction. *Biomed. Res. Int.* 2015:292683. doi: 10.1155/2015/292683

Zhang, L., Zhu, H., Oprea, T. I., Golbraikh, A., and Tropsha, A. (2008). QSAR 21odelling of the blood-brain barrier permeability for diverse organic compounds. *Pharm. Res.* 25, 1902–1914. doi: 10.1007/s11095-008-9609-0

Zhao, Y. H., Abraham, M. H., Ibrahim, A., Fish, P. V., Cole, S., Lewis, M. L., et al. (2007). Predicting penetration across the blood-brain barrier from simple descriptors and fragmentation schemes. *J. Chem. Inf. Model.* 47, 170–175. doi: 10.1021/ci600312d

Conflict of Interest: The authors declare that the research was conducted in the absence of any commercial or financial relationships that could be construed as a potential conflict of interest.

Publisher's Note: All claims expressed in this article are solely those of the authors and do not necessarily represent those of their affiliated organizations, or those of the publisher, the editors and the reviewers. Any product that may be evaluated in this article, or claim that may be made by its manufacturer, is not guaranteed or endorsed by the publisher.

frontiers | Frontiers in Aging Neuroscience

ORIGINAL RESEARCH
published: 17 May 2022
doi: 10.3389/fnagi.2022.889983

Intermittent Theta Burst Stimulation Ameliorates Cognitive Deficit and Attenuates Neuroinflammation *via* PI3K/Akt/mTOR Signaling Pathway in Alzheimer's-Like Disease Model

*Andjela Stekic[1], Milica Zeljkovic[1], Marina Zaric Kontic[2], Katarina Mihajlovic[1], Marija Adzic[1], Ivana Stevanovic[3,4], Milica Ninkovic[3,4], Ivana Grkovic[2], Tihomir V. Ilic[3], Nadezda Nedeljkovic[1] and Milorad Dragic[1]**

[1] *Laboratory for Neurobiology, Department of General Physiology and Biophysics, Faculty of Biology, University of Belgrade, Belgrade, Serbia,* [2] *Department of Molecular Biology and Endocrinology, Vinča Institute of Nuclear Sciences, National Institute of the Republic of Serbia, University of Belgrade, Belgrade, Serbia,* [3] *Medical Faculty of Military Medical Academy, University of Defence, Belgrade, Serbia,* [4] *Institute for Medical Research, Military Medical Academy, Belgrade, Serbia*

OPEN ACCESS

Edited by:
Nibaldo C. Inestrosa, Pontificia Universidad Católica de Chile, Chile

Reviewed by:
Tsung-Hsun Hsieh, Chang Gung University, Taiwan
Muhammad Faheem, Riphah International University, Pakistan

***Correspondence:**
Milorad Dragic
milorad.dragic@bio.bg.ac.rs

Specialty section:
This article was submitted to Alzheimer's Disease and Related Dementias, a section of the journal Frontiers in Aging Neuroscience

Received: *04 March 2022*
Accepted: *13 April 2022*
Published: *17 May 2022*

Citation:
Stekic A, Zeljkovic M, Zaric Kontic M, Mihajlovic K, Adzic M, Stevanovic I, Ninkovic M, Grkovic I, Ilic TV, Nedeljkovic N and Dragic M (2022) Intermittent Theta Burst Stimulation Ameliorates Cognitive Deficit and Attenuates Neuroinflammation via PI3K/Akt/mTOR Signaling Pathway in Alzheimer's-Like Disease Model. Front. Aging Neurosci. 14:889983. doi: 10.3389/fnagi.2022.889983

Neurodegeneration implies progressive neuronal loss and neuroinflammation further contributing to pathology progression. It is a feature of many neurological disorders, most common being Alzheimer's disease (AD). Repetitive transcranial magnetic stimulation (rTMS) is a non-invasive stimulation which modulates excitability of stimulated brain areas through magnetic pulses. Numerous studies indicated beneficial effect of rTMS in several neurological diseases, including AD, however, exact mechanism are yet to be elucidated. We aimed to evaluate the effect of intermittent theta burst stimulation (iTBS), an rTMS paradigm, on behavioral, neurochemical and molecular level in trimethyltin (TMT)-induced Alzheimer's-like disease model. TMT acts as a neurotoxic agent targeting hippocampus causing cognitive impairment and neuroinflammation, replicating behavioral and molecular aspects of AD. Male Wistar rats were divided into four experimental groups–controls, rats subjected to a single dose of TMT (8 mg/kg), TMT rats subjected to iTBS two times per day for 15 days and TMT sham group. After 3 weeks, we examined exploratory behavior and memory, histopathological and changes on molecular level. TMT-treated rats exhibited severe and cognitive deficit. iTBS-treated animals showed improved cognition. iTBS reduced TMT-induced inflammation and increased anti-inflammatory molecules. We examined PI3K/Akt/mTOR signaling pathway which is involved in regulation of apoptosis, cell growth and learning and memory. We found significant downregulation of phosphorylated forms of Akt and mTOR in TMT-intoxicated animals, which were reverted following iTBS stimulation. Application of iTBS produces beneficial effects on cognition in of rats with TMT-induced hippocampal neurodegeneration and that effect could be mediated *via* PI3K/Akt/mTOR signaling pathway, which could candidate this protocol as a potential therapeutic approach in neurodegenerative diseases such as AD.

Keywords: intermittent theta burst stimulation, Alzheimer's disease, trimethyltin, neurodegeneration, cognitive deficit, neuroinflammation, Akt/Erk/mTOR signaling

INTRODUCTION

Neurodegeneration is a complex pathological event characterized by a progressive loss of nerve cells and deterioration of neural functions, underlying many neurological disorders, most common being Alzheimer's disease (AD) (Erkkinen et al., 2018). Neurodegenerative disorders are often accompanied by neuroinflammatory activation of astrocytes and microglia, which transit from a physiological, quiescent state to a reactive phenotype, releasing various inflammatory factors thus actively contributing to further neuronal degeneration (Colonna and Butovsky, 2017; Brambilla, 2019). There is no known effective drug/treatment for any neurodegeneration and for many diseases the clear cause has not been fully discovered (Dugger and Dickson, 2017), potentiating the need for experimental and therapeutic approaches. One experimental approach that mimics behavioral and histopathological aspects of hippocampal degeneration seen in AD is trimethyltin-induced neurodegeneration (Geloso et al., 2011). Trimethyltin (TMT) is a potent neurotoxicant specifically targeting human and animal limbic systems, particularly hippocampal formation (Balaban et al., 1988). Animals exposed to a single dose of TMT develop a series of symptoms, including seizures, hyperactivity, hyperexcitability, aggression, and severe cognitive deficit as a consequence of neuronal death of CA3/CA1 pyramidal neurons (Balaban et al., 1988; Trabucco et al., 2009; Corvino et al., 2015; Dragić et al., 2019; Park et al., 2019). Neuronal damage begins 2–4 days post-exposure, primarily in medial and proximal CA3 region and CA1 and can be detected at the end of the first week. It progressively worsens over the next 3 weeks (Dragić et al., 2021b) when almost entire medial and proximal CA3 and CA1 have degenerated. Neuronal loss is accompanied by early activation of astrocytes and microglia leading to sustained astrocyte-derived neuroinflammation (Dragić et al., 2021a,b) and microgliosis (Koczyk and Oderfeld-Nowak, 2000; Dragić et al., 2021b). TMT activates pathogenic pathways resulting in excitotoxicity, oxidative stress, mitochondrial dysfunction, intracellular calcium overload, and gene expression associated with apoptosis and necrosis (Little et al., 2012; Corvino et al., 2013; Lattanzi et al., 2013). Experimental data confirmed the significant roles of these mechanisms in the pathogenesis of human neurodegenerations, especially of Alzheimer's disease, making TMT-induced degeneration a useful and translatable model convenient for probing diverse neuroprotective strategies (Park et al., 2011, 2019; Corvino et al., 2013; Jung et al., 2013). Repetitive transcranial magnetic stimulation (rTMS) is a safe, non-invasive neuromodulatory technique based on stimulation of cortical structures *via* electromagnetic pulses which are administered in a predefined protocol-dependent pattern. Stimulation at a certain frequency may lead to prolonged and increased cortical excitability after the period of stimulation (Thomson et al., 2020), affecting both neuronal and glial physiology (Cullen and Young, 2016). rTMS has already found use in clinical treatment for neurological and psychiatric diseases showing a beneficial effect in patients with drug-resistant depression (De Risio et al., 2020), motor symptoms of Parkinson's disease (Nardone et al., 2019), and stroke (León Ruiz et al., 2018). It has been reported that rTMS, especially in combination with cognitive training, could be effective for improving mild-to-moderate cognitive decline in AD (Rabey and Dobronevsky, 2016). However, the full cellular and molecular mechanisms underlying these effects are largely unknown and the need for more comprehensive clinical trials still exists. Previous studies have shown that rTMS can attenuate reactive gliosis (Dragic et al., 2020), reduce neuronal apoptosis by regulating the expression of Bcl-2 and Bax protein family members (Uzair et al., 2022), restore pathological downregulation/induce activation of certain signaling pathways including mTOR (Yang et al., 2021), PI3K/Akt (Hou et al., 2021), modulate the biochemical environment against oxidative-nitrogen stress at a distance from the area of stimulation (Stevanovic et al., 2020) and affect cellular and molecular mechanisms underlying different forms of synaptic plasticity such as long-term potentiation and long-term depression (Fujiki et al., 2020). Observed neuroprotective effects have put rTMS on a list of promising therapeutic approaches in the treatment of neurodegenerative disorders such as AD, but very few studies on experimental models of neurodegenerations have been performed up to date. The aim of this study was to examine effects of intermittent theta burst stimulation (iTBS), an rTMS paradigm, on different aspects of TMT-induced hippocampal neurodegeneration regarding changes in behavior and cognition, pro- and anti-inflammatory markers, oxidative stress parameters, potentially important signaling pathways which could regulate abovementioned processes. iTBS is a form of rTMS protocol which has been shown to produce similar if not greater effects on brain activity than standard rTMS. Its major advantage is reduction in administration duration and consistency in application across literature (Chung et al., 2015). Results in this field of study are crucial for understanding the mechanisms underlying iTBS effects, finding a new potential cellular and molecular treatment targets of this paradigm of rTMS which could candidate it as a new therapeutic approach in treatment of neurodegenerative disorders.

MATERIALS AND METHODS

Animals

A total of 54 2-month-old male *Wistar* rats, bred in the animal facility at Centre of Veterinary Service, Ministry of Defence, Serbia, were used in this study. Animals were housed (3–4 per cage) under the following conditions: 12 h light/dark regime, constant ambient temperature 23 ± 2°C and humidity, food and water *ad libitum*. All experimental procedures were approved by the Ethical Committee of Vinča Institute of Nuclear Sciences (Application No. 323-07-02057/2017-05) in compliance with EU Directive 2010/63/EU.

Treatment and Experimental Groups

Animals were randomly assigned into four experimental groups: Control (n = 12), TMT (n = 15), TMT + iTBS (n = 12), TMT + iTBSsh (n = 15). On day 0, animals of the TMT, TMT + iTBS and TMT+ iTBSsh group received a single intraperitoneal injection of TMT (8 mg/kg, administered in the volume of 1 mL

0.9% saline). Control group received an adequate volume of 0.9% saline solution. The animals were monitored daily for 3 weeks, and sacrificed by decapitation (Harvard apparatus, Holliston, MA, United States).

Theta Burst Stimulation Protocol

Three days after intoxication intermittent protocol of theta-burst stimulation (iTBS) was applied. We chose this particular time point as it coincides with the onset of TMT-induced symptoms (Kaur and Nehru, 2013; Dragić et al., 2019). The stimulation was performed by MagStim Rapid^2 device and a 25-mm figure-of-eight coil (MagStim Company, Whitland, United Kingdom). Applied iTBS protocol consisted of 20 trains of ten bursts (3 pulses at a frequency of 50 Hz), repeated at 5 Hz (10 s intervals between trains, with the total duration of the procedure of 192 s). Stimulation intensity (stimulator output) was set at 33%, which was just below/around the motor threshold value (Dragic et al., 2020). The motor threshold value was defined as a stimulus intensity which induces a minimal visible motor response of treated animals, most usually manifested as repetitive movement of mandible muscles mimicking chewing. The iTBS protocol did not induce any visible behavioral responses or distress to animals. Animals were gently held during the stimulation process, while left to move freely during 10-s intervals between trains. The stimulation was applied by holding the center of the coil gently above the frontal cranial bone, in close contact with the scalp. TMT + iTBS sham group (TMT + iTBSsh) was subjected to noise artifact – cage with two animals was set next to the MagStim Rapid^2 device and the rats were allowed to listen to the sound of the stimulation followed by handling manipulation similar to TMT + iTBS group (**Figure 1**).

Assessment of Behavioral and Aggression Severity Score

Aggressive behavior was monitored in freely moving rats and aggression severity score was determined as reported and described previously (Kaur and Nehru, 2013; Dragić et al., 2019). Briefly, every day (at 8:00 am) animals in a clean cage with bedding were scored according to the 1–4 scale, during a 2-min interval. The scores were as follows: (1) without symptoms, (2) shies from hand when grasped, mild tremor (3) avoids hand by running, struggles when captured or both, systemic tremor (4) leaps, struggles and bites when captured. Several animals in the TMT and TMT + iTBSsh group developed epileptic seizures during scoring, mostly triggered by sound (**Supplementary Video 1**) and repetitive rotational movements when captured by the tail (**Supplementary Video 2**), while in TMT + iTBS group those events were observed only once during 3 weeks.

Open Filed and Object Recognition Test

The observation of spontaneous behavior was evaluated by the open field test (OFT). Animals were transferred to the behavior analysis room on the last day of the experiment and left for habituation to the environment for 2 h before the analysis. The behavioral observation room was completely separated from the cages to prevent acoustic and/or optic disturbance of the animals. All materials that have been in contact with the tested animals were cleaned with 70% ethanol thereafter to prevent any olfactory cues. The animals received one 5-min session by placement in the center of the empty black arena (100 × 100 × 50 cm, **Figure 2I**) to habituate them to the apparatus. The total movement was continuously recorded. Rat activity during this period was analyzed for spontaneous, exploratory activity in the open field test (OFT). Following the OFT and habituation with the apparatus, animals were placed in the center of the arena, at an equal distance from two identical rectangular objects (uniformly yellow-colored, diameter 5 cm, height 20 cm), left to freely explore for 5 min period, and returned to their home cages (sampling phase). After each animal, both arena and objects were thoroughly cleaned with 70% alcohol to ensure complete removal of any olfactory cures which could interfere with the test. After the 1 h-delay, animals were put in the center of the arena, at equal distance from objects, with one of the familiar objects being replaced by a new conical object (uniformly red-colored, diameter 15 cm, height 20 cm) and left to explore freely for another 5 min (testing phase). The time spent with each object was set as a baseline criterion, provided that sniffing, climbing and exploration of the object lasted more than 2 s which was considered as an active exploration (animals that did not meet these criteria were omitted from the analysis). Analysis of the sampling phase was also performed to examine whether animals showed preference toward any of two identical objects (**Supplementary Figure 1**). Recognition index (RI) represents the percentage of time spent at the novel object in respect to the total time spent at both objects (Antunes and Biala, 2012). Two researchers, blind of treatment groups, analyzed the behavioral results.

Brain Tissue Preparation for Histological Techniques

Brains were carefully removed from the skull (n = 3–4/treatment group), fixed in 4% paraformaldehyde (PFA), cryoprotected and dehydrated in sucrose (10, 20, and 30%) in 0.2 M phosphate buffer pH 7.4 as described previously (Dragić et al., 2019). 25-μm thick coronal slices were cut on the cryostat, air-dried at room temperature (RT), and kept at −20°C until use.

Histochemical and Immunohistochemical Staining

The coronal sections were stained with thionine and micrographs were taken on Leitz light microscope equipped with a Leica DFC320 camera. For each experimental group, several sections at different stereotaxic anterior-posterior (AP) coordinates were taken. Immunofluorescent staining procedures were performed as described previously (Dragić et al., 2021b). Briefly, sections were washed in PBS, blocked in 5% normal donkey serum, incubated with primary antibodies (**Table 1**), overnight at 4°C. The next day, sections were washed in PBS, incubated with appropriate secondary antibody for 2 h at RT, and mounted with Mowiol medium. Micrographs were taken by a confocal laser scanning microscope (LSM 510, Carl Zeiss, GmbH, Jena, Germany), with Ar multi-line (457, 478, 488, and 514 nm), HeNe

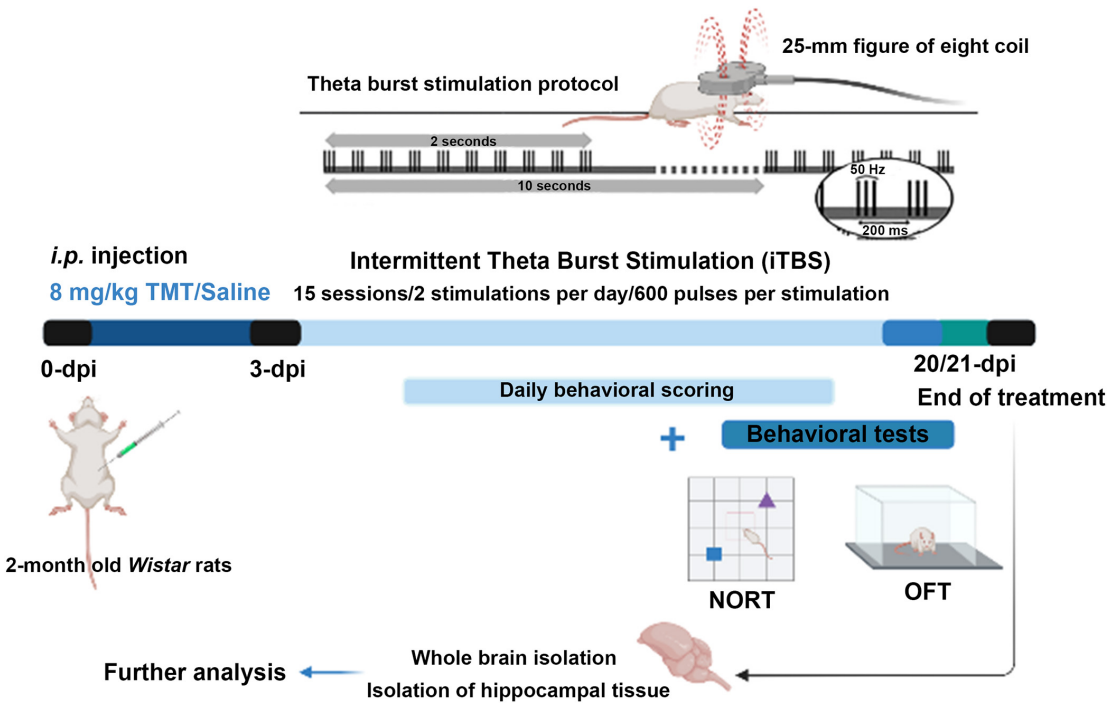

FIGURE 1 | Experimental design diagram. On day 0, animals of the TMT, TMT + iTBS, and TMT + iTBS sham group received a single intraperitoneal injection of TMT (8 mg/kg dissolved in 0.9% saline). The control group received an adequate volume of saline solution. The animals were daily scored for signs of unusual behavior for 3 weeks. Intermittent theta-burst stimulation (iTBS) was applied on 3-dpi using MagStim Rapid^2 device and a 25-mm figure-of-eight coil. Applied iTBS protocol consisted of 20 trains of ten bursts (3 pulses at a frequency of 50 Hz), repeated at 5 Hz (10 s intervals between trains, total duration of the procedure is 192 s), twice a day for 15 days in total. On the 20-/21-dpi, the behavior was evaluated by using the open field test (OFT) and novel object recognition (NORT) tests. After behavioral tests, animals were sacrificed. Whole brains and hippocampal tissue were isolated for immunohistological and immunoblot analyses.

(543 nm), HeNe (643 nm) laser at 40× and 63× (×2 digital zoom) DIC oil objectives, 40× and monochrome AxioCam ICm 1 camera (Carl Zeiss, GmbH, Jena, Germany).

Image Analysis and Semi-Quantification

Hippocampal regions of interest (CA1, mCA3, and hilus/DG region) were captured at the same region levels (ranging from AP −2.70 to −5.30 mm) and under the same conditions (40× magnification, 1024 × 1024, laser gain and exposure). The images (10–16/animal) were analyzed with ImageJ software (free download from https://imagej.net/Downloads). Correlation and interdependency between red-green channels were estimated by calculating Pearson's correlation coefficient (PCC). PCC values range from +1 (two fluorescent channels which are perfectly, linearly related) to −1 (two fluorescent channels which are perfectly, but inversely related). Values near 0 reflect distribution of two probes that are uncorrelated with one another (Dunn et al., 2011). The number of cells expressing the protein of interest was counted in the high-power field (HPF), based on an unequivocally visible cellular body with a few thicker branches and co-localization with analyzed protein. Immunoreactivity of the green signal was obtained by measuring fluorescence intensity in arbitrary units (AU). All manual quantification was performed by two independent researchers, blind of treatments. All three parameters were calculated from micrographs obtained at 40× magnification for each hippocampal region of every experimental group.

Tissue Isolation and Western Blot Analysis

Hippocampal membrane and cytosolic fractions were separated using Subcellular Protein Fractionation Kit for Tissues (Cat. No. 87790, Thermo Fisher Scientific, Waltham, MA, United States), according to the manufacturer's instructions. Briefly, homogenization of the frozen tissue samples was performed by a handheld homogenizer (Ultra-Turrax, Sigma-Aldrich, St. Louis, MO, United States) in an ice-cold cytoplasmic extraction buffer containing protease and phosphatase inhibitors. Supplied tissue strainers were used to filter tissue homogenate and obtained filtrates were centrifugated at 500 × *g* (Sorvall SL-50 T Super T21, Thermo Fisher Scientific, Waltham, MA, United States) for 5 min at 4°C. Cytoplasmic fraction remaining in supernatant was collected and the pellet was resuspended in an ice-cold membrane extraction buffer containing protease and phosphatase inhibitors, incubated on ice for 10 min and centrifuged at 3,000 × *g* for 5 min at 4°C to obtain membrane fraction remaining in supernatant after centrifugation. Protein concentration was determined using Pierce^{TM} BCA Protein Assay Kit (Cat. No. 23225, Thermo Fisher Scientific, Waltham, MA, United States) according to the manufacturer's instructions.

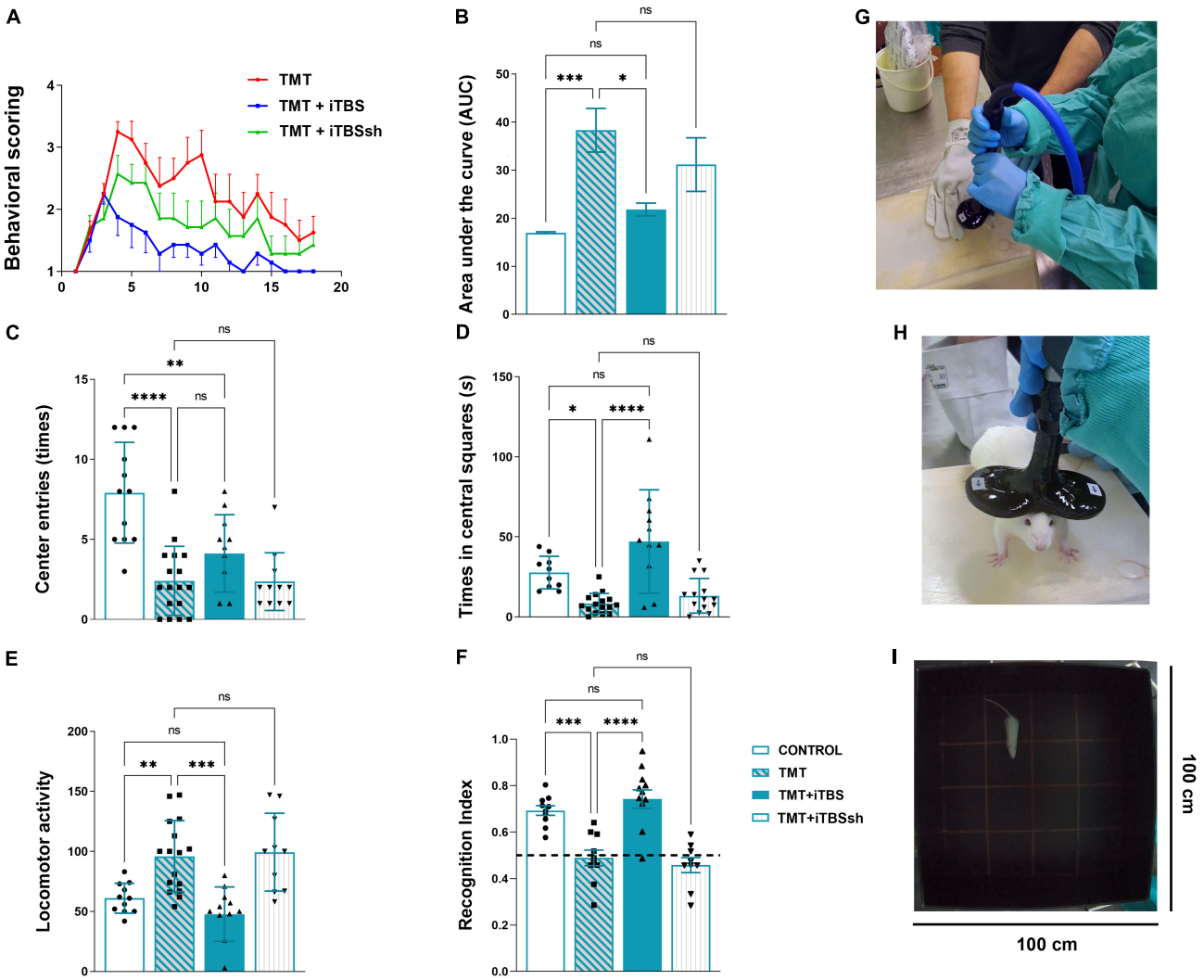

FIGURE 2 | Effect of iTBS treatment on behavior of TMT rats. **(A)** Graphic and **(B)** quantitative analysis of behavioral animal scoring. Bars represent the mean AUC ± SD. **(C,D)** Anxiety-like behavior and **(E)** motor activity, assessed in the open-field test. Bars represent **(C)** a mean number of entries, **(D)** a mean duration spent in central squares (s), and **(E)** a mean total movements, ±SD. **(F)** Recognition index determined by the novel object recognition test. Bars represent mean recognition index ± SD. Interrupted line represents 50% of recognition index, where animals showed no discrimination between novel and familiar object. Results of *post hoc* Tukey's test and significance shown inside graphs, $*p < 0.05$, $**p < 0.01$, $***p < 0.001$, $****p < 0.0001$, ns, no significance. **(G,H)** iTBS coil placement. **(I)** The behavioral testing arena. Dots in the graphs represent values of individual animals.

Western blot analyses (20–30 μg of sample proteins, n = 4–5 animals/group) were performed as previously described (Mitrović et al., 2017; Adzic and Nedeljkovic, 2018). Briefly, all samples were diluted in 6 × Laemmli buffer [4% sodium dodecyl sulfate (SDS), 0.02% bromophenol blue, 20% glycerol, 125 mmol/L Tris–HCl] and electrophoresis was run on a 10% SDS-polyacrylamide gel and proteins were transferred to PVDF membrane (0.45 mm, Millipore, Germany) using Trans-Blot® Turbo™ Transfer System (Cat. No. 1704150, Bio-Rad, Hercules, CA, United States) according to the manufacturer's instructions. Membranes were blocked in 5% non-fat dry milk (Cat. No. 42590.01, SERVA, Germany) in Tris-buffered saline containing 0.1% Tween-20 (TBST), incubated overnight at 4° C with appropriate primary antibody in TBST (**Table 1**), rinsed in TBST and incubated with adequate horseradish-peroxidase (HRP)-conjugated secondary antibody in TBST (**Table 1**) using SmartBolt apparatus. Chemiluminescent signals were detected using ECL solution (Bio-Rad, Hercules, CA, United States) by ChemiDoc-It Imager (Ultra-Violet Products Ltd., Cambridge, United Kingdom). Primary and secondary antibodies were removed by stripping protocol using mild-stripping buffer (pH 2.2) containing 0.2 mmol/L glycine, 0.1% SDS and 1% Tween-20[1] one time, so additional target protein could be blotted on the same membrane. Optical density (OD) of the specific band and actin band in each lane were quantified using the ImageJ

[1]https://www.abcam.com/protocols/western-blot-membrane-stripping-for-restaining-protocol

TABLE 1 | List of used primary and secondary antibodies.

Antibody	Source and type	Used dilution	Manufacturer
GFAP	Rabbit, polyclonal	1:500^{IF}	DAKO, Agilent Z0334, RRID:AB_10013382
C3	Goat, polyclonal	1:300^{IF}, 1:1000^{WB}	Thermo Fisher Scientific PA1-29715 RRID: AB_AB_2066730
IL-10	Goat, polyclonal	1:100^{IF}	Santa Cruz Biotechnology, sc-1783, RRID: AB_2125115
IL-1β/IL-1F2	Goat, polyclonal	1:100^{IF}	R&D Systems, AF-501-NA, RRID: AB_354508
Bax	Rabbit, polyclonal	1:1000^{WB}	Cell Signaling, #2772, RRID: AB_10695870
Bcl-2	Rabbit, polyclonal	1:1000^{WB}	Cell Signaling #2876, RRID: AB_2064177
PI3K (p85)	Rabbit, monoclonal	1:500^{WB}	Abcam, ab40755, RRID: AB_777258
p-Akt	Rabbit, polyclonal	1:1000^{WB}	Cell Signaling, #9271S, RRID: AB_329825
t-Akt	Rabbit, polyclonal	1:1000^{WB}	Cell Signaling, #9272S, RRID: AB_329827
p-mTOR	Rabbit, polyclonal	1:1000^{WB}	Cell Signaling, #5536, RRID: AB_10691552
t-mTOR	Rabbit, polyclonal	1:1000^{WB}	Cell Signaling, # 2983, RRID: AB_2105622
p-ERK 1/2	Rabbit, polyclonal	1:1000^{WB}	Cell Signaling, #9101, RRID: AB_331646
t-ERK 1/2	Rabbit, polyclonal	1:1000^{WB}	Cell Signaling, #9102, RRID: AB_330744
β-actin	Mouse, HRP-conjugated	1:5000^{WB}	Abcam, ab49900, RRID: AB_867494
Anti-goat IgG Alexa Fluor 488	Donkey, polyclonal	1:400^{IF}	Invitrogen A-11055, RRID: AB_142672
Anti-rabbit IgG Alexa Fluor 555	Donkey, polyclonal	1:400^{IF}	Invitrogen A-21428, RRID:AB_141784
Goat anti-rabbit IgG, HRP-conjugated	Goat, polyclonal	1:30000^{WB}	Abcam, ab6721, RRID: AB_955447

WB, western blot; IF, immunofluorescence.

program[2], and the ratio in each lane was expressed relative to the control, arbitrarily defined as 100% ± SEM, from n = 2–4 technical replicates.

Measurement of the Oxidative Stress

Oxidative stress was assessed by measuring several parameters in appropriate hippocampal fraction (n = 4–5 animals/group) as described in detail elsewhere (Stevanovic et al., 2020). Briefly, total superoxide dismutase activity (tSOD) was assessed by spectrophotometric determination of spontaneous epinephrine autooxidation decrease rate at 480 nm and expressed as units per milligram of total protein (U/mg). One unit is defined as an amount of enzyme required for 50% inhibition of epinephrine autooxidation (Sun and Zigman, 1978). Levels of free $O_2^{\bullet-}$ were determined by reaction based on the $O_2^{\bullet-}$ mediated reduction of nitroblue tetrazolium to monoformazan (μmol/mg protein), which is measured spectrophotometrically at 550 nm (Kono et al., 1997). Malondialdehyde (MDA) was quantified spectrophotometrically as a measurement of colored pigment formed after incubation with TBA reagent (water solution of 15% trichloroacetic acid and 0.375% TBA) at 95°C at pH 3.5. Absorbance was measured at 532 nm and results were expressed as μmol/mg protein (Girotti et al., 1991). Levels of NO were evaluated from the deproteinized samples and determined by directly measuring nitrite concentrations spectrophotometrically at 492 nm, and nitrates were converted into nitrites by cadmium reduction (Navarro-Gonzálvez et al., 1998). Total sulfhydryl groups were spectrophotometrically measured at 412 nm by Ellman's method (Ellman, 1959). Total glutathione levels (GSH + ½ GSSG, in GSH equivalents) were determined by a DNTB-GSSG reductase recycling assay. The rate of 5-thio-2-nitrobenzoic acid (TNBA) formation, which is proportional to the total glutathione concentration, was measured spectrophotometrically at 412 nm and the results were expressed as μmol/mg of proteins.

Statistical Analysis

All data were analyzed for normality and appropriate parametric statistical tests were used. One-way analysis of variance (One-way ANOVA) was performed for statistical comparison between groups, followed by Tukey's *post hoc* test for multiple comparisons between experimental groups. All values are presented as mean ± SD or SEM as indicated in Figure legends. The values of $p < 0.05$ were considered statistically significant. For all analysis and graphical presentation GraphPad Prism 9.0 (San Diego, CA, United States) software package was used. Results of *post hoc* tests are described in detail in figure legends.

RESULTS

Intermittent Theta Burst Stimulation Significantly Reduced Trimethyltin-Induced Hyperactivity, Aggressive Behavior, and Tremor

Animals were scored daily for signs of the "TMT syndrome," which include hyperactivity, aggressive behavior, and tremor (**Figure 2A**). TMT-treated animals exhibited first symptoms on the 3-day post-intoxication (dpi), which progressed over 3 weeks with several peaks and partial recoveries (**Figure 2A**, red line). We have chosen 3-dpi to start iTBS stimulation as it was the time point of the onset of the first symptoms. Control animals did not exhibit any unusual behavior and kept a score of 1 for 3 weeks (X-axis value). Animals treated with iTBS (**Figure 2A**, blue line) showed progressive and uninterrupted improvement over the 3 weeks, did not show any aggressive behavior from

[2]https://imagej.nih.gov/ij/

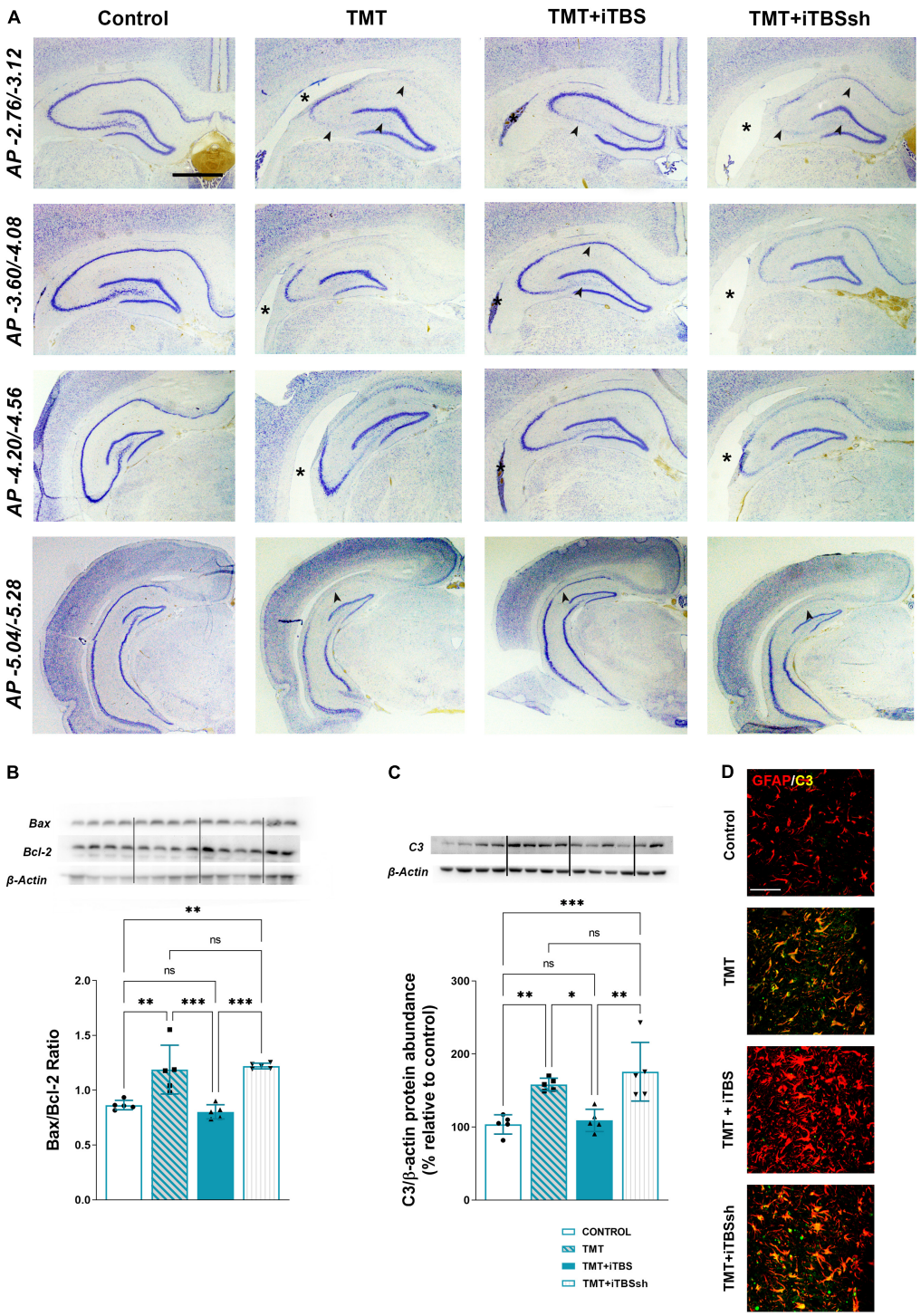

FIGURE 3 | Effect of iTBS treatment on TMT-induced neuronal death and inflammation. **(A)** Thionine-stained coronal sections at different stereotaxic anterior-posterior (*AP*) coordinates. Arrowhead indicates thinned neuronal cell layers, while asterisk marks the position of the lateral ventricle for a comparison. Scale bar = 500 μm, applies to all micrographs. Representative membrane and semi-quantitative Western blot analysis showing **(B)** relative Bax/Bcl-2 and **(C)** C3 protein abundance, expressed relative to control, arbitrary defined as 100%. Bars in **(B)** represent the ratio between Bax and Bcl-2 relative abundance, determined as mean OD ratio of the specific protein band to actin band for each group ± SEM (from $n = 5$ individual animals, in 2–4 technical replicates). Bars in **(C)** represent the mean OD of the C3 band and actin band in each group normalized to control (arbitrarily defined as 100%) ± SEM (from $n = 5$ individual animals, in 2–4 technical replicates). Results of *post hoc* Tukey's test and significance shown inside graphs: $^{*}p < 0.05$, $^{**}p < 0.01$, $^{***}p < 0.001$, $^{****}p < 0.0001$, ns, no significance. Dots in the graphs represent values of individual animals. **(D)** Double immunofluorescent staining of coronal hippocampal sections captured in the same region levels directed to GFAP (*red*) and C3 (*green*). Scale bar = 50 μm.

6-dpi, and expressed only mild tremor, which subsided in the final days of the experiment. TMT + iTBSsh group (**Figure 2A**, *green line*) presented symptoms similar to TMT group. The total score for each experimental group was obtained by averaging individual scores determined as the area under the curve (AUC) and the means were analyzed by One-way ANOVA ($F_{3,51} = 7.95$, $p < 0.0001$, **Figure 2B**). Significant difference was obtained for the comparison between TMT and TMT + iTBS ($p < 0.05$) TMT ($p < 0.001$), and iTBSsh and control ($p < 0.01$), whereas no differences were found detected between intact control group and TMT + iTBS.

Intermittent Theta Burst Stimulation Reduces Trimethyltin-Induced Hyperactivity and Anxiety-Related Behavior

The open-field test is used to evaluate the effects of iTBS on TMT-induced hyperactivity and anxiety-related behavior (**Figure 2**). Significant changes were observed regarding anxiety-related behavior, which is expressed as the number of entries (**Figure 2C**, $F_{3,46} = 14.66$, $p < 0.0001$) and the time spent in the central quadrants of the arena (**Figure 2D**, $F_{3,46} = 12.37$, $p < 0.0001$). iTBS-treated animals showed increased number in both entries and time spent in central quadrants (**Figures 2C,D**).

Changes in general locomotor activity was also observed following TMT intoxication and iTBS treatment (**Figure 2E**, $F_{3,46} = 10.48$, $p < 0.0001$). Following TMT intoxication, rats exhibited increased locomotion, while iTBS treatment reverted it to control levels (**Figure 2E**).

Intermittent Theta Burst Stimulation Improves Trimethyltin-Induced Cognitive Impairment

The effect of iTBS treatment on TMT-induced cognitive impairment was assessed by the object recognition test (**Figure 2F**). No difference was observed in exploration time and the number of approaches to the objects during the sampling phase (**Supplementary Figure 1**). A significant difference was observed during the test phase ($F_{3,42} = 19.35$, $p < 0.0001$), which suggested a notable improvement of impaired cognitive abilities in iTBS-treated animals after TMT intoxication (**Figure 2F**).

Intermittent Theta Burst Stimulation Reduced Trimethyltin-Induced Neuronal Death and Inflammation

The overall changes in the hippocampal cytoarchitecture were assessed with the use of Nissl histological staining (**Figure 3A**). Animals that received iTBS treatment (**Figure 3A**, third column)

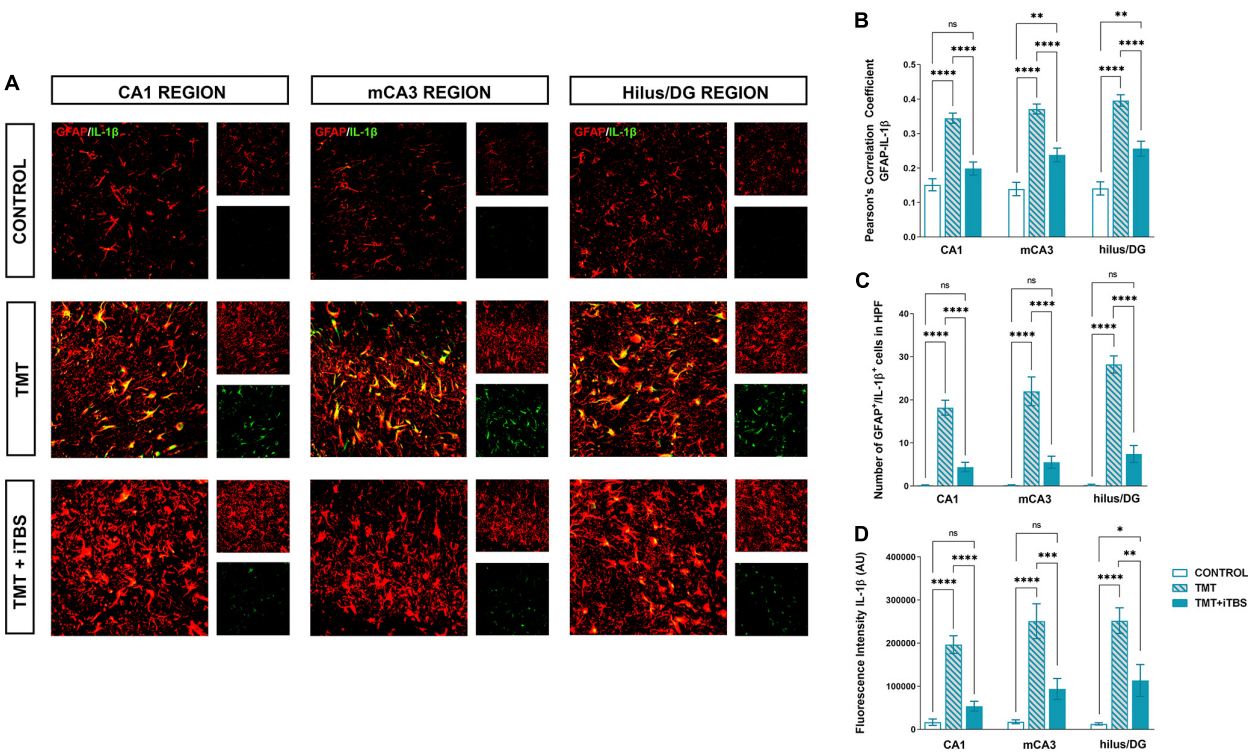

FIGURE 4 | Effect of iTBS treatment on TMT-induced astrocytic inflammation. **(A)** Double immunofluorescence staining directed to GFAP (*red*) and IL-1β (*green*) of coronal hippocampal sections captured in the same region levels. Scale bar = 50 μm. Integration of immunofluorescence intensity and quantitative analyses showing **(B)** Pearson's correlation coefficient (PCC), **(C)** number of $GFAP^+/IL\text{-}1\beta^+$ cells in high power field (HPF), and **(D)** fluorescence intensity of IL-1β in arbitrary units (AU). Bars represent the mean value ± SEM of specific parameters calculated from acquired images (10–16/animal). Results of *post hoc* Tukey's test and significance shown inside graphs: $^*p < 0.05$, $^{**}p < 0.01$, $^{***}p < 0.001$, $^{****}p < 0.0001$, ns, no significance.

showed significantly less neuronal death in respect to TMT and iTBSsh, which exhibited conspicuous neurodegeneration in CA1, medial CA3 (mCA3), and the hilar region of the dentate gyrus (hilus/DG), and extended lateral ventricles. The changes observed at the histological level were confirmed by determining the Bax/Bcl-2 abundance in the cytosolic fractions ($F_{3,16} = 16.62$ $p < 0.0001$), which pointed toward increased Bax/Bcl-2 levels in TMT and TMT + iTBS sham groups, and near the control level in TMT + iTBS group (**Figure 3B**). iTBS treatment also reverted to near control level protein expression of complement 3 (C3), which was markedly increased in TMT and iTBSsh (**Figure 3C**, $F_{3,16} = 12.29$ $p < 0.0001$). C3 was confined to reactive astrocytes, as previously shown (**Figure 3D**; Dragić et al., 2021b). Since no differences were observed between TMT and TMT + iTBSsh group at behavioral, histopathological and molecular, it has been excluded from further figures.

Intermittent Theta Burst Stimulation Alters Trimethyltin-Induced Astrocytic Inflammation

Trimethyltin induces pronounced astrocytic activation and release of IL-1β or IL-10 (Dragić et al., 2021b). Treatment with iTBS did not alter the morphology of $GFAP^+$ cells but reduced the TMT-induced increase in IL-1β-immunoreactivity (*ir*) (**Figure 4A**). To evaluate regional changes of IL-1β expression we calculated PCC (**Figure 4B**), the number of $GFAP^+$/IL-$1\beta^+$ astrocytes (**Figure 4C**), and the total intensity of the IL-1β fluorescence signal (**Figure 4D**). We found that TMT significantly increased all examined parameters in all three regions when compared to control, while iTBS treatment reduced the inflammation to levels similar to control, although astrocytes remained reactive phenotype (**Table 2**). The increase in all examined parameters measuring co-localization of GFAP and IL-10 was observed following iTBS treatment, especially in the hilus/DG (**Figure 5** and **Table 3**).

Intermittent Theta Burst Stimulation Reduces Trimethyltin-Induced Oxidative Stress

Trimethyltin intoxication is accompanied by changes in oxidative status which is the driving factor of neurodegeneration and neuroinflammation (Kang et al., 2016). iTBS reverted TMT-induced reduction in tSOD activity (**Figure 6A**, $F_{2,17} = 18.92$, $p < 0.0001$) and reverted MnSOD activity (**Figure 6B**, $F_{2,16} = 21.00$, $p < 0.0001$) to near control levels. The treatment had no impact on TMT-induced decrease in CuZnSOD activity (**Figure 6C**, $F_{2,16} = 14.42$, $p < 0.001$). The levels of pro-oxidative parameters O^{2-}, MDA and NO_2^- were examined (**Figures 6D–F**). The enhanced levels of free O^{2-} (**Figure 6D**, $F_{2,16} = 39.52$, $p < 0.0001$), MDA (**Figure 6E**, $F_{2,16} = 39.52$, $p < 0.0001$) and NO_2^- (**Figure 6F**, $F_{2,18} = 36.62$, $p < 0.0001$) following TMT intoxication were reverted by iTBS to near control level. Finally, we examined two-non enzymatic antioxidant parameters – levels of SH^- and total GSH content (**Figures 6G,H**). In TMT-treated animals, levels of SH^- did not change, but iTBS significantly increased SH level (**Figure 6G**, $F_{2,17} = 37.86$, $p < 0.0001$). iTBS also overcompensated the TMT-induced reduction of total GSH for about 50% in respect to control (**Figure 6H**, $F_{2,17} = 21.39$, $p < 0.001$).

Intermittent Theta Burst Stimulation Rescues Trimethyltin-Attenuated PI3K/Akt/mTOR and ERK1/2 Signaling

PI3K/Akt/mTOR and ERK1/2 signaling have a critical role in neurodegenerative/neuroinflammatory (Lu and Malemud, 2019). Therefore we investigated changes in protein expression of PI3K/Akt/mTOR and ERK1/2 in cytosolic fraction following TMT-induced neurodegeneration and iTBS treatment (**Figure 7**). The expression of the regulatory subunit of PI3K (p85) was slightly decreased in TMT animals, whereas iTBS significantly increased the expression (**Figure 7A**, $F_{2,12} = 17.94$, $p < 0.001$). The downstream signaling protein kinase B/Akt showed a marked decrease in p-Akt/t-Akt following TMT, while iTBS treatment reverted it to the levels similar to control (**Figure 7B**, $F_{2,12} = 12.81$, $p < 0.01$). A significant reduction in phosphorylation levels of mTOR was found after TMT-induced neurodegeneration, which was restored following iTBS treatment (**Figure 7C**, $F_{2,12} = 9.35$, $p < 0.01$). iTBS significantly increased levels of phosphorylated ERK 1/2 form, while TMT remained without the effect (**Figure 7D**, $F_{2,12} = 6.52$, $p < 0.05$).

DISCUSSION

In the present study, we evaluated the potential therapeutic use of iTBS protocol on a behavioral, histopathological, and molecular level in the Alzheimer's-like disease model induced by TMT intoxication. Acute TMT intoxication results in a well-described model of the neurodegeneration in the hippocampus and associated limbic and cortical regions (Balaban et al., 1988; Dragić et al., 2019, 2021b), and consequent cognitive impairment. That makes a model a perfect tool for studying diverse neuroprotective strategies (Koda et al., 2008; Urano and Tohda, 2010; Park et al., 2011; Kang et al., 2016), particularly in AD as the model replicates some key behavioral and molecular features of this disease (Nilsberth et al., 2002; Andjus et al., 2009; Geloso et al., 2011; Sadoughi, 2019). Given that behavioral changes occur in the initial stages after TMT exposure, they might be used to follow the efficacy of novel therapeutic strategies (Moser, 2011). We used a battery of neurobehavioral tests to screen behavior in non-stressful (activity monitoring in a cage) and a stressful environment (open field and novel object recognition test). Behavioral changes in a non-stressful environment manifested as tremor, hyperactivity and aggression became apparent at 3-dpi and peaked at 4-dpi, which is in agreement with previous data (Kaur and Nehru, 2013; Dragić et al., 2019). Thereafter, behavioral scores in TMT and iTBSsh animals spontaneously declined toward partial recovery, with two lower peaks at 10-dpi and 14-dpi, indicating ongoing neuronal degeneration (Geloso et al., 2011). The next set of neurobehavioral tests assessed animal behavior in stressful environments using OF and NORT after 21-dpi, when hippocampal neurodegeneration was shown to be at peak (Geloso et al., 2011; Dragić et al., 2021b). Animals exhibited

TABLE 2 | Results of one-way ANOVA analysis.

	Region	ANOVA results	Tukey's *post hoc* test		
			Control vs. TMT	TMT vs. TMT + iTBS	Control vs. TMT + iTBS
PCC analysis	CA1	$F_{(2,47)} = 36.23, p < 0.0001$	$p < 0.0001$	$p < 0.0001$	ns
	mCA3	$F_{(2,48)} = 40.76, p < 0.0001$	$p < 0.0001$	$p < 0.0001$	$p < 0.01$
	Hilus/DG	$F_{(2,47)} = 43.18, p < 0.0001$	$p < 0.0001$	$p < 0.0001$	$p < 0.01$
Number of $GFAP^+/IL\text{-}1\beta^+$ cells in HPF	CA1	$F_{(2,46)} = 36.32, p < 0.0001$	$p < 0.0001$	$p < 0.0001$	ns
	mCA3	$F_{(2,48)} = 36.04, p < 0.0001$	$p < 0.0001$	$p < 0.0001$	ns
	Hilus/DG	$F_{(2,45)} = 97.70, p < 0.0001$	$p < 0.0001$	$p < 0.0001$	ns
Fluorescence intensity IL-1β	CA1	$F_{(2,46)} = 41.43, p < 0.0001$	$p < 0.0001$	$p < 0.0001$	ns
	mCA3	$F_{(2,47)} = 16.22, p < 0.0001$	$p < 0.0001$	$p < 0.001$	ns
	Hilus/DG	$F_{(2,46)} = 17.10, p < 0.0001$	$p < 0.0001$	$p < 0.01$	$p < 0.05$

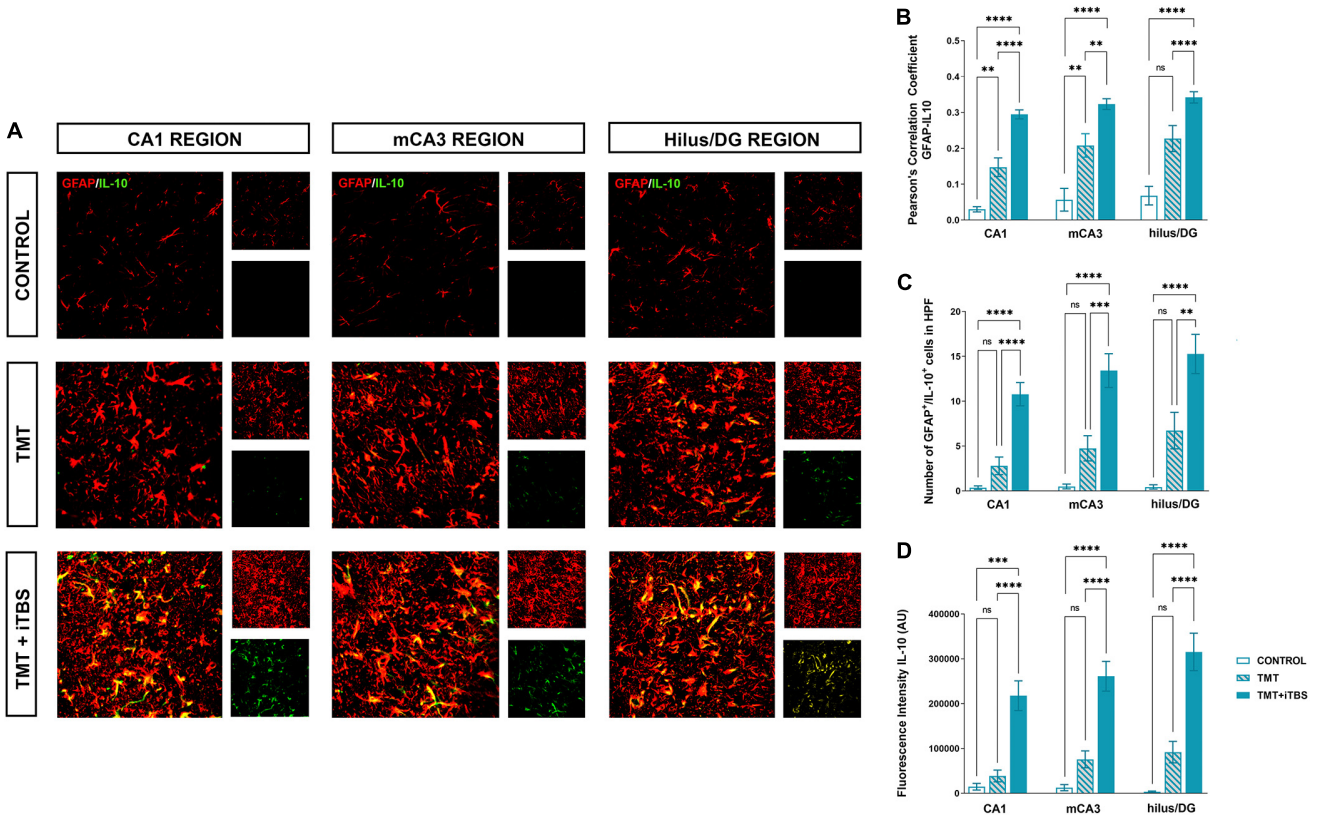

FIGURE 5 | Effect of iTBS treatment on the inflammatory status of reactive astrocytes. **(A)** Immunofluorescence staining directed to GFAP (*red*) and IL-10 (*green*) of coronal hippocampal sections captured in the same region levels and. Scale bar = 50 μm. Integration of immunofluorescence intensity and quantitative analyses showing **(B)** Pearson's correlation coefficient (PCC), **(C)** number of $GFAP^+/IL\text{-}10^+$ cells in high power field (HPF), and **(D)** fluorescence intensity of IL-10 in arbitrary units (AU). Bars represent the mean values ± SEM of specific parameters calculated from all acquired images (10–16/animal). Results of *post hoc* Tukey's test and significance shown inside graphs: $^*p < 0.05$, $^{**}p < 0.01$, $^{***}p < 0.001$, $^{****}p < 0.0001$, ns, no significance.

anxiety-like behavior and hyperlocomotion, which are typical for TMT-induced hippocampal neurodegeneration (Geloso et al., 2011; Kang et al., 2016). Since TMT-induced hippocampal degeneration results in severe cognitive deficits (Park et al., 2011, 2019; Jung et al., 2013; Kang et al., 2016), we tested short-term memory by using NORT. As anticipated, animals exposed to TMT showed a severe reduction in recognition index demonstrating impairment in processes involved in memory retention (Botton et al., 2010; Antunes and Biala, 2012). The neurotoxin primarily affects CA3 pyramidal neurons and partially CA1 pyramidal neurons, thus severing the anatomical connections between the entorhinal cortex – dentate gyrus and hippocampus proper (Balaban et al., 1988; Geloso et al., 2004, 2011). Disruption of these excitatory/inhibitory connections

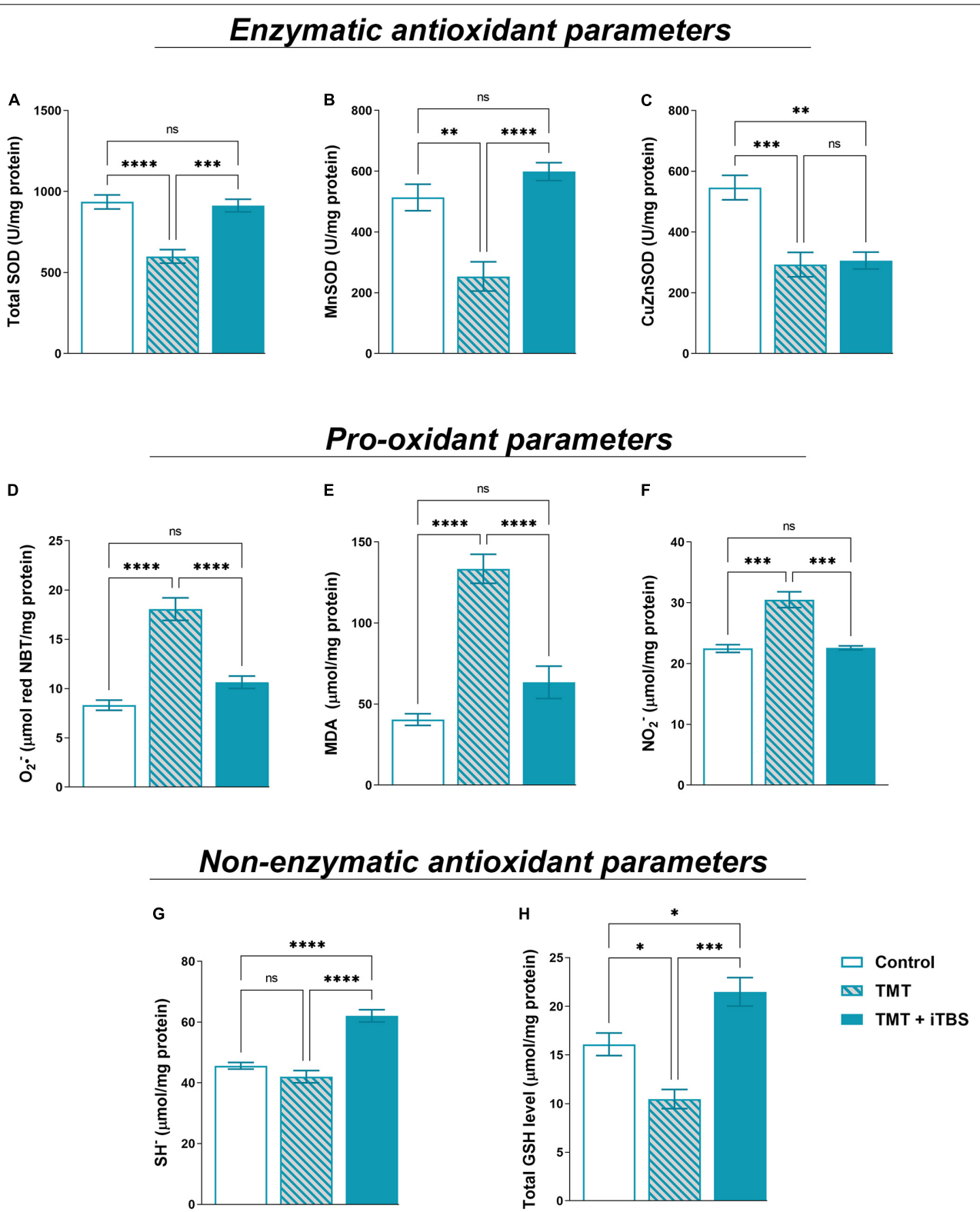

FIGURE 6 | Effect of iTBS treatment on TMT-induced oxidative stress. Spectrophotometric analysis of antioxidant parameters: **(A)** total SOD, **(B)** MnSOD, **(C)** CuZnSOD, and pro-oxidant parameters: **(D)** $O_2^{\bullet -}$, **(E)** MDA (malondialdehyde), **(F)** NO_2^- and non-enzymatic antioxidant parameters- **(G)** SH^- and **(H)** total GSH level, measured in hippocampal protein homogenates (n = 4–5 animals/group). Bars represent mean activity, expressed as U/mg protein **(A–C)**, µmol/mg protein **(D–H)**, ±SEM. Results of *post hoc* Tukey's test and significance are shown inside graphs: *$p < 0.05$, **$p < 0.01$, ***$p < 0.001$, ****$p < 0.0001$, ns, no significance.

TABLE 3 | Results of one-way ANOVA analysis.

	Region	ANOVA results	Tukey's *post hoc* test		
			Control vs. TMT	TMT vs. TMT + iTBS	Control vs. TMT + iTBS
PCC analysis	CA1	$F_{(2,46)} = 32.24, p < 0.0001$	$p < 0.0001$	$p < 0.0001$	$p < 0.01$
	mCA3	$F_{(2,49)} = 17.41, p < 0.0001$	$p < 0.01$	$p < 0.01$	$p < 0.0001$
	Hilus/DG	$F_{(2,46)} = 13.99, p < 0.0001$	ns	$p < 0.0001$	$p < 0.0001$
Number of $GFAP^+/IL\text{-}10^+$ cells in HPF	CA1	$F_{(2,47)} = 18.69, p < 0.0001$	ns	$p < 0.0001$	$p < 0.0001$
	mCA3	$F_{(2,48)} = 29.69, p < 0.0001$	ns	$p < 0.0001$	$p < 0.0001$
	Hilus/DG	$F_{(2,47)} = 17.85, p < 0.0001$	ns	$p < 0.01$	$p < 0.0001$
Fluorescence intensity IL-10	CA1	$F_{(2,46)} = 28.13, p < 0.0001$	ns	$p < 0.0001$	$p < 0.0001$
	mCA3	$F_{(2,47)} = 20.51, p < 0.0001$	ns	$p < 0.001$	$p < 0.0001$
	Hilus/DG	$F_{(2,45)} = 15.86, p < 0.0001$	ns	$p < 0.01$	$p < 0.0001$

critical for information flow in hippocampal formation is most likely responsible for aggression, hyperactivity, hyperexcitability, and cognitive impairment (Geloso et al., 2011; Lee et al., 2016). The behavioral data were corroborated with histopathology which showed extensive loss of CA3 and CA1 pyramidal neurons and consequent ventricular dilatation (Balaban et al., 1988; Koczyk and Oderfeld-Nowak, 2000; Andjus et al., 2009). As previously shown, main pro-apoptotic and anti-apoptotic markers, as well as markers of inflammation (C3, IL-1β), were dramatically increased, the latter being restricted to astrocytes as the main source of inflammatory factors (Corvino et al., 2015; Marchese et al., 2018; Dragić et al., 2021a,b). Another consequence of massive neuronal death such as that seen after TMT intoxication inevitably leads to increased production of reactive oxidative and nitrosative species (Kaur and Nehru, 2013). We demonstrated significant disturbance in pro-oxidative and anti-oxidative parameters following TMT intoxication, which are in agreement with previous results (Kaur and Nehru, 2013; Dragić et al., 2021a). Oxidative stress has been implicated in TMT-induced apoptosis and inhibition of PI3K/Akt/mTOR signaling pathways, which are important regulators of growth and cell survival as well as in the memory process (Selvaraj et al., 2012; Zhao et al., 2016). Accordingly, we found a significant reduction in phosphorylated forms of Akt and mTOR, which are also seen in other models of toxin-induced neurodegeneration (Selvaraj et al., 2012; Zhou et al., 2016) and are associated with cognitive impairment (Palumbo et al., 2021).

To the best of our knowledge, this is the first study to demonstrate that iTBS treatment notably improves motor behavior, emotional expression, cognitive abilities, and histopathological and inflammatory status after TMT-induced neurodegeneration, although some beneficial effects on cognition have been demonstrated for other rTMS protocols in animal models (Tan et al., 2013; Guo et al., 2017) and human subjects (Yin et al., 2020). One of the main problems with various rTMS paradigms is that it hugely varies pre-set parameters such as machine output strength, length of session, duration of application which makes it difficult to compare obtained results. iTBS paradigm is a powerful excitatory protocol of rTMS with consistent parameters in literature and with equal or higher efficacy with reduced time of exposure (Chung et al., 2015), which candidates it as an excellent approach in both human and animal studies. In our study, animals stimulated with iTBS had less severe symptoms with a much shorter period without seizures and aggression. Following repeated iTBS, the animals expressed less frequent and milder symptoms of "TMT syndrome," probably due to the beneficial effects on hippocampal formation, which is involved in all aspects of the behavioral expression of emotions, including aggressiveness (Vertes, 2006). Our results showed that animals stimulated with iTBS had normal locomotor behavior and reduced anxiety levels, which was previously shown in animal models of epilepsy and post-traumatic stress disorder with the use of rTMS stimulation protocols (Wang et al., 2015, 2019). It has been suggested that rTMS induces neuronal plasticity, modulates neurotransmitter and neurotrophic factors leading to LTP-like changes in stimulated areas (Uzair et al., 2022), thus improving cognitive processes (Heath et al., 2021). Prolonged stimulation with iTBS could evoke similar mechanisms and alter neuronal excitability and levels of neurotrophic factors, thus improving cognitive status in the TMT model of neurodegeneration. The cognitive and behavioral improvements can be explained by iTBS-induced changes at a cellular level. Namely, iTBS reduced apoptotic cell death in mCA3 and CA1 sectors and attenuated astrocyte-driven inflammation. Previous data demonstrate that rTMS prevents neuronal death by inhibiting several members of the Bcl-2 family, particularly pro-apoptotic factors Bax, Bad, and Bcl-xS (Guo et al., 2017; Uzair et al., 2022), which are the key mediators in TMT-induced apoptosis as well [for review see Geloso et al. (2011)]. Attenuated neuronal death following iTBS was accompanied by a reduction in pro-inflammatory factors and an increase in anti-inflammatory factors. Anti-inflammatory effects of rTMS have been demonstrated in neurological disorders and animal models (Aftanas et al., 2018; Hong et al., 2020; Clarke et al., 2021; Dragić et al., 2021c). Furthermore, rTMS was found to inhibit the polarization of astrocytes toward neurotoxic (A1-like) phenotype (Hong et al., 2020), which are also present in TMT-induced neurodegeneration (Dragić et al., 2021a,b). Reduced expression of inflammatory factors could be a result of reduced neuronal death following iTBS, but also a result of the direct effect of iTBS on glial cells (Cullen and Young, 2016; Cullen et al., 2019). It has been shown that rTMS

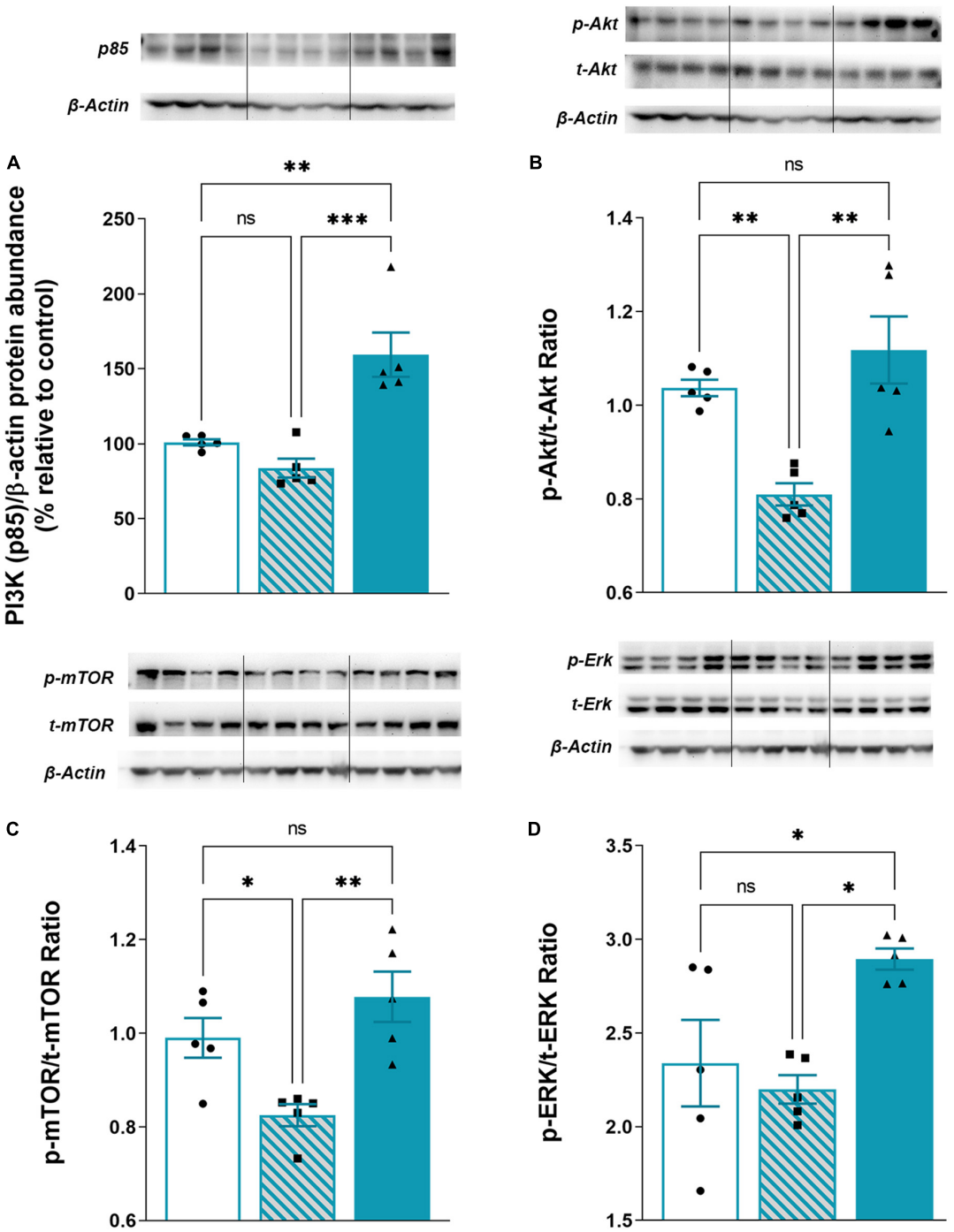

FIGURE 7 | Effect of iTBS treatment on TMT-attenuated PI3K/Akt/mTOR signaling. Representative support membrane and quantitative data of Western blot analysis showing relative protein abundance of **(A)** PI3K (p85) or phosphorylated/non-phosphorylated **(B)** p-Akt/t-Akt ratio, **(C)** p-mTOR/t-mTOR, **(D)** p-ERK/t-ERK ratio in the hippocampal cytosol. Bars represent mean value of target protein **(A)** or ratio of phosphorylated and non-phosphorylated forms **(B–D)** normalized to β-actin abundance ± SEM (from n = 4–5 individual animals, in 2–4 technical replicates), expressed relative to control (arbitrary defined as 100%). Results of *post hoc* Tukey's test and significance are shown inside graphs: *$p < 0.05$, **$p < 0.01$, ***$p < 0.001$, ****$p < 0.0001$, ns, no significance. Dots in the graphs represent values of individual animals.

affects astrocytes both *in vitro* and *in vivo*, implicating astrocytes as cellular effectors of rTMS (Cullen and Young, 2016; Clarke et al., 2021). Inflammatory phenomena are tightly coupled with the overproduction of reactive oxygen and nitrogen species, which may produce neuronal degeneration. Improvement in oxidative status following iTBS, and its antioxidative potential

(Medina-Fernández et al., 2018; Stevanovic et al., 2020) could be mediated *via* nuclear factor (erythroid-derived 2)-like 2 (Nrf2) that is involved in transcriptional regulation of antioxidative enzymes (Jaiswal, 2004). Previous studies reported that TMS increases the expression of Nrf2 in neuroinflammatory conditions (Tasset et al., 2013; Liang et al., 2021), which could also be the mechanism in TMT-mediated oxidative stress. To dissect molecular changes that could underlie favorable effects of iTBS, we investigated PI3K/Akt/mTOR and ERK 1/2 signaling as key players in the regulation of several processes, including proliferation, apoptosis, learning, and memory (Xu et al., 2020). An increase in all these kinases could be put in perspective of reduction of TMT-induced anxiety-like behavior and improvement of cognitive functions following iTBS. It has been shown that *Akt2* knockout and heterozygote mice exhibit anxiety-like behavior and impaired hippocampal-dependent learning (Palumbo et al., 2021), emphasizing the role of Akt and its downstream targets in these processes. Thus, an iTBS-induced increase in phosphorylated Akt could be a significant contributor to the reversal of selective behavioral impairments seen after TMT intoxication. Furthermore, mTOR, as a downstream target of Akt and ERK 1/2, is directly implicated in protein synthesis and involved in the process of learning and memory (Bekinschtein et al., 2007; Palumbo et al., 2021). An increase in phosphorylated mTOR and improved cognitive performance have been observed in the pharmaco-resistant model of depression following iTBS (Lee et al., 2021). Numerous studies have demonstrated that rTMS induces an increase in BDNF [for review see Uzair et al. (2022)] and the receptor tyrosine-related kinase B (TrkB) (Lee et al., 2021), both of which are reduced in TMT-induced neurodegeneration (for review see (Geloso et al., 2011)). Therefore, some of beneficial effects of iTBS may be mediated through BDNF-TrkB signaling. Increased release of BDNF and enhanced TrkB signaling may be responsible for the induction of PI3K/Akt/mTOR and favorable effects on inflammation, apoptosis, anxiety-related behavior, and cognitive improvement seen in the present study after iTBS (Stevanovic et al., 2019; Lee et al., 2021; Uzair et al., 2022). At the end, although the results of present study demonstrate significant beneficial effects of iTBS, it is noteworthy to mention some technical limitations which concern the size and manual placement of the coil, which do not allow focal stimulation of specific cortical areas; therefore the effects induced by iTBS stimulation may be the result of stimulation of both cortical and subcortical structures and their interconnections. Furthermore, due to this technical limitation it is not possible to conclude definitive mechanism and/or structures fully or partially involved in the recovery observed in this experimental paradigm. However, this approach may provide information about the potential effects of stimulation of deeper subcortical structures, which are inaccessible in human subjects.

CONCLUSION

To the best of our knowledge, this is the first study demonstrating the beneficial effects of iTBS protocol on behavioral and cognitive performance and hippocampal cytoarchitecture in the Alzheimer's-like disease model. Specifically, we found significantly reduces neuronal death, inflammation, and oxidative stress, reduced hyperactivity, aggressive behavior, and tremor, and improved cognitive status in TMT animals stimulated with iTBS protocol. Among critical signaling pathways, we demonstrated that iTBS rescued PI3K/Akt/mTOR signaling, which acts in favor of cell survival and recovery. Therefore, iTBS protocol as a paradigm of rTMS may be an excellent candidate for efficient, painless and non-invasive therapy of neurodegenerative disorders associated with cognitive deficits such as Alzheimer's disease.

DATA AVAILABILITY STATEMENT

The original contributions presented in the study are included in the article/**Supplementary Material**, further inquiries can be directed to the corresponding author/s.

ETHICS STATEMENT

The animal study was reviewed and approved by the Ethical Committee of Vinča Institute of Nuclear Sciences.

AUTHOR CONTRIBUTIONS

AS: methodology, validation, formal analysis, investigation, and writing – original draft. MZ: methodology, visualization, formal analysis, and writing – review and editing. MK and IG: methodology, formal analysis, resources, and writing – review and editing. KM, MA, IS, and MN: methodology, formal analysis, and writing – review and editing. TI: supervision, resources, and writing – review and editing. NN: project administration, supervision, funding acquisition, resources, and writing – review and editing. MD: conceptualization, methodology, validation, visualization, formal analysis, investigation, and writing – original draft. All authors contributed to the article and approved the submitted version.

FUNDING

This work was supported by the Ministry of Education, Science and Technological Development, Serbia (Grant Nos. 451-03-68/2022-14/200178 and 451-03-1/2021-16/14-0902102) and University of Defence (Grant No. MFVMA/02/22-24).

SUPPLEMENTARY MATERIAL

The Supplementary Material for this article can be found online at: https://www.frontiersin.org/articles/10.3389/fnagi.2022.889983/full#supplementary-material

REFERENCES

Adzic, M., and Nedeljkovic, N. (2018). Unveiling the role of ecto-5'-nucleotidase/CD73 in astrocyte migration by using pharmacological tools. *Front. Pharmacol.* 9:153. doi: 10.3389/fphar.2018.00153

Aftanas, L. I., Gevorgyan, M. M., Zhanaeva, S. Y., Dzemidovich, S. S., Kulikova, K. I., Al'perina, E. L., et al. (2018). Therapeutic effects of repetitive transcranial magnetic stimulation (rTMS) on neuroinflammation and neuroplasticity in patients with Parkinson's disease: a placebo-controlled study. *Bull. Exp. Biol. Med.* 165, 195–199. doi: 10.1007/s10517-018-4128-4

Andjus, P. R., Bataveljić, D., Vanhoutte, G., Mitrecic, D., Pizzolante, F., Djogo, N., et al. (2009). *In vivo* morphological changes in animal models of amyotrophic lateral sclerosis and Alzheimer's-like disease: MRI approach. *Anatom. Rec. (Hoboken, NJ : 2007)* 292, 1882–1892. doi: 10.1002/ar.20995

Antunes, M., and Biala, G. (2012). The novel object recognition memory: neurobiology, test procedure, and its modifications. *Cogn. Process.* 13, 93–110. doi: 10.1007/s10339-011-0430-z

Balaban, C. D., O'Callaghan, J. P., and Billingsley, M. L. (1988). Trimethyltin-induced neuronal damage in the rat brain: comparative studies using silver degeneration stains, immunocytochemistry and immunoassay for neuronotypic and gliotypic proteins. *Neuroscience* 26, 337–361. doi: 10.1016/0306-4522(88)90150-9

Bekinschtein, P., Katche, C., Slipczuk, L. N., Igaz, L. M., Cammarota, M., Izquierdo, I., et al. (2007). mTOR signaling in the hippocampus is necessary for memory formation. *Neurobiol. Learn. Mem.* 87, 303–307. doi: 10.1016/j.nlm.2006.08.007

Botton, P. H., Costa, M. S., Ardais, A. P., Mioranzza, S., Souza, D. O., da Rocha, J. B. T., et al. (2010). Caffeine prevents disruption of memory consolidation in the inhibitory avoidance and novel object recognition tasks by scopolamine in adult mice. *Behav. Brain Res.* 214, 254–259. doi: 10.1016/j.bbr.2010.05.034

Brambilla, R. (2019). The contribution of astrocytes to the neuroinflammatory response in multiple sclerosis and experimental autoimmune encephalomyelitis. *Acta Neuropathol.* 137, 757–783. doi: 10.1007/s00401-019-01980-7

Chung, S. W., Hoy, K. E., and Fitzgerald, P. B. (2015). Theta-burst stimulation: a new form of TMS treatment for depression? *Depress. Anxiety* 32, 182–192. doi: 10.1002/da.22335

Clarke, D., Beros, J., Bates, K. A., Harvey, A. R., Tang, A. D., and Rodger, J. (2021). Low intensity repetitive magnetic stimulation reduces expression of genes related to inflammation and calcium signalling in cultured mouse cortical astrocytes. *Brain Stimul.* 14, 183–191. doi: 10.1016/j.brs.2020.12.007

Colonna, M., and Butovsky, O. (2017). Microglia function in the central nervous system during health and neurodegeneration. *Annu. Rev. Immunol.* 35, 441–468. doi: 10.1146/annurev-immunol-051116-052358

Corvino, V., Di Maria, V., Marchese, E., Lattanzi, W., Biamonte, F., Michetti, F., et al. (2015). Estrogen administration modulates hippocampal GABAergic subpopulations in the hippocampus of trimethyltin-treated rats. *Front. Cell. Neurosci.* 9:433. doi: 10.3389/fncel.2015.00433

Corvino, V., Marchese, E., Michetti, F., and Geloso, M. C. (2013). Neuroprotective strategies in hippocampal neurodegeneration induced by the neurotoxicant trimethyltin. *Neurochem. Res.* 38, 240–253. doi: 10.1007/s11064-012-0932-9

Cullen, C. L., Senesi, M., Tang, A. D., Clutterbuck, M. T., Auderset, L., O'Rourke, M. E., et al. (2019). Low-intensity transcranial magnetic stimulation promotes the survival and maturation of newborn oligodendrocytes in the adult mouse brain. *Glia* 67, 1462–1477. doi: 10.1002/glia.23620

Cullen, C. L., and Young, K. M. (2016). How does transcranial magnetic stimulation influence glial cells in the central nervous system? *Front. Neural Circ.* 10:26. doi: 10.3389/fncir.2016.00026

De Risio, L., Borgi, M., Pettorruso, M., Miuli, A., Ottomana, A. M., Sociali, A., et al. (2020). Recovering from depression with repetitive transcranial magnetic stimulation (rTMS): a systematic review and meta-analysis of preclinical studies. *Transl. Psychiatry* 10:393. doi: 10.1038/s41398-020-01055-2

Dragić, M., Milićević, K., Adžić, M., Stevanović, I., Ninković, M., Grković, I., et al. (2021a). Trimethyltin Increases Intracellular Ca(2+) *Via* L-type voltage-gated calcium channels and promotes inflammatory phenotype in rat astrocytes *in vitro*. *Mol. Neurobiol.* 58, 1792–1805. doi: 10.1007/s12035-020-02273-x

Dragić, M., Mitrović, N., Adžić, M., Nedeljković, N., and Grković, I. (2021b). Microglial- and astrocyte-specific expression of purinergic signaling components and inflammatory mediators in the rat hippocampus during trimethyltin-induced neurodegeneration. *ASN Neuro* 13:17590914211044882. doi: 10.1177/17590914211044882

Dragić, M., Zarić, M., Mitrović, N., Nedeljković, N., and Grković, I. (2019). Two distinct hippocampal astrocyte morphotypes reveal subfield-different fate during neurodegeneration induced by trimethyltin intoxication. *Neuroscience* 423, 38–54. doi: 10.1016/j.neuroscience.2019.10.022

Dragić, M., Zeljković, M., Stevanović, I., Adžić, M., Stekić, A., Mihajlović, K., et al. (2021c). Downregulation of CD73/A(2A)R-mediated adenosine signaling as a potential mechanism of neuroprotective effects of theta-burst transcranial magnetic stimulation in acute experimental autoimmune encephalomyelitis. *Brain Sci.* 11, 736. doi: 10.3390/brainsci11060736

Dragic, M., Zeljkovic, M., Stevanovic, I., Ilic, T., Ilic, N., Nedeljkovic, N., et al. (2020). Theta burst stimulation ameliorates symptoms of experimental autoimmune encephalomyelitis and attenuates reactive gliosis. *Brain Res. Bull.* 162, 208–217. doi: 10.1016/j.brainresbull.2020.06.013

Dugger, B. N., and Dickson, D. W. (2017). Pathology of neurodegenerative diseases. *Cold Spring Harb. Perspect. Biol.* 9:a028035.

Dunn, K. W., Kamocka, M. M., and McDonald, J. H. (2011). A practical guide to evaluating colocalization in biological microscopy. *Am. J. Physiol. Cell Physiol.* 300, C723–C742. doi: 10.1152/ajpcell.00462.2010

Ellman, G. L. (1959). Tissue sulfhydryl groups. *Arch. Biochem. Biophys.* 82, 70–77. doi: 10.1016/0003-9861(59)90090-6

Erkkinen, M. G., Kim, M.-O., and Geschwind, M. D. (2018). Clinical neurology and epidemiology of the major neurodegenerative diseases. *Cold Spring Harb. Perspect. Biol.* 10:a033118. doi: 10.1101/cshperspect.a033118

Fujiki, M., Yee, K. M., and Steward, O. (2020). Non-invasive high frequency repetitive transcranial magnetic stimulation (hfrTMS) robustly activates molecular pathways implicated in neuronal growth and synaptic plasticity in select populations of neurons. *Front. Neurosci.* 14:558. doi: 10.3389/fnins.2020.00558

Geloso, M. C., Corvino, V., Cavallo, V., Toesca, A., Guadagni, E., Passalacqua, R., et al. (2004). Expression of astrocytic nestin in the rat hippocampus during trimethyltin-induced neurodegeneration. *Neurosci. Lett.* 357, 103–106. doi: 10.1016/j.neulet.2003.11.076

Geloso, M. C., Corvino, V., and Michetti, F. (2011). Trimethyltin-induced hippocampal degeneration as a tool to investigate neurodegenerative processes. *Neurochem. Int.* 58, 729–738. doi: 10.1016/j.neuint.2011.03.009

Girotti, M. J., Khan, N., and McLellan, B. A. (1991). Early measurement of systemic lipid peroxidation products in the plasma of major blunt trauma patients. *J. Trauma* 31, 32–35. doi: 10.1097/00005373-199101000-00007

Guo, F., Lou, J., Han, X., Deng, Y., and Huang, X. (2017). Repetitive transcranial magnetic stimulation ameliorates cognitive impairment by enhancing neurogenesis and suppressing apoptosis in the hippocampus in rats with ischemic stroke. *Front. Physiol.* 8:559. doi: 10.3389/fphys.2017.00559

Heath, A. M., Brewer, M., Yesavage, J., and McNerney, M. W. (2021). Improved object recognition memory using post-encoding repetitive transcranial magnetic stimulation. *Brain Stimul.* 15, 78–86. doi: 10.1016/j.brs.2021.11.009

Hong, Y., Liu, Q., Peng, M., Bai, M., Li, J., Sun, R., et al. (2020). High-frequency repetitive transcranial magnetic stimulation improves functional recovery by inhibiting neurotoxic polarization of astrocytes in ischemic rats. *J. Neuroinflamm.* 17:150. doi: 10.1186/s12974-020-01747-y

Hou, Y., Zhao, J., Yang, D., Xuan, R., Xie, R., Wang, M., et al. (2021). LF-rTMS ameliorates social dysfunction of FMR1(−/−) mice *via* modulating Akt/GSK-3β signaling. *Biochem. Biophys. Res. Commun.* 550, 22–29. doi: 10.1016/j.bbrc.2021.02.086

Jaiswal, A. K. (2004). Nrf2 signaling in coordinated activation of antioxidant gene expression. *Free Radical Biol. Med.* 36, 1199–1207. doi: 10.1016/j.freeradbiomed.2004.02.074

Jung, E.-Y., Lee, M.-S., Ahn, C. J., Cho, S.-H., Bae, H., and Shim, I. (2013). The neuroprotective effect of gugijihwang-tang on trimethyltin-induced memory dysfunction in the rat. *Evid. Based Complement. Altern. Med.* 2013:542081. doi: 10.1155/2013/542081

Kang, J. Y., Park, S. K., Guo, T. J., Ha, J. S., Lee, D. S., Kim, J. M., et al. (2016). Reversal of trimethyltin-induced learning and memory deficits by 3,5-dicaffeoylquinic acid. *Oxid. Med. Cell. Longev.* 2016:6981595. doi: 10.1155/2016/6981595

Kaur, S., and Nehru, B. (2013). Alteration in glutathione homeostasis and oxidative stress during the sequelae of trimethyltin syndrome in rat brain. *Biol. Trace Element Res.* 153, 299–308. doi: 10.1007/s12011-013-9676-x

Koczyk, D., and Oderfeld-Nowak, B. (2000). Long-term microglial and astroglial activation in the hippocampus of trimethyltin-intoxicated rat: stimulation of NGF and TrkA immunoreactivities in astroglia but not in microglia. *Int. J. Dev. Neurosci.* 18, 591–606. doi: 10.1016/s0736-5748(99)00111-2

Koda, T., Kuroda, Y., and Imai, H. (2008). Protective effect of rutin against spatial memory impairment induced by trimethyltin in rats. *Nutr. Res. (New York, NY)* 28, 629–634. doi: 10.1016/j.nutres.2008.06.004

Kono, Y., Kobayashi, K., Tagawa, S., Adachi, K., Ueda, A., Sawa, Y., et al. (1997). Antioxidant activity of polyphenolics in diets. Rate constants of reactions of chlorogenic acid and caffeic acid with reactive species of oxygen and nitrogen. *Biochim. Biophys. Acta* 1335, 335–342. doi: 10.1016/s0304-4165(96)00151-1

Lattanzi, W., Corvino, V., Di Maria, V., Michetti, F., and Geloso, M. C. (2013). Gene expression profiling as a tool to investigate the molecular machinery activated during hippocampal neurodegeneration induced by trimethyltin (TMT) administration. *Int. J. Mol. Sci.* 14, 16817–16835. doi: 10.3390/ijms140816817

Lee, C.-W., Wu, H.-F., Chu, M.-C., Chung, Y.-J., Mao, W.-C., Li, C.-T., et al. (2021). Mechanism of intermittent theta-burst stimulation in synaptic pathology in the prefrontal cortex in an antidepressant-resistant depression rat model. *Cereb. Cortex (New York, NY : 1991)* 31, 575–590. doi: 10.1093/cercor/bhaa244

Lee, S., Yang, M., Kim, J., Kang, S., Kim, J., Kim, J.-C., et al. (2016). Trimethyltin-induced hippocampal neurodegeneration: a mechanism-based review. *Brain Res. Bull.* 125, 187–199. doi: 10.1016/j.brainresbull.2016.07.010

León Ruiz, M., Rodríguez Sarasa, M. L., Sanjuán Rodríguez, L., Benito-León, J., García-Albea Ristol, E., and Arce Arce, S. (2018). Current evidence on transcranial magnetic stimulation and its potential usefulness in post-stroke neurorehabilitation: opening new doors to the treatment of cerebrovascular disease. *Neurologia (Barcelona, Spain)* 33, 459–472. doi: 10.1016/j.nrl.2016.03.008

Liang, H., Xu, C., Hu, S., Wen, G., Lin, J., Liu, T., et al. (2021). Repetitive transcranial magnetic stimulation improves neuropathy and oxidative stress levels in rats with experimental cerebral infarction through the Nrf2 signaling pathway. *Evid. Based Complement. Altern. Med.* 2021:3908677. doi: 10.1155/2021/3908677

Little, A. R., Miller, D. B., Li, S., Kashon, M. L., and O'Callaghan, J. P. (2012). Trimethyltin-induced neurotoxicity: gene expression pathway analysis, q-RT-PCR and immunoblotting reveal early effects associated with hippocampal damage and gliosis. *Neurotoxicol. Teratol.* 34, 72–82. doi: 10.1016/j.ntt.2011.09.012

Lu, N., and Malemud, C. J. (2019). Extracellular signal-regulated kinase: a regulator of cell growth, inflammation, chondrocyte and bone cell receptor-mediated gene expression. *Int. J. Mol. Sci.* 20:3792. doi: 10.3390/ijms20153792

Marchese, E., Corvino, V., Di Maria, V., Furno, A., Giannetti, S., Cesari, E., et al. (2018). The neuroprotective effects of 17β-estradiol pretreatment in a model of neonatal hippocampal injury induced by trimethyltin. *Front. Cell. Neurosci.* 12:385. doi: 10.3389/fncel.2018.00385

Medina-Fernández, F. J., Escribano, B. M., Padilla-Del-Campo, C., Drucker-Colín, R., Pascual-Leone, Á, and Túnez, I. (2018). Transcranial magnetic stimulation as an antioxidant. *Free Radical Res.* 52, 381–389.

Mitrović, N., Zarić, M., Drakulić, D., Martinović, J., Sévigny, J., Stanojlović, M., et al. (2017). 17β-estradiol-induced synaptic rearrangements are accompanied by altered ectonucleotidase activities in male rat hippocampal synaptosomes. *J. Mol. Neurosci.* 61, 412–422. doi: 10.1007/s12031-016-0877-6

Moser, V. C. (2011). Functional assays for neurotoxicity testing. *Toxicol. Pathol.* 39, 36–45. doi: 10.1177/0192623310385255

Nardone, R., Versace, V., Sebastianelli, L., Brigo, F., Golaszewski, S., Christova, M., et al. (2019). Transcranial magnetic stimulation and bladder function: a systematic review. *Clin. Neurophysiol.* 130, 2032–2037. doi: 10.1016/j.clinph.2019.08.020

Navarro-Gonzálvez, J. A., García-Benayas, C., and Arenas, J. (1998). Semiautomated measurement of nitrate in biological fluids. *Clin. Chem.* 44, 679–681. doi: 10.1093/clinchem/44.3.679

Nilsberth, C., Kostyszyn, B., and Luthman, J. (2002). Changes in APP, PS1 and other factors related to Alzheimer's disease pathophysiology after trimethyltin-induced brain lesion in the rat. *Neurotoxicity Res.* 4, 625–636. doi: 10.1080/1029842021000045471

Palumbo, S., Paterson, C., Yang, F., Hood, V. L., and Law, A. J. (2021). PKBβ/AKT2 deficiency impacts brain mTOR signaling, prefrontal cortical physiology, hippocampal plasticity and select murine behaviors. *Mol. Psychiatry* 26, 411–428. doi: 10.1038/s41380-020-00964-4

Park, H.-J., Shim, H. S., Choi, W. K., Kim, K. S., Bae, H., and Shim, I. (2011). Neuroprotective effect of lucium chinense fruit on trimethyltin-induced learning and memory deficits in the rats. *Exp. Neurobiol.* 20, 137–143. doi: 10.5607/en.2011.20.3.137

Park, S. K., Kang, J. Y., Kim, J. M., Yoo, S. K., Han, H. J., Chung, D. H., et al. (2019). Fucoidan-rich substances from ecklonia cava improve trimethyltin-induced cognitive dysfunction *via* down-regulation of amyloid β production/tau hyperphosphorylation. *Mar. Drugs* 17, 591. doi: 10.3390/md17100591

Rabey, J. M., and Dobronevsky, E. (2016). Repetitive transcranial magnetic stimulation (rTMS) combined with cognitive training is a safe and effective modality for the treatment of Alzheimer's disease: clinical experience. *J. Neural Transm. (Vienna, Austria : 1996)* 123, 1449–1455. doi: 10.1007/s00702-016-1606-6

Sadoughi, D. (2019). The effect of crocin on apoptotic, inflammatory, BDNF, Pt, and Aβ40 indicators and neuronal density of CA1, CA2, and CA3 regions of hippocampus in the model of Alzheimer suffering rats induced with trimethyltin chloride. *Comp. Clin. Path.* 28, 1403–1413. doi: 10.1007/s00580-019-02981-4

Selvaraj, S., Sun, Y., Watt, J. A., Wang, S., Lei, S., Birnbaumer, L., et al. (2012). Neurotoxin-induced ER stress in mouse dopaminergic neurons involves downregulation of TRPC1 and inhibition of AKT/mTOR signaling. *J. Clin. Invest.* 122, 1354–1367. doi: 10.1172/JCI61332

Stevanovic, I., Mancic, B., Ilic, T., Milosavljevic, P., Lavrnja, I., Stojanovic, I., et al. (2019). Theta burst stimulation influence the expression of BDNF in the spinal cord on the experimental autoimmune encephalomyelitis. *Folia Neuropathol.* 57, 129–145. doi: 10.5114/fn.2019.86294

Stevanovic, I., Ninkovic, M., Mancic, B., Milivojevic, M., Stojanovic, I., Ilic, T., et al. (2020). Compensatory neuroprotective response of thioredoxin reductase against oxidative-nitrosative stress induced by experimental autoimmune encephalomyelitis in rats: modulation by theta burst stimulation. *Molecules (Basel, Switzerland)* 25:3922. doi: 10.3390/molecules25173922

Sun, M., and Zigman, S. (1978). An improved spectrophotometric assay for superoxide dismutase based on epinephrine autoxidation. *Anal. Biochem.* 90, 81–89. doi: 10.1016/0003-2697(78)90010-6

Tan, T., Xie, J., Liu, T., Chen, X., Zheng, X., Tong, Z., et al. (2013). Low-frequency (1 Hz) repetitive transcranial magnetic stimulation (rTMS) reverses Aβ(1-42)-mediated memory deficits in rats. *Exp. Gerontol.* 48, 786–794. doi: 10.1016/j.exger.2013.05.001

Tasset, I., Pérez-Herrera, A., Medina, F. J., Arias-Carrión, O., Drucker-Colín, R., and Túnez, I. (2013). Extremely low-frequency electromagnetic fields activate the antioxidant pathway Nrf2 in a Huntington's disease-like rat model. *Brain Stimul.* 6, 84–86. doi: 10.1016/j.brs.2012.03.015

Thomson, A. C., Kenis, G., Tielens, S., de Graaf, T. A., Schuhmann, T., Rutten, B. P. F., et al. (2020). Transcranial magnetic stimulation-induced plasticity mechanisms: TMS-related gene expression and morphology changes in a human neuron-like cell model. *Front. Mol. Neurosci.* 13:528396. doi: 10.3389/fnmol.2020.528396

Trabucco, A., Di Pietro, P., Nori, S. L., Fulceri, F., Fumagalli, L., Paparelli, A., et al. (2009). Methylated tin toxicity a reappraisal using rodents models. *Arch. Ital. Biol.* 147, 141–153.

Urano, T., and Tohda, C. (2010). Icariin improves memory impairment in Alzheimer's disease model mice (5xFAD) and attenuates amyloid β-induced neurite atrophy. *Phytother. Res.* 24, 1658–1663. doi: 10.1002/ptr.3183

Uzair, M., Abualait, T., Arshad, M., Yoo, W.-K., Mir, A., Bunyan, R. F., et al. (2022). Transcranial magnetic stimulation in animal models of neurodegeneration. *Neural Regen. Res.* 17, 251–265. doi: 10.4103/1673-5374.317962

Vertes, R. P. (2006). Interactions among the medial prefrontal cortex, hippocampus and midline thalamus in emotional and cognitive processing in the rat. *Neuroscience* 142, 1–20. doi: 10.1016/j.neuroscience.2006.06.027

Wang, H.-N., Bai, Y.-H., Chen, Y.-C., Zhang, R.-G., Wang, H.-H., Zhang, Y.-H., et al. (2015). Repetitive transcranial magnetic stimulation ameliorates anxiety-like behavior and impaired sensorimotor gating in a rat model of post-traumatic stress disorder. *PLoS One* 10:e0117189. doi: 10.1371/journal.pone.0117189

Wang, S., Mao, S., Yao, B., Xiang, D., and Fang, C. (2019). Effects of low-frequency repetitive transcranial magnetic stimulation on depression- and anxiety-like behaviors in epileptic rats. *J. Integr. Neurosci.* 18, 237–243. doi: 10.31083/j.jin.2019.03.1100

Xu, F., Na, L., Li, Y., and Chen, L. (2020). Roles of the PI3K/AKT/mTOR signalling pathways in neurodegenerative diseases and tumours. *Cell Biosci.* 10:54.

Yang, J., Liang, R., Wang, L., Zheng, C., Xiao, X., and Ming, D. (2021). Repetitive transcranial magnetic stimulation (rTMS) improves the gait disorders of rats under simulated microgravity conditions associated with the regulation of motor cortex. *Front. Physiol.* 12:587515. doi: 10.3389/fphys.2021.587515

Yin, M., Liu, Y., Zhang, L., Zheng, H., Peng, L., Ai, Y., et al. (2020). Effects of rTMS treatment on cognitive impairment and resting-state brain activity in stroke patients: a randomized clinical trial. *Front. Neural Circ.* 14:563777. doi: 10.3389/fncir.2020.563777

Zhao, W., Pan, X., Li, T., Zhang, C., and Shi, N. (2016). Lycium barbarum polysaccharides protect against trimethyltin chloride-induced apoptosis *via* sonic hedgehog and PI3K/Akt signaling pathways in mouse neuro-2a cells. *Oxid .Med. Cell. Longev.* 2016:9826726. doi: 10.1155/2016/9826726

Zhou, Q., Chen, B., Wang, X., Wu, L., Yang, Y., Cheng, X., et al. (2016). Sulforaphane protects against rotenone-induced neurotoxicity *in vivo*: Involvement of the mTOR. Nrf2, and autophagy pathways. *Sci. Rep.* 6:32206. doi: 10.1038/srep32206

Conflict of Interest: The authors declare that the research was conducted in the absence of any commercial or financial relationships that could be construed as a potential conflict of interest.

Publisher's Note: All claims expressed in this article are solely those of the authors and do not necessarily represent those of their affiliated organizations, or those of the publisher, the editors and the reviewers. Any product that may be evaluated in this article, or claim that may be made by its manufacturer, is not guaranteed or endorsed by the publisher.

frontiers | Frontiers in Neuroscience

ORIGINAL RESEARCH
published: 05 July 2022
doi: 10.3389/fnins.2022.878287

Screening of Human Circular RNAs as Biomarkers for Early Onset Detection of Alzheimer's Disease

Da Zheng[1†], Rana Adnan Tahir[1†], Yan Yan[1], Juan Zhao[1], Zhenzhen Quan[1], Guixia Kang[2], Ying Han[3,4,5,6] and Hong Qing[1*]*

[1] *Key Laboratory of Molecular Medicine and Biotherapy in the Ministry of Industry and Information Technology, Department of Biology, School of Life Sciences, Beijing Institute of Technology, Beijing, China,* [2] *Key Lab of Universal Wireless Communications of Ministry of Education, Beijing University of Posts and Telecommunications, Beijing, China,* [3] *Biomedical Engineering Institute, Hainan University, Haikou, China,* [4] *Department of Neurology, Xuanwu Hospital of Capital Medical University, Beijing, China,* [5] *Center of Alzheimer's Disease, Beijing Institute for Brain Disorders, Beijing, China,* [6] *National Clinical Research Center for Geriatric Disorders, Beijing, China*

OPEN ACCESS

Edited by:
Athanasios Alexiou, Novel Global Community Educational Foundation (NGCEF), Australia

Reviewed by:
Ling-Qiang Zhu, Huazhong University of Science and Technology, China
Jie Song, Institute of Medical Biology, Chinese Academy of Medical Sciences and Peking Union Medical College, China

****Correspondence:***
Ying Han
hanying@xwh.ccmu.edu.cn
Hong Qing
hqing@bit.edu.cn
orcid.org/0000-0003-0216-4044

† These authors have contributed equally to this work

Specialty section:
This article was submitted to Neurodegeneration, a section of the journal Frontiers in Neuroscience

Received: *17 February 2022*
Accepted: *01 June 2022*
Published: *05 July 2022*

Citation:
Zheng D, Tahir RA, Yan Y, Zhao J, Quan Z, Kang G, Han Y and Qing H (2022) Screening of Human Circular RNAs as Biomarkers for Early Onset Detection of Alzheimer's Disease. Front. Neurosci. 16:878287. doi: 10.3389/fnins.2022.878287

Circular RNAs (circRNAs) are a distinctive type of endogenous non-coding RNAs, and their regulatory roles in neurological disorders have received immense attention. CircRNAs significantly contribute to the regulation of gene expression and progression of neurodegenerative disorders including Alzheimer's disease (AD). The current study aimed to identify circRNAs as prognostic and potential biomarkers in AD. The differentially expressed circRNAs among subjective cognitive decline, amnestic mild cognitive impairment, and age-matched normal donors were determined through Arraystar Human circRNA Array V2 analysis. The annotations of circRNAs-microRNA interactions were predicted by employing Arraystar's homemade microRNAs (miRNA) target prediction tool. Bioinformatics analyses comprising gene ontology enrichment, KEGG pathway, and network analysis were conducted. Microarray analysis revealed the 33 upregulated and 11 downregulated differentially expressed circRNAs (FC $\geq$ 1.5 and p-values $\leq$ 0.05). The top 10 differentially expressed upregulated and downregulated circRNAs have been chosen for further expression validation through quantitative real-time PCR and subsequently, hsa-circRNA_001481 and hsa_circRNA_000479 were confirmed experimentally. Bioinformatics analyses determined the circRNA-miRNA-mRNA interactions and microRNA response elements to inhibit the expression of miRNAs and mRNA targets. Gene ontology enrichment and KEGG pathways analysis revealed the functional clustering of target mRNAs suggesting the functional verification of these two promising circRNAs. It is concluded that human circRNA_001481 and circRNA_000479 could be utilized as potential biomarkers for the early onset detection of AD and the development of effective therapeutics.

Keywords: Alzheimer's disease, circular RNAs, miRNA, biomarker, bioinformatics, microarray analysis, gene ontology, circRNA-miRNA interactions

INTRODUCTION

Circular RNAs (circRNAs) are a peculiar group of long, non-coding endogenous RNAs characterized by the existence of covalently closed RNA loops (Salzman et al., 2012, 2013; Jeck and Sharpless, 2014). These transcripts arise through the direct back-splicing and exon skipping of precursor RNAs (Starke et al., 2015; Chen, 2016). They lack free 5′ and 3′ ends and form a circular

structure which makes them highly stable and resistant to exonuclease degradation (Wang and Wang, 2015; Chen, 2016).

Stability in expression and degradation resistance permit circRNAs in the application and development of novel clinically diagnostic biomarkers. CircRNAs also play a vital role in various diseases *via* competitively binding to the disease-related microRNAs (miRNAs; Zhang et al., 2017; Liu et al., 2018). The developmental phase and tissue-specific expressions of circRNAs signify their regulatory functions in gene expression (Wang et al., 2018). CircRNAs are widely found in eukaryotic cells and regulate gene expression *via* sponging particular miRNAs and consequently modulating their suppressive effect on RNA translation (Barrett and Salzman, 2016; Abdelmohsen et al., 2017; Han et al., 2017).

The precise understanding of circRNAs in the central nervous system (CNS) is hampered due to the lack of molecular tools required for the detection, quantification, and evaluation of circRNAs in physiologic processes and diseases such as Alzheimer's disease (AD; Lukiw, 2013). CircRNA, ciRS-7, has emerged as a sponge of miR-7 and recently identified in promoting the degradation of BACE1 and APP in an NF-κB-dependent manner (Shi et al., 2017). Recent studies suggest that ciRS-7 could be useful as a diagnostic biomarker of AD and still further experiments are needed to reveal the functions of circRNAs contributing to AD pathology (Idda et al., 2018). The ability to freely cross the blood-brain barrier makes these circRNAs potentially invasive biomarkers for CNS disorders (Lu and Xu, 2016).

Alzheimer's disease is the most common and prevalent form of dementia and one of the increasing economic and medical problems of the modern world (Alzheimer's Association, 2019). It is characterized by the irreversible degeneration of cognitive functions, thinking, behavioral, and learning abilities, and is ranked as the sixth leading cause of death in the United States (Heron, 2018). It is estimated that at least 50 million people are living with AD or other dementias globally and it could surpass 152 million by 2050 in the absence of effective therapies (Patterson, 2018). Research studies have demonstrated that AD has a slow and progressive decline in cognitive functions over several years to decades and is categorized into three main stages: subjective cognitive decline (SCD), amnestic mild cognitive impairment (aMCI), and AD (Jiang et al., 2018). SCD is described as the transitional phase in the progression of AD pathology and also an early symptomatic expression of preclinical AD (Jessen et al., 2014). The research on SCD mainly focuses to identify the specific biomarkers of AD and also verifying SCD as a risk condition for MCI or AD (Schultz et al., 2015; Snitz et al., 2015; Sun et al., 2016; Chen et al., 2019). The dynamical model of cognitive decline demonstrates a subtle cognitive decline in SCD but within the standard cognitive performance range. The further cognitive decline leads to the aMCI-AD stage and still performance declines linearly (Jessen et al., 2014). The MCI phase has been recognized as an impairment of memory or cognition domains on a standard assessment and clinical cognitive staging in the absence of biomarkers (Jack et al., 2018). Still, extensive studies are needed to determine the dynamic model of cognitive decline in various stages for a better understanding of the quantitative mechanism of AD onset and progression (Jiang et al., 2018).

The current study aimed to identify the circRNAs as diagnostic biomarkers for the early onset detection of AD through circRNA microarray profiling followed by bioinformatics analyses. Here, the results revealed that hsa_circRNA_001481 and hsa_circRNA_000479 are significantly upregulated in the blood samples at various stages of AD patients. Gene ontology enrichment, KEGG pathway, and interaction network were constructed and analyzed for these upregulated human circRNAs to reveal the gene targets. Expression profiles of human circRNAs may lead to a better understanding of molecular insights and potential mechanisms for developing diagnostic markers and therapeutic methods.

MATERIALS AND METHODS

Data Collection (Patients and Specimens)

Experiments of the current study were undertaken by the Ethics committee of Beijing Institute of Technology (BIT), Beijing, and all the samples were collected from the Xuanwu Hospital Capital Medical University, Beijing, with the consent of each subject. Blood specimen collection was divided into two phases: (i) diagnosis phase and (ii) validation phase. The first phase involved the collection of fresh blood samples from 55 participants (male: 26 and female 29). Three types of samples comprising SCD (22), aMCI (11), and AD (5) patient samples were collected along with normal controls (17) to determine the differentially expressed circRNAs. All the patients were diagnosed with transitional stages of cognitive decline through the consensus of two consultant psychiatrists based on the criteria for SCD, aMCI, and AD. It has been observed that approximately 30% of SCD patients had the habit of smoking and drinking along with hypertension. Some of the other patients having aMCI and AD also showed smoking, drinking, and a history of hypertension. Three SCD patients also had diabetes for the last 1, 3, and 12 years individually. No patient was suffering from Hepatitis or any other infectious diseases; however, heart diseases including blood pressure issues were reported in almost 13 patients. The six samples having different medical histories were selected for further circRNA microarray analyses. The second phase involves the collection of samples for the cross-validation of microarray analysis through qRT-PCR. The blood samples comprising SCD (3), aMCI (2), and AD (3) were collected in this phase. The SCD patient at the age of 70 years with no habit of smoking, drinking, or any other infectious disease along with the patient (65 years) with only a smoking habit, while third patient (76 years) suffering from heart disease and hypertension were utilized for the validation of differentially expressed circRNAs and to identify the uniform relative expression among all SCD patients. The aMCI patient with 7 years of hypertension and heart disease with an occasionally drinking habit was used for sample collection. The other aMCI with drinking and smoking habits and

hypertension was also utilized for cross-validation of circRNAs. The AD samples with no habits of smoking and drinking and with hypertension and heart disease were also utilized in this phase. The initially collected samples were utilized for the high-throughput microarray sequencing analyses followed by the initial validation of differentially expressed circRNAs through qRT-PCR. The second phase involves the collection of samples for the cross-validation of differentially expressed circRNAs and to identify the potential and coverage of circRNAs among similar transitional stages of AD samples.

Total RNA Extraction and Quality Control

Total RNA was extracted from the blood samples using TRIzol reagent (Invitrogen, NY, United States) according to the manufacturer's instructions. The concentrations were measured through OD260 by employing NanoDrop ND-1000. Denaturing agarose gel electrophoresis was utilized to evaluate the RNA purity and gDNA contamination testing.

RNA Labeling and Hybridization

Sample preparations, labeling, and array hybridization were executed under the company's standard procedures (Arraystar Inc., MD, United States). Ribonuclease R (Epicentre, Inc.) digested the total RNAs and hence removed the linear RNAs which led to the enrichment of circRNAs. A random priming method (Arraystar Super RNA Labeling Kit; Arraystar) was used to amplify and transcribe the enriched circRNAs into fluorescent cRNA. The purification of labeled cRNAs was conducted *via* the RNeasy Mini Kit (Qiagen).

NanoDrop ND-1000 was utilized to determine the precise activity and concentration of labeled cRNAs (pmol Cy3/μg cRNA). A 1 μg of each labeled cRNA was fragmented by adding 1 μl of 25 × Fragmentation Buffer and 5 μl of 10 × Blocking Agent followed by the heating of the mixture for 30 min at 60°C. Subsequently, 25 μl of 2 × Hybridization buffer was used to dilute the labeled cRNA. A total of 50 μl of hybridization solution was dispensed into the gasket slide and assembled to create the circRNA expression microarray slide. The incubation of slides was carried out at 65°C for 17 h in an Agilent Hybridization Oven. Agilent Scanner G2505C was used to wash, fix, and scan the hybridized arrays.

Circular RNAs Microarray Analysis

An Agilent feature extraction tool was employed to extract the raw data from the scanned images. The limma package of R language/software was used for quantile normalization and further data processing of raw data. Subsequently, low-intensity filtering was done to scrutinize the circRNAs from samples. The circRNAs that exhibited the "P" or "M" flags ("All Targets Value") in at least 1 out of 6 samples were kept for further differential expression analyses. Profile differences (disease versus control) and "fold change" between the groups for each circRNA were computed and its statistical significance was assessed by *t*-test. Differentially expressed circRNAs having p-values < 0.05 and fold change > 1.5 were retrieved from microarray expression profiling.

Annotation for Circular RNAs-MicroRNAs Interaction

Arraystar's homemade miRNA target prediction software was used to generate the circRNAs-microRNA interactions and annotations of all the differentially expressed circRNAs by assessing the miRanda (Enright et al., 2003) and TargetScan (Lewis et al., 2005) databases. miRNA response elements (MREs) were hunted by utilizing the Arraystar software and the top five putative target miRNAs were selected based on seed match sequences.

Quantitative Real-Time PCR

Quantitative real-time PCR (qRT-PCR) was performed to validate the overexpression of circRNAs, obtained from the microarray expression profiling. The top 10 circRNAs sorted on their fold change values were selected for qRT-PCR. The details of selected circRNAs including names, fold change values, p-values, chromosomal location, best transcript, gene symbol, and their up- or downregulation are mentioned in **Table 2**.

Total RNA was extracted from the blood samples and subsequently, reverse transcription was done to produce cDNA according to the standard protocols. SYBR green assay was utilized in qPCR to evaluate the expression levels of circRNAs. Divergent primers were designed and optimized to amplify the circular transcripts. CircRNA spliced sequences were retrieved from the database "circBase" to design the primers from Primer3 and Primer-Blast. Primers were synthesized from Sangon Biotech (Beijing, China) for qPCR. GAPDH was used as a reference to determine the relative expression of circRNAs.

Bioinformatics Analyses

Bioinformatics analyses were carried out on differentially expressed circRNAs to predict the circRNA-miRNA-gene interactions and construct the network for the identification of gene targets that may be regulated by these selected circRNAs.

The miRDB database (Chen and Wang, 2020) was utilized to predict the miRNA interactions with gene targets and top upregulated circRNAs interactions with miRNAs and gene targets were mapped to an interaction network. CircRNA-miRNA-gene interactions network was constructed by using the Cytoscape software (Shannon et al., 2003). Gene ontology enrichment analysis was conducted to construct the annotations of the genes by using DAVID (Sherman and Lempicki, 2009). Gene functions comprising cellular components, physiological processes, and molecular functions were determined. KEGG pathway analysis was also performed to determine the involvement of genes in different physiological processes. Significant enrichment scores were examined and the involvement of genes in neurological disorders and their upregulations in brain tissues were observed.

Cell Culture and Plasmid Construction

The human embryonic kidney cell lines (HEK293T) were purchased from American Type Culture Collection (ATCC, Manassas, VA, United States). The cells were cultured and maintained in Dulbecco's modified Eagle's medium containing 10% fetal bovine serum (GIBCO BRL, NY, United States)

and 0.1% penicillin/streptomycin (Gibco, United States). The cultured cells were incubated in a humidified 5% CO_2 atmosphere at 37°C.

The sequences of hsa_circRNA_001481 and hsa_circRNA_000479 were amplified through PCR and subsequently cloned into the pcDNA3.1 vector. The final constructs were validated by direct sequencing from Sangon Biotech (Shanghai, China).

Transfection and Luciferase Assay

HEK293T cells were transfected at about 80% confluence with corresponding plasmid constructs and subsequently co-transfected with miRNAs by using a transfection reagent (Lipofectamine 2000, Invitrogen) as per the manufacturer's recommendations. The miRNAs mimics of hsa_circRNA_001481 and hsa_circRNA_000479 were synthesized through Sangon Biotech, which is mentioned in **Table 3**.

The cells were seeded into 24-well culture plates in which each group contains the three biological replicates. The cells were categorized into two basic groups: the negative control (NC) group involving the transfection with pcDNA3.1 and the mimics group comprising cells transfected with all miRNAs of both circRNAs. The pGL3 luciferase reporter vector was also used in the luciferase screening assay in addition to two NCs comprising miRNAs controls and luciferase reporters with or without circRNA_001481 and circRNA_000479. The cells were harvested after 48 h of transfection and then the relative luciferase activity of each miRNA was determined through the Dual-Luciferase Reporter Assay System. This experiment was repeated independently three times to increase the reproducibility and yield reliable and accurate results.

Statistical Analysis

All the experiments were performed in triplicates and subsequent statistical analyses were performed to analyze and calculate the significance level of the data. Experimental results were expressed as mean ± standard error (SE), while group comparisons were tested through one-way ANOVA having less than 0.05 significant *p*-value. Pearson's correlation analysis was carried out to analyze the relevance of expression. GraphPad Prism 8 (GraphPad Software, 2019) and Microsoft Excel were employed to analyze the experimental data and plot the graphs.

RESULTS AND DISCUSSION

Present work focused to determine the differentially expressed human circRNAs susceptible to AD patients for the early onset detection of disease through the circRNA as a biomarker *via* microarray analysis profiling and bioinformatics analyses.

The initial diagnosis phase involved the collection of 55 blood samples comprising 22 SCD, 11 aMCI, and 5 AD patient samples along with 17 normal controls to determine the differentially expressed circRNAs. SCD is referred to as the initial manifestation of the AD continuum which is the subjective experience of worsening cognitive performance (Jessen et al., 2020). The six samples including 3 SCD, 1 aMCI, and 2 NC were selected for circRNA microarray analysis. The details of these selected samples are mentioned in **Table 1** along with their medical history. The medical history of these nominated donors shows the absence of smoking, coronary heart diseases, hepatitis, and other infectious diseases. SCD (#287) had diabetes for the last 12 years along with hypertension for 4 years while the SCD patient (#288) only had a history of specific hypertension. Participant #274 (aMCI) was suffering from a high blood pressure of around 170/90 mm Hg and later it was reduced to 140/80 mm Hg by regular medications. He also has a drinking addiction and has almost drank approximately 50 mL of liquor daily for the last 7 to 8 years.

General Microarray Profiles

The differential expression of circRNAs was measured through human circRNA microarray analysis which detected the upregulation and downregulation of circRNAs among SCD, aMCI, and NC samples. The expression of circRNAs was compared between each group and approximately 6,000 to 8,000 differentially expressed circRNAs are detected in each comparison where significant ones were scrutinized based on fold change ($\geq$1.5) and *p*-values ($\leq$0.05). A total of 33 differentially expressed upregulated and 11 downregulated circRNAs were detected in the test versus control group. The comparison between aMCI versus control revealed 926 differentially expressed upregulated and 854 downregulated circRNAs, while aMCI versus test identified 1,300 upregulated and 1,169 downregulated circRNAs (**Supplementary File 1**).

The distribution of intensities from all the samples was visualized in the box plot which compares the distribution of expression values between each group after normalization (**Figure 1A**). The expression variability of circRNAs was assessed through the scatter plots between each sample group. The scatter plots between test versus control, control versus aMCI, and test versus aMCI were constructed accordant with the fold change (**Figure 1B**). A volcano plot was constructed to determine the

TABLE 1 | Clinical details of specimens for circRNA microarray analysis.

Sr #	Clinical diagnosis	No.	Gender	Age	Medical history
1	NC	276	♀	69	
2		281	♂	62	
3	SCD	287	♀	61	12 years of Diabetes and 4 years of Hypertension
4		288	♀	75	History of Hypertension
5		275	♂	72	No Smoking, Drinking, Hypertension, or Heart disease
6	aMCI	274	♂	75	High Blood Pressure and Drinking

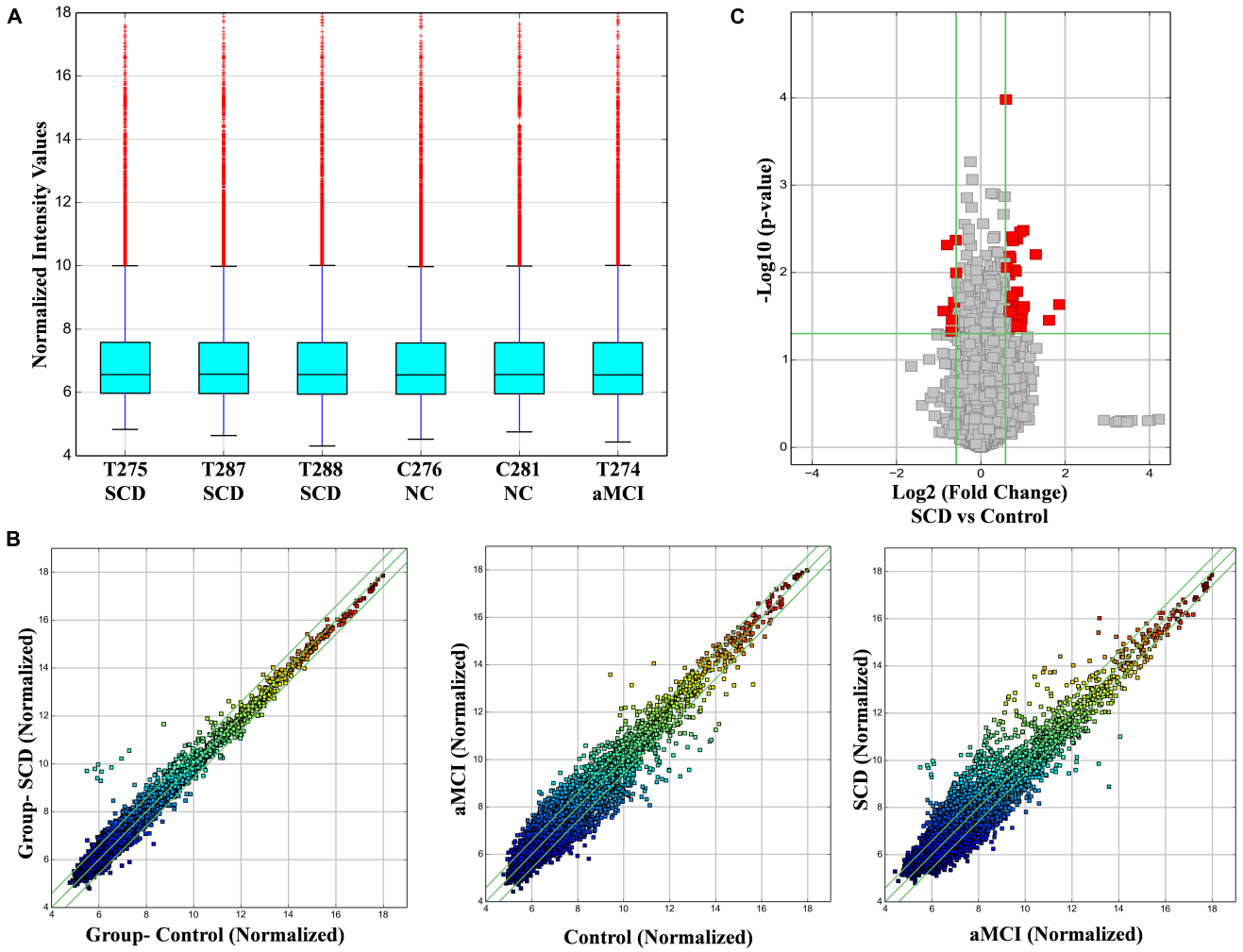

FIGURE 1 | Microarray expression analysis of human circRNAs in SCD and aMCI against control samples. **(A)** Box plot presenting the normalized intensity values of each sample which are almost the same in each sample. **(B)** The scatter plots represent the variability of expression between each sample. The values of the *X* and *Y* axes in the scatter plot are the normalized signal values of the samples (log2 scaled). The green lines are fold change lines. The CircRNAs above the top green line and below the bottom green line indicated more than a 1.5-fold change of circRNAs between the two compared samples. **(C)** Volcano plot, showing the red points that represent the differentially expressed circRNAs with statistical significance. The vertical lines correspond to 1.5-fold up and down, respectively, and the horizontal line represents a *p*-value of 0.05.

differential expression between test versus control which helped to identify the altered circRNAs with statistical significance (**Figure 1C**). Fold change and *p*-value filtering were considered in the volcano plot, thereby allowing to separate the circRNAs with variability and significance.

Hierarchical clustering was used to determine the expression levels of samples. Cluster analysis placed the samples per their expression levels and compared each group (**Figure 2**). Heat maps were used to identify the expression levels of each sample and higher expression levels of test samples were observed as compared to control and aMCI samples. Groups having similar expression levels are clustered through the dendrogram.

Fold change filtering was applied to sort out the top upregulated and downregulated differentially expressed circRNAs and selected them for subsequent validation through RT-qPCR. The top circRNAs are mentioned in **Table 2** along with annotations of circRNAs. A total of 30 circRNAs are exonic, while 2 are sense overlapping and only 1 lies in the intronic region.

The top potential binding target miRNAs of differentially expressed circRNAs were also predicted and considered as the potential binding targets as mentioned in **Table 3**.

Validation of Circular RNAs by Real-Time-qPCR

High-throughput microarray assay yielded the differentially expressed circRNAs which required verification through experimental techniques. Top altered circRNAs with relatively high fold change as mentioned in **Table 2** are selected

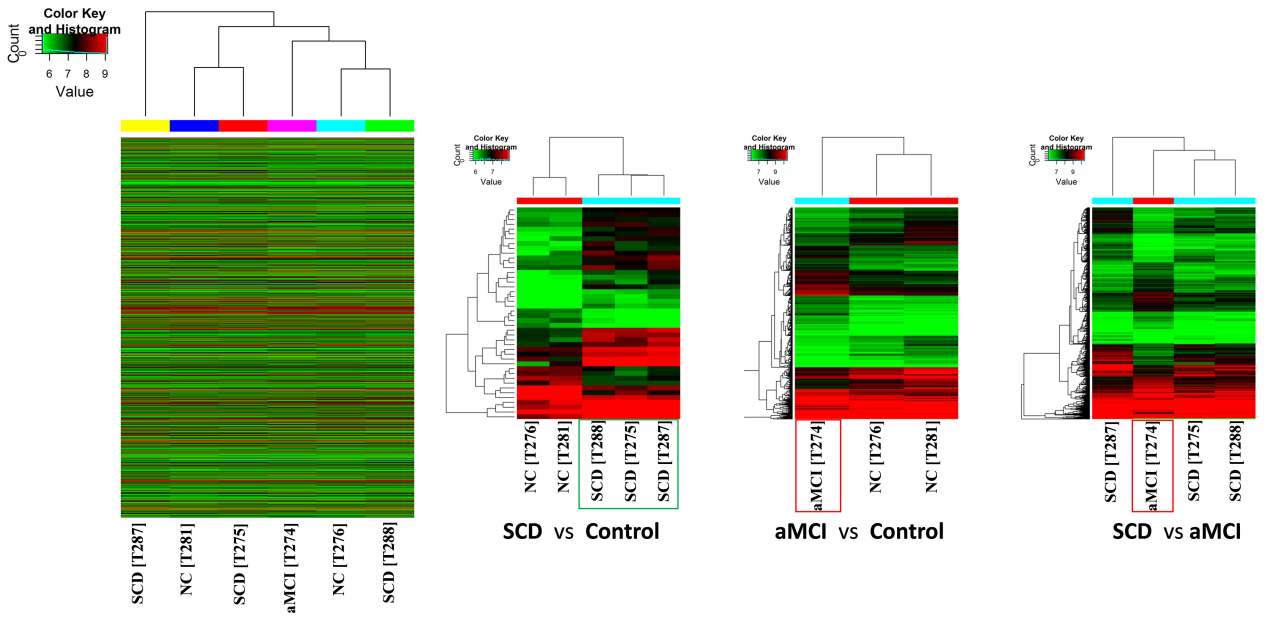

FIGURE 2 | Hierarchical cluster analysis presents the expression profiles of each group. High relative expression is indicated by red color while low relative expression is in green color. Expression profiles of similar groups were clustered and represented through the dendrogram. Heat maps of each comparison show the higher relative expression of SCD samples as compared to controls. Control samples (C276 and C281) and test samples (SCD: T275, T287, and T288 and aMCI: T274).

TABLE 2 | Top 10 (upregulated and downregulated) differentially expressed circRNAs ranked by fold change.

CircRNA	FC	*P*-value	Chr.	Best transcript	Gene symbol	Regulation
hsa_circRNA_001481	3.6248831	0.02314	Chr5	NM_198449	EMB	UP
hsa_circRNA_016545	3.0679614	0.03505	Chr1	NM_001748	CAPN2	UP
hsa_circRNA_101543	2.4627691	0.00618	Chr15	NM_017684	VPS13C	UP
hsa_circRNA_100141	2.0285053	0.02437	Chr1	NM_080391	PTP4A2	UP
hsa_circRNA_078353	2.0063117	0.00326	chr6	NM_014892	SCAF8	UP
hsa_circRNA_104062	1.9204745	0.04166	Chr6	NM_005493	RANBP9	UP
hsa_circRNA_100978	1.9727913	0.02646	Chr11	NM_152715	TBCEL	UP
hsa_circRNA_000479	1.9500463	0.03432	Chr13	NM_033255	EPSTI1	UP
hsa_circRNA_003601	1.8470151	0.02749	Chr1	NM_018056	TMEM39B	Down
hsa_circRNA_042200	1.7439849	0.00482	Chr17	NR_027160	LRRC75A-AS1	Down

TABLE 3 | Top five miRNA binding sites of top differentially expressed circRNAs.

CircRNAs	MRE1	MRE2	MRE3	MRE4	MRE5
hsa_circRNA_001481	hsa-miR-1252-5p	hsa-miR-4644	hsa-miR-548m	hsa-miR-6758-5p	hsa-miR-6797-5p
hsa_circRNA_016545	hsa-miR-5193	hsa-miR-4685-5p	hsa-miR-339-5p	hsa-miR-6836-5p	hsa-miR-4638-5p
hsa_circRNA_101543	hsa-miR-643	hsa-miR-337-3p	hsa-miR-100-3p	hsa-miR-632	hsa-miR-19b-2-5p
hsa_circRNA_100141	hsa-miR-217	hsa-miR-574-5p	hsa-miR-595	hsa-miR-1323	hsa-miR-203a-3p
hsa_circRNA_078353	hsa-miR-6787-5p	hsa-miR-3960	hsa-miR-8072	hsa-miR-3141	hsa-miR-149-3p
hsa_circRNA_104062	hsa-miR-376c-5p	hsa-miR-376b-5p	hsa-miR-150-5p	hsa-miR-891a-3p	hsa-miR-135b-5p
hsa_circRNA_100978	hsa-miR-651-3p	hsa-miR-298	hsa-miR-154-5p	hsa-miR-335-3p	hsa-miR-424-5p
hsa_circRNA_000479	hsa-miR-942-5p	hsa-miR-4753-3p	hsa-miR-6873-3p	hsa-miR-6739-3p	hsa-miR-6809-3p
hsa_circRNA_003601	hsa-miR-214-3p	hsa-miR-3619-5p	hsa-miR-761	hsa-miR-634	hsa-miR-1226-3p
hsa_circRNA_042200	hsa-miR-612	hsa-miR-661	hsa-miR-6860	hsa-miR-6774-5p	hsa-miR-1285-3p

for verification through RT-qPCR. As compared with the reference, hsa_circRNA_001481 and hsa_circRNA_000479 were significantly upregulated in the test samples (**Figure 3**).

The hsa_circRNA_001481 has been identified as significantly upregulated in SCD and aMCI compared with control samples and further verified through RT-qPCR. Upregulated expressed

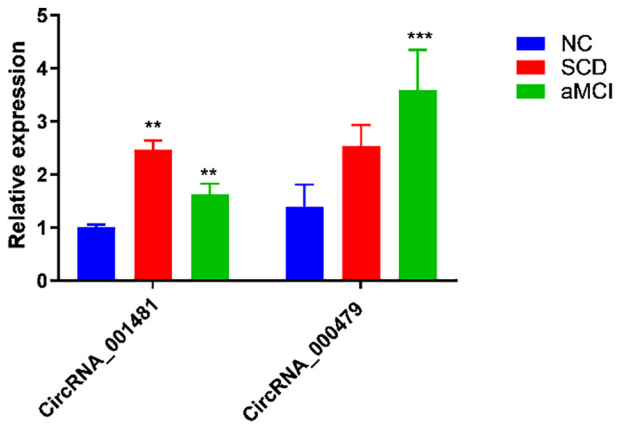

FIGURE 3 | RT-qPCR analysis of hsa_circRNA_001481 and hsa_circRNA_000479. The relative expression of SCD and aMCI are significantly upregulated in hsa_circRNA_001481 as compared to NC. The relatively higher expression in aMCI is also observed in hsa_circRNA_000479. The values are the average values of three independent experiments (**$P < 0.01$, ***$P < 0.001$).

circRNAs between control versus SCD revealed the highest fold change 3.62 of hsa_circRNA_001481, while 2.40 and 1.51 FC in control versus aMCI and SCD versus aMCI samples were identified, respectively. The hsa_circRNA_001481 is a sense-overlapping circRNA and its official gene symbol is EMB that is located on the negative strand of chromosome 5. The significant upregulation of hsa_circRNA_000479 in microarray analysis was also validated by RT-qPCR. The fold change 1.9 of this circRNA was observed in SCD versus control groups, while 2.2 was observed in the upregulation of SCD versus aMCI. This exonic circRNA is located on the negative strand of chromosome13 and its gene symbol is Epithelial stromal interaction 1 (EPSTI1).

The binding sites of these circRNAs are analyzed to mediate the interactions of miRNA with MREs and to determine the target interactions of circRNAs. The details of MREs of both hsa_circRNA_001481 and hsa_circRNA_000479 are provided in **Supplementary File 2**.

Construction of Circular RNAs-MicroRNAs-mRNA Networks

Circular RNAs act as miRNA sponges that play significant roles in various diseases. Therefore, the interaction network of circRNAs-miRNA-mRNA was predicted and constructed to identify the potential functions of differentially expressed circRNAs. miRDB and miRWalk 3.0 (also utilizes miRTarBase, miRDB, and TargetScan databases) were used to predict the miRNA targets. The miRWalk 3.0 predicts the targets through the experimentally validated interactions and machine learning algorithm. The top target genes were selected for each miRNA for the construction of circRNAs-miRNA-mRNA interactions through the bioinformatics tools, that is, Cytoscape 3.6. The target interaction network of hsa_circRNA_001481 was constructed and presented in **Figure 4A**. The upregulated hsa_circRNA_001481 was predicted to inhibit the expression level of hsa-miR-1252-5p, hsa-miR-4644, hsa-miR-548m, hsa-miR-6758-5p, and hsa-miR-6797-5p and further promote the expression of target genes. POU2AF1 and AMMECR1 genes are found as the common targets between hsa-miR-1252-5p and hsa-miR-6758-5p, and between hsa-miR-1252-5p and hsa-miR-548m, respectively.

The MREs of hsa_circRNA_001481 were predicted and shown in **Figure 4B** along with the sequence analysis. The 3′ pairing sequence of hsa_circRNA_001481, target miRNA seed type, and MRE sequence are illustrated in the 2D structure. The element matching perfectly based on their seeds are selected for each miRNA. The miR-548m exhibited

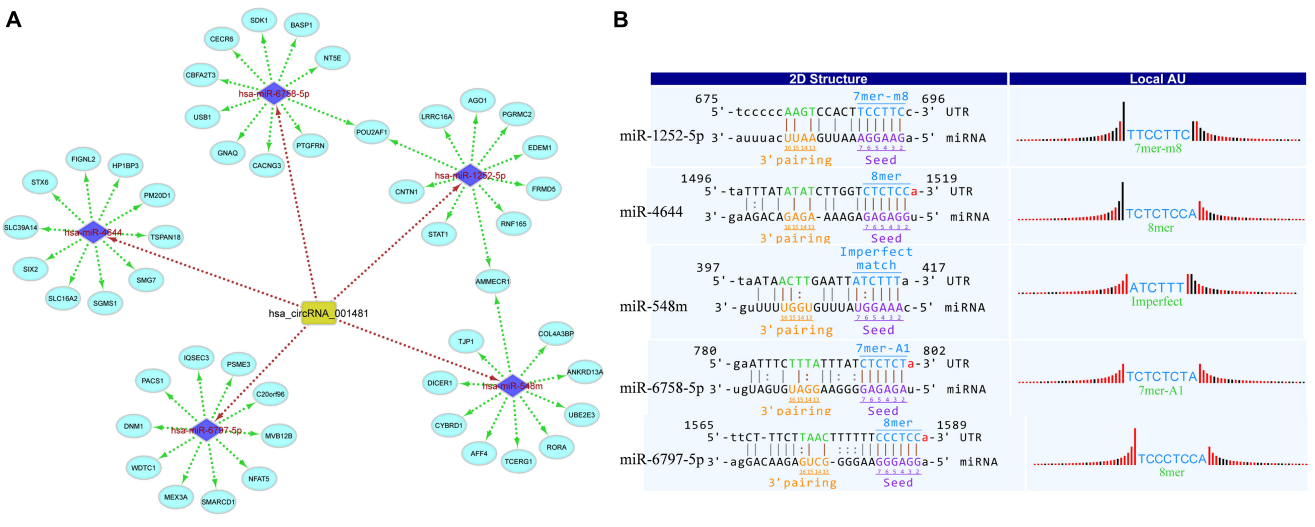

FIGURE 4 | (A) CircRNA_001481_miRNA_mRNA interaction network comprising 5 miRNAs and 50 targets. The top 10 mRNA targets of each miRNA are shown in this network constructed by Cytoscape 3.6. **(B)** Top MREs of miRNAs and 2D structure showing the MRE sequence analysis for hsa_circRNA_001481.

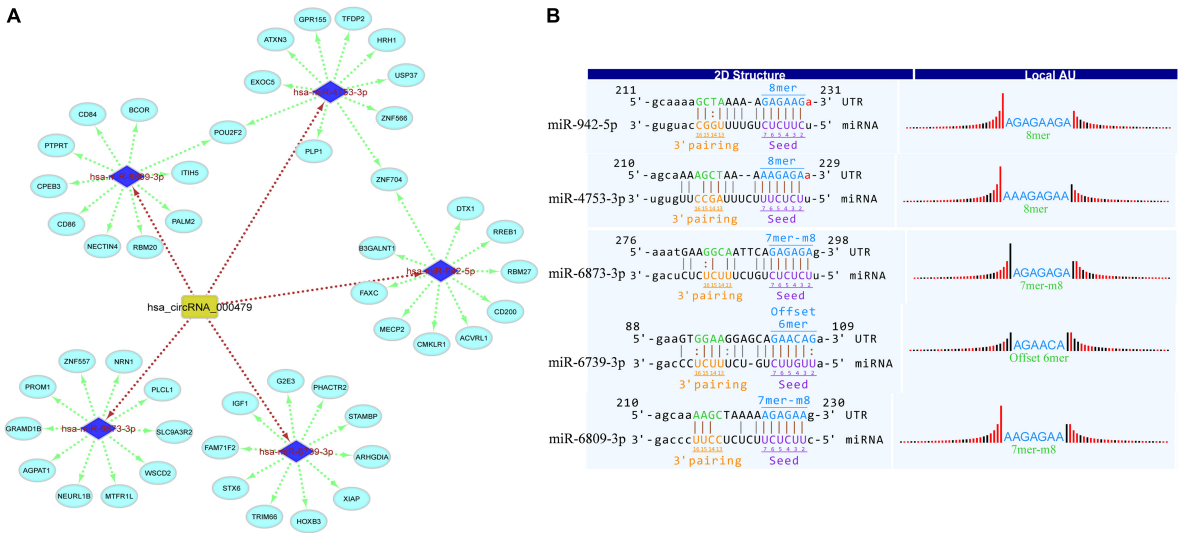

FIGURE 5 | (A) CircRNA_000479_miRNA_mRNA interaction network constructed by Cytoscape. **(B)** Top MREs of hsa_circRNA_000479 are shown, predicted by Targetscan and miRanda databases.

imperfect pairing with their predicted MRE sequence. The hsa_circRNA_000479-miRNA_mRNA network was also constructed which contains 5 miRNAs and 50 targeted genes (**Figure 5A**). The initial-miR-4753-3p displayed the common targets ZNF704 and POU2F2 with hsa-miR-942-5p and hsa-miR-6809-3p, respectively. The upregulated hsa_circRNA_000479 was also predicted to increase the expression level of miRNA target genes through the inhibition of hsa-miR-942-5p, hsa-miR-4753-3p, hsa-miR-6873-3p, hsa-miR-6739-3p, and hsa-miR-6809-3p. The 2D MRE sequence analysis of hsa_circRNA_000479 identified the target miRNA seed type, 3′ pairing sequence for hsa_circRNAs_000479, and MRE sequence as depicted in **Figure 5B**.

GO and Pathway Analysis of Target mRNAs

Both hsa_circRNA_001481 and hsa_circRNA_000479 may play key roles in the molecular mechanisms through the regulation of target mRNAs on the report of these interactions. These putative mRNAs were further investigated in GO, KEGG pathway, and tissue expression analyses for the functional characterization of these circRNAs.

The biological process, molecular function, and cellular component were predicted and analyzed in GO bioinformatics analyses (**Figure 6**). In terms of biological process, nervous system development, positive and negative regulations of transcription, and transcription from RNA polymerase II were identified as significant terms that describe a series of biological activities. Protein binding and transcription factor activity are the meaningful enrichment terms in the category of molecular function showing the functional role at the molecular level. GO Cellular component determined the nucleus and plasma membrane as significant terms elucidating the components of a cell.

The tissue expression analysis was conducted to determine the upregulation of target mRNAs at the tissue level (**Figure 7A**). The upregulations were observed in the brain, epithelium, lymph, and gastric adenocarcinoma in terms of tissue expression. The significant upregulation of these mRNAs was observed in brain tissues which accounts for almost 60% of the total genes providing evidence for the functional verification of hsa_circRNA_001481 and hsa_circRNA_000479. The KEGG pathway analysis exhibited the top three pathways' transcriptional misregulation in cancer, endocytosis, and gap junction (**Figure 7B**). Pathway analysis suggests that these genes may play a significant role in multiple metabolic events.

The GO, tissue expression, and disease analysis of differentially expressed genes (DEGs) from microarray analysis were also conducted to determine the biological functions, cellular component, molecular function, upregulated expression in tissues, and their involvement in diseases. The common DEG genes among upregulated SCD versus control, aMCI versus Control, and SCD versus aMCI were identified through the Venn diagram as represented in **Figure 8A**. The 25 genes from SCD versus Control also common with groups were utilized for their biological functions, biological process, and cellular component (**Figure 8B**). The second analysis involves all mutual DEGs between aMCI versus Control, SCD versus Control, and SCD versus aMCI, which was employed for their upregulation expression in tissues followed by disease analysis (**Figure 9**). It has been seen that the highest number of DEGs have been found in Schizophrenia in disease analysis.

Circular RNAs Act as MicroRNAs Sponges

It has been documented that cirRNAs act as miRNA sponges that competitively suppress and naturally sequester miRNA activity (Hansen et al., 2013). As presumed, CircRNAs can

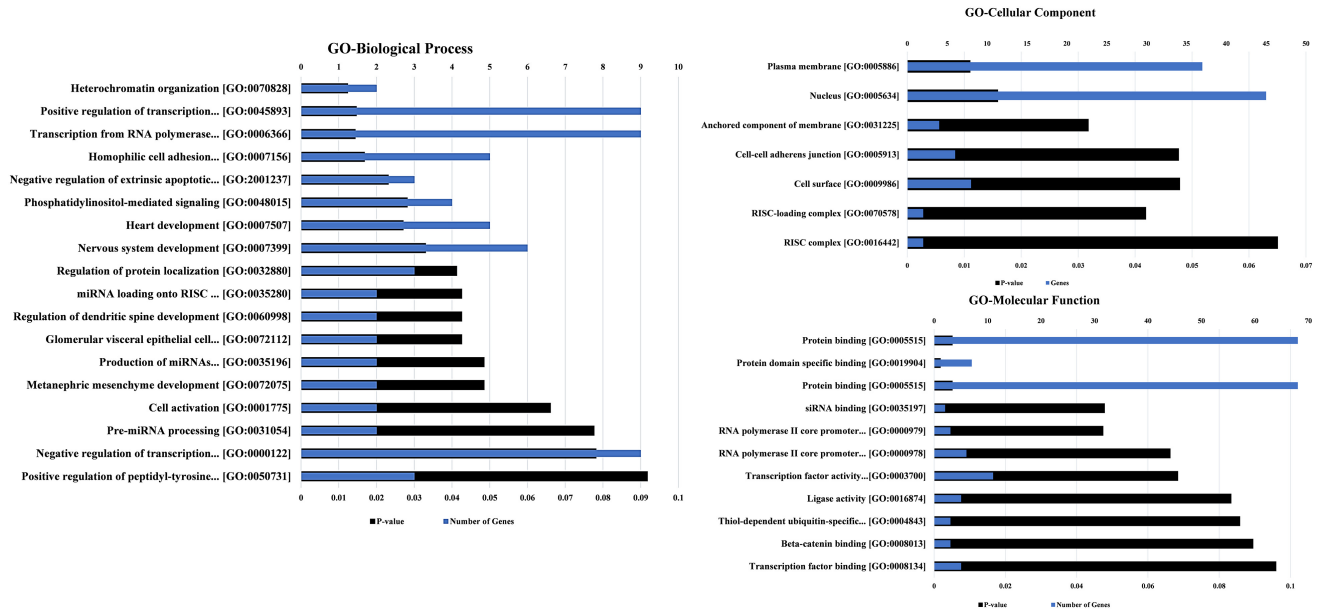

FIGURE 6 | The GO annotations for biological process, molecular function, and cellular component of the predicted mRNAs regulated by both scrutinized circRNAs. The GO annotations along with the number of genes and *P*-value are also mentioned in the chart. The lowest *p*-value is utilized for sorting the GO terms in the figure.

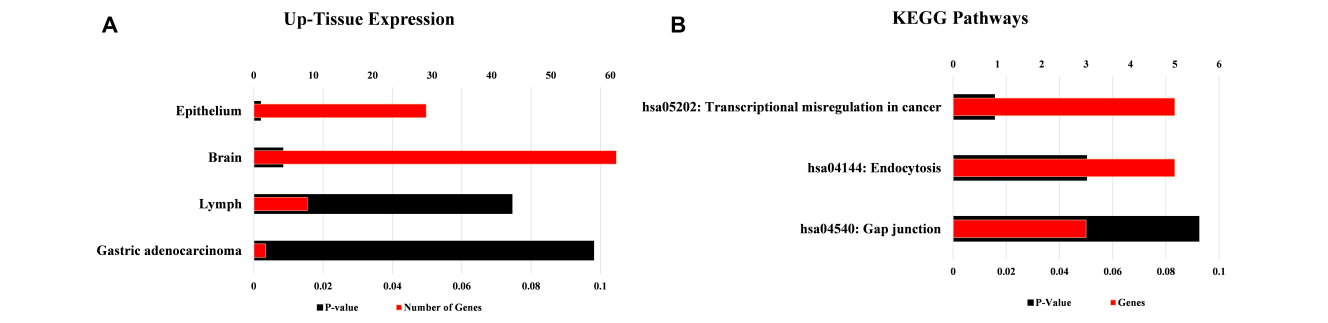

FIGURE 7 | Functional annotations of target mRNAs. **(A)** Up-tissue expression of target mRNAs regulated by these both circRNAs. **(B)** KEGG pathway analysis of these targets' mRNAs.

also function as a decoy to regulate the mRNA expression similarly. It has been proposed and investigated that either hsa_circRNA_001481 or hsa_circRNA_000479 function as competing endogenous RNAs to target miRNAs and suppress their expression. The miRNAs having binding sites at the 3′ UTR region of hsa_circRNA_001481 are hsa-miR-1252-5p, hsa-miR-4644, hsa-miR-548m, hsa-miR-6758-5p, and hsa-miR-6797-5p were determined through bioinformatics analysis as mentioned above. Similarly, hsa-miR-942-5p, hsa-miR-4753-3p, hsa-miR-6873-3p, hsa-miR-6739-3p, and hsa-miR-6809-3p were identified as the target binding miRNAs of hsa_circRNA_000479. Luciferase screening assay was conducted to verify corresponding miRNAs binding to hsa_circRNA_001481 and hsa_circRNA_000479. The miRNAs mimics were co-transfected with the luciferase reporter by utilizing HEK293T cells and determined the expression level with and without circRNAs. The relative luciferase activities were calculated and plotted on a graph through GraphPad Prism8 as shown in **Figure 10**. It has been seen that hsa_circRNA_001481 significantly reduced the expression of hsa-miR-548m ($P < 0.0004$), hsa-miR-1252-5p ($P < 0.0008$), and hsa-miR-4644 ($P < 0.05$) as compared to the controls. Luciferase activities indicate that hsa_circRNA_001481 may function as a sponge for hsa-miR-548m, hsa-miR-1252-5p, and hsa-miR-4644 to regulate the expression level of EMB. There were no convincing variations in the expression level of hsa-miR-6758-5p and hsa-miR-6797-5p that do not show any effect of hsa_circRNA_001481.

The relative luciferase activities of hsa_circRNA_000479 against five miRNAs mimics were calculated and it has been observed that hsa_circRNA_000479 reduced the luciferase reporter activities of hsa-miR-942-5p ($P < 0.0455$), hsa-miR-4753-3p ($P < 0.0001$), and hsa-miR-6739-3p ($P < 0.0001$) as compared with NCs. Luciferase screening suggests

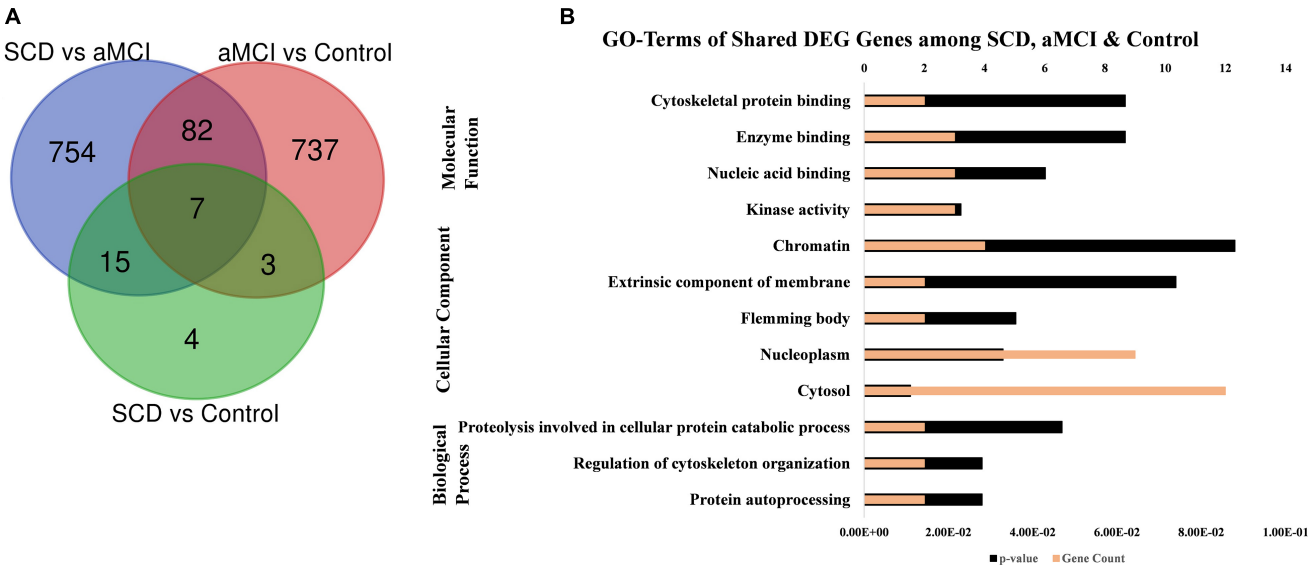

FIGURE 8 | GO annotations of upregulated DEGs among SCD, aMCI, and control groups. **(A)** Venn diagram showing the common upregulated DEG among SCD versus aMCI, aMCI versus control, and SCD versus control. **(B)** GO terms including biological process, molecular function, and cellular component of DEGs (25) from SCD versus control, also share with other SCD versus aMCI and aMCI versus control groups.

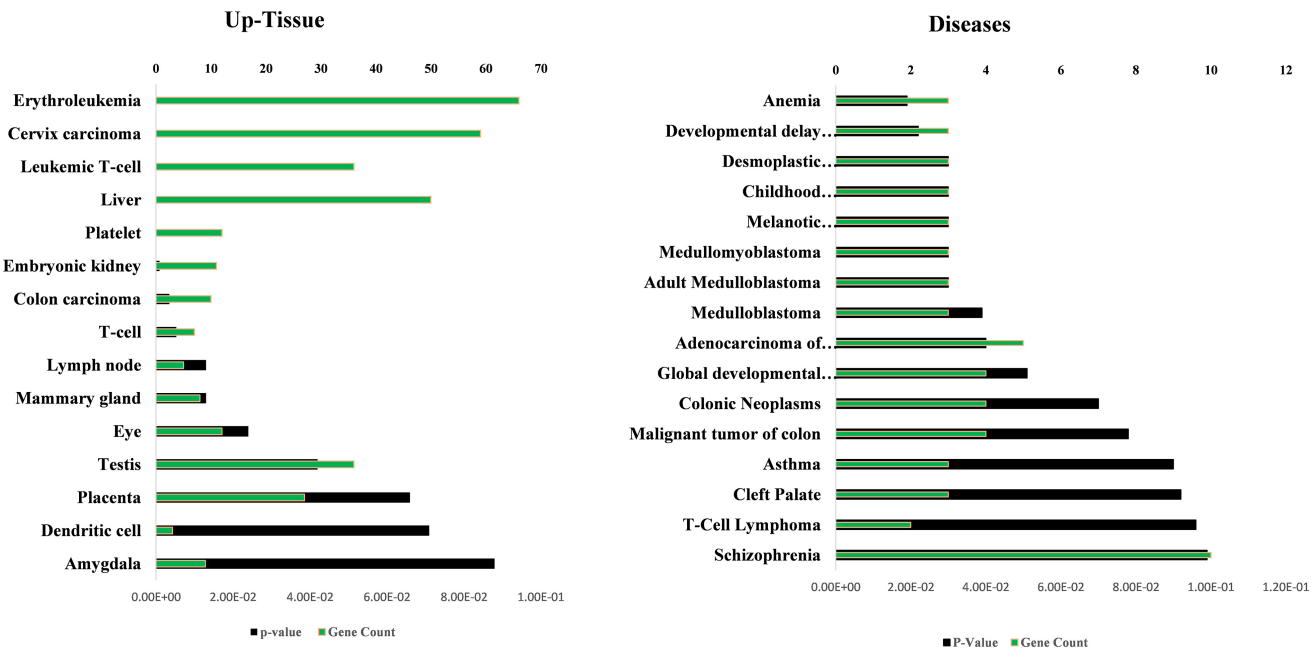

FIGURE 9 | Up-tissue expression and involvement in diseases of all the mutual DEGs (107) between SCD versus aMCI, aMCI versus control, and SCD versus control. The annotation terms are mentioned with a number of genes along with significance (*p*-value).

that hsa_circRNA_000479 may function as a sponge for hsa-miR-942-5p, hsa-miR-4753-3p, and hsa-miR-6739-3p to regulate the expression level of EPSTI1. However, the hsa_circRNA_000479 did not show the sponge properties for hsa-miR-6873-3p and hsa-miR-6809-3p, and hence no expression level differences were detected for both these miRNAs.

The aggregation and differential expression of circRNAs in neural tissues in the course of aging through neural genes have received immense attention in neurosciences (Ashwal-Fluss et al., 2014; Westholm et al., 2014). The highly expressed thousands of circRNAs in the mammalian brain have been reported in the advanced sequencing studies of dissected brain

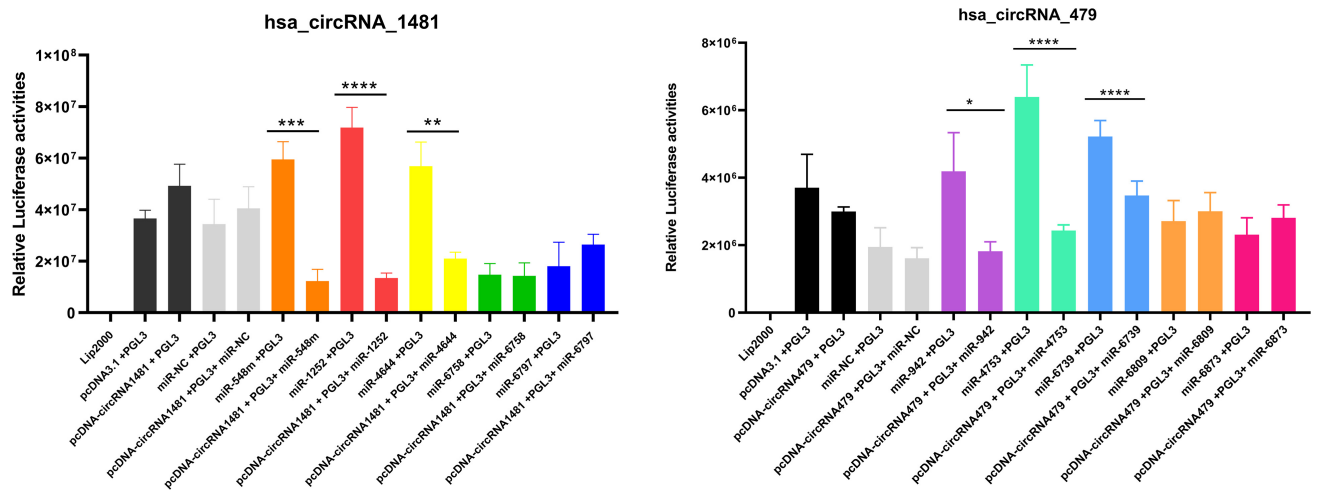

FIGURE 10 | The relative luciferase activities of hsa_circRNA_1481 and hsa_circRNA_000479 showing the expression level of each miRNA. The relative luciferase activities were calculated in HEK293T cells co-transfected by five miRNA mimics are depicted in the bar graph (*$P < 0.05$, **$P < 0.01$, ***$P < 0.001$, and ****$P < 0.0001$). Experimental results are expressed as mean ± standard error.

tissues and differentiated neuronal cell lines. These circRNAs are highly conserved between humans and rodents, developmentally regulated, and enriched in synaptic fractions in neurons (Rybak-Wolf et al., 2015; You et al., 2015).

A study by Rybak-Wolf et al. (2015) has identified a large number of upregulated circRNAs in neuronal differentiation and most of them originated from host genes, involved in neuronal functions. Furthermore, You et al. (2015) utilized an RNA *in situ* hybridization technique to validate the synaptic localization of circRNAs and found the enrichment of circRNAs with a majority of them derived from the genes that encode synaptic proteins in brain samples.

Many circRNAs have been reported and documented in neurological disorders including AD, schizophrenia, Parkinson's disease, and multiple sclerosis (Lukiw, 2013). CircRNA study has become a research hotspot due to their significant roles in disease progression (Zhang et al., 2018) and systematic research is underway to reveal the functional roles of circRNAs and elaborate on the regulation patterns of the human transcriptome (Guo et al., 2014; Rybak-Wolf et al., 2015).

It has been clearly stated from numerous genome-wide surveys that the circRNAs normally arise during the transcription process rather than the circumstantial expression of this type of ncRNAs (Guo et al., 2014; Rybak-Wolf et al., 2015). The dynamic expression of circRNAs in the brain indicates that their accumulation and expression are age-dependent (Westholm et al., 2014). The resistance ability of circRNAs against RNase cleavage extends their stability which enables circRNAs as a preferable choice for molecular markers as compared to linear RNAs (Enuka et al., 2015). The dynamic expression of circRNAs and their transcriptomic analyses in neurodegenerative disorders needs to be performed and demonstrated effectively. The reduced expression of circRNA for miRNA-7 has been reported in AD brains while it comprises tandem antimiRNA-7 sequences (Lukiw, 2013).

In the current investigation, the expression profiles of circRNAs among SCD, aMCI, and AD were discovered to screen the circRNAs mainly through microarray analysis followed by the bioinformatics approaches. SCD is defined as the experience of worsening or more frequent confusion or memory loss. It is a form of cognitive impairment and one of the earliest noticeable symptoms of AD and related dementias. The objectives of the current study were also to identify the potential biomarkers for early onset detection of AD. The three samples of the main SCD group were taken for microarray analysis with a smaller number of samples from other groups. The reliability of differential expressed data is extensively verified through further experimental and computational analyses and techniques. The top 10 differentially expressed up- and downregulated circRNAs extracted from microarray analysis were further validated through qRT-PCR, and hsa-circRNA_001481 and hsa_circRNA_000479 were confirmed with a high degree of sensitivity and specificity. Therefore, the current study is not limited to samples but extensive analyses were carried out to validate the novel potential circRNAs as biomarkers for the early onset detection of AD. In future, the studies will be conducted with a greater number of samples to identify and analyze the novel potential circRNAs.

Our findings have indicated that hsa-circRNA_001481 was significantly upregulated in SCD and aMCI expression profile as compared to the healthy controls highlighting it as a potential biomarker for early stage AD patients.

The EMB gene harbors nine exons that encode an embigin protein having a 30-kDa molecular weight when unglycosylated and its chromosomal location is 5q11.1 (Ozawa et al., 1988). Embigin is involved in the formation of neuromuscular junctions, cell migration, and early embryonic development depending upon neural cell adhesion molecules (Zhou et al., 2020). Embigin upholds the catalytic activity of MCT2 for synergistic transfer of lactic acid between neurons and glial

cells (Wilson et al., 2005), which plays a vital role in long-term procedural memory formation and brain energy metabolism (Pérez-Escuredo et al., 2016).

GWAS study showed the genome-wide significance of the EMB gene with mRNA expression level in cis genetic linkage with rs10940346 associated with schizophrenia (Li et al., 2017). EMB as a susceptible gene for schizophrenia has been confirmed and consistent with the GWAS results (Li et al., 2017; Pardiñas et al., 2018). The polymorphism at 3′-UTR of EMB is prominently linked with schizophrenia in the Chinese Han population but its effect on EMB expression still needs to be elucidated (Zhou et al., 2020).

The hsa_circRNA_000479 also exhibited a higher specificity and sensitivity that might be a non-invasive biomarker for early stage AD patient screening tests. EPSTI1, an interferon response gene was initially recognized in breast cancer that induces stromal fibroblast (Gudjonsson et al., 2003). Mo and Chae (2017) have described the possible role of EPSTI1 as a candidate gene for systematic lupus erythematosus and highlighted that variants at EPSTI1 could be utilized as potential genetic markers for systematic lupus erythematosus susceptibility.

Luo et al. (2016) have conducted a study to determine and compare the expression patterns of AD and vascular dementia (VaD) from peripheral blood samples. A set of signature genes were extracted in the experiment including EPSTI1, which might be the potential biomarkers for early detection of AD and VaD (Luo et al., 2016).

The circRNAs have the potential to be utilized as diagnostic and prognostic biomarkers for various complex disorders due to their high abundance in the human body and their excellent stability (Zhang et al., 2018). An average half-live of circRNAs is 48 h as compared to 10 h for mRNAs in the resistance to RNA endonucleases cleavage (Jeck and Sharpless, 2014). The circRNAs have been extensively studied to determine their potential as non-invasive biomarkers for human diseases but still, many complex mechanisms and functions remain elusive (Li et al., 2015; Memczak et al., 2015; Zhang et al., 2018). The circRNA transcripts are preferable molecules for the actual detection of neurological disorders due to their high abundance in peripheral blood and brain, compared to other tissues. Particularly, circRNA-based detection might be an appropriate approach for neurodegenerative diseases as disruptions of circRNAs-miRNA binding are reported in AD (Lukiw, 2013).

The miRNAs play a vital role in the regulation of gene expression through posttranscriptional regulation, hereby it gained much attention for a better understanding of miRNAs regulatory mechanisms. Recently, miRNA sponging has been identified as one of the key functions of circRNAs that leads to the inhibitory activity of miRNAs (Qi et al., 2015; Meng et al., 2017).

mRNAs and circRNAs utilize MREs for competitively binding to inadequately targeted miRNAs and construct the regulatory network of competing for endogenous RNA (Jeck and Sharpless, 2014). The translation process interrupts due to the binding of mRNA with miRNAs; however, circRNAs remain resistant and stable from the degradation by RNA exonucleases (Panda, 2018; Yu and Liu, 2019). CircRNAs may transport or store miRNAs momentarily, and modulate the expression of miRNA-associated target genes (Duk and Samsonova, 2021). Many studies have documented the significance of miRNAs in the elucidation of molecular pathology in different diseases (Misir et al., 2020a,b). CircRNAs as miRNA sponges and circRNAs-miRNAs-mRNAs networks may deliver a vital role in understanding and modulating the expression of miRNA-related genes in different diseases (Zhao et al., 2019).

The accumulation of circRNAs appears in the brain with time, and so their metabolism can be associated with healthy aging. Age-dependent accumulation of circRNA transcripts has been determined in Drosophila neural tissue (Westholm et al., 2014) and demonstrating that the function of circRNAs is a well-conserved genomic feature for brain physiology. The circRNA transcriptome is also widely reshaped through porcine and human brain development (Szabo et al., 2015; Venø et al., 2015). The fact that the expression patterns of circRNAs are affected during aging or neurodegeneration processes could be determined to identify and study the more promising circRNAs biomarkers for human diseases and their clinical implementation.

CONCLUSION

The current study reported the preferentially expressed profiles of circRNAs from the blood samples susceptible to AD individuals. Human microarray analysis followed by bioinformatics approaches revealed the hsa_circRNA_001481 and hsa_circRNA_000479 as differentially expressed circRNAs that could be utilized for early diagnosis of AD. The precise expression and stability of numerous circRNAs enable them to model candidates as diagnostic tools in neurodegenerative disorders and aging. The circRNAs-based effective therapeutic approaches and diagnostic biomarkers could be developed for AD through the molecular insights of circRNAs in disease development. Collectively, circRNAs are novel promising and favorable biomarkers for human diseases owing to distinct functional and structural features. Recent advances in Biotechnology and Bioinformatics will assist to determine the increasingly circRNAs as potential biomarkers for clinical applications.

DATA AVAILABILITY STATEMENT

The original contributions presented in this study are included in the article/**Supplementary Material**, further inquiries can be directed to the corresponding authors.

ETHICS STATEMENT

The studies involving human participants were reviewed and approved by Han Ying, Department of Neurology, Xuanwu Hospital of Capital Medical University, Beijing, China. The

patients/participants provided their written informed consent to participate in this study.

AUTHOR CONTRIBUTIONS

HQ, YH, and ZQ conceived, designed, and supervised the experiments and manuscript. DZ, RT, and YY conducted the sampling and further lab experiments. RT performed the computational analyses and drafted the manuscript. All authors contributed to the article and approved the submitted version.

FUNDING

This work was supported by the National Natural Science Foundation of China (Grant nos. 81870844, 92049102, 61633018, and 82020108013).

SUPPLEMENTARY MATERIAL

The Supplementary Material for this article can be found online at: https://www.frontiersin.org/articles/10.3389/fnins.2022.878287/full#supplementary-material

REFERENCES

Abdelmohsen, K., Panda, A. C., Munk, R., Grammatikakis, I., Dudekula, D. B., De, S., et al. (2017). Identification of HuR target circular RNAs uncovers suppression of PABPN1 translation by CircPABPN1. *RNA Biol.* 14, 361–369. doi: 10.1080/15476286.2017.1279788

Alzheimer's Association (2019). 2019 Alzheimer's disease facts and figures. *Alzheimer's Dement.* 15, 321–387.

Ashwal-Fluss, R., Meyer, M., Pamudurti, N. R., Ivanov, A., Bartok, O., Hanan, M., et al. (2014). circRNA biogenesis competes with pre-mRNA splicing. *Mol. Cell* 56, 55–66. doi: 10.1016/j.molcel.2014.08.019

Barrett, S. P., and Salzman, J. (2016). Circular RNAs: analysis, expression and potential functions. *Development* 143, 1838–1847. doi: 10.1242/dev.128074

Chen, L.-L. (2016). The biogenesis and emerging roles of circular RNAs. *Nat. Rev. Mol. Cell Biol.* 17:205. doi: 10.1038/nrm.2015.32

Chen, X., Farrell, M. E., Moore, W., and Park, D. C. (2019). Actual memory as a mediator of the amyloid-subjective cognitive decline relationship. *Alzheimers Dement.* 11, 151–160. doi: 10.1016/j.dadm.2018.12.007

Chen, Y., and Wang, X. (2020). miRDB: an online database for prediction of functional microRNA targets. *Nucleic acids Res.* 48, D127–D131. doi: 10.1093/nar/gkz757

Duk, M., and Samsonova, M. (2021). The Pros and Cons of Circular RNAs as miRNA Sponges. *Biophysics* 66, 8–16.

Enright, A. J., John, B., Gaul, U., Tuschl, T., Sander, C., and Marks, D. S. (2003). MicroRNA targets in Drosophila. *Genome Biol.* 5:R1.

Enuka, Y., Lauriola, M., Feldman, M. E., Sas-Chen, A., Ulitsky, I., and Yarden, Y. (2015). Circular RNAs are long-lived and display only minimal early alterations in response to a growth factor. *Nucleic Acids Res.* 44, 1370–1383. doi: 10.1093/nar/gkv1367

GraphPad Software (2019). One-Way ANOVA Followed by Dunnett's Multiple Comparisons Test Was Performed Using GraphPad Prism Version 8.0.0 for Windows. San Diego: GraphPad Software.

Gudjonsson, T., Rønnov-Jessen, L., Villadsen, R., Bissell, M. J., and Petersen, O. W. (2003). To create the correct microenvironment: three-dimensional heterotypic collagen assays for human breast epithelial morphogenesis and neoplasia. *Methods* 30, 247–255. doi: 10.1016/s1046-2023(03)00031-8

Guo, J. U., Agarwal, V., Guo, H., and Bartel, D. P. (2014). Expanded identification and characterization of mammalian circular RNAs. *Genome Biol.* 15:409. doi: 10.1186/s13059-014-0409-z

Han, D., Li, J., Wang, H., Su, X., Hou, J., Gu, Y., et al. (2017). Circular RNA circMTO1 acts as the sponge of microRNA-9 to suppress hepatocellular carcinoma progression. *Hepatology* 66, 1151–1164. doi: 10.1002/hep.29270

Hansen, T. B., Jensen, T. I., Clausen, B. H., Bramsen, J. B., Finsen, B., Damgaard, C. K., et al. (2013). Natural RNA circles function as efficient microRNA sponges. *Nature* 495:384. doi: 10.1038/nature11993

Heron, M. P. (2018). Deaths: leading causes for 2016. *Natl. Vital Stat. Rep.* 67, 1–77.

Idda, M. L., Munk, R., Abdelmohsen, K., and Gorospe, M. (2018). Noncoding RNAs in Alzheimer's disease. *Wiley Interdiscip. Rev. RNA.* 9:e1463.

Jack, C. R. Jr., Bennett, D. A., Blennow, K., Carrillo, M. C., Dunn, B., Haeberlein, S. B., et al. (2018). NIA-AA research framework: toward a biological definition of Alzheimer's disease. *Alzheimer's Dement.* 14, 535–562. doi: 10.1016/j.jalz.2018.02.018

Jeck, W. R., and Sharpless, N. E. (2014). Detecting and characterizing circular RNAs. *Nat. Biotechnol.* 32:453.

Jessen, F., Amariglio, R. E., Buckley, R. F., van der Flier, W. M., Han, Y., Molinuevo, J. L., et al. (2020). The characterisation of subjective cognitive decline. *Lancet Neurol.* 19, 271–278. doi: 10.1016/S1474-4422(19)30368-0

Jessen, F., Amariglio, R. E., Van Boxtel, M., Breteler, M., Ceccaldi, M., Chételat, G., et al. (2014). A conceptual framework for research on subjective cognitive decline in preclinical Alzheimer's disease. *Alzheimer's Dement.* 10, 844–852. doi: 10.1016/j.jalz.2014.01.001

Jiang, L., Sui, D., Qiao, K., Dong, H.-M., Chen, L., and Han, Y. (2018). Impaired functional criticality of human brain during Alzheimer's disease progression. *Sci. Rep.* 8:1324 . doi: 10.1038/s41598-018-19674-7

Lewis, B. P., Burge, C. B., and Bartel, D. P. (2005). Conserved seed pairing, often flanked by adenosines, indicates that thousands of human genes are microRNA targets. *Cell* 120, 15–20. doi: 10.1016/j.cell.2004.12.035

Li, Y., Zheng, Q., Bao, C., Li, S., Guo, W., Zhao, J., et al. (2015). Circular RNA is enriched and stable in exosomes: a promising biomarker for cancer diagnosis. *Cell Res.* 25, 981–984. doi: 10.1038/cr.2015.82

Li, Z., Chen, J., Yu, H., He, L., Xu, Y., Zhang, D., et al. (2017). Genome-wide association analysis identifies 30 new susceptibility loci for schizophrenia. *Nat. Genet.* 49:1576. doi: 10.1038/ng.3973

Liu, W., Ma, W., Yuan, Y., Zhang, Y., and Sun, S. (2018). Circular RNA hsa_circRNA_103809 promotes lung cancer progression via facilitating ZNF121-dependent MYC expression by sequestering miR-4302. *Biochem. Biophys. Res. Commun.* 500, 846–851. doi: 10.1016/j.bbrc.2018.04.172

Lu, D., and Xu, A.-D. (2016). Mini review: circular RNAs as potential clinical biomarkers for disorders in the central nervous system. *Front. Genet.* 7:53. doi: 10.3389/fgene.2016.00053

Lukiw, W. (2013). Circular RNA (circRNA) in Alzheimer's disease (AD). *Front. Genet.* 4:307. doi: 10.3389/fgene.2013.00307

Luo, H., Han, G., Wang, J., Zeng, F., Li, Y., Shao, S., et al. (2016). Common aging signature in the peripheral blood of vascular dementia and Alzheimer's disease. *Mol. Neurobiol.* 53, 3596–3605. doi: 10.1007/s12035-015-9288-x

Memczak, S., Papavasileiou, P., Peters, O., and Rajewsky, N. (2015). Identification and characterization of circular RNAs as a new class of putative biomarkers in human blood. *PLoS One* 10:e0141214. doi: 10.1371/journal.pone.0141214

Meng, S., Zhou, H., Feng, Z., Xu, Z., Tang, Y., Li, P., et al. (2017). CircRNA: functions and properties of a novel potential biomarker for cancer. *Mol. Cancer* 16:94. doi: 10.1186/s12943-017-0663-2

Misir, S., Aliyazicioglu, Y., Demir, S., Turan, I., and Hepokur, C. (2020a). Effect of Turkish propolis on miRNA expression, cell cycle, and apoptosis in human breast cancer (MCF-7) cells. *Nutri. Cancer* 72, 133–145. doi: 10.1080/01635581.2019.1616100

Misir, S., Hepokur, C., Aliyazicioglu, Y., and Enguita, F. J. (2020b). Circular RNAs serve as miRNA sponges in breast cancer. *Breast Cancer* 27, 1048–1057. doi: 10.1007/s12282-020-01140-w

Mo, J.-S., and Chae, S.-C. (2017). EPSTI1 polymorphisms are associated with systemic lupus erythematosus. *Genes Genomics* 39, 445–451.

Ozawa, M., Huang, R.-P., Furukawa, T., and Muramatsu, T. (1988). A teratocarcinoma glycoprotein carrying a developmentally regulated carbohydrate marker is a member of the immunoglobulin gene superfamily. *J. Biol. Chem.* 263, 3059–3062.

Panda, A. C. (2018). Circular RNAs act as miRNA sponges. *Circular RNAs* 1087, 67–79.

Pardiñas, A. F., Holmans, P., Pocklington, A. J., Escott-Price, V., Ripke, S., Carrera, N., et al. (2018). Common schizophrenia alleles are enriched in mutation-intolerant genes and in regions under strong background selection. *Nat. Genet.* 50, 381–389.

Patterson, C. (2018). *World Alzheimer Report 2018: the State of the Art of Dementia Research: New Frontiers*. London, U. K: Alzheimer's Disease International.

Pérez-Escuredo, J., Van Hée, V. F., Sboarina, M., Falces, J., Payen, V. L., Pellerin, L., et al. (2016). Monocarboxylate transporters in the brain and in cancer. *Biochim. Biophys. Acta(BBA)-Mol. Cell Res.* 1863, 2481–2497. doi: 10.1016/j.bbamcr.2016.03.013

Qi, X., Zhang, D.-H., Wu, N., Xiao, J.-H., Wang, X., and Ma, W. (2015). ceRNA in cancer: possible functions and clinical implications. *J. Medical Genet.* 52, 710–718. doi: 10.1136/jmedgenet-2015-103334

Rybak-Wolf, A., Stottmeister, C., Glažar, P., Jens, M., Pino, N., Giusti, S., et al. (2015). Circular RNAs in the mammalian brain are highly abundant, conserved, and dynamically expressed. *Mol. Cell* 58, 870–885. doi: 10.1016/j.molcel.2015.03.027

Salzman, J., Chen, R. E., Olsen, M. N., Wang, P. L., and Brown, P. O. (2013). Cell-type specific features of circular RNA expression. *PLoS Genet.* 9:e1003777. doi: 10.1371/journal.pgen.1003777

Salzman, J., Gawad, C., Wang, P. L., Lacayo, N., and Brown, P. O. (2012). Circular RNAs are the predominant transcript isoform from hundreds of human genes in diverse cell types. *PLoS One* 7:e30733. doi: 10.1371/journal.pone.0030733

Schultz, S. A., Oh, J. M., Koscik, R. L., Dowling, N. M., Gallagher, C. L., Carlsson, C. M., et al. (2015). Subjective memory complaints, cortical thinning, and cognitive dysfunction in middle-age adults at risk of AD. *Alzheimers Dement.* 1, 33–40. doi: 10.1016/j.dadm.2014.11.010

Shannon, P., Markiel, A., Ozier, O., Baliga, N. S., Wang, J. T., Ramage, D., et al. (2003). Cytoscape: a software environment for integrated models of biomolecular interaction networks. *Genome Res.* 13, 2498–2504. doi: 10.1101/gr.1239303

Sherman, B. T., and Lempicki, R. A. (2009). Systematic and integrative analysis of large gene lists using DAVID bioinformatics resources. *Nat. Protocols* 4:44. doi: 10.1038/nprot.2008.211

Shi, Z., Chen, T., Yao, Q., Zheng, L., Zhang, Z., Wang, J., et al. (2017). The circular RNA ciRS-7 promotes APP and BACE1 degradation in an NF-κB-dependent manner. *FEBS J* 284, 1096–1109. doi: 10.1111/febs.14045

Snitz, B. E., Lopez, O. L., McDade, E., Becker, J. T., Cohen, A. D., Price, J. C., et al. (2015). Amyloid-β imaging in older adults presenting to a memory clinic with subjective cognitive decline: a pilot study. *J. Alzheimer's Dis.* 48, S151–S159. doi: 10.3233/JAD-150113

Starke, S., Jost, I., Rossbach, O., Schneider, T., Schreiner, S., Hung, L.-H., et al. (2015). Exon circularization requires canonical splice signals. *Cell Rep.* 10, 103–111. doi: 10.1016/j.celrep.2014.12.002

Sun, Y., Dai, Z., Li, Y., Sheng, C., Li, H., Wang, X., et al. (2016). Subjective cognitive decline: mapping functional and structural brain changes—a combined resting-state functional and structural MR imaging study. *Radiology* 281, 185–192. doi: 10.1148/radiol.2016151771

Szabo, L., Morey, R., Palpant, N. J., Wang, P. L., Afari, N., Jiang, C., et al. (2015). Statistically based splicing detection reveals neural enrichment and tissue-specific induction of circular RNA during human fetal development. *Genome Biol.* 16:126.

Venø, M. T., Hansen, T. B., Venø, S. T., Clausen, B. H., Grebing, M., Finsen, B., et al. (2015). Spatio-temporal regulation of circular RNA expression during porcine embryonic brain development. *Genome Biol.* 16:245. doi: 10.1186/s13059-015-0801-3

Wang, Q., Qu, L., Chen, X., Zhao, Y.-H., and Luo, Q. (2018). Progress in understanding the relationship between circular RNAs and neurological disorders. *J. Mol. Neurosci.* 65, 546–556. doi: 10.1007/s12031-018-1125-z

Wang, Y., and Wang, Z. (2015). Efficient backsplicing produces translatable circular mRNAs. *RNA* 21, 172–179. doi: 10.1261/rna.048272.114

Westholm, J. O., Miura, P., Olson, S., Shenker, S., Joseph, B., Sanfilippo, P., et al. (2014). Genome-wide analysis of drosophila circular RNAs reveals their structural and sequence properties and age-dependent neural accumulation. *Cell Rep.* 9, 1966–1980. doi: 10.1016/j.celrep.2014.10.062

Wilson, M. C., Meredith, D., Fox, J. E. M., Manoharan, C., Davies, A. J., and Halestrap, A. P. (2005). Basigin (CD147) Is the Target for Organomercurial Inhibition of Monocarboxylate Transporter Isoforms 1 and 4 the ancillary protein for the insensitive MCT2 is EMBIGIN (gp70). *J. Biol. Chem.* 280, 27213–27221. doi: 10.1074/jbc.M411950200

You, X., Vlatkovic, I., Babic, A., Will, T., Epstein, I., Tushev, G., et al. (2015). Neural circular RNAs are derived from synaptic genes and regulated by development and plasticity. *Nat. Neurosci.* 18:603. doi: 10.1038/nn.3975

Yu, L., and Liu, Y. (2019). circRNA_0016624 could sponge miR-98 to regulate BMP2 expression in postmenopausal osteoporosis. *Biochem. Biophys. Res. Commun.* 516, 546–550. doi: 10.1016/j.bbrc.2019.06.087

Zhang, Y., Liu, H., Li, W., Yu, J., Li, J., Shen, Z., et al. (2017). CircRNA_100269 is downregulated in gastric cancer and suppresses tumor cell growth by targeting miR-630. *Aging* 9:1585. doi: 10.18632/aging.101254

Zhang, Z., Yang, T., and Xiao, J. (2018). Circular RNAs: promising biomarkers for human diseases. *EBioMedicine* 34, 267–274.

Zhao, W., Dong, M., Pan, J., Wang, Y., Zhou, J., Ma, J., et al. (2019). Circular RNAs: a novel target among non-coding RNAs with potential roles in malignant tumors. *Mol. Medicine Rep.* 20, 3463–3474. doi: 10.3892/mmr.2019.10637

Zhou, J., Ma, C., Wang, K., Li, X., Zhang, H., Chen, J., et al. (2020). Rare and common variants analysis of the EMB gene in patients with schizophrenia. *BMC Psychiat* 20:1–11. doi: 10.1186/s12888-020-02513-3

Conflict of Interest: The authors declare that the research was conducted in the absence of any commercial or financial relationships that could be construed as a potential conflict of interest.

Publisher's Note: All claims expressed in this article are solely those of the authors and do not necessarily represent those of their affiliated organizations, or those of the publisher, the editors and the reviewers. Any product that may be evaluated in this article, or claim that may be made by its manufacturer, is not guaranteed or endorsed by the publisher.

frontiers | Frontiers in Aging Neuroscience

REVIEW
published: 08 July 2022
doi: 10.3389/fnagi.2022.879114

Nanomedicines in the Management of Alzheimer's Disease: Current View and Future Prospects

Hitesh Chopra[1], Shabana Bibi[2,3], Inderbir Singh[1], Mohammad Amjad Kamal[4,5,6,7], Fahadul Islam[6], Fahad A. Alhumaydhi[8], Talha Bin Emran[6,9]* and Simona Cavalu[10]**

[1] Chitkara College of Pharmacy, Chitkara University, Punjab, India, [2] Department of Biosciences, Shifa Tameer-e-Millat University, Islamabad, Pakistan, [3] Yunnan Herbal Laboratory, College of Ecology and Environmental Sciences, Yunnan University, Kunming, China, [4] Institutes for Systems Genetics, Frontiers Science Center for Disease-Related Molecular Network, West China Hospital, Sichuan University, Chengdu, China, [5] King Fahd Medical Research Center, King Abdulaziz University, Jeddah, Saudi Arabia, [6] Department of Pharmacy, Faculty of Allied Health Sciences, Daffodil International University, Dhaka, Bangladesh, [7] Enzymoics, Novel Global Community Educational Foundation, Hebersham, NSW, Australia, [8] Department of Medical Laboratories, College of Applied Medical Sciences, Qassim University, Buraydah, Saudi Arabia, [9] Department of Pharmacy, BGC Trust University Bangladesh, Chittagong, Bangladesh, [10] Faculty of Medicine and Pharmacy, University of Oradea, Oradea, Romania

Alzheimer's disease (AD) is a kind of dementia that creates serious challenges for sufferers' memory, thinking, and behavior. It commonly targeting the aging population and decay the brain cells, despite attempts have been performed to enhance AD diagnostic and therapeutic techniques. Hence, AD remains incurable owing to its complex and multifactorial consequences and still there is lack of appropriate diagnostics/therapeutics option for this severe brain disorder. Therefore, nanotechnology is currently bringing new tools and insights to improve the previous knowledge of AD and ultimately may provide a novel treatment option and a ray of hope to AD patients. Here in this review, we highlighted the nanotechnologies-based findings for AD, in both diagnostic and therapeutic aspects and explained how advances in the field of nanotechnology/nanomedicine could enhance patient prognosis and quality of life. It is highly expected these emerging technologies could bring a research-based revolution in the field of neurodegenerative disorders and may assist their clinical experiments and develop an efficacious drug for AD also. The main aim of review is to showcase readers the recent advances in nanotechnology-based approaches for treatment and diagnosing of AD.

Keywords: Alzheimer's disease, neurodegenerative disorders, nanotechnology, nanomedicine, dementia, aging

OPEN ACCESS

Edited by:
Angelina Angelova, UMR 8612 Institut Galien Paris Sud (IGPS), France

Reviewed by:
Piera Di Martino, University of Camerino, Italy
Abu Montakim Tareq, University of Houston, United States
Chy Mohammad Monirul Hasan, National University of Malaysia, Malaysia
Ahmed Rakib, University of Tennessee Health Science Center (UTHSC), United States

***Correspondence:**
Shabana Bibi
shabana.bibi.stmu@gmail.com
Talha Bin Emran
talhabmb@bgctub.ac.bd
Simona Cavalu
simona.cavalu@gmail.com

Specialty section:
This article was submitted to Alzheimer's Disease and Related Dementias, a section of the journal Frontiers in Aging Neuroscience

Received: *18 February 2022*
Accepted: *17 June 2022*
Published: *08 July 2022*

Citation:
Chopra H, Bibi S, Singh I, Kamal MA, Islam F, Alhumaydhi FA, Emran TB and Cavalu S (2022) Nanomedicines in the Management of Alzheimer's Disease: Current View and Future Prospects. Front. Aging Neurosci. 14:879114. doi: 10.3389/fnagi.2022.879114

INTRODUCTION

Alzheimer's disease (AD) is frequently linked to memory loss and other critical cognitive abilities (Anand et al., 2014). The most common cause of dementia in the world is AD (Alzheimer's Association, 2022). Although growing older is an established risk factor, AD is not a natural aspect of becoming older. Since the symptoms of AD grow with time, it's important to monitor progress (Soliman et al., 2021; Walia et al., 2021). Although there is presently no cure for the condition, it may be slowed down by the use of medicines. AD is the result of a complex interplay of factors. The pathogenesis of this disease is still being re-examined (Tran and Ha-Duong, 2015). Cortical atrophy and the loss of neurons in the parietal and temporal lobes are hallmarks of AD (Walia et al., 2021).

The brain's ventricles also grow in size when brain mass diminishes (Tiwari et al., 2019). Slowly, the person's cognition alters as a result of brain tissue alterations.

Patients with Alzheimer's have higher quantities of extracellular amyloid in their brains compared to those with normal aging (Liu et al., 2015a). Neocortical and amygdala neurofibrillary tangles and nucleus basalis of meynert neurofibrillary tangles have also been reported (Serrano-Pozo et al., 2011). Beta-amyloid (Aβ) is dissolved and eliminated from the brain in a healthy brain. The Aβ protein may fold in on itself if it is not reabsorbed. Plaques are formed as a result of the proteins interacting with one another. More brain tissue is damaged as a consequence of the inflammatory response caused by these plaques (Reitz and Mayeux, 2014). Thalamus, dorsal tegmentum, locus ceruleus, paramedian reticular region, and the hypothalamus lateral nuclei may all be affected (Reitz and Mayeux, 2014).

Reduced choline acetyltransferase activity in the cerebral cortex and hippocampus, besides the death of cholinergic neurons along the cholinergic projection route to the hippocampus, are thought to be the root causes of these degenerative changes (Reitz and Mayeux, 2014). Above seventy-five percent of the patients here are over the age of 75 (Alzheimer's Association, 2022). It is reported that, an estimated 8 million AD-patients are present worldwide (Alzheimer's Association, 2022) and 115.4 million, AD-patients might be added by 2050, a threefold increase. People over 65 have a prevalence of 6%, people over 80 have a prevalence of 20%, and people over 95 have a prevalence of almost 95%. Adults patients die from AD as the sixth greatest cause of death (Alzheimer's Association, 2022). A total of 7–9 years is the typical time span between the beginning of symptoms and the patient's death.

Neuronal and synapses are compromised in AD, and neurofibrillary tangles, senile plaques, and neurodegeneration are pathological hallmarks (Wilson, 2011). Tau proteins are hyperphosphorylated, resulting in neurofibrillary tangles (also known as tau tangles), which are paired helical filaments. Axons are the most common location for tau proteins. Hyperphosphorylation of these proteins is the result of cellular dysregulation. Neurofibrillary tangles have a devastating effect on axonal integrity and the transport of neurotransmitters (Sun et al., 2003). As the Aβ protein accumulates on the exterior of neurons, it forms senile plaques. Cleavage of Aβ precursor protein (APP) through proteolytic cleavage results in the production of Aβ. The APP, which is found in the brain, is involved in neurogenesis, synaptic formation, cell signaling, axonal transport, and plasticity. When secretases, such as β-secretase and γ-secretase, are used to release Aβ peptides with 40 or 42 amino acids from APP, Aβ oligomers and finally Aβ plaques are formed, and these plaques are then processed in further ways. Deposition of Aβ plaques and neurofibrillary tangles causes nerve cell deterioration and death. The pathophysiology of AD has been described in **Figure 1**.

Cholinergic neurotransmission is essential for a variety of cognitive functions, including memory, learning, attention, sleep, and sensory perception, as well as the stress response. Deficits in acetylcholine (ACh), a neurotransmitter critical to cognitive function, have been linked to AD (Francis, 2005). A deficiency in cholinergic transmission may have a significant impact on both cognition and behavior, so be aware of this possibility (Hampel et al., 2018; DeTure and Dickson, 2019).When cortex is disrupted, cholinergic input also gets affected. CA3 cholinergic receptors have been shown to affect information and memory encoding (Rogers and Kesner, 2004). Brain activity in Alzheimer's sufferers was found to be lower than normal. Because of this, the cholinergic theory acquired a lot of support. Synaptic transmission and plasticity are greatly influenced by NMDA (N-methyl-D-aspartate receptor) receptors (Liu et al., 2019; Lituma et al., 2021). It seems that they help neurons survive by activating a neuronal survival pathway (Hardingham et al., 2002). Neuronal death and degeneration have been linked to NMDA receptor blockade (Ikonomidou et al., 1999). Synaptic NMDA receptor signaling has a detrimental effect on the survival of neurons when it is insufficiently expressed. Neuronal injury and neuronal death result from over activation of glutamatergic signaling (Rothman and Olney, 1986). Neuronal cell loss begins in memory and learning-related regions of the brain and extends throughout the body (Brunholz et al., 2012). Genetic mutations are responsible for a small number of cases of AD. There are mutations in the APP and PS1 and PS2 protein genes (presenilin 1 and 2) (Li et al., 2016; Duncan et al., 2018; Dehury et al., 2019). APP and presenilin gene mutations are seen in familial AD, i.e., PS1 and PS2 are present, but not tau. Several variables have a role in the development of the illness, and age is one of them. The average age of patient is 65 years old when they expected the first diagnosed. AD is more likely to develop in those with a family history of the disease, as do those who have the apolipoprotein E allele 4 (König and Stögmann, 2021). The primary aim of review is to present the readers the current treatment and diagnosing strategies for AD for more targeted approach.

METHODOLOGY

The literature review was conducted using various search engines such as PubMed,[1] Science direct,[2] Scopus,[3] Google scholar.[4] The studies from the years 2010–2022 were chosen with key terms such as "Alzheimer's disease,", "neurological disorders," "amyloid," "nanoparticles," "polymeric micelles," "dendrimers," "nanotechnology," and "liposomes". The papers which were indexed in the above-mentioned search engines were only.

WHY NANOTECHNOLOGY IS IMPORTANT FOR THE RESEARCH OF ALZHEIMER'S DISEASE

The neuronal "milieu" is protected from external chemicals by the blood–brain barrier (BBB), ensuring chemical balance in

[1]https://pubmed.ncbi.nlm.nih.gov/
[2]https://www.sciencedirect.com/
[3]https://www.scopus.com/
[4]https://scholar.google.com/

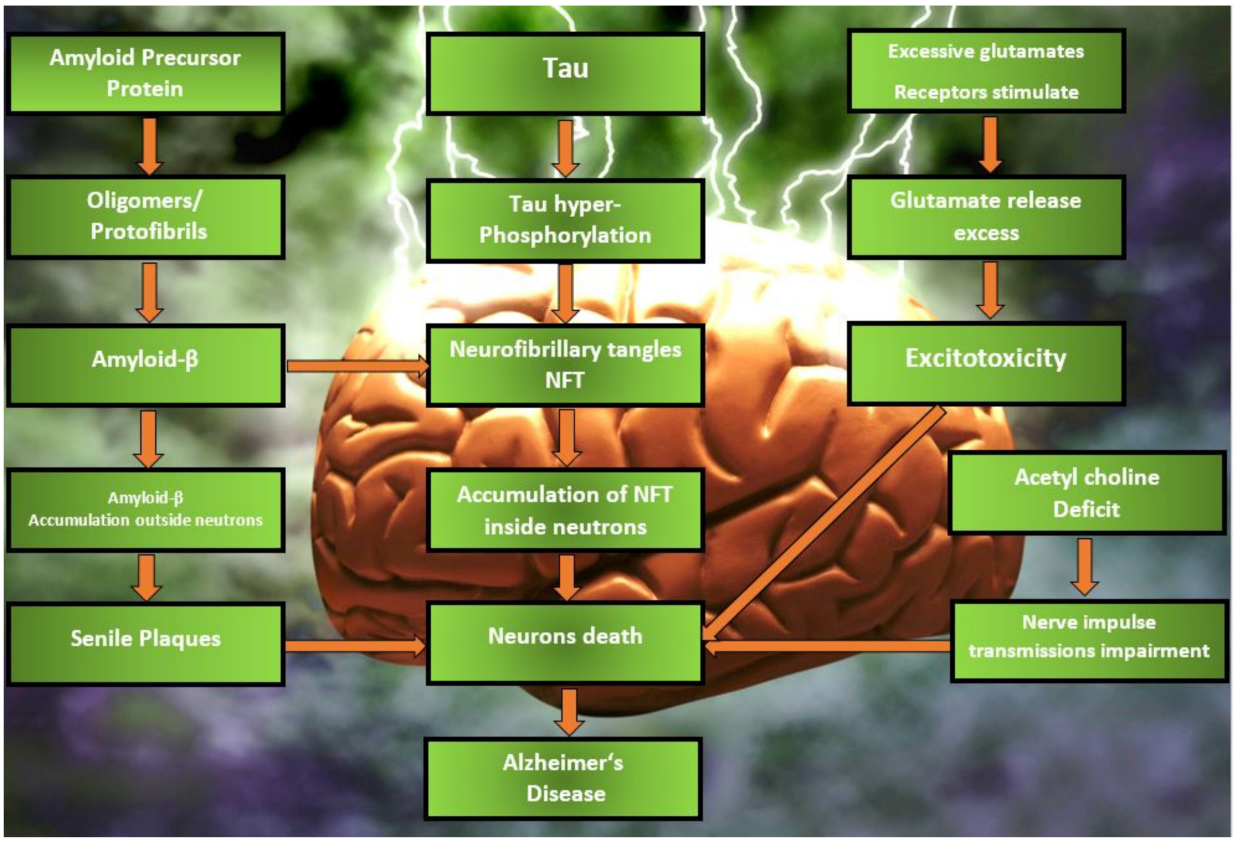

FIGURE 1 | Different phases of pathophysiology of AD.

neuronal circuits and synaptic transmission. The primary contact between the blood and the brain is established by the endothelial cells of the cerebral capillaries, which constitute this barrier. The BBB is the most significant impediment to the development of novel CNS therapeutics and biologics. Pharmaceuticals, including most tiny compounds, do not typically enter or exit the BBB (Cavalu et al., 2020a). Numerous efforts have been made over the last decade to address this critical issue by devising various techniques to facilitate medication transport over the BBB. In recent years, nanotechnology-based approaches have grown in prominence due to their ability to circumvent the restrictions imposed by BBB crossing. Controlled medication delivery and release for a variety of CNS diseases may be achieved using a variety of lipidic, polymeric, inorganic, and other kinds of nanoparticles (NPs) (Cavalu et al., 2020b).

As a result, NP-based treatments for AD have mostly focused on preventing Aβ from aggregating or sequestering the peptide in order to reduce its brain level (the so-called "sink effect") (Matsuoka et al., 2003). Sink-effect-capable nanoliposomes (NL) with phosphatidic acid or cardiolipin were developed by Gobbi et al. (2010). Studying these NL *in vitro*, researchers found that they were highly sensitive to Aβ and had its protective effect (Bereczki et al., 2011). The findings of Mourtas et al. (2011) and Canovi et al. (2011) show that NL coated with an anti-A monoclonal antibody, which has strong affinity for Aβ either *in vitro* or *ex vivo* on post-mortem AD brain tissues, may suppress Aβ aggregation *in vitro* and *in vivo* (Taylor et al., 2011). The capacity of fullerenes C60 to prevent Aβ fibrillization is being studied in a similar fashion (Podolski et al., 2007).

By shielding neurons from oxidative damage, NPs may alleviate the symptoms of AD. They may be used as anti-oxidative agents, but they have toxic effects that are especially dangerous for those with liver and brain impairment. Several studies have shown that NP may be used to address these issues (Liu et al., 2009b). The iron chelator 2-methyl-N-(2'-aminoethyl)-3-hydroxyl-4 pyridinone was found to be able to protect neurons from Aβ toxicity and prevent Aβ aggregation *in vitro*, without affecting cell growth or proliferation, as demonstrated by Liu et al. (2009a).

DRUG LOADED NANOMEDICINES FOR ALZHEIMER'S DISEASE

Liposomes

When it comes to delivering medication over the BBB, the phospholipid bilayer of liposomes is the most likely answer. Nonetheless, the BBB is not permitted to be crossed. In order to increase liposomal carrier transport across the BBB, many surface changes have (Spuch and Navarro, 2011). The BBB's

surface may include several proteins, peptide, antibody, and other ligand receptors. The use of surface-active ligands, such as those present in these compounds, facilitates transcytosis. Cationic liposome absorption into the BBB is also occurring at the same time as transcytosis. To facilitate their passage through the body, liposomes are coated with nutrients such as glucose (Noble et al., 2014). Once in the brain, the liposomes begin the process of passive diffusion, which is activated by the brain's own passive efflux (Noble et al., 2014). The rate at which the chemical is released is unaffected. When the patient's physiological conditions change, fresh techniques have been created that adapt to these changes and manage the drug's release accordingly. Liposome drug release may be triggered by pH variations, enzyme activity, or changes in glutathione levels, to name just (Cavalu et al., 2002; Andresen et al., 2005; Malam et al., 2009). Amyloid peptides interact with ACh, causing amyloid plaque to disintegrate and reducing inflammation in the brain. This helps to preserve healthy neurons as well as treat AD once it has been released.

Liposomes can be modified using ligands for the internalization of active, as BBB have negative charge and electrostatic interactions takes place (Joshi et al., 2014, 2015). PEG11 or polysaccharides may be added to the surface of liposomes to enhance their pharmacokinetic profile, enabling them to remain in circulation for longer periods of time and increasing their distribution into the brain (by inhibiting their rapid clearance *via* the RES12). Despite the fact that "stealth" liposomes were able to significantly shorten the time it takes for liposomes to circulate, there is no guarantee that liposomes will cross the BBB. There are a number of recent approaches for "stealth" liposomes to add extra features, such as physiologically active ligands such as peptides, antibodies or small compounds that bind directly to receptors or target transporters overexpressed on brain endothelial cells. As a result of the specificity of receptor and ligand interactions, receptor-mediated transcytosis has been identified as the most successful and often used method for liposome delivery to the brain. The most often targeted receptor is TfR13, a transmembrane glycoprotein found in abundance in brain endothelial cells. There have been studies using tf14-functionalized liposomes for BBB targeting, however, endogenous Tf prevents them from binding to the receptor (Chen et al., 2014), therefore antibodies against TfR (which binds to the receptors at discrete sites) have been used to eliminate ligand competition (Markoutsa et al., 2012; Mourtas et al., 2014). Another iron-binding glycoprotein found in mammals, lactoferrin, which binds to Lf15 receptors and is found in abundance on the BBB, has also been used to functionalize liposomes. Using receptor-mediated transcytosis, lactoferrin-modified liposomes have been generated as functionalized nanocarriers for BBB crossing (Chen et al., 2010).

Curcumin and two BBB piercing peptides were combined with the preceding research to determine whether a synergistic effect could be achieved by combining the two BBB penetrating peptides, and to test if curcumin interfered with the functioning of the BBB targeting ligands (Papadia et al., 2017b). Curcumin derivative and two BBB binding ligands are added to the surface of multifunctional liposomes (targeting transferrin and LDL receptors). For Aβ inhibition, the liposomes were tested in hCMEC/D3 cells with surface-modified liposomes. These surface-modified liposomes were analyzed for the influence of one or more alterations on the BBB targeting and amyloid binding properties of these liposomes. Studies on FVB and APP/PS1 transgenic mice also shown that curcumin derivatives did not interfere with BBB specific ligands' ability to function (Papadia et al., 2017a,b). An AD nanomedicine made of PEGylated immuno liposomes and two monoclonal antibodies (MAbs) targeting the transferrin receptor and Aβ peptide was developed. Streptavidin-biotin complex and maleimide conjugation were used to affix OX26, an anti-transferrin receptor mAb, and 19B8 to the liposome surface. After being administered intravenously to male Wistar rats, these immunoliposomes were taken up by porcine brain capillary endothelial cells and successfully permeated the BBB *in vivo*. The extracellular trafficking of 19B8 across the BBB was made possible by the disease's persistently leaky BBB. A potential technique for AD treatments was found to be the use of immunoliposomes with two ligand-targeting antibodies (Loureiro et al., 2015).

Rivastigmine and CPP-loaded liposomes may be used to treat AD, according to Yang et al. (2013) experiment. It exhibited cognitive and behavioral development, had fewer side effects, and increased the concentration of medication in the brain, resulting in great therapeutic efficacy in this treatment modality. Beta sheet blocker peptide may be added to liposome vehicles to prevent Aβ protein buildup in the brains of AD patients (Birks and Harvey, 2018). If NPs are supplied intranasally, researchers say that all of the liposomes encapsulated with rivastigmine showed effective drug transport to the brain and high BBB penetration. Nanoformulations of monoclonal antibodies have shown promising outcomes in the treatment of AD. Research with monoclonal antibodies tagged with curcumin showed that they were able to attach strongly to the neurotic plaques in the brain tissue of AD patients and prevent the formation of Aβ peptide. It was shown that curcumin-loaded liposomes were capable of discoloring the accumulated Aβ in mice (Qizilbash et al., 1998). It was shown that the breakdown of Ach by the enzyme Acetyl choline esterase (AChE) could not occur in the presence of rivastigmine-loaded liposomes in solution with sodium taurocholate, according to another study on these liposomes. To improve AChE inhibitor effectiveness, folic acid may be supplied in liposome form through intranasal route. Because the reticuloendothelial system is protected by PEG-coated liposomes, they are very successful in the treatment of AD. To that end, glutathione PEGylated liposomes have been shown to improve medication absorption across the BBB. Infusion of rivastigmine-tagged liposomes and rivastigmine solution into an artificial AD model treated with aluminum chloride indicated the improvement in deteriorated memory that was encouraged by aluminum chloride.

Glutathione (GSH) and ApoE were both transported to the AD-specific location when treated with active ligands by Kuo et al. (2021). It has been shown that increasing the Stearic acid (SA) percentage in liposomes while reducing the PC proportion affected the entrapment efficiency of drugs and the stability of liposomes overall. By enhancing the

TABLE 1 | Latest researches citing use of liposomes for treatment of AD.

Active drug	Outcome	References
Icariin and Tanshinone IIA	The pharmacodynamic analysis *in vivo* demonstrated that Ang2-ICA/TSIIA liposomes could improve AD-like pathological features in APP/PS1 mice, including inhibiting neuroinflammation and oxidative stress, reducing apoptosis, protecting neurons, and improving cognitive function	Monteiro et al., 2022
Hydroxy-α-Sanshool	Liposomes were not significantly toxic to the nasal mucosa and effectively alleviated D-galactose-induced learning memory deficits and protected mouse hippocampal neuronal cells	Li et al., 2022
Imatinib Mesylate	The liposomes effectively improved the brain deposition of drug in brain from formulation compared to pure drug solution as indicated by AUC from *in vivo* experiments	Saka et al., 2021
Transferrin-Pep63	Pep63 effectively inhibited the binding between EphB2 and Aβ oligomers after release from liposomes and rescued NMDA receptors trafficking, the basis of synaptic plasticity	Yang et al., 2021
Rosemary extract	All optimal Nano-Liposomes samples showed statistically significant higher antioxidant capacity (>94.15%) compared to Rosemary extract (90.04%)	Shalabalija et al., 2021

BBB permeability of medicines, GSH-ApoE-PC-liposomes boosted the brain-targeting capacity. ApoE-coated liposomes improved endocytosis of Curcumin (CURC), Quercitin (QU), epigallocatechin gallate(EGCG), rosmarinic acid(RA), and phosphatidylcholine(PC) into SK-N-MC cells *via* engulfing with low-density lipoprotein receptor (LDLR), as shown in this study. To identify A, liposome-encapsulated PC had to rely on a binding affinity that was very particular. Anti-apoptotic effects of GSH, ApoE, CuRC, EGCG, and PC liposomes were shown by immunofluorescence labeling and western blot analysis in $A\beta_{1-42}$ infected cells following treatment with GSH-ApoE–CURC–QU–EGCG-RA-PC liposomes. The GSH-ApoE-PC-liposome triple targeting formulation was used to penetrate the BBB and deliver CURC, QU, EGCG, and RA to the AD-specific location concurrently. A multifunctional GSH-ApoE-CURC-QU-EGCG-RA-PC-liposomes method for AD control was discovered in this study.

Researchers developed non-invasive method of analysis of AD based on liposomes (Monteiro et al., 2022). An Aβ40 peptide liposome encapsulated in dipalmitoyl phosphatidyl glycerol (DPPG) liposomes and attached to a polyethylene imine-coated screen-printed carbon electrode is used to detect autoantibodies against Aβ40, a possible biomarker in plasma samples. Immunosensing utilizing a 2-bilayer PEI/DPPG + anti-Aβ40 autoantibody was able to distinguish plasma and CSF from plasma and CSF samples from three patients with AD by applying currents at 0.45 V. In addition, the CSF voltammograms were able to distinguish healthy samples from those of patients with higher performance. Hence, the ability to identify AD in plasma samples from patients with a confirmed diagnosis, which definitely has larger notoriety, was a first step toward the primary goal: a successful diagnosis of AD in the preclinical stage and plasma. The comparison of peripheral blood and CSF in diagnostic techniques is also critical. Some other studies citing the use of liposomes has been listed in **Table 1**.

Nanoparticles

Chitosan Nanoparticles

Chitosan (CH) is a naturally derived cationic polysaccharide composed of glucosamine and N-acetylglucosamine copolymers (Chen et al., 2010). It is a deacetylated chitin found in lobster, crab, and shrimp shells. The enzyme lysozyme hydrolyzes chitosan into non-carcinogenic, non-toxic, and non-immunogenetic amine sugar compounds that may be absorbed and destroyed by the human body. Chitosan is self-medicating, lowering cholesterol, and promoting ulcer healing and wound healing (Chopra et al., 2020, 2021b, 2022a,b,c; Singh Bakshi et al., 2022). Chitosan NPs are smaller than 70 nm, resulting in a greater surface-to-volume ratio (Cavalu et al., 2018). Chitosan's drug encapsulation efficiency rises with decreasing molecular weight (Xu and Du, 2003; Yang and Hon, 2009). However, research shows that chitosan breakdown rises with molecular weight decrease (Szymańska and Winnicka, 2015).

SpBMP-9, a peptide generated from bone morphogenetic protein-9 (BMP-9), has recently been delivered to the central nervous system (CNS) *via* an alginate-Chitosan NP-based method (Lauzon et al., 2018). Peptide SpBMP-9 (derived from the growth factor BMP-9) is a short peptide that has been shown to stimulate cholinergic neuron development and inhibit GSK3a (a kinase of tau protein) (Beauvais et al., 2016). Peptide-loaded Alg/CS-based NPs enhanced the viability of SH-SY5Y cells when compared to controls. Higher neurite outgrowth and enhanced expression of neuronal markers (such as vesicular acetylcholine transporter (VAchT) and neuron specific enolase (NSE)) were evidence that released SpBMP-9 from NPs stimulated SH-SY5Y cells' differentiation into adult neurons.

Elnaggar et al. (2015) synthesized piperine-loaded chitosan NPs in another investigation. After loading with piperine, the chitosan NPs produced in this work had an average diameter of 230 nm. Dialysis (for 2 h) of piperine-loaded chitosan NPs indicated that the controlled release of piperine was greater than that of unbound piperine in the *in vitro* investigation. Using an animal model of senile dementia of the Alzheimer's type (SDAT), researchers have also undertaken *in vivo* experiments on the cognitive impairments caused by colchicine. Increased AChE secretion in AD brains may be attributed to the increased production of free radicals by colchicine. Cognitive impairment is exacerbated by an increased amount of AChE in the brain, which lowers brain Ach concentrations. Thus, Elnaggar et al. (2015) concluded that piperine-loaded chitosan NPs might be a suitable option to improve cognitive impairment in the brains of patients with AD based on *in vivo* experiments.

Chitosan NPs have been shown to be effective in the intranasal administration of FDA-approved AD medications like Rivastigmine in multiple studies. Research by Fazil et al. (2012) examined the bioavailability of Rivastigmine into the brains of Wistar rats. Diffusion-based mechanisms were found *in vitro*, however *in vivo* experiments demonstrated that the drug was better retained in brain regions when administered as a solution rather than pure. Tween-80 coating of chitosan NPs with Rivastigmine was shown to be more effective in reversing amnesia in Swiss albino mice than chitosan NPs without coating by Nagpal et al. (2013). In contrast to the rapid biphasic release seen with Rivastigmine alone, adding coated or uncoated NPs produced a more gradual biphasic release. As an alternative, trimethyl chitosan (TMC) covalently attached to surface-modified polylactide (PLGA) NPs has been shown to transport Coenzyme Q10 to APP/PS1 transgenic mice (Wang et al., 2010). Memory was much improved, and it was hypothesized that the NP system was able to penetrate the BBB through adsorption-mediated transcytosis and that it was less hazardous.

In spite of the promise of Growth Factors (GF) for treating AD, only a few studies have been undertaken on their entrance into the brain, and most of the studies that have been published have employed chitosan solutions rather than NPs in their research. Nanocapsules of chitosan-based nanocapsules, such as BMP-2 and bFGF, may effectively encapsulate and release GFs like these (Lai et al., 2013). Sprague Dawley rats' brains absorbed BDNF in a chitosan solution (0.25 percent w/v) 13 times quicker than did BDNF alone, as shown by Vaka et al. (2012). A spray solution containing the chitosan chitin was shown to be more effective than intravenous injections in terms of brain/serum concentration ratio and acetyltransferase activity, as well as reducing memory impairment (Feng et al., 2012). Because of this, chitosan seems to have the potential to be an ideal carrier for therapeutic GFs across the BBB. To further understand how NPs aid in the delivery of GF, more research is required.

The chitosan NPs' surface charge is also an important factor that might influence their therapeutic efficacy. The presence of amine groups on the C6 position of the pyranose ring in chitosan gives it a cationic character, which may be favorable or harmful in biomedical applications. Using this positive charge, chitosan NPs may be easily synthesized, for example by self-assembly or ionotropic gelation (Jiang et al., 2018). The negatively charged sialic acid moiety of the mucosa is electrostatically bound by the hydrophilic and cationic amino groups, which aid the polymer's mucoadhesivity. Additional evidence suggests that the negative charge of chitosan NPs may play a role in both their cellular absorption and their dispersibility (Jiang et al., 2018). It is possible that the finding that PEG-modified chitosan NPs in MTT tests were less hazardous to cells than uncoated chitosan NPs may suggest that excessive positive charge attributable to free amine groups might affect the integrity of membranes to the point of causing cell death (Malhotra et al., 2013). Chitosan's cationic nature may potentially impair the encapsulation effectiveness of cationic drugs. Since the degree of dispersion of individual particles is significantly influenced by electrostatic repulsion, surface charge on chitosan-based drug nanocarriers is also critical for their stability. The mild electrostatic repulsive interactions between individual particles explain why NPs with negative surface charge display poor aggregation stability (Ormanci et al., 2014). It is because of this that the RES macrophages can rapidly aggregate and remove these particles from the bloodstream. API nanocarriers with high positive surface charges, on the other hand, are unfavorable because they are more easily phagocytized than NPs with lower positive charges (He et al., 2010) and because they were demonstrated to have an acute toxic impact on the BBB right away. Therefore, nanoparticles for the treatment of AD must have a tiny positive surface charge in order to enhance blood circulation and reduce BBB toxicity (Ormanci et al., 2014). Finally, the surface charge of chitosan NPs has a significant influence on Aβ aggregation (Zhang and Neau, 2001; Chang et al., 2018), however the precise impact of positive and negative charges has been disputed (Cabaleiro-Lago et al., 2010; Assarsson et al., 2014a; Liu et al., 2015b). Although positive NPs have been shown to prevent Aβ fibrillogenesis in a few investigations, their Aβ aggregation-stimulating impact has been observed in others (Luo et al., 2013; Assarsson et al., 2014b). The suppression of Xu et al. (2009), Chan et al. (2012) as well as the promotion of Elbassal et al. (2016), Kim et al. (2016) of Aβ fibrillogenesis have both been linked to negative charges. Most likely the NPs' ability to prevent or promote amyloid-beta aggregation relies on a variety of parameters, including surface charge, hydrophobicity and pH, and the kind of Aβ species.

PLGA Based Nanoparticles

Nigella sativa seed essential oil has been shown to have a bioactive ingredient known as Thymoquinone (TQ), which has been shown to have a wide range of medicinal applications (Javidi et al., 2016). Several early pharmacological studies have been conducted to investigate the therapeutic usage of TQ and additional study is needed to determine its usefulness in neurological illnesses. TQ has recently been shown to have high promise in the treatment of AD by Abulfadl et al. (2018). To achieve any meaningful therapeutic effect, TQ's short bioavailability and rapid elimination hinder its potential to be developed in any traditional dosage form due to its high lipophilicity and strong plasma protein binding (99%) (Alkharfy et al., 2015). The targeted drug delivery system (TDDS) is effective, but the BBB and other cerebrospinal barriers limit the spread of any foreign particles between the CNS and blood. However, these protective barriers are extremely important for normal CNS physiology. Reducing medication delivery systems' capacity to treat brain illnesses may be hindered because to several limitations. In order to transport drugs over the BBB without diminishing their potency, TDDS is needed (Pires et al., 2009). Polysorbate-80 (P-80) coated NPs containing TQ might be a viable and reliable technique of delivering nanoscale delivery to the brain over the BBB (Yusuf et al., 2021). When hydrolyzed into its harmless endogenous metabolites, such as glycolic acid and lactic acid, Poly(lactic-co-glycolic acid) (PLGA) is a biodegradable polymer (Kumari et al., 2010). However, while PLGA is a commonly utilized polymer for CNS specific drug administration, its hydrophobic nature tends to opsonize and remove it *via* the reticulo-endothelial system (RES) (Sempf et al., 2013). Surfactant P-80, a non-toxic,

non-ionic, biodegradable, and hydrophilic surfactant, is ideally suited to achieve this job because its coating protects PLGA NPs from being opsonized and eliminated (Kreuter et al., 2002). P-80 inhibits P-glycoprotein efflux by adsorbing apolipoproteins to the surface of the cell and mimicking LDL to pass the BBB through receptor-mediated endocytosis. TQ release from the PLGA matrix may be explained by a variety of processes, including matrix degradation and drug diffusion (Fredenberg et al., 2011; Kamaly et al., 2016). The autocatalytic hydrolytic breakdown of PLGA to lactic and glycolic acid is a major support for drug release from matrix through diffusion via pore creation (diffusion). High porosity and strong drug diffusion may be achieved by autocatalytic breakdown of the matrix. TQ from P-80-TQN was readily released due to P-80 coating's hydrophilicity (Tıŋlı Aydın et al., 2016). An initial quick burst lasted for two hours, followed by a persistent release for P-80-TQN's biphasic release paradigm. One possibility is that the early burst of TQ is a consequence of TQ restricted to the outer surface. Due of the PLGA matrix swelling and disintegration, it may have been responsible for the early burst of TQ (Zhang and Feng, 2006; Tıŋlı Aydın et al., 2016). TQ and PLGA interaction may have resulted in further sluggish release, which may have limited the release of TQ. The TQ acts primarily by inhibiting enzyme Xanthine-oxidase and reducing the production of superoxide radicals, while semi-TQ produced by cytochrome 450 reductase provides electron deficient platforms at 1 and 4th positions, providing electron deficient centers for superoxide radicals (As shown in **Figure 2**). Both processes have the potential to lower the amount of superoxide radicals produced as a result of decreased OS and AD.

As an anti-oxidant and anti-inflammatory, curcumin has been studied as a possible biological treatment for a variety of health concerns (Chopra et al., 2021a), including cancer, sepsis, heart, and brain illnesses, including AD (Yallapu et al., 2010, 2012; Chopra et al., 2016). During human clinical studies, cur substance was shown to be very safe, with no serious side effects at the higher dosage (4 g/day). Intermolecular hydrogen bonds may also be used to interact with Aβ and iron in plaques without the need of additional chemical linkers. The non-polar regions of Aβ plaques form hydrophobic interactions with the symmetrical phenyl and methoxyl groups of cur molecular chains, allowing them to attach readily to Aβ plaques. Cur's hydroxyl and diketone groups connect to the polar regions of Aβ plaques by hydrogen bonding, further stabilizing the bonds. Researchers prepared, curcumin and Se NPs loaded PLGA nanospheres for targeting AD (Huo et al., 2019).Neuroimaging of Alzheimer's-treated mice was used to assess the nanospheres' capacity to recognize Aβ plaque. These transgenic mice (5XFAD) were utilized in this study because of their ability to display plaque, which increased significantly in quantity as the animal became older, fluorescence intensity was minimal in both Cur and Cur/PLGA groups. In contrast, the Se/Cur-PLGA nanospheres show an increased fluorescence intensity, which confirms that Se NPs on the nanospheres surface helped to improve BBB penetration. Astonishingly, Se/Cur-PLGA was spread throughout the brain slice of the mice, compared to Cur-PLGA. When the Se/Cur-PLGA nanospheres were found mostly on the plaques, it can be directly shown that these nanospheres were attached to Aβ plaques by traversing the BBB in its entirety. Additional neuroprotective features of Cur compounds include their high levels of antioxidant and anti-inflammatory activity as well as their ability to neutralize amyloid and tau hyperphosphorylation. It is possible for curcumin molecules to interact with Aβ oligomers *via* hydrophobic contacts in the non-polar regions of Aβ oligomers and the hydrophobic chains of curcumin. Hydrogen interaction between the polar regions of Aβ oligomers and curcumin's hydroxyl groups may further solidify these hydrophobic connections. Aβ oligomer toxicity in AD may be reversed by curcumin molecules, which act as an obstructive agent.

Dhas and Mehta (2021) prepared flavonoid, i.e., Curcumin based PLGA NPs for AD for reducing oxidative stress. Cur's low solubility, rapid metabolism, and bioavailability have limited its use in medicine because of these three things. Not only does Cur have a low solubility, but it has a low solubility at different pH ranges, like 11 ng/ml in water at pH 5, 0.0004 mg/ml in water at pH 7.4. Under normal conditions, Cur breaks down quickly. The main product is trans-6-(4-hydroxy-3-methoxyphenyl)-24-dioxo-5-hexenal, which is also broken down into ferulic acid, feruloyl methane, and vanillin. Cur is also prone to photodegradation, which could make it difficult to store for a long time. Due of its biocompatibility, biodegradability, and non-toxicity, PLGA was chosen as the study's main material. It can readily be functionalized across the surface with other materials and has a high drug loading capacity (Khan et al., 2018; Mehta et al., 2019). Chitosan (CH), a cationic mucoadhesive polymer, was also included in the research since it has the potential to produce gels by absorbing water, which will aid in prolonging the duration of action at the site of action. According to several reports, CH aids in the opening of tight junctions and improves medication penetration through the nasal mucosa when administered orally (Islam et al., 2015). It is therefore possible to use CH to enhance the residence duration and improve medication permeability by using this material as a shell material.

Therapeutic and biological uses of AuNPs have garnered significant interest. For the therapy of neurodegenerative illnesses, AuNPs have been identified as a viable option. Aβ aggregation is inhibited, and Aβ fibrils are dissociated, which has a synergistic impact on suppressing and dissociating Aβ faults. Their distinctive optical characteristics, chemical stability, electrical conductivity, biocompatibility, and catalytic activity are just some of their many other impressive attributes. Both their surface area and their protein-binding adsorption capability are huge. They may be used to identify Aβproteins by combining with antibodies. Increased signal and improved electron transfer efficiency are also a result of their incorporation (Elbassal et al., 2017; Muller et al., 2017; Song et al., 2018; Cao et al., 2019; Qiao et al., 2021). Consequently, they have been frequently used in the development of AD biomarker biosensors (Meenambal and Srinivas Bharath, 2020). AuNPs-based AD diagnostic techniques would benefit greatly from these exceptional qualities and traits.

A number of trials have been done to find an effective way to prevent the aggregation and fibrillation of Aβ in AD. One of

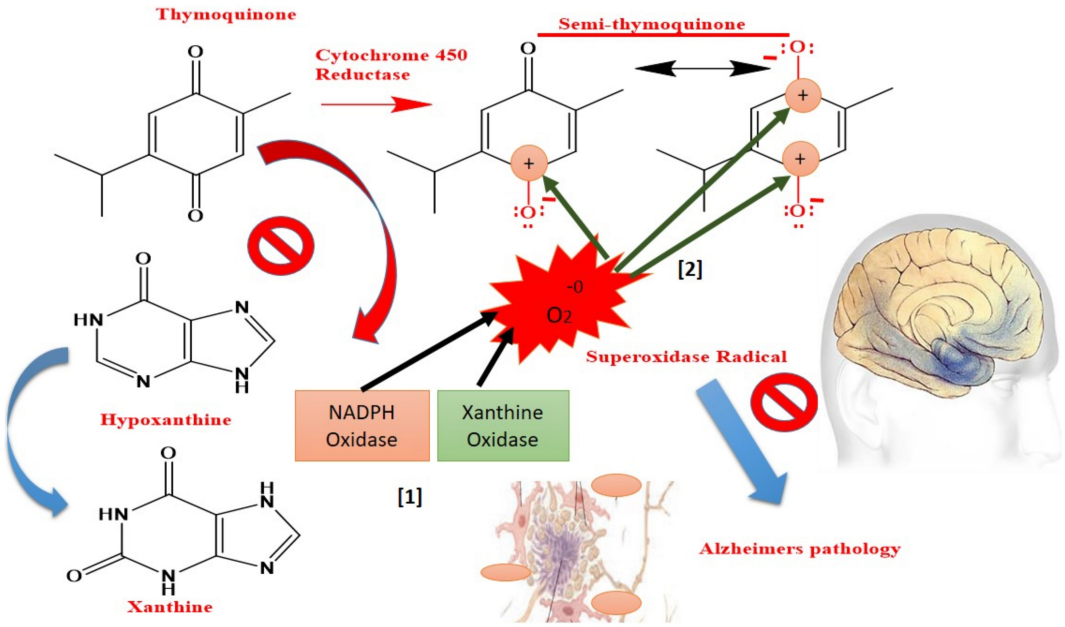

FIGURE 2 | Mechanism of "Thymoquinone" drug toward oxidative stress-mediated AD symptoms.

AD's most striking pathological features is the accumulation of A peptides into insoluble amyloid fibrils (Pradhan et al., 2018). AD may benefit from the use of Aβ aggregation inhibitors. The A fibrils may be destabilized *in vitro* by a variety of drugs, which prevent Aβ aggregation and neurotoxicity. The inhibitory effects of NPs have been extensively explored. Protein aggregation may be effectively inhibited by the functional NPs. Preformed fibrils may be disintegrated by light-activated AuNPs containing peptides. When the nanocarrier is properly surface functionalized, harmful ions are prevented from being released from the nanocarrier (Meenambal and Srinivas Bharath, 2020). NPs may break tiny fibers and prevent them from aggregating. By slowing down the nucleation process, small AuNPs may prevent Aβ aggregation and fibrillation in experiments. As a result, the synthesis of AuNPs may give theoretical insights for therapeutic candidates to treat AD.

An amyloid fibril formation inhibitory effect is shown for gold nanoparticles (AuNP) coated with metal-phenolic networks (MPN). Studies have shown that MPN may work synergistically to prevent amyloid aggregation (Zhang et al., 2019). Metal ions accelerate Aβ aggregation and promote the creation of neurotoxic reactive oxygen species, which lead to the beginning of AD. Despite the fact that metal chelators may block these effects, most of these chelators cannot traverse the BBB or distinguish metal ions associated with toxic Aβ plaques from those in normal biological systems. They can only reduce these effects. AuNPs may be used in the biomedical area because of their high BBB permeability, anti-Aβ aggregation, and great biocompatibility. Molecular interactions have a strong influence on the production of amyloid in the human body. In biological systems, the interfaces are often not flat and exhibit a wide range of sizes and shapes. Because of the enrichment impact toward Aβ, they have the ability to significantly speed up fibrillation. Binding sites are also increased. The fibrillation kinetics may be further altered by interactions with Aβ peptides at these locations. Gao et al. found that large AuNPs accelerated Aβ fibrillation, but smaller ones slowed it down (Gao et al., 2017). Peptide chains were reduced in aggregates generated by AuNPs, and the smaller NPs showed the highest inhibitory effectiveness (Hou et al., 2020). The findings suggested that particle size may have a significant impact on protein folding when adsorbed on NPs.

It is also vital to consider the form of AuNPs in the transport of drugs, bio-labeling and internalization. Gold nanospheres (AuNSs) and gold nanocubes (AuCubes) were created through seed-mediated development of AuNPs by Wang et al. (2019) (AuNCs). Although their surface structures differed, their surface chemistry was quite similar (Wang et al., 2019). Two AuNPs were used to study the secondary structure and fibrillation kinetics of Aβ (1–40) using different microscopic and spectroscopic methods. It is also possible to change the form of NPs to monitor the flow rate, cell absorption, and systemic dispersion of the drug-loaded nanocarrier in the body (Meenambal and Srinivas Bharath, 2020).

The secondary structure of the fibrils generated by AuNPs is influenced by their shape. Peptide secondary structure may be studied using the FTIR. An amyloid fibril's sheet structure, in which the chain folds perpendicular to the long axis of the fibrils, is prevalent. It has been shown that AuNPs may increase sheet content and lead to the development of amyloid fibrils (Wang et al., 2019). It was found that the size, surface charge, concentration, and shape of AuNPs had an influence on the integrity of BBB. AuNPs are attached to Aβ structures in a selective manner. Although these AuNPs conjugates have been widely exploited as photothermal absorbers for putative AD

therapy, their overall negative charge could prevent them from passing across the BBB. The integrity of the BBB was severely compromised by the presence of small AuNPs (Ruff et al., 2017). AuNPs, a nanotechnology-based brain delivery system, may hold the key to better brain treatment (Teleanu et al., 2018).

Antibody Decorated Nanoparticles

Adverse events like as meningoencephalitis may occur as a result of administering immunotherapy dosages to treat AD (Moretto et al., 2007; Hoskin et al., 2019). The best option to using immunotherapy to identify and dissolve protein aggregates in brain cells is to use NPs coated with antibodies for particular target proteins. Antibodies coated with metal oxide NPs are used in secondary ion mass spectrometry to image proteins related with AD in the brain (Moon et al., 2020). Amyloid-bearing cells in AD have been targeted using nano-vehicles coated with chitosan and Aβ fragments. Contrast chemicals such as FITC and Alexa Fluor are used to enhance NP-Aβ absorption across the BBB (Agyare et al., 2008). Class A receptor activator XD4 (W20/XD4-SPIONs) and A oligomer-specific scFv-AbW20 coupled to superparamagnetic iron oxide NPs (SPIONs) show promising outcomes in the treatment of AD (Liu et al., 2020a). Superparamagnetic iron oxide NPs linked with A-oligomer-specific antibody and class A scavenger receptor activator reveal excellent early diagnostic potential for AD (Liu et al., 2020b).

Magnetic Nanoparticles

Typically, gadolinium-based contrast agents are accessible as biocompatible chelates of Gd3 +, which prevent any competitive inhibition of biological processes that involve calcium ions from occurring during the procedure. Despite the fact that various Gd-based contrast agents are commercially available, their clinical use has been discontinued owing to the danger of nephrogenic systemic fibrosis as a result of the buildup of Gd in the tissues of patients. IONPs are considered to be a safer alternative to gadolinium in MRI contrast agents. Because the IONPs are more effective than gadolinium, they may be used at lower concentrations to achieve the same relaxation changes in the surrounding water molecules. In part because of their smaller size, they exhibit superparamagnetism, with each molecule serving as a separate magnetic domain, and as a result, they get magnetized to a higher degree when compared to the same number of Gd-DTPA NPs, which are routinely utilized as T1 contrast agents (Blasiak et al., 2013). In order to achieve certain qualities such as biocompatibility and solubility, IONPs may be functionalized with desired motif sequences. They are able to target brain areas that would otherwise be inaccessible due to their tiny size when paired with their small size. However, although the nephrotoxicity of gadolinium NPs is a source of worry, it has been hypothesized that the IONPs get absorbed into the body's iron stores after a few days in the system (Daldrup-Link, 2017). In this way, they may be used in longitudinal investigations of follow-up detection tools after therapeutic therapies. The FDA-approved IONPs have core sizes ranging from 50 to 200 nm, good biodistribution, and biocompatibility, and many of them were approved for clinical use, including Resovist®, Clariscan®, and Feridex®, before being removed from the market (Cardona et al., 2016). They are traditionally synthesized by co-precipitating a mix of Fe^{2+} and Fe^{3+} salts such as $FeCl_2.4H_2O$ and $FeCl_3.6H_2$. The NPs precipitate and are magnetically collected, after which they are dried under high pressure and temperature in a vacuum (Mohammadi and Barikani, 2014). Additional factors influencing the selection of appropriate IONPs include their bioconjugation, decreased size, stability, solubility, and biocompatibility when exposed to physiological circumstances, to mention a few. They may be endowed with specialized capabilities by selectively attaching to functional patterns found in antibodies, carbohydrates, proteins, and tiny biomolecules, among other substances. Fe^{3+} ions have a larger r1 relaxivity than other ions, indicating that IONPs have the potential to be developed as both T1 and T2 contrast agents. After MRI, the existence of IONPs in the tissue is often verified using histological staining, such as Perl Blue, in the majority of pre-clinical research investigations.

In order to see amyloid structures in the sick brain, anti- Aβ antibodies have been conjugated to IONPs. Intranasal injection of NU-4 antibodies, which are designed to precisely target harmful soluble A oligomers, was reported to bind (24–48)-unit Aβ oligomers in the brains of AD animals after intranasal delivery (Viola et al., 2015). These antibodies were also discovered utilizing magnetic resonance imaging (MRI) when probed on probable AD human brain slices and a 5xFAD mouse model. IONPs that were dual functionalized with the amyloid-binding dye Congo Red and the antioxidant Rutin were shown to aggregate with Aβ plaques in the brains of AD transgenic mice and to relieve memory impairments (Hu et al., 1994). In order to detect aggregation in the sick brain, IONPs were conjugated to A(1–42) peptides, which were chosen because of their natural affinity for Aβ plaques. Following intravenous injections of these probes into the transgenic mice's brains, MRI images and immunolabeling investigations revealed that they were present in AD-associated brain areas such as the cortex and hippocampus (Wadghiri et al., 2013). Other characteristics of AD may be detected and diagnosed using magnetic NPs. For example, under the influence of alternating magnetic fields, IONPs functionalized with anti-tau antibodies may identify tau proteins in the blood plasma of AD patients (Chiu et al., 2014).

According to Pansieri et al. (2018) findings, MNPs might be used to easily detect amyloidosis by imaging the amyloidogenic plaque or fibril depositions on the surface of the cell. Under optimal circumstances, this approach has been shown to be safe and non-toxic, according to the research. It is still necessary to explore the biocompatibility of free or functionalized MNPs in terms of medical significance, as well as their functionality. Nasr et al. (2018) tried to accomplish *in vivo* AD detection and developed magnetic NPs that could pass the BBB and detect the presence of A plaques. With the use of functionalized magnetic fields created by electromagnetic coils, Amin et al. (2017) devised a way for delivering FMNPs into normal mice brains. FMNPs shown the capacity to cross the BBB and reach the cortex and hippocampus of the brain. FeO MNPs coated with dextran containing osmotin were used to extend the effect to target Aβ in mice. It was shown to be beneficial in preventing synaptic

loss caused by Aβ accumulation, expression of BACE-1 a, and other factors.

Dendrimers

There are three elements to dendrimers: a central core, branches, and functional groups on the macromolecule's surface. They take the form of a tree-like nanostructure. Macromolecular complexes containing nucleic acids or encapsulated drugs are effective because of their functional groups. To address the specific needs of the surface functional moieties, dendrimers are multivalent molecules that have a known structure and a fixed size (Mignani et al., 2013). With its hydrophilic functional groups, it has a lower viscosity than its linear polymer counterparts, and it is also more easily soluble in water. As a result, dendrimers may be engineered with a wide range of chemical modifications such as organic and inorganic groups attached to the branching site. Dendrimers are utilized in gene therapy in lieu of traditional viral vectors. When studied in mammalian cell types and animal models, dendrimers have showed encouraging outcomes. By endocytosis, it carries DNA into the nucleus, where it may be transcribed into the appropriate gene and product. Dendrimer-based treatment has an unusual benefit in that it does not stimulate the immune system (Lohan et al., 2017).

Another prominent polymeric carrier is dendrimer, which has gained favor in recent years as a means of gaining access to the cerebral cortex. Dendrimers have a number of benefits over other drug delivery systems, including high density, monodispersity, controlled size, and a high degree of surface functioning. These characteristics make them particularly well suited for site-specific drug administration. Many other kinds of dendrimers have been created using composite biomaterials like as PAMAM49, PPI50, carbosilane, PLL51, and triazine, among other things. Among the polymers used in biomedical applications, PAMAM is the most widely used and accepted because to its high biocompatibility, flexibility, and cheap cost (Igartúa et al., 2020). PAMAM dendrimer was administered with tacrine, an approved anti-AD medicine, according to Igartúa et al. (2020), with the goal of improving the therapeutic effectiveness of the therapy while simultaneously reducing the toxicity profile. Tacrine and dendrimers (DG 4.0 and 4.5) were mixed together in methanol, and the interaction between the two substances was investigated. The toxicological profile was examined using human RBC52 for *ex vivo* toxicity, cell culture experiments (Neuro-2a cell culture) for *in vitro* toxicity, and zebrafish larvae for *in vivo* toxicity. The results of the investigations were published in the journal Toxicology. When cells were treated with 300 micrograms of tacrine, the researchers discovered a substantial drop in cell viability. In contrast, when tacrine was delivered in conjunction with 1.8 mM of DG 4.0 or 4.5, no signs of toxicity were seen (Igartúa et al., 2020). They have previously used PAMAM dendrimer for carbamazepine brain delivery in order to increase drug solubility, decrease dosage and dosing frequency, lessen side effects, and lower the cost of treatment. Compaction with PAMAM dendrimer results in a large increase in the solubility of the medication, by almost thrice. Additionally, the formulation was proven to be safe in *ex vivo* human blood cell, *in vitro* N2a cell, and an *in vivo* zebrafish model (Igartúa et al., 2018). The brain targeting efficacy of Lf53 conjugated PAMAM dendrimers for administering memantine (NMDA antagonist) in an *in vivo* AD mice model was investigated in another comparable study. The 1HNMR confirmed that the Lf-PAMAM conjugation occurred as a result of a chemical process. The combination of Lf with PAMAM results in a considerable increase in the size of the drug-loaded PAMAM dendrimer, which rises from 11.5 to 131.7 nm. Since lactoferrin has cationic properties, it raises the zeta potential, which, when combined with surface coating, allows for slower drug release rates and longer durations of action than would otherwise be possible. The Lf conjugated dendrimer efficiently carried the medicine to the brain with enhanced bioavailability and shown improvement in memory and behavioral function in an AD animal model, according to the researchers (Gothwal et al., 2019). Another fascinating piece of research established the application of PEL54 dendrimer for brain delivery of flurbiprofen, an anti-inflammatory medicine licensed by the US Food and Drug Administration to treat AD. The dendrons were first created by solid-phase peptide synthesis and were then combined with flurbiprofen to create the final product. Mass spectroscopy and Fourier transform infrared spectroscopy were used to validate the interaction of the polymer and the medication. The formulation was tested for cell viability using bEnd.3 cells, and the results revealed that the system was very biocompatible. Incorporating the drug into the PEL dendrimer improved penetration through the BBB and hydrolysis of the drug transported the drug to the targeted spot.

Quantum Dots

Peptides containing 39–42 amino acids, the majority of which are $A\beta_{1-40}$ and $A\beta_{1-42}$, are found in humans. In order to generate Aβ plaques, the abundance of $A\beta_{1-40}$ and $A\beta_{1-42}$ and their fibril-forming abilities lead to the creation of Aβ-peptides. AD is caused by the aggregation of Aβ peptides, mature fibrils, and soluble oligomers (Roychaudhuri et al., 2009). However, because of the accompanying toxicity and development of resistance, there are only a few authorized medications that can be used to treat AD (Gorain et al., 2020). Peptides, organic compounds, and synthetic peptides have showed promising outcomes in AD in preclinical investigations by removing aggregates or preventing the production of aggregates. Due to limited BBB penetration, a reduced *in vivo* stability and less effectiveness, they have no use for AD treatment (Takahashi and Mihara, 2008). Modern AD treatments use GQDs because of their capacity to suppress Aβ plaque development while simultaneously protecting cells from the harmful effects of A oligomers due to their tiny size (2–10 nm) and minimal cytotoxicity, making them very effective. Aβ plaques may be inhibited by hydrophobic interactions between carbon materials and $A_{\beta\ 1-42}$ peptides, which lowers the negative surface potential and enhances the inhibitory efficacy of QDs (Mahmoudi et al., 2013; Liu et al., 2015c).

Tramiprosate linked covalently with GQDs inhibited A aggregation in AD in a synergistic manner (Mahmoudi et al., 2013). Glycine-proline-glutamate (Gly-Pro-Glu, GPE) was coupled with GQDs to generate GQDG nanomaterial, which inhibited the aggregation of A1-42 fibrils in APP/PS1 transgenic mice when intravenously delivered. With its tiny size and high

surface area, GQDG can pass the MDCK cell monolayer and preferentially bind to the hydrophobic group $A_{\beta\ 1-42}$ protein, which promotes their inhibition, as well as improve memory and learning capacity in mice receiving AD therapy (Xiao et al., 2016).

The unique properties of QDs allow them to overcome the limitations of conventional dyes and imaging techniques. Early detection of AD by the use of QDs is possible, since they can track the *in vivo* states of Aβ aggregation in mice in a variety of ways. Healthy mice and transgenic mice with human APP695swe and APP717 V–F mutations receive intracerebroventricular administration of fluorescent QD probes coupled with an anti-A antibody. Fluorescence microscopy and *in vivo* imaging indicated lower fluorescence intensity in APP transgenic mice compared to APP transgenic animals in the hippocampus, cerebral cortex, sagittal septum, and striatum of A1–42 fluorescent mice (Feng et al., 2013).

This ApoE-significant biomarker in AD might be detected electrochemically using CdSe@ZnS QDs as a sensing carrier. The immune-complex assay was used on a chip with flow mode to evaluate ApoE. AD biomarker tosyl-activated magnetic beads platform consists of a PDMS polydimethylsiloxane-polycarbonate microfluidic chip with integrated screen-printed electrodes. SqWave anodic stripping voltammetry demonstrated that CdSe@ZnS QDs had a lower detection limit and greater accuracy for diluted human plasma (Medina-Sánchez et al., 2014). The CdSe@ZnS QDs were manufactured by the same research group for the detection of apolipoprotein E (ApoE). For comparison research, Alexa 647 was used to assess the sandwich immunocomplex microarray. The experiment was carried out under the same circumstances as the standard enzyme-linked immunosorbent test (ELISA) targeting ApoE was used as a reference. In microarray assays, QDs have a lower limit of detection than Alexa microarray and ELISA, respectively, according to the findings of the excitation wavelength results (Morales-Narváez et al., 2012).

SUMMARY

Though administration of nanomaterials in *in vitro*, *in vivo* based preclinical studies showed significant improvement in the AD models, but still their clinical translation is somewhat lacking to demonstrate. There is a depressing truth that the first-line medications for clinical AD treatment only relieve symptoms but fail to prevent or reverse the course of AD. This is why so much time and money has been invested in understanding the pathophysiology of Alzheimer's disease and creating viable treatment options. As a result of the disease's many pathogenic variables and targets, including A, tau hyperphosphorylation, microglia, ROS, metal ions, and others, disease-modifying therapeutic methods are focused on a variety of approaches. In light of the failure of single-target treatments, it seems that multi-target combination therapies, which administer numerous medications simultaneously, have the brightest chances for treating AD. Nanomaterials have been shown to be capable of delivering many medications (e.g., chemical compounds, genes, peptides, and antibodies) at the same time, indicating a prospective use for the treatment of AD. There are some groundbreaking researches done in treatment or diagnosing AD using nanomaterials. For example, In Chinese patent, CN110559454B (2022) CRT (cathode ray tube) targeting peptides and QSH (quadrupole superparamagnetic ferrite) targeting peptides are used to modify a medicine-carrying nano micelle, which is used to transport an anti-amyloid protein and superparamagnetic ferrite medication for the treatment of Alzheimer's disease. MRI imaging tracing and Alzheimer's disease diagnosis and therapy are integrated into the nano composite medicine. The invention combines QSH targeting peptide and CRT targeting peptide to allow drug-loaded nano-micelles to pass through the blood-brain barrier by targeting both AD protein and transferrin. By targeting both AD protein and transferrin simultaneously, the concentration of a targeted site drug can be increased while the action time of the drug can be prolonged. In another patent, CN108685875A Anti-Alzheimer's disease nano grain-pharmaceutical compositions are the subject of this invention, which focuses on preparations and applications in the pharmaceutical area (CN108685875A, 2022). Anti-AD combination treatments are now possible thanks to the present invention, which addresses a technological issue by extracting natural lipoproteins nanoparticles and AD medication recombination. Bio-imitability, safety, high drug load, efficient brain targeting, high affinity and targeting for amyloid protein are some of the features of the natural nano grain-pharmaceutical composition provided by the invention. The preparation conditions are mild, the process simple and the composition is easily industrialized. As a matter of fact, the patent CN110507830A, innovation focuses on a specific kind of nano-probe and its manufacture for Alzheimer's disease pathogenic protein (CN110507830A, 2022). It's a polyethyleneglycol derivative, as well as a phenothiazine derivative, that's used to make the multi-modal nano-probe of the current invention. In the core of the nano-probe is an extra-small ferrite nanometer particle, and the outside layer is a polyethylene glycol segment that is connected with the phenothiazine derivative. In addition to its unique near-infrared fluorescent label enhancement effect and T1–T2 nuclear magnetic resonance image Contrast improved effect, the multi-modal nano-probe may be particular in combination with beta-amyloid protein patch. In addition to its compact size, superior biocompatibility, radiation-free properties, and a range of without possible neurotoxicity, the probe has a strong application potential in the early detection of Alzheimer's disease.

Based on clinical trials, https://clinicaltrials.gov/ was assessed on dated June 16, 2022, it was found that 2852 clinical trials were registered as recruiting and not recruiting filter, however only 1 study NCT03806478 was registered as nanomaterial based technique (Mirani et al., 2017). APH-1105 NPs is investigational drug product which is sterile, pyrogen free lyophilized powder for nose to brain administration. However this study in phase 2, stage and is documented to complete in 2024. Based on above mentioned clinical settings it can be said that there is vast difference between preclinical and clinical translation. This can also be accounted based on nanotoxicity arising from

nanomaterials that has not be regulated by government agency and there are no strict guidelines for it. As the clinical trials, has been missing these has been no FDA approved drugs for it.

FUTURE DIRECTIONS AND CONCLUSION

According to this study, nanotechnology may be used to fight AD. However, further *in vivo* studies are needed to assess the safety of nanotherapeutic methods. Studies on the pharmacokinetic and pharmacodynamic characteristics are needed before the medications are tested in humans. There are still many investigations that are restricted to *in vitro* or animal model studies. The goal of this study was to summaries current nanomedicine breakthroughs in the treatment of AD. CNS illnesses, such as AD, need more effective, non-toxic nanomedicine formulations. To summaries, nanomaterials have the potential to open up a world of possibilities for both current chemicals and new formulations, paving the path for the future development of innovative therapeutic interventions for AD. As a result of the failure of single-target medicines, multi-target combination therapies seem to provide the best hope for treating Alzheimer's disease. Nanomaterials have been shown to be capable of delivering many medications (e.g., chemical compounds, genes, peptides, and antibodies) at the same time, indicating a possible therapeutic option for AD. Based on the crosstalk between distinct therapeutic targets, the rationale of several combination treatment techniques was examined in this study in order to give reference points for future drug design.

In theory, treating the fundamental cause of AD should lead to positive memory and cognitive enhancement, as well as a reduction in neurodegenerative damage. Although gene therapy seems to be a potential alternative treatment technique, it still has certain drawbacks especially *in vivo* due to a lack of selectivity, limited efficiency, and direct host exposure to the non-viral transport vector. However, even though *ex vivo* gene therapy may minimize the risk of these difficulties, it has a number of downsides, largely due to its delivery technique and more intrusive process. Clinical trials for AD have a reported failure rate of 99.6% (Cummings, 2018). This is thought to be owing to the many pathways involved in most studies and a lack of knowledge about the mechanisms at play. The key to establishing a treatment approach for AD is figuring out how the disease's hereditary predisposition interacts with the disease's downstream molecular process. The ideal success rate of immunotherapy is also disappointingly low, since most clinical studies were forced to stop owing to uneven outcomes or the onset of significant side effects. In addition, most active and passive immunotherapy aimed at mild-to-moderate AD, with limited benefit in cognition in more severe patients. However, immunotherapy is unable to restore cognitive function and cognitive decline that develops at a later stage of AD. The high surface-to-volume ratio and lipophilic characteristics of nano-based treatments, on the other hand, present a potential approach for drug delivery across the BBB. Nanoengineered systems have showed good physicochemical qualities, which have led to a number of studies reporting that NPs have been effectively changed to encapsulate highly antioxidant or anti-inflammatory bioactive substances into specified brain regions (Babazadeh et al., 2020). Toxicology studies have shown that nanoparticle formulations may be harmful, but they haven't been able to establish this yet in human trials, which is why further research is needed (Sharifi et al., 2012; Mirani et al., 2017; Cummings, 2018; Babazadeh et al., 2020; CN110507830A, 2022). If they could afford it at all, most people would have had little choice but to look for more affordable treatment choices. It is thus determined that more study and pricing control are important to further examine and tap into the efficacy of each therapy method, as well as to evaluate the probable efficacies of combinatorial use of all three aspects against AD. There is a long way to go, but we are confident that fresh trials will lead to the discovery of a novel medication for AD that will eliminate the disease.

AUTHOR CONTRIBUTIONS

All authors listed have made a substantial, direct, and intellectual contribution to the work, and approved it for publication.

FUNDING

Funding's for publication of this manuscript are provided by University of Oradea, Romania, by an Internal project.

REFERENCES

Abulfadl, Y. S., El-Maraghy, N. N., Ahmed, A. E., Nofal, S., Abdel-Mottaleb, Y., and Badary, O. A. (2018). Thymoquinone alleviates the experimentally induced Alzheimer's disease inflammation by modulation of TLRs signaling. *Hum. Exp. Toxicol.* 37, 1092–1104. doi: 10.1177/0960327118755256

Agyare, E. K., Curran, G. L., Ramakrishnan, M., Yu, C. C., Poduslo, J. F., and Kandimalla, K. K. (2008). Development of a smart nano-vehicle to target cerebrovascular amyloid deposits and brain parenchymal plaques observed in Alzheimer's disease and cerebral amyloid angiopathy. *Pharm. Res.* 25, 2674–2684. doi: 10.1007/s11095-008-9688-y

Alkharfy, K. M., Ahmad, A., Khan, R., and Al-Shagha, W. M. (2015). Pharmacokinetic plasma behaviors of intravenous and oral bioavailability of thymoquinone in a rabbit model. *Eur. J. Drug Metab. Pharmacokinet.* 40, 319–323. doi: 10.1007/s13318-014-0207-8

Alzheimer's Association (2022). *Alzheimer's Disease Facts and Figures Report*. Available online at: https://www.alz.org/alzheimers-dementia/facts-figures (accessed February 17, 2022).

Alzheimer's Association (2022). *What is Alzheimer's Disease? Symptoms & Causes*. Available online at: https://www.alz.org/alzheimers-dementia/what-is-alzheimers (accessed February 17, 2022).

Amin, F. U., Hoshiar, A. K., Do, T. D., Noh, Y., Shah, S. A., Khan, M. S., et al. (2017). Osmotin-loaded magnetic nanoparticles with electromagnetic guidance

for the treatment of Alzheimer's disease. *Nanoscale* 9, 10619–10632. doi: 10.1039/C7NR00772H

Anand, R., Gill, K. D., and Mahdi, A. A. (2014). Therapeutics of Alzheimer's disease: past, present and future. *Neuropharmacology* 76, 27–50. doi: 10.1016/j.neuropharm.2013.07.004

Andresen, T. L., Jensen, S. S., and Jørgensen, K. (2005). Advanced strategies in liposomal cancer therapy: problems and prospects of active and tumor specific drug release. *Prog. Lipid Res.* 44, 68–97. doi: 10.1016/j.plipres.2004.12.001

Assarsson, A., Hellstrand, E., Cabaleiro-Lago, C., and Linse, S. (2014a). Charge dependent retardation of amyloid β aggregation by hydrophilic proteins. *ACS Chem. Neurosci.* 5, 266–274. doi: 10.1021/cn400124r

Assarsson, A., Linse, S., and Cabaleiro-Lago, C. (2014b). Effects of polyamino acids and polyelectrolytes on amyloid β fibril formation. *Langmuir* 30, 8812–8818. doi: 10.1021/la501414j

Babazadeh, A., Mohammadi Vahed, F., and Jafari, S. M. (2020). Nanocarrier-mediated brain delivery of bioactives for treatment/prevention of neurodegenerative diseases. *J. Control. Release* 321, 211–221. doi: 10.1016/j.jconrel.2020.02.015

Beauvais, S., Drevelle, O., Lauzon, M. A., Daviau, A., and Faucheux, N. (2016). Modulation of MAPK signalling by immobilized adhesive peptides: effect on stem cell response to BMP-9-derived peptides. *Acta Biomater.* 31, 241–251. doi: 10.1016/j.actbio.2015.12.005

Bereczki, E., Re, F., Masserini, M. E., Winblad, B., and Pei, J. J. (2011). Liposomes functionalized with acidic lipids rescue Aβ-induced toxicity in murine neuroblastoma cells. *Nanomedicine* 7, 560–571. doi: 10.1016/j.nano.2011.05.009

Birks, J. S., and Harvey, R. J. (2018). Donepezil for dementia due to Alzheimer's disease. *Cochrane Database Syst. Rev.* 6:CD001190.

Blasiak, B., Barnes, S., Foniok, T., Rushforth, D., Matyas, J., Ponjevic, D., et al. (2013). Comparison of T2 and T2*-weighted MR molecular imaging of a mouse model of glioma. *BMC Med. Imaging* 13:20. doi: 10.1186/1471-2342-13-20/TABLES/2

Brunholz, S., Sisodia, S., Lorenzo, A., Deyts, C., Kins, S., and Morfini, G. (2012). Axonal transport of APP and the spatial regulation of APP cleavage and function in neuronal cells. *Exp. Brain Res.* 217, 353–364. doi: 10.1007/s00221-011-2870-1

Cabaleiro-Lago, C., Quinlan-Pluck, F., Lynch, I., Dawson, K. A., and Linse, S. (2010). Dual effect of amino modified polystyrene nanoparticles on amyloid β protein fibrillation. *ACS Chem. Neurosci.* 1, 279–287. doi: 10.1021/cn900027u

Canovi, M., Markoutsa, E., Lazar, A. N., Pampalakis, G., Clemente, C., Re, F., et al. (2011). The binding affinity of anti-Aβ1-42 MAb-decorated nanoliposomes to Aβ1-42 peptides in vitro and to amyloid deposits in post-mortem tissue. *Biomaterials* 32, 5489–5497. doi: 10.1016/j.biomaterials.2011.04.020

Cao, Y., Wei, Z., Li, M., Wang, H., Yin, L., Chen, D., et al. (2019). Formulation, pharmacokinetic evaluation and cytotoxicity of an enhanced- penetration paclitaxel nanosuspension. *Curr. Cancer Drug Targets* 19, 338–347. doi: 10.2174/1568009618666180629150927

Cardona, F. A., Urquiza, E. S., De La Presa, P., Tobón, S. H., Pal, U., Fraijo, P. H., et al. (2016). Enhanced magnetic properties and MRI performance of bi-magnetic core-shell nanoparticles. *RSC Adv.* 6, 77558–77568. doi: 10.1039/c6ra14265f

Cavalu, S., Antoniac, I. V., Mohan, A., Bodog, F., Doicin, C., Mates, I., et al. (2020a). Nanoparticles and nanostructured surface fabrication for innovative cranial and maxillofacial surgery. *Materials* 13:5391. doi: 10.3390/ma13235391

Cavalu, S., Bisboaca, S., Mates, I. M., Pasca, P. M., Laslo, V., Costea, T., et al. (2018). Novel formulation based on chitosan-Arabic gum nanoparticles entrapping propolis extract production, physico-chemical and structural characterization. *Rev. Chim.* 69, 3756–3760. doi: 10.37358/rc.18.12.6836

Cavalu, S., Damian, G., and Dansoreanu, M. (2002). EPR study of non-covalent spin labeled serum albumin and hemoglobin. *Biophys. Chem.* 99, 181–188. doi: 10.1016/S0301-4622(02)00182-5

Cavalu, S., Fritea, L., Brocks, M., Barbaro, K., Murvai, G., Costea, T. O., et al. (2020b). Novel hybrid composites based on PVA/SeTiO2 nanoparticles and natural hydroxyapatite for orthopedic applications: correlations between structural, morphological and biocompatibility properties. *Materials* 13:2077. doi: 10.3390/ma13092077

Chan, H. M., Xiao, L., Yeung, K. M., Ho, S. L., Zhao, D., Chan, W. H., et al. (2012). Effect of surface-functionalized nanoparticles on the elongation phase of beta-amyloid (1–40) fibrillogenesis. *Biomaterials* 33, 4443–4450. doi: 10.1016/j.biomaterials.2012.03.024

Chang, S. H., Wu, C. H., and Tsai, G. J. (2018). Effects of chitosan molecular weight on its antioxidant and antimutagenic properties. *Carbohydr. Polym.* 181, 1026–1032. doi: 10.1016/j.carbpol.2017.11.047

Chen, H., Tang, L., Qin, Y., Yin, Y., Tang, J., Tang, W., et al. (2010). Lactoferrin-modified procationic liposomes as a novel drug carrier for brain delivery. *Eur. J. Pharm. Sci.* 40, 94–102. doi: 10.1016/j.ejps.2010.03.007

Chen, Y. C., Chiang, C. F., Chen, L. F., Liang, P. C., Hsieh, W. Y., and Lin, W. L. (2014). Polymersomes conjugated with des-octanoyl ghrelin and folate as a BBB-penetrating cancer cell-targeting delivery system. *Biomaterials* 35, 4066–4081. doi: 10.1016/j.biomaterials.2014.01.042

Chiu, M. J., Chen, Y. F., Chen, T. F., Yang, S. Y., Yang, F. P. G., Tseng, T. W., et al. (2014). Plasma tau as a window to the brain-negative associations with brain volume and memory function in mild cognitive impairment and early Alzheimer's disease. *Hum. Brain Mapp.* 35, 3132–3142. doi: 10.1002/hbm.22390

Chopra, D., Ray, L., Dwivedi, A., Tiwari, S. K., Singh, J., Singh, K. P., et al. (2016). Photoprotective efficiency of PLGA-curcumin nanoparticles versus curcumin through the involvement of ERK/AKT pathway under ambient UV-R exposure in HaCaT cell line. *Biomaterials* 84, 25–41. doi: 10.1016/j.biomaterials.2016.01.018

Chopra, H., Bibi, S., Kumar, S., Khan, M. S., Kumar, P., and Singh, I. (2022a). Preparation and evaluation of chitosan/PVA based hydrogel films loaded with honey for wound healing application. *Gels* 8:111. doi: 10.3390/GELS8020111

Chopra, H., Dey, P. S., Das, D., Bhattacharya, T., Shah, M., Mubin, S., et al. (2021a). Curcumin nanoparticles as promising therapeutic agents for drug targets. *Molecules* 26:4998. doi: 10.3390/molecules26164998

Chopra, H., Kumar, S., and Singh, I. (2020). "Bioadhesive hydrogels and their applications," in *Bioadhesives in Drug Delivery*, eds K. L. Mittal, I. S. Bakshi, and J. K. Narang (Hoboken, NJ: Wiley), 147–170.

Chopra, H., Kumar, S., and Singh, I. (2021b). Biopolymer-based scaffolds for tissue engineering applications. *Curr. Drug Targets* 22, 282–295. doi: 10.2174/1389450121999201102140408

Chopra, H., Kumar, S., and Singh, I. (2022b). Strategies and therapies for wound healing: a review. *Curr. Drug Targets* 23, 87–98. doi: 10.2174/1389450122666210415101218

Chopra, H., Singh, I., Kumar, S., Bhattacharya, T., Rahman, M. H., Akter, R., et al. (2022c). Comprehensive review on hydrogels. *Curr. Drug Deliv.* 19, 658–675. doi: 10.2174/1567201818666210601155558

CN108685875A (2022). *A kind of Natural Nano Grain-Pharmaceutical Composition of Anti-Alzheimer's Disease and Its Preparation Method and Application – Google Patents*. Available online at: https://patents.google.com/patent/CN108685875A/en?q=alzheimer+disease+nano&oq=alzheimer+disease+nano (accessed June 16, 2022).

CN110507830A (2022). *A Kind of Nano-Probe and Its Preparation for Alzheimer Disease Pathogenic Protein – Google Patents*. Available online at: https://patents.google.com/patent/CN110507830A/en?q=alzheimer+disease+nano&oq=alzheimer+disease+nano (accessed June 16, 2022).

CN110559454B (2022). *Nano Composite Medicine for Diagnosing and Treating Alzheimer's Disease – Google Patents*. Available online at: https://patents.google.com/patent/CN110559454B/en?q=alzheimer+disease+nano&oq=alzheimer+disease+nano (accessed June 16, 2022).

Cummings, J. (2018). Lessons learned from alzheimer disease: clinical trials with negative outcomes. *Clin. Transl. Sci.* 11, 147–152. doi: 10.1111/cts.12491

Daldrup-Link, H. E. (2017). Ten things you might not know about iron oxide nanoparticles. *Radiology* 284:616. doi: 10.1148/RADIOL.2017162759

Dehury, B., Tang, N., Blundell, T. L., and Kepp, K. P. (2019). Structure and dynamics of γ-secretase with presenilin 2 compared to presenilin 1. *RSC Adv.* 9, 20901–20916. doi: 10.1039/c9ra02623a

DeTure, M. A., and Dickson, D. W. (2019). The neuropathological diagnosis of Alzheimer's disease. *Mol. Neurodegener.* 14, 1–8. doi: 10.1186/s13024-019-0333-5

Dhas, N., and Mehta, T. (2021). Intranasal delivery of chitosan decorated PLGA core /shell nanoparticles containing flavonoid to reduce oxidative stress in the treatment of Alzheimer's disease. *J. Drug Deliv. Sci. Technol.* 61:102242. doi: 10.1016/j.jddst.2020.102242

Duncan, R. S., Song, B., and Koulen, P. (2018). Presenilins as drug targets for Alzheimer's disease—recent insights from cell biology and electrophysiology

as novel opportunities in drug development. *Int. J. Mol. Sci.* 19:1621. doi: 10.3390/IJMS19061621

Elbassal, E. A., Liu, H., Morris, C., Wojcikiewicz, E. P., and Du, D. (2016). Effects of charged cholesterol derivatives on Aβ40 amyloid formation. *J. Phys. Chem. B* 120, 59–68. doi: 10.1021/acs.jpcb.5b09557

Elbassal, E. A., Morris, C., Kent, T. W., Lantz, R., Ojha, B., Wojcikiewicz, E. P., et al. (2017). Gold nanoparticles as a probe for amyloid-β oligomer and amyloid formation. *J. Phys. Chem. C* 121, 20007–20015. doi: 10.1021/acs.jpcc.7b05169

Elnaggar, Y. S., Etman, S. M., Abdelmonsif, D. A., and Abdallah, O. Y. (2015). Intranasal piperine-loaded chitosan nanoparticles as brain-targeted therapy in Alzheimer's disease: optimization, biological efficacy, and potential toxicity. *J. Pharm. Sci.* 104, 3544–3556. doi: 10.1002/jps.24557

Fazil, M., Md, S., Haque, S., Kumar, M., Baboota, S., Kaur Sahni, J., et al. (2012). Development and evaluation of rivastigmine loaded chitosan nanoparticles for brain targeting. *Eur. J. Pharm. Sci.* 47, 6–15. doi: 10.1016/j.ejps.2012.04.013

Feng, C., Zhang, C., Shao, X., Liu, Q., Qian, Y., Feng, L., et al. (2012). Enhancement of nose-to-brain delivery of basic fibroblast growth factor for improving rat memory impairments induced by co-injection of β-amyloid and ibotenic acid into the bilateral hippocampus. *Int. J. Pharm.* 423, 226–234. doi: 10.1016/j.ijpharm.2011.12.008

Feng, L., Long, H. Y., Liu, R. K., Sun, D. N., Liu, C., Long, L. L., et al. (2013). A quantum dot probe conjugated with Aβ antibody for molecular imaging of Alzheimer's disease in a mouse model. *Cell. Mol. Neurobiol.* 33, 759–765. doi: 10.1007/s10571-013-9943-6

Francis, P. T. (2005). The interplay of neurotransmitters in Alzheimer's disease. *CNS Spectr.* 10, 6–9. doi: 10.1017/s1092852900014164

Fredenberg, S., Wahlgren, M., Reslow, M., and Axelsson, A. (2011). The mechanisms of drug release in poly(lactic-co-glycolic acid)-based drug delivery systems – a review. *Int. J. Pharm.* 415, 34–52. doi: 10.1016/j.ijpharm.2011.05.049

Gao, G., Zhang, M., Gong, D., Chen, R., Hu, X., and Sun, T. (2017). The size-effect of gold nanoparticles and nanoclusters in the inhibition of amyloid-β fibrillation. *Nanoscale* 9, 4107–4113. doi: 10.1039/c7nr00699c

Gobbi, M., Re, F., Canovi, M., Beeg, M., Gregori, M., Sesana, S., et al. (2010). Lipid-based nanoparticles with high binding affinity for amyloid-β1–42 peptide. *Biomaterials* 31, 6519–6529. doi: 10.1016/j.biomaterials.2010.04.044

Gorain, B., Rajeswary, D. C., Pandey, M., Kesharwani, P., Kumbhar, S. A., and Choudhury, H. (2020). Nose to brain delivery of nanocarriers towards attenuation of demented condition. *Curr. Pharm. Des.* 26, 2233–2246. doi: 10.2174/1381612826666200313125613

Gothwal, A., Kumar, H., Nakhate, K. T., Ajazuddin, Dutta, A., Borah, A., et al. (2019). Lactoferrin coupled lower generation PAMAM dendrimers for brain targeted delivery of memantine in aluminum-chloride-induced Alzheimer's disease in mice. *Bioconjug. Chem.* 30, 2573–2583. doi: 10.1021/acs.bioconjchem.9b00505

Hampel, H., Mesulam, M. M., Cuello, A. C., Farlow, M. R., Giacobini, E., Grossberg, G. T., et al. (2018). The cholinergic system in the pathophysiology and treatment of Alzheimer's disease. *Brain* 141, 1917–1933. doi: 10.1093/brain/awy132

Hardingham, G. E., Fukunaga, Y., and Bading, H. (2002). Extrasynaptic NMDARs oppose synaptic NMDARs by triggering CREB shut-off and cell death pathways. *Nat. Neurosci.* 5, 405–414. doi: 10.1038/nn835

He, C., Hu, Y., Yin, L., Tang, C., and Yin, C. (2010). Effects of particle size and surface charge on cellular uptake and biodistribution of polymeric nanoparticles. *Biomaterials* 31, 3657–3666. doi: 10.1016/j.biomaterials.2010.01.065

Hoskin, J. L., Sabbagh, M. N., Al-Hasan, Y., and Decourt, B. (2019). Tau immunotherapies for Alzheimer's disease. *Expert Opin. Investig. Drugs* 28, 545–554. doi: 10.1080/13543784.2019.1619694

Hou, K., Zhao, J., Wang, H., Li, B., Li, K., Shi, X., et al. (2020). Chiral gold nanoparticles enantioselectively rescue memory deficits in a mouse model of Alzheimer's disease. *Nat. Commun.* 11, 1–1. doi: 10.1038/s41467-020-18525-2

Hu, B., Dai, F., Fan, Z., Ma, G., Tang, Q., and Zhang, X. (1994). Nanotheranostics: congo red/Rutin-MNPs with enhanced magnetic resonance imaging and H2O2-Responsive therapy of Alzheimer's disease in APPswe/PS1dE9 transgenic mice. *J. Chem. Educ.* 71:290. doi: 10.1002/adma.201502227

Huo, X., Zhang, Y., Jin, X., Li, Y., and Zhang, L. (2019). A novel synthesis of selenium nanoparticles encapsulated PLGA nanospheres with curcumin molecules for the inhibition of amyloid β aggregation in Alzheimer's disease. *J. Photochem. Photobiol. B Biol.* 190, 98–102. doi: 10.1016/j.jphotobiol.2018.11.008

Igartúa, D. E., Martinez, C. S., Del V Alonso, S., and Prieto, M. J. (2020). Combined therapy for Alzheimer's disease: tacrine and PAMAM dendrimers Co-administration reduces the side effects of the drug without modifying its activity. *AAPS PharmSciTech* 21, 1–4. doi: 10.1208/s12249-020-01652-w

Igartúa, D. E., Martinez, C. S., Temprana, C. F., Alonso, S. D. V., and Prieto, M. J. (2018). PAMAM dendrimers as a carbamazepine delivery system for neurodegenerative diseases: a biophysical and nanotoxicological characterization. *Int. J. Pharm.* 544, 191–202. doi: 10.1016/j.ijpharm.2018.04.032

Ikonomidou, C., Bosch, F., Miksa, M., Bittigau, P., Vockler, J., Dikranian, K., et al. (1999). Blockade of NMDA receptors and apoptotic neurodegeneration in the developing brain. *Science* 283, 70–74. doi: 10.1126/science.283.5398.70

Islam, M., Park, T.-E., Reesor, E., Cherukula, K., Hasan, A., Firdous, J., et al. (2015). Mucoadhesive chitosan derivatives as novel drug carriers. *Curr. Pharm. Des.* 21, 4285–4309. doi: 10.2174/1381612821666150901103819

Javidi, S., Razavi, B. M., and Hosseinzadeh, H. (2016). A review of neuropharmacology effects of *Nigella sativa* and its main component, thymoquinone. *Phytother. Res.* 30, 1219–1229. doi: 10.1002/ptr.5634

Jiang, Z., Dong, X., and Sun, Y. (2018). Charge effects of self-assembled chitosan-hyaluronic acid nanoparticles on inhibiting amyloid β-protein aggregation. *Carbohydr. Polym.* 461, 11–18. doi: 10.1016/j.carres.2018.03.001

Joshi, S., Singh-Moon, R. P., Ellis, J. A., Chaudhuri, D. B., Wang, M., Reif, R., et al. (2015). Cerebral hypoperfusion-assisted intra-arterial deposition of liposomes in normal and glioma-bearing rats. *Neurosurgery* 76, 92–100. doi: 10.1227/NEU.0000000000000552

Joshi, S., Singh-Moon, R., Wang, M., Chaudhuri, D. B., Ellis, J. A., Bruce, J. N., et al. (2014). Cationic surface charge enhances early regional deposition of liposomes after intracarotid injection. *J. Neuro-Oncol.* 120, 489–497. doi: 10.1007/s11060-014-1584-1

Kamaly, N., Yameen, B., Wu, J., and Farokhzad, O. C. (2016). Degradable controlled-release polymers and polymeric nanoparticles: mechanisms of controlling drug release. *Chem. Rev.* 116, 2602–2663. doi: 10.1021/acs.chemrev.5b00346

Khan, N., Ameeduzzafar, Khanna, K., Bhatnagar, A., Ahmad, F. J., and Ali, A. (2018). Chitosan coated PLGA nanoparticles amplify the ocular hypotensive effect of forskolin: statistical design, characterization and in vivo studies. *Int. J. Biol. Macromol.* 116, 648–663. doi: 10.1016/j.ijbiomac.2018.04.122

Kim, Y., Park, J. H., Lee, H., and Nam, J. M. (2016). How do the size, charge and shape of nanoparticles affect amyloid β aggregation on brain lipid bilayer? *Sci. Rep.* 6, 1–4. doi: 10.1038/srep19548

König, T., and Stögmann, E. (2021). Genetics of Alzheimer's disease. *Wien. Med. Wochenschr.* 171, 249–256. doi: 10.1007/s10354-021-00819-9

Kreuter, J., Shamenkov, D., Petrov, V., Ramge, P., Cychutek, K., Koch-Brandt, C., et al. (2002). Apolipoprotein-mediated transport of nanoparticle-bound drugs across the blood-brain barrier. *J. Drug Target.* 10, 317–325. doi: 10.1080/10611860290031877

Kumari, A., Yadav, S. K., and Yadav, S. C. (2010). Biodegradable polymeric nanoparticles based drug delivery systems. *Colloids Surf. B Biointerfaces* 75, 1–8. doi: 10.1016/j.colsurfb.2009.09.001

Kuo, Y. C., Ng, I. W., and Rajesh, R. (2021). Glutathione-and apolipoprotein E-grafted liposomes to regulate mitogen-activated protein kinases and rescue neurons in Alzheimer's disease. *Mater. Sci. Eng. C* 127:112233. doi: 10.1016/j.msec.2021.112233

Lai, R. F., Li, Z. J., Zhou, Z. Y., Feng, Z. Q., and Zhao, Q. T. (2013). Effect of rhBMP–2 sustained–release nanocapsules on the ectopic osteogenesis process in sprague–dawley rats. *Asian Pac. J. Trop. Med.* 6, 884–888. doi: 10.1016/S1995-7645(13)60157-1

Lauzon, M. A., Marcos, B., and Faucheux, N. (2018). Characterization of alginate/chitosan-based nanoparticles and mathematical modeling of their SpBMP-9 release inducing neuronal differentiation of human SH-SY5Y cells. *Carbohydr. Polym.* 181, 801–811. doi: 10.1016/j.carbpol.2017.11.075

Li, N., Liu, K., Qiu, Y., Ren, Z., Dai, R., Deng, Y., et al. (2016). Effect of presenilin mutations on APP cleavage; insights into the pathogenesis of FAD. *Front. Aging Neurosci.* 8:51. doi: 10.3389/FNAGI.2016.00051/BIBTEX

Li, R., Lu, F., Sun, X., He, L., Duan, H., Peng, W., et al. (2022). Development and in vivo evaluation of hydroxy-α-sanshool intranasal liposomes as a potential remedial treatment for Alzheimer's disease. *Int. J. Nanomedicine* 17:185. doi: 10.2147/IJN.S339979

Lituma, P. J., Kwon, H. B., Alviña, K., Luján, R., and Castillo, P. E. (2021). Presynaptic NMDA receptors facilitate short-term plasticity and BDNF release at hippocampal mossy fiber synapses. *Elife* 10:e66612. doi: 10.7554/eLife.66612

Liu, A. K., Chang, R. C., Pearce, R. K., and Gentleman, S. M. (2015a). Nucleus basalis of Meynert revisited: anatomy, history and differential involvement in Alzheimer's and Parkinson's disease. *Acta Neuropathol.* 129, 527–540. doi: 10.1007/s00401-015-1392-5

Liu, G., Men, P., Kudo, W., Perry, G., and Smith, M. A. (2009a). Nanoparticle–chelator conjugates as inhibitors of amyloid-β aggregation and neurotoxicity: a novel therapeutic approach for Alzheimer disease. *Neurosci. Lett.* 455, 187–190. doi: 10.1016/j.neulet.2009.03.064

Liu, G., Men, P., Perry, G., and Smith, M. A. (2009b). Development of iron chelator–nanoparticle conjugates as potential therapeutic agents for Alzheimer disease. *Prog. Brain Res.* 180, 97–108. doi: 10.1016/S0079-6123(08)80005-2

Liu, H., Ojha, B., Morris, C., Jiang, M., Wojcikiewicz, E. P., Rao, P. P., et al. (2015b). Positively charged chitosan and N-trimethyl chitosan inhibit Aβ40 fibrillogenesis. *Biomacromolecules* 16, 2363–2373. doi: 10.1021/acs.biomac.5b00603

Liu, J., Chang, L., Song, Y., Li, H., and Wu, Y. (2019). The role of NMDA receptors in Alzheimer's disease. *Front. Neurosci.* 13:43. doi: 10.3389/fnins.2019.00043

Liu, X. G., Zhang, L., Lu, S., Liu, D. Q., Huang, Y. R., Zhu, J., et al. (2020a). Superparamagnetic iron oxide nanoparticles conjugated with Aβ oligomer-specific scFv antibody and class A scavenger receptor activator show therapeutic potentials for Alzheimer's Disease. *J. Nanobiotechnology* 18:60. doi: 10.1186/s12951-020-00723-1

Liu, X. G., Zhang, L., Lu, S., Liu, D. Q., Zhang, L. X., Yu, X. L., et al. (2020b). Multifunctional superparamagnetic iron oxide nanoparticles conjugated with Aβ oligomer-specific scFv antibody and class a scavenger receptor activator show early diagnostic potentials for Alzheimer's disease. *Int. J. Nanomedicine* 15:4919. doi: 10.2147/IJN.S240953

Liu, Y., Xu, L. P., Dai, W., Dong, H., Wen, Y., and Zhang, X. (2015c). Graphene quantum dots for the inhibition of β amyloid aggregation. *Nanoscale* 7, 19060–19065. doi: 10.1039/c5nr06282a

Lohan, S., Raza, K., Mehta, S. K., Bhatti, G. K., Saini, S., and Singh, B. (2017). Anti-Alzheimer's potential of berberine using surface decorated multi-walled carbon nanotubes: a preclinical evidence. *Int. J. Pharm.* 530, 263–278. doi: 10.1016/j.ijpharm.2017.07.080

Loureiro, J. A., Gomes, B., Fricker, G., Cardoso, I., Ribeiro, C. A., Gaiteiro, C., et al. (2015). Dual ligand immunoliposomes for drug delivery to the brain. *Colloids Surf. B Biointerfaces* 134, 213–219. doi: 10.1016/j.colsurfb.2015.06.067

Luo, J., Yu, C. H., Yu, H., Borstnar, R., Kamerlin, S. C., Graüslund, A., et al. (2013). Cellular polyamines promote amyloid-beta (Aβ) peptide fibrillation and modulate the aggregation pathways. *ACS Chem. Neurosci.* 4, 454–462. doi: 10.1021/cn300170x

Mahmoudi, M., Quinlan-Pluck, F., Monopoli, M. P., Sheibani, S., Vali, H., Dawson, K. A., et al. (2013). Influence of the physiochemical properties of superparamagnetic iron oxide nanoparticles on amyloid β protein fibrillation in solution. *ACS Chem. Neurosci.* 4, 475–485. doi: 10.1021/cn300196n

Malam, Y., Loizidou, M., and Seifalian, A. M. (2009). Liposomes and nanoparticles: nanosized vehicles for drug delivery in cancer. *Trends Pharmacol. Sci.* 30, 592–599.

Malhotra, M., Tomaro-Duchesneau, C., and Prakash, S. (2013). Synthesis of TAT peptide-tagged PEGylated chitosan nanoparticles for siRNA delivery targeting neurodegenerative diseases. *Biomaterials* 34, 1270–1280. doi: 10.1016/j.biomaterials.2012.10.013

Markoutsa, E., Papadia, K., Clemente, C., Flores, O., and Antimisiaris, S. G. (2012). Anti-Aβ-MAb and dually decorated nanoliposomes: effect of Aβ1-42 peptides on interaction with hCMEC/D3 cells. *Eur. J. Pharm. Biopharm.* 81, 49–56. doi: 10.1016/j.ejpb.2012.02.006

Matsuoka, Y., Saito, M., LaFrancois, J., Saito, M., Gaynor, K., Olm, V., et al. (2003). Novel therapeutic approach for the treatment of Alzheimer's disease by peripheral administration of agents with an affinity to β-amyloid. *J. Neurosci.* 23, 29–33. doi: 10.1523/jneurosci.23-01-00029.2003

Medina-Sánchez, M., Miserere, S., Morales-Narváez, E., and Merkoçi, A. (2014). On-chip magneto-immunoassay for Alzheimer's biomarker electrochemical detection by using quantum dots as labels. *Biosens. Bioelectron.* 54, 279–284. doi: 10.1016/J.BIOS.2013.10.069

Meenambal, R., and Srinivas Bharath, M. M. (2020). Nanocarriers for effective nutraceutical delivery to the brain. *Neurochem. Int.* 140:104851. doi: 10.1016/j.neuint.2020.104851

Mehta, T. A., Shah, N., Parekh, K., Dhas, N., and Patel, J. K. (2019). "Surface-modified PLGA nanoparticles for targeted drug delivery to neurons," in *Surface Modification of Nanoparticles for Targeted Drug Delivery*, ed. Y. V. Pathak (Cham: Springer), 33–71. doi: 10.1007/978-3-030-06115-9_3

Mignani, S., El Kazzouli, S., Bousmina, M., and Majoral, J. P. (2013). Expand classical drug administration ways by emerging routes using dendrimer drug delivery systems: a concise overview. *Adv. Drug Deliv. Rev.* 65, 1316–1330. doi: 10.1016/j.addr.2013.01.001

Mirani, B., Pagan, E., Currie, B., Siddiqui, M. A., Hosseinzadeh, R., Mostafalu, P., et al. (2017). An advanced multifunctional hydrogel-based dressing for wound monitoring and drug delivery. *Adv. Healthc. Mater.* 6:1700718. doi: 10.1002/adhm.201700718

Mohammadi, A., and Barikani, M. (2014). Synthesis and characterization of superparamagnetic Fe3O 4 nanoparticles coated with thiodiglycol. *Mater. Charact.* 90, 88–93. doi: 10.1016/j.matchar.2014.01.021

Monteiro, J. C. Jr., Yokomichi, A. L., de Carvalho Bovolato, A. L., Schelp, A. O., Ribeiro, S. J., Deffune, E., et al. (2022). Alzheimer's disease diagnosis based on detection of autoantibodies against Aβ using Aβ40 peptide in liposomes. *Clin. Chim. Acta* 531, 223–229. doi: 10.1016/J.CCA.2022.04.235

Moon, D. W., Park, Y. H., Lee, S. Y., Lim, H., Kwak, S. H., Kim, M. S., et al. (2020). Multiplex protein imaging with secondary ion mass spectrometry using metal oxide nanoparticle-conjugated antibodies. *ACS Appl. Mater. Interfaces* 12, 18056–18064. doi: 10.1021/acsami.9b21800

Morales-Narváez, E., Montón, H., Fomicheva, A., and Merkoçi, A. (2012). Signal enhancement in antibody microarrays using quantum dots nanocrystals: application to potential Alzheimer's disease biomarker screening. *Anal. Chem.* 84, 6821–6827. doi: 10.1021/ac301369e

Moretto, N., Bolchi, A., Rivetti, C., Imbimbo, B. P., Villetti, G., Pietrini, V., et al. (2007). Conformation-sensitive antibodies against Alzheimer amyloid-β by immunization with a thioredoxin-constrained B-cell epitope peptide. *J. Biol. Chem.* 282, 11436–11445. doi: 10.1074/jbc.M609690200

Mourtas, S., Canovi, M., Zona, C., Aurilia, D., Niarakis, A., La Ferla, B., et al. (2011). Curcumin-decorated nanoliposomes with very high affinity for amyloid-β1-42 peptide. *Biomaterials* 32, 1635–1645. doi: 10.1016/j.biomaterials.2010.10.027

Mourtas, S., Lazar, A. N., Markoutsa, E., Duyckaerts, C., and Antimisiaris, S. G. (2014). Multifunctional nanoliposomes with curcumin–lipid derivative and brain targeting functionality with potential applications for Alzheimer disease. *Eur. J. Med. Chem.* 80, 175–183. doi: 10.1016/j.ejmech.2014.04.050

Muller, A. P., Ferreira, G. K., Pires, A. J., de Bem Silveira, G., de Souza, D. L., Brandolfi, J., et al. (2017). Gold nanoparticles prevent cognitive deficits, oxidative stress and inflammation in a rat model of sporadic dementia of Alzheimer's type. *Mater. Sci. Eng. C* 77, 476–483. doi: 10.1016/j.msec.2017.03.283

Nagpal, K., Singh, S. K., and Mishra, D. N. (2013). Optimization of brain targeted chitosan nanoparticles of Rivastigmine for improved efficacy and safety. *Int. J. Biol. Macromol.* 59, 72–83. doi: 10.1016/J.IJBIOMAC.2013.04.024

Nasr, S. H., Kouyoumdjian, H., Mallett, C., Ramadan, S., Zhu, D. C., Shapiro, E. M., et al. (2018). Detection of β-amyloid by sialic acid coated bovine serum albumin magnetic nanoparticles in a mouse model of Alzheimer's disease. *Small* 14:1701828. doi: 10.1002/SMLL.201701828

Noble, G. T., Stefanick, J. F., Ashley, J. D., Kiziltepe, T., and Bilgicer, B. (2014). Ligand-targeted liposome design: challenges and fundamental considerations. *Trends Biotechnol.* 32, 32–45. doi: 10.1016/j.tibtech.2013.09.007

Ormanci, O., Akin, I., Sahin, F., Yucel, O., Simon, V., Cavalu, S., et al. (2014). Spark plasma sintered Al2O3-YSZ-TiO2 composites: processing, characterization and in vivo evaluation. *Mater. Sci. Eng. C Mater. Biol. Appl.* 40, 16–23. doi: 10.1016/j.msec.2014.03.041

Pansieri, J., Gerstenmayer, M., Lux, F., Mériaux, S., Tillement, O., Forge, V., et al. (2018). Magnetic nanoparticles applications for amyloidosis study and detection: a review. *Nanomaterials* 8:740. doi: 10.3390/nano8090740

Papadia, K., Giannou, A. D., Markoutsa, E., Bigot, C., Vanhoute, G., Mourtas, S., et al. (2017a). Multifunctional LUV liposomes decorated for BBB and amyloid targeting-B. In vivo brain targeting potential in wild-type and APP/PS1 mice. *Eur. J. Pharm. Sci.* 102, 180–187. doi: 10.1016/j.ejps.2017.03.010

Papadia, K., Markoutsa, E., Mourtas, S., Giannou, A. D., La Ferla, B., Nicotra, F., et al. (2017b). Multifunctional LUV liposomes decorated for BBB and amyloid targeting. A. in vitro proof-of-concept. *Eur. J. Pharm. Sci.* 101, 140–148. doi: 10.1016/j.ejps.2017.02.019

Pires, A., Fortuna, A., Alves, G., and Falcão, A. (2009). Intranasal drug delivery: how, why and what for? *J. Pharm. Pharm. Sci.* 12, 288–311. doi: 10.18433/J3NC79

Podolski, I. Y., Podlubnaya, Z. A., Kosenko, E. A., Mugantseva, E. A., Makarova, E. G., Marsagishvili, L. G., et al. (2007). Effects of hydrated forms of C60 fullerene on amyloid β-peptide fibrillization in vitro and performance of the cognitive task. *J. Nanosci. Nanotechnol.* 7, 1479–1485. doi: 10.1166/jnn.2007.330

Pradhan, N., Jana, N. R., and Jana, N. R. (2018). Inhibition of protein aggregation by iron oxide nanoparticles conjugated with glutamine-and proline-based osmolytes. *ACS Appl. Nano Mater.* 1, 1094–1103. doi: 10.1021/acsanm.7b00245

Qiao, Y., Wei, Z., Qin, T., Song, R., Yu, Z., Yuan, Q., et al. (2021). Combined nanosuspensions from two natural active ingredients for cancer therapy with reduced side effects. *Chin. Chem. Lett.* 32, 2877–2881. doi: 10.1016/j.cclet.2021.03.049

Qizilbash, N., Whitehead, A., Higgins, J., Wilcock, G., Schneider, L., and Farlow, M. (1998). Dementia trialists' collaboration, dementia trialists' collaboration. Cholinesterase inhibition for Alzheimer disease: a meta-analysis of the tacrine trials. *JAMA* 280, 1777–1782. doi: 10.1001/jama.280.20.1777

Reitz, C., and Mayeux, R. (2014). Alzheimer disease: epidemiology, diagnostic criteria, risk factors and biomarkers. *Biochem. Pharmacol.* 88, 640–651. doi: 10.1016/j.bcp.2013.12.024

Rogers, J. L., and Kesner, R. P. (2004). Cholinergic modulation of the hippocampus during encoding and retrieval of tone/shock-induced fear conditioning. *Learn. Mem.* 11, 102–107. doi: 10.1101/lm.64604

Rothman, S. M., and Olney, J. W. (1986). Glutamate and the pathophysiology of hypoxic–ischemic brain damage. *Ann. Neurol.* 19, 105–111. doi: 10.1002/ana.410190202

Roychaudhuri, R., Yang, M., Hoshi, M. M., and Teplow, D. B. (2009). Amyloid β-protein assembly and Alzheimer disease. *J. Biol. Chem.* 284, 4749–4753. doi: 10.1074/jbc.R800036200

Ruff, J., Hüwel, S., Kogan, M. J., Simon, U., and Galla, H. J. (2017). The effects of gold nanoparticles functionalized with ß-amyloid specific peptides on an in vitro model of blood–brain barrier. *Nanomedicine NBM* 13, 1645–1652. doi: 10.1016/j.nano.2017.02.013

Saka, R., Chella, N., and Khan, W. (2021). Development of imatinib mesylate-loaded liposomes for nose to brain delivery: in vitro and in vivo evaluation. *AAPS PharmSciTech* 22, 1–10. doi: 10.1208/s12249-021-02072-0

Sempf, K., Arrey, T., Gelperina, S., Schorge, T., Meyer, B., Karas, M., et al. (2013). Adsorption of plasma proteins on uncoated PLGA nanoparticles. *Eur. J. Pharmacol.* 85, 53–60. doi: 10.1016/j.ejpb.2012.11.030

Serrano-Pozo, A., Frosch, M. P., Masliah, E., and Hyman, B. T. (2011). Neuropathological alterations in Alzheimer disease. *Cold Spring Harb. Perspect. Med.* 1:a006189. doi: 10.1101/cshperspect.a006189

Shalabalija, D., Mihailova, L., Crcarevska, M. S., Karanfilova, I. C., Ivanovski, V., Nestorovska, A. K., et al. (2021). Formulation and optimization of bioinspired rosemary extract loaded PEGylated nanoliposomes for potential treatment of Alzheimer's disease using design of experiments. *J. Drug Deliv. Sci. Technol.* 63:102434. doi: 10.1016/j.jddst.2021.102434

Sharifi, S., Behzadi, S., Laurent, S., Forrest, M. L., Stroeve, P., and Mahmoudi, M. (2012). Toxicity of nanomaterials. *Chem. Soc. Rev.* 41, 2323–2343. doi: 10.1039/c1cs15188f

Singh Bakshi, I., Chopra, H., Sharma, M., Kaushik, D., and Pahwa, R. (2022). Haryanto Herbal bioactives for wound healing application. *Herb. Bioact. Drug Deliv. Syst.* 1, 259–282. doi: 10.1016/B978-0-12-824385-5.00003-0

Soliman, H. M., Ghonaim, G. A., Gharib, S. M., Chopra, H., Farag, A. K., Hassanin, M. H., et al. (2021). Exosomes in Alzheimer's disease: from being pathological players to potential diagnostics and therapeutics. *Int. J. Mol. Sci.* 22:10794. doi: 10.3390/ijms221910794

Song, M., Sun, Y., Luo, Y., Zhu, Y., Liu, Y., and Li, H. (2018). Exploring the mechanism of inhibition of au nanoparticles on the aggregation of amyloid-β(16-22) peptides at the atom level by all-atom molecular dynamics. *Int. J. Mol. Sci.* 19:1815. doi: 10.3390/ijms19061815

Spuch, C., and Navarro, C. (2011). Liposomes for targeted delivery of active agents against neurodegenerative diseases (Alzheimer's disease and Parkinson's disease). *J. Drug Deliv.* 2011:469679. doi: 10.1155/2011/469679

Sun, L., Liu, S. Y., Zhou, X. W., Wang, X. C., Liu, R., Wang, Q., et al. (2003). Inhibition of protein phosphatase 2A-and protein phosphatase 1-induced tau hyperphosphorylation and impairment of spatial memory retention in rats. *Neuroscience* 118, 1175–1182. doi: 10.1016/s0306-4522(02)00697-8

Szymańska, E., and Winnicka, K. (2015). Stability of chitosan—a challenge for pharmaceutical and biomedical applications. *Mar. Drugs* 13, 1819–1846. doi: 10.3390/MD13041819

Takahashi, T., and Mihara, H. (2008). Peptide and protein mimetics inhibiting amyloid beta-peptide aggregation. *Acc. Chem. Res.* 41, 1309–1318. doi: 10.1021/AR8000475

Taylor, M., Moore, S., Mourtas, S., Niarakis, A., Re, F., Zona, C., et al. (2011). Effect of curcumin-associated and lipid ligand-functionalized nanoliposomes on aggregation of the Alzheimer's Aβ peptide. *Nanomedicine* 7, 541–550. doi: 10.1016/j.nano.2011.06.015

Teleanu, D. M., Chircov, C., Grumezescu, A. M., Volceanov, A., and Teleanu, R. I. (2018). Blood-brain delivery methods using nanotechnology. *Pharmaceutics* 10:269. doi: 10.3390/pharmaceutics10040269

Tıŀlı Aydın, R. S., Kaynak, G., and GümüşderelioØlu, M. (2016). Salinomycin encapsulated nanoparticles as a targeting vehicle for glioblastoma cells. *J. Biomed. Mater. Res.* 104, 455–464. doi: 10.1002/jbm.a.35591

Tiwari, S., Atluri, V., Kaushik, A., Yndart, A., and Nair, M. (2019). Alzheimer's disease: pathogenesis, diagnostics, and therapeutics. *Int. J. Nanomed.* 14, 5541–5544. doi: 10.2147/IJN.S200490

Tran, L., and Ha-Duong, T. (2015). Exploring the Alzheimer amyloid-β peptide conformational ensemble: a review of molecular dynamics approaches. *Peptides* 69, 86–91. doi: 10.1016/j.peptides.2015.04.009

Vaka, S. R., Murthy, S. N., Balaji, A., and Repka, M. A. (2012). Delivery of brain-derived neurotrophic factor via nose-to-brain pathway. *Pharm. Res.* 29, 441–447. doi: 10.1007/s11095-011-0572-9

Viola, K. L., Sbarboro, J., Sureka, R., De, M., Bicca, M. A., Wang, J., et al. (2015). Towards non-invasive diagnostic imaging of early-stage Alzheimer's disease. *Nat. Nanotechnol.* 10, 91–98. doi: 10.1038/nnano.2014.254

Wadghiri, Y. Z., Li, J., Wang, J., Hoang, D. M., Sun, Y., Xu, H., et al. (2013). Detection of amyloid plaques targeted by bifunctional USPIO in Alzheimer's disease transgenic mice using magnetic resonance microimaging. *PLoS One* 8:e57097. doi: 10.1371/journal.pone.0057097

Walia, V., Kaushik, D., Mittal, V., Kumar, K., Verma, R., Parashar, J., et al. (2021). Delineation of neuroprotective effects and possible benefits of antioxidantstherapy for the treatment of Alzheimer's diseases by targeting mitochondrial-derived reactive oxygen species: bench to bedside. *Mol. Neurobiol.* 59, 657–680. doi: 10.1007/s12035-021-02617-1

Wang, W., Han, Y., Fan, Y., and Wang, Y. (2019). Effects of gold nanospheres and nanocubes on amyloid-β peptide fibrillation. *Langmuir* 35, 2334–2342. doi: 10.1021/acs.langmuir.8b04006

Wang, Z. H., Wang, Z. Y., Sun, C. S., Wang, C. Y., Jiang, T. Y., and Wang, S. L. (2010). Trimethylated chitosan-conjugated PLGA nanoparticles for the delivery of drugs to the brain. *Biomaterials* 31, 908–915. doi: 10.1016/j.biomaterials.2009.09.104

Wilson, B. (2011). Therapeutic compliance of nanomedicine in Alzheimer's disease. *Nanomedicine* 6, 1137–1139. doi: 10.2217/nnm.11.114

Xiao, S., Zhou, D., Luan, P., Gu, B., Feng, L., Fan, S., et al. (2016). Graphene quantum dots conjugated neuroprotective peptide improve learning and memory capability. *Biomaterials* 102, 220–230. doi: 10.1016/j.biomaterials.2016.08.021

Xu, Y., and Du, Y. (2003). Effect of molecular structure of chitosan on protein delivery properties of chitosan nanoparticles. *Int. J. Pharm.* 250, 215–226. doi: 10.1016/S0378-5173(02)00548-3

Xu, Y., Takai, M., and Ishihara, K. (2009). Protein adsorption and cell adhesion on cationic, neutral, and anionic 2-methacryloyloxyethyl phosphorylcholine

copolymer surfaces. *Biomaterials* 30, 4930–4938. doi: 10.1016/j.biomaterials.2009.06.005

Yallapu, M. M., Gupta, B. K., Jaggi, M., and Chauhan, S. C. (2010). Fabrication of curcumin encapsulated PLGA nanoparticles for improved therapeutic effects in metastatic cancer cells. *J. Colloid Interface Sci.* 351, 19–29. doi: 10.1016/j.jcis.2010.05.022

Yallapu, M. M., Jaggi, M., and Chauhan, S. C. (2012). Curcumin nanoformulations: a future nanomedicine for cancer. *Drug Discov. Today* 17, 71–80. doi: 10.1016/j.drudis.2011.09.009

Yang, H. C., and Hon, M. H. (2009). The effect of the molecular weight of chitosan nanoparticles and its application on drug delivery. *Microchem. J.* 92, 87–91. doi: 10.1016/J.MICROC.2009.02.001

Yang, X., Li, X., Liu, L., Chen, Y. H., You, Y., Gao, Y., et al. (2021). Transferrin-Pep63-liposomes accelerate the clearance of Aβ and rescue impaired synaptic plasticity in early Alzheimer's disease models. *Cell Death Discov.* 7, 1–3. doi: 10.1038/s41420-021-00639-1

Yang, Z. Z., Zhang, Y. Q., Wang, Z. Z., Wu, K., Lou, J. N., and Qi, X. R. (2013). Enhanced brain distribution and pharmacodynamics of rivastigmine by liposomes following intranasal administration. *Int. J. Pharm.* 452, 344–354. doi: 10.1016/j.ijpharm.2013.05.009

Yusuf, M., Khan, M., Alrobaian, M. M., Alghamdi, S. A., Warsi, M. H., Sultana, S., et al. (2021). Brain targeted Polysorbate-80 coated PLGA thymoquinone nanoparticles for the treatment of Alzheimer's disease, with biomechanistic insights. *J. Drug Deliv. Sci. Technol.* 61:102214. doi: 10.1016/j.jddst.2020.102214

Zhang, H., and Neau, S. H. (2001). In vitro degradation of chitosan by a commercial enzyme preparation: effect of molecular weight and degree of deacetylation. *Biomaterials* 22, 1653–1658. doi: 10.1016/S0142-9612(00)00326-4

Zhang, W., Christofferson, A. J., Besford, Q. A., Richardson, J. J., Guo, J., Ju, Y., et al. (2019). Metal-dependent inhibition of amyloid fibril formation: synergistic effects of cobalt-tannic acid networks. *Nanoscale* 11, 1921–1928. doi: 10.1039/c8nr09221d

Zhang, Z., and Feng, S. S. (2006). In vitro investigation on poly(lactide)-tween 80 copolymer nanoparticles fabricated by dialysis method for chemotherapy. *Biomacromolecules* 7, 1139–1146. doi: 10.1021/bm050953v

Conflict of Interest: The authors declare that the research was conducted in the absence of any commercial or financial relationships that could be construed as a potential conflict of interest.

Publisher's Note: All claims expressed in this article are solely those of the authors and do not necessarily represent those of their affiliated organizations, or those of the publisher, the editors and the reviewers. Any product that may be evaluated in this article, or claim that may be made by its manufacturer, is not guaranteed or endorsed by the publisher.

frontiers | Frontiers in Aging Neuroscience

ORIGINAL RESEARCH
published: 11 July 2022
doi: 10.3389/fnagi.2022.893018

Dietary Alterations in Impaired Mitochondrial Dynamics Due to Neurodegeneration

Ghulam Md Ashraf[1,2], Stylianos Chatzichronis[3], Athanasios Alexiou[3,4]*, Gazala Firdousi[5], Mohammad Amjad Kamal[6,7,8,9] and Magdah Ganash[10]*

[1] Pre-clinical Research Unit, King Fahd Medical Research Center, King Abdulaziz University, Jeddah, Saudi Arabia, [2] Department of Medical Laboratory Technology, Faculty of Applied Medical Sciences, King Abdulaziz University, Jeddah, Saudi Arabia, [3] Department of Science and Engineering, Novel Global Community Educational Foundation, Hebersham, NSW, Australia, [4] AFNP Med Austria, Wien, Austria, [5] Department of Health Sciences, Novel Global Community Educational Foundation, Hebersham, NSW, Australia, [6] Institutes for Systems Genetics, Frontiers Science Center for Disease-Related Molecular Network, West China Hospital, Sichuan University, Chengdu, China, [7] King Fahd Medical Research Center, King Abdulaziz University, Jeddah, Saudi Arabia, [8] Department of Pharmacy, Faculty of Allied Health Sciences, Daffodil International University, Dhaka, Bangladesh, [9] Enzymoics, Novel Global Community Educational Foundation, Hebersham, NSW, Australia, [10] Department of Biology, Faculty of Science, King Abdulaziz University, Jeddah, Saudi Arabia

OPEN ACCESS

Edited by:
Wenquan Zou,
Case Western Reserve University, United States

Reviewed by:
Dimitra Dafou,
Aristotle University of Thessaloniki, Greece
Gunter Peter Eckert,
University of Giessen, Germany

***Correspondence:**
Athanasios Alexiou
alexiou@ngcef.net
Ghulam Md Ashraf
gashraf@kau.edu.sa

Specialty section:
This article was submitted to Alzheimer's Disease and Related Dementias, a section of the journal Frontiers in Aging Neuroscience

Received: *09 March 2022*
Accepted: *20 June 2022*
Published: *11 July 2022*

Citation:
Ashraf GM, Chatzichronis S, Alexiou A, Firdousi G, Kamal MA and Ganash M (2022) Dietary Alterations in Impaired Mitochondrial Dynamics Due to Neurodegeneration. Front. Aging Neurosci. 14:893018. doi: 10.3389/fnagi.2022.893018

Alzheimer's disease is still an incurable disease with significant social and economic impact globally. Nevertheless, newly FDA-approved drugs and non-pharmacological techniques may offer efficient disease treatments. Furthermore, it is widely accepted that early diagnosis or even prognosis of Alzheimer's disease using advanced computational tools could offer a compelling alternative way of management. In addition, several studies have presented an insight into the role of mitochondrial dynamics in Alzheimer's development. In combination with diverse dietary and obesity-related diseases, mitochondrial bioenergetics may be linked to neurodegeneration. Considering the probabilistic expectations of Alzheimer's disease development or progression due to specific risk factors or biomarkers, we designed a Bayesian model to formulate the impact of diet-induced obesity with an impaired mitochondrial function and altered behavior. The applied probabilities are based on clinical trials globally and are continuously subject to updating and redefinition. The proposed multiparametric model combines various data types based on uniform probabilities. The program simulates all the variables with a uniform distribution in a sample of 1000 patients. First, the program initializes the variable age (30–95) and the four different diet types ("HFO_diet," "Starvation," "HL_diet," "CR") along with the factors that are related to prodromal or mixed AD (ATP, MFN1, MFN2, DRP1, FIS1, Diabetes, Oxidative_Stress, Hypertension, Obesity, Depression, and Physical_activity). Besides the known proteins related to mitochondrial dynamics, our model includes risk factors like Age, Hypertension, Oxidative Stress, Obesity, Depression, and Physical Activity, which are associated with Prodromal Alzheimer's. The outcome is the disease progression probability corresponding to a random individual ID related to diet choices and mitochondrial

dynamics parameters. The proposed model and the programming code are adjustable to different parameters and values. The program is coded and executed in Python and is fully and freely available for research purposes and testing the correlation between diet type and Alzheimer's disease progression regarding various risk factors and biomarkers.

Keywords: Alzheimer's disease, bayesian inference, dietary, mitochondrial dynamics, Python programming language, simulation

INTRODUCTION

Mitochondria are vital organelles across every nucleated cell that generate energy in the form of ATP *via* the oxidative phosphorylation (OXPHOS) system (Saada, 2014). Mitochondria are defined as dynamic organelles that have been through coordinated cycles of fission and fusion, referred to as mitochondrial dynamics. Mitochondrial dynamics are ongoing processes of mitochondrial fusion, fission, biogenesis, and mitophagy that work together to maintain optimal cellular bioenergetics and reactive oxygen species (ROS) homeostasis (Archer, 2013). These mitochondrial dynamics regulate the number, distribution, and morphology of mitochondria in the cell and thus play critical roles in various mitochondrial functions such as energy production, metabolism, intracellular signaling, and apoptosis. Mitochondrial fusion is carried out by the dynamin-like GTPases regulatory mitofusin proteins mfn1, mfn2, and Opa1 (Itoh et al., 2013; Mishra and Chan, 2016). Mfn1 and Mfn2 are outer membranous proteins found on the outer side of the mitochondrial membrane, whereas OPA1 is a transmembrane protein found within the inner mitochondrial membrane (IMM) (Ni et al., 2015) that plays a role in mitochondrial quality regulation, which is mediated by mitophagy (Natarajan et al., 2020). Mitophagy corresponds to removing damaged or unnecessary mitochondria using autophagic machinery. Mitophagy is critical for mitochondrial quality control and homeostasis maintenance (Liao et al., 2017). Mitochondrial fission is required to form new mitochondria, excluding damaged mitochondria. Mitochondrial fission is essential for mitochondrial replication and the removal of damaged organelles *via* selective autophagy (Liao et al., 2017). The dynamin-related GTPase dynamin-related protein 1 (Drp1) is recruited by Fis1 protein from the cytosol to the mitochondrial outer membrane during mitochondrial fission (Cho et al., 2013). In contrast, mitochondrial fusion results in tubular or elongated mitochondria, which allow material exchange between mitochondria and can compensate for functional defects. Mfn1 and Mfn2 are responsible for mitochondrial outer membrane (MOM) fusion (Suárez-Rivero et al., 2017). OPA1 is responsible for mitochondrial inner membrane (MIM) fusion (Griparic et al., 2004; Suárez-Rivero et al., 2017). The OPA1 protein is involved in various functions, including respiratory chain and potential membrane maintenance, cristae organization and apoptosis control, and mtDNA maintenance (Griparic et al., 2004; Ni et al., 2015).

Mitochondrial morphology is dynamic and responsive to metabolic changes. Mitochondrial fusion is linked to increased ATP production, whereas fusion inhibition is linked to impaired OXPHOS, mtDNA depletion, and ROS production. OPA1 deficiency causes mitochondrial fragmentation and cell death in pancreatic cells, impairing insulin secretion and systemic glucose homeostasis. Alterations in mitochondrial dynamics can result in disease neuropathies characterized by impaired mitochondrial fusion and transport or significant optic atrophy caused by reduced mitochondrial fusion (Züchner et al., 2004). Mitochondrial dynamics shed new light on the pathophysiology of mitochondrial disorders and other diseases associated with mitochondrial dysfunction, such as diabetes, heart failure, and neurodegenerative diseases like Alzheimer's disease (AD) (Alexiou et al., 2018a,b).

Additionally, different dietary elements have been suggested to affect AD and mitochondrial function and their dynamic behavior, such as Omega 3 (PUFA), Ketogenic Diet, and saturated fatty acid. Increased fat oxidation, energy expenditure, and reduced-fat deposition are potential effects of omega 3 PUFAs that could help prevent obesity and related metabolic disorders (DeFronzoand Tripathy, 2009). The capacity of omega 3 polyunsaturated fatty acids (PUFAs) to reduce inflammation, a characteristic of obesity and related metabolic disorders is well established (Buckley and Howe, 2010; Lalia and Lanza, 2016; Lepretti et al., 2018). Insulin resistance is closely linked to the emergence of inflammatory pathways, mitochondrial dysfunction, oxidative damage, and ER stress. The positive modulatory effects of omega 3 PUFAs on Mfn2 may explain the improvement of mitochondrial performance and the stimulation of fusion events related to maintaining the mitochondrial-associated endoplasmic reticulum membrane integrity, given Mfn2's unique position as an ER-mitochondria bridge (Lepretti et al., 2018). Amyloid plaques, including beta-amyloid peptides (A-βeta), are the neuropathological hallmarks of AD (Mattson, 2004). According to recent studies, soluble oligomeric forms of Aβ may play a vital role in the etiology of AD. Amyloid Precursor Protein Processing (APP) is inextricably linked to cellular membranes, and membrane biophysical characteristics are crucial (Chen et al., 2017). PUFAs play an essential role in defining cell membrane fluidity. There is evidence that membrane fluidity influences APP processing regulation in multiple ways (Afshordel et al., 2015; Gammone et al., 2019), while A-βeta reduces membrane fluidity and thus stimulates its production, starting a vicious cycle (Pagani and Eckert, 2011). Recent *in vitro* findings suggest that the positive effects of docosahexaenoic acid (DHA), found in fish oil, are linked to mitochondria and APP processing modulation and significantly impact mitochondrial membrane phospholipid composition and function (Chen et al., 2017).

Modern biodata is characterized by abundance and diversity, including nucleic acid structures, gene expression levels,

molecular interactions maps, gene maps, prediction of proteins' unfolding, mutants identification, and pattern and motifs recognition mainly based on mathematical and computational models of low complexity and high efficiency. Mathematical Biology includes many interdisciplinary fields applied to modeling a natural phenomenon or mechanism, such as Theory of Algorithms, Data Mining, Genetic Algorithms, Neural Networks, Artificial Intelligence, and Machine Learning, Combined Learning Mathematics, Bayesian Statistics, Stochastic Analysis, Pattern Recognition, and Simulation. Theoretical models are a set of rules and laws that represent this phenomenon. When these rules or laws are expressed in mathematical relations, we refer to a mathematical model, a structure that approaches the properties of a random phenomenon through a simplification process. Mathematical modeling enables the analysis and monitoring of complex biological processes revealing any possible connections or disruptions that may lead, for example, to the development of a hypothesis related to a disease etiology or a drug discovery (Fischer, 2008). However, sometimes the limitations in the accuracy and the complexity of a mathematical model in Biology may lead to insufficient clinical application. Therefore, in this study, we formulate the probabilistic expectations of AD development or progression due to specific risk factors or biomarkers related to the impact of diet-induced obesity with an impaired mitochondrial function and altered behavior. We designed and programmed a Bayesian model to formulate and test diet type and AD progression correlation regarding various risk factors and biomarkers.

THE KETOGENIC DIET OFFERS A PREVENTIVE ABILITY FOR ALZHEIMER'S DISEASE

In ketogenic diets (KD), fats are in huge quantity, proteins are comparatively low, and carbohydrates are in insufficient quantity, which results in protein and carbohydrates' limited metabolism and the metabolic rate of fats being high (Allen et al., 2014; Lima et al., 2014). The ketogenic diet is used to treat neurodegenerative diseases such as AD because ketone bodies such as acetoacetate (AA) and -hydroxybutyrate (-OHB) reduce oxidative stress and improve mitochondrial biogenesis and function (Branco et al., 2016). The ketogenic diet makes it a viable alternative energy precursor. Furthermore, this diet may aid in the reduction of amyloid plaque accumulation as well as the reversal of amyloid-beta toxicity (Broom et al., 2019). KD may address these metabolic issues while protecting against A plaques associated with AD. Recent memory loss is associated with amyloid-βeta (Aβ) peptide deposition and hippocampal neuronal death in AD. *In vitro* studies suggest that the ketogenic diet can help with this, as -OHB has been shown to protect against toxicity in cultured hippocampal neurons (Branco et al., 2016). Evidence suggests that brain ketone uptake is not impaired in AD, unlike glucose.

INFLUENCE OF DIETARY SATURATED FATTY ACID ON MITOCHONDRIAL DYNAMICS

Different fat sources (high lard diet) in a high-fat diet affected serum levels of metabolites associated with the development of obesity and obesity-related diseases differently. A high-fat, saturated-fatty-acid-rich diet (high lard, HL, diet) resulted in hepatic fat accumulation and insulin resistance and impaired mitochondrial function, increased ROS production, and decreased production of mitochondrial motility proteins (Lionetti et al., 2014; Putti et al., 2015; Chen et al., 2018). Mfn2 expression was reduced in the skeletal muscles of obese Zucker rats and type 2 diabetic patients (Bach et al., 2005; Hernández-Alvarez et al., 2010; Putti et al., 2015). Besides that, saturated fatty acids have been shown *in vitro* to induce fission processes in differentiated C2C12 skeletal muscle cells, associated with mitochondrial dysfunction (Jheng et al., 2012). *In vivo*, smaller mitochondria and increased mitochondrial fission machinery have been observed in the skeletal muscles of genetically obese rats and those with diet-induced obesity, as previously described (Jheng et al., 2012). Rats fed high-lard (L rats) and high-fish-oil (F rats) diets presented similar increases in energy intake in comparison with the intake of rats fed standard diets (N rats) (Lionetti et al., 2014). L rats significantly gained additional bodyweight than F rats (Lionetti et al., 2014). Serum TG and ALT levels were significantly higher in L rats than in N rats and both parameters were lower in F rats than in L rats, with TG levels not differing between F and N rats (Lionetti et al., 2014). L and F rats also displayed significantly higher serum glucose levels than N rats. In contrast, the serum insulin level and the HOMA index value were highest in L rats, with TG levels not differing between F and N rats (Lionetti et al., 2014). Compared to high lard feeding, high fish oil feeding was associated with the development of obesity, dyslipidemia, insulin resistance, and a lower degree of liver injury. Protection against ROS damage through mild uncoupling markers of mitochondrial oxidative stress was evaluated (Lionetti et al., 2014). Because once compared to both N and F rats, L rats generated more mitochondrial ROS due to their lower basal/total aconitase activity ratio. Similarly, to their significantly higher H_2O_2 production in isolated mitochondria. The administration of a high-fat diet to rats increases the activity of AgRP neurons and significantly disrupts systemic energy metabolism (Figlewicz et al., 2013). Mfn2 deletion in these neurons prevents these adverse metabolic effects: fat mass was reduced, insulin and glucose levels were legitimized, and obesity was avoided (Dietrich et al., 2013). A high-fat diet caused mitochondrial fragmentation in AgRP neurons, leading to the hypothesis that reduced mitochondrial fusion contributes to neuronal regulation of whole-body energy metabolism and behavior patterns. A high-fat diet suppresses POMC neurons, which produce various peptide hormones that reduce appetite, food intake, and body weight (Wai and Langer, 2016). Unlike the effects in AgRP neurons, genetic ablation of Mfn2 in POMC neurons results in severe obesity characterized by overeating, low energy expenditure, and endocrine dysregulation. Mfn2 POMC

deletion did not disrupt whole-body energy homeostasis, whereas Mfn1 POMC deletion did.

MITOCHONDRIAL DYNAMICS IN ALZHEIMER'S DISEASE

The fusion events are significant because they enable mitochondria to mix their contents, facilitating many vital functions like an equal distribution of metabolites, mtDNA repair, protein complementation, autophagy promotion, and isolation of damaged mitochondrial segments (Twig et al., 2008). On the other hand, the fission events enhance mitochondrial distribution along the cytoskeletal tracks and divide mitochondria equally into two daughter cells. Any malfunctioning in this process may result in programmed cell death. Fusion and fission, motility, transport, and mitophagy consist of the other three essential aspects of mitochondrial dynamics. These points are especially critical in neurons as they require mitochondria at the sites far from the cell body, and they are essential for functioning in cells of smaller size. A significant decrease in the mitochondrial movement has been reported when there are defects in fusion and fission. The decline in brain mitochondria' normal functioning with increasing age has been associated with increased mitochondrial biogenesis (Grimm and Eckert, 2017).

Neurodegenerative diseases are observed to be associated with mitochondrial dysfunction, illustrating the importance of mitochondrial dynamics for human health. Mitochondria's fusion and fission process maintain significant mitochondrial from and integrity. So, dysfunctions in mitochondrial fusion or fission may also contribute to neurological disorders. Motor neuron diseases characterized by progressive axonal degeneration have altered mitochondrial transport through the cytoskeleton. Mitochondria must be adequately positioned to meet the demands of the cell. Accordingly, mitochondria are delivered to areas of the axon where metabolic demand is high, such as synapses, active cones, and branches, or areas where axonal protein synthesis occurs (Babic et al., 2015). Alzheimer's disease is one example of how mitochondrial transport has been linked to pathophysiological alterations (Magrané et al., 2014). In neurons, mitochondrial fission and fusion are essential for mitochondrial transport (Sheng and Cai, 2012). Fission is affected by Drp1 inhibition because it leads to enlarged mitochondria that cannot be adequately localized to dendrites or axons, and it suppresses synaptic formation and function (Chen et al., 2007; Kageyama et al., 2012; Itoh et al., 2013).

Mitophagy defects can cause the mitochondrial respiratory function to be lost in Drp1-null neurons, and Drp1 may be deficient in HeLa cells due to oxidative damage to mitochondrial components. ROS generation can be exacerbated by impaired respiration (Kageyama et al., 2012; Itoh et al., 2013). Although the processes underlying these alterations are unknown, there could be direct consequences of amyloid-beta (Ab), as AB fragments increased in mitochondria and mitochondrial mass decreased in cultured neurons' neurites. S-nitrosylation-mediated enhancement of Drp1 activity is required for this mechanism (Cho et al., 2009). Mitochondrial morphological abnormalities, displayed as fragmented mitochondria with damaged inner membrane structures, have been progressively observed in neurons from AD patients and AD animal models overexpressed or treated with Aβ or tau (DuBoff et al., 2012; Manczak and Reddy, 2012; Li et al., 2016). Outward deposition of amyloid plaques is followed by accumulation of intraneuronal neurofibrillary tangles of hyperphosphorylated tau on a pathological level. It is linked to the loss of synapses, which leads to neuronal death (Huang and Mucke, 2012).

The lack of mitochondria or fusion and fission regulators in neurites and concurrent abnormalities in axon repair and axonal transport implies that mitochondrial and neuronal dysfunction in AD may be ascribed to mitochondrial trafficking impairment (Gao et al., 2017). Nonetheless, faulty mitochondrial morphology and transport in cell bodies, axons, and synaptic terminals produce localized energy in AD. Deficiency causes or exacerbates neuron malfunction and destruction in AD. As a result, aberrant mitochondrial dynamics could be critical in mitochondrial malfunction and neuronal dysfunction in the AD brain (Huang and Mucke, 2012).

MATERIALS AND METHODS

Experimental Method

In this research paper, a new mathematical model is designed to formulate the correlation of AD progression with diverse diets and its mitochondrial dynamics side effects. The computational implementation was made in the Python programming language, and the Bayesian inference was applied in simulating data.

Bayesian theory is based on probability theory. Even though many supporters of the Classical approach oppose the Bayesian Inference due to the weak approach of prior distributions, the Markov Chain Monte Carlo theory was provided as a solution for this problem for disease assessments with satisfactory results (Tzoufras, 2009). Bayesian statistics uses random variables to predefine the prior distribution of the desired model and calculate the posterior distribution $f(\theta \mid y)$. This posterior distribution can be expressed as (Vidakovic, 2011; Højsgaard, 2012):

$$f(\theta|y) = \frac{f(y|\theta)f(\theta)}{f(y)} \propto f(y|\theta)f(\theta), \quad (1)$$

including both the prior and the observed data by the expression of the prior distribution $f(\theta)$ and the likelihood $f(y \mid \theta)$ (Alexiou et al., 2017) as follows:

$$f(y|\theta) = \prod_{i=1}^{n} f(y_i|\theta), \quad (2)$$

Considering the probabilistic expectations of AD development or progression due to specific risk factors or biomarkers (**Table 1**), we designed a Bayesian model to formulate the impact of diet-induced obesity with an impaired mitochondrial function and altered behavior (Putti et al., 2015; Alexiou et al., 2017). The applied probabilities are based on clinical trials globally and are continuously subject to updating and redefinition (Alexiou et al., 2017). Therefore the proposed

model and the programming code are adjustable to different parameters and values.

The proposed Bayesian model is presented in an acyclic graph (**Figure 1**), and the related variables are formulated using the uniform distribution:

$$p(x|\alpha) \sim U(0,\alpha) = \begin{cases} \frac{1}{a} & if\ 0 \le x \le a \\ 0 & otherwise \end{cases} \quad (3)$$

For the Bayesian inference, we mainly apply a conjugate prior in medical experiments, where this conjugate prior to the uniform distribution is the Pareto distribution (Tenenbaum, 1998):

$$p(a) \sim Pa(b,K) = \begin{cases} \frac{Kb^K}{a^{K+1}} & if\ a \ge b \\ 0 & otherwise \end{cases} \quad (4)$$

RESULTS

The program is coded and executed in Python and is fully and freely available for research purposes and testing the correlation between diet type and AD progression regarding various risk factors and biomarkers. The proposed multiparametric model combines various data types based on uniform probabilities. The calculated error is the Monte Carlo Error that measures the variability of each estimation due to simulation, increasing the model's accuracy almost to 100% (Alexiou et al., 2017). Furthermore, in this Bayesian model, every biomarker (knots in the graph) can be linked with more than one other biomarker in the form of False | False, False | True, True | False, True | True (Alexiou et al., 2017).

The program simulates all the variables with a uniform distribution in a sample of 1,000 patients. First, the program initializes age (30–95) and the four different diet types ("HFO_diet," "Starvation," "HL_diet," "CR") along with the factors that are related to prodromal or mixed AD (ATP, MFN1, MFN2, DRP1, FIS1, Diabetes, Oxidative_Stress, Hypertension, Obesity, Depression, and Physical_activity). Then, the program executes the simulation according to the probabilities of **Table 1**, assigning values 1 or 0 in the case of a positive (abnormal) or not positive biomarker. The outcome is a table with the probability of AD development or progression related to diet choices and mitochondrial dynamics parameters (**Table 2**).

TABLE 1 | The relevant probabilities affecting Alzheimer's disease progression related to age and factors that influence Obesity and Mitochondrial Dynamics, according to the literature (Christen, 2000; Modrego and Ferrández, 2004; Wang et al., 2009; Israeli-Korn et al., 2010; Barnes and Yaffe, 2011; Alzheimer's Association, 2015; Alexiou et al., 2017; Mantzavinos and Alexiou, 2017).

Biomarker	Relevant probability affecting AD progression
Age (> 85)	38%
Age (75–84)	43%
Age (65–74)	15%
Age (< 65)	4%
Hypertension	∼20%
Oxidative Stress	25–30%
Obesity	3.4%
Depression	13.2%
Physical Activity	17.7%
DRP1	74.3%
OPA1	61.4%
MFN1	27.8%
MFN2	33.6%
FIS1	60%

The model represents specific proteins or diets' negative or positive impact on developing AD. The symbol (-) shows that the parent node increases the possibility of the child node occurring. The symbol (+) shows that the current node is a deterrent factor for activating the next node. In the experimentation, zeros and ones were used as the result of an activation function that checks if the node's current state is efficient enough to activate the next node. These calculations have included all the factors, with corresponding prior probabilities applied to uniformed distributed data. Results show different combinations of those factors that produce specific patients' profiles and cases. Besides the known proteins related to mitochondrial dynamics, our model includes risk factors like Age, Hypertension, Oxidative Stress, Obesity, Depression, and Physical Activity, which are associated with Prodromal AD.

Strong evidence suggests the necessity of an optimized bioenergetics balance between mitochondrial fusion and fission (Putti et al., 2015). Therefore we present a few cases generated from our simulation accordingly to the corresponding theory and the relevant probabilities affecting AD progression related to age and other factors (**Table 1**).

Case 1: Subject with decreased oxidative stress due to HFO diets resulting in increased mfn2 expression and ATP levels and promoting fusion within a risk group due to the age (age > 60):

$$P(Prodromal/Mixed\ AD \mid HFO) = \frac{P(Prodromal/Mixed\ AD \mid HFO)P(Prodromal/Mixed)}{P(HFO)} = 0.2$$

Case 2: Subject with abnormal mitochondrial fission proteins (fis1 increased) and mfn2 (decreased) associated with high fat diet-induced obesity (HL diet), leading to an increased ROS:

$$P(Prodromal/Mixed\ AD \mid HL) = \frac{P(Prodromal/Mixed\ AD \mid HL)P(Prodromal/Mixed)}{P(HL)} = 0.614$$

Case 3: Subject with increased mfn1 and opa1 due to starvation-induced mitochondrial fusion, which increases ATP, within a risk group due to the age (age > 60):

$$P(Prodromal/Mixed\ AD \mid SR) = \frac{P(Prodromal/Mixed\ AD \mid SR)P(Prodromal/Mixed)}{P(SR)} = 0.278$$

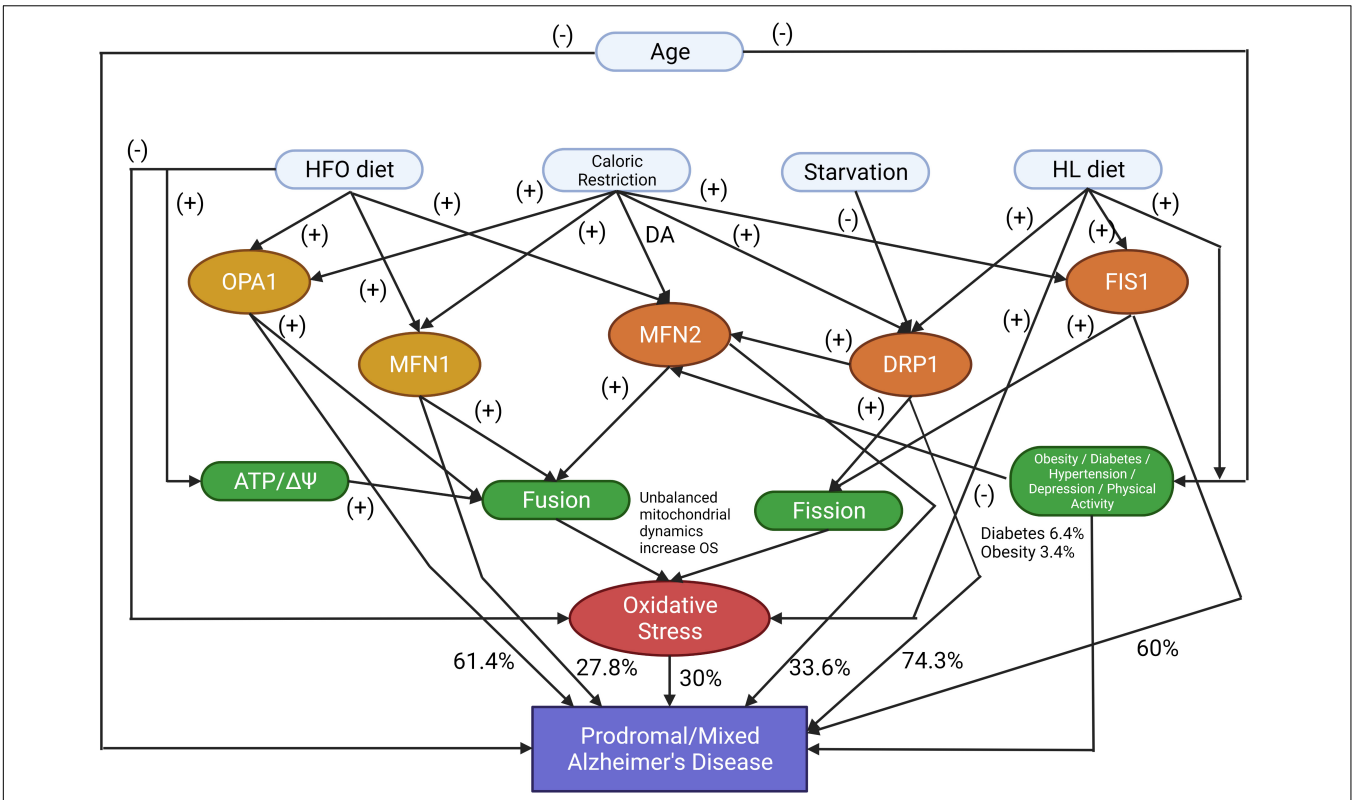

FIGURE 1 | The proposed model identifies the markers that affect Prodromal or Mixed Alzheimer's disease development or progression (DA, Don't Affect; HFO diet, a high-fat diet rich in fish oil; HL diet, a high-fat diet rich in saturated fatty acids). The symbol (-) shows that the parent node increases the possibility of the child node occurring. The symbol (+) shows that the current node is a deterrent factor for activating the next node.

TABLE 2 | Randomly selected results from the simulation of the 1,000 patients, in accordance with the five cases above.

Case	atp	opa1	mfn1	mfn2	drp1	fis1	db	os	ht	ob	dp	pa	diet	age	fusion	fission	AD
1	0	0	0	0	0	0	1	0	1	0	1	0	HFO	63	0	0	0.2
2	1	1	1	1	0	1	1	0	0	1	0	1	HL	31	1	1	0.614
3	1	0	1	0	0	0	0	0	0	1	1	0	starv	70	0	0	0.278
4	1	1	0	1	0	1	0	0	1	0	1	1	CR	86	1	1	0.614
5	0	0	0	0	0	0	1	0	1	0	0	0	0	80	0	0	0.743

The probabilities refer to the development or progression of Prodromal/Mixed AD as defined by the "Research criteria for diagnosing AD: revising the NINCDS-ADRDA criteria" (Dubois et al., 2007). Keys: [atp, adenosine triphosphate; opa1, optic atrophy-1; mfn1, mitofusin-1; mfn2, mitofusin-2; drp1, dynamin-related protein; fis1, mitochondrial fission 1; db, diabetes; os, oxidative stress; ht, hypertension; ob, obesity; dp, depression; pa, physical activity; diet (type), starv (starvation); high-fat diet rich in fish oil (HFO), high-fat diet rich in saturated fatty acids (HL), Caloric Restriction (CR)], fusion and fission corresponds to the mitochondrial dynamics and AD to AD.

Case 4: Subject with an increased mitochondrial population, based on a Caloric Restriction diet type leading to abnormal fis1 and drp1 (increased) and normal mfn1, mfn2, opa1 levels within a risk group due to the age (age > 60):

$$P(Prodromal/_{Mixed}\, AD \mid CR)$$

$$= \frac{P(Prodromal/_{Mixed}\, AD \mid CR)P(Prodromal/_{Mixed})}{P(CR)} = 0.614$$

Case 5: Subject within a risk group due to the age (age > 60), with problems related to a certain quality of life factors (diabetes and hypertension) but with no other evidence of abnormal biomarkers. The model calculates the probability of leading to AD due to these factors:

$$P(Prodromal/_{Mixed}\, AD \mid quality\ of\ life\ factors)$$

$$= \frac{P(Prodromal/_{Mixed}\, AD \mid quality\ of\ life\ factors)}{P(quality\ of\ life\ factors)} \frac{P(Prodromal/_{Mixed})}{} = 0.743$$

DISCUSSION

Mitochondrial dysfunction and oxidative stress are significant causes of neurodegeneration. Both processes produce high levels of ROS, which are detrimental to all cellular macromolecules,

including nucleic acid, lipid, and protein damage (Lauritzen et al., 2016). Plenty of studies confirm that mitochondrial dysfunction is the most likely underlying mechanism of cortical contractility, especially in areas of the brain involved in learning and memory, such as the hippocampus (Stefanova et al., 2016). Mitochondrial changes can increase the production and accumulation of amyloid-β, which is directly toxic to mitochondria, and delay the neurodegenerative process. Tau hyperphosphorylation, which causes a concatenation of events, causes neurodegenerative disease, synaptic damage, and neuronal cell death, and is a detrimental feature of AD (Grimm et al., 2016). As a result, KD may provide neuroprotection by improving mitochondrial function through biochemical changes caused by inhibition of glycolysis and increased KB (ketone body) formation (Rusek et al., 2019). In addition, KB can affect mitochondrial homeostasis by altering calcium-induced membrane permeability transitions (MPTs) and preventing pores from opening.

Furthermore, certain polyunsaturated fatty acids (PUFAs) such as eicosapentaenoic acid, arachidonic acid, and docosahexaenoic acid suppress ROS production, reduce inflammatory mediators, and block voltage-gated sodium and calcium channels. In addition, it can promote neuronal cell membrane stimulation (McDonald and Cervenka, 2018). A high-fat diet is a primary etiology of overweight, obesity, and inflammation, leading to high levels of circulating free fatty acids, which stimulates the formation of amyloid and tau filaments. A high-fat diabetic diet promotes the etiology of AD, and a diet high in docosahexaenoic acid (DHA) prevents AD (Cole et al., 2010; Pugazhenthi et al., 2017).

Several lately published studies provide tools for an efficient early diagnosis or even prognosis of AD development or progression based on the Bayesian Inference or Machine Learning Techniques (Mantzavinos and Alexiou, 2017; Ali et al., 2019; Ashraf and Alexiou, 2019, 2022; De Velasco Oriol et al., 2019; Alexiou et al., 2020; Tan et al., 2021; Mirzaei and Adeli, 2022).

This article presents the first attempt in the literature to simulate the side effects of dietary types in the mitochondrial population, highly correlated to AD and other related neurodegenerative disorders. Furthermore, it provides a freely accessed programming code for reusing and expanding the experimental procedures.

In **Table 2**, several defined cases reveal the potential presence of Prodromal/Mixed AD due to specific biomarkers. Our base study (Putti et al., 2015) showed that HL is highly correlated to altered mitochondrial dynamics and increased ROS production. On the contrary, HFO positively affects mitochondrial functionality, reduces ROS production, and promotes mitochondrial fusion. In addition, the HFO diet can lead to decreased lipid accumulation, obesity, and insulin sensibility compared to HL (Lionetti et al., 2013; Putti et al., 2015). The results of **Table 2** fit the theory of the highly correlated dietary types and mitochondrial dynamics, while mitochondrial fission and fusion seem to be depending on the high-fat diet and starvation (**Table 2**).

Further analysis and observational studies could also validate the model with patient data. This program is an assistive research tool for AD prognosis, but alternative prognostic tools must not replace the clinician's diagnosis.

DATA AVAILABILITY STATEMENT

The original contributions presented in this study are included in the article/supplementary material, further inquiries can be directed to the corresponding authors.

AUTHOR CONTRIBUTIONS

AA and GF wrote the manuscript. AA and SC performed the analysis and data collection. SC designed the programming code. GA and MG provided the funding. MG, GA, and MK provided critical feedback and edited the manuscript. All authors revised the manuscript and agreed to its final form.

FUNDING

This project was funded by the Deanship of Scientific Research (DSR) at King Abdulaziz University, Jeddah, under the grant No. G: 1440-141-1346. We thank DSR for technical and financial support.

REFERENCES

Afshordel, S., Hagl, S., Werner, D., Röhner, N., Kögel, D., Bazan, N. G., et al. (2015). Omega-3 polyunsaturated fatty acids improve mitochondrial dysfunction in brain aging–impact of Bcl-2 and NPD-1 like metabolites. *Prostagl. Leukotr. Essent. Fatty Acids* 92, 23–31. doi: 10.1016/j.plefa.2014.05.008

Alexiou, A., Chatzichronis, S., and Ashraf, G. M. (2020). "Chapter 23 – The prediction of Alzheimer's disease," in *Diagnosis and Management in Dementia: The Neuroscience of Dementia*, Vol. 1, eds C. R. Martin and V. R. Preedy (Amsterdam: Elsevier), 365–378. doi: 10.1016/B978-0-12-815854-8.00023-9

Alexiou, A., Mantzavinos, V. D., Greig, N. H., and Kamal, M. A. (2017). A Bayesian Model for the Prediction and Early Diagnosis of Alzheimer's Disease. *Front. Aging Neurosci.* 9:77. doi: 10.3389/fnagi.2017.00077

Alexiou, A., Nizami, B., Khan, F. I., Soursou, G., Vairaktarakis, C., Chatzichronis, S., et al. (2018a). Mitochondrial Dynamics and Proteins Related to Neurodegenerative Diseases. *Curr. Prot. Pept. Sci.* 19, 850–857. doi: 10.2174/1389203718666170810150151

Alexiou, A., Soursou, G., Yarla, N. S., and Md Ashraf, G. (2018b). Proteins Commonly Linked to Autism Spectrum Disorder and Alzheimer's Disease. *Curr. Prot. Pept. Sci.* 19, 876–880. doi: 10.2174/1389203718666170911145321

Ali, M. A., Alexiou, A., and Ashraf, G. M. (2019). "Biotechnology and Bioinformatics Applications in Alzheimer's Disease," in *Biological, Diagnostic and Therapeutic Advances in Alzheimer's Disease*, eds G. Ashraf and A. Alexiou (Singapore: Springer), doi: 10.1007/978-981-13-9636-6_12

Allen, B. G., Bhatia, S. K., Anderson, C. M., Eichenberger-Gilmore, J. M., Sibenaller, Z. A., and Mapuskar, K. A. (2014). Ketogenic diets as an adjuvant cancer therapy: history and potential mechanism. *Redox Biol.* 2, 963–970. doi: 10.1016/j.redox.2014.08.002

Alzheimer's Association (2015). Alzheimer's Disease Facts and Figures Alzheimer's & Dementia. *Alzheimers Dement* 11, 1–88.

Archer, S. L. (2013). Mitochondrial dynamics—mitochondrial fission and fusion in human diseases. *New Engl. J. Med.* 369, 2236–2251.

Ashraf, G. M., and Alexiou, A. (2019). *Biological, Diagnostic and Therapeutic Advances in Alzheimer's Disease - Non-Pharmacological Therapies for Alzheimer's Disease*. New York, NY: Springer, ISBN: 978-981-13-9635-9 doi: 10.1007/978-981-13-9636-6,

Ashraf, G. M., and Alexiou, A. (2022). *Autism Spectrum Disorder and Alzheimer's Disease - Advances in Research*. New York, NY: Springer Nature, doi: 10.1007/978-981-16-4558-7

Babic, M., Russo, G. J., Wellington, A. J., Sangston, R. M., Gonzalez, M., and Zinsmaier, K. E. (2015). Miro's N-terminal GTPase domain is required for transport of mitochondria into axons and dendrites. *J. Neurosci.* 35, 5754–5771. doi: 10.1523/JNEUROSCI.1035-14.2015

Bach, D., Naon, D., Pich, S., Soriano, F. X., Vega, N., Rieusset, J., et al. (2005). Expression of Mfn2, the Charcot-Marie-Tooth neuropathy type 2A gene, in human skeletal muscle: effects of type 2 diabetes, obesity, weight loss, and the regulatory role of tumor necrosis factor alpha and interleukin-6. *Diabetes* 54, 2685–2693. doi: 10.2337/diabetes.54.9.2685

Barnes, D. E., and Yaffe, K. (2011). The projected impact of risk factor reduction on Alzheimer's disease prevalence. *Lancet. Neurol.* 10, 819–828. doi: 10.1016/S1474-4422(11)70072-2

Branco, A. F., Ferreira, A., Simoes, R. F., Magalhães-Novais, S., Zehowski, C., Cope, E., et al. (2016). Ketogenic diets: from cancer to mitochondrial diseases and beyond. *Eur. J. Clin. Investig.* 46, 285–298.

Broom, G. M., Shaw, I. C., and Rucklidge, J. J. (2019). The ketogenic diet as a potential treatment and prevention strategy for Alzheimer's disease. *Nutrition* 60, 118–121.

Buckley, J. D., and Howe, P. R. (2010). Long-chain omega-3 polyunsaturated fatty acids may be beneficial for reducing obesity—a review. *Nutrients* 2, 1212–1230. doi: 10.3390/nu2121212

Chen, D., Li, X., Zhang, L., Zhu, M., and Gao, L. (2018). A high-fat diet impairs mitochondrial biogenesis, mitochondrial dynamics, and the respiratory chain complex in rat myocardial tissues. *J. Cell. Biochem.* 119, 9602–9602. doi: 10.1002/jcb.27068

Chen, G. F., Xu, T. H., Yan, Y., Zhou, Y. R., Jiang, Y., Melcher, K., et al. (2017). Amyloid beta: structure, biology and structure-based therapeutic development. *Acta Pharmacol. Sin.* 38, 1205–1235.

Chen, H., McCaffery, J. M., and Chan, D. C. (2007). Mitochondrial fusion protects against neurodegeneration in the cerebellum. *Cell* 130, 548–562. doi: 10.1016/j.cell.2007.06.026

Cho, B., Choi, S. Y., Cho, H. M., Kim, H. J., and Sun, W. (2013). Physiological and pathological significance of dynamin-related protein 1 (drp1)-dependent mitochondrial fission in the nervous system. *Exp. Neurob.* 22:149. doi: 10.5607/en.2013.22.3.149

Cho, D. H., Nakamura, T., Fang, J., Cieplak, P., Godzik, A., Gu, Z., et al. (2009). S-nitrosylation of Drp1 mediates beta-amyloidrelated mitochondrial fission and neuronal injury. *Science* 324, 102–105.

Christen, Y. (2000). Oxidative stress and Alzheimer disease. *Am. J. Clin. Nutr.* 71, 621S–629S. doi: 10.1093/ajcn/71.2.621s

Cole, G. M., Ma, Q. L., and Frautschy, S. A. (2010). Dietary fatty acids and the aging brain. *Nutrit. Rev.* 68(Suppl._2), S102–S111. doi: 10.1111/j.1753-4887.2010.00345.x

De Velasco Oriol, J., Vallejo, E. E., Estrada, K., and Gerardo, J. (2019). Benchmarking machine learning models for late-onset alzheimer's disease prediction from genomic data. *BMC Bioinform.* 20:709. doi: 10.1186/s12859-019-3158-x

DeFronzo, R. A. and Tripathy, D. (2009). Skeletal muscle insulin resistance is the primary defect in type 2 diabetes. *Diabetes Care* 32, 157–163.

Dietrich, M. O., Liu, Z. W., and Horvath, T. L. (2013). Mitochondrial dynamics controlled by mitofusins regulate Agrp neuronal activity and diet-induced obesity. *Cell* 155, 188–199. doi: 10.1016/j.cell.2013.09.004

DuBoff, B., Gotz, J., and Feany, M. B. (2012). Tau promotes neurodegeneration via Drp1 mislocalization in vivo. *Neuron* 75, 618–632. doi: 10.1016/j.neuron.2012.06.026

Dubois, B., Feldman, H. H., Jacova, C., Dekosky, S. T., Barberger-Gateau, P., Cummings, J., et al. (2007). Research criteria for the diagnosis of Alzheimer's disease: revising the NINCDS-ADRDA criteria. *Lancet Neurol.* 6, 734–746. doi: 10.1016/S1474-4422(07)70178-3

Figlewicz, D. P., Jay, J. L., Acheson, M. A., Magrisso, I. J., West, C. H., Zavosh, A., et al. (2013). Moderate high fat diet increases sucrose self-administration in young rats. *Appetite* 61, 19–29. doi: 10.1016/j.appet.2012.09.021

Fischer, H. P. (2008). Mathematical modeling of complex biological systems: from parts lists to understanding systems behavior. *Alcohol. Res. Health* 31, 49–59.

Gammone, M. A., Riccioni, G., Parrinello, G., and D'Orazio, N. (2019). Omega-3 polyunsaturated fatty acids: benefits and endpoints in sport. *Nutrients* 11:46.

Gao, J., Wang, L., Liu, J., Xie, F., Su, B., and Wang, X. (2017). Abnormalities of mitochondrial dynamics in neurodegenerative diseases. *Antioxidants* 6:25.

Grimm, A., and Eckert, A. (2017). Brain aging and neurodegeneration: from a mitochondrial point of view. *J. Neurochem.* 143, 418–431.

Grimm, A., Friedland, K., and Eckert, A. (2016). Mitochondrial dysfunction: the missing link between aging and sporadic Alzheimer's disease. *Biogerontology* 17, 281–296.

Griparic, L., van der Wel, N. N., Orozco, I. J., Peters, P. J., and van der Bliek, A. M. (2004). Loss of the intermembrane space protein mgm1/opa1 induces swelling and localized constrictions along the lengths of mitochondria. *J. Biol. Chem.* 279, 18792–18798. doi: 10.1074/jbc.M400920200

Hernández-Alvarez, M. I., Thabit, H., Burns, N., Shah, S., Brema, I., Hatunic, M., et al. (2010). Subjects with early-onset type 2 diabetes show defective activation of the skeletal muscle PGC-1α/Mitofusin-2 regulatory pathway in response to physical activity. *Diabetes Care* 33, 645–651. doi: 10.2337/dc09-1305

Højsgaard, S. (2012). Graphical independence networks with the gRain package for R. *J Stat Softw.* 46, 1–26. doi: 10.18637/jss.v046.i10

Huang, Y., and Mucke, L. (2012). Alzheimer mechanisms and therapeutic strategies. *Cell* 148, 1204–1222.

Israeli-Korn, S. D., Masarwa, M., Schechtman, E., Abuful, A., Strugatsky, R., Avni, S., et al. (2010). Hypertension increases the probability of Alzheimer's disease and of mild cognitive impairment in an Arab community in northern Israel. *Neuroepidemiology* 34, 99–105. doi: 10.1159/000264828

Itoh, K., Nakamura, K., Iijima, M., and Sesaki, H. (2013). Mitochondrial dynamics in neurodegeneration. *Trends Cell Biol.* 23, 64–71.

Jheng, H. F., Tsai, P. J., Guo, S. M., Kuo, L. H., Chang, C. S., Su, I. J., et al. (2012). Mitochondrial fission contributes to mitochondrial dysfunction and insulin resistance in skeletal muscle. *Mol. Cell. Biol.* 32, 309–319. doi: 10.1128/MCB.05603-11

Kageyama, Y., Zhang, Z., Roda, R., Fukaya, M., Wakabayashi, J., Wakabayashi, N., et al. (2012). Mitochondrial division ensures the survival of postmitotic neurons by suppressing oxidative damage. *J. Cell Biol.* 197, 535–551. doi: 10.1083/jcb.201110034

Lalia, A. Z., and Lanza, I. R. (2016). Insulin-Sensitizing Effects of Omega-3 Fatty Acids: lost in Translation? *Nutrients* 8:329. doi: 10.3390/nu8060329

Lauritzen, K. H., Hasan-Olive, M. M., Regnell, C. E., Kleppa, L., Scheibye-Knudsen, M., Gjedde, A., et al. (2016). A ketogenic diet accelerates neurodegeneration in mice with induced mitochondrial DNA toxicity in the forebrain. *Neurobiol. Aging* 48, 34–47. doi: 10.1016/j.neurobiolaging.2016.08.005

Lepretti, M., Martucciello, S., Burgos Aceves, M. A., Putti, R., and Lionetti, L. (2018). Omega-3 fatty acids and insulin resistance: focus on the regulation of mitochondria and endoplasmic reticulum stress. *Nutrients* 10:350. doi: 10.3390/nu10030350

Li, X. C., Hu, Y., Wang, Z. H., Luo, Y., Zhang, Y., Liu, X. P., et al. (2016). Human wild-type full-length tau accumulation disrupts mitochondrial dynamics and the functions via increasing mitofusins. *Sci. Rep.* 6:24756. doi: 10.1038/srep24756

Liao, C., Ashley, N., Diot, A., Morten, K., Phadwal, K., Williams, A., et al. (2017). Dysregulated mitophagy and mitochondrial organization in optic atrophy due to OPA1 mutations. *Neurology* 88, 131–142. doi: 10.1212/WNL.0000000000003491

Lima, P. A., Sampaio, L. P., and Damasceno, N. R. (2014). Neurobiochemical mechanisms of a ketogenic diet in refractory epilepsy. *Clinics* 69, 699–705. doi: 10.6061/clinics/2014(10)09

Lionetti, L., Mollica, M. P., Donizzetti, I., Gifuni, G., Sica, R., Pignalosa, A., et al. (2014). High-lard and high-fish-oil diets differ in their effects on function and dynamic behaviour of rat hepatic mitochondria. *PLoS One* 9:e92753. doi: 10.1371/journal.pone.0092753

Lionetti, L., Sica, R., Mollica, M. P., and Putti, R. (2013). High-lard and high-fish oil diets differ in their effects on insulin resistance development, mitochondrial

morphology and dynamic behaviour in rat skeletal muscle. *Food Nutr. Sci.* 4, 105–112. doi: 10.4236/fns.2013.49A1017

Magrané, J., Cortez, C., Gan, W. B., and Manfredi, G. (2014). Abnormal mitochondrial transport and morphology are common pathological denominators in SOD1 and TDP43 ALS mouse models. *Hum. Mole. Genet.* 23, 1413–1424. doi: 10.1093/hmg/ddt528

Manczak, M., and Reddy, P. H. (2012). Abnormal interaction between the mitochondrial fission protein Drp1 and hyperphosphorylated tau in Alzheimer's disease neurons: implications for mitochondrial dysfunction and neuronal damage. *Hum. Mole. Genet.* 21, 2538–2547. doi: 10.1093/hmg/dds072

Mantzavinos, V., and Alexiou, A. (2017). Biomarkers for Alzheimer's Disease Diagnosis. *Curr. Alzheimer Res.* 14, 1149–1154.

Mattson, M. P. (2004). Pathways towards and away from Alzheimer's disease. *Nature* 430, 631–639.

McDonald, T. J., and Cervenka, M. C. (2018). Ketogenic diets for adult neurological disorders. *Neurotherapeutics* 15, 1018–1031.

Mirzaei, G., and Adeli, H. (2022). Machine learning techniques for diagnosis of alzheimer disease, mild cognitive disorder, and other types of dementia. *Biomed. Sign. Proc. Control* 72:103293. doi: 10.1016/j.bspc.2021.103293

Mishra, P., and Chan, D. C. (2016). Metabolic regulation of mitochondrial dynamics. *J. Cell Biol.* 212, 379–387.

Modrego, P. J., and Ferrández, J. (2004). Depression in Patients with Mild cognitive impairment increases the risk of developing dementia of Alzheimer typea prospective cohort study. *Arch. Neurol.* 61, 1290–1293. doi: 10.1001/archneur.61.8.1290

Natarajan, V., Chawla, R., Mah, T., Vivekanandan, R., Tan, S. Y., Sato, P. Y., et al. (2020). Mitochondrial dysfunction in age-related metabolic disorders. *Proteomics* 20:1800404.

Ni, H. M., Williams, J. A., and Ding, W. X. (2015). Mitochondrial dynamics and mitochondrial quality control. *Redox Biol.* 4, 6–13. doi: 10.1016/j.redox.2014.11.006

Pagani, L., and Eckert, A. (2011). Amyloid-Beta interaction with mitochondria. *Internat. J. Alzheimer's Dis.* 2011:925050. doi: 10.4061/2011/925050

Pugazhenthi, S., Qin, L., and Reddy, P. H. (2017). Common neurodegenerative pathways in obesity, diabetes, and Alzheimer's disease. *Biochimica et biophysica acta* 1863, 1037–1045.

Putti, R., Sica, R., Migliaccio, V., and Lionetti, L. (2015). Diet impact on mitochondrial bioenergetics and dynamics. *Front. Physiol.* 6:109. doi: 10.3389/fphys.2015.00109

Rusek, M., Pluta, R., Ułamek-Kozioł, M., and Czuczwar, S. J. (2019). Ketogenic diet in Alzheimer's disease. *Internat. J. Mole. Sci.* 20:3892. doi: 10.3390/ijms20163892

Saada, A. (2014). Mitochondria: mitochondrial OXPHOS (dys) function ex vivo–The use of primary fibroblasts. *Internat. J. Biochem. Cell Biol.* 48, 60–65. doi: 10.1016/j.biocel.2013.12.010

Sheng, Z. H., and Cai, Q. (2012). Mitochondrial transport in neurons: impact on synaptic homeostasis and neurodegeneration. *Nat. Rev. Neurosci.* 13, 77–93.

Stefanova, N. A., Muraleva, N. A., Maksimova, K. Y., Rudnitskaya, E. A., Kiseleva, E., Telegina, D. V., et al. (2016). An antioxidant specifically targeting mitochondria delays progression of Alzheimer's disease-like pathology. *Aging* 8:2713. doi: 10.18632/aging.101054

Suárez-Rivero, J. M., Villanueva-Paz, M., la Cruz-Ojeda, D., De la Mata, M., Cotán, D., Oropesa-Avila, M., et al. (2017). Mitochondrial dynamics in mitochondrial diseases. *Diseases* 5:1.

Tan, M. S., Cheah, P. L., Chin, A. V., Looi, L. M., and Chang, S. W. (2021). A review on omics-based biomarkers discovery for Alzheimer's disease from the bioinformatics perspectives: statistical approach vs machine learning approach. *Comp. Biol. Med.* 139:104947. doi: 10.1016/j.compbiomed.2021.104947

Tenenbaum, J. (1998). Bayesian modeling of human concept learning. *Adv. Neural. Inform. Proc. Syst.* 1998:11.

Twig, G., Hyde, B., and Shirihai, O. S. (2008). Mitochondrial fusion, fission and autophagy as a quality control axis: the bioenergetic view. *Biochimica et Biophysica Acta* 1777, 1092–1097. doi: 10.1016/j.bbabio.2008.05.001

Tzoufras, I. (2009). *Bayesian Modeling UsingWinb*. ugs. Hoboken, NJ: Wiley.

Vidakovic, B. (2011). *Statistics for Bioengineering Sciences*. New York,NY: Springer.

Wai, T., and Langer, T. (2016). Mitochondrial dynamics and metabolic regulation. *Trends Endocrinol. Metabol.* 27, 105–117.

Wang, X., Su, B., Lee, H. G., Li, X., Perry, G., Smith, M. A., et al. (2009). Impaired balance of mitochondrial fission and fusion in Alzheimer's disease. *J. Neurosci.* 29, 9090–9103. doi: 10.1523/JNEUROSCI.1357-09.2009

Züchner, S., Mersiyanova, I. V., Muglia, M., Bissar-Tadmouri, N., Rochelle, J., Dadali, E. L., et al. (2004). Mutations in the mitochondrial GTPase mitofusin 2 cause Charcot-Marie-Tooth neuropathy type 2A. *Nat. Genet.* 36, 449–451. doi: 10.1038/ng1341

Conflict of Interest: AA holds an unpaid position on the scientific board of the company AFNP Med Austria.

The remaining authors declare that the research was conducted in the absence of any commercial or financial relationships that could be construed as a potential conflict of interest.

Publisher's Note: All claims expressed in this article are solely those of the authors and do not necessarily represent those of their affiliated organizations, or those of the publisher, the editors and the reviewers. Any product that may be evaluated in this article, or claim that may be made by its manufacturer, is not guaranteed or endorsed by the publisher.

frontiers | Frontiers in Neuroscience

ORIGINAL RESEARCH
published: 25 July 2022
doi: 10.3389/fnins.2022.915122

Effect of Date Palm (*Phoenix dactylifera*) Phytochemicals on $A\beta_{1-40}$ Amyloid Formation: An *in-silico* Analysis

Qamar Zia[1,2], Md Tabish Rehman[3], Md Amiruddin Hashmi[4], Sahabjada Siddiqui[5], Abdulaziz Bin Dukhyil[1], Mohammad Z. Ahmed[3], Azfar Jamal[2,6], Saeed Banawas[1,2,7], Sami G. Almalki[1], Mohammad Owais[4], Hamad Qasem Aldhafeeri[1], Ibrahim M. Ibrahim[8], Wael Alturaiki[1], Mohamed F. AlAjmi[3], Mohammed Alsieni[8] and Yaser E. Alqurashi[6]*

[1] Department of Medical Laboratory Sciences, College of Applied Medical Sciences, Majmaah University, Al Majmaah, Saudi Arabia, [2] Health and Basic Sciences Research Center, Majmaah University, Al Majmaah, Saudi Arabia, [3] Department of Pharmacognosy, College of Pharmacy, King Saud University, Riyadh, Saudi Arabia, [4] Interdisciplinary Biotechnology Unit, Faculty of Life Sciences, Aligarh Muslim University, Aligarh, India, [5] Department of Biotechnology, Era's Lucknow Medical College and Hospital, Era University, Lucknow, India, [6] Department of Biology, College of Science Al-Zulfi, Majmaah University, Majmaah, Saudi Arabia, [7] Department of Biomedical Sciences, Oregon State University, Corvallis, OR, United States, [8] Department of Pharmacology, Faculty of Medicine, King Abdulaziz University, Jeddah, Saudi Arabia

OPEN ACCESS

Edited by:
Asma Perveen, Glocal University, India

Reviewed by:
Sajal Kumar Halder, Jahangirnagar University, Bangladesh
Parijat Kabiraj, Mayo Clinic, United States
Mubashir Hassan, The Research Institute at the Nationwide Children's Hospital, United States

***Correspondence:**
Qamar Zia
qamarbiotech@gmail.com;
qamarzia@mu.edu.sa

Specialty section:
This article was submitted to Neurodegeneration, a section of the journal Frontiers in Neuroscience

Received: *07 April 2022*
Accepted: *23 June 2022*
Published: *25 July 2022*

Citation:
Zia Q, Rehman MT, Hashmi MA, Siddiqui S, Bin Dukhyil A, Ahmed MZ, Jamal A, Banawas S, Almalki SG, Owais M, Aldhafeeri HQ, Ibrahim IM, Alturaiki W, AlAjmi MF, Alsieni M and Alqurashi YE (2022) Effect of Date Palm (Phoenix dactylifera) Phytochemicals on $A\beta_{1-40}$ Amyloid Formation: An in-silico Analysis. Front. Neurosci. 16:915122. doi: 10.3389/fnins.2022.915122

Alzheimer's disease (AD) is a neurodegenerative disease and the most prevalent form of dementia. The generation of oxygen free radicals and oxidative damage is believed to be involved in the pathogenesis of AD. It has been suggested that date palm, a plant rich in phenolic compounds and flavonoids, can provide an alternative treatment to fight memory loss and cognitive dysfunction due to its potent antioxidant activity. Thus, we studied the effect of flavonoids present in date palm on $A\beta_{1-40}$ amyloid formation using molecular docking and molecular dynamics simulation. AutoDock. Myricetin was used as a positive control drug. The flavonoids Diosmetin, Luteolin, and Rutin were found to be potent inhibitors of aggregation (docking energies ≤ -8.05 kcal mol^{-1}) targeting $A\beta_{1-40}$ fibrils (both 2LMO and 6TI5), simultaneously. Further screening by physicochemical properties and drug-likeness analysis suggested that all flavonoids except Rutin followed Lipinski's rule of five. Rutin was, thus, taken as a negative control (due to its violation of Lipinski's rule) to compare its dynamics with Diosmetin. Diosmetin exhibited the highest positive scores for drug likeness. Since Luteolin exhibited moderate drug-likeness and better absorption properties, it was also included in molecular dynamics simulation. Molecular dynamics of shortlisted compounds (Rutin, Diosmetin, and Luteolin) were performed for 200 ns, and the results were analyzed by monitoring root mean square deviations (RMSD), root mean square fluctuation (RMSF) analysis, the radius of gyration (Rg), and solvent accessible surface area (SASA). The results proved the formation of a stable protein-compound complex. Based on binding energies and non-bonded interactions, Rutin and Luteolin emerged as better lead molecules than Diosmetin. However, high MW (610.5), lowest absorption rate (16.04%), and more than one violation of Lipinski's rule make Rutin a less likely candidate as an anti-amyloidogenic agent. Moreover, among non-violators of Lipinski's rule, Diosmetin exhibited a greater

absorption rate than Luteolin as well as the highest positive scores for drug-likeness. Thus, we can conclude that Diosmetin and Luteolin may serve as a scaffold for the design of better inhibitors with higher affinities toward the target proteins. However, these results warrant *in-vitro* and *in-vivo* validation before practical use.

Keywords: Alzheimer's disease, *Phoenix dactylifera* (date palm), molecular docking (MD), phytochemicals (alkaloids/lignans), drug likeness and bioactivity

INTRODUCTION

Alzheimer's disease (AD), a progressive neurodegenerative disorder, is most prevalent among the elderly and encompasses cognitive dysfunction, intellectual decline, and personality changes (Yamada et al., 1999). AD is typically associated with granulovacuolar degeneration, amyloid precursor protein (APP) derived amyloid-beta (Aβ) peptide deposition in extracellular tissue, and neurofibrillary tangles (NFTs) within the neurons. AD and other forms of dementia are ranked as the 7th leading cause of death globally according to the World Health Organization (WHO) (WHO Fact Sheet, 2020), with 40–50 million individuals currently living with dementia (Nichols et al., 2019). The prevalence of dementia in Saudi Arabia is estimated at 6.4%, with number of cases projected to nearly triple by 2060 [Ministry of Health (MoH), KSA, 2022] . As the elderly population ages, Alzheimer's, a form of dementia, is likely to become a more significant healthcare issue, if proactive measures are not taken (Alzheimer's Association Report, 2020).

Although the pathogenesis of AD is complex, increased oxidative distress forms the basis for neurodegeneration (Markesbery and Carney, 1999). Memory-related brain structures are particularly susceptible to oxidative stress because they require a high amount of oxygen (Floyd, 1992; Coyle and Puttfarcken, 1993). Highly reactive oxygen free radicals generated during high metabolic activity in the brain are toxic to neuronal cells; thus, believed to be involved in the etiology of the disease. Aging increases chronic oxidative stress, a major risk factor for Alzheimer's (Lee et al., 2022).

Several epidemiological studies investigating the effect of dietary components on AD are in the early stages. Nonetheless, fruit- and vegetable-rich diet may provide an effective alternative to AD by improving age-related memory decline and cognitive dysfunction associated with AD (Dominguez and Barbagallo, 2018). In the animal model, the antioxidant nutrients appear to protect neurons from oxidative damage and inflammatory responses. Histological studies also indicated that mice fed with antioxidant supplements exhibit less neuronal cell death (Joseph et al., 1998; Guerrero et al., 1999).

Fruits of the date palm (*Phoenix dactylifera* L. Arecaceae) represent a vital component of the diet and a staple food in Arabian countries. Date fruit is listed in folk remedies for the treatment of various diseases (Duke, 1992). In addition, date palm fruits have demonstrated immunomodulatory (Puri et al., 2000), antibacterial (Sallal and Ashkenani, 1989), antihyperlipidemic (Salah and Al-Maiman, 2005), hepatoprotective (Saafi et al., 2011), renal protective (Al Qarawi et al., 2008), anticancerous (Ishurda and John, 2005), antifungal (Sallal et al., 1996; Shraideh et al., 1998), and antimutagenic activities (Vayalil, 2002). The importance of dates in human nutrition derives from its valuable ingredients, such as carbohydrates, dietary fiber, salts, vitamins, and proteins (Vayalil, 2002). Besides nutritional value, date fruits are rich in antioxidants and phenolic compounds with free radical activity. An aqueous extract of date palm (ADFE) has recently shown promising neuroprotective activity in different models of neurodegeneration (Asadi-Shekaari et al., 2008; Zangiabadi et al., 2011; Badeli et al., 2016).

This study was designed to investigate the anti-amyloidogenic property of flavonoids present in date palm extract. We tested several date palm compounds against the $A\beta_{1-40}$ fibrils, responsible for the formation of amyloid. We also evaluated drug-likeness and toxicity potential of these chemicals Molecular docking was then performed to ascertain the best ligand. Next, we assessed its binding potential and stability in molecular dynamics studies. This study suggests that Diosmetin may be used as a novel inhibitor of protein aggregation and can act as a neuroprotective agent.

MATERIALS AND METHODS

Preparation of Proteins and Ligands

The protein targets used in this study [2LMO: structural model of a 40-residue β-amyloid fibril, and 6TI5: structural model of $A\beta_{1-40}$ fibrils] were downloaded from the PDB RCSB database (www.rcsb.org). It was noted that there are no water molecules and heteroatoms in the pdb files of 2LMO and 6TI5. Thus, prior to molecular docking, the proteins were pre-processed only by assigning Kollman charges using AutoDock Tool (ADT). The structure of protein molecules was finally energy minimized by MMFF (Merck Molecular Force Field) using Discovery Studio. The 2D structures of ligands namely, Apigenin (CID: 5280443), Cianidanol (CID: 9064), Diadzein (CID: 5281708), Diosmetin (CID:5281612), Ferulic acid (CID: 445858), Formonometin (CID:5280378), Gallic acid (CID:370), Genistein (CID:5280961), Gycitein (CID:5317750), Luteolin (CID:5280445), Quercetin (CID:5280343), Rutin (CID:5280805), Sinapic acid (CID:637775), and Vanillic acid (CID:8468) were downloaded from PubChem database and prepared for molecular docking by assigning bond orders and angles using ADT. Gasteiger partial charges were defined in ADT, and the

energies of all the ligands were minimized using UFF (Universal Force Field).

Molecular Docking

The interaction between proteins and ligands was determined by conducting molecular docking using AutoDock4.2 (Morris et al., 2009; Alsaleem et al., 2020; Al-Shabib et al., 2020). All the ligands were individually docked with each of the target proteins in separate docking runs. The molecular docking was performed inside a grid box covering the whole protein molecule i.e., a blind docking approach was adopted. For 2LMO, the dimension of the grid box was set to 50.7 × 77.7 × 58.9 Å, centered at 13.8 × 69.8 × 72.3 Å with 0.375 Å spacing between the grid points. Similarly, the dimension of the grid box for 6TI5 was set to 45.4 × 52.1 × 58.6 Å, centered at −1.1 × 6.0 × 1.6 Å with 0.375 Å spacing. Molecular docking was performed using LGA (Lamarck Genetic Algorithm) and Solis-Wets local search methods During molecular docking, LGA is generally used as the global search method, while the Solis-Wets method is directed for the local search. Solis and Wets local search act as a kind of cross-validation of the free energy model (Morris et al., 1998). For each run, 2.5×10^6 energy calculations were computed and a total of 10 docking runs were performed. The population size, translational step, quaternions, and torsions were set as 150, 0.2, 5, and 5 respectively. The van der Waals' and electrostatic parameters were calculated with the help of a distance-dependent dielectric function. We have also performed molecular docking using DockThor using the default setting to reconfirm the results of AutoDock4.2 (Guedes et al., 2021). The docking affinity or dissociation constant (K_d) of ligands for proteins was estimated from docking energy (ΔG) using the following relation as reported earlier (Ahmed et al., 2021).

$$\Delta G = -RT \ln K_d \quad (1)$$

where, R and T were universal gas constant (1.987 cal/mol-K) and temperature (298 K) respectively.

Calculation of Physicochemical Properties and Prediction of Toxicity Potential

Drug-likeness, mutagenic, tumorigenic, reproductive, and irritant effects of drug-toxicity risk parameters were analyzed by OSIRIS Data Warrior V5.2.1 software (https://openmolecules.org/datawarrior/) (Siddiqui et al., 2020; Iqbal et al., 2022). All of the 14 active constituents of date palm were also evaluated using Lipinski's rule of five (Lipinski, 2004). The drug-likeness parameters *viz.* MW ≤ 500, logP ≤ 5, number of hydrogen bond donors (NOHNH) ≤ 5 and hydrogen bond acceptor sites (NON) ≤ 10, topological polar surface area (TPSA) (≤140 Å^2), and number of the rotatable bond (≤10) were measured. The absorption % was calculated as: % Absorption = 109 – [0.345×Topological Polar Surface Area] (Zhao et al., 2002).

Molecular Dynamics Simulation

The molecular dynamics (MD) simulation of the 2LMO and 6TI5 protein and their respective complexes with Diosmetin, Luteolin, and Rutin exhibiting the lowest binding energies were performed in the aqueous environment. The MD simulations were carried out in Gromacs-2018.1 using the Amber99SB-ILDN force field (Van Der Spoel et al., 2005). All the 3 ligand molecules were extracted from their respective complexes with 2LMO and 6TI5 and their topologies were generated in the AmberTools21 using the AM1-BCC charge model with Antechamber packages (Sousa Da Silva and Vranken, 2012). Both the 2LMO and 6TI5 protein alone and their complexes with Diosmetin, Luteolin, and Rutin were first solvated using the TIP3P water model followed by the neutralization of charges of each system by adding an equal number of counter sodium/chlorine ions. All systems were minimized to a maximum of 50,000 steps using the steepest descent minimization to remove the weak Van der Waals contacts. The first equilibration of all systems (NVT equilibration) was done using a V-rescale thermostat at 300 K and constant volume for 200 ps at a coupling constant of 0.1 ps (Bussi et al., 2007). The second equilibration (NPT equilibration) was performed using Parrinello–Rahman barostat at 1.0 bar and 300 K for 200 ps having a coupling constant of 2 ps (Parrinello and Rahman, 1981). The Coulombs and Lennard Johns interaction had a cutoff distance of 1.4 nm with an integration time step of 2 fs (Darden et al., 1993). The electrostatic interaction was governed using PME (Particle Mesh Ewald) and the Fourier transformation had a grid spacing of 0.16 nm (Essmann et al., 1995). Finally, 200 ns production MD simulation of a total of eight systems, including 2LMO and 6TI5 protein alone and the respective complexes for each protein with Diosmetin, Luteolin, and Rutin, was performed in which 20,000 frames of each trajectory were recorded. The trajectories were subjected to PBC corrections before the analysis. The MM-PBSA analysis for the interaction of the three ligand molecules with the 2LMO and 6TI5 protein was performed for the evaluation of the binding energies (Kumari et al., 2014).

RESULTS AND DISCUSSION

In AD, isoforms of different lengths of β-amyloid protein (Aβ) derived from endoproteolytic cleavage of the transmembrane APP, are the main components of senile plaques (Henning-Knechtel et al., 2020). Aβ monomers aggregate into different forms of oligomers, which can then form fibrillar polypeptide aggregates found in the brains of Alzheimer's disease patients (Chen et al., 2017). The 40-residue peptide $A\beta_{1-40}$ represents the most abundant Aβ isoform in the brain (Mori et al., 1992; Selkoe and Hardy, 2016). It has been established that high $A\beta_{1-40}$ levels are associated with a greater mortality rate in the elderly (Lehmann et al., 2020). Therefore, we have selected $A\beta_{1-40}$ as our model protein. Since diverse conformations of the same protein are available, we choose to perform our studies on two different conformers of the same target ($A\beta_{1-40}$) namely, 2LMO and 6TI5.

Dates are a good source of energy, vitamins, and important elements, such as phosphorus, iron, potassium, and a significant amount of calcium (Aljaloud et al., 2020). Dates have been reported to have high antioxidant contents and activities (Saleh et al., 2011; Mistrello et al., 2014; Al-Jasass et al., 2015;

TABLE 1 | Molecular docking scores of selected palm date phytochemicals.

S. No.	Compound name	PubChem ID	Formula	AutoDock docking energy (kcal mol^{-1})		DockThor docking energy (kcal mol^{-1})	
				2LMO	6TI5	2LMO	6TI5
1.	Apigenin	5280443	$C_{15}H_{10}O_5$	−8.0	−7.2	−8.4	−7.1
2.	Cianidanol	9064	$C_{15}H_{14}O_6$	−8.3	−7.3	−8.2	−7.2
3.	Diadzein	5281708	$C_{15}H_{10}O_4$	−7.6	−7.9	−8.3	−7.3
4.	Diosmetin	5281612	$C_{16}H_{12}O_6$	−8.5	−7.7	−8.6	−7.8
5.	Ferulic acid	445858	$C_{10}H_{10}O_4$	−6.3	−6.2	−6.8	−6.7
6.	Formononetin	5280378	$C_{16}H_{12}O_4$	−7.9	−8.5	−8.4	−7.2
7.	Gallic acid	370	$C_7H_6O_5$	−6.2	−5.6	−6.3	−6.6
8.	Genistein	5280961	$C_{15}H_{10}O_5$	−7.6	−7.8	−8.9	−7.7
9	Gycitein	5317750	$C_{16}H_{12}O_5$	−7.7	−7.1	−8.5	−7.2
10.	Luteolin	5280445	$C_{15}H_{10}O_6$	−8.5	−7.7	−8.7	−7.9
11.	Quercetin	5280343	$C_{15}H_{10}O_7$	−8.2	−8.0	−7.1	−6.9
12.	Rutin	5280805	$C_{27}H_{30}O_{16}$	−8.7	−8.5	−8.9	−8.3
13.	Sinapic acid	637775	$C_{11}H_{12}O_5$	−6.3	−5.5	−6.9	−6.8
14.	Vanillic acid	8468	$C_8H_8O_4$	−6.5	−5.6	−6.8	−6.5
15.	Myricetin (Control)	5281672	$C_{15}H_{10}O_8$	−8.5	−7.6	−8.5	−7.6

Shahdadi et al., 2015). Studies with various varieties of dates have shown the presence of both free and bound phenolic acids (Al-Farsi et al., 2005) that are responsible for their potent antioxidant property. Moreover, date varieties from different regions had different levels and patterns of phenolic acids. Various phenolic acids (Luteolin, quercetin, Rutin, apigenin, (+)-catechin, and (–)-epicatechin, gallic, p-hydroxybenzoic, vanillic, caffeic, syringic, sinapic, coumaric, ferulic and protocatechuic acid) have been tentatively identified (Al-Shwyeh, 2019). Here, we speculated whether date palm fruits growing in Saudi Arabia can inhibit the formation of the Aβ1-40 fibril. For this, we evaluated the drug-likeness and toxicity potential of common date palm phytocomponents. The best ones were then subjected to molecular docking and simulation studies to identify the paramount compound that can be used against $A\beta_{1-40}$ fibrils. We have included Myricetin as a control/standard ligand in molecular docking with both target proteins. Also, we have performed molecular docking using DockThor to confirm the results obtained using AutoDock.

Docking of Natural Compounds of Date Palm Fruits Against 2LMO and 6TI5

In this study, the binding affinities of various natural compounds as promising anti-aggregation lead molecules against $A\beta_{1-40}$ were determined by molecular docking. The computational screening revealed the AutoDock docking energies of the studied ligands were in the range of −6.2– −8.7 kcal/mol, and −5.5– −8.5 kcal/mol for 2LMO and 6TI5, respectively (**Table 1**). Moreover, the docking energies obtained from DockThor server were in the range of −6.3– −8.9 kcal/mol for 2LMO and −6.5– −8.3 kcal/mol for 6TI5 (**Table 1**). Based on the docking score of ligands from AutoDock, Diosmetin, Genistein, Gycitein, Luteolin, and Rutin had binding energies ≤ -8.5 kcal/mol (docking energy of Myricetin) against 2LMO. Likewise, Diosmetin, Genistein, Luteolin, and Rutin displayed docking energies ≤ -7.6 kcal/mol (docking energy of Myricetin) against 6TI5. Further analysis by comparing the docking energies of ligands obtained from DockThor revealed that three ligands (Diosmetin, Luteolin, and Rutin) showed binding energies of ≤ -8.5 kcal/mol (which is the docking energy of the control ligand i.e., Myricetin) against 2LMO. Similarly, Diadzein, Diosmetin, Formononetin, Genistein, Luteolin, Quercetin, and Rutin displayed binding energies of ≤ -7.6 kcal/mol (docking energy of Myricetin) against 6TI5. An analysis of these results showed that Diosmetin, Luteolin, and Rutin were the most promising natural compounds targeting both 2LMO and 6TI5, simultaneously. Hence, a detailed interaction and molecular dynamics simulation of Diosmetin, Luteolin, and Rutin was further studied.

Prediction of Physicochemical Properties, Drug-Likeness, and Toxicity Potentials

Analysis of toxicity risk assessment provides the initial knowledge of probable side effects of phytocomponents that may be utilized in lead discovery and development. The prediction of different properties of phytocomponents at an early stage is a vital step in leading discovery and development. The OSIRIS Data Warrior V5.2.1 program was used to assess the toxicological characteristics and drug-likeness of date palm phytochemicals. Lipinski's rule explains the molecular characteristics of a chemical that are critical for lead optimization and selectivity of a possible orally active therapeutic candidate in clinical applications (Lipinski, 2004). In general, an orally active drug should have no more than one Lipinski violation, otherwise, its bioavailability will be reduced. Among all compounds, Rutin displayed three violations of Lipinski's rule of five (**Table 2**). The lowest absorption rate (16.04%) was expected for Rutin due to its

TABLE 2 | Physicochemical properties of palm date phytochemicals.

S. No.	Compound name	% Absorption (> 50%)	TPSA ()(< 160)	MW(< 500)	c logP (< 5)	HA	HBD (≤ 5)	HBA(≤ 10)	RB (≤ 10)	ROF violation
1.	Apigenin	77.64	90.89	270.2	2.46	20	3	5	1	0
2.	Cianidanol	70.92	110.4	290.3	1.37	21	5	6	1	0
3.	Diadzein	84.61	70.67	254.2	2.56	19	2	4	1	0
4.	Diosmetin	74.45	100.1	300.3	2.28	22	3	6	2	0
5.	Ferulic acid	85.96	66.76	194.2	1.25	14	2	4	3	0
6.	Formononetin	88.41	59.67	268.3	3.1	20	1	4	2	0
7.	Gallic acid	75.19	97.98	170.1	0.59	12	4	5	1	0
8.	Genistein	77.64	90.89	270.2	2.27	20	3	5	1	0
9.	Glycitein	81.43	79.9	284.3	2.38	21	2	5	2	0
10.	Luteolin	70.66	111.1	286.2	1.97	21	4	6	1	0
11.	Quercetin	63.68	131.4	302.2	1.68	22	5	7	1	0
12.	Rutin	16.04	269.4	610.5	−1.06	43	10	16	6	3
13.	Sinapic acid	82.78	76	224.2	1.26	16	2	5	4	0
14.	Vanillic acid	85.96	66.76	168.2	1.19	12	2	4	2	0

Percentage Absorption was calculated as: % Absorption = 109 – [0.345×Topological Polar Surface Area]; TPSA, MW, HA, HBD, HBA, RB and ROF stands for total polar surface area, molecular weight, number of heavy atoms, number of hydrogen bond donors, number of hydrogen bond acceptors, number of rotatable bonds, and Lipinski's rule of five.

high MW (610.5), making it a less likely candidate as an anti-amyloidogenic agent. Moreover, all of the compounds having a molecular mass of <500 g/mol, showed high gastrointestinal absorption and zero violation of Lipinski's rule. Among non-violators of Lipinski's rule, Quercetin exhibited the lowest absorption rate. Considering the analyzed physicochemical properties and absorption potential, a further toxicological investigation was carried out and found that Formononetin, Sinapic acid, Cianidanol, Diosmetin, Rutin, and Luteolin exhibited no toxicity for all the tested parameters (**Table 3**). However, the dug-likeness was very low for Formononetin. Diosmetin exhibited the highest positive scores for drug likeness. This stimulated us to explore its property to ameliorate AD and was, therefore, selected for molecular docking and molecular dynamics simulation analysis. We also studied Rutin as a negative control (due to its violation of Lipinski's rule) to compare its dynamics with Diosmetin. Since Luteolin exhibited moderate drug-likeness and better absorption properties, it was also included in molecular dynamics simulation.

Molecular Docking Analysis

Interaction of 2LMO With Phytochemicals

An analysis of molecular docking showed that Rutin, Diosmetin, and Luteolin were bound to a cavity created between different multiple chains of aggregated $A\beta_{1-40}$ protein i.e. the 2LMO model (**Figures 1A,B**). The 2LMO–Rutin complex was primarily stabilized by hydrogen bonding and hydrophobic interactions. Rutin formed four hydrogen bonds with C:ASN27:HD22 (2.69 Å), C:LYS28:HN (2.42 Å), D:ALA30:O (2.54 Å), and I:VAL40:OXT (2.38 Å). Also, Rutin interacted with J:VAL39:CG2 (3.56 Å), C:LYS28:C, O;GLY29:N (4.16Å), and J:VAL39 (4.22 Å) through four hydrophobic interactions (**Figure 1C**). Some residues, such as D:ASN27, D:SER26, K:VAL39, D:GLY29, D:LYS28, E:GLY:29, E:ILE31, K:GLY38, E:ALA30, C:GLY29, J:GLY38, D:ILE31, I:GLY38, C:ILE31, B:ILE31, B:GLY29, and J:VAL40, are further stabilized 2LMO-Rutin complex by van der Waals' interactions. The binding free energy and the corresponding dissociation constant of 2LMO-Rutin were −8.7 kcal mol^{-1}, and 2.40×10^6 M^{-1} (**Table 4**).

The Diosmetin-2LMO complex is stabilized mainly through hydrogen bonding and hydrophobic interactions (**Figure 1D**). The amino acid residues of 2LMO, namely I:GLY38:HN (2.77 Å), D:ALA30:O (2.48 Å), and I:GLY38:O (2.05 Å) formed three hydrogen bonds with Diosmetin (**Table 2**). In addition, D:ILE31 (5.32 Å) and J:VAL39 (3.52 Å, 4.42 Å, and 5.23 Å) interacted with Diosmetin through one and three hydrophobic interactions, respectively. The 2LMO-Diosmetin complex was further stabilized by van der Waals' interactions with B:ASN27, B:GLY29, C:GLY29, C:ILE31, D:LYS28, D:GLY29, E:GLY29, E:ALA30, E:ILE31, H:GLY38, I;GLY37, I:VAL39, I:VAL40, and J:GLY38. The binding energy of 2LMO-Diosmetin complex formation was estimated to be −8.5 kcal mol^{-1} while the dissociation constant was 1.72×10^6 M^{-1} (**Table 4**).

The 2LMO–Luteolin complex was stabilized by hydrogen bonding and hydrophobic interactions. Luteolin formed four hydrogen bonds with I:GLY38:HN (2.84 Å), E:GLY29:O (2.57 Å), E:GLY29:O (2.38 Å), and C:GLY29:CA (3.36 Å). Also, Luteolin interacted with C:ILE31 (5.49 Å), J:VAL39 (3.57 Å), J:VAL39 (4.43 Å), D:ILE31 (5.22 Å), and J:VAL39 (5.36 Å) through four hydrophobic interactions (**Figure 1E**). Some residues, such as B:ASN27, B:GLY29, D:LYS28, D:GLY29, D:ALA30, E:ALA30, E:ILE31, H:GLY38, I:VAL39, J:GLY37, I:VAL40, and J:GLY38, are further stabilized 2LMO–Luteolin complex by van der Waals' interactions. The binding free energy and the corresponding dissociation constant of 2LMO-Luteolin were−8.5 kcal mol^{-1} and 1.72×10^6 M^{-1} (**Table 4**).

Interaction of 6TI5 With Phytochemicals

In the case of molecular docking with 6TI5, Rutin, Diosmetin, and Luteolin were found to occupy the cavity created due to the formation of fibril i.e., 6TI5 model (**Figures 2A,B**). It has been found that Rutin interacted with 6TI5 through

TABLE 3 | Drug-likeness and toxicity potential of palm date phytochemicals.

S. No.	Compound name	Druglikeness properties				
		Druglikeness	**Mutant**	**Tumorigenic**	**Reproductive effective**	**Irritant**
1.	Apigenin	0.28194	High	None	None	None
2.	Cianidanol	0.31525	None	None	None	None
3.	Diadzein	−0.09385	None	None	High	None
4.	Diosmetin	0.40331	None	None	None	None
5.	Ferulic acid	0.27506	High	High	High	None
6.	Formononetin	0.036465	None	None	None	None
7.	Gallic acid	−1.8442	High	None	High	None
8.	Genistein	−0.09385	High	High	High	None
9.	Glycitein	0.036465	None	None	High	None
10.	Luteolin	0.28194	None	None	None	None
11.	Quercetin	−0.08283	High	High	None	None
12.	Rutin	1.9337	None	None	None	None
13.	Sinapic acid	0.27506	None	None	None	None
14.	Vanillic acid	−1.597	High	None	None	None

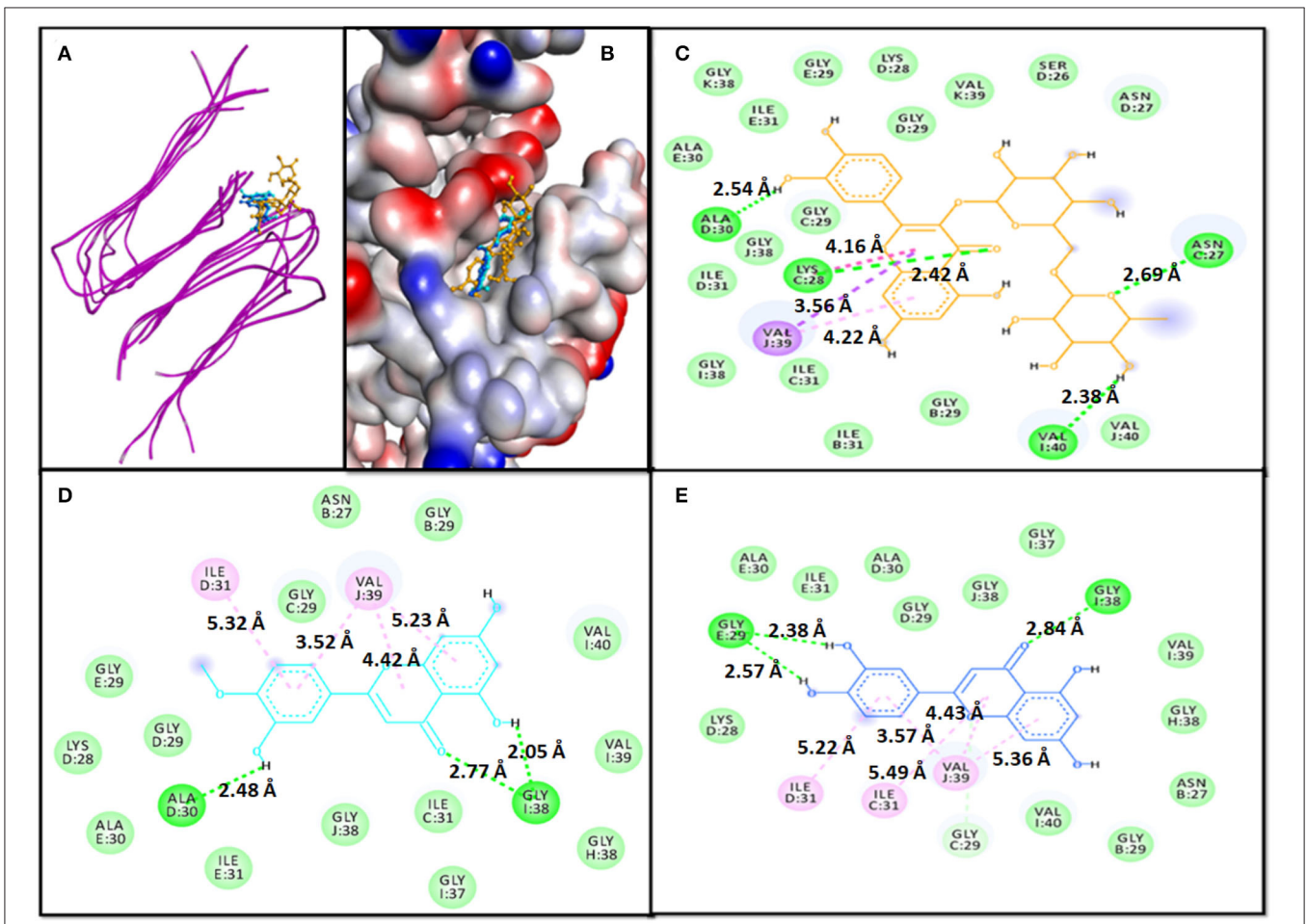

FIGURE 1 | Molecular docking of 2LMO with phytochemicals. **(A)** 2D representation of the binding of phytochemical to 2LMO, **(B)** 3D representation of the binding of phytochemical to 2LMO, **(C)** Interaction between 2LMO and Rutin, **(D)** Interaction between 2LMO and Diosmetin, and **(E)** Interaction between 2LMO and Luteolin.

TABLE 4 | Parameters for the interaction of target proteins (2LMO and 6TI5) with Rutin, Diosmetin, and Luteolin as determined by molecular docking.

Interaction between donor and acceptor atoms	Distance (Å)	Nature of interaction	Binding energy (ΔG), kcal mol^{-1}	Binding affinity (K_d), M^{-1}
2LMO-Rutin				
C:ASN27:HD22 - LIG:O	2.69	Hydrogen Bond	−8.7	2.40×10^6
C:LYS28:HN - LIG:O	2.42	Hydrogen Bond		
LIG:H - D:ALA30:O	2.54	Hydrogen Bond		
LIG:H - I:VAL40:OXT	2.38	Hydrogen Bond		
J:VAL39:CG2 - LIG	3.56	Hydrophobic (Pi-Sigma)		
C:LYS28:C,O;GLY29:N - LIG	4.16	Hydrophobic (Amide-Pi		
LIG - J:VAL39	4.22	Stacked)		
		Hydrophobic (Pi-Alkyl)		
2LMO-Diosmetin				
I:GLY38:HN - LIG:O	2.77	Hydrogen Bond	−8.5	1.72×10^6
LIG:H - D:ALA30:O	2.48	Hydrogen Bond		
LIG:H - I:GLY38:O	2.05	Hydrogen Bond		
LIG - J:VAL39	3.52	Hydrophobic (Pi-Alkyl)		
LIG - J:VAL39	4.42	Hydrophobic (Pi-Alkyl)		
LIG - D:ILE31	5.32	Hydrophobic (Pi-Alkyl)		
LIG - J:VAL39	5.23	Hydrophobic (Pi-Alkyl)		
2LMO-Luteolin				
I:GLY38:HN - LIG:O	2.84	Hydrogen Bond	−8.5	1.72×10^6
LIG:H - E:GLY29:O	2.57	Hydrogen Bond		
LIG:H - E:GLY29:O	2.38	Hydrogen Bond		
C:GLY29:CA - LIG:O	3.36	Hydrogen Bond		
LIG - C:ILE31	5.49	Hydrophobic (Pi-Alkyl)		
LIG - J:VAL39	3.57	Hydrophobic (Pi-Alkyl)		
LIG - J:VAL39	4.43	Hydrophobic (Pi-Alkyl)		
LIG - D:ILE31	5.22	Hydrophobic (Pi-Alkyl)		
LIG - J:VAL39	5.36	Hydrophobic (Pi-Alkyl)		
6TI5-Rutin				
M:HIS13:ND1 - LIG:O	2.95	Hydrogen Bond	−8.5	1.72×10^6
LIG:H - F:ALA30:O	2.94	Hydrogen Bond		
LIG:H - K:VAL12:O	2.07	Hydrogen Bond		
F:LYS28:CE - LIG:O	3.20	Carbon Hydrogen Bond		
LIG:C - K:GLU11:OE2	3.48	Carbon Hydrogen Bond		
LIG - E:ILE31	4.93	Hydrophobic (Pi-Alkyl)		
6TI5-Diosmetin				
LIG:H - M:GLU11:O	2.38	Hydrogen Bond	−7.7	4.44×10^5
K:GLU11:OE2 - LIG	3.98	Electrostatic (Pi-Anion)		
K:GLU11:OE2 - LIG	3.38	Electrostatic (Pi-Anion)		
L:GLU11:OE2 – LIG	4.22	Electrostatic (Pi-Anion)		
6TI5-Luteolin				
LIG:H - L:VAL12:O	2.44	Hydrogen Bond	−7.7	4.44×10^5
LIG:H - M:GLU11:O	2.35	Hydrogen Bond		
LIG:H - J:VAL12:O	2.49	Hydrogen Bond		
LIG:H - K:GLU11:O	2.11	Hydrogen Bond		
K:GLU11:OE2 - LIG	4.05	Electrostatic (Pi-Anion)		
K:GLU11:OE2 - LIG	3.35	Electrostatic (Pi-Anion)		
L:GLU11:OE2 – LIG	4.32	Electrostatic (Pi-Anion)		

three conventional hydrogen bonds, two carbon hydrogen bonds, and one hydrophobic interaction with E:ILE:31 (4.93 Å). The conventional hydrogen bonds were formed by M:HIS31:ND1 (2.95 Å), F:ALA30:O (2.94 Å), and K:VAL12:O (2.07 Å), while carbon hydrogen bonds were formed by F:LYS28:CE (3.20 Å), and K:GLU11:OE2 (3.48 Å) (**Figure 2C**). The 6TI5-Rutin interaction was further stabilized by D:ILE:31, E:ALA30, F:ILE31, I:GLU11, I:HIS13, J:GLU11, J:HIS13, K:HIS13, K:VAL40, L:GLU11, L:VAL12, L:HIS13, M:GLU11, M:VAL40, and N:VAL40, through van der Waals' interaction. Moreover, the binding free energy of Rutin-6TI5 interaction was estimated as −8.5 kcal mol^{-1}, and the corresponding binding affinity was 4.44×10^5 M^{-1} (**Table 4**).

The 6TI5-Diosmetin interaction was favored by one conventional hydrogen bond and three electrostatic interactions

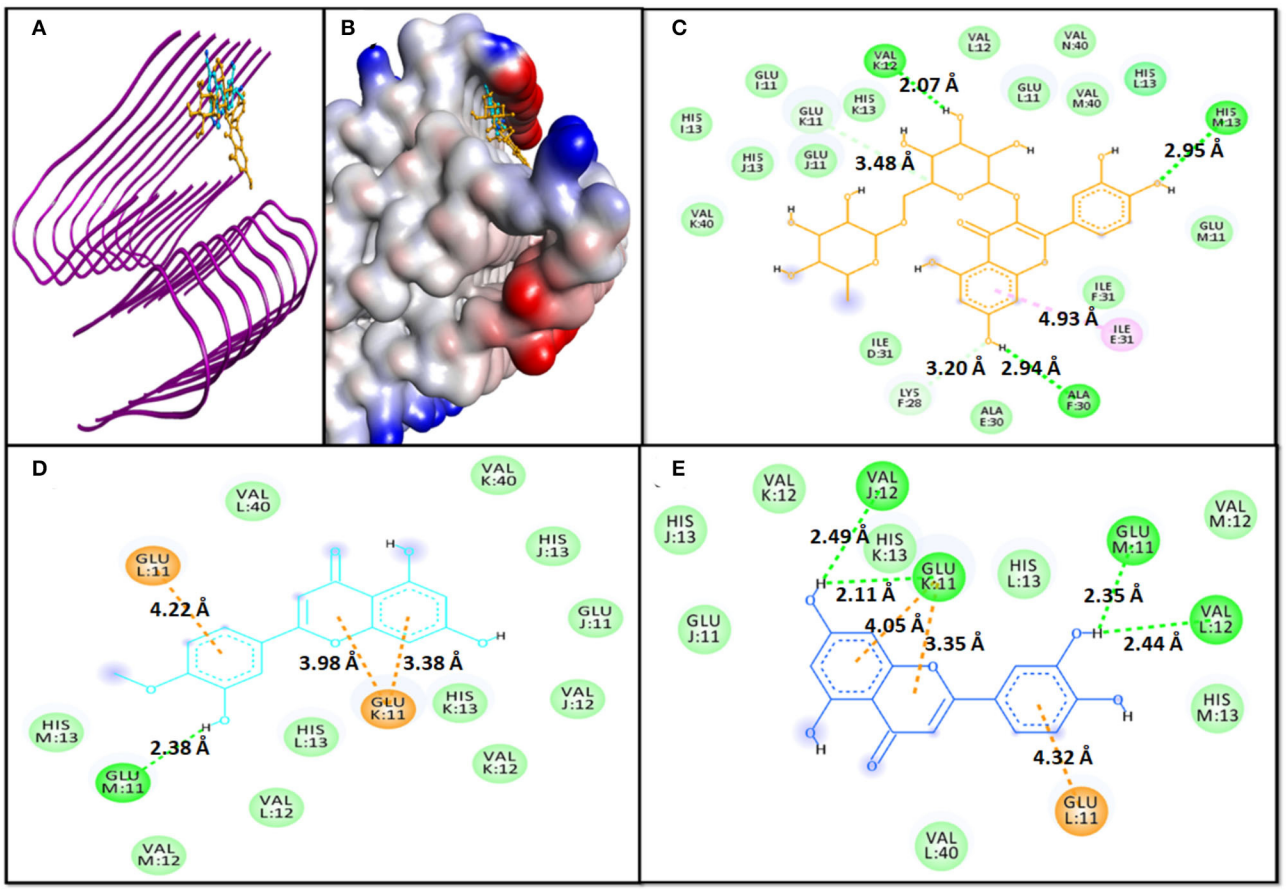

FIGURE 2 | Molecular docking of 6TI5 with phytochemicals. **(A)** 2D representation of the binding of phytochemical to 6TI5, **(B)** 3D representation of the binding of phytochemical to 6TI5, **(C)** Interaction between 6TI5 and Rutin, **(D)** Interaction between 6TI5 and Diosmetin, and **(E)** Interaction between 6TI5 and Luteolin.

(Pi-Anion). The hydrogen bond was formed by M:GLU11:O (2.38 Å), while the electrostatic interactions were formed by K:GLU11:OE2 (3.98 Å, 3.38 Å, and 4.22 Å) (**Figure 2D**). Further, the Diosmetin-6TI5 complex was stabilized by van der Waals' interactions with residues J:GLU11, J:VAL12, J:HIS13, K:VAL12, K:HIS13, K:VAL40, L:VAL12, L:HIS13, L:VAL40, M:VAL12, and M:HIS13. The binding free energy and the corresponding binding affinity of Diosmetin-6TI5 interaction were−7.7 kcal mol^{-1} and 4.44 × 10^5 M^{-1} (**Table 4**).

The 6TI5-Luteolin interaction was favored by four hydrogen bonds and three electrostatic interactions (Pi-Anion). The hydrogen bond was formed by L:VAL12:O (2.44 Å), M:GLU11:O (2.35 Å), and J:VAL12:O (2.49 Å). Likewise, three electrostatic interactions were formed by K:GLU11:OE2 (4.05 Å, 3.35 Å, and 4.32 Å) (**Figure 2E**). Further, the Luteolin-6TI5 complex was stabilized by van der Waals' interactions with residues J:GLU11, J:HIS13, K:VAL12, K:HIS13, L:HIS13, L:VAL40, M:VAL12, and M:HIS13. The binding free energy and the corresponding binding affinity of Luteolin-6TI5 interaction were −7.7 kcal mol^{-1} and 4.44 × 10^5 M^{-1} (**Table 4**).

Molecular Dynamics Simulation Analysis

Root Mean Square Deviation and Root Mean Square Fluctuation Analysis

The docked complexes of the 2LMO protein with Diosmetin, Luteolin, and Rutin were simulated in an aqueous environment to study their dynamics and stability. RMSD is a measure of deviation in the initial frame of protein or protein-ligand complex that occurred during the course of MD simulation. The RMSD plot of 2LMO and 6TI5 protein and their complexes with Diosmetin, Luteolin, and Rutin are shown in **Figure 3**. The RMSD of the backbone atoms of each system was calculated for preliminary analysis of the MD simulation data. The RMSD was calculated with respect to their respective initial conformations. The RMSD of 2LMO depicts some variations initially but was found to be stable after 50 ns of simulation. The 2LMO–Diosmetin complex was found to be stable after 60 ns of simulation time. Similarly, the 2LMO–Luteolin and 2LMO–Rutin complexes attained stability in their structural deviation after 40 and 20 ns of simulation time, respectively. The average RMSD of 2LMO, 2LMO-Diosmetin, 2LMO–Luteolin, and 2LMO-Rutin were found to be at 0.78, 0.81, 0.85, and

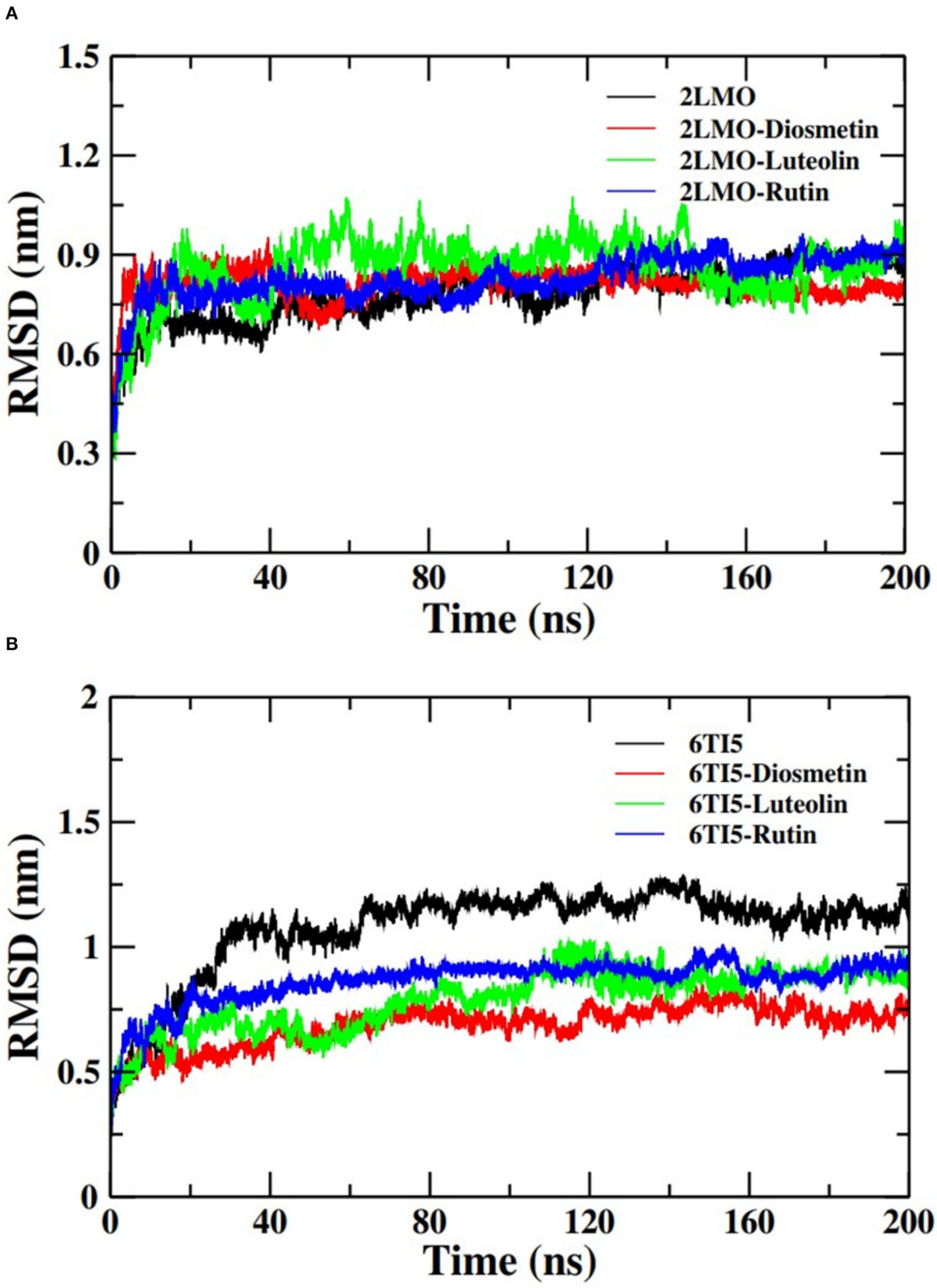

FIGURE 3 | Root mean square deviation (RMSD) of the backbone atoms of **(A)** 2LMO and its complexes with Diosmetin, Luteolin and Rutin and **(B)** 6TI5 and its complexes with Diosmetin, Luteolin and Rutin over 200 ns of MD simulation.

0.82 nm, respectively. Further, the RMSD of the backbone atoms of 6TI5 was found to be stable after 35 ns of MD simulation. Similarly, the three complexes of 6TI5 with diosmetion, Luteolin, and Rutin were found to be stable after 20 ns of simulation time. The average RMSD of 6TI5, 6TI5-Diosmetin, 6TI5-Luteolin, and 6TI5-Rutin were calculated to be 1.07, 0.68, 0.78, and 0.86 nm, respectively. However, RMSD plots revealed relatively greater values that attain equilibration after reaching a particular magnitude of deviation. This reason for such higher RMSD values can be further explained by the residue RMSF plot (**Supplementary Figures 1**, **2**). The RMSF plot clearly indicates higher fluctuations in the residues ranging from 20 to 30 amino acids, as well as the C and N terminal residues of 2LMO and 6TI5. These regions define the loop of the protein and exhibit relatively greater RMSF values in some of the chains. This change in RMSF values (relatively higher or lower) is the plausible reason for structural deviations in the respective complexes, resulting in high RMSD values. Several studies have reported a higher value of RMSD of the backbone atoms of Abeta-1-40 protein (Minicozzi et al., 2014; Turner et al., 2019). The native structure of $A\beta_{1-40}$ shows higher RMSD (1.4–1.6 nm), which is its characteristic property $A\beta_{1-40}$ (Minicozzi et al., 2014). In a similar study, RMSD of $A\beta_{1-40}$ was shown to fall in the range of around 1 nm (Turner et al., 2019). Aligning to these previously reported findings, the RMSD values in our study for the $A\beta_{1-40}$ show a comparable range which is stable over the entire course of MD simulation. Moreover, the high RMSD values are also due to fluctuations (RMSF) contributed by the loop regions of the protein as explained earlier. In brief, the data from both the plots clearly indicate that the structures subjected to molecular dynamic simulations attain stability in the aqueous medium after a certain period of simulation time and there isn't any major structural deviation over the course of 200 ns of MD simulation.

Radius of Gyration Analysis

Moving forward, the analysis proceeded with calculating the Rg of the C_α atoms of the 2LMO and 6TI5 protein and its complex with Diosmetin, Luteolin, and Rutin (**Figure 4**). Rg indicates the stability of the complexes as a function of the collective mass-weighted root mean square distance of atoms during the molecular dynamic simulation from the center of mass. It is a measure of the overall compactness and 3-D structure of a protein in different conditions and is generally used to access the conformational and folding behavior of proteins (Hashmi et al., 2021). The average Rg of 2LMO, 2LMO-Diosmetin, 2LMO-Luteolin, and 2LMO-Rutin was found to be 1.55, 1.54, 1.60, and 1.52 nm, respectively. Similarly, the average Rg for the 6TI5, 6TI5-Diosmetin, 6TI5-Luteolin, and 6TI5-Rutin was found to be 1.48, 1.50, 1.57, and 1.56 nm, respectively. It should be pointed out that the change in Rg values was not very significant, indicating the formation of stable protein-ligand complexes, conferring the stability of the complexed systems over the course of MD simulations.

Solvent Accessible Surface Area Analysis

Further analysis of the MD simulation data was performed by calculating SASA and the energies of all systems. SASA is a parameter to analyze the nature of structural compactness of proteins and their complexes with the ligand molecules by calculating the area of the protein surface interacting with the continuum solvent (Ahmad et al., 2021). The measurement of SASA is fundamental to understanding the folding-unfolding pathway of a protein in an altered environment or due to the binding of ligand molecules. Here, we have measured SASA of 2LMO and 6TI5 in the presence of Rutin and Diosmetin (**Figure 5**). The SASA of 2LMO, 2LMO-Diosmetin, 2LMO-Luteolin, and 2LMO-Rutin complexes was found to be constant throughout the simulation. The average SASA of 2LMO, 2LMO-Diosmetin, 2LMO-Luteolin, and 2LMO-Rutin was determined as 84.28, 83.30, 87.73, and 82.30 nm^2, respectively. Similarly, the SASA of 6TI5 and its complexes with the three ligand molecules were found to be uniform throughout the course of the MD simulation. The average SASA of 6TI5, 6TI5-Diosmetin, 6TI5-Luteolin, and 6TI5-Rutin were found to be 81.05, 78.74, 76.81, and 78.00 nm^2, respectively. The data shows the stable nature of the proteins (2LMO and 6TI5) with all their complexes in aqueous conditions suggesting that the structure has not compacted or expanded significantly. Moreover, the physicochemical parameters, such as potential and total energies of the system, were also calculated. The total and potential energies of the systems (**Figures 6**, **7**) for both the proteins (2LMO and 6TI5) and their respective complexes with Diosmetin, Luteolin, and Rutin remained constant throughout the simulation, further verifying the stable nature of all systems.

Hydrogen Bond Analysis

The interaction of the ligand molecules Diosmetin, Luteolin, and Rutin with 2LMO and 6TI5 proteins was studied by determining the hydrogen bond profiles between the respective complexes (**Table 4**). The residues, including Gly(A), Gly(B), Val(B), Tyr(C), and His(D), in the 2LMO–Diosmetin complex exhibit 12.86, 9.76, 75.43, 13.05, and 6.54% existence of hydrogen bond formation over the course of 200 ns of MD simulation. Similarly, in case of 2LMO–Luteolin complex, residues Met(A), Gly(A), Gln(B), and Gln(C) contributes with 10.46, 12.44, 8.55, 8.27% existence for H-bond formation. The Val(B) in the 2LMO-Luteolin complex shows more than 40 % H-bond existence. Further, the residues Gly(A), Gln(C), and Tyr(C) in the 2LMO-Rutin complex exhibit 66.87, 32.75, and 61.42% existence of H-bond formation. Val(A) also contributes significantly with >40% H-bond existence in the 2LMO-Rutin complex.

We also studied the hydrogen bond existence map of 6TI5-Diosmetin, 6TI5-Luteolin, and 6TI5-Rutin. Glu22 in the 6TI5-Diosmetin complex shows >15% H-bond existence and Phe19 has 7.44% of H-bond existence. Similarly, in the 6TI5-Luteolin complex, Glu11 and Glu22 show H-bond formation having 5.71 and 7.42% existence. There is significant H-bond formation observed in the 6TI5-Rutin complex. His13 and Gly37 show H-bond formation exhibiting 61.5 and 42.18% existence. In addition, Gln15 also shows >25% of H-bond

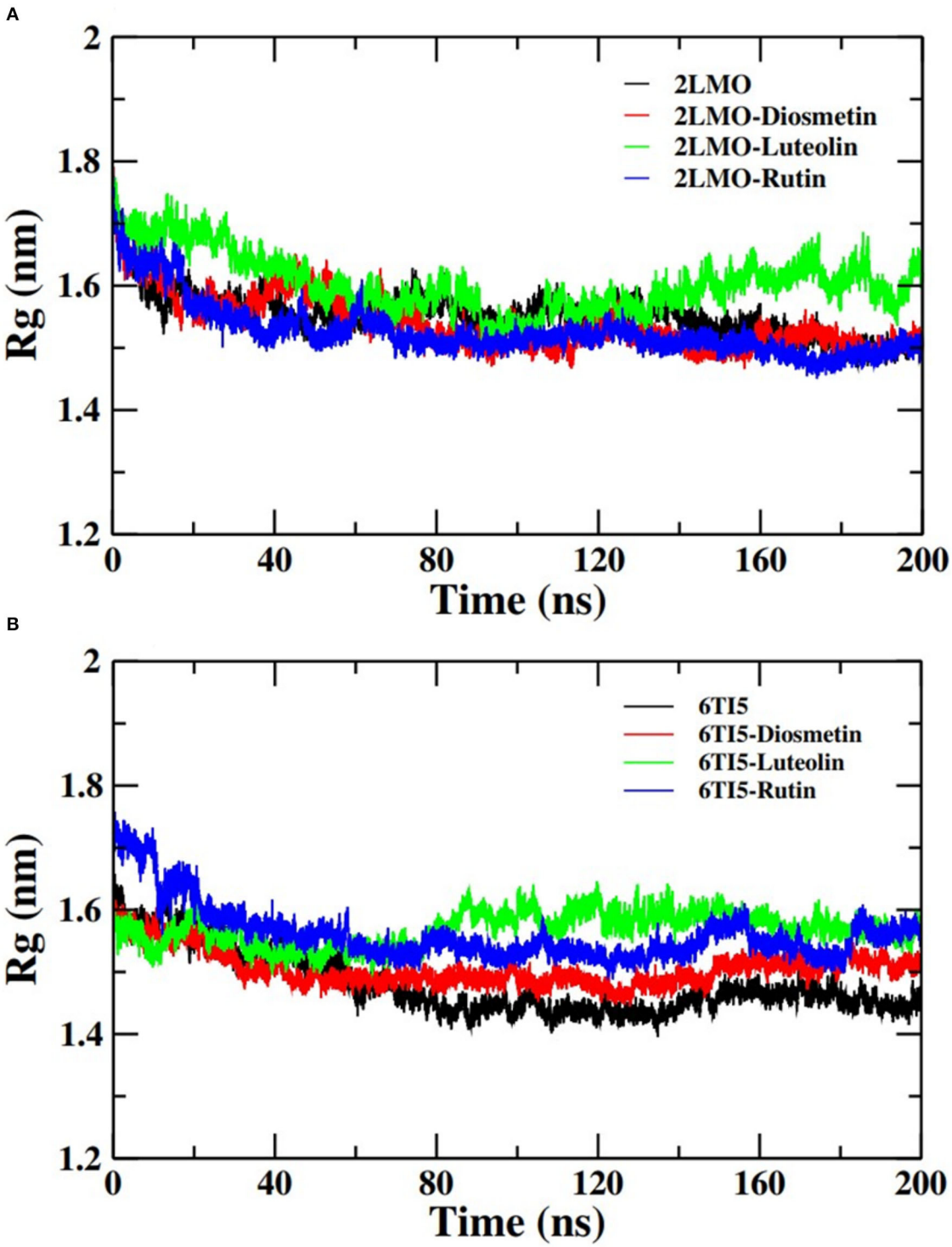

FIGURE 4 | Radius of gyration (Rg) of backbone atoms of **(A)** 2LMO and its complexes with Diosmetin, Luteolin and Rutin and **(B)** 6TI5 and its complexes with Diosmetin, Luteolin and Rutin over the course of 200 ns of simulation time.

existence in the 6TI5-Rutin complex. The high percent of hydrogen bond formation between the 2LMO-Rutin and 6TI5-Rutin complexes is due to more polar functional groups in Rutin compared to disometin and Luteolin which order facilitates more possibility of hydrogen bond formation with the protein residues.

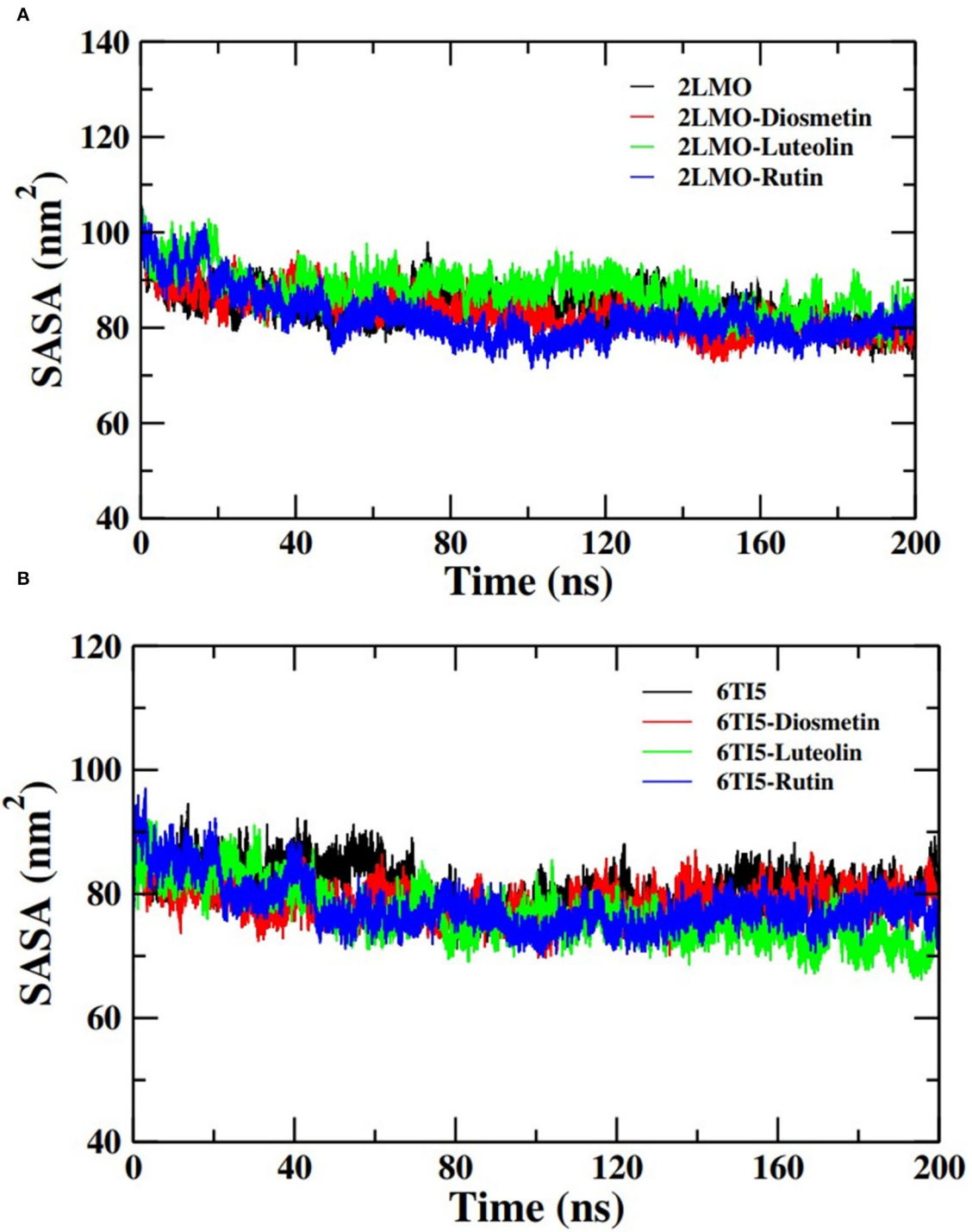

FIGURE 5 | Solvent accessible surface area (SASA) of **(A)** 2LMO and its complexes with Diosmetin, Luteolin and Rutin and **(B)** 6TI5 and its complexes with Diosmetin, Luteolin and Rutin over the course of 200 ns of simulation time.

Evaluation of the Energies Involved in Binding (MM-PBSA Calculations)

The different binding energies involved in the interaction of both the proteins (2LMO and 6TI5) with the respective ligand (Diosmetin, Luteolin, and Rutin) molecules were determined using MM-PBSA calculations. For MM-PBSA calculations, 500 frames were taken out from the last 50 ns MD simulation trajectory of 2LMO and its three complexes at uniform intervals.

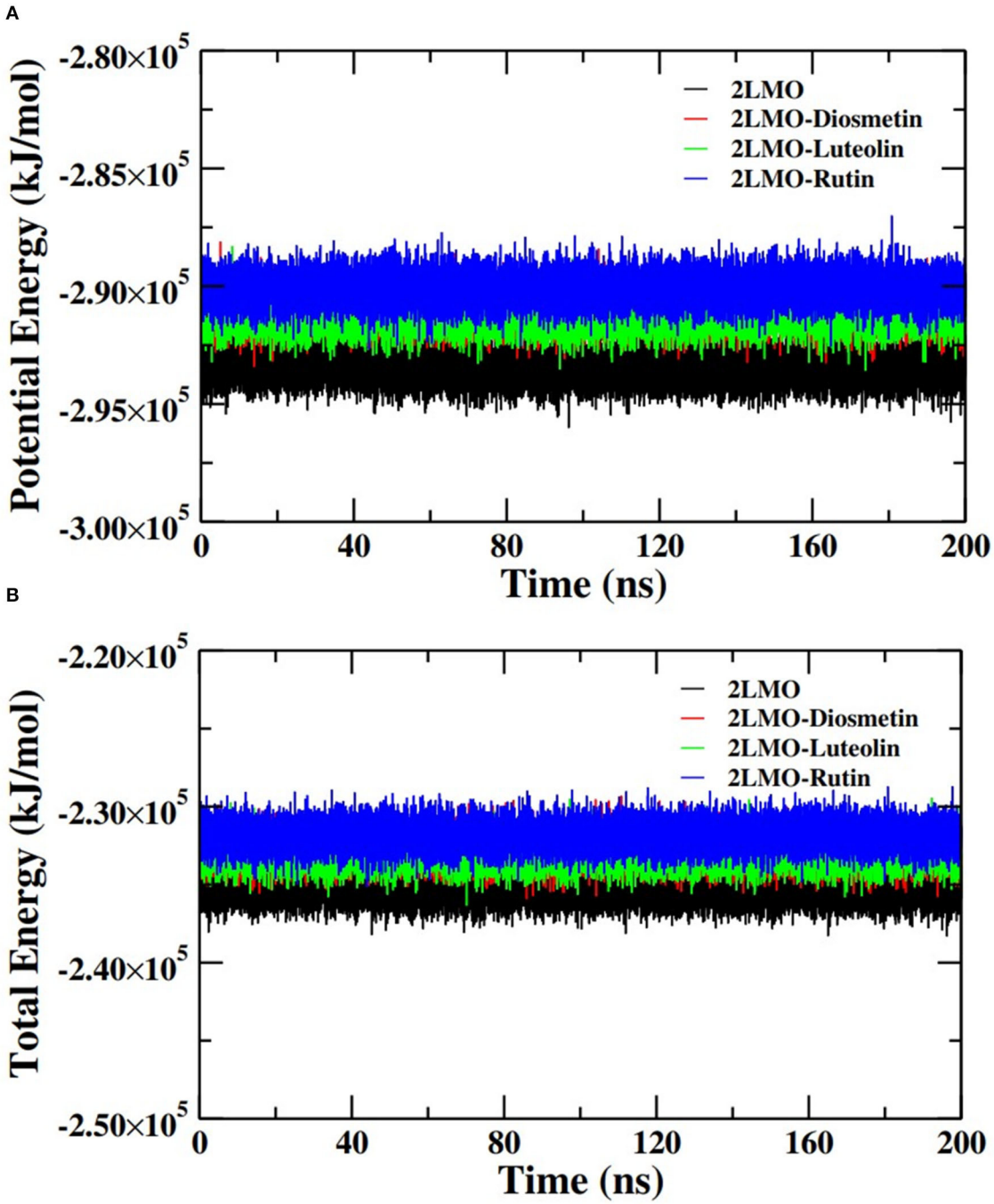

FIGURE 6 | (A) Potential energy (PE) and **(B)** total energy (TE) of the systems of 2LMO and its complexes with Diosmetin, Luteolin and Rutin as a function of time.

Similarly, 500 frames from the last 50 ns were extracted for three complexes with 6TI5 protein. The protein-ligand interactions are influenced by the non-covalent forces. These forces include van der Waals forces, hydrophobic interactions, hydrogen bonds, and electrostatic interactions. These forces have either a positive or negative contribution to the overall binding (Siddiqui et al., 2019). The binding energies for the interaction of 2LMO with the respective ligand molecules (Diosmetin, Luteolin, and Rutin) at subsequent intervals of 10 ns are enlisted in **Table 5**. The binding of all ligands is mostly favored by van der Waals forces and electrostatic interactions. Moreover, there is very less contribution of solvent accessible surface area energy in the interaction of the ligand molecules with the protein (2LMO). On contrary, polar solvation energy

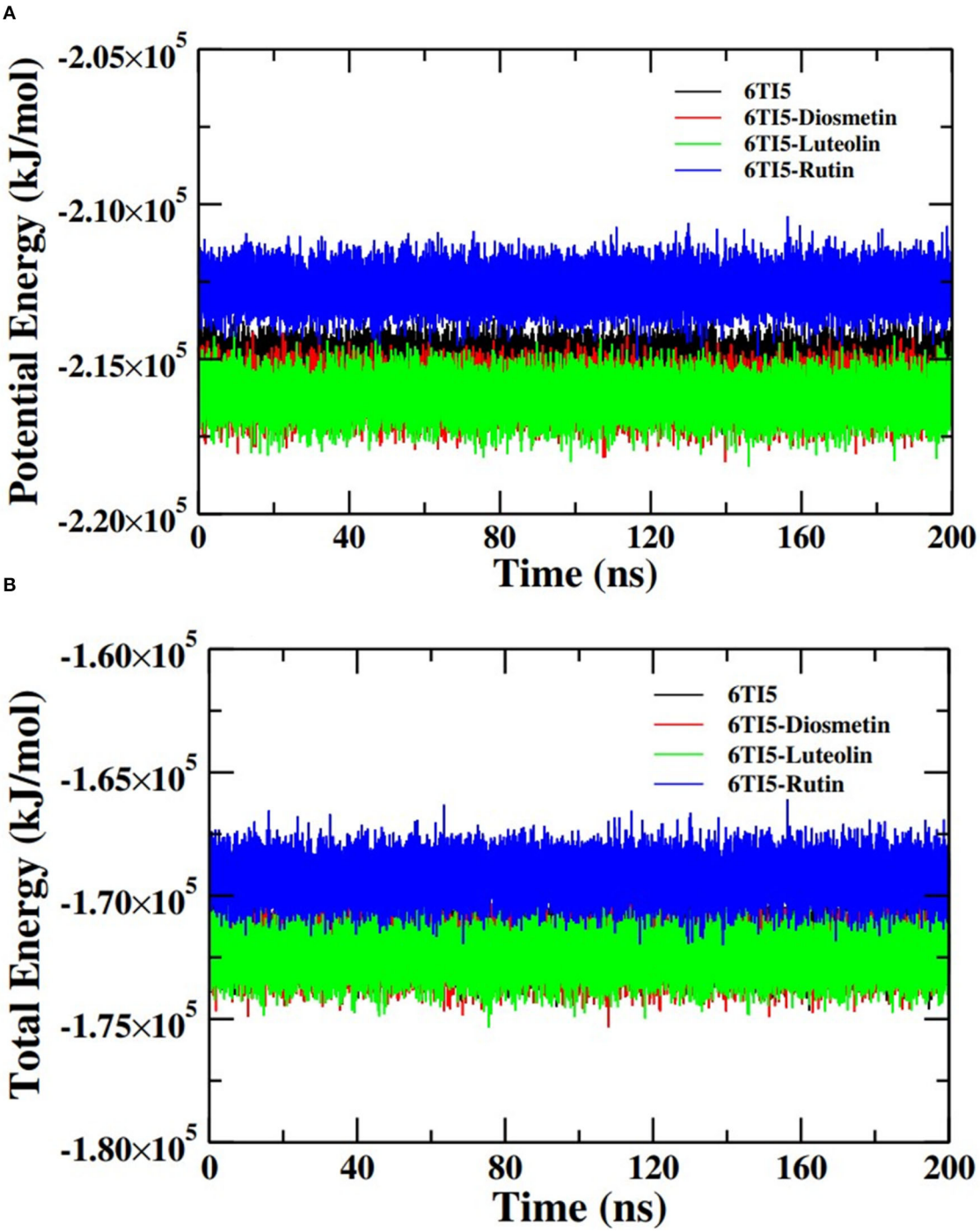

FIGURE 7 | (A) Potential energy (PE) and **(B)** total energy (TE) of the systems of 6TI5 and its complexes with Diosmetin, Luteolin and Rutin as a function of time.

impaired the binding of three compounds with the protein. Since polar solvation energy is the energy due to the interaction of the solute with the continuum solvent. Therefore, more the polar functional groups in the ligand molecules (for e.g., Rutin), more will be the polar solvation energy, thereby having a negative contribution to the collective binding energy of the complexes. Among the three complexes of 2LMO, 2LMO-Rutin shows an effective and stronger binding affinity compared to the other two complexes of 2LMO. Similarly, for the complexes of 6TI5, MM-PBSA calculations were performed and the calculated energies at an interval of 10 ns are shown in **Table 6**. As evident from the data, Rutin has a greater binding

TABLE 5 | Binding free energies (kJ/mol) determined by MM-PBSA calculations of the last 50 ns of trajectories of 2LMO in complex with Rutin, Diosmetin, and Luteolin.

Binding free energies	150–160 ns	160–170 ns	170–180 ns	180–190 ns	190–200 ns
2LMO-Rutin					
ΔE_{vdW}	−244.22 ± 20.32	−243.00 ± 21.05	−253.71 ± 22.52	−263.23 ± 23.41	−261.63 ± 21.14
ΔE_{ele}	−179.66 ± 36.67	−213.85 ± 31.05	−235.88 ± 37.97	−213.93 ± 52.09	−201.20 ± 31.87
ΔE_{PSE}	330.08 ± 28.84	357.82 ± 31.47	377.45 ± 30.82	360.24 ± 40.64	346.89 ± 24.97
ΔE_{SASA}	−25.21 ± 1.28	−25.26 ± 1.06	−26.49 ± 1.06	−26.30 ± 1.02	−26.60 ± 1.08
ΔE_{BE}	−119.01± 18.42	−124.30 ± 19.53	−138.64 ± 21.85	−143.23 ± 16.63	−142.54 ± 19.12
2LMO-Diosmetin					
ΔE_{vdW}	−172.29 ± 13.71	−161.60 ± 11.07	−158.18 ± 11.53	−162.90 ± 15.21	−167.30 ± 12.34
ΔE_{ele}	−83.97 ± 38.55	−31.85 ± 12.01	−26.40 ± 14.70	−22.82 ± 13.35	−17.11 ± 11.64
ΔE_{PSE}	180.94 ± 38.84	119.51 ± 8.19	117.27 ± 11.02	115.35 ± 11.20	119.54 ± 10.77
ΔE_{SASA}	−16.40 ± 0.80	−16.01 ± 0.81	−16.09 ± 0.76	−16.26 ± 0.78	−16.44 ± 0.79
ΔE_{BE}	−91.72 ± 15.02	−89.95 ± 12.47	−83.39 ± 11.01	−86.62 ± 13.44	−81.32 ± 14.68
2LMO-Luteolin					
ΔE_{vdW}	−97.80 ± 17.03	−90.46 ± 13.11	−83.20 ± 15.60	−62.91 ± 26.20	−75.76 ± 26.63
ΔE_{ele}	−102.83 ± 19.60	−92.10 ± 15.55	−101.58 ± 10.68	−53.50 ± 44.37	−53.87 ± 44.70
ΔE_{PSE}	153.07 ± 24.38	120.43 ± 17.30	135.88 ± 10.67	85.55 ± 51.90	96.36 ± 42.40
ΔE_{SASA}	−13.45 ± 1.17	−12.01 ± 0.68	−12.14 ± 0.92	−9.24 ± 3.12	−9.83 ± 2.14
ΔE_{BE}	−61.02 ± 16.93	−74.15 ± 13.51	−61.04 ± 12.32	−40.09 ± 22.59	−43.12 ± 17.26

ΔE_{vdW}, van der Waal energy; ΔE_{ele}, Electrostatic energy; ΔE_{PSE}, Polar solvation energy; ΔE_{SASA}, Solvent accessible surface area energy; ΔE_{BE}, Binding energy.

TABLE 6 | Binding free energies (kJ/mol) determined by MM-PBSA calculations of the last 50 ns of trajectories of 6TI5 in complex Diosmetin, Luteolin, and Rutin.

Binding free energies	150–160 ns	160–170 ns	170–180 ns	180–190 ns	190–200 ns
6TI5-Rutin					
ΔE_{vdW}	−174.24 ± 1.71	−184.51 ± 1.51	−178.18 ± 1.52	−175.50 ± 1.50	−184.40 ± 1.52
ΔE_{ele}	−80.49 ± 2.66	−89.77 ± 2.39	−100.94 ± 2.68	−81.68 ± 1.41	−71.00 ± 1.23
ΔE_{PSE}	191.27 ± 3.38	222.09 ± 3.70	227.91 ± 3.33	200.65 ± 1.40	185.82 ± 1.87
ΔE_{SASA}	−18.00 ± 0.12	−18.85 ± 0.15	−18.73 ± 0.12	−18.14 ± 0.13	−18.54 ± 0.13
ΔE_{BE}	−81.16 ± 2.71	−70.68 ± 2.77	−69.82 ± 1.72	−74.68 ± 1.51	−88.14 ± 1.40
6TI5-Diosmetin					
ΔE_{vdW}	−79.50 ± 1.04	−78.52 ± 1.18	−79.31 ± 1.23	−78.50 ± 1.17	−71.57 ± 1.50
ΔE_{ele}	−43.93 ± 1.62	−58.86 ± 2.11	−48.42 ± 2.26	−59.50 ± 2.47	−57.52 ± 3.12
ΔE_{PSE}	66.76 ± 1.74	81.94 ± 1.61	72.01 ± 2.19	90.62 ± 3.26	89.59 ± 3.28
ΔE_{SASA}	−9.20 ± 0.10	−9.54 ± 0.07	−9.57 ± 0.08	−9.82 ± 0.07	−9.39 ± 0.09
ΔE_{BE}	−65.80 ± 1.62	−64.97 ± 1.47	−65.29 ± 2.02	−57.20 ± 2.19	−48.83 ± 2.83
6TI5-Luteolin					
ΔE_{vdW}	−83.69 ± 0.89	−77.34 ± 0.91	−81.71 ± 1.12	−71.58 ± 1.11	−67.91 ± 1.43
ΔE_{ele}	−20.45 ± 0.84	−24.58 ± 0.94	−24.34 ± 0.96	−55.64 ± 4.47	−107.00 ± 5.08
ΔE_{PSE}	87.77 ± 1.38	77.07 ± 1.24	82.24 ± 1.52	110.67 ± 4.44	176.81 ± 5.40
ΔE_{SASA}	−9.50 ± 0.08	−9.26 ± 0.07	−9.67 ± 0.11	−9.80 ± 0.11	−11.34 ± 0.12
ΔE_{BE}	−25.82 ± 1.08	−34.13 ± 1.10	−33.54 ± 1.01	−26.20 ± 1.22	−9.41 ± 1.50

ΔE_{vdW}, van der Waal energy; ΔE_{ele}, Electrostatic energy; ΔE_{PSE}, Polar solvation energy; ΔE_{SASA}, Solvent accessible surface area energy; ΔE_{BE}, Binding energy.

for 6TI5 compared to the other two (Diosmetin, Luteolin) molecules. Therefore, Rutin among the three ligand molecules is considered to be an effective drug molecule possessing an efficient binding affinity for the two (2LMO and 6TI5) target proteins.

CONCLUSION

Based on binding energies and non-bonded interactions, as well as molecular dynamics simulation, Rutin and Luteolin emerged as better lead molecules than Diosmetin. However,

high MW (610.5), lowest absorption rate (16.04%), and more than one violation of Lipinski's rule make Rutin a less likely candidate as an anti-amyloidogenic agent. Moreover, among non-violators of Lipinski's rule, Diosmetin exhibited a greater absorption rate than Luteolin as well as the highest positive scores for drug likeness, while Luteolin exhibited moderate drug-likeness. Thus, we can conclude that Diosmetin and Luteolin may serve as a scaffold for the design of better inhibitors with higher affinities toward the target proteins. Our study may open a new vista for the analysis of the neuroprotective potential of these candidate drugs through *in vitro* and *in vivo* techniques.

DATA AVAILABILITY STATEMENT

The raw data supporting the conclusions of this article will be made available by the authors, without undue reservation.

AUTHOR CONTRIBUTIONS

Conceptualization: QZ. Methodology: QZ, MR, SS, and MH. Software: MR, SS, and MH. Validation: QZ and MR. Data analysis: MR, SS, AB, MZA, and AJ. Writing—original draft preparation: QZ, MR, MH, AB, AJ, and MZA. Writing—review and editing: QZ, MR, SS, AJ, SB, and MO. Writing—revision: QZ, HA, SB, II, SA, MA, YA, and WA. Visualization: QZ, MZA, and MFA. Supervision: QZ and MO. Project administration: QZ, AB, SB, and MFA. Funding acquisition: QZ, II, SA, MA, YA, and WA. All authors have read and agreed to the published version of the manuscript.

FUNDING

This research was funded by Deputyship for Research and Innovation, Ministry of Education in Saudi Arabia, Grant Number IFP-2020-40.

ACKNOWLEDGMENTS

The authors are very thankful to the Deanship of Scientific Research at the Majmaah University for providing the facilities.

SUPPLEMENTARY MATERIAL

The Supplementary Material for this article can be found online at: https://www.frontiersin.org/articles/10.3389/fnins.2022.915122/full#supplementary-material

REFERENCES

Ahmad, S., Arsalan, A., Hashmi, A., Khan, M. A., Siddiqui, W. A., and Younus, H. (2021). A comparative study based on activity, conformation and computational analysis on the inhibition of human salivary aldehyde dehydrogenase by phthalate plasticizers: implications in assessing the safety of packaged food items. *Toxicol* 462, 152947. doi: 10.1016/j.tox.2021.152947

Ahmed, M. Z., Zia, Q., Haque, A., Alqahtani, A. S., Almarfadi, O. M., et al. (2021). Aminoglycosides as potential inhibitors of SARS-CoV-2 main protease: an in silico drug repurposing study on FDA-approved antiviral and anti-infection agents. *J. Infect. Public Health*. 14, 611–619. doi: 10.1016/j.jiph.2021.01.016

Al Qarawi, A. A., Abdel-Rahman, H., Mousa, H. M., Ali, B. H., and El-Mougy, S. A. (2008). Nephroprotective action of Phoenix dactylifera in gentamicin-induced nephrotoxicity. *Pharm. Biol.* 46, 227–230. doi: 10.1080/13880200701739322

Al-Farsi, M., Alasalvar, C., Morris, A., Baron, M., and Shahidi, F. (2005). Comparison of antioxidant activity, anthocyanins, carotenoids, and phenolics of three native fresh and sun-dried date (*Phoenix dactylifera L.)* varieties grown in Oman. *J. Agri. Food Chem*. 53, 7592-7599. doi: 10.1021/jf050579q

Aljaloud, S., Colleran, H. L. and Ibrahim, S. A. (2020). Nutritional value of date fruits and potential use in nutritional bars for athletes. *Food Nutri. Sci*. 11, 463–480. doi: 10.4236/fns.2020.116034

Al-Jasass, F. M., Siddiq, M., and Sogi, D. S. (2015). Antioxidants activity and color evaluation of date fruit of selected cultivars commercially available in the United States. *Adv. Chem*. 2015, 1–5 doi: 10.1155/2015/567203

Alsaleem, M. S., Alwahaibi, I. H., Rehman, M. T., AlAjmi, M. F., Alkahtani, R. A., and Abdelmageed, W. (2020). Phenolic compounds of Heliotropium europaenum and their biological activities. *Pharmacogn. Mag.* 16, S108–S116. doi: 10.4103/pm.pm_376_19

Al-Shabib, N. A., Khan, J. M., Malik, A., Rehman, M. T., AlAjmi, M. F., Husain, F. M., et al. (2020). Investigating the effect of food additive azo dye "tartrazine" on BLG fibrillation under in-vitro condition. A biophysical and molecular docking study. *J. King Saud Uni. Sci.* 32, 2034–2040. doi: 10.1016/j.jksus.2020.02.017

Al-Shwyeh, H. A. (2019). Date palm (*Phoenix dactylifera L.*) fruit as potential antioxidant and antimicrobial agents. *J. Pharm. Bioallied. Sci*. 11, 1–11. doi: 10.4103/JPBS.JPBS_168_18

Alzheimer's Association Report. (2020). Alzheimer's disease facts and figures. *Alzheimer's Dement* 16, 391–460. doi: 10.1002/alz.12068

Asadi-Shekaari, M., Marzieh, P., Shahriar, D., Zahed, S. K., and Pari, K. T. (2008). Neuroprotective effects of aqueous date fruit extract on focal cerebral ischemia in rats. *Pak. J. Med. Sci*. 24, 661–665.

Badeli, H., Shahrokhi, N., KhoshNazar, M., Asadi-Shekaari, M., Shabani, M., et al. (2016). Aqueous date fruit efficiency as preventing traumatic brain deterioration and improving pathological parameters after traumatic brain injury in male rats. *Cell J.* 18, 416–424. doi: 10.22074/cellj.2016.4570

Bussi, G., Donadio, D., and Parrinello, M. (2007). Canonical sampling through velocity rescaling. *J. Chem. Phy*. 126, 014101. doi: 10.1063/1.2408420

Chen, G.f., Xu, T.h., Yan, Y., et al. (2017). Amyloid beta: structure, biology and structure-based therapeutic development. *Acta. Pharmacol. Sin*. 38, 1205–1235. doi: 10.1038/aps.2017.28

Coyle, J. T., and Puttfarcken, P. (1993). Oxidative stress, glutamate, and neurodegenerative disorders. *Science* 262, 689–695. doi: 10.1126/science.7901908

Darden, T., York, D., and Pedersen, L. (1993). Particle mesh ewald: an N-log (N) method for Ewald sums in large systems. *J. Chem. Phys*. 98, 10089–10092. doi: 10.1063/1.464397

Dominguez, L. J., and Barbagallo, M. (2018). Nutritional prevention of cognitive decline and dementia. *Acta. Biomed*. 89, 276–290. doi: 10.23750/abm.v89i2.7401

Duke, J. A. (1992). *Handbook of Phytochemicals of GRAS Herbs and Other Economic Plants*. Boca Raton, FL: CRC Press.

Essmann, U., Perera, L., Berkowitz, M. L., Darden, T., Lee, H., and Pedersen, L. G. (1995). A smooth particle mesh Ewald method. *J. Chem. Phys*. 103, 8577–8593. doi: 10.1063/1.470117

Floyd, R. A. (1992). Antioxidants, oxidative stress, and degenerative neurological disorders. *Proc. Soc. Exp. Biol. Med*. 222, 236–245. doi: 10.1046/j.1525-1373.1999.d01-140.x

Guedes, I. A., Costa, L. S. C., dos Santos, K. B., Karl, A. L. M., Rocha, G. K., Teixeira, I. M., et al. (2021). Drug design and repurposing with DockThor-VS web server focusing on SARS-CoV-2 therapeutic targets and their non-synonym variants. *Sci. Rep*. 11, 5543. doi: 10.1038/s41598-021-84700-0

Guerrero, A. L., Dorado-Martinez, C., Rodriguez, A., Pedroza-Rios, K., Borgonio-Perez, G., and Rivas-Arancibia, S. (1999). Effects of vitamin E on ozone-induced memory deficits and lipid peroxidation in rats. *Neuroreport* 10, 1689–1692. doi: 10.1097/00001756-199906030-00012

Hashmi, M. A., Malik, A., Arsalan, A., Khan, M. A., and Younus, H. (2021). Elucidation of kinetic and structural properties of eye lens ζ-crystallin: an invitro and insilico approach. *J. Biomol. Struct. Dys*. 20, 1–15. doi: 10.1080/07391102.2021.2017351

Henning-Knechtel, A., Kumar, S., Wallin, C., Król, S., Wärmländer, S. K. T. S., et al. (2020). Designed cell-penetrating peptide inhibitors of amyloid-beta aggregation and cytotoxicity. *Cell Rep. Phy. Sci*. 1, 100014. doi: 10.1016/j.xcrp.2020.100014

Iqbal, D., Rizvi, S. M. D., Rehman, M. T., Khan, M. S., Bin Dukhyil, A., AlAjmi, M. F., et al. (2022). Soyasapogenol-B as a potential multitarget therapeutic agent for neurodegenerative disorders: Molecular docking and dynamics study. *Entropy* 24, 593. doi: 10.3390/e24050593

Ishurda, O., and John, F. K. (2005). The anti-cancer activity of polysaccharide prepared from Libyan dates (*Phoenix dactylifera L.). Carbohydr. Polym*. 59, 531-535. doi: 10.1016/j.carbpol.2004.11.004

Joseph, J. A., Shukitt-Hale, B., Denisova, N. A., Prior, R. L., Cao, G., et al. (1998). Long-term dietary strawberry, spinach, or vitamin E supplementation retards the onset of age-related neuronal signal-transduction and cognitive behavioral deficits. *J. Neurosci*. 18, 8047–8055. doi: 10.1523/JNEUROSCI.18-19-08047.1998

Kumari, R., Kumar, R., and Lynn, A. (2014). g_mmpbsa —A GROMACS tool for high-throughput MM-PBSA calculations. *J. Chem. Inf. Model* 54, 1951–1962. doi: 10.1021/ci500020m

Lee, J.-M., Lee, J. H., Song, M. K., and Kim, Y.-J. (2022). NXP032 ameliorates aging-induced oxidative stress and cognitive impairment in mice through activation of Nrf2 signaling. *Antioxidants* 11, 130. doi: 10.3390/antiox11010130

Lehmann, S., Dumurgier, J., Ayrignac, X., Marelli, C., Alcolea, D., Ormaechea, J. F., et al. (2020). Alzheimer's disease neuroimaging initiative (ADNI). Cerebrospinal fluid a beta 1-40 peptides increase in Alzheimer's disease and are highly correlated with phospho-tau in control individuals. *Alzheimers Res. Ther*. 12, 123. doi: 10.1186/s13195-020-00696-1

Lipinski, C. A. (2004). Lead- and drug-like compounds: the rule-of-five revolution. *Drug Discov. Today Technol*. 1, 337–341. doi: 10.1016/j.ddtec.2004.11.007

Markesbery, W. R., and Carney, J. M. (1999). Oxidative alterations in Alzheimer's disease. *Brain Pathol* 9, 133-146. doi: 10.1111/j.1750-3639.1999.tb00215.x

Minicozzi, V., Chiaraluce, R., Consalvi, V., Giordano, C., Narcisi, C., Punzi, P., et al. (2014). Computational and experimental studies on β-sheet breakers targeting Aβ1–40 fibrils. *J. Biol. Chem*. 289, 11242–11252. doi: 10.1074/jbc.M113.537472

Ministry of Health (MoH), KSA. (2022). Available online at: https://www.moh.gov.sa/en/HealthAwareness/healthDay/2022/Pages/HealthDay-2022-09-21-001.aspx Pages/HealthDay-2020-09-21.aspx (accessed May 20, 2022).

Mistrello, J., Sirisena, S. D., Ghavamic, A., Marshalld, R. J., and Krishnamoorthy, S. (2014). Determination of the antioxidant capacity, total phenolic and avonoid contents of seeds from three commercial varieties of culinary dates. *Int. J. Food Stud*. 3, 34–44. doi: 10.7455/ijfs/3.1.2014.a3

Mori, H., Takio, K., Ogawara, M., and Selkoe, D. J. (1992). Mass spectrometry of purified amyloid beta protein in Alzheimer's disease. *J. Biol. Chem*. 267, 17082–17086. doi: 10.1016/S0021-9258(18)41896-0

Morris, G. M., Goodsell, D. S., Halliday, R. S., Huey, R., Hart, W. E., Belew, R. K., et al. (1998). Automated docking using a lamarckian genetic algorithm and an empirical binding free energy function. *J. Compu. Chem*. 19, 1639–1662.

Morris, G. M., Huey, R., Lindstrom, W., Sanner, M. F., Belew, R. K., Goodsell, D. S., et al. (2009). Autodock4 and AutoDockTools4: automated docking with selective receptor flexiblity. *J. Comput. Chem*. 16, 2785–2791. doi: 10.1002/jcc.21256

Nichols, E., Szoeke, C. E., Vollset, S. E., Abbasi, N., Abd-Allah, F., Abdela, J., et al. (2019). GBD 2016 dementia collaborators. global, regional, and national burden of Alzheimer's disease and other dementias, 1990–2016: a systematic analysis for the global burden of disease study. *Lancet Neurol*. 18, 88–106. doi: 10.1016/S1474-4422(18)30403-4

Parrinello, M., and Rahman, A. (1981). Polymorphic transitions in single crystals: a new molecular dynamics method. *J. Appl. Phy*. 52, 7182–7190. doi: 10.1063/1.328693

Puri, A., Sahai, R., Singh, K. L., Saxena, R. P., Tandon, J. S., and Saxena, K. C. (2000). Immunostimulant activity of dry fruits and plant materials used in Indian traditional medical system for mothers after child birth and invalids. *J. Ethnopharmacol*. 71, 89–92. doi: 10.1016/S0378-8741(99)00181-6

Saafi, E. B., Louedi, M., Elfeki, A., Zakhama, A., Najjar, M.,F/, Hammami, M., et al. (2011). Protective effect of date palm fruit extract (*Phoenix dactylifera L.*) on dimethoate induced-oxidative stress in rat liver. *Exp. Toxicol. Pathol*. 63, 433–441. doi: 10.1016/j.etp.2010.03.002

Salah, A., and Al-Maiman, S. A. (2005). Effect of date palm (Phoenix dactylifera) seed fibers on plasma lipids in rats. *J. King Saud. Univ*. 17, 117–123.

Saleh, E. A., Tawfik, M. S., and Abu-Tarboush, H. M. (2011). Phenolic contents and antioxidant activity of various date palm (*Phoenix dactylifera L.*) fruits from Saudi Arabia. *Food Nutr. Sci*. 02, 1134–1141. doi: 10.4236/fns.2011.210152

Sallal, A. K., and Ashkenani, A. (1989). Effect of date extract on growth and spore germination of *Bacillus subtilis*. *Microbios* 59, 203–210.

Sallal, A. K., El-Teen, K. H., and Abderrahman, S. (1996). Effect of date extract on growth and morphology of Candida albicans. *Biomed. Lett* 53, 179–184.

Selkoe, D. J., and Hardy, J. (2016). The amyloid hypothesis of Alzheimer's disease at 25 years. *EMBO Mol. Med*. 8, 595–608. doi: 10.15252/emmm.201606210

Shahdadi, F., Mirzaei, H. O., and Daraei Garmakhany, A. (2015). Study of phenolic compound and antioxidant activity of date fruit as a function of ripening stages and drying process. *J. Food Sci. Technol*. 52, 1814–1819. doi: 10.1007/s13197-013-1177-6

Shraideh, Z. A., Abu-Elteen, K. H., and Sallal, A. K. (1998). Ultrastructural effects of date extract on Candida albicans. *Mycopathol*. 142, 119–123 doi: 10.1023/A:1006901019786

Siddiqui, S., Ameen, F., Jahan, I., Nayeem, S. M., and Tabish, M. (2019). A comprehensive spectroscopic and computational investigation on the binding of the anti-asthmatic drug triamcinolone with serum albumin. *New J. Chem*. 43, 4137–4151. doi: 10.1039/C8NJ05486J

Siddiqui, S., Upadhyay, S., Ahmad, R., Gupta, A., Srivastava, A., Trivedi, A., et al. (2020). Virtual screening of phytoconstituents from miracle herb *nigella sativa* targeting nucleocapsid protein and papain-like protease of SARS-CoV-2 for COVID-19 treatment. *J. Biomol. Struct. Dyn*. 40, 3928–3948. doi: 10.1080/07391102.2020.1852117

Sousa Da Silva, A. W., and Vranken, W. F. (2012). ACPYPE - antechamber python parser interface. *BMC Res Notes* 5, 367. doi: 10.1186/1756-0500-5-367

Turner, M., Mutter, S. T., Kennedy-Britten, O. D., and Platts, J. A. (2019). Molecular dynamics simulation of aluminium binding to amyloid-β and its effect on peptide structure. *PLoS ONE* 14, e0217992. doi: 10.1371/journal.pone.0217992

Van Der Spoel, D., Lindahl, E., Hess, B., Groenhof, G., Mark, A. E., and Berendsen, H. J. C. (2005). GROMACS: fast, flexible, and free. *J Compu Chem* 26, 1701–1718. doi: 10.1002/jcc.20291

Vayalil, P. K. (2002). Antioxidant and antimutagenic properties of aqueous extract of date fruit (Phoenix dactylifera L. *Arecaceae). J. Agric. Food Chem*. 50, 610-617. doi: 10.1021/jf010716t,

WHO Fact Sheet (2020). Available online at: https://www.who.int/news-room/fact-sheets/detail/the-top-10-causes-of-death (accessed March20, 2022).

Yamada, K., Tanaka, T., Han, D., Senzaki, K., Kameyama, T., and Nabeshima, T. (1999). Protective effects of idebenone and α-tocopherol on β-amyloid-(1-42)-induced learning and memory deficits in rats: implication of oxidative stress in β-amyloid-induced neurotoxicity *in vivo*. *Eur. J. Neurosci*. 11, 83–90. doi: 10.1046/j.1460-9568.1999.00408.x

Zangiabadi, N., Asadi-Shekaari, M., Sheibani, V., Jafari, M., Shabani, M., et al. (2011). Date fruit extract is a neuroprotective agent in diabetic peripheral neuropathy in streptozotocin-induced diabetic rats: a multimodal analysis. *Oxidative Med. Cell Longevity* 2011, 976948. doi: 10.1155/2011/976948

Zhao, Y. H., Abraham, M. H., Le, J., Hersey, A., Luscombe, C. N., Beck, G., et al. (2002). Rate-limited steps of human oral absorption

and QSAR studies. *Pharm. Res* 19, 1446–1457. doi: 10.1023/A:1020444330011

Conflict of Interest: The authors declare that the research was conducted in the absence of any commercial or financial relationships that could be construed as a potential conflict of interest.

Publisher's Note: All claims expressed in this article are solely those of the authors and do not necessarily represent those of their affiliated organizations, or those of the publisher, the editors and the reviewers. Any product that may be evaluated in this article, or claim that may be made by its manufacturer, is not guaranteed or endorsed by the publisher.

frontiers | Frontiers in Aging Neuroscience

TYPE Original Research
PUBLISHED 22 August 2022
DOI 10.3389/fnagi.2022.878276

OPEN ACCESS

EDITED BY
Mercè Pallàs,
University of Barcelona, Spain

REVIEWED BY
Hoon Kim,
Sunchon National University, South Korea
Rehan Khan,
Institute of Nano Science and Technology (INST), India
Anas Shamsi,
Jamia Millia Islamia, India

*CORRESPONDENCE
Nobendu Mukerjee
nabendu21@rkmvccrahara.org
Ghulam Md Ashraf
ashraf.gm@gmail.com
Arabinda Ghosh
dra.ghosh@gauhati.ac.in

†These authors have contributed equally to this work

SPECIALTY SECTION
This article was submitted to Alzheimer's Disease and Related Dementias, a section of the journal Frontiers in Aging Neuroscience

RECEIVED 17 February 2022
ACCEPTED 07 July 2022
PUBLISHED 22 August 2022

Repurposing food molecules as a potential BACE1 inhibitor for Alzheimer's disease

Nobendu Mukerjee[1,2*†], Anubhab Das[3†], Rahul D. Jawarkar[4†], Swastika Maitra[5†], Padmashree Das[6], Melvin A. Castrosanto[7], Soumyadip Paul[1], Abdul Samad[8], Magdi E. A. Zaki[9], Sami A. Al-Hussain[9], Vijay H. Masand[10], Mohammad Mehedi Hasan[11], Syed Nasir Abbas Bukhari[12], Asma Perveen[13], Badrah S. Alghamdi[14,15,16], Athanasios Alexiou[17,18], Mohammad Amjad Kamal[19,20,21,22], Abhijit Dey[23], Sumira Malik[24], Ravindra L. Bakal[4], Adel Mohammad Abuzenadah[20,25], Arabinda Ghosh[26*] and Ghulam Md Ashraf[15,25*]

[1]Department of Microbiology, Ramakrishna Mission Vivekananda Centenary College, Khardaha, India, [2]Department of Health Sciences, Novel Global Community Educational Foundation, Hebersham, NSW, Australia, [3]Institute of Health Sciences, Presidency University, Kolkata, India, [4]Department of Medicinal Chemistry, Dr. Rajendra Gode Institute of Pharmacy, Amravati, India, [5]Department of Microbiology, Adamas University, Kolkata, India, [6]Central Silk Board, Guwahati, India, [7]Institute of Chemistry, University of the Philippines Los Baños, Los Baños, Philippines, [8]Department of Pharmaceutical Chemistry, Faculty of Pharmacy, Tishk International University, Erbil, Iraq, [9]Department of Chemistry, Faculty of Science, Imam Mohammad Ibn Saud Islamic University, Riyadh, Saudi Arabia, [10]Department of Chemistry, Vidya Bharati Mahavidyalaya, Amravati, India, [11]Department of Biochemistry and Molecular Biology, Faculty of Life Sciences, Mawlana Bhashani Science and Technology University, Tangail, Bangladesh, [12]Department of Pharmaceutical Chemistry, College of Pharmacy, Jouf University, Sakaka, Saudi Arabia, [13]Glocal School of Life Sciences, Glocal University, Saharanpur, India, [14]Department of Physiology, Faculty of Medicine, King Abdulaziz University, Jeddah, Saudi Arabia, [15]Pre-Clinical Research Unit, King Fahd Medical Research Center, King Abdulaziz University, Jeddah, Saudi Arabia, [16]The Neuroscience Research Unit, Faculty of Medicine, King Abdulaziz University, Jeddah, Saudi Arabia, [17]Department of Science and Engineering, Novel Global Community Educational Foundation, Hebersham, NSW, Australia, [18]AFNP Med, Vienna, Austria, [19]Institutes for Systems Genetics, Frontiers Science Center for Disease-Related Molecular Network, West China Hospital, Sichuan University, Chengdu, China, [20]King Fahd Medical Research Center, King Abdulaziz University, Jeddah, Saudi Arabia, [21]Department of Pharmacy, Faculty of Allied Health Sciences, Daffodil International University, Dhaka, Bangladesh, [22]Enzymoics, Novel Global Community Educational Foundation, Hebersham, NSW, Australia, [23]Department of Life Sciences, Presidency University, Kolkata, India, [24]Amity Institute of Biotechnology, Amity University, Jharkhand, Ranchi, India, [25]Department of Medical Laboratory Sciences, Faculty of Applied Medical Sciences, King Abdulaziz University, Jeddah, Saudi Arabia, [26]Microbiology Division, Department of Botany, Gauhati University, Guwahati, India

Alzheimer's disease (AD) is a severe neurodegenerative disorder of the brain that manifests as dementia, disorientation, difficulty in speech, and progressive cognitive and behavioral impairment. The emerging therapeutic approach to AD management is the inhibition of β-site APP cleaving enzyme-1 (BACE1), known to be one of the two aspartyl proteases that cleave β-amyloid precursor protein (APP). Studies confirmed the association of high BACE1 activity with the proficiency in the formation of β-amyloid-containing neurotic plaques, the characteristics of AD. Only a few FDA-approved BACE1 inhibitors

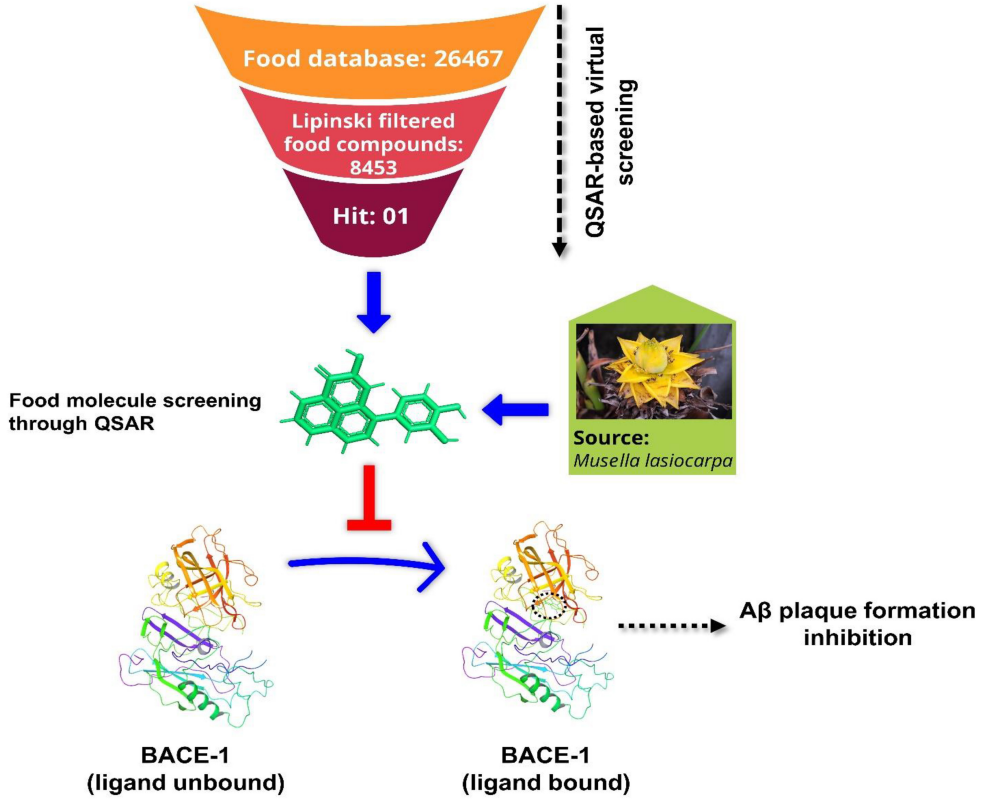

GRAPHICAL ABSTRACT
Food molecules as a potential BACE1 inhibitor against Alzheimer's disease.

are available in the market, but their adverse off-target effects limit their usage. In this paper, we have used both ligand-based and target-based approaches for drug design. The QSAR study entails creating a multivariate GA-MLR (Genetic Algorithm-Multilinear Regression) model using 552 molecules with acceptable statistical performance (R^2 = 0.82, Q^2_{loo} = 0.81). According to the QSAR study, the activity has a strong link with various atoms such as aromatic carbons and ring Sulfur, acceptor atoms, sp2-hybridized oxygen, etc. Following that, a database of 26,467 food compounds was primarily used for QSAR-based virtual screening accompanied by the application of the Lipinski rule of five; the elimination of duplicates, salts, and metal derivatives resulted in a truncated dataset of 8,453 molecules. The molecular descriptor was calculated and a well-validated 6-parametric version of the QSAR model was used to predict the bioactivity of the 8,453 food compounds. Following this, the food compounds whose predicted activity (pKi) was observed above 7.0 M were further docked into the BACE1 receptor which gave rise to the Identification of 4-(3,4-Dihydroxyphenyl)-2-hydroxy-1H-phenalen-1-one (PubChem I.D: 4468; Food I.D: FDB017657) as a hit molecule (Binding Affinity = −8.9 kcal/mol, pKi = 7.97 nM, Ki = 10.715 M). Furthermore, molecular dynamics simulation for 150 ns and molecular mechanics generalized born and surface area (MMGBSA) study aided in identifying structural motifs involved in interactions with the BACE1 enzyme. Molecular docking and QSAR yielded complementary and congruent results. The validated analyses

can be used to improve a drug/lead candidate's inhibitory efficacy against the BACE1. Thus, our approach is expected to widen the field of study of repurposing nutraceuticals into neuroprotective as well as anti-cancer and anti-viral therapeutic interventions.

KEYWORDS

beta-site APP cleaving enzyme 1, BACE1, Alzheimer's disease, glioblastoma, QSAR, molecular docking, MD simulations, golden lotus banana

Introduction

Alzheimer's disease (AD) is a devastating mental illness, which leads to an irreversible, progressive brain disorder that slowly destroys memory skills and learning abilities (De Strooper and Karran, 2016). Though the disease progression and risk factors of AD are not completely understood, a large number of evidence suggest the formation of amyloid-beta (Aβ) is central to the pathophysiology of AD (Vassar et al., 1999). AD progression stages vary from mild to severe in middle-aged people to older persons detected with cognitive tests (Hall et al., 2019). During the preclinical stage of AD, patients seem to be symptom-free, but neurodegenerative changes occur in the brain. Abnormal accumulation of Aβ-containing plaques and hyperphosphorylated tau throughout the brain causes healthy neurons to exhibit loss of synaptic connections, ion-channel dysfunctions, and severe deterioration in neuronal health. This ultimately leads to neuronal cell death and cognitive decline in elderly persons (Musi et al., 2018; Sebastián-Serrano et al., 2018). This progressive accumulation of Aβ is caused by imbalances in the levels of Aβ production, aggregation, and clearance (Murphy and LeVine, 2010; Jabir et al., 2021). Moreover, alterations in synaptic plasticity and integral neuronal circuitries severely hamper neurogenesis.

The Special Report examines MCI, including Alzheimer's, from the perspectives of consumers and primary care providers. AD affects 6.5 million Americans who are 65 years old or older. By 2060, this figure may increase to 13.8 million unless medical advances prevent, slow down, or cure AD. A total of 121,499 AD deaths were reported on official death certificates in 2019. According to one COVID-19 report, AD is the sixth most common cause of death in the United States in 2019 and will move up to the seventh most common cause in 2020 and 2021. Among Americans 65 and older, AD is the seventh most common cause of death. Between 2000 and 2019, mortality from HIV, heart disease, and stroke all dropped, whereas AD deaths rose by 145 percent. In 2021, 16 billion hours of care were supplied by over 11 million family members and other unpaid caregivers. These statistics demonstrate a decrease in carers and an increase in the amount of care that each caregiver who is still working gives. $271,6 billion was spent on unpaid dementia care in 2021. Family caregivers now have a higher risk of emotional discomfort as well as poorer mental and physical health due to COVID-19. Caregivers of dementia are also impacted by COVID-19. To safeguard their own health and the health of their families, several caregivers have resigned. However, there is a need for more dementia carers. Medicaid payments are more than 22 times greater than Medicare payments, and payments to beneficiaries 65 and older with AD or other dementias are approximately three times more than payments to beneficiaries without these illnesses. Hospice, long-term care, and healthcare for dementia patients will cost $321 billion in 2022. A poll by the Alzheimer's Association indicates MCI obstacles. The study revealed low MCI knowledge, a lack of desire to seek medical attention for symptoms, and challenges with MCI diagnosis. According to survey findings, clinical trial participation should be increased together with MCI awareness and diagnosis, particularly in impoverished communities (Alzheimer's Association, 2012).

Aβ is a neurotoxic aggregate produced by the consecutive proteolysis of β-amyloid precursor protein (APP) by two aspartyl proteases, beta-site APP cleaving enzyme, Beta-Secretase (BACE1), and finally by γ secretase (Sinha et al., 1999; Vassar et al., 1999; Yan et al., 1999; Cui et al., 2011; Zhang et al., 2011). BACE1 is a novel target, a type 1 transmembrane aspartic protease, related to the pepsin and retroviral aspartic protease families (Moussa-Pacha et al., 2020), having 501 amino acids and is predominantly expressed in the human brain (Zacchetti et al., 2007; Hassan et al., 2018).

As there is a strong association between Aβ accumulation and AD, the primary therapeutic strategy for the treatment of AD targets lowering the concentration of Aβ. One such strategy that has come up in recent findings involves inhibiting the enzymes that generate Aβ in the first place. BACE1 antisense oligonucleotide treatment to APP overexpressing cells is reportedly responsible for a decreased production of β-secretase cleaved APP fragments. Recent studies suggest that the levels of BACE1 protein and their activity were raised to approximately double in patients with AD where BACE1 might initiate or enhance AD pathogenesis. Several studies proved that BACE1 is a vital drug target and active site of the enzyme (Sinha et al., 1999; Vassar et al., 1999; Dingwall, 2001;

Fukumoto et al., 2002; Yang et al., 2003; Li and Südhof, 2004). It is covered by a flexible antiparallel β-hairpin, called a flap (Hussain et al., 2000). It is elucidated that the flap can control substrate access to the receptor site and set the substrate into the perfect orientation for the catalytic process (Lin et al., 2000). Hence, the inhibition of proteases such as BACE1 may represent modifying treatment for AD by controlling the production of Aβ (Tresadern et al., 2011; Arif et al., 2020). Therefore, BACE1 inhibitors may be used to treat AD.

Natural compounds have been investigated for many years for their ability to target a range of *trans*-acetyl peptidases in the search for new medications with fewer side effects due to their high biocompatibility. Apart from their benefits, the majority of natural compounds have a variety of disadvantages, including a high molecular weight, low stability, and in many cases, insufficient solubility. These difficulties can be resolved by using computer-assisted research to generate more effective and selective inhibitors. They are less harmful and more readily absorbed into the body than manufactured drugs. Computational techniques enable the modeling and screening of such compounds in a cost-effective and informative manner from a vast library of choices. The binding sites for various bioactive substances in BACE1 protein were predicted, and their interactions were explored utilizing the Food database and molecular docking. *Musella lasiocarpa*'s bioactive component, 4-(3,4-Dihydroxyphenyl)-2-hydroxy-1H-phenalen-1-one, is found to be the potential inhibitor of BACE1. *M. lasiocarpa*, also known as Chinese Dwarf Banana, is the only species in the genus Musella, which belongs to the family of Musaceae. Some novel compounds have also been isolated from this plant, which showed remarkable *in vitro* anticancer activities and some degree of antimicrobial activity (Bo et al., 2000; Dong et al., 2011).

These results demonstrate the potential of the *M. lasiocarpa* as a source of novel drugs, nutraceuticals, and functional foods. The result from this study will inspire the perspective of natural compounds and computer-aided drug discovery and, in the long run, significantly reduce the time required to research and build new lead compounds with specified biological activity and structural variety.

Methodology

QSAR modeling

Organization for economic corporation and development guidelines and a standard protocol recommended by different researchers, which involved sequential execution of (1) data collection and its curation, (2) structure generation and calculation of molecular descriptors, (3) objective feature selection (OFS), (4) splitting the dataset into training and external validation sets, and (5) subjective feature selection involving building a regression model and validation of the developed model, has been followed to build a widely applicable QSAR model for the BACE1 inhibitory activity. This also ensures thorough validation and successful application of the model.

Selection of data set

The data set of BACE1 inhibitory activity used for building, training, and validating the QSAR model in the present work was downloaded from the Chembl database (accessed on 22nd December 2021)[1], which is a free and publicly accessible database. Initially, the data set comprised of 552 molecules (Davies et al., 2015). Then, as a part of data curation, entries with ambiguous Ki values, duplicates, salts, metal-based inhibitors, etc., were omitted. The final data set comprises structurally diverse 371 molecules with remarkable variation in structural scaffolds, which were tested experimentally for potency in terms of Ki (nM). A collection of 371 molecules with various structural configurations with mentioned enzyme inhibitory concentration (Ki) was decided on for the existing work (O'Boyle et al., 2011; Tosco et al., 2011; Fujita and Winkler, 2016). The Ki values ranging from 0.47 to 1,400 nM have been transformed to pKi (pKi = – logKi) earlier than real QSAR evaluation for ease of dealing with the data. Five least and five most active molecules are depicted in **Figure 1** to illustrate the version in bio-activity with chemical features. The SMILES strings with mentioned Ki and pKi values for all of the molecules are depicted inside **Supplementary Table 1** with the **Supplementary material**.

Molecular structure drawing and optimization

Drawing the 2D structures of all 371 and converting them to their corresponding 3D structures was done using ChemSketch 12 Freeware and Open Babel 2.4, (O'Boyle et al., 2011) both free and open-source software, respectively.[2] After that, the MMFF94 force field available in TINKER (default setting) and Open3DAlign is used for optimization and molecular alignment, respectively.

Molecular descriptor calculation and objective feature selection

PyDescriptor has over 30,000 molecular descriptors for each molecule (Masand and Rastija, 2017). Molecular descriptors with near constant values (>95%) and resonance ($|R|$) > 0.95 were eliminated using OFS in QSARINS v2.2.4 (Gramatica et al., 2013, 2014). This work removed duplicate molecular descriptors and prevented collisions of multicollinearity and hypothetical variables in the Genetic Algorithm multiple linear regression (GA-MLR) model. Only 3,281 molecular descriptors

1 https://www.ebi.ac.uk/chembl/g/#search_results/all/query bace 1

2 www.acdlabs.com

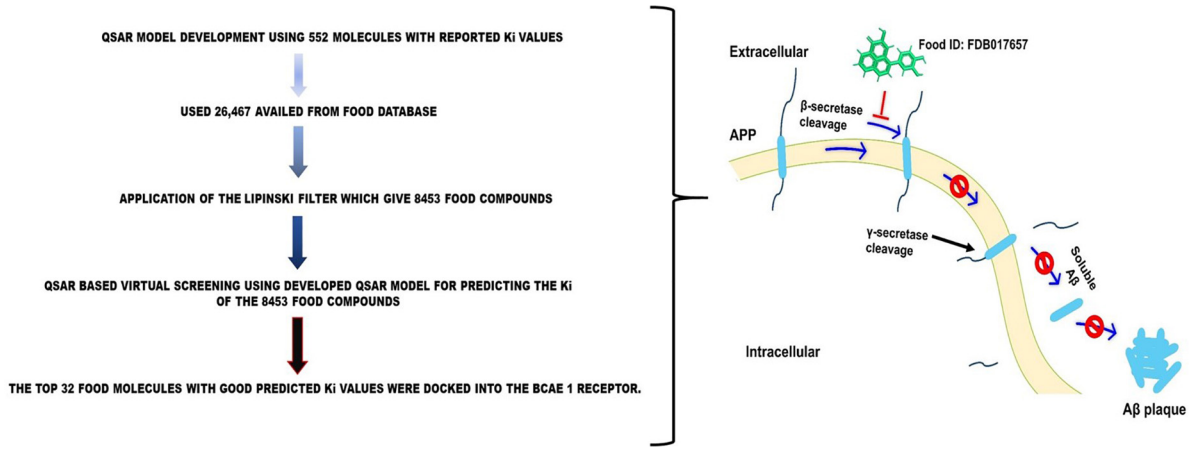

FIGURE 1
Schematic representation of the inhibition of Aβ plaque formation by FDB017657.

were found in the reduced pool of molecular descriptors generated after OFS processing.

Subjective feature selection, QSAR model development, and validation

A reduced set of molecular descriptors consisting of 1D to 3D descriptors, molecular properties and charge descriptors, etc., covers a fairly complete descriptor space. A statistically robust genetic algorithm (GA) based on multiple linear regression (MLR) was deployed to run the QSAR model using the subjective feature selection (SFS) task in QSARINS v2.2.4. Models derived according to the organization for economic corporation and development (OECD) principles have been subjected to rigorous internal and external statistical validation, scrambling, and range analysis. The QSAR deployment process goes through the following steps:

To generate a QSAR model from the split data set, a random split operation is performed in QSARINS v2.2.4 to split the given data set into 80% training set (297 molecules) and 20% predictions (74 molecules set). A total of 297 molecules in the training set were used to develop the QSAR model, and external validation was performed on 74 molecules in the prediction set (Gramatica et al., 2013).

The GA-MLR-based QSAR model was built with the default setting QSARINS v2.2.4. Subjective feature selection was performed by setting Q^2_{LOO} as a fitness feature. The Q^2_{LOO} score increased significantly to six variables but then increased slightly. Therefore, to avoid overfitting the model, SFS was limited to a set of seven descriptors. This helped to get a simple and informative QSAR model (see **Supplementary Table 2** in **Supplementary information**) for additional information on the six selected molecular descriptors present in the QSAR).

A good QSAR model which has been properly validated using various methods such as cross-validation, external validation, Y-randomization, and applicability domain (Williams plot) is useful for future utilization in virtual screening, molecular optimization, and decision making, etc. The following statistical parameters and their recommended threshold values are routinely used to validate a model (Bellacasa et al., 2013; Roskoski, 2013; Fujita and Winkler, 2016; Gramatica, 2020): $R^2_{tr} \geq 0.6$, $Q^2_{loo} \geq 0.5$, $Q^2_{LMO} \geq 0.6$, $R^2 > Q^2$, $R^2_{ex} \geq 0.6$, $RMSE_{tr} < RMSE_{cv}$, $\Delta K \geq 0.05$, CCC ≥ 0.80, $Q^2_{-Fn} \geq 0.60$, $r^2_m \geq 0.5$, $(1-r^2/r_o^2) < 0.1$, $0.9 \leq k \leq 1.1$ or $(1-r^2/r_o^2) < 0.1$, $0.9 \leq k' \leq 1.1$,$(r_o^2 - r'^2_o|) < 0.3$, $RMSE_{ex}$, MAE_{ex}, R^2_{ex}, Q^{2F1}, Q^2_{F2}, Q^2_{F3}, and low R^2_{Yscr}, RMSE and MAE. The formulae for calculating these statistical parameters are available in **Supplementary Table 3** in the **Supplementary material**. In addition, the Williams plot was plotted to evaluate the applicability domain of the QSAR model.

QSAR-based virtual screening

A database of 26,467 food compounds was downloaded from FooDB (accessed December 28, 2021)[3], primarily for QSAR-based virtual screening (VS) accompanied through the utility of Lipinski rule of five; the elimination of duplicates, salts, and metal derivatives resulted in a truncated dataset of 8,453 molecules. Therefore, the 8,453-food molecule was mainly used for VS-based QSAR. Prior to the calculation of the molecular descriptor, the 3D molecular system was organized within the same Method as a modeling set. Next, the molecular descriptor was calculated and a well-validated 6-parametric version of the QSAR model was used to predict the bioactivity of the new compound (Gramatica, 2013; Neves et al., 2018; Zaki et al., 2021; Jawarkar et al., 2022; Mukerjee et al., 2022). (The calculated

3 http://foodb.ca/

molecular descriptors along with the predicted pKi and Ki values with smiles strings are given in **Supplementary Table 4** in the **Supplementary material**).

Virtual screening of natural compounds using molecular docking

The structure-based virtual screening of the compounds was performed using AutoDock vina Version 1.1.2 (Trott and Olson, 2010). Binding sites of BACE1 for screening were predicted using DoGSiteScorer (Volkamer et al., 2012) and information about the binding site of the native ligand. The size of the grid box was set to be 96 × 52 × 56 Å for BACE1, centered around the identified binding site. The compounds with the best binding affinity (kcal/mol) corroborating ligand-based screening in the QSAR analysis were selected for the studies.

Preparation of protein and ligand molecule

The target of interest BACE1 (PDB I.D: 2ZHV) crystallographic structure was discovered in the Protein Data Bank's structural database, and a molecular editor with an open-source license was used to import the structure (Discovery studio visualizer 4.0)[4] (**Figure 2**). To get the structure optimized, the UCSF Chimera utilized the steepest descent to find 1,000 steps, followed by the conjugate gradient of energy minimization approach to optimize the structure of 4-(3,4-dihydroxyphenyl)-2-hydroxy-1H-phenalen-1-one (PubChem I.D: 4468; Food I.D: FDB017657) was acquired from Food Database after screening and QSAR. This dataset was imported into the DS visualizer and saved as PDB files.

The FOOD database was used to obtain the library of ligands by screening the metabolites of *M. lasiocarpa* (Bonvino et al., 2018). The smiles notation and the three-dimensional structures of the selected ligands were downloaded in SDF format from the PubChem database (Kim et al., 2019), and further ligand structure files were converted to PDB format using Open Babel software (O'Boyle et al., 2011). The energy minimization of the ligands was performed in UCSF Chimera software (Pettersen et al., 2004) using the Amber ff 14 sb force field. The receptor used in the study is receptor tyrosine kinase; RCSB Protein Data Bank (PDB) (Berman et al., 2000) was used to download receptors BACE1 with PDB I.D: 2ZHV, Resolution: 1.85 Å. The protein structure was prepared by removing ligand, water molecules, and metal ions. Polar hydrogens were added, and non-polar hydrogens were merged. Finally, Kollman charges were added to the protein molecule before converting to PDBQT format by AutoDock Tools (v.1.5.6) of the MGL software package (Forli et al., 2016).

4 https://www.rcsb.org/structure/2ZHV

Molecular docking for validation of docking score

The best hits from the QSAR modeling and virtual screening were re-docked against BACE1 (PDB I.D: 2ZHV). Protein and ligand preparations were done using AutoDock Tools (v.1.5.6) (Forli et al., 2016). Gasteiger charges were added to the ligand molecules prior converting to the PDBQT format. Online server DoGSiteScorer and the information about the binding site residues of native ligand were used to construct the grid box. The grid box of dimensions 96 × 52 × 56 Å for BACE1 with 0.375 Å grid spacing was constructed using auto grid 4.2. Semi-flexible docking was done keeping the receptor molecule rigid and ligands flexible. Molecular docking was done via AutoDock 4.2 (Morris et al., 2009) using the Lamarckian Genetic Algorithm (LGA) scoring function with the number of GA runs = 100, population size = 550, and a maximum number of evaluations = 24,000,000.

Molecular dynamics simulation (MD-simulation) and free energy landscape (FEL) analysis

The MD simulations studies were carried out in triplicate on dock complexes for BACE1 (PDB I.D: 2ZHV) with FDB017657 using the Desmond 2020.1 from Schrödinger, LLC. The triplicate samplings were made using the same parameters for each MD run to obtain the reproducibility of the results. The OPLS-2005 force field (Bowers et al., 2006; Chow et al., 2008; Shivakumar et al., 2010) and explicit solvent model with the stocktickerSPC water molecules were used in this system (Jorgensen et al., 1983). Na^+ ions were added to neutralize the charge of 0.15 M, and NaCl solutions were added to the system to simulate the physiological environment. Initially, the system was equilibrated using an NVT ensemble for 150 ns to retrain over the protein- FDB017657 complex. Following the previous step, a short run of equilibration and minimization was carried out using an NPT ensemble for 12 ns. The NPT ensemble was set up using the Nose-Hoover chain coupling scheme (Martyna et al., 1994) with the temperature at 27°C, the relaxation time of 1.0 ps, and pressure of 1 bar maintained in all the simulations. A time step of 2fs was used. The Martyna–Tuckerman–Klein chain coupling scheme (Martyna et al., 1992) barostat method was used for pressure control with a relaxation time of 2 ps. The particle mesh Ewald method (Toukmaji and Board, 1996) was used to calculate long-range electrostatic interactions, and the Radius for the Coulomb interactions was fixed at 9Å. RESPA integrator was used for a time step of 2 fs for each trajectory to calculate the bonded forces. The root means square deviation (RMSD), radius of gyration (Rg), root mean square fluctuation (RMSF),

and the number of hydrogen (H-bonds) were calculated to monitor the stability of the MD simulations. The free energy landscape of protein folding on the FDB017657 bound complex was measured using geo_measures v 0.8 (Kagami et al., 2020). Geo_measures include a powerful library of g_sham and form the MD trajectory against RMSD and Radius of gyration (Rg) energy profile of folding recorded in a 3D plot using matplotlib python package.

Molecular mechanics generalized born and surface area (MMGBSA) calculations

During MD simulations of BACE1 complexed with FDB017657, the binding free energy (Gbind) of docked complexes was calculated using the premier molecular mechanics generalized Born surface area (MM-GBSA) module (Schrodinger suite, LLC, New York, NY, United States, 2017-4). The binding free energy was calculated using the OPLS 2005 force field, VSGB solvent model, and rotamer search methods (Piao et al., 2019). After the MD run, 10 ns intervals were used to choose the MD trajectories frames. The total free energy binding was calculated using equation 1:

$$\Delta Gbind = Gcomplex - (Gprotein + Gligand) \quad (1)$$

Where, ΔGbind = binding free energy, Gcomplex = free energy of the complex, Gprotein = free energy of the target protein, and Gligand = free energy of the ligand. The MMGBSA outcome trajectories were analyzed further for post-dynamics structure modifications.

Dynamic cross-correlation and principal component (PCA) analysis

During a 150 ns MD simulation, a dynamic cross-correlation matrix (DCCM) was constructed across all C-atoms for all complexes to examine domain correlations. During a 150 ns simulation of the BACE1 (PDB I.D- 2ZHV) complexed with FDB017657, PCA analysis was used to recover the global movements of the trajectories. To calculate the PCA, a covariance matrix was created as stated. For conformational analysis of the FDB017657 in bound complex, 20 alternative conformational modes of the main component as movements of trajectories were calculated, and a comparison of the first highest mode (PC2) with PC10 was investigated. Geo measures v 0.8 was used to calculate the free energy landscape of protein folding on an FDB017657-bound complex (Kagami et al., 2020). The MD trajectory versus PC2 and PC10 energy folding profiles were recorded in a 3D plot using the matplotlib python package using Geo measures, which includes a comprehensive library of g_sham.

Results

The present QSAR analysis is performed using a moderate-size data set comprising structurally diverse compounds with experimentally measured Ki in the range from 0.47 to 1,400 nM. Thus, it covers a sufficiently broad chemical and data range. This helped to derive a properly validated (Martin and Muchmore, 2012; Gramatica et al., 2013; Masand et al., 2015; Fujita and Winkler, 2016) genetic algorithm unified with multilinear regression (GA-MLR) model to collect or extend thorough information about the pharmacophoric features that control the desired bio-activity (Descriptive QSAR) and having adequate external predictive capability (Predictive QSAR). The six variable-based GA-MLR QSAR model along with selected internal and external validation parameters (see **Supplementary material** for additional parameters) is as follows:

QSAR Model (Divided Set: Training Set-80% and Prediction Set-20%):

pKi = 4.415 (± 0.236) + 0.046 (± 0.017) * com_lipohyd_5A + 0.12 (± 0.027) * faccC3B + 0.353 (± 0.105) * aroC_sumpc + 0.273 (± 0.034) * N_acc_5B + 0.109 (± 0.02) * aroC_ringS_6B + 0.269 (± 0.04) * fsp3OringC8B +

Statistical parameters related to fitting, double cross-validation, and Y-scrambling for the *de novo* QSAR model with thresholds for some parameters (bottom of table) are shown in **Table 1**.

Thresholds for some important statistical parameters: $R^2 \geq 0.6$, $Q^2_{LOO} \geq 0.5$, $Q^2_{LMO} \geq 0.6$, $R^2 > Q^2$, $R^2_{ex} \geq 0.6$, $RMSE_{tr} < RMSE_{cv}$, $\Delta K \geq 0.05$, CCC ≥ 0.80, $Q^2_{Fn} \geq 0.60$, $r^2m \geq 0.6$, $0.9 \leq k \leq 1.1$ and $0.9 \leq k' \leq 1.1$ at RMSE≈2, MAE 4 ≈04 R^2_{adj} of fitting parameter R^2, etc.) The threshold is significantly exceeded, confirming the adequacy of the number of molecular descriptors in the model and the statistical acceptability of the QSAR model. The values of Q^2_{LOO}, Q^2_{LMO}, etc., (internal validation parameters) confirm the statistical robustness of the QSAR model. The high values of the external test parameters R^2_{ex}, Q^2_{F1}, Q^2_{F2}, Q^2_{F3}, etc., emphasize the external predictability of the QSAR model. The coverage area of the model (Applicability Domain) is determined from Williams plots for the QSAR model (see **Figure 3**). Almost all statistical parameters reached values well above the accepted threshold, and the minimal correlation between the selected molecular descriptors precluded the possibility of random development of the QSAR model. This data confirms the statistical reliability and high external predictability of the developed QSAR models.

A nicely proven correlation among salient capabilities of the molecules represented through molecular descriptors, and their bioactivity expands statistics approximately mechanistic elements of molecules, specificity, and quantity (presence or even absence) of various structural developments for preferred bioactivity. Although, withinside the QSAR analysis, we've as compared the Ki values of various molecules in correlation and as an impact of a specific molecular descriptor, a similar

TABLE 1 Statistical parameters for the developed QSAR model.

Statistical parameters	Model
Fitting	
R^2	0.8120
R^2_{adj}	0.8168
R^2-R^2_{adj}	0.0037
LOF	0.1807
K_{xx}	0.2382
Delta K	0.0928
$RMSE_{tr}$	0.4079
MAE_{tr}	0.3276
RSS_{tr}	49.5888
CCC_{tr}	0.9014
s	0.4128
F	221.7565
Internal validation	
Q^2_{LOO}	0.8120
R^2-Q^2_{LOO}	0.0085
$RMSE_{cv}$	0.4175
MAE_{cv}	0.3352
$PRESS_{cv}$	51.9415
CCC_{cv}	0.8968
Q^2_{LMO}	0.8123
R^2_{Yscr}	0.0197
RMSE AV $_{Yscr}$	0.9534
$Q^{2\ Yscr}$	−0.0283
External validation	
$RMSE_{ext}$	0.4604
MAEext	0.3803
$PRESS_{ext}$	15.4724
R^2_{ext}	0.7829
Q^2-F1	0.7832
Q^2-F2	0.7819
Q^2-F3	0.7714
CCC_{ext}	0.8742
r^2_m aver.	0.6607
r^2_m delta	0.1977
k′	0.9967
K	0.9999
Clos′	0.0496
Clos	0.0000

or contrary impact of different molecular descriptors or unknown descriptors has a dominant impact in figuring out the general Ki value of a molecule cannot be neglected. In different words, a single molecular descriptor is incapable of absolutely explaining the experimental Ki value for this sort of numerous set of molecules. That is, the successful usage of the advanced QSAR model is based on the concomitant usage of molecular descriptors.

Mechanistic interpretation

com_lipohyd_5A (occurrence of the lipo-hydrophobic atoms within 5A from the center of mass of the molecule) Since this descriptor received a positive coefficient in the developed QSAR model, increasing the value of the molecular descriptor com_lipohyd_5A was observed to increase BACE1 inhibitory activity. This can be observed by comparing the compound 368 (pKi = 7.75, com_lipohyd_5A = 14) with 48 (pKi = 6.37, com_lipohyd_5A = 13) for which an increase in the value of the molecular descriptor com_lipohyd_5A from 13 for the molecule 48 to the 14 will give rise to increase in pKi value by about 1 unit (about ten-fold increase in BACE1 inhibitory activity). This observation is further reinforced by the following pair of molecules; 243 (pKi = 7.35, com_lipohyd_5A = 8) and 134 (pKi = 6.93, com_lipohyd_5A = 7), 211 (pKi = 7.92, com_lipohyd_5A = 12) and 207 (pKi = 7.58, com_lipohyd_5A = 11), 189 (pKi = 8.4, com_lipohyd_5A = 15) and 255 (pKi = 8.19, com_lipohyd_5A = 10), 262 (pKi = 5.52, com_lipohyd_5A = 15) and 115 (pKi = 4.97, com_lipohyd_5A = 13), etc. Shifting the molecular descriptor com_lipohyd_5A with com_lipohyd_6A statistically improves the performance (R: 0.84) of the developed QSAR model, while replacing com_lipohyd_5A with com_lipohyd_4A statistically drops the performance of the QSAR model (R: 0.81). This observation underscores the importance of the molecular descriptor com_lipohyd_5A. In addition, the optimum distance between lipo-hydrophobic atoms from the center of mass of the molecule should be maintained at 6 Å to show better inhibitory activity against BACE1.

faccC3B (occurrence of the carbon atom exactly at three bonds from the acceptor atom). If the same descriptor exists in two or four bonding at the same time, it will be removed during the calculation of faccC3B. This descriptor received a positive sign in the developed QSAR model. Therefore, further increases in faccC3B value increase the inhibitory efficacy of BACE1 inhibitors. Comparison of the compound 331 (pKi = 7.6, faccC3B = 7) with 142 (pKi = 6.87, faccC3B = 6) illustrate the influence of the molecular descriptor faccC3B. If the value of the molecular descriptor faccC3B is enhanced from 6 for the molecule 142 to 7 will upsurge the pki value by about 1 unit (about 10-fold amplification in the BACE1 inhibitory activity). Following pair from **Figures 3C,D** of molecules support this observation; 295 (pKi = 8.72, faccC3B = 6) and 255 (pKi = 8.19, faccC3B = 4), 262 (pKi = 5.52, faccC3B = 3) and 115 (pKi = 4.97, faccC3B = 2), 258 (pKi = 8.7, faccC3B = 9) and 274 (pKi = 7.58, faccC3B = 8), 128 (pKi = 6.28, faccC3B = 3) and 60 (pKi = 6.1, faccC3B = 2), 169 (pKi = 8.7, faccC3B = 9) and 286 (pKi = 7.55, faccC3B = 7), etc.

This shows that simple carbon atoms along the 3-bond acceptor atom are essential for inhibitory efficacy, but the molecular descriptors faccC3B and fdonC3B (frequency of carbon atoms exactly 3 bonds away from the donor atom). Or

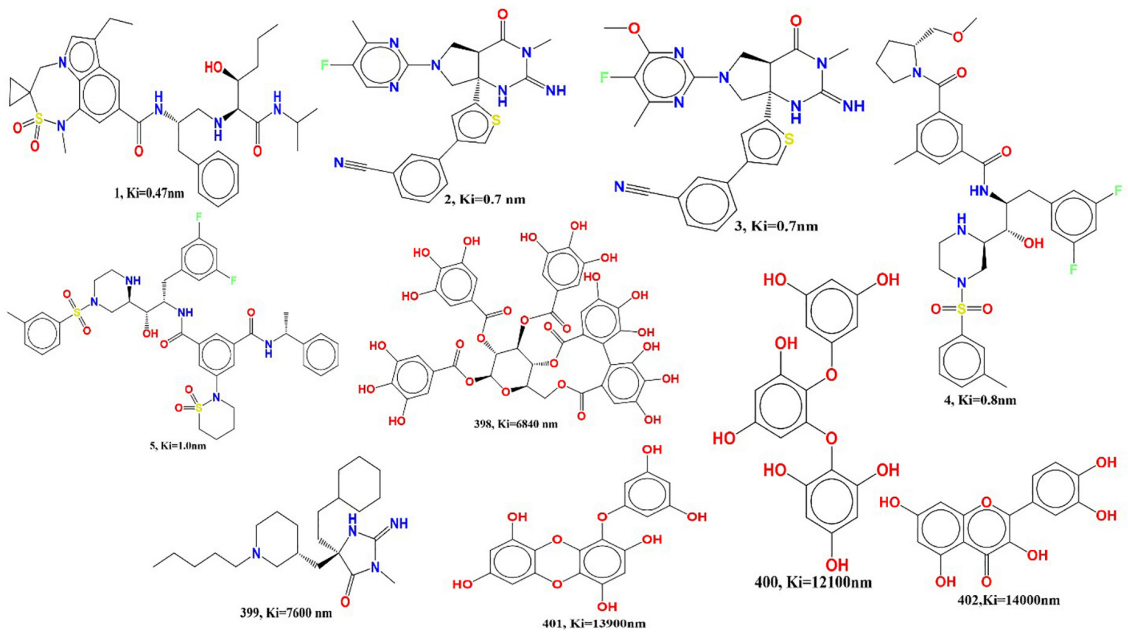

FIGURE 2
Variations in activity and chemical structure in the present dataset of BACE1 inhibitors.

fdonlipo5B (an acceptor atom with exactly 5 bonds from the donor atom) greatly improves the statistical detection power of the developed QSAR model (fdonC3B, R: 0.89) (fdonlipo5B, R: 0.88). This observation shows that the inhibitory effect can be enhanced by replacing the acceptor atom with a donor atom with 3 bonds of the same topology distance, or by moving the carbon atom to any lipophilic atom along the donor by a distance of five bonds. This observation shows that the carbon atom is more important along the donor atom located at the optimum distance of the three bonds. Therefore, since most H-bond donors or acceptors are nitrogen or oxygen, the presence of donor atoms close to the carbon atom may help to enhance the interaction with the polar residues of the receptor (BACE1). In addition, the descriptor also shows the important role that carbon atoms definitely play in lipophilicity.

aroC_sumpc (sum of partial charges on aromatic carbon atoms in the range of + 0.2 and −0.2). A positive coefficient for aroC_sumpc indicates that the higher the value of this descriptor, the better the activity profile. The presence of a large number of carbon atoms makes the molecule lipophilic, while the presence of positively or negatively charged carbon atoms causes various types of hydrophobic interactions with the receptor (BACE1), such as pi-alkyl, pi-cation, and pi-pi stacking. This observation underscores the importance of the molecular descriptor aroC_sumpc. This observation is supported by comparing the following pairs of molecules: 316 (pKi = 8.5, aroC_sumpc = 0.224000013) and 23 (pKi = 7.4, aroC_sumpc = −0.088000003), 159 (pKi = 9, aroC_sumpc = 0.013999997) and 298 (pKi = 8.5, aroC_sumpc = −0.197999999), 369 (pKi = 9, aroC_sumpc = 0.356000006) and 109 (pKi = 8.14, aroC_sumpc = −0.32299999), etc. This observation pointed out that negatively charged carbons are not favorable for BACE1 inhibitory activity, hence, ring carbon atom with neutral or positively charged possesses a better BACE1 inhibitory activity.

Subsequently, shifting the molecular descriptor aroC_sumpc to the molecular descriptor ringC_sumpc (sum of partial charges of the ring carbon atom) for future drug optimization increases the statistical power (R: 0.88) of the developed QSAR model. Furthermore, assuming that the molecular descriptor aroC_sumpc is replaced with the molecular descriptor aroCminus_sumpc (sum of partial charges of negatively charged aromatic carbon atoms), this reduces the statistical power (R: 0.75) of the QSAR model. Therefore, incorporating the ring carbon atom (ringC_sumpc) is a better choice for future optimization of hits to the lead molecule for better inhibitory activity of BACE1.

N_acc_5B (occurrence of acceptor atom within 5 bonds from the nitrogen atom). The molecular descriptor N_acc_5B indicates that the acceptor atom is within the four bonds of the nitrogen atom. This molecular descriptor has a positive coefficient in the developed QSAR model, so increasing the number of such combinations can enhance BACE1 inhibition. The effect of N_acc_5B can be explained by comparing the molecule 258 (pKi = 8.7, N_acc_5B = 5) and 57 (pKi = 6.4, N_acc_5B = 3). For molecule 57, if the value of the molecule descriptor increase from 3 to 5 will further amplify the pKi value

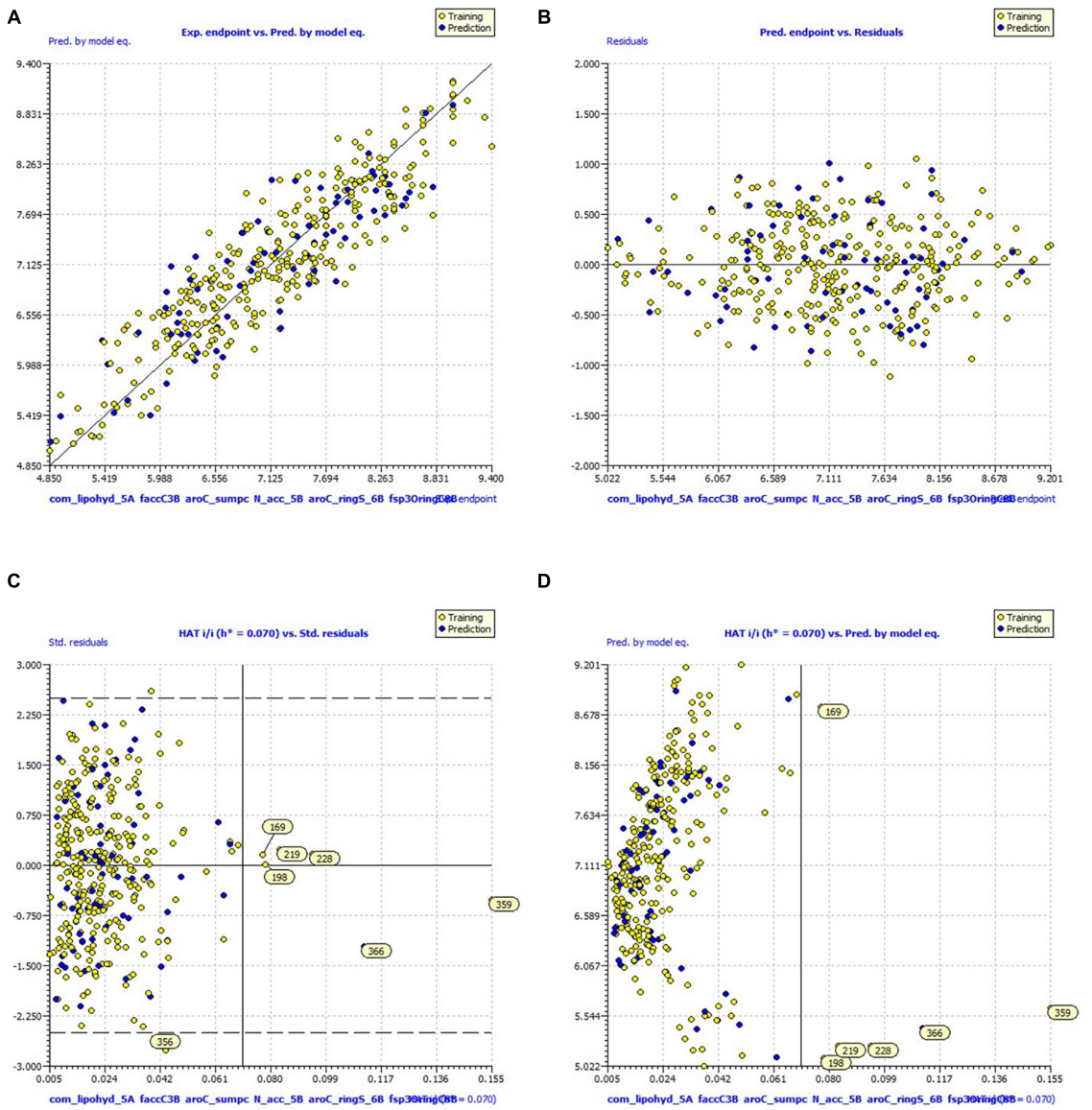

FIGURE 3
Graph for **(A)** experimental vs. predicted pKi **(B)** experimental vs. residuals **(C)** Williams plot for applicability domain **(D)** Insubria Plot.

by about 2 units, therefore, enhancing the BACE1 inhibitory activity by about 20 folds. These descriptors pointed out the importance of the nitrogen atom in BACE1 inhibitory activity. Moreover, additional molecular pair also illustrate the effect of N_acc_5B on BACE1 inhibitory activity include; 250 (pKi = 7.64, N_acc_5B = 5) and 55 (pKi = 6.52, N_acc_5B = 3), 189 (pKi = 8.4, N_acc_5B = 5) and 252 (pKi = 7.57, N_acc_5B = 4), 297 (pKi = 8.0, N_acc_5B = 8) and 102 (pKi = 7.17, N_acc_5B = 7), 312 (pKi = 8.5, N_acc_5B = 4) and 213 (pKi = 6.2, N_acc_5B = 3), etc.

The shift of the molecular descriptor N_acc_5B by the molecular descriptor N_acc_2B (the occurrence of acceptor atoms within two bonds from the nitrogen atom) strongly affects the statistical performance (R: 0.86) of the developed QSAR model (N_don_5B). This observation shows that the subsequent descriptor is N_acc_2B, which is useful as a better alternative to future drug optimization and to enhance the BACE1 inhibitor activity. Again, it is suggested that the optimum distance between the acceptor atom and the nitrogen atom may be two bonds.

On the other hand, replacing the molecular descriptor N_acc_5B with the molecular descriptor N_don_5B (the appearance of a donor atom within 5 bonds from the nitrogen atom) significantly increases the statistical power (R: 0.85)

of the developed QSAR model. This remark reveals two strategies for future optimization, consisting of reducing the topological distance from five bonds to two bonds according to the N_acc_2B descriptor, and replacement of acceptors with donors by maintaining the optimal distance of five bonds. This observation underscores the importance of nitrogen atoms and acceptor/donor properties for better inhibitory activity of BACE1.

aroC_ringS_6B (occurrence of the ring sulfur atoms within six bonds from the aromatic carbon atoms). The positive coefficient of the developed QSAR model descriptor justifies the increase in the value of the aroC_ringS_6B descriptor and further enhances the BACE1 inhibitory activity. Shifting the molecular descriptor aroC_ringS_6B by fringSringC3B (frequency of ring carbon atoms in exactly three bonds from the ring sulfur atom) significantly increases the statistical power (R:0.91) of the QSAR model. By comparing the molecule 222 (pKi = 8.0, aroC_ringS_6B = 1) and 362 (pKi = 7.75, aroC_ringS_6B = 0), the influence of aroC_ringS_6B as illustrated in the Figures 4A–J. Moreover, amplification in the value of the molecular descriptor aroC_ringS_6B from 0 to 1 for the molecule will uplift the pKi value by about 0.75 units (about 7 fold increase in the BACE1 inhibitory activity). Another pair of molecules also illustrate the effect of aroC_ringS_6B on BACE1 inhibitory activity include; 256 (pKi = 8.5, aroC_ringS_6B = 2) and 2 (pKi = 7.5, aroC_ringS_6B = 1), 295 (pKi = 8.7, aroC_ringS_6B = 2) and 324 (pKi = 7.3, aroC_ringS_6B = 0), 189 (pKi = 8.4, aroC_ringS_6B = 2) and 254 (pKi = 8.1, aroC_ringS_6B = 1), 144 (pKi = 7.8, aroC_ringS_6B = 2) and 140 (pKi = 7.0, aroC_ringS_6B = 0), etc.

Furthermore, replacing the molecular descriptor aroC_ringS_6B with fringSringC5B (frequency of ring carbon atoms in exactly five bonds from the ring sulfur atom) shows an increase in the statistical power (r: 0.94) of the developed QSAR model. On the other hand, replacing the molecular descriptor aroC_ringS_6B with fringSC6B (frequency of carbon atoms appearing in exactly 6 bonds from the ring sulfur atom) significantly reduces the statistical power (R: 0.80) of the QSAR model. This observation emphasizes the importance of the ring carbon atom and the ring sulfur atom. Furthermore, it can be concluded that reducing the topology bond distance from six to five bonds strongly affects the inhibitory activity of BACE1. Therefore, in future drug designs, it is recommended to keep the optimal distance between the ring carbon and the ring sprue atom at five bonds in order to increase the inhibitory activity of base 1. Aromatic and heterocyclic rings are very powerful motifs in drug discovery with target proteins such as the classical arene-arene interactions (π stacking), π-sulfur interactions, and arene-cation interaction. It offers many unique and powerful interactions such as bonds (end-face interactions) and recently identified π cations.

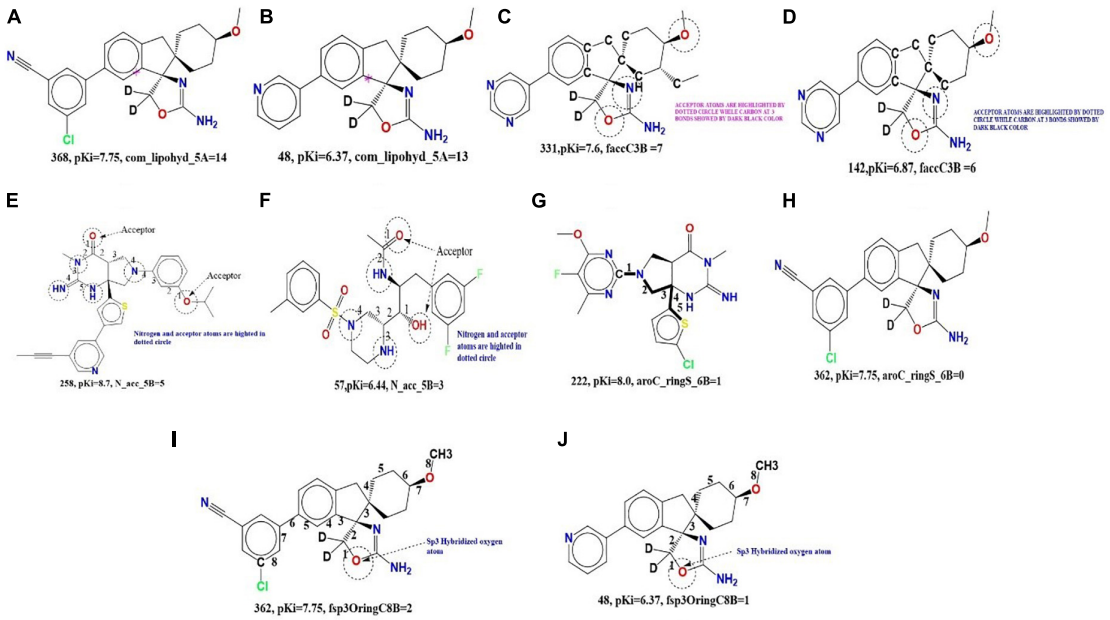

FIGURE 4
(A,B) Depiction of molecular descriptor com_lipohyd_5A for the compound 368 and 48 (pink star in the in both molecules indicates center of mass of the molecule). **(C,D)** Depiction of molecular descriptor faccC3B for the compound 331 and 48. **(E,F)** Illustration of the molecular descriptor N_acc_5B for the molecule 258 and 57. **(G,H)** Presentation of the molecular descriptor aroC_ringS_6B for the molecule 222 and 362. **(I,J)** Illustration of molecular descriptor fsp3OringC8B for the molecule 362 and 48.

fsp3OringC8B (frequency of occurrence of the ring carbon atom exactly at eight bonds from the sp3 oxygen atom) If the same ring carbon atom occurs simultaneously in seven or nine bonds, it will be bypassed in the fsp3OringC8B calculation. This molecular descriptor has a positive coefficient in the developed QSAR model, so increasing its value can improve the Ki value.

The effect of fsp3OringC8B can be assessed by comparing the molecule 362 9 (pKi = 7.75, fsp3OringC8B = 2) with 48 (pKi = 6.37, fsp3OringC8B = 1). Increasing the value of fsp3OringC8B for molecule 1 to 2 for molecule 48 will upsurge the pKi value by 1.38unit (about 13-fold amplification in the BACE1 inhibitory potential). Following pair of molecules also explain the effect of fsp3OringC8B on BACE1 inhibitory activity; 211 (pKi = 7.9, fsp3OringC8B = 3) and 207 (pKi = 7.5, fsp3OringC8B = 1), 299 (pKi = 8.7, fsp3OringC8B = 2) and 255 (pKi = 8.1, fsp3OringC8B = 1), 352 (pKi = 8.4, fsp3OringC8B = 2) and 30 (pKi = 6.0, fsp3OringC8B = 0), 110 (pKi = 7.5, fsp3OringC8B = 4) and 66 (pKi = 6.5, fsp3OringC8B = 0), etc. Replacing the fsp3OringC8B molecular descriptor with the fsp3OringC9B descriptor significantly reduces the statistical power (R: 0.78) of the developed QSAR model.

This observation underscores the importance of the molecular descriptor fsp3OringC8B. Therefore, future drug designs need to maintain the optimal distance between sp3 hybridized oxygen and ring carbon atoms at eight bonds in order to achieve better BACE1 inhibitory activity. Most oxygen atoms act as either acceptors or ether linkage, which can confer lipophilicity on the molecule. This may help to enhance both polar and hydrophobic interactions with the BACE1 receptor.

Molecular docking for validation of docking score

In molecular docking analysis of the BACE1 with FDB017657 in Autodock output, a dock complex displayed the best conformation. Receptors and ligands were saved in the.pdbqt format for subsequent usage using the MGL 1.5.6 suite. Vina was launched from a command prompt using the command line. In the setup, the default grid point spacing was 0.525 and the exhaustiveness was set to 8. The output files were in.pdbqt format, and they were analyzed using PyMol and the Discovery studio visualizer 2021. The ligand-binding was validated and optimized using the co-crystal ligand. Both the receptor and ligands were made by combining 48 polar hydrogen bonds and detecting 1 rotatable bond and adding Kollman and Gasteiger charges. Finally, both receptor and ligand molecules were stored in the.pdbqt format. With the values $X = -1.655$, $Y = 57.005$, and $Z = 133.83$, a grid box was produced with a spacing of 0.375. Docking experiments of the protein-ligand complex were carried out using Genetic Algorithm (GA) parameters were set with 100, population size was made 300 with a maximum number of evaluates was set to low at 2,500,000 and maximum generations of 27,000. Further docking experiments of the protein–ligand complex were carried out using the Lamarckian Genetic Algorithm (LGA) to obtain the lowest free energy of binding (G). The 2ZHV-FDB017657 complex showed free energy of binding (ΔG) −8.9 kcal/mol, inhibitory concentration (Ki) 990.57 μM, ligand efficiency −1.26, total internal energy −1.45 kJ/mol, and torsional energy 0.3 kJ/mol. The docking scores are mentioned in Table 2.

TABLE 2 Screening of phytochemicals based on their best binding energy.

Protein-ligand	Binding affinity (kcal/mol)
2zhv_8265	−4.8
2zhv_8263	−4.7
2zhv_8262	−7.3
2zhv_8079	−4.7
2zhv_7888	−5
2zhv_7701	−6.4
2zhv_7594	−6.3
2zhv_7334	−2.9
2zhv_7032	−4.9
2zhv_6574	−5.1
2zhv_5179	−5.6
2zhv_4844	−7.6
2zhv_4817	−5.6
2zhv_4693	−4.9
2zhv_4688	−5.8
2zhv_4605	−5.5
2zhv_4468	**−8.9**
2zhv_4340	−7.6
2zhv_4009	−5.7
2zhv_3981	−4.6
2zhv_3805	−4.7
2zhv_3207	−5.7
2zhv_2839	−4.8
2zhv_1976	−5.4
2zhv_1749	−5.7
2zhv_734	−7.3
2zhv_686	−6.7
2zhv_673	−8.3
2zhv_603	−6.5
2zhv_442	−4.5
2zhv_41	−3.8
2zhv_4	−5.6

The principal residues making the binding pocket around 4-(3,4-dihydroxyphenyl)-2-hydroxy-1H-phenalen-1-one (Food I.D: FDB017657) are comprised of THR72, THR231, GLY230, ASP228, GLY34, ILE118, SER35, PHE108, ASP106, LYS107, GLY74, and GLN73 by Van der Waals interaction forces; ASP32

is involved in conventional hydrogen bonding, while TYR71 is involved in forming a conventional Pi-Pi bond (Figure 5, left).

Molecular dynamics simulation (MD) and free energy landscape analysis

Molecular dynamics and simulation (MD) studies were carried out to determine the stability and convergence of the 4-(3,4-Dihydroxyphenyl)-2-hydroxy-1H-phenalen-1-one (PubChem I.D: 4468; Food I.D: FDB017657) bound BACE1 (PDB I.D: 2ZHV) complex. Each simulation of 150 ns displayed stable conformation while comparing the root mean square deviation (RMSD) values.

The Root Mean Square Deviation (RMSD) is a metric for calculating the average change in the displacement of a group of atoms in relation to a reference frame. It is calculated for each and every frame of the trajectory. The RMSD for frame x is:

$$RMSD_X = \sqrt{\frac{1}{N}\sum_{i=1}^{N}(r_i'(t_X)) - r_i(t_{ref}))^2}$$

where N is the number of atoms in the atom selection; t_{ref} is the reference time (the first frame is usually used as the reference and is treated as time $t = 0$); and where r' is the position of the selected atoms after superimposing on the reference frame in frame x, where frame x is recorded at time t_x. Every frame in the simulation trajectory is subjected to the same technique (Maiorov and Crippen, 1994).

For characterizing local changes along the protein chain, the Root Mean Square Fluctuation (RMSF) is useful. The RMSF for residue i is:

$$RMSF_i = \sqrt{\frac{1}{T}\sum_{t=1}^{T} < (r_i'(t)) - r_i(t_{ref}))^2 >}$$

The angle brackets indicate that the average of square distance is taken over the selection of atoms in the residue. where T is the trajectory time over which the RMSF is calculated, t_{ref} is the reference time, r_i is the position of residue I r′ is the position of atoms in residue I after superposition on the reference. Its simulation paths of Desmond were examined. MD trajectory analysis was used to calculate the root mean square deviation (RMSD), root mean square fluctuation (RMSF), and protein–ligand interactions. Protein RMSD: The graphs depict the evolution of a protein's RMSD (left Y-axis). The RMSD is estimated based on the atom selection once all protein frames are aligned on the reference frame backbone.

The Cα-backbone of BACE1 bound to 4-(3,4-dihydroxyphenyl)-2-hydroxy-1H-phenalen-1-one (PubChem I.D: 4468; Food I.D: FDB017657) exhibited a deviation of 0.4 Å (Figure 6A). RMSD plots are within the acceptable range signifying the stability of proteins in the FDB017657 bound state before and after simulation and it can also be suggested that FDB017657 bound BACE1 (PDB I.D: 2ZHV) is quite stable in the complex might be due to significant binding of the ligand.

The radius of gyration is the measure of the compactness of the protein. FDB017657 bound proteins displayed a lowering of radius of gyration (Rg) (Figure 6B; R1, R2, R3). The lowering of Rg indicates the compactness of the protein–ligand complex. From the overall quality analysis from RMSD and Rg, it can be suggested that FDB017657 bound to the protein targets posthumously in the binding cavities and plays a significant role in the stability of the proteins.

The plots for root mean square fluctuations (RMSF) displayed a significant RMSF in BACE1 protein at a few residues at the specific time function of 150 ns. Peaks show sections of the protein that fluctuate the greatest during the simulation on the RMSF plot. Typically, the tails (N- and C-terminal) of proteins change more than any other portion of the protein. Secondary structural parts such as alpha helices and beta strands are usually more rigid than the unstructured portion of the protein and fluctuate less than loop areas. The residues with higher peaks belong to loop areas or N and C-terminal zones, as determined by MD trajectories (Figure 6C). The stability of ligand binding to the protein is shown by low RMSF values of binding site residues. From the triplicate runs of BACE1, as shown in Figure 6C, a few fluctuating peaks can be seen although mostly the complex is found to be stabilized as shown in Figure 6C. The RMSF values are acceptable for stabilizing the protein–ligand complex. Therefore, in RMSF plots, it can be suggested that the protein structures were stable during simulation in FDB017657 bound conformation.

The average hydrogen bonds formed between FDB017657 and the respective protein, BACE1 (PDB I.D: 2ZHV), during the 150 ns simulation were also recorded (Figure 6D). From 0 ns to 150 ns a formation of hydrogen bonding was found throughout the simulation and the same for triplicate MD simulation of FDB017657 with BACE1 (Figure 6D). Moreover, the pattern of two hydrogen bond formation with BACE1 (PDB I.D: 2ZHV), in docking was corroborated by the number of hydrogen plot analyses after 150 ns molecular dynamics (Figure 6D). The amount of hydrogen bonds between BACE1 with FDB017657 has strengthened the binding and facilitated to conform to a more stable complex during the simulation.

Throughout the simulation, protein interactions with the ligand can be observed. As seen in the graph above, these interactions can be classified and summarized by type. Hydrogen bonds, hydrophobic, ionic, and water bridges are the four forms of protein–ligand interactions (or "contacts"). Each interaction type has a number of subtypes that can be examined using Maestro's "Simulation Interactions Diagram" panel (see Figure 7A). The stacked bar charts are standardized over the course of the trajectory. Some protein residues may make several interactions of the same subtype with the ligand, values above 1.0 are feasible. As shown in Figure 7A, the majority of

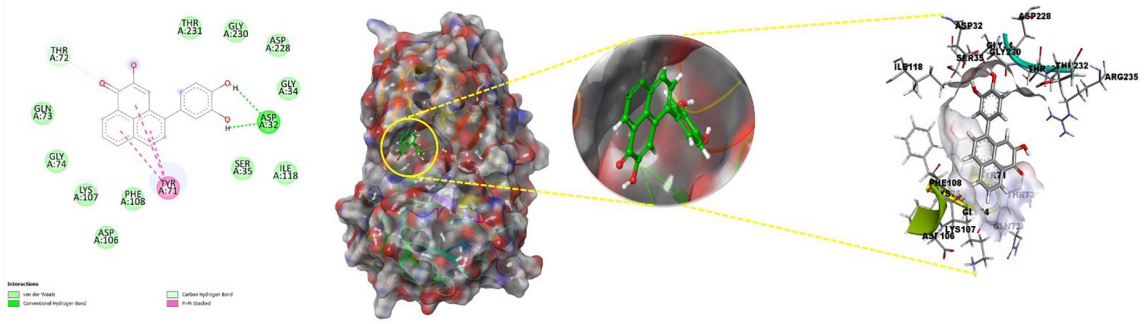

FIGURE 5
Best docked pose of FDB017657 with 2ZHV displaying 2D interaction plot on the **left panel**. Pink dashed lines indicate the Pi-Alkyl bond and residues embedded in the light green sphere, indicating involvement in Van der Waals interactions. On the **center panel**, surface view of 2ZHV displays binding cavity of FDB017657, and **right panel** displays the zoomed-out binding pocket having amino acid residues at 3Å surrounding the FDB017657 molecule.

the significant ligand–protein interactions discovered by MD are hydrogen bonds and hydrophobic interactions. For 2ZHV-FDB017657, complex residues VAL_31, ASP_32, TYR_71, and THR_72 are the most important ones in terms of H-bonds.

Individual ligand atom interactions with protein residues are depicted in Figure 7B. Interactions that occur for more than 30.0% of the simulation period in the chosen trajectory (0.00 through 150.0 ns) are displayed. From Figure 7B, it can be concluded that the amino acid residues: PHE108, TRP76, TYR71, and VAL69 involve a hydrophobic interaction, LYS107, ARG128 possess a positive charge bonding with the ligand, GLN73, SER35, and ASN37 are involved in polar interactions, and ASP32 and ASP228 are involved in negatively charged interaction with the ligand, FDB017657 in 150 ns simulation time scale.

Throughout the simulation, the existence of protein secondary structural elements (SSE) such as alpha helices and beta strands is examined to ensure that they are not present. The plot shown in Figure 7C depicts the distribution of SSE by residue index over the complete protein structure, and it encompasses the full protein structure. In contrast to the charts, which show the summary of the SSE composition for each trajectory frame during the course of the simulation, the graphs at the bottom show the evolution of each residue and its SSE assignment throughout the experiment. Throughout the simulation, alpha-helices and beta-strands are monitored as secondary structure elements (SSE). The left graph shows the distribution of SSE across the protein structure by the residue index. The top image highlights the SSE composition for each trajectory frame throughout the simulation, while the bottom plot tracks each residue's SSE assignment through time.

It can be observed from Figure 7D, how each rotatable bond (RB) in the ligand alters its conformation throughout the simulation on the ligand torsions map (0.00 through 150.15 ns). The top panel shows a two-dimensional schematic of a ligand with color-coded rotatable bonds. There includes a dial plot as well as bar plots in the same color for each rotatable bond torsion. The evolution of the torsion's conformation during the simulation is depicted using dial (or radial) graphs. The simulation's time evolution is depicted radially outwards from the simulation's start point at the center of the radial plot. The data from the dial plots are summarized in the bar plots, which show the torsion probability density in the data. Alternatively, if torsional potential data is available, the graphic will also indicate the rotatable bond's potential (by summing the potential of the related torsions) kcal/mol. The potential values are given as kcal/mol and plotted on the graph's left *Y*-axis. The histogram and torsion potential correlations can reveal the conformational strain that the ligand is under in order to maintain a protein-bound conformational state.

The stepwise trajectory analysis of every 25 ns of simulation of FDB017657 with BACE1 displayed the positional alteration with reference to the 0 ns structure (Figure 8). It has been observed that the ligand, FDB017657 has possessed a structural angular movement at the end frame to achieve its conformational stability and convergence.

The free energy landscape (FEL) of achieving global minima of Cα backbone atoms of proteins with respect to RMSD and radius of gyration (Rg) is displayed in Figure 9, BACE1 bound to the ligand, FDB017657 achieved the global minima (lowest free energy state) at 1.1 Å and Rg 20.9 Å (Figure 9). The FEL envisaged a deterministic behavior of BACE1 to the lowest energy state owing to its high stability and best conformation at FDB017657 bound state.

Molecular mechanics generalized born and surface area calculations

To assess the binding energy of ligands to protein molecules, the MMGBSA technique is commonly employed. The binding free energy of each BACE1– FDB017657 complex, as well

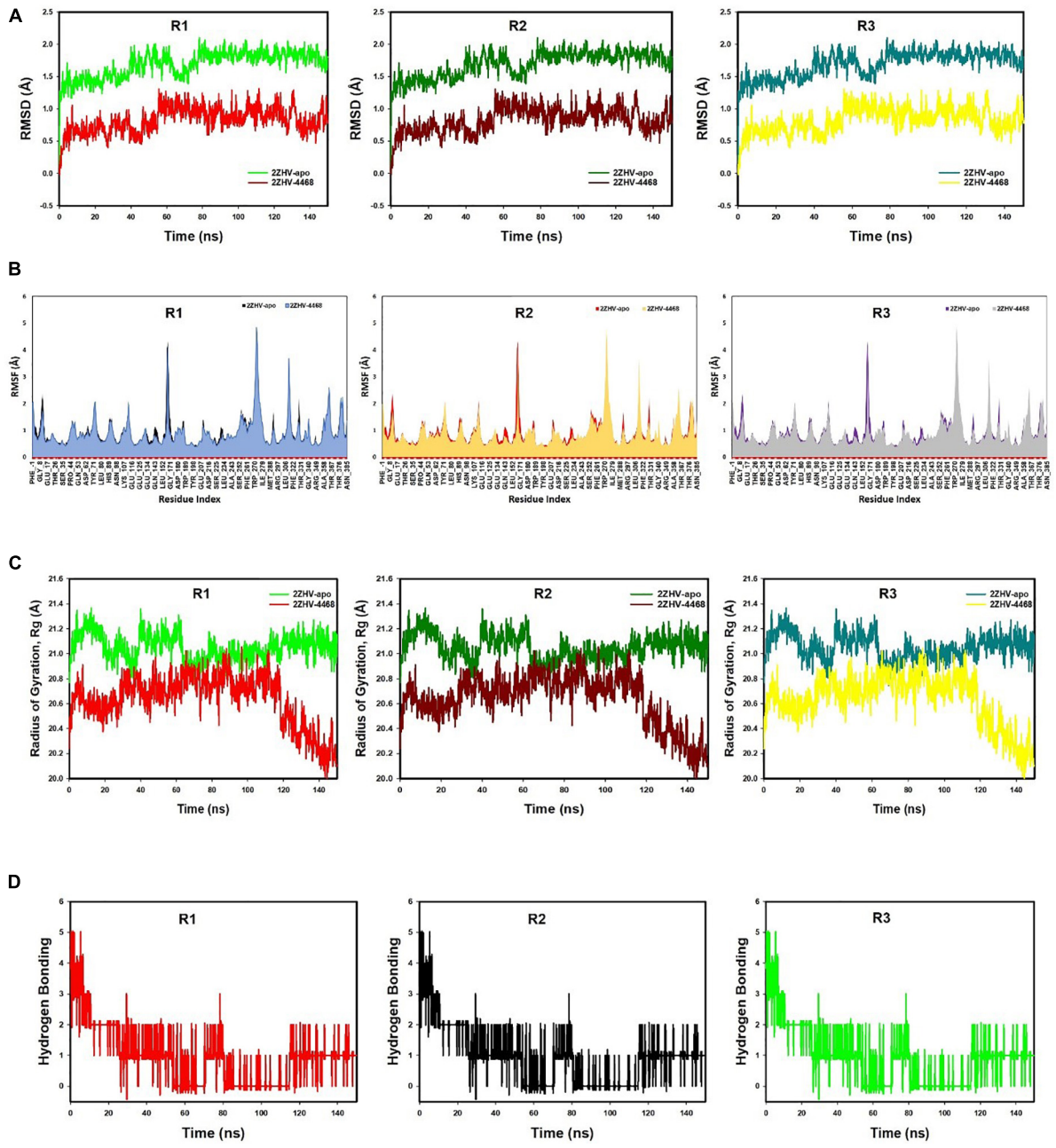

FIGURE 6

(A) MD simulation trajectory analysis of Root Mean Square Divisions (RMSD) of FDB017657 bound with 2ZHV, i.e., BACE1 150 ns time frame in triplicate displayed: R1 (replicate 1) RMSD plot of FDB017657 bound BACE1 (PDB I.D: 2ZHV) (red) with control protein BACE1 (PDB I.D: 2ZHV) (light green); R2 (replicate 2) RMSD plot of FDB017657 bound BACE1 (PDB I.D: 2ZHV) (dark maroon) with control protein BACE1 (PDB I.D: 2ZHV) (juniper green); R3 (replicate 3) RMSD plot of FDB017657 bound BACE1 (PDB I.D: 2ZHV) (lemon yellow) with control protein BACE1 (PDB I.D: 2ZHV) (cyan). **(B)** MD simulation trajectory analysis of Root Mean Square Fluctuations (RMSF) of FDB017657 bound with BACE1 (PDB I.D: 2ZHV) at 150 ns time frame in triplicate displayed: R1 (replicate 1) RMSF plot of FDB017657 bound BACE1 (PDB I.D: 2ZHV) (navy blue) with control protein BACE1 (PDB I.D: 2ZHV) (black); R2 (replicate 2) RMSF plot of FDB017657 bound BACE1 (PDB I.D: 2ZHV) (canary yellow) with control protein BACE1 (PDB I.D: 2ZHV) (red); R3 (replicate 3) RMSF plot of FDB017657 bound BACE1 (PDB I.D: 2ZHV) (gray) with control protein BACE1 (PDB I.D: 2ZHV) (purple). **(C)** MD simulation trajectory analysis of Radius of gyration (Rg) of FDB017657 bound with BACE1 (PDB I.D: 2ZHV) at 150 ns time frame in triplicate displayed: R1 (replicate 1) Rg plot of FDB017657 bound BACE1 (PDB I.D: 2ZHV) (red) with control protein BACE1 (PDB I.D: 2ZHV) (light green); R2 (replicate 2) Rg plot of FDB017657 bound BACE1 (PDB I.D: 2ZHV) (dark maroon) with control protein BACE1 (PDB I.D: 2ZHV) (juniper green); R3 (replicate 3) Rg plot of FDB017657 bound BACE1 (PDB I.D: 2ZHV) (cyan) with control protein BACE1 (PDB I.D: 2ZHV) (lemon yellow). **(D)** MD simulation trajectory analysis of Hydrogen Bonding (H-Bonds) of FDB017657 bound with BACE1 (PDB I.D: 2ZHV) at 150 ns time frame in triplicate displayed: R1 (replicate 1) H-Bond plot of FDB017657 bound BACE1 (PDB I.D: 2ZHV) (red); R2 (replicate 2) H-Bond plot of FDB017657 bound BACE1 (PDB I.D: 2ZHV) (black); R3 (replicate 3) H-Bond plot of FDB017657 bound BACE1 (PDB I.D: 2ZHV) (light green).

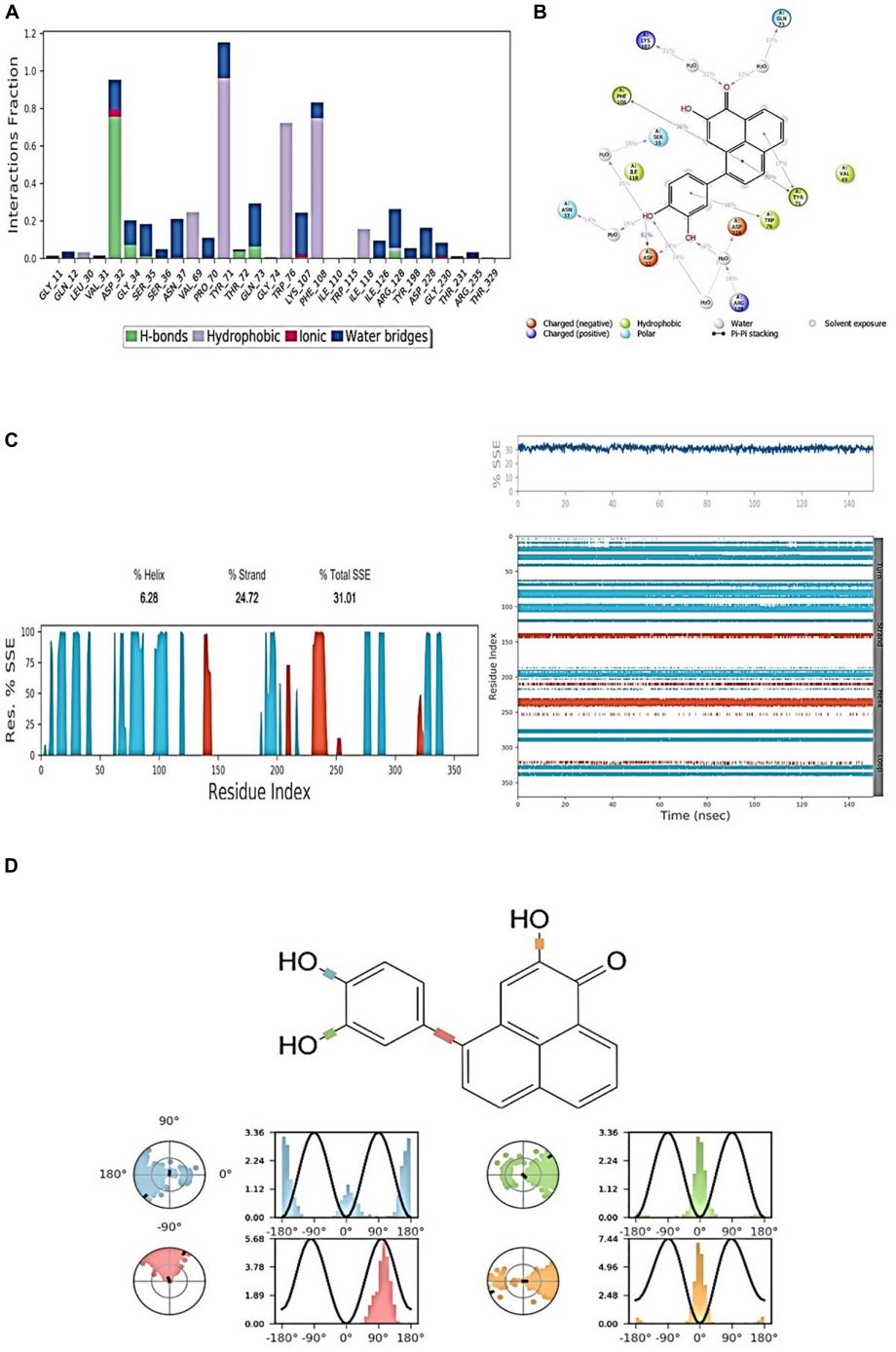

FIGURE 7
(A) Protein-ligand contact histogram (H-bonds, Hydrophobic, Ionic, Water bridges) of the ligand, FDB017657 bound with 2ZHV recorded in a 150 ns simulation interval. **(B)** Ligand atom interactions with the protein residues of 2ZHV bound with FDB017657. **(C)** Secondary Structure element distribution by residue index throughout the protein structure. Red indicates alpha helices, and blue indicate beta-strands of 2ZHV bound with FDB017657. **(D)** Ligand torsion profile.

as the impact of other non-bonded interaction energies, were estimated. With BACE1, the ligand FDB017657 has a binding energy of −53.4670 kcal/mol. Non-bonded interactions like G_{bind}Coulomb, G_{bind}Covalent, G_{bind}Hbond, G_{bind}Lipo, G_{bind}SolvGB, and G_{bind}vdW govern Gbind. Across all types of interactions, the G_{bind}vdW, G_{bind}Lipo, and G_{bind}Coulomb energies contributed the most to the average binding energy. On the other side, the G_{bind}SolvGB and Gbind Covalent

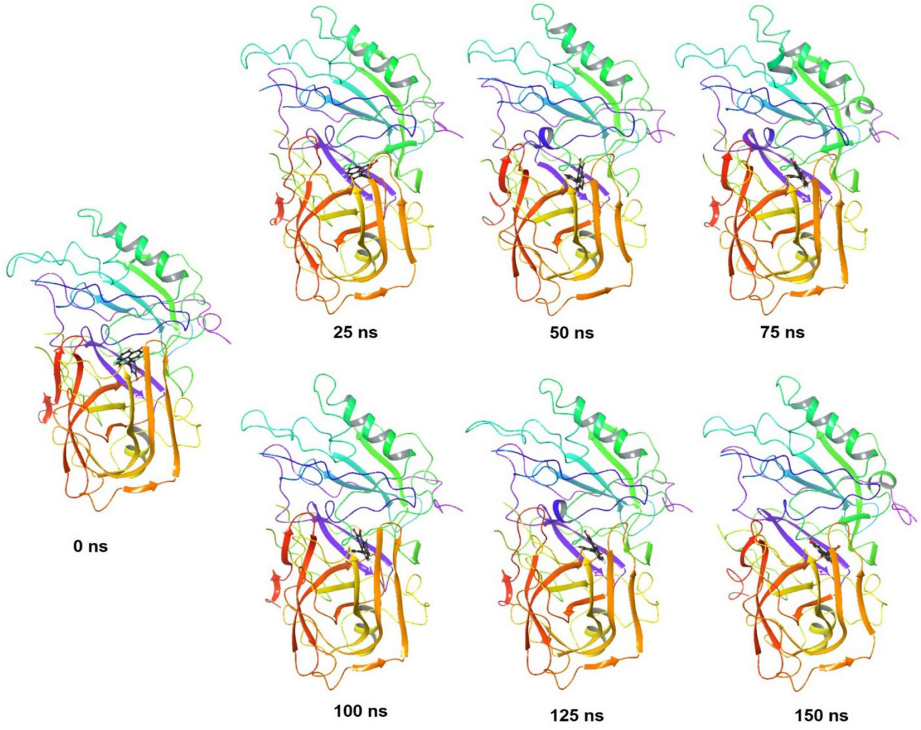

FIGURE 8
Stepwise trajectory analysis for every 25 ns displaying the protein, BACE1 (PDB I.D: 2ZHV) and ligand conformation during 150 ns of simulation of 4-(3,4-Dihydroxyphenyl)-2-hydroxy-1H-phenalen-1-one (PubChem I.D: 4468; Food I.D: FDB017657).

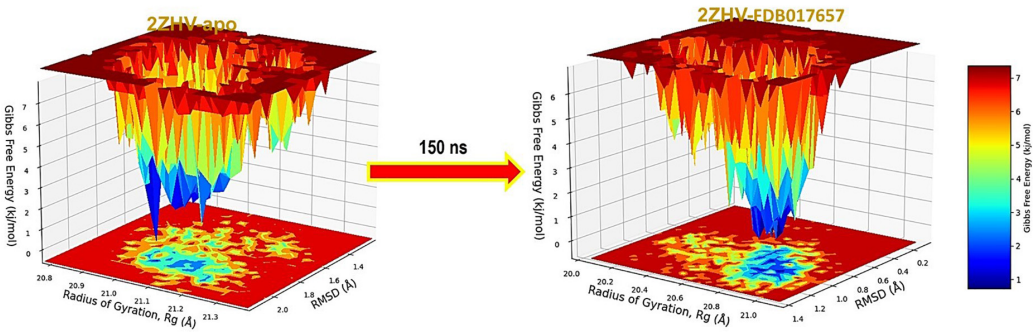

FIGURE 9
Free Energy Landscape displaying the achievement of global minima (ΔG, kJ/mol) of BACE1 in presence of FDB017657 with respect to their RMSD (nm) and Radius of gyration (Rg, nm).

energies contributed the least to the final average binding energies. Furthermore, the G_{bind}Hbond interaction values of BACE1–FDB017657 complexes demonstrated stable hydrogen bonds with amino acid residues. In all of the compounds, G_{bind}SolvGB and G_{bind}Covalent exhibited unfavorable energy contributions and so opposed binding. Figure 10 (left panel) reveals that between pre-simulation (0 ns) and post-simulation (0 ns), FDB017657 in the binding pocket of BACE1 has undergone a large angular change in the pose (curved to straight) (150 ns). These conformational changes lead to better binding pocket acquisition and interaction with residues, which leads to enhanced stability and binding energy (mentioned in Table 3).

Thus, MM-GBSA calculations resulted from MD simulation trajectories well justified with the binding energy obtained from docking results; moreover, the last frame (150 ns) of MMGBSA displayed the positional change of FDB017657 as compared to the 0 ns trajectory signifying the better binding

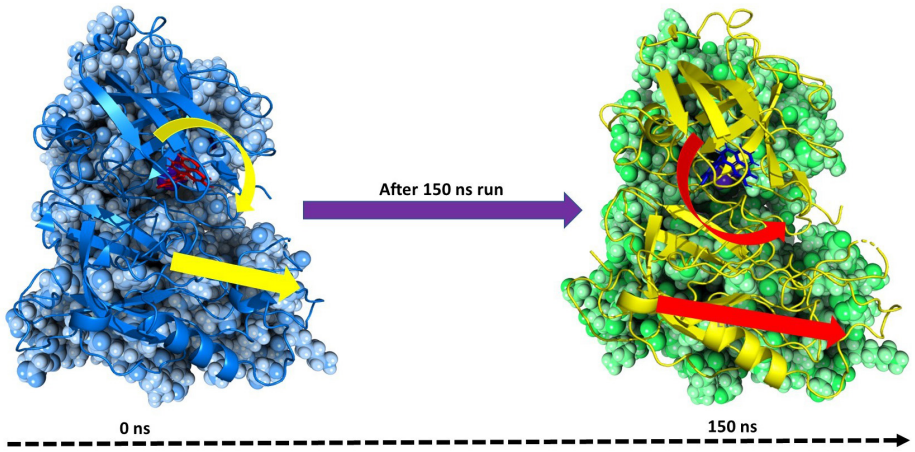

FIGURE 10
MMGBSA trajectory (0 ns, before simulation and 150 ns, after simulation) exhibited conformational changes of FDB017657 upon binding with the protein 2ZHV. The arrows indicate the overall positional variation (movement and pose) of FDB017657 at the binding site cavity.

pose for best fitting in the binding cavity of the protein (see Figure 10).

Therefore, it can be suggested that the FDB017657 molecule has a good affinity for the major target BACE1.

Dynamic cross-correlation, principal component analysis (PCA), and energy calculations

Molecular dynamics simulation trajectories are analyzed for dynamic cross-correlation among the domains within protein chains bound with the FDB017657 molecule. For correlative dynamic motion, the cross-correlation matrices of BACE1 were generated and displayed in Figure 11. The blue blocks displayed in the figure indicated the residues having high correlated movement and red having the least correlation. The amino acid residues of FDB017657 bound BACE1 showed the concerted movement of residues (Figure 11).

Principal component analysis (PCA) determines the relationship between statistically meaningful conformations (major global motions) sampled during the trajectory. PCA of the MD simulation trajectories for BACE1 bound to the FDB017657 molecule was analyzed to interpret the randomized global motion of the atoms of amino acid residues. The internal coordinates mobility into three-dimensional space in the spatial time of 150 ns were recorded in a covariance matrix and the rational motion of each trajectory is interpreted in the form of orthogonal sets or Eigen vectors. In the BACE1 trajectory, PCA indicates statistically significant conformations. It is possible to identify the major motions within the trajectory as well as the critical motions required for conformational changes. In BACE1 bound to FDB017657, two different clusters along the PC1 and PC2 planes are exhibited that indicate a non-periodic conformational shift (Figure 12A). While these global motions are periodic because the groupings along the PC3 and PC4 planes do not totally cluster separately (Figure 12B). Moreover, a high periodic global motion was observed along the PC9 and PC10 planes due to the grouping of trajectories in a single cluster at the center of the PCA plot (Figure 12C). Centering of the trajectories in a single cluster indicates the periodic motion of MD trajectories due to stable conformational global motion.

TABLE 3 Binding energy calculation of FDB017657 with 2ZHV and non-bonded interaction energies from MMGBSA trajectories.

Energies (kcal/mol)	2ZHV
ΔG_{bind}	-53.467 ± 3.001
ΔG_{bind}Lipo	-22.124 ± 2.448
ΔG_{bind}vdW	33.667 ± 0.0701
ΔG_{bind}Coulomb	-9.827 ± 5.083
$\Delta G_{bind}H_{bond}$	-1.465 ± 0.775
ΔG_{bind}SolvGB	-8.989 ± 1.695
ΔG_{bind}Covalent	-1.079 ± 1.049

The energy profiles of the protein, BACE1 and FDB017657 complex systems, were determined to display the stability of the entire system. In this regard, the total energy (ETOT) of the BACE1 bound FDB017657 system was shown to be very stable with an average total energy of −69.00 kcal/mol (green). However, van der Waal's energy (vdW) displayed to be merged over the total energy with an average energy of −40.00 kcal/mol and contemplated as a principal contributor to the stability of the BACE1-FDB017657 complex (cyan). In addition, Coulombic interactions played a minor role in the system stability and contributed to an average energy of −32.00 kcal/mol (red), (see Figure 12D).

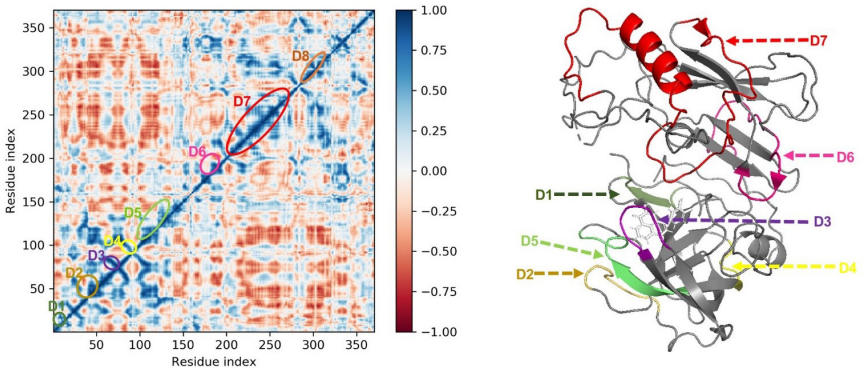

FIGURE 11
Dynamic Cross Correlation matrix (DCCM) of 2ZHV and correlated amino acids conformed into secondary structural domains (colored) and non-correlated domains (gray) of 2ZHV.

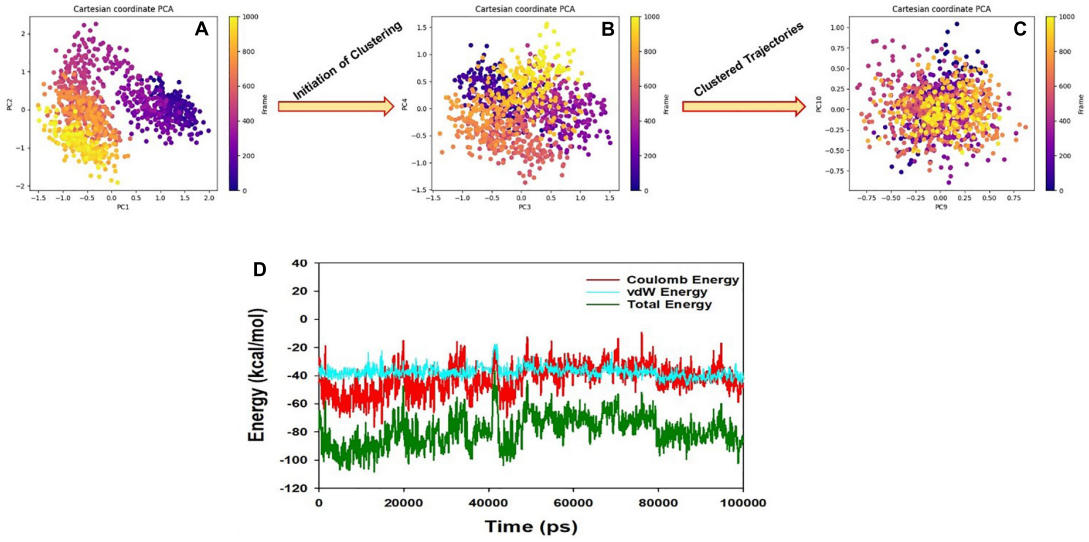

FIGURE 12
(A) PCA of 2ZHV- FDB017657 showing a stable configuration. **(B)** Energy plot of protein BACE1 and FDB017657 complex system during the entire simulation event of 150 ns. **(C,D)** The change in PCA movements. The total energy (dark green), van der Waal's energy (cyan) and Coulomb energy (red) of the entire system indicate the stability of the individual systems bound to FDB017657 molecule.

Discussion

Proteolytic processing of APP by BACE1 is the rate-determining step in Aβ production, hence BACE1 is employed as a therapeutic target for creating innovative lead compounds in AD in this study. According to the earlier reports, it was suggested that the enzyme BACE1 is also associated with different types of cancers and viruses in conjunction with AD. In this study, we have tried to reveal the potential of naturally available food molecules to bind the BACE1's active site in a highly specific binding pattern. The aim of our study is toward the development of a drug from food compounds with the help of computational biology as it has the additional advantage regarding safety, and lesser chance of side effects. The low toxicity profile of natural products inspired by small-molecule inhibitors may prove to be a great asset during the frenetic development period of drug discovery when time is of the essence. Current state-of-the-art computational approaches can be used to identify structural and pharmacophoric properties of active natural compounds that can be used as drugs. Our results suggest that the selected 8,453 compounds from the Food database are majorly phenols and naphthol metabolites having a high potential of showing inhibitory activity against BACE1. The Food database is a recent database that proved the potential of food metabolites that we use in our daily life and found its

major application in developing different therapeutics treating depressive disorders and others.

A nicely proven correlation among salient capabilities of the molecules represented through molecular descriptors, and their bioactivity expands statistics approximately mechanistic elements of molecules, specificity, and quantity (presence or even absence) of various structural developments for preferred bioactivity. Although, with the QSAR analysis, we've compared the Ki values of various molecules in correlation and as an impact of a specific molecular descriptor, a similar or contrary impact of different molecular descriptors or unknown descriptors has a dominant impact in figuring out the general Ki value of a molecule can't be neglected. In other words, a single molecular descriptor is incapable of absolutely explaining the experimental Ki value for this sort of numerous sets of molecules. That is, the successful usage of the advanced QSAR model is based on the concomitant usage of molecular descriptors.

A QSAR model with multiple chemical descriptors is built using a dataset of 371 compounds. The resulting model was rigorously verified for fitting and internal validation to prove its strong external prediction capacity and resilience. In addition, virtual screening using QSAR yielded a novel food molecule with a better Ki value of 10.715 nM. Combined QSARs and molecular docking studies offered complimentary information and helped discover prodigious and under-privileged chemical characteristics that might be leveraged to change a molecule to produce better BACE1 inhibitors with higher Ki values. In the future, structural modifications that result in augmented values for the molecular descriptors with positive coefficients in the developed model for the anti-BACE1 activity will be performed to generate novel hits suitable for construction and *in vitro* evaluation as anti-Alzheimer's (AD) disease therapy. These reports already demonstrated the potential of this plant as a source of novel drugs, nutraceuticals, and functional foods. Our present study perhaps supports a further avenue for *in vivo* and clinical trial of the food molecule, 4-(3,4-dihydroxyphenyl)-2-hydroxy-1H-phenalen-1-one to target BACE1 for any future scope to treat the AD along with viruses and cancer.

Data availability statement

The original contributions presented in this study are included in the article/**Supplementary material**, further inquiries can be directed to the corresponding authors.

Author contributions

NM and ADa performed the concept design. NM, AG, SwM, and RJ designed and carried out the experimental procedures. NM, AG, RJ, RB, MC, and VM done the analysis. NM, ADa, PD, AP, GM, SB, BA, and SA-H done the manuscript preparation. NM, ADe, GM, MK, AAl, ADa, SuM, AMA, and MZ edited the manuscript. All authors contributed to the article and approved the submitted version.

Funding

This research work was funded by the Institutional Fund Projects under grant no. IFPDP-85-22. This research work was funded by the Institutional Fund Projects under grant no. (IFPDP-85-22). Therefore, authors gratefully acknowledge technical and financial support from Ministry of Education and Deanship of Scientific Research (DSR), King Abdulaziz University, Jeddah, Saudi Arabia.

Conflict of interest

AA is honorary associated with the scientific board of the company AFNP Med in Austria.

The remaining authors declare that the research was conducted in the absence of any commercial or financial relationships that could be construed as a potential conflict of interest.

Publisher's note

Supplementary material

The Supplementary Material for this article can be found online at: https://www.frontiersin.org/articles/10.3389/fnagi.2022.878276/full#supplementary-material

SUPPLEMENTARY TABLE 1
Smileskipki.

SUPPLEMENTARY TABLE 2
Descriptor used in QSAR.

SUPPLEMENTARY TABLE 3
Formulas for calculation of model parameters.

SUPPLEMENTARY TABLE 4
Food molecules predicted pki and descriptors.

References

Alzheimer's Association (2012). 2012 Alzheimer's disease facts and figures. *Alzheimer's Dement.* 8, 131–168.

Arif, N., Subhani, A., Hussain, W., and Rasool, N. (2020). In silico inhibition of BACE-1 by selective phytochemicals as novel potential inhibitors: Molecular docking and DFT studies. *Curr. Drug Disc. Technol.* 17, 397–411. doi: 10.2174/1570163816666190214161825

Bellacasa, R. P., Karachaliou, N., Estrada-Tejedor, R., Teixidó, J., Costa, C., and Borrell, J. I. A. L. K. (2013). and ROS1 as a joint target for the treatment of lung cancer: A review. *Transl. Lung Cancer Res.* 2, 72–86.

Berman, H. M., Westbrook, J., Feng, Z., Gilliland, G., Bhat, T. N., Weissig, H., et al. (2000). The protein data bank. *Nucleic Acids Res.* 28, 235–242. doi: 10.1093/nar/28.1.235

Bo, Q., Runhua, L., Hanqing, W., Min, W., Wenpeng, L., and Jinlun, X. (2000). Chemical constituents from Musella lasiocarpa (Franch.) CY Wu. *Nat. Product Res. Develop.* 12, 41–44.

Bonvino, N. P., Liang, J., McCord, E. D., Zafiris, E., Benetti, N., Ray, N. B., et al. (2018). OliveNet^{TM}: A comprehensive library of compounds from Olea europaea. *Database* 2018:bay016. doi: 10.1093/database/bay016

Bowers, K. J., Chow, D. E., Xu, H., Dror, R. O., Eastwood, M. P., Gregersen, B. A., et al. (2006). "Scalable algorithms for molecular dynamics simulations on commodity clusters," in *SC'06: Proceedings of the 2006 ACM/IEEE Conference on Supercomputing*, (Tampa, FL: IEEE), 43–43. doi: 10.1109/SC.2006.54

Chow, E., Rendleman, C. A., Bowers, K. J., Dror, R. O., Hughes, D. H., Gullingsrud, J., et al. (2008). *Desmond performance on a cluster of multicore processors*. New York, NY: DE Shaw Research Technical Report DESRES/TR–2008-01.

Cui, H., Hung, A. C., Klaver, D. W., Suzuki, T., Freeman, C., Narkowicz, C., et al. (2011). Effects of heparin and enoxaparin on APP processing and aβ production in primary cortical neurons from Tg2576 mice. *PLoS One* 6:e23007. doi: 10.1371/journal.pone.0023007

Davies, M., Nowotka, M., Papadatos, G., Dedman, N., Gaulton, A., and Atkinson, F. (2015). ChEMBL web services: Streamlining access to drug discovery data and utilities. *Nucleic Acids Res.* 45, D945–D954. doi: 10.1093/nar/gkv352

De Strooper, B., and Karran, E. (2016). The cellular phase of Alzheimer's disease. *Cell* 164, 603–615. doi: 10.1016/j.cell.2015.12.056

Dingwall, C. (2001). Spotlight on BACE: The secretases as targets for treatment in Alzheimer disease. *J. Clin. Invest.* 108, 1243–1246. doi: 10.1172/JCI14402

Dong, L. B., He, J., Li, X. Y., Wu, X. D., Deng, X., Xu, G., et al. (2011). Chemical constituents from the aerial parts of Musella lasiocarpa. *Nat. Products Bioprospect.* 1, 41–47. doi: 10.1007/s13659-011-0007-7

Forli, S., Huey, R., Pique, M. E., Sanner, M. F., Goodsell, D. S., and Olson, A. J. (2016). Computational protein–ligand docking and virtual drug screening with the AutoDock suite. *Nat. Protocols* 11, 905–919. doi: 10.1038/nprot.2016.051

Fujita, T., and Winkler, D. A. (2016). Understanding the Roles of the "Two QSARs". *J. Chem. Inf. Model* 56, 269–274. doi: 10.1021/acs.jcim.5b00229

Fukumoto, H., Cheung, B. S., Hyman, B. T., and Irizarry, M. C. (2002). β-Secretase protein and activity are increased in the neocortex in Alzheimer disease. *Arch. Neurol.* 59, 1381–1389. doi: 10.1001/archneur.59.9.1381

Gramatica, P. (2013). On the development and validation of QSAR models. *Methods Mol. Biol.* 930, 499–526. doi: 10.1007/978-1-62703-059-5_21

Gramatica, P. (2020). Principles of QSAR Modeling. *Int. J. Quant. Struct. Property Relation.* 5, 61–97. doi: 10.4018/IJQSPR.2020070101.oa1

Gramatica, P., Cassani, S., and Chirico, N. (2014). QSARINS-Chem: Insubria Datasets and New QSAR/QSPR Models for Environmental Pollutants in QSARINS. *J. Comput. Chem. Softw. News Updates* 35, 1036–1044. doi: 10.1002/jcc.23576

Gramatica, P., Chirico, N., Papa, E., Kovarich, S., and Cassani, S. (2013). QSARINS: A New Software for the Development, Analysis, and Validation of QSAR MLR Models. *J. Comp. Chem. Softw. News Updates* 34, 2121–2132. doi: 10.1002/jcc.23361

Hall, A., Pekkala, T., Polvikoski, T., Van Gils, M., Kivipelto, M., Lötjönen, J., et al. (2019). Prediction models for dementia and neuropathology in the oldest old: The Vantaa 85+ cohort study. *Alzheimer's Res. Ther.* 11, 1–2. doi: 10.1186/s13195-018-0450-3

Hassan, M., Shahzadi, S., Seo, S. Y., Alashwal, H., Zaki, N., and Moustafa, A. A. (2018). Molecular docking and dynamic simulation of AZD3293 and solanezumab effects against BACE1 to treat Alzheimer's disease. *Front. Comput. Neurosci.* 12:34. doi: 10.3389/fncom.2018.00034

Hussain, I., Powell, D. J., Howlett, D. R., Chapman, G. A., Gilmour, L., Murdock, P. R., et al. (2000). ASP1 (BACE2) cleaves the amyloid precursor protein at the β-secretase site. *Mol. Cell. Neurosci.* 16, 609–619. doi: 10.1006/mcne.2000.0884

Jabir, N. R., Rehman, M. T., Alsolami, K., Shakil, S., Zughaibi, T. A., Alserihi, R. F., et al. (2021). Concatenation of molecular docking and molecular simulation of BACE-1, γ-secretase targeted ligands: In pursuit of Alzheimer's treatment. *Ann. Med.* 53, 2332–2344. doi: 10.1080/07853890.2021.2009124

Jawarkar, R. D., Bakal, R. L., Zaki, M. E. A., Al-Hussain, S., Ghosh, A., Gandhi, A., et al. (2022). QSAR based virtual screening derived identification of a novel hit as a SARS CoV-229E 3CLpro Inhibitor: GA-MLR QSAR modeling supported by molecular Docking, molecular dynamics simulation and MMGBSA calculation approaches. *Arab. J. Chem.* 15:103499. doi: 10.1016/j.arabjc.2021.103499

Jorgensen, W. L., Chandrasekhar, J., Madura, J. D., Impey, R. W., and Klein, M. L. (1983). Comparison of simple potential functions for simulating liquid water. *J. Chem. Phys.* 79, 926–935. doi: 10.1063/1.445869

Kagami, L. P., das Neves, G. M., Timmers, L. F. S. M., Caceres, R. A., and Eifler-Lima, V. L. (2020). Geo-Measures: A Pymol plugin for protein structure ensembles analysis. *Comp. Biol. Chem.* 87:107322. doi: 10.1016/j.compbiolchem.2020.107322

Kim, S., Chen, J., Cheng, T., Gindulyte, A., He, J., He, S., et al. (2019). PubChem 2019 update: Improved access to chemical data. *Nucleic Acids Res.* 47, D1102–D1109. doi: 10.1093/nar/gky1033

Li, Q., and Südhof, T. C. (2004). Cleavage of amyloid-β precursor protein and amyloid-β precursor-like protein by BACE 1. *J. Biol. Chem.* 279, 10542–10550. doi: 10.1074/jbc.M310001200

Lin, X., Koelsch, G., Wu, S., Downs, D., Dashti, A., and Tang, J. (2000). Human aspartic protease memapsin 2 cleaves the β-secretase site of β-amyloid precursor protein. *Proc. Natl. Acad. Sci.* 97, 1456–1460. doi: 10.1073/pnas.97.4.1456

Maiorov, V. N., and Crippen, G. M. (1994). Significance of root-mean-square deviation in comparing three-dimensional structures of globular proteins. *J. Mol. Biol.* 235, 625–634. doi: 10.1006/jmbi.1994.1017

Martin, Y. C., and Muchmore, S. W. (2012). Frozen out: Molecular modeling in the age of cryocrystallography. *J. Comput. Aided Mol. Design* 26, 91–92.

Martyna, G. J., Klein, M. L., and Tuckerman, M. (1992). Nosé–Hoover chains: The canonical ensemble via continuous dynamics. *J. Chem. Phys.* 97, 2635–2643. doi: 10.1063/1.463940

Martyna, G. J., Tobias, D. J., and Klein, M. L. (1994). Constant pressure molecular dynamics algorithms. *J. Chem. Phys.* 101, 4177–4189. doi: 10.1063/1.467468

Masand, V. H., Mahajan, D. T., Alafeefy, A. M., Bukhari, S. N., and Elsayed, N. N. (2015). Optimization of antiproliferative activity of substituted phenyl 4-(2-oxoimidazolidin-1-yl) benzenesulfonates: QSAR and CoMFA analyses. *Eur. J. Pharm. Sci.* 77, 230–237.

Masand, V. H., and Rastija, V. (2017). PyDescriptor : A new PyMOL plugin for calculating thousands of easily understandable molecular descriptors. *Chemom. Intell. Labor. Syst.* 169, 12–18. doi: 10.1016/j.chemolab.2017.08.003

Morris, G. M., Huey, R., Lindstrom, W., Sanner, M. F., Belew, R. K., Goodsell, D. S., et al. (2009). AutoDock4 and AutoDockTools4: Automated docking with selective receptor flexibility. *J. Comp. Chem.* 30, 2785–2791. doi: 10.1002/jcc.21256

Moussa-Pacha, N. M., Abdin, S. M., Omar, H. A., Alniss, H., and Al-Tel, T. H. (2020). BACE1 inhibitors: Current status and future directions in treating Alzheimer's disease. *Med. Res. Rev.* 40, 339–384. doi: 10.1002/med.21622

Mukerjee, N., Das, A., Maitra, S., Ghosh, A., Khan, P., Alexiou, A., et al. (2022). Dynamics of natural product lupenone as a potential fusion inhibitor against the spike complex of novel semliki forest virus. *PLoS One* 17:e0263853. doi: 10.1371/journal.pone.0263853

Murphy, M. P., and LeVine, III. H. (2010). Alzheimer's disease and the amyloid-beta peptide. *J. Alzheimers Dis.* 19, 311–323. doi: 10.3233/JAD-2010-1221

Musi, N., Valentine, J. M., Sickora, K. R., Baeuerle, E., Thompson, C. S., Shen, Q., et al. (2018). Tau protein aggregation is associated with cellular senescence in the brain. *Aging cell* 17:e12840. doi: 10.1111/acel.12840

Neves, B. J., Braga, R. C., Melo-Filho, C. C., Moreira-Filho, J. T., Muratov, E. N., and Andrade, C. H. (2018). QSAR-Based Virtual Screening: Advances and Applications in Drug Discovery. *Front. Pharmacol.* 9:1275. doi: 10.3389/fphar.2018.01275

O'Boyle, N. M., Banck, M., James, C. A., Morley, C., Vandermeersch, T., and Hutchison, G. R. (2011). Open Babel: An open chemical toolbox. *J. Cheminform.* 3:33. doi: 10.1186/1758-2946-3-33

Pettersen, E. F., Goddard, T. D., Huang, C. C., Couch, G. S., Greenblatt, D. M., Meng, E. C., et al. (2004). UCSF Chimera—a visualization system for exploratory research and analysis. *J. Comp. Chem.* 25, 1605–1612. doi: 10.1002/jcc.20084

Piao, L., Chen, Z., Li, Q., Liu, R., Song, W., Kong, R., et al. (2019). Molecular dynamics simulations of wild type and mutants of SAPAP in complexed with Shank3. *Int. J. Mol. Sci.* 20:224. doi: 10.3390/ijms20010224

Roskoski, R. Jr. (2013). Anaplastic lymphoma kinase (ALK): Structure, oncogenic activation, and pharmacological inhibition. *Pharmacol. Res.* 68, 68–94. doi: 10.1016/j.phrs.2012.11.007

Sebastián-Serrano, Á, Diego-García, D., and Díaz-Hernández, M. (2018). The neurotoxic role of extracellular tau protein. *Int. J. Mol. Sci.* 19:998. doi: 10.3390/ijms19040998

Shivakumar, D., Williams, J., Wu, Y., Damm, W., Shelley, J., and Sherman, W. (2010). Prediction of absolute solvation free energies using molecular dynamics free energy perturbation and the OPLS force field. *J. Chem. Theory Comp.* 6, 1509–1519. doi: 10.1021/ct900587b

Sinha, S., Anderson, J. P., Barbour, R., Basi, G. S., Caccavello, R., Davis, D., et al. (1999). Purification and cloning of amyloid precursor protein β-secretase from human brain. *Nature* 402, 537–540. doi: 10.1038/990114

Tosco, P., Balle, T., and Shiri, F. (2011). Open3DALIGN: An open-source software aimed at unsupervised ligand alignment. *J. Comp.Aided Mol. Design* 25, 777–783. doi: 10.1007/s10822-011-9462-9

Toukmaji, A. Y., and Board, J. A. Jr. (1996). Ewald summation techniques in perspective: A survey. *Comp. Phys. Commun.* 95, 73–92. doi: 10.1016/0010-4655(96)00016-1

Tresadern, G., Delgado, F., Delgado, O., Gijsen, H., Macdonald, G. J., Moechars, D., et al. (2011). Rational design and synthesis of aminopiperazinones as β-secretase (BACE) inhibitors. *Bioorgan. Med. Chem. Lett.* 21, 7255–7260. doi: 10.1016/j.bmcl.2011.10.050

Trott, O., and Olson, A. J. (2010). AutoDock Vina: Improving the speed and accuracy of docking with a new scoring function, efficient optimization, and multithreading. *J. Comput. Chem.* 31, 455–461. doi: 10.1002/jcc.21334

Vassar, R., Bennett, B. D., Babu-Khan, S., Kahn, S., Mendiaz, E. A., Denis, P., et al. (1999). β-Secretase cleavage of Alzheimer's amyloid precursor protein by the transmembrane aspartic protease BACE. *Science* 286, 735–741. doi: 10.1126/science.286.5440.735

Volkamer, A., Kuhn, D., Grombacher, T., Rippmann, F., and Rarey, M. (2012). Combining global and local measures for structure-based druggability predictions. *J. Chem. Inf. Model* 52, 360–372. doi: 10.1021/ci200454v

Yan, R., Bienkowski, M. J., Shuck, M. E., Miao, H., Tory, M. C., Pauley, A. M., et al. (1999). Membrane-anchored aspartyl protease with Alzheimer's disease β-secretase activity. *Nature* 402, 533–537. doi: 10.1038/990107

Yang, L. B., Lindholm, K., Yan, R., Citron, M., Xia, W., Yang, X. L., et al. (2003). Elevated β-secretase expression and enzymatic activity detected in sporadic Alzheimer disease. *Nat. Med.* 9, 3–4. doi: 10.1038/nm0103-3

Zacchetti, D., Chieregatti, E., Bettegazzi, B., Mihailovich, M., Sousa, V. L., Grohovaz, F., et al. (2007). BACE1 expression and activity: Relevance in Alzheimer's disease. *Neurodegener. Dis.* 4, 117–126. doi: 10.1159/000101836

Zaki, M. E. A., Al-Hussain, S. A., Masand, V. H., Akasapu, S., Bajaj, S. O., El-Sayed, N. N. E., et al. (2021). Identification of Anti-SARS-CoV-2 Compounds from Food Using QSAR-Based Virtual Screening, Molecular Docking, and Molecular Dynamics Simulation Analysis. *Pharmaceuticals* 14:357. doi: 10.3390/ph14040357

Zhang, Y. W., Thompson, R., Zhang, H., and Xu, H. (2011). APP processing in Alzheimer's disease. *Mol. Brain* 4:3. doi: 10.1186/1756-6606-4-3

CITATION

Mukerjee N, Das A, Jawarkar RD, Maitra S, Das P, Castrosanto MA, Paul S, Samad A, Zaki MEA, Al-Hussain SA, Masand VH, Hasan MM, Bukhari SNA, Perveen A, Alghamdi BS, Alexiou A, Kamal MA, Dey A, Malik S, Bakal RL, Abuzenadah AM, Ghosh A and Md Ashraf G (2022) Repurposing food molecules as a potential BACE1 inhibitor for Alzheimer's disease. *Front. Aging Neurosci.* 14:878276. doi: 10.3389/fnagi.2022.878276

frontiers | Frontiers in Aging Neuroscience

TYPE Review
PUBLISHED 07 September 2022
DOI 10.3389/fnagi.2022.977411

OPEN ACCESS

EDITED BY
Elliott Jay Mufson,
Barrow Neurological Institute,
United States

REVIEWED BY
Hitesh Chopra,
Chitkara University, India
Rehan Khan,
Institute of Nano Science
and Technology, India

*CORRESPONDENCE
Tariq Maqbool
tmwani@uok.edu.in
Gulam Md. Ashraf
ashraf.gm@gmail.com

SPECIALTY SECTION
This article was submitted to
Alzheimer's Disease and Related
Dementias,
a section of the journal
Frontiers in Aging Neuroscience

RECEIVED 24 June 2022
ACCEPTED 18 August 2022
PUBLISHED 07 September 2022

CITATION
Mumtaz I, Ayaz MO, Khan MS,
Manzoor U, Ganayee MA, Bhat AQ,
Dar GH, Alghamdi BS, Hashem AM,
Dar MJ, Ashraf GM and Maqbool T
(2022) Clinical relevance
of biomarkers, new therapeutic
approaches, and role
of post-translational modifications
in the pathogenesis of Alzheimer's
disease.
Front. Aging Neurosci. 14:977411.
doi: 10.3389/fnagi.2022.977411

Clinical relevance of biomarkers, new therapeutic approaches, and role of post-translational modifications in the pathogenesis of Alzheimer's disease

Ibtisam Mumtaz[1], Mir Owais Ayaz[2,3], Mohamad Sultan Khan[4], Umar Manzoor[5], Mohd Azhardin Ganayee[1,6], Aadil Qadir Bhat[2,3], Ghulam Hassan Dar[7], Badrah S. Alghamdi[8,9], Anwar M. Hashem[10,11], Mohd Jamal Dar[2,3], Gulam Md. Ashraf[9,12]* and Tariq Maqbool[1]*

[1]Laboratory of Nanotherapeutics and Regenerative Medicine, Department of Nanotechnology, University of Kashmir, Srinagar, India, [2]Laboratory of Cell and Molecular Biology, Department of Cancer Pharmacology, CSIR-Indian Institute of Integrative Medicine, Jammu, India, [3]Centre for Scientific and Innovative Research, Ghaziabad, Utter Pradesh, India, [4]Neurobiology and Molecular Chronobiology Laboratory, Department of Animal Biology, School of Life Sciences, University of Hyderabad, Hyderabad, India, [5]Laboratory of Immune and Inflammatory Disease, Jeju Research Institute of Pharmaceutical Sciences, Jeju National University, Jeju, South Korea, [6]Department of Chemistry, Indian Institute of Technology Madras, Chennai, India, [7]Sri Pratap College, Cluster University Srinagar, Jammu and Kashmir, India, [8]Department of Physiology, Neuroscience Unit, Faculty of Medicine, King Abdulaziz University, Jeddah, Saudi Arabia, [9]Pre-clinical Research Unit, King Fahd Medical Research Center, King Abdulaziz University, Jeddah, Saudi Arabia, [10]Department of Medical Microbiology and Parasitology, Faculty of Medicine, King Abdulaziz University, Jeddah, Saudi Arabia, [11]Vaccines and Immunotherapy Unit, King Fahd Medical Research Center, King Abdulaziz University, Jeddah, Saudi Arabia, [12]Department of Medical Laboratory Sciences, Faculty of Applied Medical Sciences, King Abdulaziz University, Jeddah, Saudi Arabia

Alzheimer's disease (AD) is a neurodegenerative disorder that causes progressive loss of cognitive functions like thinking, memory, reasoning, behavioral abilities, and social skills thus affecting the ability of a person to perform normal daily functions independently. There is no definitive cure for this disease, and treatment options available for the management of the disease are not very effective as well. Based on histopathology, AD is characterized by the accumulation of insoluble deposits of amyloid beta (Aβ) plaques and neurofibrillary tangles (NFTs). Although several molecular events contribute to the formation of these insoluble deposits, the aberrant post-translational modifications (PTMs) of AD-related proteins (like APP, Aβ, tau, and BACE1) are also known to be involved in the onset and progression of this disease. However, early diagnosis of the disease as well as the development of effective therapeutic approaches is impeded by lack of proper clinical biomarkers. In this review, we summarized the current status and clinical relevance of biomarkers from cerebrospinal fluid (CSF), blood and

extracellular vesicles involved in onset and progression of AD. Moreover, we highlight the effects of several PTMs on the AD-related proteins, and provide an insight how these modifications impact the structure and function of proteins leading to AD pathology. Finally, for disease-modifying therapeutics, novel approaches, and targets are discussed for the successful treatment and management of AD.

KEYWORDS

Alzheimer's disease, AD-related proteins, biomarkers, post translational modifications, AD therapeutics

Introduction

Alzheimer's disease (AD) is a neurodegenerative disorder associated with diminished regenerative capacity of neurons and impaired cognitive functions including learning and memory (Galimberti and Scarpini, 2012; Haque and Levey, 2019; Chatterjee et al., 2020). Nearly 35 million people are suffering from AD worldwide and is estimated to be doubled by 2030 (Alzheimer's Association, 2019; Haque and Levey, 2019). The nature of this disease demands proper and long-term medical care which has accounted for an estimated cost of $195 billion in 2019 and is expected to rise to $1 trillion by 2050 (Alzheimer's Association, 2019). Various factors contribute to AD-related dementia and impairment of cognitive functions, however, extracellular amyloid beta (Aβ) plaques and intracellular aggregates of hyperphosphorylated tau proteins also called neurofibrillary tangles (NFTs) are the two major histopathological hallmarks of AD (Mayeux and Stern, 2012; Xu et al., 2012; Kametani and Hasegawa, 2018; Janeiro et al., 2021).

Abbreviations: AD, Alzheimer's disease; AGES, Advanced Glycation End Products; APP, Amyloid Precursor Protein; Aβ, Amyloid Beta; BACE, β-Site APP Cleavage Enzyme; BBB, Blood Brain Barrier; BDNF, Brain Derived Neurotropic Factor; BMAL, Brain and muscle ARNT-like; Cas9, CRISPR-associated protein 9; CLOCK, Circadian Locomotor Output Cycles Kaput Protein; CNS, Central Nervous System; CR, Circadian rhythms; CREB, Cyclic AMP Responsive Element Binding; CRF, Corticotropin Releasing Factor; CRISPR, Clustered Regularly Interspaced Short Palindromic Repeats; CRY, Cryptochrome Circadian Regulators; CSF, Cerebrospinal Fluid; ELISA, Enzyme-Linked Immunosorbent Assay; ER, Endoplasmic Reticulum; EV, Extracellular vesicles; EXOs, Exosomes; FAD, Familial Alzheimer's disease; GSSG, Glutathione Disulphide; HATs, Histone Acetyltransferases; HDACs, Histone Deacetylases; IGF, Insulin like Growth Factor; LOD, Limit of Detection; LP-MS, liquid chromatography-mass spectroscopy; MARCKS, Myristoylated Alanine-Rich C Kinase Substrate; miRNAs, micro RNAs; MP-MSCs-EXOS, Exosomes from Multipluripotent mesenchymal cells; MTBR, Microtubule Binding Region; NCS, Neuronal Stem Cells; NEP, Neprilysin; NET, Novel exosome-based therapeutics; NFTs, Neurofibrillary Tangles; NMT, N-myristoyltransferases; PER, Period Circadian Regulators; PHFs, Paired Helical Filaments; PKA, Protein Kinase A; PSEN, Presenilin; PTMs, Post-Translational Modifications; ROS/RNS, Reactive Oxygen/Nitrogen Species; SCN, Suprachiasmatic Nucleus; SCRD, Sleep and Circadian Rhythm Dysfunction; SiRNAs, Small Interfering RNAs; SUMO, Small Ubiquitin-like Modifier.

Accumulation of amyloid beta (Aβ) plaques and NFTs initiate a cascade of events, resulting firstly in synaptic dysfunction, axonal degeneration and impaired cellular communication, and followed subsequently as the disease progresses by gliosis, neurodegeneration and widespread neuronal death (Wang et al., 2013; Hampel et al., 2015; Li et al., 2015; Pini et al., 2016; Knezevic et al., 2018). Although accumulation of Aβ deposits and NFTs are the pathological hallmarks of AD and have drawn the special attention of researchers in the search for biological markers, it is clear now that the disease begins decades before the onset of any clinical symptoms. To predict, diagnose, or monitor the progression of AD disease biomarkers are considered useful in every step of patient care. As disease symptoms are subjective, biomarkers provide an objective, measurable way to characterize the disease. Biomarkers for Alzheimer's disease aim to facilitate early disease prognosis and makes it possible to determine the progression of disease during initial stage and evaluate response to existing and future treatments. Also, biomarkers are likely to predict clinical benefit and support accelerated or traditional drug approval, respectively. There is an unmet need for identification of such clinical biomarker for Alzheimer's disease.

Major proteins and enzymes involved in Alzheimer's progression: Role of amyloid-beta precursor protein, secretase, Tau, beta-site amyloid-beta precursor protein-cleaving enzyme, Apo E, PS1/2, and microglia

Amyloid-beta precursor protein and secretase enzymes

Amyloid-beta precursor protein (APP) encoded by a gene *APP* (located on chromosome 21) is a ubiquitous type-1

transmembrane protein with three splice variants: APP695, APP751, and APP770 expressed mostly in neurons, astrocytes, and vascular endothelial cells respectively (Miura et al., 2020; Zhao et al., 2020). Although the exact functions of APP are not known, however, its expression increases during differentiation of neurons and synapse formation, and declines once mature connections are established, suggesting the role of APP in aging and development (Chen et al., 2017). Under normal conditions, APP undergoes non-pathogenic processing by involving two important enzymes α-and γ-secretase. These enzymes cleave the APP within the Aβ domain resulting into non-amyloidogenic fragments along with soluble amyloid precursor protein fragments α (sAPPα) and C-terminal fragments (CTFs). In diseased conditions, a different set of enzymes including β-and γ-secretase to cleave the APP in such a way that it generates the neurotoxic Aβ peptides (40–42 amino acid long peptides), along with soluble amyloid precursor protein fragments β (sAPPβ) and CTFs (Nesterova et al., 2019). Various studies have shown a link between the mutations of *APP* and AD; for example 10–15% cases of early-onset-familial Alzheimer's disease (EOFAD) are reported to be caused by APP gene mutations (Hooli and Tanzi, 2016). Such mutations appear to influence the biology of Aβ by promoting local oligomer/fibril formation or changing the propensity of Aβ to bind to other proteins and affecting Aβ clearance. This ability of APP to undergo cleavage using different set of enzymes to form either soluble or pathogenic amyloid-beta (Aβ) peptides makes APP as a main target protein in AD progression. Any mutation in APP and in the proteins that regulate APP endocytosis and processing in neurons leading to disturbed APP-related intracellular signaling pathways can be used as a biomarker during early stages of AD.

Tau protein

Tau is a microtubule-associated protein involved in the stabilization of microtubules by promoting their polymerization. The association of tau protein with the microtubules is involved in regulating the axonal transport as well as neuronal cytoskeleton (Zhou et al., 2018). Six different isoforms of tau are usually expressed in normal mature human brains however they are found to be abnormally hyperphosphorylated in AD brains. Any unusual alterations in the structural conformation or phosphorylation events of tau impact its binding affinity with microtubule which leads to its toxic aggregation in the form of neurofibrillary tangles (NFTs) and paired helical filaments (PHFs). These NFTs which on aggregation attain the shape of PHFs are one among the major hallmarks seen in pathology of AD (Augustinack et al., 2002). Tau phosphorylation and its detailed role in the pathogenesis is included elsewhere under post-translational modifications (PTMs) in AD. Importantly, Hyper-phosphorylated tau is considered to be promising biomarker for monitoring the disease progression in AD.

Beta-site amyloid-beta precursor protein-cleaving enzyme

Beta-Site APP-cleaving enzyme (BACE) is a ubiquitously expressed membrane-bound aspartyl protease. It uses its proteolytic activity for the production of neuro-pathogenic Aβ peptides. There are four splice variants of BACE with 501, 476, 457, and 432 amino acids. Among these variants 501 variant is having the highest degree of proteolytic activity on Aβ amyloid substrate (Mowrer and Wolfe, 2008). The production of Aβ peptides from its precursor APP occurs in two sequential proteolytic cleavages. First cleavage is catalyzed by BACE in which BACE cleaves the ectodomain of APP generating a C99 membrane-bound C-terminal fragment and the second proteolytic reaction is carried out by γ-secretase which further processes a C99 fragment leading to the formation of Aβ peptides (Bolduc et al., 2016). In AD patients BACE is highly expressed in various parts of the brain especially in brain cortex and cerebrospinal fluid (CSF) (Hampel et al., 2020). The increased expression of BACE can serve as an early biomarker in detection of AD (Blennow et al., 2010; Evin et al., 2010), and its increased expression has been directly co-related with the age of the patient and stress level (O'brien and Wong, 2011). BACE1 protein concentrations and rates of enzyme activity are promising candidates among biological markers in clinical trials investigating the role of BACE1 inhibitors in regulating APP processing.

Apolipoprotein E

In the central nervous system (CNS), apolipoprotein E (ApoE) is mostly synthesized and produced by astrocytes to transport cholesterol to neurons *via* ApoE receptors (Bu, 2009). ApoE is composed of 299 amino acids and exists in three isoforms in humans; ApoE2, ApoE3, and ApoE4. The single amino acid differences alter the structure of these isoforms and influences their functional abilities (Frieden and Garai, 2012). The ApoE4 isoform represents the most significant risk factor for late-onset Alzheimer disease (LOAD) (Corder et al., 1993; Mahoney-Sanchez et al., 2016). The individuals carrying the rare E2 variant are less likely to develop AD and E3 represents the most common but non-pathogenic isoform of ApoE (Serrano-Pozo et al., 2015). Although number of studies have been conducted to understand the mechanism of action of different variants of ApoE, but further investigation and research is needed to fully understand the differential effects of ApoE isoforms on Aβ aggregation and clearance in AD pathogenesis (Kim et al., 2009; Husain et al., 2021). In an interesting study, the total ApoE and ApoE4 plasma proteins were assessed using Australian Imaging, Biomarkers and Lifestyle (AIBL) study of aging and the result were assessed by Positron Emission Tomography (PET) using Pittsburgh compound B (PiB). The levels of these plasma proteins were compared with cerebral

Aβ load, and it was found that both the total ApoE as well as ApoE4 levels are significantly lowered in AD patients. From ApoE genotyping, the protein (ApoE) levels were significantly lower among E4 homozygous individuals and in *APOE* E3/E4 heterozygote carriers, ApoE4 levels decreased, indicating that ApoE3 levels increase with disease. This study suggests that ApoE, ApoE3, and ApoE4 can be used as AD biomarkers and possible therapeutic drug targets (Gupta et al., 2011; Soares et al., 2012).

Presenilin 1

Presenilin 1 protein encoded by *PSEN1* gene is located on chromosome 14 and forms an important component of the γ-secretase complex, which cleaves APP into Aβ fragments (Steiner et al., 2008). It is mostly expressed in endoplasmic reticulum and helps in protein processing (Bezprozvanny and Mattson, 2008). The importance of PSEN1 gene in AD is evident from the fact that it accounts for about 50% cases of early-onset Alzheimer's disease (EOAD), with complete penetrance (Giri et al., 2016). Mutation in PSEN1 leads to mutations in γ-secretase and increase in the Aβ42/40 ratio resulting in cotton wool plague formation (Zhang et al., 2015; Miki et al., 2019). Only few mutations are insertions and deletions, majority of *PSEN1* mutations are missense. PSEN1 mutations not only affect the activity of γ-secretase enzyme but also directly affect the neuronal functioning by controlling the activity of GSK-3β and kinesin I (Giri et al., 2016). More than 295 pathogenic mutations have been identified in *PSEN1*, of which 70% mutations occur in exons 5, 6, 7, and 8. Studies using genetically modified mice have shown that mutations in PSEN1 lead to impaired Aβ production and increased ratio of Aβ42/Aβ40 (Xia et al., 2015). Recent studies that investigated potential relationships between the molecular composition of FAD-linked Aβ profiles and disease severity by analyzing Aβ profiles generated by 25 mutant PSEN1/GSECs that span a wide range of AAOs, revealed that full spectrum of Aβ profiles (including Aβ37, Aβ38, Aβ40, Aβ42, and Aβ43) better reflects mutation pathogenicity. Furthermore, this study suggested Aβ(37 + 38 + 40)/Aβ(42 + 43) ratio better at predicting the age at disease onset (Petit et al., 2022). Presently, PSEN1 gene is considered as the most common cause of familial Alzheimer's disease (FAD). However, a recent studies (Sun et al., 2017) contradicts the role of *PSEN1* in AD progression by increasing the Aβ42 production (Hardy and Selkoe, 2002) and therefore is a matter of a debate in the scientific world.

Presenilin 2

Presenilin 2 protein encoded by *PSEN2* gene is located on chromosome 1 is similar in structure and function to *PSEN1* (Ridge et al., 2013). Similar to PSEN1, it also forms the important component of the γ secretase complex and any mutation in *PSEN2* alters the activity of γ secretase leading to elevated ratio of Aβ42/40 (Wakabayashi and De Strooper, 2008). Despite close homology between the two, mutations in PSEN2 are less toxic and less common than PSEN1, but neuritic plaque accumulation and neurofibrillary tangle (NFT) formation have been found in some people with *PSEN2* mutations (Giri et al., 2016). Efforts to develop disease-modifying therapies for AD have been heavily focused on the amyloid hypothesis but repeated failures in late-stage clinical trials based on these hypotheses heighten the urgency to explore alternative approaches. Thus, therapeutic strategies aimed at restoring secretase activities by involving modifications or mutations at the levels of PSN1 and PSN2 offer a valid and complementary approach to develop disease modifying treatments for FAD.

Microglial role in Alzheimer's disease

Microglia, a type of neuroglia (glial cells), forms the innate immune system of our central nervous system (CNS). Proliferation, activation, and concentration of these glial cells in the brain around amyloid plaques, is a prominent feature of AD. Data from human genetic studies also suggest the role of these cells in AD progression. Under normal conditions, microglia protect against AD, however, impaired microglial activities lead to increased risk of AD progression. Activated microglial cells can be harmful and mediate loss of synaptic junctions *via* complement-dependent mechanisms, increase tau phosphorylation and enhance inflammatory responses against neurons leading to activation of neurotoxic astrocytes (Hansen et al., 2018). The role of microglia in forming neuritic plaques was described long back by Alois Alzheimer himself (Alzheimer et al., 1995; Graeber et al., 1997) and further studies have shown the involvement of both reactive astrocytes and microglia in deposition of Aβ plagues (Verkhratsky et al., 2016). In AD patients, the microglia interact with the amyloid peptides, APP, and neurofibrillary tangles during early phase of AD, and their activation promote Aβ clearance through microglia's scavenger receptors, and thus acts as a hurdle in the progression of AD. The Aβ activation induced continuous activation of microglia involving CD36, Fc receptors, toll-like receptors (TLRs), and complement receptors advanced glycation end products (RAGE), promote Aβ production while hampering Aβ clearance, which ultimately causes neuronal damage (Wang et al., 2015). In a study done on post-mortem brain sections taken from AD patient, it was found that increased microglia activation begins with amyloid NP deposition and the increase was found to be directly related to the part of brain involved in AD (Xiang et al., 2006). Thus, activation of microglia in brain tissues, such as hippocampi, can serve as an inflammatory biomarker for AD.

Major sources and methods for isolation of potential biomarkers for Alzheimer's disease

One of the major challenges in the treatment of Alzheimer's disease is the lack of sensitive and specific biomarkers. Multiple studies have argued that AD begins decades before the onset of clinical symptoms and accumulation of Aβ deposits and NFTs-pathological hallmarks of AD. Clinically relevant biomarkers are expected to be useful in detecting the preclinical as well as symptomatic stages of AD. Such clinically relevant biomarkers used in the validation of AD are structured through a road map called the Strategic Biomarker Roadmap (SBR), initiated in 2017 and according to recent reports is still valid for the assessment of biomarkers of tauopathy, as well as that of the other diagnostic biomarkers of AD and related disorders (Boccardi et al., 2021). Moreover, biomarkers would be significantly helpful to predict, diagnose, or monitor the progression of AD disease during initial stage, and in evaluating response to existing and future treatments. Till date different methods have been followed to access and isolate the different biomarkers for AD.

Potential biomarkers for Alzheimer's disease from cerebrospinal fluid

Although advanced neuroimaging techniques have been very useful in assessing structural and physiological changes in the brains of AD patients, clinical biomarkers still represent the most convenient and direct means to monitor the disease state. Despite the fact that PET and cerebrospinal fluid (CSF) biomarkers are useful information for the diagnosis of AD, these methods have limited use due to their sophistication, invasiveness, and high cost. In the search for biological markers of AD, Aβ42, t-Tau, and p-Tau have drawn the special attention of researchers. Various types of brain specific biomarkers associated with AD are shown in **Figure 1**, CSF specific biomarkers for AD are listed in **Table 1** and diagnostic platforms based on four chief biomarkers for AD along with various parameter are listed in **Table 2**. Aβ42, T-tau and P-tau biomarkers can predict progression from preclinical to clinical AD (Mattsson et al., 2018). The levels and variations of Aβ in CSF have been an essential hallmark feature of AD-type dementia (d'Abramo et al., 2020). It has been suggested that the ratio of CSF Aβ42/Aβ40 can be a superior biomarker because this ratio is quite useful in the differentiation of AD from other non-Alzheimer's related cognitive changes like the subcortical deficits related to vascular diseases. Aβ42 levels in the CSF are generally lower in comparison to the controls and Aβ42 levels decrease substantially with an increase in disease progression (d'Abramo et al., 2020). The other biomarkers like YKL-40 (Chitinase-3-protein like), VILIP-1 (VLP-1) and, NFL are associated with glial inflammation, neuronal damage and non-specific marker for neurodegeneration respectively can also be used for the diagnosis but the limit of detection (LOD) and accuracy should be validated first in order to gain the specificity (Gaiottino et al., 2013; Olsson et al., 2016).

Potential biomarkers for Alzheimer's disease from blood

Blood-based biomarkers are more cost-effective than PET imaging, less invasive than CSF testing, and can be used as viable first-line tools in the multi-stage diagnostic processes (d'Abramo et al., 2020). Since blood testing is a part of clinical routines all over the world which require no special or further training, therefore, blood-based biomarkers for AD are more promising. Although, a lot of progress has been made in understanding the role of biomarkers in the pathophysiology of AD (**Tables 1**, **2**), there is still a need for the development of blood-based biomarkers that can help in the early diagnosis of AD and to understand disease progression. Tau and β-Site APP Cleavage Enzyme 1 (BACE 1) to some levels are useful in this context (Snyder et al., 2014). Tau levels in the blood can be used to predict the onset of future cognitive decline and the levels of BACE1 activity in the blood can also be used to predict the progression of mild cognitive impairment to AD dementia (Hampel et al., 2018). Aβ peptides like Aβ1-42, Aβ1-40, and Aβ1-17 as well as tau are important blood biomarkers to detect AD and its progression. These peptides in plasma can be detected by immunoprecipitation and mass spectroscopy (Pannee et al., 2014; Ovod et al., 2017). It has been found that the plasma levels of Aβ-42, Aβ1-40, and Aβ1-42/Aβ1-40 are low in AD patients but show a significant correlation with CSF levels (Janelidze et al., 2016a). Blood levels of Aβ1-17 also play an important role in the diagnosis of AD. The ratio of free to cell-bound Aβ1-17 levels in the blood helped to understand the difference between healthy individuals and individuals with mild AD with high specificity and sensitivity (Snyder et al., 2014). Tau proteins in plasma have been quantified by sensitive immunoassay techniques and found to be increased in AD patients compared to controls (Zetterberg et al., 2013; Neergaard et al., 2018). Phosphorylated tau (p-tau) proteins are leading blood biomarkers that identify AD, and its underlying pathology. It also highlights future risks of AD. Plasma p-tau (p-tau217 and p-tau181) highlights AD in dementia cases with high accuracy and can also be validated by neuropathological studies. AD progression can be strongly predicted by even baseline increases of p-tau biomarkers However, assay platform comparisons and effects of covariates and accurate biomarker cut-offs for p-tau and Aβ are still lacking necessitating more studies in this direction in the context of Strategic Biomarker Roadmap (Ashton et al., 2021). Moreover, Aβ1–42, Aβ1–40 and phosphorylated tau represent

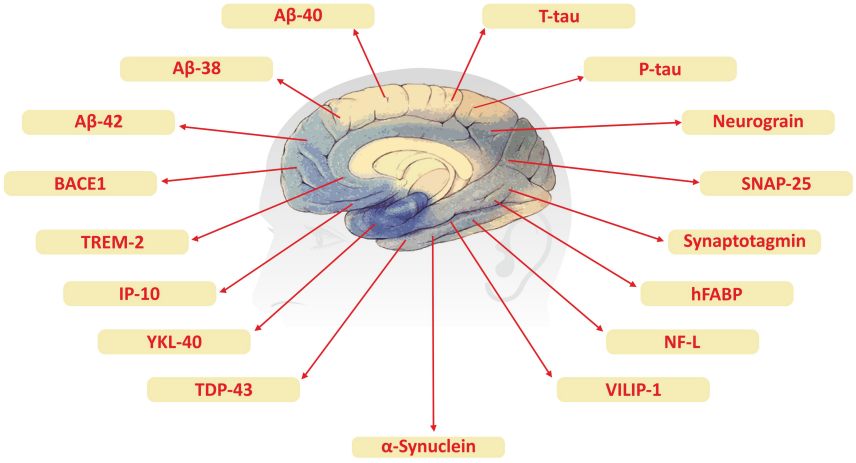

FIGURE 1
Brain specific biomarker associated with Alzheimer's disease.

post-translationally modified protein species this explains the involvement of PTMs as biomarkers in AD (Henriksen et al., 2014). Furthermore, recent studies suggested Aβ37/42 ratio could become an improved Aβ biomarker for Alzheimer's disease of pathogenicity and clinical diagnosis (Liu et al., 2022). Other proteins like axonal protein and neurofilament light (NF-L) are found to be increased in the serum of AD patients and have been found to be comparable with plasma Aβ1–42/Aβ1–40 (Mattsson et al., 2017). However, high NFL-1 concentration in plasma is not associated only with AD but also with other neurodegenerative disorders (Progressive supranuclear palsy and corticobasal syndrome). Recently, investigators questioned if a panel of blood-based biomarkers instead of an individual biomarker could be more useful in the detection of AD. In this direction, O'Bryant used a different set of 30 serum proteins to develop an algorithm that could detect AD with 80% sensitivity and 91% specificity (O'Bryant et al., 2010). It was reported that a panel of three blood markers von Willebrand factor, cortisol, and oxidized LDL antibodies identified using multivariate data analysis, could distinguish between AD patients and normal ones with more than 80% accuracy (Laske et al., 2011). To some level, microRNAs and PTMs can also serve as biomarkers for AD. Alterations in microRNAs levels are reported to be associated with AD pathology and efforts are being made to monitor the changes in the individual miRNAs in blood as biomarkers (Henriksen et al., 2014). A decrease in miR-132-3p levels has been reported to be associated with AD due to the hyper-phosphorylation of tau (Lau et al., 2013). Interestingly, miR-125b and miR-26b have been reported to be increased in AD patients and both are associated with tau phosphorylation (Absalon et al., 2013; Ma et al., 2017). Blood biomarkers are reliable and promising in AD detection Anything that may interfere with the detection of AD biomarkers when their concentration is low in blood is taken care of by modern diagnostic platforms that work with high dilution and high amplification of the specific signal which allows the detection of picomolar/ml or even lesser concentrations of the target biomarker. It was shown that detection by immunoprecipitation followed by liquid chromatography-mass spectroscopy (IP-MS) is a high precision assay for plasma Aβ42-40 ratio, which predicts brain amyloidosis with 90% accuracy (d'Abramo et al., 2020). Recent clinic trials based on biomarker identification for Alzheimer's disease are listed in **Table 3**.

Extracellular vesicles associated with Alzheimer's disease

Extracellular vesicles (EV) or exosomes (EXOs) were initially considered as cellular trash bags. These lipid-based membrane-bound biological nanoparticles have now emerged as a new paradigm of cell-to-cell communication which has implications for both normal and pathological physiology (Raposo and Stahl, 2019). Recently, extracellular vesicles have been widely used as biomarkers and are found to play an important role in the pathogenesis of Alzheimer's disease. The presence of disease-related proteins in these extracellular vesicles from AD patients have been actively studied to use them as biomarkers to predict the development of AD before the appearance of clinical symptoms (Lin et al., 2019). They are excreted in the urine and saliva of both healthy and diseased individuals which makes them an excellent choice for diagnostics in diseases like AD as compared to other invasive methods which require lumbar puncture or brain autopsy for diagnosis (Watson et al., 2019). EVs are released from various cell types including the cells associated with neuron-glia communication, neuronal progression, and regeneration

TABLE 1 Biomarkers for Alzheimer's disease (AD) in cerebrospinal fluid (CSF).

Biomarker	Concerned diagnosis	References
Aβ42	CSF	Olsson et al., 2016; Wellington et al., 2016
Aβ40	Coupled with CSF	Olsson et al., 2016; Wellington et al., 2016; Janelidze et al., 2016b
Aβ38	AD and dementia.	Olsson et al., 2016; Janelidze et al., 2016b
sAPPα	Associated with dementia	Olsson et al., 2016
sAPPβ	Combination with CSF	Olsson et al., 2016
t-Tau and p-Tau	CSF	Olsson et al., 2016
NFL	CSF	Olsson et al., 2016
NSE	CSF	Olsson et al., 2016
VLP-1	CSF	Olsson et al., 2016
HFABP	CSF	Olsson et al., 2016
Albumin-ratio	CSF and dementia	Wellington et al., 2016
YKL-40	CSF	Olsson et al., 2016; Wellington et al., 2016
MCP-1	AD and dementia	Olsson et al., 2016; Wellington et al., 2016
GFAP	CSF and dementia	Olsson et al., 2016; Wellington et al., 2016
Neurogranin	AD	Janelidze et al., 2016b
sTREM2	CSF	Suárez-Calvet et al., 2016
Alpha-synuclein	AD	Majbour et al., 2017

from CNS (Surgucheva et al., 2012; Bronisz et al., 2014; Janas et al., 2016). It is widely accepted that EVs are good biomarkers but their nature, regulation, sorting and molecular composition need to be further investigated. Interestingly, the role of exosomes in stimulating aggregation of amyloid-beta (Aβ) peptides *in vitro* and *in vivo* was demonstrated and as was their role in the uptake of Aβ by cultured astrocytes and microglia under *in vitro* conditions (Dinkins et al., 2014). By preventing the secretion of EVs *via* inhibition of neutral sphingomyelinase 2 (nSMase2), a key regulatory enzyme generating ceramide from sphingomyelin, with GW4869, they observed a significant reduction of Aβ plaques in the mice brain. Moreover, exosomal markers such as Alix and flotillins have been found to be associated with the amyloid plaques of the brain of post-mortem tissues of human AD patients when compared to post-mortem samples of healthy individuals, thereby reflecting specific association of EVs with amyloid plaques (Hu et al., 2016). Further, an increase in levels of tau in exosomes have been reported in CSF at an early phase of AD (Saman et al., 2012; Asai et al., 2015). Levels of several exosomal miRNAs that are altered in AD points to their roles in regulating certain events related to AD neurodegeneration as the ability of miRNAs to target genes related to tau phosphorylation, APP processing, and apoptosis is already known (Liu et al., 2014; Ma et al., 2017). The miRNA-193b and miRNA-125b-5p are the two most common exosomal miRNAs identified and are reported to be expressed differentially in exosomes isolated from serum, plasma and CSF of AD patients (Soares Martins et al., 2021). Therefore, miRNA-193b and miRNA-125b-5p are thought to be potential putative peripheral biomarkers of AD pathogenesis. EVs as potential biomarkers for AD can open up a wide arena of discoveries associated with it; however, a proper evaluation and correlation is needed for it as well.

Circadian genes associated with Alzheimer's disease

It has been reported that that the levels of the main risk factor for AD progression i.e., Aβ in the brain are regulated by circadian rhythms and the sleep-wake cycle (Kang et al., 2009). Circadian rhythms (CR) are biological clocks that coordinate internal time with the external environment to regulate various physiological processes like the sleep-wake cycle, mental, behavioral and physical changes. Circadian rhythms are managed by a molecular clock in the suprachiasmatic nucleus (SCN) that resides in the anterior part of the hypothalamus. Molecular clockwork consists of different core clock genes such as period circadian regulators 1 and 2 (PER1 and PER2), circadian locomotor output cycles kaput protein (CLOCK), brain and muscle ARNT-like 1 (BMAL1), cryptochrome circadian regulators 1 and 2 (CRY1 and CRY2), These genes are organized in a transcription-translation feedback loop that oscillates every 24 h. Any mutation or alteration in these genes or their subsequent proteins has functional impacts on the CR (Shkodina et al., 2021). Disruptions in CR cause cognitive impairment, psychiatric illness, metabolic syndromes, and are thus considered as a significant risk factor in the onset of cerebrovascular and neurodegenerative disorders such as Alzheimer's, Parkinson's, and Huntington's diseases. Moreover, disrupted sleep wake-cycle and alterations in circadian rhythms are seen to lead to AD progression by dysfunctional tau metabolism. This is achieved by changing the conformation and solubility of tau in the brain involving the post-translational modifications by decreasing the activity of major regulators of tau phosphorylation, especially cyclin-dependent kinase 5 (cdk-5) (Di Meco et al., 2014). During the early development of AD, there is a disruption in the normal expression of clock genes (especially *Cry1*, *Cry2,* and *Per1*) not only in the central pacemaker but also in other brain areas like the cortex, hippocampus, and cerebellum supporting circadian regulation (Bellanti et al., 2017). Since sleep and circadian rhythm dysfunction (SCRD) are very common in the early stage of AD, it is considered as a potential early biomarker for detecting AD. A proper understanding of the circadian clock

TABLE 2 Sensing platforms based on four chief biomarkers associated with Alzheimer's disease (AD) and their limit of detection (LOD).

Sensing platform	Biomarker	Protein form	Limit of detection	Dynamic range	Sensitivity	Specificity	References
IP-MS	**High performance** plasma amyloid-β biomarkers for Alzheimer's disease	APP 669-711/Aβ142	2.5Da	∼180 ng/ml	96.7% (AUC)	81.0% (AUC)	Nakamura et al., 2018
IMR	**Assay of plasma** phosphorylated tau protein (threonine 181) and total tau protein in early-stage Alzheimer's disease	Tau	0.0028 pg/ml	0.001–10,000 pg/ml	0.793 (ROC)	0.836 (ROC)	Yang et al., 2018
Digital-ELISA	**Plasma neurofilament** light as a potential biomarker of neurodegeneration in Alzheimer's disease	NFL	0.62 pg/ml	unknown	0.84 (ROC)	0.78 (ROC)	Lewczuk et al., 2018
ELISA	**C-terminal neurogranin** is increased in cerebrospinal fluid but unchanged in plasma in Alzheimer's disease	Neurogranin	3 pg/ml	3–2,000 pg/ml	x	x	De Vos et al., 2015

and investigations of core clock components including *Bmal1*, *Clock*, *Per1*, *Per2*, *Cry1*, *Cry2*, *Rev-erbα*, and *Rorα* by genomic, proteomic, and metabolomic studies and its influence on several key processes involved in neurodegeneration might be helpful to be manipulated at early stages to promote healthy brain aging and decrease the chances of AD progression on one hand and uncover their potential use as biomarkers and hallmarks of circadian disruption during early stages of Alzheimer's disease progression.

Post-translational modifications in Alzheimer's disease

Translated messages in the form of protein undergo important modifications usually after their synthesis. These post translational modifications (PTMs) usually occur in the various cellular compartments like the Endoplasmic reticulum, Golgi complex, Nucleus, as well as Cytoplasm (Blom et al., 2004). PTM's play an important role in regulating the structure, localization and, activity of proteins (Deribe et al., 2010). PTMs impact the hydrophobicity of proteins and induce changes in their structural conformations and thus define protein function as well as their interactions with other proteins (Ravid and Hochstrasser, 2008; Ardito et al., 2017). PTMs involve the addition of varied chemical moieties to a target protein that include phosphate, acyl, methyl, and glycosyl groups catalyzed by specific enzymes. PTMs not only define the structural integrity of proteins, these modifications usually cause the proteins to lose or enhance their normal function as well (Santos and Lindner, 2017). Unusual PTMs of various proteins like APP, secretases, tau, various kinases, and phosphatases are linked to the development of neurodegenerative diseases. The appearance of NFTs, senile plaques and aggregation of toxic amyloid β peptides are some of the hallmarks of abnormal PTMs in Alzheimer's disease. These posttranslational protein modifications are associated with memory weakening, cognitive impairments, reduced synaptic plasticity and thus rapid progression to AD (Chong et al., 2018). Exploring post-translational modifications and understanding their molecular mechanism will open a window to develop effective and rational therapeutic interventions to counter these neurodegenerative disorders. Various PTMs associated with AD are shown in **Figure 2**. PTM specific modifications associated with AD vs. normal brain are also shown in **Figure 3** and discussed in detail here.

Phosphorylation

Phosphorylation is one of the most frequently occurring PTMs in proteome biology, and about 30% of proteins undergo such modifications (Sacco et al., 2012). It involves the addition of a phosphate group to amino acids particularly to serine, threonine and tyrosine residues (Humphrey et al., 2015). This modification impacts the structure and function of proteins and determines their fate in terms of signaling, trafficking as well as metabolism; thus playing an important part in regulating the normal physiological processes (Ravid and Hochstrasser, 2008). Protein phosphorylation is one of the most predominant PTMs that drives enormous cellular cascades in living cells.

TABLE 3 List of natural products and synthetic drugs tested for identification of a reliable clinical biomarker in various clinical trials of Alzheimer's disease.

Therapy	Drug	Stage of AD	Used as (mechanism of action)	References
Anti-amyloid therapy	Solanezumab	Mild	Monoclonal antibody (mAb)	Honig et al., 2018
	Verubecestat	Mild to Moderate stages	BACE inhibitor	Villarreal et al., 2017; Egan et al., 2018
	Verubecestat	Prodromal stage	BACE inhibitor	
	Atabecestat	Preclinical stage		Novak et al., 2020
	Lanabecestat	Early stage		Wessels et al., 2020
	Lanabecestat	Mild stage		
	Aducanumab	Early AD	mAb	Beshir et al., 2022
	CNP520	Preclinical stage	BACE inhibitor	Neumann et al., 2018
	Plasma exchange with albumin 1 Ig	Mild to Moderate stages	Plasma exchange	Boada et al., 2019
	ALZT-OP1a + ALZT-OP1	Preclinical stage	Mast cell stabilizer, anti-inflammatory	Lozupone et al., 2022
	ANAVEX2–73		Anti-tau, Anti-amyloid	
	Crenezumab		mAb	Salloway et al., 2018; Avgerinos et al., 2021
	E2609 (elenbecestat)		BACE inhibitor	Huang et al., 2020; Patel et al., 2022
	Gantenerumab	Prodromal to moderate stage	mAb	Klein et al., 2019
	Gantenerumab and Solanezumab	Early stages		Salloway et al., 2021
	GV-971 (sodium oligomannurarate)	Mild to moderate stage	Aβ aggregation inhibitor	Wang T. et al., 2020
	Solanezumab	Dominantly inherited AD	mAb	Salloway et al., 2021
Non-Anti-amyloid therapy	AC-1204	Mild to Late (severe) stage	Induction of ketosis	Dewsbury et al., 2021
	AGB101 (levetiracetam)	Mild stage	SV2A modulator	Cummings et al., 2020; Tampi et al., 2021
	Aripiprazole	Early stage	Partial agonist at dopamine D2 and 5-HT 1A receptors	Zheng et al., 2020
	AVP-786	Early stage	Sigma-1 receptor agonist, Anti-NMDA receptor	Khoury et al., 2021
	AXS-05	Early stage	Sigma-1 receptor agonist; Anti-NMDA receptor and dopamine-norepinephrine reuptake inhibitor	Huang et al., 2020; Nagata et al., 2022
	Azeliragon	Mild stage	Microglial activation inhibitor, antagonist of the receptor for glycation end products	Burstein et al., 2018; Yang et al., 2021
	OPC-34712 (brexpiprazole)	Mild stage	Agonist of serotonin, 5-hydroxytryptamine1A and dopamine D2 receptors and an antagonist of serotonin 5-hydroxytryptamine2A	Liu et al., 2018; Zarini-Gakiye et al., 2020
	Coconut oil	Early stage	Reduction in ADP-ribosylation factor 1 protein expression	Chatterjee et al., 2020
	COR388	Mild to moderate	Bacterial protease inhibitor	Detke et al., 2020; Seymour and Zhang, 2021
	Escitalopram	Mild stage	Serotonin reuptake inhibitor	Sheline et al., 2020
	Gabapentin Enacarbil	moderate to late stage	Glutamate receptor-independent mechanisms	Liu et al., 2021
	Ginkgo biloba	Early stage	Antioxidant and anti-amyloid aggregation	Vellas et al., 2012; Liu et al., 2021; Xie et al., 2022
	Guanfacine	Healthy but old aged	Alpha-2A-adrenoceptor agonist, a potent 5-HT2B receptor agonist	Barcelos et al., 2018
	Icosapent ethyl (IPE)	Late stage	Omega-3 fatty acids protect neurons from disease	Cummings et al., 2018
	Idalopirdine	Late stage	5-HT6 receptor antagonist	Hung and Fu, 2017
	RVT-101 (intepirdine)	mild to moderate	5-HT6 receptor antagonist	Huang et al., 2020; Akhondzadeh, 2017
	Insulin	Mild stage	Affects metabolism	Craft et al., 2017

(Continued)

TABLE 3 (Continued)

Therapy	Drug	Stage of AD	Used as (mechanism of action)	References
	ITI-007 (lumateperone)	mild to moderate	5-HT2A antagonist	Porsteinsson and Antonsdottir, 2017; Cooper and Gupta, 2020
	Losartan, amlodipine, aerobic exercise training, and etc.	mild to moderate	Anti-Angiotensin II receptor, Anti-calcium channel, cholesterol agent	Cummings et al., 2019; Ihara and Saito, 2020
				Szabo-Reed et al., 2019
	Masitinib	mild to moderate	Tyrosine kinase inhibitor	Folch et al., 2015; Ettcheto et al., 2021
	Methylphenidate	——	Dopamine reuptake inhibitor	Khaksarian et al., 2021
	Mirtazapine	——	Alpha-1 antagonist	Correia and Vale, 2021
	MK-4305 (suvorexant)	Mild stage	Orexin antagonist	Zhou F. et al., 2020
	EVP-6124	——	Selective α7 nicotinic acetylcholine receptor partial agonist	Potasiewicz et al., 2020
	Nabilone	Early to mild stage	Anti-cannabinoid receptors 1 and 2	Ruthirakuhan et al., 2020
	Nilvadipine	mild to moderate	Dihydropyridine calcium channel blocker	Lawlor et al., 2018
	AVP-923 (nuedexta)	Moderate to late stage	Uncompetitive NMDA glutamate receptor antagonist, a sigma-1 receptor agonist, and a serotonin and nor epinephrine reuptake inhibitor	Khoury et al., 2021; Liu et al., 2021; Khoury, 2022
	Pioglitazone	Early to Mild stage	Peroxisome proliferator-activated receptor gamma (PPARγ) agonists	Galimberti and Scarpini, 2017
	Troriluzole	Mild to moderate	Glutamate modulator	Yiannopoulou and Papageorgiou, 2020
	TRx0237 (LMTX)	Preclinical or early stage	Tau stabilizers and aggregation inhibitors	Panza et al., 2016
	Vitamin D3	Early stage	Vitamin-D receptor Agonist	Yamini et al., 2018
	Zolpidem zoplicone	Old aged persons	Allosteric modulator of GABA-A receptors	Wu, 2017

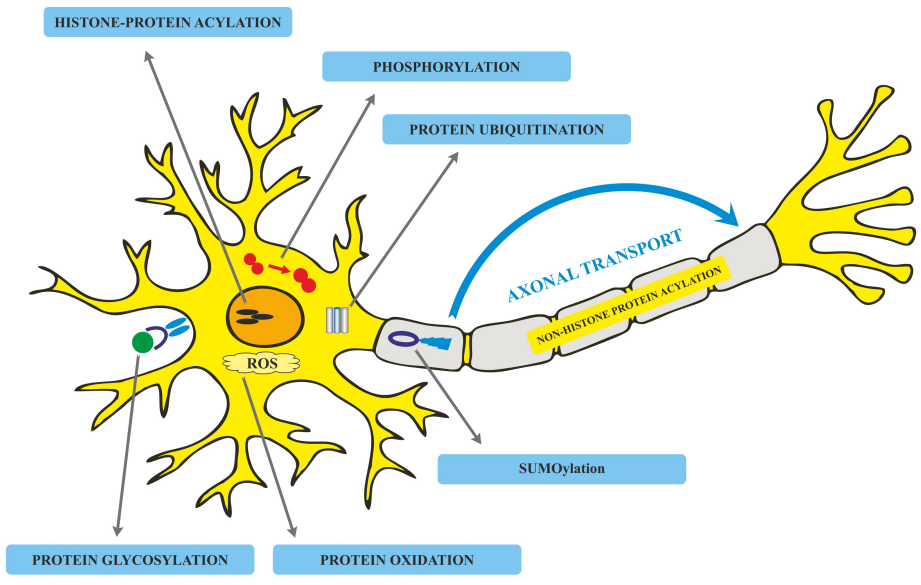

FIGURE 2
Various post-translational modifications (PTMs) associated with Alzheimer's disease.

The phosphorylation of proteins is reversible and very specific. These events of phosphorylation and dephosphorylation are catalyzed by diverse kinases. A variety of kinases like Akt, Erk, and PKA. GSK3β and Cdks have been found to be overexpressed with enhanced activity accompanied by a significant drop in phosphatases activity in AD patients (Alquezar et al., 2021).

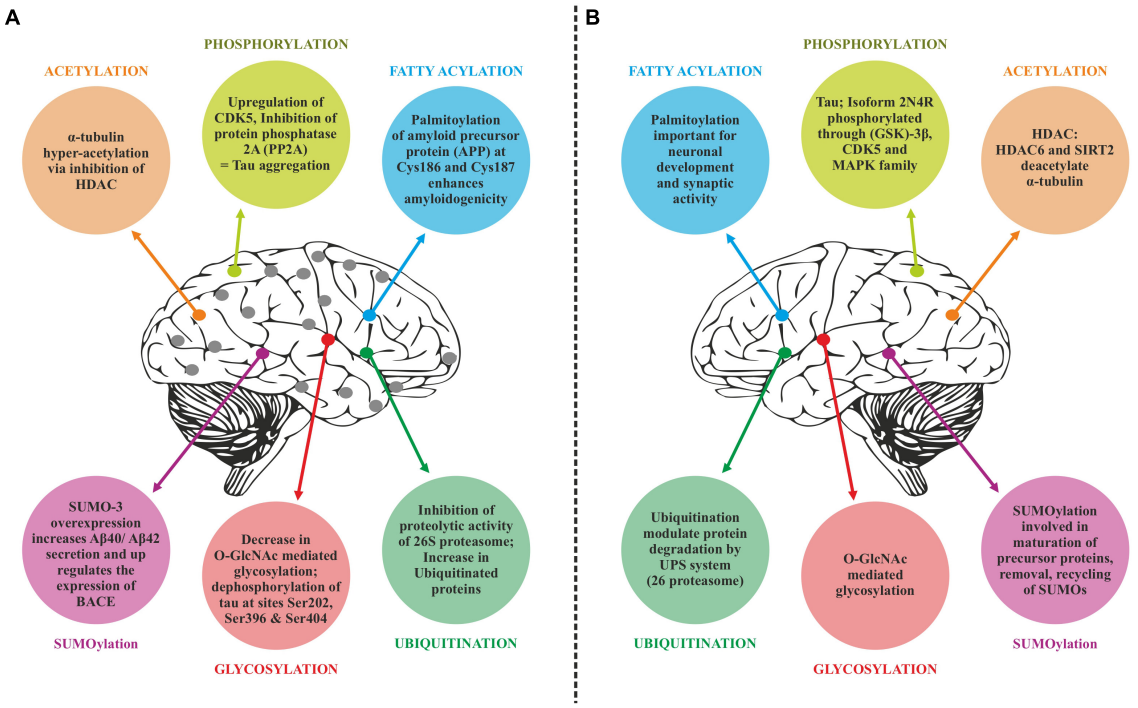

FIGURE 3
Post-translational modifications (PTM) specific modifications associated with Alzheimer's disease vs. normal brain. **(A)** PTMs associated with Alzheimer's disease. **(B)** Normal PTMs.

Accumulating evidence report that various proteins on altered phosphorylation in these neuro disorders drive the cell death signaling cascades (Suprun, 2019).

Tau phosphorylation

Tau is involved in the stabilization of microtubules, as mentioned earlier. Six different isoforms of tau are usually expressed in normal mature human brain which are found to be hyperphosphorylation in AD brains. These six isoforms of tau protein with varied amino acid chain length (331 to 441) emanate from alternative splicing of a single gene. Tau protein has different domains like N terminal projection domain ranging from 1 to 165 amino acids, proline rich domain from 166 to 242, microtubule binding region (MTBR) starting from 243 to 367 as well as carboxy terminal domain 368–441. Tau proteins bear 85 phosphorylation sites; with nearly half of them found to undergo phosphorylation and the majority of these phosphorylated stretches are found in proline rich domain of tau protein, flanking microtubule binding region (Goedert et al., 1989; Hanger et al., 2009). These phosphorylation events and isoform expression are developmentally regulated and it determines the complexity of embryonic cytoskeleton plasticity (Hanger et al., 2007). However, any unusual alterations in its structural conformation or in phosphorylation events impact its binding affinity with microtubule. Tau phosphorylation is residue specific and is mediated by different types of kinases. These kinases are proline rich domain specific kinases like GSK-3, Cdk5, and AMPK, non-proline directed phosphorylating kinases as well as Fyn kinases (Iqbal et al., 2016). Phosphorylation of tau protein by GSK3β at residues other than that of microtubule binding region like, thr231 pro232, and s214 has been found to impede its association with the microtubule thus affecting its anterograde transport (**Figure 4**). This residue specific phosphorylation leads to the induction of some conformational alterations which in turn lead to hyperphosphorylation of tau protein. It has been found that phosphorylation of Ser 404 accommodated by C-terminal domain alters the tau conformation (Luna-Munoz et al., 2007). Although GSK3B has been found to phosphorylate 36 residues of tau protein, however, preferable sites spotted by 2D phosphor-peptide mapping include Ser199, Thr231 as well as Ser413, respectively. Besides aforementioned mapping, monoclonal antibody technology has been applied to spot the phosphorylation sites that play a role in AD pathology, and it has been found that phosphorylation at specific motifs like Thr212/Ser214 and Thr231/Ser235 are exclusively seen in PHF (Ebneth et al., 1998; Despres et al., 2017). Interestingly phosphorylation of tau proteins at ser293 and ser305 neutralizes its ability to form aggregates without affecting tubulin polymerization. GSK3β like other kinases recognizes primed target proteins as it has been noted that Thr231 residue of tau proteins needs to be primed by other kinases like

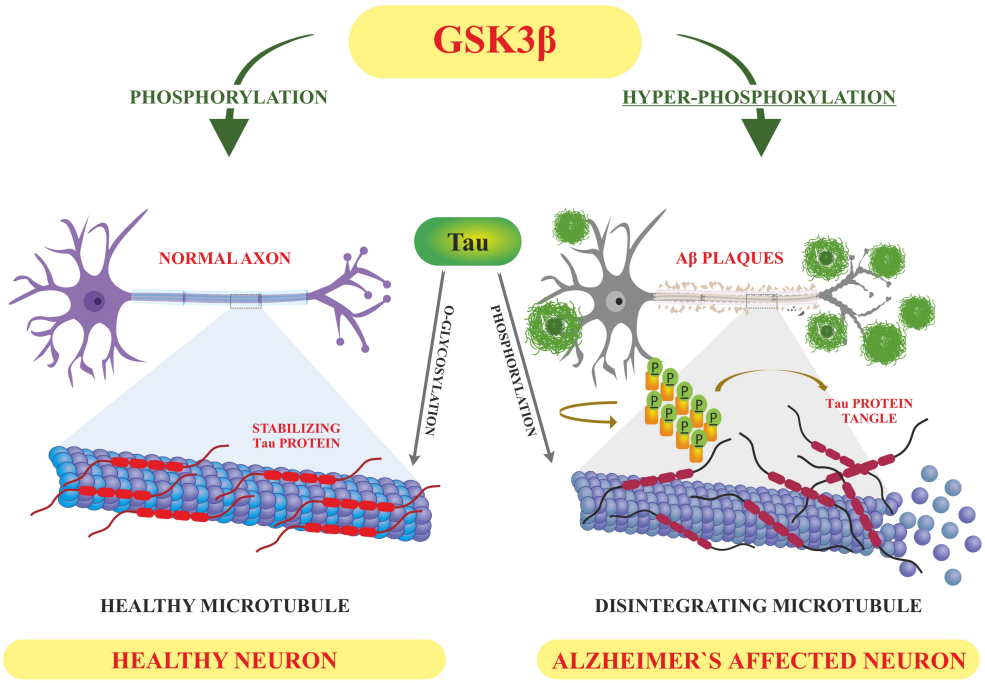

FIGURE 4
Displaying how the altered post-translational modifications (PTM) leads to Alzheimer's pathology-based on the literature surveyed GSK3β dependent hyperphosphorylation of tau proteins results in accumulation of NFT'S and deposition of Aβ plaques–hallmarks of Alzheimer's disease whereas O-linked glycosylation of tau proteins hampers its aggregation thus promoting normal polymerization processes.

Cdk5 which is followed by GSK3b mediated phosphorylation. This phosphorylation of tau protein, in turn, impacts its binding ability with the microtubules thus hampering their polymerization and other neuronal functions (Stoothoff and Johnson, 2005). Cdk5 another proline region-specific kinase involved in hyperphosphorylation of tau hampers the ability of tau protein to bind and stabilize microtubules leading to the disruption of axonal transport and neuronal death-an important contributor to the pathology of neurodegenerative diseases like AD (Piedrahita et al., 2010). Growing evidences report that dephosphorylated tau protects nuclear DNA from heat damage and other kinds of oxidative stress insults however tau in hyperphosphorylated form is believed to halt protective functionalities associated with non-phosphorylated forms in neuronal entities (Sultan et al., 2011). Cdk5 isoform is expressed in the brain, unlike cell cycle-related Cdks serine/threonine kinase, shows affinity toward the proline rich domain and phosphorylates some preferable residues like Ser202, Thr205, Ser235, and Ser404; which are found to be essential in regulating Tau-Mt binding. Cdk5 is activated by neuron specific p35 and p39 proteins-which are not considered to be cyclins. Thus, Cdk5 mostly acts in neural cells and is activated by binding to neuronally enriched activators, p35 and p39, to display its functions predominantly in post-mitotic neurons. While the defect of Cdk5 is disparaging to the CNS, its hyperactivation is also lethal to neurons. Some studies have also unraveled the various roles of cdk5 in neuronal remodeling as well as modulation of synaptic transmission (Fleming and Johnson, 1995; Cruz et al., 2003). Fyn, a tyrosine kinase, phosphorylates tyr18 residue and has been reported to precede the deposition of NFT as well as PHF associated with AD pathology (Lee et al., 2004). Exhaustive research has been carried out and it has been observed that hyperphosphorylation of tau protein makes it susceptible to aggregation and leads to the formation of tau assembly *in vitro* conditions whereas dephosphorylation events reverse its assembly to normal levels as well as stabilizes microtubules back. Coordinated interactions of kinase as well as phosphatases have been seen to maintain the phosphorylation status of tau protein and imbalance in such interplay usually drives its aggregations associated with several tauopathies. Various *in vitro* studies have been carried out which unraveled the involvement of specific phosphatases involved in the regulation of phosphorylation in AD. It has been found that PP1, PP2A as well as PP5 are residue specific and dephosphorylates the tau protein at particular residues like ser199, ser20, thr212, and ser409 respectively, thus maintaining the balance between kinase and phosphatase action (Liu et al., 2005). These phosphates also drive the positive feedback cycles by regulating the ERK/MAPK signaling cascade that otherwise activates the GSK3β which progresses the aggregation of tau

proteins. Among these phosphates PP2A is most extensively studied as it regulates about 70% of tau dephosphorylation in the human brain. Besides phosphorylation, tau proteins undergo other post translational modifications like acylation and glycosylation playing a role in standard microtubule dynamics (Qian et al., 2010). Emerging evidences suggest that overexpression of GSK3β as well as other kinases like Cdk5 plays a part in the progression of these neurodegenerative disorders like AD thus gaining a special interest in treating these disorders by employing therapeutic intervention in the form of specific inhibitors which can inactivate these kinases. Lithium-One of the most commonly used GSK3β inhibitor that inactivates the gsk3b by enhancing its ser-9 inhibitory phosphorylation which acts as a pseudo substrate and prevents its activity (Zhang et al., 2003). It has been reported that the application of lithium treatment in some experimental murine models that are overexpressing human APP, showed some encouraging results in retarding the neuropathology and cognitive impairments (Hu et al., 2009; Undurraga et al., 2019). Lithium is the only GSK-3β inhibitor that has been in clinical use for a significant time. However, we know that lithium lacks target specificity, and shows adverse side effects and high toxicity. Although two molecules AZD-1080 (AstraZeneca) and NP-12/Tideglusib (Noscria) reached the clinic in 2006, AZD-1080 was later on abandoned due to its nephrotoxicity as observed in phase I clinical trial while as NP-12 is currently in phase IIb trials for Alzheimer's disease and paralysis supranuclear palsy. Meanwhile presently, an increasing number of GSK-3β inhibitors are being tested in preclinical models, and it is anticipated that some of the potent inhibitors will enter clinical trials (Eldar-Finkelman and Martinez, 2011). Recent developments in the field of small-molecule inhibitors of CDKs have led to several compounds with anticancer potencies both *in vitro* and *in vivo* and models of cancer. However, the specificity of the inhibitors, which inhibit close isoforms, is not fully achieved yet, especially for CDK5, which is involved in neurodegenerative diseases (Łukasik et al., 2021). Other specific inhibitors have been developed with improved therapeutic effects, some of which are non-ATP competitive inhibitors that are selective and significantly less toxic than others like L803-mts as well as TDZD-8, VP0.7 (Kaidanovich-Beilin et al., 2004; Kaidanovich-Beilin and Eldar-Finkelman, 2006). Other conventional ATP competitive inhibitors include paullones, indirubin, SB415286 and SB216763 as well as AR-A014418 respectively (Leost et al., 2000; Bhat et al., 2007). Tau phosphorylation as well as amyloid beta deposition is impeded by treating the transgenic mouse models that are overexpressing APP, as well as reducing the memory weakening in the Morris water maze (Serenó et al., 2009; Ly et al., 2012). A recent finding suggests that selective GSK3 inhibitor SAR502250 is effective in contributing toward neuroprotection as well as diminish behavioral impairments in rodent models with neuropsychiatric abnormalities. Treatment of P301L human transgenic mice with this inhibitor was seen to reduce the tau phosphorylation thus impairs the formation of tau aggregates. Besides implications of specific inhibitors, genetic knockdowns of GSK isoforms have been also shown to recover cognitive abnormalities associated with various murine models. So these findings suggest that intervention of these kinase inhibitors can possibly act as disease modifying tactics to encounter AD related conditions (Griebel et al., 2019).

Acetylation

Alzheimer's disease (AD), also known as a protein misfolding disease, is a degenerative and incurable terminal disease of the central Nervous system (CNS) characterized by the presence of two main types of protein aggregates that include amyloid plaques and NFTs. Both genetic and non-genetic (environmental) factors are involved in the development of AD (Singh and Li, 2012; Tönnies and Trushina, 2017). However, the exact gene-environment interactions involved in the development of AD have not been delineated yet. Epigenetic changes are involved in integrating genetic and environmental interactions. These epigenetic processes are thus considered heritable changes in gene expression without causing any change in the coding sequence of genes. Most common epigenetic alterations reported that impact phenotypic outcomes include histone modifications like acetylation, phosphorylation, methylation, ubiquitination, ADP ribosylation, and SUMOylation; DNA methylation and non-coding RNA (Miller and Grant, 2013). These epigenetic changes regulate gene expression by altering the chromatin structure thereby increasing access to transcription factors (Venkatesh and Workman, 2015). The histone modifications involve acetylation and deacetylation of histone proteins which are the chief protein components of chromatin in the form of histone octamers. Each histone octamer consists of four core histones which include H2A, H2B, H3, and H4 (Shahbazian and Grunstein, 2007). These positively charged histone octamers wrap around negatively charged DNA to form nucleosomes-the basic components of chromatin structure. Acetylation and deacetylation of these histones define the chromatin configuration. Acetylation at the N-terminal tails of H3 and H4 histones neutralizes their positive charge thereby reducing the binding of histone to DNA. Acetylation of core histones, considered as the markers of an open configuration of chromatin, opens up the chromatin to facilitate gene transcription (Struhl, 1998). On the other hand, deacetylation does the opposite. Thus, we can say that histone acetylation promotes transcriptional activation, while as histone deacetylation leads to transcriptional repression of genes. These histone modifications regulate critical cellular processes that include cell proliferation, differentiation, apoptosis, inflammation, neuronal plasticity, and metabolic

reprogramming (Thiel et al., 2004). During the process of histone acetylation, Histone Acetyltransferases (HATs) transfer an acetyl group from acetyl coenzyme A to the lysine residues present at the N-terminal domains of core histones. This acetylation neutralizes the positive charge in histones and thus reduces affinity between histones and negatively charged phosphates in DNA. Therefore, it opens up chromatin to promote the transcriptional activity of genes (Bannister and Kouzarides, 2011). In contrast to this, histone deacetylase (HDAC) removes the acetyl groups from histones which results in silencing of gene expression. Thus, both histone acetyl transferases (HATs) and histone deacetylases (HDACs) play an important role in chromatin remodeling (Kuo and Allis, 1998). HATs are broadly divided into two classes based on their subcellular localization: A-type HATs, and the B-type HATs which are seen in the nucleus and cytoplasm respectively (Mersfelder, 2008). A-type HATs are further divided into three subclasses based on their structural homology: (1) GNAT family represented by Gnc5, PCAF, and ELP3; (2) MYST family containing Tip60, MOZ/MYST3, MORF/MYST4, HBO1/MYST2, and HMOF/MYST1; and (3) p300/CBP family containing p300 and CBP. Multiple studies have been conducted to investigate the role of these HATS in the etiology of AD (Lu et al., 2015; Li et al., 2021). HAT activity of Tip60 was shown to regulate the expression of genes that are related to behavior, learning, memory, and neuronal apoptosis in Drosophila (Xu et al., 2014). Similarly, HAT activity of CBP and p300 is related to long-term memory and neuronal survival. An interesting study was conducted in behavior-trained rats where hyperacetylated H2B/H4 in the promoters of the synaptic-plasticity-related genes was observed upon expression of CBP/p300 and PCAF (Chatterjee et al., 2013). Furthermore, AD pathological contexts also show a critical CBP/p300 loss with histone H3 deacetylation (Rouaux et al., 2003). A genome-wide study was conducted to examine the histone H3 acetylation pattern in the entorhinal cortex of AD patient samples and compared with the control subjects using chromatin immunoprecipitation and highly parallel sequencing (Marzi et al., 2018; MacBean et al., 2020). Genes involved in the progression of AD like amyloid-β and tau showed highly enriched acetylated peaks. Ramamurthy E. et al. carried out cell type-specific histone acetylation pattern analysis of AD patients and controls and observed differential acetylation peaks in the early onset risk genes (*APP, PSEN1, PSEN2, and BACE1*), and late onset genes *(BIN1, PICALM, CLU, ADAM10, ADAMTS4, SORL1,* and *FERMT2*) associated with the pathogenesis of AD (Marzi et al., 2018; Ramamurthy et al., 2020).

The histone deacetylases are also classified into four groups based on their homology to yeast enzymes: Class I HDACs consist of HDACs 1, 2, 3, and 8; Class II HDACs which are further divided into two subclasses, class IIa including HDACs 4, 5, 7, 9, and class IIb HDACs 6, 10; Class III HDACs which include SirT1-7; and class IV HDAC that has a single member-HDAC11 (Seto and Yoshida, 2014). Although class I HDACs are ubiquitously expressed, in comparison to HDAC1, HDAC2 and –3 show the highest expression levels in brain regions associated with memory and learning, such as the amygdala, hippocampus, and cortical areas (Volmar and Wahlestedt, 2015). The subcellular localization and expression levels of individual HDAC isoforms differ in different cell types during various stages of AD progression. HDAC2 is reported to negatively regulate memory and synaptic plasticity (Guan et al., 2009). The mice overexpressing HDAC2 showed hypoacetylation of histone H4 on their K12 and K5 residues. These mice also showed memory impairment and decreased number of synapses (Kumar et al., 2005). Since HDAC2 shows high levels of expression in the post-mortem brain samples of AD patients. HDAC2 downregulation by using short-hairpin-RNA restored the memory impairment and synaptic plasticity in CK-p25 mice indicating the critical nature of HDAC in memory formation and synaptic plasticity (Gräff et al., 2012). In another study, HDAC3 was shown to be critical for regulating synaptic plasticity in a single neuron or neuronal populations. Some established human neural cell culture models with familial AD (FAD) mutations showed a significant increase in HDAC4 levels in response to Aβ deposition in this cell model (Citron, 2010). Targeting HDAC4 by the selective inhibitor TasQ rescued the expression of genes involved in regulating neuronal memory/synaptic plasticity (Mielcarek et al., 2015). While high levels of HDAC6 protein were seen in the cortices and hippocampi of AD post mortem brain samples, reducing endogenous levels of HDAC6 were reported to restore learning and memory ability in the mouse model of AD. This happens partly because HDAC6 is shown to significantly decrease tau aggregation and promote tau clearance *via* acetylation (Fan et al., 2018). Thus, several studies have demonstrated that abnormal acetylation of core histones is involved in the etiology of AD. In addition to histones, altered acetylation of non-histone proteins which include NF-κb, p53, alpha tubulin and tau have also been reported in the pathogenesis of AD. Tau acetylation is mediated by p300 and CBP histone acetyl transferases at different residues. Acetylation of tau reduces its solubility and thus affects its intrinsic propensity to aggregate. Intracellular tau acetylated at Lys280, preferably by CBP, is seen during all stages of AD disease. Tau acetylation is known to suppress the degradation of phosphorylated tau (Chen et al., 2001; Park et al., 2013). Moreover, both acetylated and hyperphosphorylated-tau were reported to show similar spatial distribution pattern. Conversely,HDAC6 activity promotes deacetylation tau, which then contributes to enhanced tau-microtubule interactions and microtubule stability (Carlomagno et al., 2017).

Histone deacetylases (HDAC) inhibitors for the treatment of AD: A growing body of evidence considers HDAC proteins as therapeutic targets for the treatment of AD. HDAC inhibitors

may be alternative drugs to potentially protect against the impairment of cognition in AD patients. It is suggested that HDAC inhibitors may be a good alternative to conventional drugs to potentially improve the cognition features in AD patients (Xu et al., 2011). It has been shown that inhibitors targeting HDACs are involved in improving memory and cognition in the mouse model of AD. In AD animal models, HDAC inhibitors show neuroprotective activities, and thus provide a promising strategy for the treatment of AD (Sun et al., 2017). However, care should be taken when using pan-HDAC inhibitors (non-selective HDAC inhibitors) to treat AD because these HDAC inhibitors are poorly selective and often cause some undesired side effects (Cheng et al., 2015; Sun et al., 2017). Thus, evaluating the role of individual HDAC isoforms fin memory, learning and in the pathogenesis of AD becomes all the more important for the discovery and development of more selective HDAC inhibitors. Isoform selective HDAC inhibitors may, however, greatly eliminate side effects and toxicities associated with pan inhibitors and offer improved efficacy (Balasubramanian et al., 2009).

Glycosylation

Glycosylation involves the attachment of specialized forms of sugars called glycans to the target proteins through glycosidic bonding like N and O linkages (Spiro, 2002). Glycans are the sugar moieties linked to protein, lipids or other molecular entities and their structural complexity varies depending on the type of monocarbide core it bears. These glycans regulate the various functionalities associated with the normal functioning of cells like cellular signaling (Varki, 2017). These tissue specific glycosylation patterns have also been reported. Unusual alterations in such modification have implications for different diseases including several neurodegenerative disorders (Abou-Abbass et al., 2016). Nearly 50% of proteins have been observed to undergo such modifications. Glycosylation of proteins usually occurs in the ER and Golgi complex to facilitate the trafficking of proteins to different locations like mitochondria, cytoplasm, plasma membrane, nucleus etc., (Kizuka et al., 2017). This modification is usually catalyzed by enzymes to add glycans to target proteins through glycosidic bonding. Based on the type of glycosidic bonding between sugar moiety and target protein, it is categorized into N-linked and O-linked modifications (Shental-Bechor and Levy, 2008; Haukedal and Freude, 2021). N-linked glycosylation involves the attachment of N-acetyl glucosamine to the asparagine residues of target proteins through β-1N linkages. This modification starts with the synthesis of glycan (14 carbon moiety) from N acetyl glucosamine and mannose sugar, which undergoes further sugar modification, followed by the transfer of modified sugar chain to a particular protein thus acquiring complex form. This whole process is carried out by a specific set of enzymes like mannosidases and glucosidases of ER as well as glycosyltransferases of the Golgi complex (Moremen et al., 2012; Reily et al., 2019). On the other hand, O-linked glycosylation occurs in the several cellular compartments like cytoplasm, nucleus and mitochondria and involves the linking of O-glycans usually in the form of N-acetyl galactosamine or N-acetyl glucosamine to target proteins through Ser/Thr residues without undergoing any kind of alteration in the form of trimming of precursor sugar as is seen in N linked type. Many other sugar modifications are also reported which are carried out by enzymes like glycosyl transferases. These modifications involve the addition of galactose, N acetyl glucosamine, sialic acid etc., to target proteins (Clausen and Bennett, 1996; Akasaka-Manya and Manya, 2020). These sugar modifications usually determine the stereochemistry of target proteins which in turn define the structural organization as well as protein stability (Shental-Bechor and Levy, 2008). In the progression of Alzheimer's disease (AD), glycosylation is associated with tauopathies. Several proteins like APP and BACE1 are seen to be glycosylated in tauopathy patients (Kizuka et al., 2015). It has been seen that O-glycosylation of tau hampers its aggregation without causing any kind of obstruction in its normal polymerization activity (Mietelska-Porowska et al., 2014). Thus, it has been proposed that glycosylation of tau plays a protective role by blocking tau aggregation. Few O-linked glycosylation sites have been spotted in tau protein at residues which are targets of tau phosphorylation as well. These residues include S400, S238, and S409 (Yuzwa et al., 2011). Unlike O-glycosylation, N-type modifications of tau protein have been observed to affect the subcellular localization of tau protein in AD patients (Alquezar et al., 2021). Transgenic mice models of AD have shown a significant disparity in O-GlcNAcylation and phosphorylation with tau protein being hyperphosphorylated at specific serine residues followed by a drop in O-GlcNAcylation levels (Bourré et al., 2018). Both O-linked glycosylation and phosphorylation of tau protein are well-adjusted in normal conditions and it has been observed that hyperphosphorylated protein shows a decreased glycosylation thus impacting its nuclear localization (Lefebvre et al., 2003). Thus we can say that O-glycosylation competes with phosphorylation and shields tau protein from hyperphosphorylation at particular stretches of serine residues by Protein Kinase A (PKA), therefore playing a protective role in normal brain functions. However, it has been found that N-glycosylation helps tau phosphorylation by hampering dephosphorylation or by activating PKA mediated tau phosphorylation, and thus promotes the progression of pathology associated with Alzheimer's disease (Liu et al., 2004). Altered glycosylation patterns of many other proteins involved in the progression of neuro disorders like APP have been reported as well. Glycosylated APP has been reported in CSF of patients showing AD pathology (Schedin-Weiss et al., 2014). It has been reported that N-bonded glycan display modulation of amyloid beta production and structural variations in such

glycans alters APP transport as well as trafficking. O-linked glycosylation of APP directs it to plasma membranes to promote the processing of APP through non-toxic, non-amyloidogenic pathways, thus lowering the production of toxic amyloid beta peptides (Chun et al., 2015a). N-glycans are also involved in the trafficking and secretion of APP. It has been shown that blocking the activity of mannosidase hampers the production of hybrid and complex forms of N glycan which affects APP transport and other proteins to the synaptic membrane (Bieberich, 2014). Recently site-directed mutagenesis approach has shown that specific O-glycosylation at Thr576, directs its transport toward the plasma membrane and the subsequent endocytosis of APP elevates Aβ levels (Chun et al., 2015b). Treatment of experimental 5XFAD mice with a small molecule inhibitor blocking the glycosylation of gamma secretase lead to reduced production of AB peptides, thus slowing the progression of neuroinflammation followed by recovery in memory impairments (Kim et al., 2013). Patients displaying AD pathology have been found to contain BACE1 post translationally altered with bisecting GlcNAc however blocking this modification using knockout approach slows down APP processing followed by reduced amyloid deposition. Experimental knockout Mgat3-gene mice have been shown to alleviate cognitive abnormalities as well as deposition of amyloid beta aggregates (Elder et al., 2010; Haukedal and Freude, 2021). Besides these enzyme dependent modifications, there are enzyme independent post translational modifications called glypiations which involve the covalent attachment of sugars to lysine residue of target proteins. This alteration usually produces advanced glycation end products (AGES) which are speculated as glycotoxins playing a role in age related diseases (Cho et al., 2007). It has been observed that glycation modifications cause aggregation of the tau proteins by hampering the ubiquitination process required for tau degradation. Moreover. this modification usually reduces the binding affinity of tau protein toward microtubule thus affecting polymerization followed by defective axonal transport and other synaptic functions (Ko et al., 1999).

Fatty acylation

The attachment of long chain fatty acids like palmitate (16 carbon saturated fatty acid) and myristate (14 carbon saturated fatty acid) by amide and thioester linkages respectively is called fatty acylation (Lanyon-Hogg et al., 2017). The mechanism of fatty acylation tunes various cellular processes such as protein-protein interactions, membrane targeting, and intercellular as well as intracellular signaling. Dysregulation in the process of fatty acylation leads to the development of disease conditions including neuronal defects (Wright et al., 2010; Tate et al., 2015). Of all the three lipid modifications viz myristylation, prenylation and palmitoylation; myristoylation and palmitoylation are the most common acylation processes and only palmitoylation is reversible (Resh, 2016).

Palmitoylation

S-Palmitoylation is a vital post-translational modification that is important for the function and trafficking of various synaptic proteins. Palmitoylation reactions are carried out by palmitoyl acyltransferases (PATs) that catalyze the attachment of palmitate (16 carbon) covalently to cysteine residues through thioester bonds (Cho and Park, 2016). Palmitoylation (addition of sulfhydryl group to palmitoyl group) is important for synaptic activity and an increase in palmitoylation contributes to pathogenesis of AD to a large extent (Bhattacharyya et al., 2013). BACE 1 or β-secretase, a 501 amino acid type 1 transmembrane aspartic acid protease, associated with the retroviral aspartic β-secretase protease and pepsin family, leads to APP cleavage in the amyloidogenic pathway generating Aβ including pathogenic Aβ42 (Vassar et al., 2009). S-Palmitoylation of BACE 1 takes place at specific Cys residues viz Cys-474, 478, and 485, out of which Cys 474 is a part of the transmembrane domain. Mutations that change these cysteine residues to alanine cause displacement of BACE1 from the lipid rafts without affecting the processing of APP and produce peptides of amyloid (Vetrivel et al., 2009). S-Palmitoylation of BACE1 and its role in Alzheimer's disease was studied by developing a gene knock-in transgenic AD mice, where the cysteine residues of S-palmitoylation were changed to alanine residues. The lack of S-Palmitoylation of BACE 1 was observed to reduce the cerebral amyloid burden in AD mice significantly, it also reduced cognitive defects. This suggests that the intrinsic S-palmitoylation of BACE 1 has an impact on the pathogenesis of amyloid and further cognitive decline (Andrew et al., 2017). Palmitoylation targets APP to the lipid rafts and enhances its BACE-1 mediated cleavage which ultimately increases the amyloidogenic processing. Palmitoylation inhibitors impair the processing of APP and α and β (a family of proteolytic enzymes that cleave APP to produce amyloid beta peptides). Acyl Coenzyme A Cholesterol acyltransferase (ACAT) inhibitor, known to redistribute cellular cholesterol, inhibits APP palmitoylation and significantly reduces Aβ generation (Bhattacharyya et al., 2013).

Myristoylation

Myristoylation, is a eukaryotic post and co-translational modification, is the covalent attachment of myristic acid, a 14-carbon saturated fatty acid, to the N-terminal glycine of proteins. Proteins that are destined to be myristoylated begin with the sequence Met-Gly. N-M-T acts on myristoyl coenzyme A and transfers myristate from it to N-terminal glycine to a varied range of substrate proteins. These myristoylated proteins play critical roles in many signaling pathways to mediate protein-protein and protein-membrane interactions, subcellular

targeting of proteins etc. Myristoylation is mediated by the enzymes commonly known as N-myristoyltransferases (N-M-T). In vertebrates myristoylation is carried out by NMT1 and NMT2-members of the GCN5 acetyltransferase superfamily, expressed in nearly all tissues and are reported to be involved in the progression and development of various pathological conditions which include Alzheimer's disease, cancer, epilepsy etc., (Thinon et al., 2014). A key event in AD is the cleavage of APP by β-secretase to generate APP C99, which then undergoes additional cleavages by γ-secretase to produce Aβ40 and Aβ42 peptides (Su et al., 2010). The presenilin-1 (PSEN1) and presenilin-2 (PSEN2) genes encodes the major component of γ secretase responsible for APP cleavage resulting in the subsequent formation of Aβ peptides (Delabio et al., 2014) and altered APP processing is usually seen in AD patients carrying PSEN mutation. It has been shown that calmyrin, a calcium binding myristoylated protein, plays a versatile role in intracellular signaling and is also important in the functioning of presenilin (Stabler et al., 1999). Calmyrin preferentially interacts and colocalizes with PSEN2. The co-expression of calmyrin and PSEN2 in Hela cells were reported to modify the subcellular distribution of these proteins and cause cell death, thus suggesting that these two proteins act in concert in pathways that regulate cell death (Stabler et al., 1999). PSEN2 and calmyrin mutually regulate each other; calmyrin regulates the PSEN2 function when it detects changes in calcium homeostasis, on the other hand, PSEN2 proteins may disrupt calcium homeostasis altering the calcium binding capacity of calmyrin. Also, the overexpression of presenilins causes perturbations in calcium balance (Guo et al., 1996; Keller et al., 1998). Any imbalance in the regulation of calcium could be fatal to the cell because calcium plays a central role in various cellular processes and in apoptosis (McConkey and Orrenius, 1997).

Normally, APP, β-and γ-secretases and phosphatidylinositol 4, 5-bisphosphate (PIP2), which is an signaling lipid moiety for endocytosis, are located on the lipid rafts. Also, It has been shown that endocytotic invagination of the membrane causes smaller lipid rafts to fuse to form larger rafts where APP, β, and γ secretases come together, this combination brings APP, β, and γ secretases in close proximity to one another causing APP cleavage thus, inducing the amyloidogenic pathway in AD (Su et al., 2010). The myristoylated alanine-rich C kinase substrate (MARCKS) usually binds to the membranes to shield PIP2 from taking a part in endocytosis. This process halts endocytosis, thus reducing the Aβ production (van Rheenen et al., 2005). Phosphorylation of MARCKS by protein kinase C (PKC) or its interaction with Ca2 + leads to its release from the membrane into the cytoplasm, thus releasing PIP2 and promoting endocytosis again, and subsequent generation of Aβ40 and Aβ42 peptides in AD (Arbuzova et al., 2002). Thus, MARCKS provides a novel therapeutic option for reducing the generation of Aβ40 and Aβ42 peptides by regulating the pathway of endocytosis.

Ubiquitination

Ubiquitin is a greatly conserved 8.6 kDa regulatory protein composed of 76 amino acids found in almost all tissues of eukaryotes encoded by UBB, UBC, UBA52, and RPS27A genes (Kimura and Tanaka, 2010). Ubiquitination interchangeable with ubiquitylation is the addition of ubiquitin to a substrate protein. Ubiquitination is known to mark proteins for degradation; it can affect their function and alter protein sub-cellular localization as well (Mukhopadhyay and Riezman, 2007). Ubiquitination is regulated by three main enzymes viz (E1) Ubiquitin activating enzymes, (E2) Ubiquitin conjugating enzymes and (E3) Ubiquitin ligase. Ubiquitination can take place by either the addition of a single ubiquitin protein (mono-ubiquitination) or a chain of ubiquitin proteins (Polyubiquitination) (Mukhopadhyay and Riezman, 2007). These modifications generally occur at the side chain of lysine residues or the N-terminal methionine, although lately cysteine, serine and threonine residues have also been recognized as places for ubiquitination (McClellan et al., 2019). The site, length, and attachment of these ubiquitin proteins help to determine the fate and stability of a substrate (Ramesh et al., 2020). As EI, E2, and E3 enzymes help in the attachment of ubiquitin proteins, the deubiquitinases (DUBs) detach ubiquitin proteins from the substrates (Schmidt et al., 2021). Interestingly, Ubiquitin, protein can itself be post-translationally modified with acetylation and phosphorylation for enhanced diversity and regulation. The ubiquitin proteasomal degradation pathway is one of the major routes responsible for the clearance of misfolded proteins to maintain protein homeostasis. Any perturbation of the ubiquitination degradation pathway leads to toxic aggregation of species promoting the onset of various neurodegenerative diseases including Alzheimer's (Zhang et al., 2017). AD is mainly caused by the unusual accumulation of misfolded proteins and peptides which result in the formation of amyloid plaques and NFTs, respectively. APP, BACE1 and tau proteins are the major targets of abnormal modification by ubiquitination (Perluigi et al., 2016). β-secretase/BACE1 leads to APP cleavage in the amyloidogenic pathway generating Aβ. The therapeutic inhibition/regulation of β-secretase would therefore reduce the production of all forms of beta-amyloid including the pathogenic Aβ42 (Vassar et al., 2009). The regulation of BACE1 level is done by the ubiquitination and proteasome degradation system. Tau is a protein is also rich in lys residues thus has high susceptibility toward ubiquitination. The central role of tau ubiquitination is to regulate tau clearance by proteasomal or lysosomal autophagy system (Gonzalez-Santamarta et al., 2020).

Further, the presenilin (PSEN) proteins are known to play an essential role in AD pathogenesis by mediating the intramembranous cleavage of APP generating (Aβ) (Oikawa and Walter, 2019). In order to sort APP into the endosome and allow their processing by PSEN, ubiquitination of its lysine residues present in its cytosolic domain is carried out by E3 ligases.

These ligases are active in Alzheimer's and they ubiquitinate at Lys 649/650/651/678 of ACR. Any mutation that changes these lysine residues to arginine hinders the ubiquitination of APP and increases Aβ40 levels (Williamson et al., 2017; **Figure 5**). Apart from this, Lys 203 and Lys 382 of BACE1 are also important ubiquitination sites for degradation. Mutations at these sites also disrupt the degradation of BACE1, thus increasing the production of Aβ (Wang et al., 2012). BACE1 is ubiquitinated by an E3 ligase known as FbX2 *via* trp280 which causes it to degrade through the proteasome pathway. In turn, the expression level of FbX2 gets affected by PGC-1α [Peroxisome proliferator-activated receptor gamma (PPARγ) coactivator-1α] which is known to promote the degradation of BACE 1 through the ubiquitin degradation system (Ramesh et al., 2020). The AD brain has altered expression levels of both FbX2 and PGC-1α and any supplementation of FbX2 externally reduces the levels of BACE1 and also improves synaptic function (Gong et al., 2010). This suggests that FbX2 has a role in the reduction of Aβ levels.

The ubiquitination of tau is also an important factor to study AD pathology. NFTs and paired helical filaments (PHFs) which were derived from the Alzheimer's affected brain at an early stage, depicted that tau is hyperphosphorylated and ubiquitinated at lys-6,11, and 48. These residues thus have a significant role in AD pathogenesis. While lys48 linked polyubiquitination targets tau to proteasomal degradation, lys6 linked polyubiquitination prevents its degradation and thus hinders the clearance of PHFs (Mayeux and Stern, 2012). As already known that dUbs are the species that mediate deubiquitination, the only dUb that has been reported to target tau is the Otub1, a cysteine protease. Otub1 is reported to prevent the degradation of tau by removing Lys48 polyubiquitin chains from the endogenous tau. This removal of the Lys 48 polyubiquitin chain prevents degradation of tau in primary neurons derived from transgenic mouse models, which suggests that Otub 1 has a necessary role in regulating tau ubiquitination (Juang et al., 2012).

SUMOylation

SUMOylation, a reversible post-translational protein modification, occurs by the binding of an 11KDa, Small Ubiquitin-like Modifier (SUMO) peptide to the lysine residues of target proteins. SUMOylation helps in the normal functioning of proteins by regulating the transactivation of transcription factors, localization of proteins and protein-protein interactions to subcellular regions (Zhang and Sarge, 2008; Feligioni et al., 2015). Similar to the ubiquitination pathway, the SUMOylation process also requires a SUMO-EI activating enzyme, a SUMO-E2 conjugating enzyme and a SUMO-E3 ligase to complete the cycle. Various SUMO paralogues (SUMO-1,2,3,4, and 5) get expressed in a tissue specific manner. The subtypes SUMO2 and SUMO3 share sequence homology of around 95% therefore, they are more commonly called SUMO2/3. SUMO1 and SUMO2/3 are predominantly expressed in brains, SUMO4 in lymph nodes, spleen and kidney while SUMO5 is expressed in the testis (Liang et al., 2016). In AD patients, the expression of SUMO-related proteins are altered, for example the post-mortem brain sections taken from Alzheimer's patients

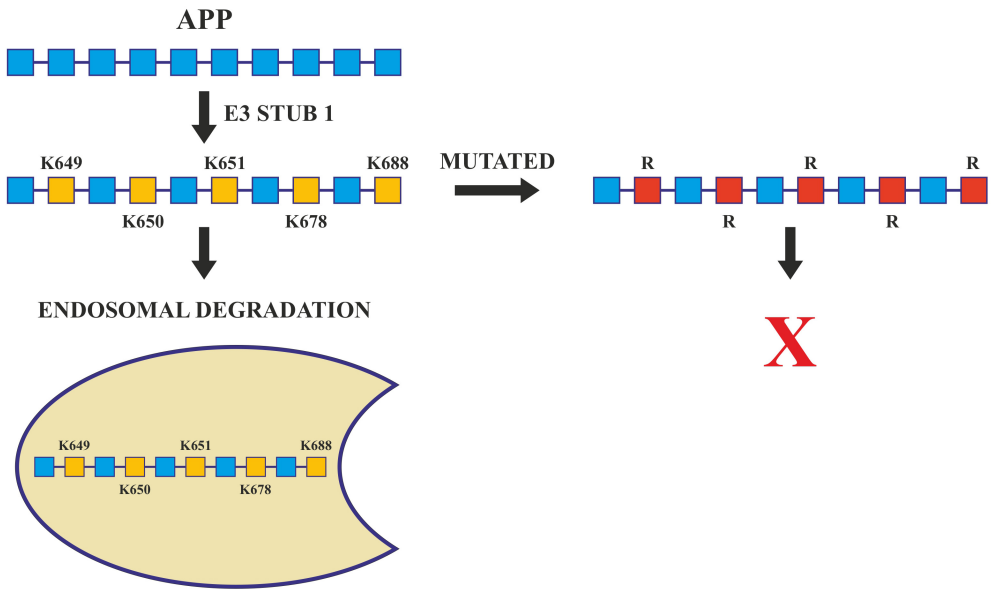

FIGURE 5
Ubiquitination in Alzheimer's disease. Ubiquitination of APP by E3 ligase (Stub1) targets it to endosomal degradation. Mutations at lysine residues inhibit the ubiquitination and endosomal degradation of APP increasing the amyloid burden.

showed enhanced SUMO3 labeling in the hippocampal region (learning and memory) (Li et al., 2003). SENP3 (a SUMO-specific proteases 3), which takes part in the maturation of native SUMO as well as de-SUMOylation process has been reported to get down-regulated in the inferior parietal lobes of sporadic Alzheimer's patients (Weeraratna et al., 2007). In addition, the proteins like tau, AβPP, GSK3β, BACE1, and JNK which are involved in AD are SUMO targets (Feligioni and Nisticò, 2013). As already known the abnormal intracellular accumulation is an important hallmark in the progression of AD and is an important target for SUMOylation studies. SUMO1 modification of tau happens on K340, through which tau binds with microtubules (Dorval and Fraser, 2006). SUMOylation and phosphorylation of tau are known to stimulate each other reciprocally. Increased SUMOylation enhances phosphorylation and vice-versa. The SUMOylated/Phosphorylated tau does not bind to tubulin thus making it unable to promote microtubule assembly, and it also removes normal tau from the microtubule assembly, which therefore serves as a template for the transition of normal tau into a misfolded protein (Luo H.B. et al., 2014). SUMOylation of tau also leads to increased formation of NFTs by either competing with ubiquitination or by enhancing the aggregation of tau (Luo Y. et al., 2014).

In APP processing, SUMOylation helps in its trafficking, its modulation and finally in its amyloidogenic processing. Both SUMO1 and SUMO2, SUMOylates APP *in vitro* on lysines 587 and 595 which reduces Aβ levels in Hela cells overexpressing APP (Martins et al., 2016). Apart from tau and APP, BACE 1 SUMOylation also has a significant role to play in AD pathogenesis. BACE 1, cleaves APP during late or early endosome for Aβ generation. SUMOylation of BACE1 at Lys 501, increases the stability and enhances its protease activity resulting in the processing of APP and ultimately excessive Aβ production. Mutation at this SUMOylation site (lys501) causes BACE1 to degrade which confirms that lys501 is important in stabilizing BACE1 upon SUMOylation (Ramesh et al., 2020; **Figure 6**).

Histone deacetylases play critical roles in the modulation of various cellular processes like chromatin remodeling, DNA repair and transcription (Seto and Yoshida, 2014). SUMOylation of HDACs at lys444 and lys476 decrease the amyloid burden (**Figure 5**). HDACs particularly HDAC1 maintains genomic integrity in cultured neurons and the mouse brain (Pao et al., 2020). Co-localization studies done *in vivo* and *in vitro,* have revealed that the SUMOylation of HDAC1 in the hippocampal CA2 region gets increased in the presence of PIAS1(Protein inhibitor of STAT1). HDAC1 SUMOylation also gets enhanced when Aβ is administered directly in the rat hippocampus (Tao et al., 2017). Furthermore, it has been reported that the Corticotropin Releasing Factor (CRF), Insulin like Growth Factor (IGF-1) and Brain Derived Neurotropic Factor (BDNF) increased the SUMOylation in the CA2 region of HDAC1 of the rat brain. SUMOylation of HDAC1 results in the suppression of HDAC1 and CREB (Cyclic AMP Responsive Element Binding). CREB then binds to the region of the promoter of Mcl-2 (a family of proteins having a role in apoptosis) and enhances its expression. HDAC1 SUMOylation promotes cellular apoptosis, enhances the amyloid burden and relieves memory and synaptic deficits in PSEN/APP mice (Tao et al., 2017).

Deamidation

Deamidation is a spontaneous and non-enzymatic post translational modification which takes place at the side chains of asparagine and glutamine (Dunkelberger et al., 2012). Protein and peptides can undergo deamidation of glutaminyl (Gln) and asparaginyl (Asn) to produce glutamyl and aspartyl residues which cause changes in the structure of the protein because of the addition of negative charge. It influences protein stability, structure, folding, and aggregation. Studies done *in vivo* and *in vitro* have shown that deamidation rates are dependent upon the pH, primary sequence, and three dimensional structure of the protein, buffer ions, ionic strength, and temperature etc., (Robinson and Robinson, 2001). Although deamidation of proteins has been found to be involved in the process of amyloid formation, however, the role of deamidation in the formation of Alzheimer's plaques is still not very well understood One hypothesis is that deamidation can contribute to the development of plaque through the isomerization of Asp to iso-Asp that might prevent the damaged peptides to degrade properly (Dunkelberger et al., 2012). As an example, the Tottori Japanese mutation (Asn-7) and the Lowa mutation (Asn-23) are two common Aβ mutations that have been found to deaminate to iso-Asp in AD patients (Wakutani et al., 2004). Under physiological conditions, the process of deamidation takes place through the formation of a 5-membered succinimide ring (intermediate) facilitated by the protein L-isoaspartate-*O*-methyltransferase (PIMT), which can restore iso-aspartate to succinimide by transferring methyl from S-adenosyl-methionine (SAM) to the side chain of iso-Asp. These 5-membered rings then hydrolyze into aspartic or iso-aspartic acid (from asparagine) or glutamic or iso-glutamic acid (from glutamine) (Dunkelberger et al., 2012). Deamidation produces L-forms of the products, but they also have the potential to racemize to D-forms through the succinimide intermediate. The ratio of normal to iso-products is 1:3 (Dunkelberger et al., 2012). This isomerization increases the length of the backbone by a CH2 group resulting in the addition of a rotable bond in the backbone of the peptide (Dunkelberger et al., 2012) which therefore, causes serious structural changes leading to the augmentation of Alzheimer's pathogenesis (Roher et al., 1993). It has been shown that different Aβ biochemical pools have different amounts of N-terminus Isomerization. The membrane fractions and insoluble plaques in AD brains

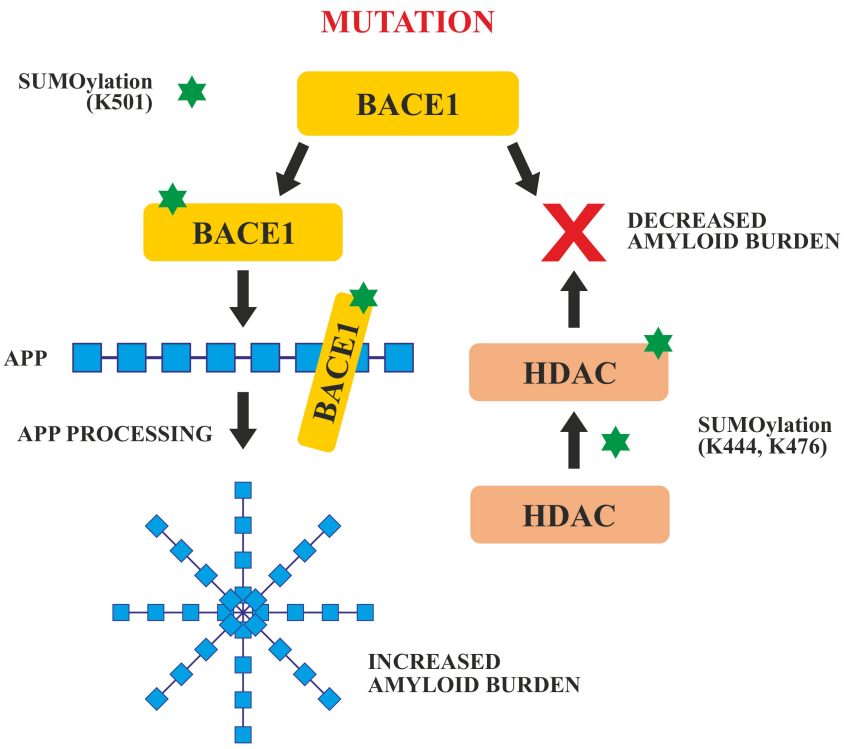

FIGURE 6
SUMOylation of BACE1 and HDAC. SUMOylation at Lys 501 enhances the activity of BACE1 which enhances APP cleavage and increases amyloid burden. Any mutation in the BACE 1 SUMOylation site decreases the amyloid burden. SUMOylation of HDAC at Lys 444 and Lys 476 also decreases the amyloid burden.

have nearly 85% isomerized $A\beta_{1-15}$, whereas the soluble and vesicular portions have lower isomerization percentage [42 (Bronisz et al., 2014)]. Moreover, on deamidation some otherwise non-amyloidogenic proteins have been reported to convert to amyloidogenic which also leads to Alzheimer's disease (Nilsson et al., 2002).

Oxidative/nitrosative stress

The imbalance between the creation of reactive oxygen/nitrogen species (ROS/RNS) and the ability of the cell's antioxidant defense to neutralize them is known as oxidative stress. The brain requires a lot of oxygen to function correctly and is highly vulnerable to the action of ROS. Furthermore, the brain is abundant in polyunsaturated fatty acids (PUFAs) that are at risk of peroxidation or free radical attack. Moreover, there is a high quantity of iron, a powerful ROS catalyst, and other antioxidant molecules present in the brain. The etiology of several neurodegenerative disorders, including Alzheimer's disease, has been linked to an increase in oxidative stress. The increase of Aβ peptide and hyperphosphorylated tau protein in the brain during the progression of Alzheimer's disease has been suggested to have significant pro-oxidant effects, either directly or indirectly. Through activation of NADPH oxidase and inducible nitric oxide synthase (iNOS), amyloid-β could induce reactive oxygen species (ROS) production from cortical neurons, as a result, superoxide anion ($O2^-$) and nitric oxide are formed, which leads to the production of hydrogen peroxide (H_2O_2) and peroxynitrite (ONOO) (Medeiros et al., 2007). Amyloid-β disrupts the mitochondrial electron transport by negatively regulating the key enzymes involved in the electron transport chain such as cytochrome C oxidase which leads to the increase in superoxide anion ($O2^-$) and later on its conversion into hydrogen peroxide (H_2O_2) thus exacerbating oxidative stress (Yan et al., 2013). Aβ induced oxidative stress also leads to the activation of different signaling pathways, for example, p38 a member of mitogen-activated protein kinases (MAPKs) family is activated during Aβ-mediated oxidative stress (Zhu et al., 2000). When compared to control individuals, late AD patients had higher levels of several lipid peroxidation markers such as 4-hydroxyhexanal (HHE), F2-isoprostane, and F4-neuroprostane. Peroxidation of lipids harms mitochondria by impairing respiration by releasing electrophilic aldehydes (Kuhla et al., 2007). Protein oxidation indicators such as protein carbonyls and 3-nitrotyrosine (3-NT) were also shown to be higher in MCI and AD patients (Alzheimer's Association, 2019).

Significant increases in the levels of DNA oxidation marker 8-hydroxy guanosine (8-OH-dG) were seen in CSF of Alzheimer's patients when compared with control (Lovell et al., 1999). Oxidation of different proteins in the brain alters the function of enzymes responsible for the proper neuron and glial function, for example, Glutamine synthetase and creatine kinases undergo oxidative modifications during oxidative stress that leads to excitotoxicity altering the concentrations of glutamate and decrease in energy metabolism in AD (Moreira et al., 2005). As a result of oxidative stress, Aβ, and tau have been shown to undergo a variety of changes. Tau helps to organize microtubules by actively interacting with newly generated microtubules. Modification of tau by oxidative stress leads to the disruption of microtubule organization in AD patients (Heston and White, 1978). Levels of different metal ions such as Cu^{2+} and Zn^{2+} are tightly regulated for different functions of the brain and also prevent the oxidative stress resulting from the interaction of Fe^{2+} or Cu^{2+} with oxygen to generate free radicals. In AD the homeostasis is disrupted and leads to oxidative stress (Deibel et al., 1996).

In AD patients various stress responses or antioxidant genes are activated during oxidative stress such as heme-oxygenase 1, which degrades the prooxidant heme into antioxidant biliverdin, carbon monoxide and free iron. These antioxidants play central neuro-protective roles in AD (Maines, 2000; Pini et al., 2016) Gene expression of Mn^{-}, Cu-, and Zn-superoxide dismutase (Mn^{-} and Cu, Zn-SOD), catalase (CAT), glutathione peroxidase (GSH-Px), and glutathione reductase (GSSG-R) is enhanced (Aksenov et al., 1998). Superoxide dismutase (SOD) is an enzyme that catalyzes the conversion of superoxide radicals to H2O2 and oxygen (O2) as part of the body's initial defense against ROS (Balmuş et al., 2017). In both MCI and AD patients, serum SOD activity was lower than in controls. GSH reacts with oxidized products or ROS either catalyzed by glutathione peroxidase (GPx) or on its own or leads to the formation of glutathione disulphide (GSSG). Glutathione reductase can then convert the GSSG back to reduced GSH (GR). According to various human brain studies, damaged brain areas of Alzheimer's patients have a decreased ratio of reduced to oxidized glutathione (GSH/GSSG) (Benzi and Moretti, 1995; Li et al., 2015). α-tocopherol (Vitamin E) an endogenous antioxidant protects lipid peroxidation because of its lipophilic nature. Reduced Levels of α-tocopherol were present in the plasma of mild AD patients compared to control (Brigelius-Flohé and Traber, 1999; Baldeiras et al., 2008). Higher vitamin E levels in the blood have also been linked to a lower incidence of Alzheimer's disease in older people (Mangialasche et al., 2010). Ascorbic acid (vitamin C) is one of the most significant water-soluble antioxidants required for the reactivation of Vitamin E, and its levels in plasma are lower in MCI and AD patients as compared to controls (Rinaldi et al., 2003). Different studies have reported that N-3 PUFA's is having a strong neuroprotective effect in humans in the early stages of AD development, corresponding to MCI. Enriching brain cells with N-3 PUFA causes a low-level oxidative/nitrosative stress, which will boost antioxidant activities and hence have a neuro-protective impact (Barone et al., 2014). Zhang et al. have recently reported that in both *in vitro* and *in vivo* models n-3 PUFAs induces neuroprotective effects through targeting Nrf2 and upregulating heme oxygenase-1 (HO-1) (Zhang et al., 2014).

Therapeutic prospects for the treatment of Alzheimer's disease

Some of the approaches that can be adopted for the treatment of AD include:

1. Novel exosomes-based therapeutics (NET): Several intriguing properties of exosomes, such as immunological inertness and the natural ability of EVs to transfer cargo between the cells makes them unique natural biological vehicles to cross the biological barriers such as the blood-brain barrier (BBB), which increases their therapeutic potential exponentially for delivering drugs particularly non-coding RNAs across the brain, resulting in silencing of disease-causing genes in the neurological disorders (Familtseva et al., 2019). Further, in mouse studies, it was demonstrated that Neprilysin (NEP) deficient mice showed elevated levels of Aβ, which relates NEP to the degradation of Aβ in the brain (Farris et al., 2003). When MSC-derived exosomes with NEP activity were administered intravenously, it led to reduction in the deposition of Aβ plaques in AD mice, a promising approach in AD therapeutics (Ding et al., 2018). Apart from their role as biomarkers exosomes have also emerged as promising vehicles for pharmaceuticals and they are also reported to play a neuroprotective role in neurodegenerative illnesses and traumatic brain injuries. E.g., exosomes derived from multipluripotent mesenchymal stem cells (MP-MSCs-EXOS), support functional recovery in these illnesses by inhibiting apoptosis and neuroinflammation (Alzheimer et al., 1995). However, the lack of techniques to isolate tissue specific EVs and lack of standard methodology to isolate EVs from different biological fluids are some of the critical challenges that needs to be overcome before utilizing the properties of EVs in treating various challenging diseases. For example, BACE 1 is an important therapeutic target for lowering Aβ levels in AD by specifically silencing BACE1 using small interfering RNAs (siRNAs), significant reduction of Aβ levels were seen (Zhou Y. et al., 2020). Thus, exosome based nanocarrier systems could be employed as effective therapeutic strategies in AD.
2. CRISPR/Cas9 based gene-editing: This approach has demonstrated a great potential for the treatment of AD

and other diseases by correcting specific gene sequences (DiCarlo et al., 2017; Schneller et al., 2017; German et al., 2019; Mirza and Karim, 2019; Karimian et al., 2020; Xu et al., 2020; Bhardwaj et al., 2021). In a study using CRISPR/Cas9, gene editing of endogenous APP at the extreme C-terminus inhibited interactions of APP and BAC1 within the endosomes, thereby the most important cleavage event in Aβ generation was avoided in Sporadic AD (Das et al., 2013; Sun et al., 2019). Thus, CRISPR/Cas9 technology could be used to correct increased Aβ production or mutations in APP, PSEN-1, and PSEN-2 genes, which are known to be a causative factor in familial AD, and is a promising tool and has potential for therapeutics in AD. However, further studies are required to establish off-targets and safety of this approach.

3. Nanotherapeutic approaches: Functionalized and tailored nanomaterials have been designed that have the ability to cross the BBB easily and act on the target cells and cellular components like cellular proteins, peptides, and nucleic acids (Tsou et al., 2017; Furtado et al., 2018). Interestingly, nanomaterial-based drugs are considered promising due to their small size and multidimensional therapeutic abilities, and various nano-formulations such as carbon nanotubes, quantum dots, dendrimers, fullerenes, and tailor-made gold nanoparticles help in the targeted delivery of drugs in the targeted cells in AD brain to reduce synaptic impairment (Karthivashan et al., 2018; Farheen et al., 2021; Khan et al., 2021). Interestingly, the amyloid-β-derived peptides prevented *in vitro* tau aggregation and their inhibitory effect on tau and non-toxic nature points to their therapeutic importance in overcoming AD (Hampel et al., 2015; Kametani and Hasegawa, 2018; Abeysinghe et al., 2020; Farheen et al., 2021). Nanomaterials help in hindering amyloid protein growth and its accumulation due to their highly sensitive molecular detection and identification (Elbassal et al., 2017; Li et al., 2019; Jara-Guajardo et al., 2020; Gorantla et al., 2021). Due to their ability to cross BBB, nanomaterials have been used to identify AD biomarkers, and to study the beta-amyloid protein and tau proteins pathological mechanism (Kametani and Hasegawa, 2018). Another approach in nanotherapeutics is the use of nano-phytomedicine which is the conjugation of nanoparticles and medicinal plants, or their components. The antioxidative, anti-inflammatory, anticholinesterase and, anti-amyloid properties of phytochemicals make them promising therapeutic agents (Bhattacharya et al., 2022). For example, curcumin loaded poly lactic-co-glycolic-acid (PLGA) nanoparticles system has been shown to enhance the action of curcumin and when targeted to the neuroblastoma cell line for the treatment of Alzheimer's disease they were reported to reduce oxidative damage of the cells. Further, it has been reported that the NPs-Cur delivery system enhances the action of curcumin on several pathways implicated in the pathophysiology of AD by either inhibiting M1-microglial activation or by reducing the expression of apolipoprotein J or clusterin (Chopra et al., 2021). Therefore, nanotechnology-based approaches, with all its advantages already discussed, to target various therapeutic targets in AD including PTMs provides an excellent strategy to manage the progression and decrease the burden of AD.

4. Reactive oxygen species have been shown to be one of the primary drivers in the pathogenesis of AD. Because of the protective effects of phytochemicals against oxidative stress-induced cell apoptosis, they are being explored as potential therapeutic agents for treating or preventing neurodegenerative diseases. Phytochemicals show neuro-protective effects and due to their various effects as anti-inflammatory and antioxidative activities (Palmal et al., 2014). For example, Salidroside, one of the main bioactive ingredients of R. Crenulata, was reported to improve the proliferation and neuronal differentiation of NSCs in the hippocampus of STZ-treated rats, where it acts by scavenging ROS to protect Neural Stem Cells (NSCs) from necrosis and apoptosis (Zhang et al., 2007; Uddin et al., 2021). Another example is Curcumin, which is a polyphenolic natural compound. It has shown its beneficial therapeutic effect in AD and related conditions in various preclinical and clinical studies. The findings from these studies suggested that the curcumin treatment counteracts the deleterious effects of oxidative stress and reverses memory (Walia et al., 2021). Several other phytochemicals have been reported to be involved in slowing down the onset and progression of AD and in improving cognitive functions. However, further research is needed to bring these phytochemicals to a clinical stage, where they can be used as effective antioxidants and/or anti-inflammatory agents for the treatment of AD. Plant derived phytochemicals combined with nanotherapeutics approaches have great potential in targeted therapies for AD and are quite prnset and progressioomising.
5. Another promising therapeutic approach is using antibody-based immunotherapy against Aβ to initiate its clearance or to reduce its neurotoxicity. Recently, Aducanumab, a human monoclonal antibody, when administered intravenously into transgenic mouse models of AD, was shown to selectively target the aggregated forms of Aβ by entering the brain and binding to parenchymal Aβ thereby reducing the soluble and in-soluble forms of Aβ in a dose dependent manner (Qu et al., 2012). Therefore, monoclonal antibody based immuno therapeutics hold a great promise in treating AD, besides other novel therapeutic approaches discussed above.

Future direction

Considering the complex nature of human health and disease, a single gene, protein, glycan or a phosphorylated site may be inadequate as a precise biomarker for diagnosis and for knowing the effective possible cure for any specific disease, so the need of the hour is to establish methods to develop PTM signatures and to develop PTM specific diagnostic and therapeutic interventions for the treatment of AD. Emerging technological approaches like metabolomics, lipidomics, and proteomics hold a great promise and intriguing role in identifying and predicting the progression of neurodegenerative diseases like AD by exploring changes occurring in cells, tissues, and biofluids; structure and function of AD-related proteins, protein-protein interactions (Schumacher-Schuh et al., 2021) and so there is a need to employ these technological approaches for reliable biomarker-based diagnostics and therapeutic interventions. Recently, Huo et al. used targeted multiomics strategy to assess blood and brain samples from different cohorts and reported different serum metabolites that play an important role in predicting cognitive decline in AD patients, as well as other brain metabolites related to neuropathological measurements (Huo et al., 2020). Multiomics profiling analysis of a group of elderly patients with normal cognition, mild cognitive impairments as well as with dementia have unraveled new pathways associated with AD pathology including homeostasis, extracellular matrix signaling as well as immune responses, which enabled researchers to define combination of molecules that could be useful in predicting cognitive impairments as well as omics signatures associated with AD pathology (Clark et al., 2021). Such approaches have made it possible to identify various transcripts and metabolites associated with metabolism of fatty acids and inflammation in AD patients showing disturbances in blood brain barrier and unusual exchange of metabolites. Moreover, new compounds related to AD pathology have been identified by lipidomic analysis in AD patients that include sphingolipids, phospholipids, and ceramides, which have been found to be linked with some neuronal deuteriations like memory impairments, hippocampus volume loss and rapid progression of AD (Han et al., 2011; Mielke et al., 2012). AD is multifactorial disease with varied parameters, of which certain belongs to metabolic changes and some are environmental as well. In order to enhance the specificity of certain biomarkers at varied geographical levels, we need to enhance the proteome analysis of AD patients with accurate and precise detections Untargeted proteome analysis is need of an hour at various AD hit geographical locations to achieve this goal of differential detections and to develop AD therapeutics. A common database generated based on proteome data from plaques or from sera of patients can not only provide an insight of whole protein compositions but also help us to differentiate the proteome of subjects having underlying disease as well giving clear image of changes associated with AD. By using TMT-LC/LC-MS/MS platforms, seven deep proteomic datasets have been developed recently, which identified > 8,000 proteins from 192 subjects (Bai et al., 2020; Higginbotham et al., 2020; Wang Z. et al., 2020; Sathe et al., 2021). These data sets of AD proteome could be used as control data for other geographical locations. After developing the data-sets from various geographical locations, we need to pool the data by high-throughput screening and develop an AI based system which can easily detect the changes in proteins associated with certain factor. So that we can easily make the datasets more reliable and the biomarkers associated with it.

To help identify new biomarkers for AD, molecular profiling which is based on integration of systems biology with high-throughput technology is the best way forward in this direction and these platforms are going to be a valuable tool in AD diagnostics. It is believed that systems biology-based approaches/platforms will help uncover the exact mechanisms involved in the pathogenesis of AD and help understand about triggering factors involved in the onset and progression of the disease (Sevigny et al., 2016). This, in turn, will enable researchers to design disease modifying therapies inhibiting key steps of pathogenesis, and thereby hindering the occurrence and progression of the disease (Hampel et al., 2015; Abeysinghe et al., 2020). Furthermore, it is hoped that recent developments in the identification of biomarkers like miRNAs in exosomes and understanding of circadian clock genes and their dysregulation at different stages will prove to be potential future generation biomarkers, which can revolutionize AD diagnostics. However, more research and validation are needed in this direction.

Conclusion

Biomarkers play a central role in the diagnosis of any disease, but the lack of clinically relevant biomarkers that can provide information about early disease stages as well as its subsequent progression has complicated development of effective treatments for AD. Several candidates as potential biomarkers for early diagnosis of AD are being studied worldwide. We have reviewed the recent literature related to most the advanced technical developments in the identification of biomarkers, like PTM signatures, levels of miRNAs in exosomes and have highlighted the need to understand circadian clock genes and their dysregulations at different stages, which are expected to be potential new generation biomarkers that can revolutionize AD diagnostics. The main hallmarks of AD include accumulation of insoluble proteins primarily composed of amyloid-β plaques and NFTs in the brain. In this review, we have described in detail how aberrant post-translational modifications of AD-related proteins like APP, Aβ, tau, and BACE1 are involved in impairing their normal function resulting in onset and progression

of AD. Finally, we also discussed recent developments and therapeutic approaches for AD based on targeted siRNA/miRNA therapeutics, exosome-based drug carriers, nanoparticle-based targeted therapies, CRISPR/Cas9 based gene-editing, monoclonal antibody-based immunotherapies, and phytochemicals which are highly promising interventions that can be employed for the management and treatment of AD in future.

Author contributions

TM and GA conceptualized the idea, developed the contents for this review, and approved the revised final manuscript. IM, MD, and TM prepared the first draft. IM, MA, MK, UM, MG, AB, GD, BA, and AH contributed in writing different sections/sub-section. IM, MA, AB, MK, and UM contributed in the preparation of original figures and tables. TM, GA, MD, IM, MA, MK, and UM contributed in critical revision of the manuscript.

Funding

We are gratefully and acknowledge the technical and financial support from the Ministry of Education and Deanship of Scientific Research (DSR), King Abdulaziz University, Jeddah, Saudi Arabia, under the Institutional Fund Projects Grant No. IFPDP-72-22. Research funding by the University Grants Commission (UGC), New Delhi, India, under BSR Grant No. F.30-357, 2017 (BSR) to TM and Research Fellowship (JRF) by CSIR, New Delhi, India, to IM is gratefully acknowledged.

Acknowledgments

TM acknowledges the help and support received from the University of Kashmir, India.

Conflict of interest

The authors declare that the research was conducted in the absence of any commercial or financial relationships that could be construed as a potential conflict of interest.

Publisher's note

References

Abeysinghe, A., Deshapriya, R., and Udawatte, C. (2020). Alzheimer's disease; a review of the pathophysiological basis and therapeutic interventions. *Life Sci.* 256:117996. doi: 10.1016/j.lfs.2020.117996

Abou-Abbass, H., Abou-El-Hassan, H., Bahmad, H., Zibara, K., Zebian, A., Youssef, R., et al. (2016). Glycosylation and other PTMs alterations in neurodegenerative diseases: Current status and future role in neurotrauma. *Electrophoresis* 37, 1549–1561. doi: 10.1002/elps.201500585

Absalon, S., Kochanek, D. M., Raghavan, V., and Krichevsky, A. M. (2013). MiR-26b, upregulated in Alzheimer's disease, activates cell cycle entry, tau-phosphorylation, and apoptosis in postmitotic neurons. *J. Neurosci.* 33, 14645–14659. doi: 10.1523/JNEUROSCI.1327-13.2013

Akasaka-Manya, K., and Manya, H. (2020). The Role of APP O-glycosylation in Alzheimer's Disease. *Biomolecules* 10:1569. doi: 10.3390/biom10111569

Akhondzadeh, S. (2017). New hopes for treatment of Alzheimer's disease. *Avicenna J. Med. Biotechnol.* 10:1.

Aksenov, M. Y., Tucker, H. M., Nair, P., Aksenova, M. V., Butterfield, D. A., Estus, S., et al. (1998). The expression of key oxidative stress-handling genes in different brain regions in Alzheimer's disease. *J. Mol. Neurosci.* 11, 151–164. doi: 10.1385/JMN:11:2:151

Alquezar, C., Arya, S., and Kao, A. W. (2021). Tau post-translational modifications: Dynamic transformers of tau function, degradation, and aggregation. *Front. Neurol.* 11:595532. doi: 10.3389/fneur.2020.595532

Alzheimer, A., Stelzma, R. A., Schnitzlein, H. N., and Murllagh, F. R. (1995). An english I'ranslation of Alzheimer's 1907 paper,"ijber eine eigenartige erlranliung der hirnrinde". *Clin. Anat.* 8, 429–431. doi: 10.1002/ca.980080612

Alzheimer's Association. (2019). 2019 Alzheimer's disease facts and figures. *Alzheimers Dement.* 15, 321–387. doi: 10.1016/j.jalz.2019.01.010

Andrew, R. J., Fernandez, C. G., Stanley, M., Jiang, H., Nguyen, P., Rice, R. C., et al. (2017). Lack of BACE1 S-palmitoylation reduces amyloid burden and mitigates memory deficits in transgenic mouse models of Alzheimer's disease. *Proc. Natl. Acad. Sci. U.S.A.* 114, E9665–E9674. doi: 10.1073/pnas.1708568114

Arbuzova, A., Schmitz, A. A., and Vergères, G. (2002). Cross-talk unfolded: MARCKS proteins. *Biochem. J.* 362, 1–12. doi: 10.1042/bj3620001

Ardito, F., Giuliani, M., Perrone, D., Troiano, G., and Lo Muzio, L. (2017). The crucial role of protein phosphorylation in cell signaling and its use as targeted therapy. *Int. J. Mol. Med.* 40, 271–280. doi: 10.3892/ijmm.2017.3036

Asai, H., Ikezu, S., Tsunoda, S., Medalla, M., Luebke, J., Haydar, T., et al. (2015). Depletion of microglia and inhibition of exosome synthesis halt tau propagation. *Nat. Neurosci.* 18, 1584–1593. doi: 10.1038/nn.4132

Ashton, N., Leuzy, A., Karikari, T., Mattsson-Carlgren, N., Dodich, A., Boccardi, M., et al. (2021). The validation status of blood biomarkers of amyloid and phospho-tau assessed with the 5-phase development framework for AD biomarkers. *Eur. J. Nucl. Med. Mol. Imaging* 48, 2140–2156. doi: 10.1007/s00259-021-05253-y

Augustinack, J. C., Schneider, A., Mandelkow, E.-M., and Hyman, B. T. (2002). Specific tau phosphorylation sites correlate with severity of neuronal cytopathology in Alzheimer's disease. *Acta Neuropathol.* 103, 26–35. doi: 10.1007/s004010100423

Avgerinos, K. I., Ferrucci, L., and Kapogiannis, D. (2021). Effects of monoclonal antibodies against amyloid-β on clinical and biomarker outcomes and adverse

event risks: A systematic review and meta-analysis of phase III RCTs in Alzheimer's disease. *Ageing Res. Rev.* 68:101339. doi: 10.1016/j.arr.2021.101339

Bai, B., Wang, X., Li, Y., Chen, P.-C., Yu, K., Dey, K. K., et al. (2020). Deep multilayer brain proteomics identifies molecular networks in Alzheimer's disease progression. *Neuron* 105, 975.–991. doi: 10.1016/j.neuron.2019.12.015

Balasubramanian, S., Verner, E., and Buggy, J. J. (2009). Isoform-specific histone deacetylase inhibitors: The next step? *Cancer Lett.* 280, 211–221. doi: 10.1016/j.canlet.2009.02.013

Baldeiras, I., Santana, I., Proença, M. T., Garrucho, M. H., Pascoal, R., Rodrigues, A., et al. (2008). Peripheral oxidative damage in mild cognitive impairment and mild Alzheimer's disease. *J. Alzheimers Dis.* 15, 117–128. doi: 10.3233/JAD-2008-15110

Balmuş, I.-M., Strungaru, S.-A., Ciobica, A., Nicoara, M.-N., Dobrin, R., Plavan, G., et al. (2017). Preliminary data on the interaction between some biometals and oxidative stress status in mild cognitive impairment and Alzheimer's disease patients. *Oxid. Med. Cell. Longev.* 2017:7156928. doi: 10.1155/2017/7156928

Bannister, A. J., and Kouzarides, T. (2011). Regulation of chromatin by histone modifications. *Cell Res.* 21, 381–395. doi: 10.1038/cr.2011.22

Barcelos, N. M., Van Ness, P. H., Wagner, A. F., MacAvoy, M. G., Mecca, A. P., Anderson, G. M., et al. (2018). Guanfacine treatment for prefrontal cognitive dysfunction in older participants: A randomized clinical trial. *Neurobiol. Aging* 70, 117–124. doi: 10.1016/j.neurobiolaging.2018.05.033

Barone, E., Di Domenico, F., Mancuso, C., and Butterfield, D. A. (2014). The Janus face of the heme oxygenase/biliverdin reductase system in Alzheimer disease: It's time for reconciliation. *Neurobiol. Dis.* 62, 144–159. doi: 10.1016/j.nbd.2013.09.018

Bellanti, F., Iannelli, G., Blonda, M., Tamborra, R., Villani, R., Romano, A., et al. (2017). Alterations of clock gene RNA expression in brain regions of a triple transgenic model of Alzheimer's disease. *J. Alzheimers Dis.* 59, 615–631. doi: 10.3233/JAD-160942

Benzi, G., and Moretti, A. (1995). Age-and peroxidative stress-related modifications of the cerebral enzymatic activities linked to mitochondria and the glutathione system. *Free Radic. Biol. Med.* 19, 77–101. doi: 10.1016/0891-5849(94)00244-E

Beshir, S. A., Aadithsoorya, A., Parveen, A., Goh, S. S. L., Hussain, N., and Menon, V. (2022). Aducanumab therapy to treat Alzheimer's disease: A narrative review. *Int. J. Alzheimers Dis.* 2022:9343514. doi: 10.1155/2022/9343514

Bezprozvanny, I., and Mattson, M. P. (2008). Neuronal calcium mishandling and the pathogenesis of Alzheimer's disease. *Trends Neurosci.* 31, 454–463. doi: 10.1016/j.tins.2008.06.005

Bhardwaj, S., Kesari, K. K., Rachamalla, M., Mani, S., Ashraf, G. M., Jha, S. K., et al. (2021). CRISPR/Cas9 gene editing: New hope for Alzheimer's disease therapeutics. *J. Adv. Res.* doi: 10.1016/j.jare.2021.07.001 [Epub ahead of print].

Bhat, R. V., Berg, S., Burrows, J., and Lindquist, J. (2007). "GSK-3 inhibitors for the treatment of Alzheimer's disease," in *Alzheimer's disease. topics in medicinal chemistry*, eds L. F. Lau and M. A. Brodney (Berlin: Springer), doi: 10.1007/7355_2007_015

Bhattacharya, T., Soares, G. A. B. E., Chopra, H., Rahman, M. M., Hasan, Z., Swain, S. S., et al. (2022). Applications of phyto-nanotechnology for the treatment of neurodegenerative disorders. *Materials* 15:804. doi: 10.3390/ma15030804

Bhattacharyya, R., Barren, C., and Kovacs, D. M. (2013). Palmitoylation of amyloid precursor protein regulates amyloidogenic processing in lipid rafts. *J. Neurosci.* 33, 11169–11183. doi: 10.1523/JNEUROSCI.4704-12.2013

Bieberich, E. (2014). Synthesis, processing, and function of N-glycans in N-glycoproteins. *Adv. Neurobiol.* 9, 47–70. doi: 10.1007/978-1-4939-1154-7_3

Blennow, K., Hampel, H., Weiner, M., and Zetterberg, H. (2010). Cerebrospinal fluid and plasma biomarkers in Alzheimer disease. *Nat. Rev. Neurol.* 6, 131–144. doi: 10.1038/nrneurol.2010.4

Blom, N., Sicheritz-Pontén, T., Gupta, R., Gammeltoft, S., and Brunak, S. (2004). Prediction of post-translational glycosylation and phosphorylation of proteins from the amino acid sequence. *Proteomics* 4, 1633–1649. doi: 10.1002/pmic.200300771

Boada, M., López, O., Núñez, L., Szczepiorkowski, Z. M., Torres, M., Grifols, C., et al. (2019). Plasma exchange for Alzheimer's disease management by albumin replacement (AMBAR) trial: Study design and progress. *Alzheimers Dement.* 5, 61–69. doi: 10.1016/j.trci.2019.01.001

Boccardi, M., Dodich, A., Albanese, E., Gayet-Ageron, A., Festari, C., and Ramusino, M. (2021). The strategic biomarker roadmap for the validation of Alzheimer's diagnostic biomarkers: Methodological update. *Eur. J. Nucl. Med. Mol. Imaging* 48, 2070–2085. doi: 10.1007/s00259-020-05120-2

Bolduc, D. M., Montagna, D. R., Seghers, M. C., Wolfe, M. S., and Selkoe, D. J. (2016). The amyloid-beta forming tripeptide cleavage mechanism of γ-secretase. *Elife* 5:e17578. doi: 10.7554/eLife.17578

Bourré, G., Cantrelle, F.-X., Kamah, A., Chambraud, B., Landrieu, I., and Smet-Nocca, C. (2018). Direct crosstalk between O-GlcNAcylation and phosphorylation of tau protein investigated by NMR spectroscopy. *Front. Endocrinol.* 9:595. doi: 10.3389/fendo.2018.00595

Brigelius-Flohé, R., and Traber, M. G. (1999). Vitamin E: Function and metabolism. *FASEB J.* 13, 1145–1155. doi: 10.1096/fasebj.13.10.1145

Bronisz, A., Wang, Y., Nowicki, M. O., Peruzzi, P., Ansari, K. I., Ogawa, D., et al. (2014). Extracellular vesicles modulate the glioblastoma microenvironment via a tumor suppression signaling network directed by miR-1. *Cancer Res.* 74, 738–750. doi: 10.1158/0008-5472.CAN-13-2650

Bu, G. (2009). Apolipoprotein E and its receptors in Alzheimer's disease: Pathways, pathogenesis and therapy. *Nat. Rev. Neurosci.* 10, 333–344. doi: 10.1038/nrn2620

Burstein, A., Sabbagh, M., Andrews, R., Valcarce, C., Dunn, I., and Altstiel, L. (2018). Development of Azeliragon, an oral small molecule antagonist of the receptor for advanced glycation endproducts, for the potential slowing of loss of cognition in mild Alzheimer's disease. *J. Prev. Alzheimers Dis.* 5, 149–154. doi: 10.14283/jpad.2018.18

Carlomagno, Y., Chung, D. C., Yue, M., Castanedes-Casey, M., Madden, B. J., Dunmore, J., et al. (2017). An acetylation–phosphorylation switch that regulates tau aggregation propensity and function. *J. Biol. Chem.* 292, 15277–15286. doi: 10.1074/jbc.M117.794602

Chatterjee, P., Fernando, M., Fernando, B., Dias, C. B., Shah, T., Silva, R., et al. (2020). Potential of coconut oil and medium chain triglycerides in the prevention and treatment of Alzheimer's disease. *Mech. Ageing Dev.* 186:111209. doi: 10.1016/j.mad.2020.111209

Chatterjee, S., Mizar, P., Cassel, R., Neidl, R., Selvi, B. R., Mohankrishna, D. V., et al. (2013). A novel activator of CBP/p300 acetyltransferases promotes neurogenesis and extends memory duration in adult mice. *J. Neurosci.* 33, 10698–10712. doi: 10.1523/JNEUROSCI.5772-12.2013

Chen, G.-F., Xu, T.-H., Yan, Y., Zhou, Y.-R., Jiang, Y., Melcher, K., et al. (2017). Amyloid beta: Structure, biology and structure-based therapeutic development. *Acta Pharmacol. Sin.* 38, 1205–1235. doi: 10.1038/aps.2017.28

Chen, Lf, Fischle, W., Verdin, E., and Greene, W. C. (2001). Duration of nuclear NF-κB action regulated by reversible acetylation. *Science* 293, 1653–1657. doi: 10.1126/science.1062374

Cheng, X., Liu, Z., Liu, B., Zhao, T., Li, Y., and Alam, H. B. (2015). Selective histone deacetylase 6 inhibition prolongs survival in a lethal two-hit model. *J. Surg. Res.* 197, 39–44. doi: 10.1016/j.jss.2015.02.070

Cho, E., and Park, M. (2016). Palmitoylation in Alzheimer? s disease and other neurodegenerative diseases. *Pharmacol. Res.* 111, 133–151. doi: 10.1016/j.phrs.2016.06.008

Cho, S.-J., Roman, G., Yeboah, F., and Konishi, Y. (2007). The road to advanced glycation end products: A mechanistic perspective. *Curr. Med. Chem.* 14, 1653–1671. doi: 10.2174/092986707780830989

Chong, F. P., Ng, K. Y., Koh, R. Y., and Chye, S. M. (2018). Tau proteins and tauopathies in Alzheimer's disease. *Cell. Mol. Neurobiol.* 38, 965–980. doi: 10.1007/s10571-017-0574-1

Chopra, H., Dey, P. S., Das, D., Bhattacharya, T., Shah, M., Mubin, S., et al. (2021). Curcumin nanoparticles as promising therapeutic agents for drug targets. *Molecules* 26:4998. doi: 10.3390/molecules26164998

Chun, Y. S., Kwon, O.-H., Oh, H. G., Kim, T.-W., McIntire, L. B., Park, M. K., et al. (2015b). Threonine 576 residue of amyloid-β precursor protein regulates its trafficking and processing. *Biochem. Biophys. Res. Commun.* 467, 955–960. doi: 10.1016/j.bbrc.2015.10.037

Chun, Y. S., Park, Y., Oh, H. G., Kim, T.-W., Yang, H. O., Park, M. K., et al. (2015a). O-GlcNAcylation promotes non-amyloidogenic processing of amyloid-β protein precursor via inhibition of endocytosis from the plasma membrane. *J. Alzheimers Dis.* 44, 261–275. doi: 10.3233/JAD-140096

Citron, M. (2010). Alzheimer's disease: Strategies for disease modification. *Nat. Rev. Drug Discov.* 9, 387–398. doi: 10.1038/nrd2896

Clark, C., Dayon, L., Masoodi, M., Bowman, G. L., and Popp, J. (2021). An integrative multi-omics approach reveals new central nervous system pathway alterations in Alzheimer's disease. *Alzheimers Res. Ther.* 13, 1–19. doi: 10.1186/s13195-021-00814-7

Clausen, H., and Bennett, E. P. (1996). A family of UDP-GalNAc: Polypeptide N-acetylgalactosaminyl-transferases control the initiation of mucin-type O-linked glycosylation. *Glycobiology* 6, 635–646. doi: 10.1093/glycob/6.6.635

Cooper, D., and Gupta, V. (2020). *Lumateperone*. Tampa, FL: StatPearls.

Corder, E. H., Saunders, A. M., Strittmatter, W. J., Schmechel, D. E., Gaskell, P. C., Small, G., et al. (1993). Gene dose of apolipoprotein E type 4 allele and the risk of Alzheimer's disease in late onset families. *Science* 261, 921–923. doi: 10.1126/science.8346443

Correia, A. S., and Vale, N. (2021). Antidepressants in Alzheimer's disease: A focus on the role of mirtazapine. *Pharmaceuticals (Basel)* 14:930. doi: 10.3390/ph14090930

Craft, S., Claxton, A., Baker, L. D., Hanson, A. J., Cholerton, B., Trittschuh, E. H., et al. (2017). Effects of regular and long-acting insulin on cognition and Alzheimer's disease biomarkers: A pilot clinical trial. *J. Alzheimers Dis.* 57, 1325–1334. doi: 10.3233/JAD-161256

Cruz, J. C., Tseng, H.-C., Goldman, J. A., Shih, H., and Tsai, L.-H. (2003). Aberrant Cdk5 activation by p25 triggers pathological events leading to neurodegeneration and neurofibrillary tangles. *Neuron* 40, 471–483. doi: 10.1016/S0896-6273(03)00627-5

Cummings, J., Lee, G., Ritter, A., and Zhong, K. (2018). Alzheimer's disease drug development pipeline: 2018. *Alzheimers Dement.* 4, 195–214. doi: 10.1016/j.trci.2018.03.009

Cummings, J., Lee, G., Ritter, A., Sabbagh, M., and Zhong, K. (2020). Alzheimer's disease drug development pipeline: 2020. *Alzheimers Dement.* 6:e12050. doi: 10.1002/trc2.12050

Cummings, J., Lee, G., Ritter, A., Sabbagh, M., Zhong, K., Research, D. T., et al. (2019). Alzheimer's disease drug development pipeline: 2019. *Alzheimers Dement.* 5, 272–293. doi: 10.1016/j.trci.2019.05.008

d'Abramo, C., D'adamio, L., and Giliberto, L. (2020). Significance of blood and cerebrospinal fluid biomarkers for Alzheimer's disease: Sensitivity, specificity and potential for clinical use. *J. Pers. Med.* 10:116. doi: 10.3390/jpm10030116

Das, U., Scott, D. A., Ganguly, A., Koo, E. H., Tang, Y., and Roy, S. (2013). Activity-induced convergence of APP and BACE-1 in acidic microdomains via an endocytosis-dependent pathway. *Neuron* 79, 447–460. doi: 10.1016/j.neuron.2013.05.035

De Vos, A., Jacobs, D., Struyfs, H., Fransen, E., Andersson, K., Portelius, E., et al. (2015). C-terminal neurogranin is increased in cerebrospinal fluid but unchanged in plasma in Alzheimer's disease. *Alzheimers Dement.* 11, 1461–1469. doi: 10.1016/j.jalz.2015.05.012

Deibel, M., Ehmann, W., and Markesbery, W. (1996). Copper, iron, and zinc imbalances in severely degenerated brain regions in Alzheimer's disease: Possible relation to oxidative stress. *J. Neurol. Sci.* 143, 137–142. doi: 10.1016/S0022-510X(96)00203-1

Delabio, R., Rasmussen, L., Mizumoto, I., Viani, G.-A., Chen, E., Villares, J., et al. (2014). PSEN1 and PSEN2 gene expression in Alzheimer's disease brain: A new approach. *J. Alzheimers Dis.* 42, 757–760. doi: 10.3233/JAD-140033

Deribe, Y. L., Pawson, T., and Dikic, I. (2010). Post-translational modifications in signal integration. *Nat. Struct. Mol. Biol.* 17, 666–672. doi: 10.1038/nsmb.1842

Despres, C., Byrne, C., Qi, H., Cantrelle, F.-X., Huvent, I., Chambraud, B., et al. (2017). Identification of the Tau phosphorylation pattern that drives its aggregation. *Proc. Natl. Acad. Sci. U.S.A.* 114, 9080–9085. doi: 10.1073/pnas.1708448114

Detke, M., Lynch, C., Holsinger, L., Kapur, S., Hennings, D., Raha, D., et al. (2020). COR388 for the treatment of Alzheimer's disease (4098). *Neurology* 94:4098.

Dewsbury, L. S., Lim, C. K., and Steiner, G. (2021). The efficacy of ketogenic therapies in the clinical management of people with neurodegenerative disease: A systematic review. *Adv. Nutr.* 12, 1571–1593. doi: 10.1093/advances/nmaa180

Di Meco, A., Joshi, Y. B., and Praticò, D. (2014). Sleep deprivation impairs memory, tau metabolism, and synaptic integrity of a mouse model of Alzheimer's disease with plaques and tangles. *Neurobiol. Aging* 35, 1813–1820. doi: 10.1016/j.neurobiolaging.2014.02.011

DiCarlo, J. E., Sengillo, J. D., Justus, S., Cabral, T., Tsang, S. H., and Mahajan, V. B. (2017). CRISPR-cas genome surgery in ophthalmology. *Transl. Vis. Sci. Technol.* 6:13. doi: 10.1167/tvst.6.3.13

Ding, M., Shen, Y., Wang, P., Xie, Z., Xu, S., Zhu, Z., et al. (2018). Exosomes isolated from human umbilical cord mesenchymal stem cells alleviate neuroinflammation and reduce amyloid-beta deposition by modulating microglial activation in Alzheimer's disease. *Neurochem. Res.* 43, 2165–2177. doi: 10.1007/s11064-018-2641-5

Dinkins, M. B., Dasgupta, S., Wang, G., Zhu, G., and Bieberich, E. (2014). Exosome reduction in vivo is associated with lower amyloid plaque load in the 5XFAD mouse model of Alzheimer's disease. *Neurobiol. Aging* 35, 1792–1800. doi: 10.1016/j.neurobiolaging.2014.02.012

Dorval, V., and Fraser, P. E. (2006). Small ubiquitin-like modifier (SUMO) modification of natively unfolded proteins tau and α-synuclein. *J. Biol. Chem.* 281, 9919–9924. doi: 10.1074/jbc.M510127200

Dunkelberger, E. B., Buchanan, L. E., Marek, P., Cao, P., Raleigh, D. P., and Zanni, M. T. (2012). Deamidation accelerates amyloid formation and alters amylin fiber structure. *J. Am. Chem. Soc.* 134, 12658–12667. doi: 10.1021/ja3039486

Ebneth, A., Godemann, R., Stamer, K., Illenberger, S., Trinczek, B., Mandelkow, E.-M., et al. (1998). Overexpression of tau protein inhibits kinesin-dependent trafficking of vesicles, mitochondria, and endoplasmic reticulum: Implications for Alzheimer's disease. *J. Cell Biol.* 143, 777–794. doi: 10.1083/jcb.143.3.777

Egan, M. F., Kost, J., Tariot, P. N., Aisen, P. S., Cummings, J. L., Vellas, B., et al. (2018). Randomized trial of verubecestat for mild-to-moderate Alzheimer's disease. *N. Engl. J. Med.* 378, 1691–1703. doi: 10.1056/NEJMoa1706441

Elbassal, E. A., Morris, C., Kent, T. W., Lantz, R., Ojha, B., Wojcikiewicz, E. P., et al. (2017). Gold nanoparticles as a probe for amyloid-β oligomer and amyloid formation. *J. Phys. Chem. C* 121, 20007–20015. doi: 10.1021/acs.jpcc.7b05169

Eldar-Finkelman, H., and Martinez, A. (2011). GSK-3 inhibitors: Preclinical and clinical focus on CNS. *Front. Mol. Neurosci.* 4:32. doi: 10.3389/fnmol.2011.00032

Elder, G. A., Gama Sosa, M. A., and De Gasperi, R. (2010). Transgenic mouse models of Alzheimer's disease. *Mt. Sinai. J. Med.* 77, 69–81. doi: 10.1002/msj.20159

Ettcheto, M., Cano, A., Sanchez-López, E., Verdaguer, E., Folch, J., Auladell, C., et al. (2021). Masitinib for the treatment of Alzheimer's disease. *Neurodegener. Dis. Manag.* 11, 263–276. doi: 10.2217/nmt-2021-0019

Evin, G., Barakat, A., and Masters, C. L. (2010). BACE: Therapeutic target and potential biomarker for Alzheimer's disease. *Int. J. Biochem. Cell Biol.* 42, 1923–1926. doi: 10.1016/j.biocel.2010.08.017

Familtseva, A., Jeremic, N., and Tyagi, S. C. (2019). Exosomes: Cell-created drug delivery systems. *Mol. Cell. Biochem.* 459, 1–6. doi: 10.1007/s11010-019-03545-4

Fan, S.-J., Huang, F.-I., Liou, J.-P., and Yang, C.-R. (2018). The novel histone de acetylase 6 inhibitor, MPT0G211, ameliorates tau phosphorylation and cognitive deficits in an Alzheimer's disease model. *Cell Death Dis.* 9, 1–14. doi: 10.1038/s41419-018-0688-5

Farheen, Khan, M. A., Ashraf, G. M., Bilgrami, A. L., and Rizvi, M. (2021). New horizons in the treatment of neurological disorders with tailorable gold nanoparticles. *Curr. Drug Metab.* 22, 931–938. doi: 10.2174/1389200222666210525123416

Farris, W., Mansourian, S., Chang, Y., Lindsley, L., Eckman, E. A., Frosch, M. P., et al. (2003). Insulin-degrading enzyme regulates the levels of insulin, amyloid β-protein, and the β-amyloid precursor protein intracellular domain in vivo. *Proc. Natl. Acad. Sci. U.S.A.* 100, 4162–4167. doi: 10.1073/pnas.0230450100

Feligioni, M., and Nisticò, R. (2013). SUMO: A (oxidative) stressed protein. *Neuromolecular Med.* 15, 707–719. doi: 10.1007/s12017-013-8266-6

Feligioni, M., Marcelli, S., Knock, E., Nadeem, U., Arancio, O., and Fraser, P. E. (2015). SUMO modulation of protein aggregation and degradation. *AIMS Mol. Sci.* 2, 382–410. doi: 10.3934/molsci.2015.4.382

Fleming, L. M., and Johnson, G. V. (1995). Modulation of the phosphorylation state of tau in situ: The roles of calcium and cyclic AMP. *Biochem. J.* 309, 41–47. doi: 10.1042/bj3090041

Folch, J., Petrov, D., Ettcheto, M., Pedros, I., Abad, S., Beas-Zarate, C., et al. (2015). Masitinib for the treatment of mild to moderate Alzheimer's disease. *Expert Rev. Neurother.* 15, 587–596. doi: 10.1586/14737175.2015.1045419

Frieden, C., and Garai, K. (2012). Structural differences between apoE3 and apoE4 may be useful in developing therapeutic agents for Alzheimer's disease. *Proc. Natl. Acad. Sci. U.S.A.* 109, 8913–8918. doi: 10.1073/pnas.1207022109

Furtado, D., Björnmalm, M., Ayton, S., Bush, A. I., Kempe, K., and Caruso, F. (2018). Overcoming the blood–brain barrier: The role of nanomaterials in treating neurological diseases. *Adv. Mater.* 30:1801362. doi: 10.1002/adma.201801362

Gaiottino, J., Norgren, N., Dobson, R., Topping, J., Nissim, A., Malaspina, A., et al. (2013). Increased neurofilament light chain blood levels in neurodegenerative neurological diseases. *PLoS One* 8:e75091. doi: 10.1371/journal.pone.0075091

Galimberti, D., and Scarpini, E. (2012). Progress in Alzheimer's disease. *J. Neurol.* 259, 201–211. doi: 10.1007/s00415-011-6145-3

Galimberti, D., and Scarpini, E. (2017). Pioglitazone for the treatment of Alzheimer's disease. *Expert Opin. Investig. Drugs* 26, 97–101. doi: 10.1080/13543784.2017.1265504

German, D. M., Mitalipov, S., Mishra, A., and Kaul, S. (2019). Therapeutic genome editing in cardiovascular diseases. *JACC: Basic Transl. Sci.* 4, 122–131. doi: 10.1016/j.jacbts.2018.11.004

Giri, M., Zhang, M., and Lü, Y. (2016). Genes associated with Alzheimer's disease: An overview and current status. *Clin. Interv. Aging* 11:665. doi: 10.2147/CIA.S105769

Goedert, M., Spillantini, M., Jakes, R., Rutherford, D., and Crowther, R. (1989). Multiple isoforms of human microtubule-associated protein tau: Sequences and localization in neurofibrillary tangles of Alzheimer's disease. *Neuron* 3, 519–526. doi: 10.1016/0896-6273(89)90210-9

Gong, B., Chen, F., Pan, Y., Arrieta-Cruz, I., Yoshida, Y., Haroutunian, V., et al. (2010). SCFFbx2-E3-ligase-mediated degradation of BACE1 attenuates Alzheimer's disease amyloidosis and improves synaptic function. *Aging Cell* 9, 1018–1031. doi: 10.1111/j.1474-9726.2010.00632.x

Gonzalez-Santamarta, M., Quinet, G., Reyes-Garau, D., Sola, B., Roué, G., and Rodriguez, M. S. (2020). Resistance to the proteasome inhibitors: Lessons from multiple myeloma and mantle cell lymphoma. *Adv. Exp. Med. Biol.* 1233, 153–174. doi: 10.1007/978-3-030-38266-7_6

Gorantla, N. V., Sunny, L. P., Rajasekhar, K., Nagaraju, P. G., Cg, P. P., Govindaraju, T., et al. (2021). Amyloid-β-derived peptidomimetics inhibits tau aggregation. *ACS Omega.* 6, 11131–11138. doi: 10.1021/acsomega.9b03497

Graeber, M., Kösel, S., Egensperger, R., Banati, R., Müller, U., Bise, K., et al. (1997). Rediscovery of the case described by alois Alzheimer in 1911: Historical, histological and molecular genetic analysis. *Neurogenetics* 1, 73–80. doi: 10.1007/s100480050011

Gräff, J., Rei, D., Guan, J.-S., Wang, W.-Y., Seo, J., Hennig, K. M., et al. (2012). An epigenetic blockade of cognitive functions in the neurodegenerating brain. *Nature* 483, 222–226. doi: 10.1038/nature10849

Griebel, G., Stemmelin, J., Lopez-Grancha, M., Boulay, D., Boquet, G., Slowinski, F., et al. (2019). The selective GSK3 inhibitor, SAR502250, displays neuroprotective activity and attenuates behavioral impairments in models of neuropsychiatric symptoms of Alzheimer's disease in rodents. *Sci. Rep.* 9, 1–15. doi: 10.1038/s41598-019-54557-5

Guan, J.-S., Haggarty, S. J., Giacometti, E., Dannenberg, J.-H., Joseph, N., Gao, J., et al. (2009). HDAC2 negatively regulates memory formation and synaptic plasticity. *Nature* 459, 55–60. doi: 10.1038/nature07925

Guo, Q., Furukawa, K., Sopher, B. L., Pham, D. G., Xie, J., Robinson, N., et al. (1996). Alzheimer's PS-1 mutation perturbs calcium homeostasis and sensitizes PC12 cells to death induced by amyloid β-peptide. *Neuroreport* 8, 379–383. doi: 10.1097/00001756-199612200-00074

Gupta, V., Laws, S. M., Villemagne, V. L., Ames, D., Bush, A. I., Ellis, K. A., et al. (2011). Plasma apolipoprotein E and Alzheimer disease risk: The AIBL study of aging. *Neurology* 76, 1091–1098. doi: 10.1212/WNL.0b013e318211c352

Hampel, H., Lista, S., Vanmechelen, E., Zetterberg, H., Giorgi, F. S., Galgani, A., et al. (2020). β-Secretase1 biological markers for Alzheimer's disease: State-of-art of validation and qualification. *Alzheimers Res. Ther.* 12, 1–14. doi: 10.1186/s13195-020-00686-3

Hampel, H., O'Bryant, S. E., Molinuevo, J. L., Zetterberg, H., Masters, C. L., Lista, S., et al. (2018). Blood-based biomarkers for Alzheimer disease: Mapping the road to the clinic. *Nat. Rev. Neurol.* 14, 639–652. doi: 10.1038/s41582-018-0079-7

Hampel, H., Schneider, L. S., Giacobini, E., Kivipelto, M., Sindi, S., Dubois, B., et al. (2015). Advances in the therapy of Alzheimer's disease: Targeting amyloid beta and tau and perspectives for the future. *Expert Rev. Neurother.* 15, 83–105. doi: 10.1586/14737175.2015.995637

Han, X., Rozen, S., Boyle, S. H., Hellegers, C., Cheng, H., Burke, J. R., et al. (2011). Metabolomics in early Alzheimer's disease: Identification of altered plasma sphingolipidome using shotgun lipidomics. *PLoS One* 6:e21643. doi: 10.1371/journal.pone.0021643

Hanger, D. P., Anderton, B. H., and Noble, W. (2009). Tau phosphorylation: The therapeutic challenge for neurodegenerative disease. *Trends Mol. Med.* 15, 112–119. doi: 10.1016/j.molmed.2009.01.003

Hanger, D. P., Byers, H. L., Wray, S., Leung, K.-Y., Saxton, M. J., Seereeram, A., et al. (2007). Novel phosphorylation sites in tau from Alzheimer brain support a role for casein kinase 1 in disease pathogenesis. *J. Biol. Chem.* 282, 23645–23654. doi: 10.1074/jbc.M703269200

Hansen, D. V., Hanson, J. E., and Sheng, M. (2018). Microglia in Alzheimer's disease. *J. Cell Biol.* 217, 459–472. doi: 10.1083/jcb.201709069

Haque, R. U., and Levey, A. I. (2019). Alzheimer's disease: A clinical perspective and future nonhuman primate research opportunities. *Proc. Natl. Acad. Sci. U.S.A.* 116, 26224–26229. doi: 10.1073/pnas.1912954116

Hardy, J., and Selkoe, D. J. (2002). The amyloid hypothesis of Alzheimer's disease: Progress and problems on the road to therapeutics. *Science* 297, 353–356. doi: 10.1126/science.1072994

Haukedal, H., and Freude, K. K. (2021). Implications of glycosylation in Alzheimer's disease. *Front. Neurosci.* 14:625348. doi: 10.3389/fnins.2020.625348

Henriksen, K., O'Bryant, S. E., Hampel, H., Trojanowski, J. Q., Montine, T. J., Jeromin, A., et al. (2014). The future of blood-based biomarkers for Alzheimer's disease. *Alzheimers Dement.* 10, 115–131. doi: 10.1016/j.jalz.2013.01.013

Heston, L., and White, J. (1978). Pedigrees of 30 families with Alzheimer disease: Associations with defective organization of microfilaments and microtubules. *Behav. Genet.* 8, 315–331. doi: 10.1007/BF01067395

Higginbotham, L., Ping, L., Dammer, E. B., Duong, D. M., Zhou, M., Gearing, M., et al. (2020). Integrated proteomics reveals brain-based cerebrospinal fluid biomarkers in asymptomatic and symptomatic Alzheimer's disease. *Sci. Adv.* 6:eaaz9360. doi: 10.1126/sciadv.aaz9360

Honig, L. S., Vellas, B., Woodward, M., Boada, M., Bullock, R., Borrie, M., et al. (2018). Trial of solanezumab for mild dementia due to Alzheimer's disease. *N. Engl. J. Med.* 378, 321–330. doi: 10.1056/NEJMoa1705971

Hooli, B., and Tanzi, R. E. (2016). *The genetic basis of Alzheimer's disease: Findings from genome-wide studies. Genomics, circuits, and pathways in clinical neuropsychiatry*. New York, NY: Elsevier, 547–571. doi: 10.1016/B978-0-12-800105-9.00034-2

Hu, G., Yang, L., Cai, Y., Niu, F., Mezzacappa, F., Callen, S., et al. (2016). Emerging roles of extracellular vesicles in neurodegenerative disorders: Focus on HIV-associated neurological complications. *Cell Death Dis.* 7:e2481. doi: 10.1038/cddis.2016.336

Hu, S., Begum, A. N., Jones, M. R., Oh, M. S., Beech, W. K., Beech, B. H., et al. (2009). GSK3 inhibitors show benefits in an Alzheimer's disease (AD) model of neurodegeneration but adverse effects in control animals. *Neurobiol. Dis.* 33, 193–206. doi: 10.1016/j.nbd.2008.10.007

Huang, L.-K., Chao, S.-P., and Hu, C.-J. (2020). Clinical trials of new drugs for Alzheimer disease. *J. Biomed. Sci.* 27, 1–13. doi: 10.1186/s12929-019-0609-7

Humphrey, S. J., James, D. E., and Mann, M. (2015). Protein phosphorylation: A major switch mechanism for metabolic regulation. *Trends Endocrinol. Metab.* 26, 676–687. doi: 10.1016/j.tem.2015.09.013

Hung, S.-Y., and Fu, W.-M. (2017). Drug candidates in clinical trials for Alzheimer's disease. *J. Biomed. Sci.* 24, 1–12. doi: 10.1186/s12929-017-0355-7

Huo, Z., Yu, L., Yang, J., Zhu, Y., Bennett, D. A., and Zhao, J. (2020). Brain and blood metabolome for Alzheimer's dementia: Findings from a targeted metabolomics analysis. *Neurobiol. Aging* 86, 123–133. doi: 10.1016/j.neurobiolaging.2019.10.014

Husain, M. A., Laurent, B., and Plourde, M. (2021). APOE and Alzheimer's disease: From lipid transport to physiopathology and therapeutics. *Front. Neurosci.* 15:630502. doi: 10.3389/fnins.2021.630502

Ihara, M., and Saito, S. (2020). Drug repositioning for Alzheimer's disease: Finding hidden clues in old drugs. *J. Alzheimers Dis.* 74, 1013–1028. doi: 10.3233/JAD-200049

Iqbal, K., Liu, F., and Gong, C.-X. (2016). Tau and neurodegenerative disease: The story so far. *Nat. Rev. Neurol.* 12, 15–27. doi: 10.1038/nrneurol.2015.225

Janas, A. M., Sapoń, K., Janas, T., Stowell, M. H., and Janas, T. (2016). Exosomes and other extracellular vesicles in neural cells and neurodegenerative diseases. *Biochim. Biophys. Acta* 1858, 1139–1151. doi: 10.1016/j.bbamem.2016.02.011

Janeiro, M. H., Ardanaz, C. G., Sola-Sevilla, N., Dong, J., Cortés-Erice, M., Solas, M., et al. (2021). Biomarkers in Alzheimer's disease. *Adv. Lab. Med. Av. En Med. Lab.* 2, 27–37. doi: 10.1515/almed-2020-0090

Janelidze, S., Hertze, J., Zetterberg, H., Landqvist Waldö, M., Santillo, A., Blennow, K., et al. (2016b). Cerebrospinal fluid neurogranin and YKL-40 as biomarkers of Alzheimer's disease. *Ann. Clin. Transl. Neurol.* 3, 12–20. doi: 10.1002/acn3.266

Janelidze, S., Stomrud, E., Palmqvist, S., Zetterberg, H., Van Westen, D., Jeromin, A., et al. (2016a). Plasma β-amyloid in Alzheimer's disease and vascular disease. *Sci. Rep.* 6, 1–11. doi: 10.1038/srep26801

Jara-Guajardo, P., Cabrera, P., Celis, F., Soler, M., Berlanga, I., Parra-Muñoz, N., et al. (2020). Gold nanoparticles mediate improved detection of β-amyloid aggregates by fluorescence. *Nanomaterials* 10:690. doi: 10.3390/nano10040690

Juang, Y.-C., Landry, M.-C., Sanches, M., Vittal, V., Leung, C. C., Ceccarelli, D. F., et al. (2012). OTUB1 co-opts Lys48-linked ubiquitin recognition to suppress E2 enzyme function. *Mol. Cell* 45, 384–397. doi: 10.1016/j.molcel.2012.01.011

Kaidanovich-Beilin, O., and Eldar-Finkelman, H. (2006). Long-term treatment with novel glycogen synthase kinase-3 inhibitor improves glucose homeostasis in ob/ob mice: Molecular characterization in liver and muscle. *J. Pharmacol. Exp. Ther.* 316, 17–24. doi: 10.1124/jpet.105.090266

Kaidanovich-Beilin, O., Milman, A., Weizman, A., Pick, C. G., and Eldar-Finkelman, H. (2004). Rapid antidepressive-like activity of specific glycogen synthase kinase-3 inhibitor and its effect on β-catenin in mouse hippocampus. *Biol. Psychiatry* 55, 781–784. doi: 10.1016/j.biopsych.2004.01.008

Kametani, F., and Hasegawa, M. (2018). Reconsideration of amyloid hypothesis and tau hypothesis in Alzheimer's disease. *Front. Neurosci.* 12:25. doi: 10.3389/fnins.2018.00025

Kang, M. J., Hsu, M., Krajbich, I. M., Loewenstein, G., McClure, S. M., Wang, J. T.-Y., et al. (2009). The wick in the candle of learning: Epistemic curiosity activates reward circuitry and enhances memory. *Psychol. Sci.* 20, 963–973. doi: 10.1111/j.1467-9280.2009.02402.x

Karimian, A., Gorjizadeh, N., Alemi, F., Asemi, Z., Azizian, K., Soleimanpour, J., et al. (2020). CRISPR/Cas9 novel therapeutic road for the treatment of neurodegenerative diseases. *Life Sci.* 259:118165. doi: 10.1016/j.lfs.2020.118165

Karthivashan, G., Ganesan, P., Park, S.-Y., Kim, J.-S., and Choi, D.-K. (2018). Therapeutic strategies and nano-drug delivery applications in management of ageing Alzheimer's disease. *Drug Deliv.* 25, 307–320. doi: 10.1080/10717544.2018.1428243

Keller, J. N., Guo, Q., Holtsberg, F., Bruce-Keller, A., and Mattson, M. P. (1998). Increased sensitivity to mitochondrial toxin-induced apoptosis in neural cells expressing mutant presenilin-1 is linked to perturbed calcium homeostasis and enhanced oxyradical production. *J. Neurosci.* 18, 4439–4450. doi: 10.1523/JNEUROSCI.18-12-04439.1998

Khaksarian, M., Mirr, I., Kordian, S., Nooripour, R., Ahangari, N., Masjedi-Arani, A., et al. (2021). A comparison of methylphenidate (MPH) and combined methylphenidate with crocus sativus (Saffron) in the treatment of children and adolescents with ADHD: A randomized, double-blind, parallel-group, clinical trial. Iran. *J. Psychiatry Behav. Sci.* 15:e108390. doi: 10.5812/ijpbs.108390

Khan, N. H., Mir, M., Ngowi, E. E., Zafar, U., Khakwani, M. M. A. K., Khattak, S., et al. (2021). Nanomedicine: A Promising way to manage Alzheimer's disease. *Front. Bioeng. Biotechnol.* 9:630055. doi: 10.3389/fbioe.2021.630055

Khoury, R. (2022). Deuterated dextromethorphan/quinidine for agitation in Alzheimer's disease. *Neural Regen. Res.* 17:1013. doi: 10.4103/1673-5374.324842

Khoury, R., Marx, C., Mirgati, S., Velury, D., Chakkamparambil, B., and Grossberg, G. (2021). AVP-786 as a promising treatment option for Alzheimer's disease including agitation. *Expert Opin. Pharmacother.* 22, 783–795. doi: 10.1080/14656566.2021.1882995

Kim, C., Nam, D. W., Park, S. Y., Song, H., Hong, H. S., Boo, J. H., et al. (2013). O-linked β-N-acetylglucosaminidase inhibitor attenuates β-amyloid plaque and rescues memory impairment. *Neurobiol. Aging* 34, 275–285. doi: 10.1016/j.neurobiolaging.2012.03.001

Kim, J., Basak, J. M., and Holtzman, D. M. (2009). The role of apolipoprotein E in Alzheimer's disease. *Neuron* 63, 287–303. doi: 10.1016/j.neuron.2009.06.026

Kimura, Y., and Tanaka, K. (2010). Regulatory mechanisms involved in the control of ubiquitin homeostasis. *J. Biochem.* 147, 793–798. doi: 10.1093/jb/mvq044

Kizuka, Y., Kitazume, S., and Taniguchi, N. (2017). N-glycan and Alzheimer's disease. *Biochim. Biophys. Acta Gen. Subj.* 1861, 2447–2454. doi: 10.1016/j.bbagen.2017.04.012

Kizuka, Y., Kitazume, S., Fujinawa, R., Saito, T., Iwata, N., Saido, T. C., et al. (2015). An aberrant sugar modification of BACE 1 blocks its lysosomal targeting in A lzheimer's disease. *EMBO Mol. Med.* 7, 175–189. doi: 10.15252/emmm.201404438

Klein, G., Delmar, P., Voyle, N., Rehal, S., Hofmann, C., Abi-Saab, D., et al. (2019). Gantenerumab reduces amyloid-β plaques in patients with prodromal to moderate Alzheimer's disease: A PET substudy interim analysis. *Alzheimers Res. Ther.* 11, 1–12. doi: 10.1186/s13195-019-0559-z

Knezevic, D., Mizrahi, R. J., and Psychiatry, B. (2018). Molecular imaging of neuroinflammation in Alzheimer's disease and mild cognitive impairment. *Prog. Neuropsychopharmacol. Biol. Psychiatry* 80, 123–131. doi: 10.1016/j.pnpbp.2017.05.007

Ko, L. W., Ko, E. C., Nacharaju, P., Liu, W.-K., Chang, E., Kenessey, A., et al. (1999). An immunochemical study on tau glycation in paired helical filaments. *Brain Res.* 830, 301–313. doi: 10.1016/S0006-8993(99)01415-8

Kuhla, B., Haase, C., Flach, K., Lüth, H.-J., Arendt, T., and Münch, G. (2007). Effect of pseudophosphorylation and cross-linking by lipid peroxidation and advanced glycation end product precursors on tau aggregation and filament formation. *J. Biol. Chem.* 282, 6984–6991. doi: 10.1074/jbc.M609521200

Kumar, A., Choi, K.-H., Renthal, W., Tsankova, N. M., Theobald, D. E., Truong, H.-T., et al. (2005). Chromatin remodeling is a key mechanism underlying cocaine-induced plasticity in striatum. *Neuron* 48, 303–314. doi: 10.1016/j.neuron.2005.09.023

Kuo, M. H., and Allis, C. D. (1998). Roles of histone acetyltransferases and deacetylases in gene regulation. *Bioessays* 20, 615–626. doi: 10.1002/(SICI)1521-1878(199808)20:8<615::AID-BIES4>3.0.CO;2-H

Lanyon-Hogg, T., Faronato, M., Serwa, R. A., and Tate, E. W. (2017). Dynamic protein acylation: New substrates, mechanisms, and drug targets. *Trends Biochem. Sci.* 42, 566–581. doi: 10.1016/j.tibs.2017.04.004

Laske, C., Leyhe, T., Stransky, E., Hoffmann, N., Fallgatter, A. J., and Dietzsch, J. (2011). Identification of a blood-based biomarker panel for classification of Alzheimer's disease. *Int. J. Neuropsychopharmacol.* 14, 1147–1155. doi: 10.1017/S1461145711000459

Lau, P., Bossers, K., Janky, R. S., Salta, E., Frigerio, C. S., Barbash, S., et al. (2013). Alteration of the micro RNA network during the progression of Alzheimer's disease. *EMBO Mol. Med.* 5, 1613–1634. doi: 10.1002/emmm.201201974

Lawlor, B., Segurado, R., Kennelly, S., Olde Rikkert, M. G., Howard, R., Pasquier, F., et al. (2018). Nilvadipine in mild to moderate Alzheimer disease: A randomised controlled trial. *PLoS Med.* 15:e1002660. doi: 10.1371/journal.pmed.1002660

Lee, G., Thangavel, R., Sharma, V. M., Litersky, J. M., Bhaskar, K., Fang, S. M., et al. (2004). Phosphorylation of tau by fyn: Implications for Alzheimer's disease. *J. Neurosci.* 24, 2304–2312. doi: 10.1523/JNEUROSCI.4162-03.2004

Lefebvre, T., Ferreira, S., Dupont-Wallois, L., Bussiere, T., Dupire, M.-J., Delacourte, A., et al. (2003). Evidence of a balance between phosphorylation and O-GlcNAc glycosylation of Tau proteins—a role in nuclear localization. *Biochim. Biophys. Acta.* 1619, 167–176. doi: 10.1016/S0304-4165(02)00477-4

Leost, M., Schultz, C., Link, A., Wu, Y. Z., Biernat, J., Mandelkow, E. M., et al. (2000). Paullones are potent inhibitors of glycogen synthase kinase-3β and cyclin-dependent kinase 5/p25. *Eur. J. Biochem.* 267, 5983–5994. doi: 10.1046/j.1432-1327.2000.01673.x

Lewczuk, P., Ermann, N., Andreasson, U., Schultheis, C., Podhorna, J., Spitzer, P., et al. (2018). Plasma neurofilament light as a potential biomarker of neurodegeneration in Alzheimer's disease. *Alzheimers Res. Ther.* 10, 1–10. doi: 10.1186/s13195-018-0404-9

Li, S.-Q., Yu, Y., Han, J.-Z., Wang, D., Liu, J., Qian, F., et al. (2015). Deficiency of macrophage migration inhibitory factor attenuates tau hyperphosphorylation in mouse models of Alzheimer's disease. *J. Neuroinflammation* 12:177. doi: 10.1186/s12974-015-0396-3

Li, Y., Huang, H., Zhu, M., Bai, H., and Huang, X. (2021). Roles of the MYST family in the pathogenesis of Alzheimer's disease via histone or non-histone acetylation. *Aging Dis.* 12:132. doi: 10.14336/AD.2020.0329

Li, Y., Lim, E., Fields, T., Wu, H., Xu, Y., Wang, Y. A., et al. (2019). Improving sensitivity and specificity of amyloid-β peptides and tau protein detection with antibiofouling magnetic nanoparticles for liquid biopsy of Alzheimer's disease. *ACS Biomater. Sci. Eng.* 5, 3595–3605. doi: 10.1021/acsbiomaterials.9b00086

Li, Y., Wang, H., Wang, S., Quon, D., Liu, Y.-W., and Cordell, B. (2003). Positive and negative regulation of APP amyloidogenesis by sumoylation. *Proc. Natl. Acad. Sci. U.S.A.* 100, 259–264. doi: 10.1073/pnas.0235361100

Liang, Y.-C., Lee, C.-C., Yao, Y.-L., Lai, C.-C., Schmitz, M. L., and Yang, W.-M. (2016). SUMO5, a novel poly-SUMO isoform, regulates PML nuclear bodies. *Sci. Rep.* 6, 1–15. doi: 10.1038/srep26509

Lin, S.-Y., Hsu, W.-H., Lin, C.-C., Lin, C.-L., Yeh, H.-C., and Kao, C.-H. (2019). Association of transfusion with risks of dementia or Alzheimer's disease: A population-based cohort study. *Front. Psychiatry* 10:571. doi: 10.3389/fpsyt.2019.00571

Liu, C.-G., Song, J., Zhang, Y.-Q., and Wang, P.-C. (2014). MicroRNA-193b is a regulator of amyloid precursor protein in the blood and cerebrospinal fluid derived exosomal microRNA-193b is a biomarker of Alzheimer's disease. *Mol. Med. Rep.* 10, 2395–2400. doi: 10.3892/mmr.2014.2484

Liu, F., Grundke-Iqbal, I., Iqbal, K., and Gong, C. X. (2005). Contributions of protein phosphatases PP1, PP2A, PP2B and PP5 to the regulation of tau phosphorylation. *Eur. J. Neurosci.* 22, 1942–1950. doi: 10.1111/j.1460-9568.2005.04391.x

Liu, F., Iqbal, K., Grundke-Iqbal, I., Hart, G. W., and Gong, C.-X. (2004). O-GlcNAcylation regulates phosphorylation of tau: A mechanism involved in Alzheimer's disease. *Proc. Natl. Acad. Sci. U.S.A.* 101, 10804–10809. doi: 10.1073/pnas.0400348101

Liu, K. Y., Borissova, A., Mahmood, J., Elliott, T., Knowles, M., Bentham, P., et al. (2021). Pharmacological treatment trials of agitation in Alzheimer's disease: A systematic review of clinicaltrials. Gov registered trials. *Alzheimers Dement.* 7:e12157. doi: 10.1002/trc2.12157

Liu, L., Lauro, B. M., He, A., Lee, H., Bhattarai, S., Wolfe, M. S., et al. (2022). Identification of the Aβ37/42 peptide ratio in CSF as an improved Aβ biomarker for Alzheimer's disease. *Alzheimers Dement.* doi: 10.1002/alz.12646 [Epub ahead of print].

Liu, X.-A., Das, B., Chen, Y., Chen, Z., Avchalumov, Y., Tian, X., et al. (2018). *Recent advances in Alzheimer's drug discovery research*. Sharjah: Bentham Science, 26. doi: 10.2174/9781681085609118070005

Lovell, M. A., Gabbita, S. P., and Markesbery, W. R. (1999). Increased DNA oxidation and decreased levels of repair products in Alzheimer's disease ventricular CSF. *J. Neurochem.* 72, 771–776. doi: 10.1046/j.1471-4159.1999.0720771.x

Lozupone, M., Berardino, G., Mollica, A., Sardone, R., Dibello, V., Zupo, R., et al. (2022). ALZT-OP1: An experimental combination regimen for the treatment of Alzheimer's disease. *Expert Opin. Investig. Drugs* 31, 759–771. doi: 10.1080/13543784.2022.2095261

Lu, X., Wang, L., Yu, C., Yu, D., and Yu, G. (2015). Histone acetylation modifiers in the pathogenesis of Alzheimer's disease. *Front. Cell. Neurosci.* 9:226. doi: 10.3389/fncel.2015.00226

Łukasik, P., Baranowska-Bosiacka, I., Kulczycka, K., and Gutowska, I. (2021). Inhibitors of cyclin-dependent kinases: Types and their mechanism of action. *Int. J. Mol. Sci.* 22:2806. doi: 10.3390/ijms22062806

Luna-Munoz, J., Chavez-Macias, L., Garcia-Sierra, F., and Mena, R. (2007). Earliest stages of tau conformational changes are related to the appearance of a sequence of specific phospho-dependent tau epitopes in Alzheimer's disease 1. *J. Alzheimers Dis.* 12, 365–375. doi: 10.3233/JAD-2007-12410

Luo, H.-B., Xia, Y.-Y., Shu, X.-J., Liu, Z.-C., Feng, Y., Liu, X.-H., et al. (2014). SUMOylation at K340 inhibits tau degradation through deregulating its phosphorylation and ubiquitination. *Proc. Natl. Acad. Sci. U.S.A.* 111, 16586–16591. doi: 10.1073/pnas.1417548111

Luo, Y., Ma, B., Nussinov, R., and Wei, G. (2014). Structural insight into tau protein's paradox of intrinsically disordered behavior, self-acetylation activity, and aggregation. *J. Phys. Chem. Lett.* 5, 3026–3031. doi: 10.1021/jz501457f

Ly, P. T., Wu, Y., Zou, H., Wang, R., Zhou, W., Kinoshita, A., et al. (2012). Inhibition of GSK3β-mediated BACE1 expression reduces Alzheimer-associated phenotypes. *J. Clin. Investig.* 123, 224–235. doi: 10.1172/JCI64516

Ma, X., Liu, L., and Meng, J. (2017). MicroRNA-125b promotes neurons cell apoptosis and Tau phosphorylation in Alzheimer's disease. *Neurosci. Lett.* 661, 57–62. doi: 10.1016/j.neulet.2017.09.043

MacBean, L. F., Smith, A. R., and Lunnon, K. (2020). Exploring beyond the DNA sequence: A review of epigenomic studies of DNA and histone modifications in dementia. *Curr. Genet. Med. Rep.* 8, 79–92. doi: 10.1007/s40142-020-00190-y

Mahoney-Sanchez, L., Belaidi, A. A., Bush, A. I., and Ayton, S. (2016). The complex role of apolipoprotein E in Alzheimer's disease: An overview and update. *J. Mol. Neurosci.* 60, 325–335. doi: 10.1007/s12031-016-0839-z

Maines, M. (2000). The heme oxygenase system and its functions in the brain. *Cell. Mol. Biol.* 46, 573–585.

Majbour, N. K., Chiasserini, D., Vaikath, N. N., Eusebi, P., Tokuda, T., Van De Berg, W., et al. (2017). Increased levels of CSF total but not oligomeric or phosphorylated forms of alpha-synuclein in patients diagnosed with probable Alzheimer's disease. *Sci. Rep.* 7, 1–8. doi: 10.1038/srep40263

Mangialasche, F., Kivipelto, M., Mecocci, P., Rizzuto, D., Palmer, K., Winblad, B., et al. (2010). High plasma levels of vitamin E forms and reduced Alzheimer's disease risk in advanced age. *J. Alzheimers Dis.* 20, 1029–1037. doi: 10.3233/JAD-2010-091450

Martins, W. C., Tasca, C. I., and Cimarosti, H. (2016). Battling Alzheimer's disease: Targeting SUMOylation-mediated pathways. *Neurochem. Res.* 41, 568–578. doi: 10.1007/s11064-015-1681-3

Marzi, S. J., Leung, S. K., Ribarska, T., Hannon, E., Smith, A. R., Pishva, E., et al. (2018). A histone acetylome-wide association study of Alzheimer's disease identifies disease-associated H3K27ac differences in the entorhinal cortex. *Nat. Neurosci.* 21, 1618–1627. doi: 10.1038/s41593-018-0253-7

Mattsson, N., Andreasson, U., Zetterberg, H., Blennow, K., and Initiative, A. (2017). Association of plasma neurofilament light with neurodegeneration in patients with Alzheimer disease. *JAMA Neurol.* 74, 557–566. doi: 10.1001/jamaneurol.2016.6117

Mattsson, N., Smith, R., Strandberg, O., Palmqvist, S., Schöll, M., Insel, P. S., et al. (2018). Comparing 18F-AV-1451 with CSF t-tau and p-tau for diagnosis of Alzheimer disease. *Neurology.* 90, e388–e395. doi: 10.1212/WNL.0000000000004887

Mayeux, R., and Stern, Y. (2012). Epidemiology of Alzheimer disease. *Cold Spring Harb. Perspect. Med.* 2:a006239. doi: 10.1101/cshperspect.a006239

McClellan, A. J., Laugesen, S. H., and Ellgaard, L. (2019). Cellular functions and molecular mechanisms of non-lysine ubiquitination. *Open Biol.* 9:190147. doi: 10.1098/rsob.190147

McConkey, D. J., and Orrenius, S. (1997). The role of calcium in the regulation of apoptosis. *Biochem. Biophys. Res. Commun.* 239, 357–366. doi: 10.1006/bbrc.1997.7409

Medeiros, R., Prediger, R. D., Passos, G. F., Pandolfo, P., Duarte, F. S., Franco, J. L., et al. (2007). Connecting TNF-α signaling pathways to iNOS expression in a mouse model of Alzheimer's disease: Relevance for the behavioral and synaptic deficits induced by amyloid β protein. *J. Neurosci.* 27, 5394–5404. doi: 10.1523/JNEUROSCI.5047-06.2007

Mersfelder, E. L. P. (2008). *Structural and functional characterization of yeast histone acetyltransferase-1*. Columbus, OH: The Ohio State University.

Mielcarek, M., Zielonka, D., Carnemolla, A., Marcinkowski, J. T., and Guidez, F. J. (2015). HDAC4 as a potential therapeutic target in neurodegenerative diseases: A summary of recent achievements. *Front. Cell Neurosci.* 9:42. doi: 10.3389/fncel.2015.00042

Mielke, M. M., Bandaru, V. V. R., Haughey, N. J., Xia, J., Fried, L. P., Yasar, S., et al. (2012). Serum ceramides increase the risk of Alzheimer disease: The women's health and aging study II. *Neurology* 79, 633–641. doi: 10.1212/WNL.0b013e318264e380

Mietelska-Porowska, A., Wasik, U., Goras, M., Filipek, A., and Niewiadomska, G. (2014). Tau protein modifications and interactions: Their role in function and dysfunction. *Int. J. Mol. Sci.* 15, 4671–4713. doi: 10.3390/ijms15034671

Miki, T., Yokota, O., Haraguchi, T., Ikeuchi, T., Zhu, B., Takenoshita, S., et al. (2019). Young adult-onset, very slowly progressive cognitive decline with spastic paraparesis in Alzheimer's disease with cotton wool plaques due to a novel presenilin1 G417S mutation. *Acta Neuropathol. Commun.* 7, 1–15. doi: 10.1186/s40478-019-0672-z

Miller, J. L., and Grant, P. A. (2013). The role of DNA methylation and histone modifications in transcriptional regulation in humans. *Epigenetics* 61, 289–317. doi: 10.1007/978-94-007-4525-4_13

Mirza, Z., and Karim, S. (2019). Advancements in CRISPR/Cas9 technology—focusing on cancer therapeutics and beyond. *Semin. Cell Dev. Biol.* 96, 13–21. doi: 10.1016/j.semcdb.2019.05.026

Miura, S., Yoshihisa, A., Misaka, T., Yamaki, T., Kojima, T., Toyokawa, M., et al. (2020). Amyloid precursor protein 770 is specifically expressed and released from platelets. *J. Biol. Chem.* 295, 13194–13201. doi: 10.1074/jbc.RA120.012904

Moreira, P. I., Honda, K., Liu, Q., Aliev, G., Oliveira, C. R., Santos, M. S., et al. (2005). Alzheimer's disease and oxidative stress: The old problem remains unsolved. *Cent. Nerv. Syst. Agents Med. Chem.* 5, 51–62. doi: 10.2174/1568015053202714

Moremen, K. W., Tiemeyer, M., and Nairn, A. V. (2012). Vertebrate protein glycosylation: Diversity, synthesis and function. *Nat. Rev. Mol. Cell Biol.* 13, 448–462. doi: 10.1038/nrm3383

Mowrer, K. R., and Wolfe, M. S. (2008). Promotion of BACE1 mRNA alternative splicing reduces amyloid β-peptide production. *J. Biol. Chem.* 283, 18694–18701. doi: 10.1074/jbc.M801322200

Mukhopadhyay, D., and Riezman, H. (2007). Proteasome-independent functions of ubiquitin in endocytosis and signaling. *Science* 315, 201–205. doi: 10.1126/science.1127085

Nagata, T., Shinagawa, S., Nakajima, S., Noda, Y., and Mimura, M. (2022). Pharmacotherapeutic combinations for the treatment of Alzheimer's disease. *Expert Opin. Pharmacother.* 23, 727–737. doi: 10.1080/14656566.2022.2042514

Nakamura, A., Kaneko, N., Villemagne, V. L., Kato, T., Doecke, J., Doré, V., et al. (2018). High performance plasma amyloid-β biomarkers for Alzheimer's disease. *Nature* 554, 249–254. doi: 10.1038/nature25456

Neergaard, J. S., Dragsbæk, K., Christiansen, C., Karsdal, M. A., Brix, S., and Henriksen, K. (2018). Two novel blood-based biomarker candidates measuring degradation of tau are associated with dementia: A prospective study. *PLoS One* 13:e0194802. doi: 10.1371/journal.pone.0194802

Nesterova, A. P., Yuryev, A., Klimov, E. A., Zharkova, M., Shkrob, M., Ivanikova, N. V., et al. (2019). *Disease pathways: An atlas of human disease signaling pathways*. New York, NY: Elsevier.

Neumann, U., Ufer, M., Jacobson, L. H., Rouzade-Dominguez, M. L., Huledal, G., Kolly, C., et al. (2018). The BACE-1 inhibitor CNP 520 for prevention trials in Alzheimer's disease. *EMBO Mol. Med.* 10:e9316. doi: 10.15252/emmm.201809316

Nilsson, M. R., Driscoll, M., and Raleigh, D. P. (2002). Low levels of asparagine deamidation can have a dramatic effect on aggregation of amyloidogenic peptides: Implications for the study of amyloid formation. *Protein Sci.* 11, 342–349. doi: 10.1110/ps.48702

Novak, G., Streffer, J. R., Timmers, M., Henley, D., Brashear, H. R., Bogert, J., et al. (2020). Long-term safety and tolerability of atabecestat (JNJ-54861911), an oral BACE1 inhibitor, in early Alzheimer's disease spectrum patients: A randomized, double-blind, placebo-controlled study and a two-period extension study. *Alzheimers Res. Ther.* 12, 1–16. doi: 10.1186/s13195-020-00614-5

O'brien, R. J., and Wong, P. C. (2011). Amyloid precursor protein processing and Alzheimer's disease. *Annu. Rev. Neurosci.* 34:185. doi: 10.1146/annurev-neuro-061010-113613

O'Bryant, S. E., Xiao, G., Barber, R., Reisch, J., Doody, R., Fairchild, T., et al. (2010). A serum protein–based algorithm for the detection of Alzheimer disease. *Arch. Neurol.* 67, 1077–1081. doi: 10.1001/archneurol.2010.215

Oikawa, N., and Walter, J. (2019). Presenilins and γ-secretase in membrane proteostasis. *Cells* 8:209. doi: 10.3390/cells8030209

Olsson, B., Lautner, R., Andreasson, U., Öhrfelt, A., Portelius, E., Bjerke, M., et al. (2016). CSF and blood biomarkers for the diagnosis of Alzheimer's disease: A systematic review and meta-analysis. *Lancet Neurol.* 15, 673–684. doi: 10.1016/S1474-4422(16)00070-3

Ovod, V., Ramsey, K. N., Mawuenyega, K. G., Bollinger, J. G., Hicks, T., Schneider, T., et al. (2017). Amyloid β concentrations and stable isotope labeling kinetics of human plasma specific to central nervous system amyloidosis. *Alzheimers Dement.* 13, 841–849. doi: 10.1016/j.jalz.2017.06.2266

Palmal, S., Maity, A. R., Singh, B. K., Basu, S., Jana, N. R., and Jana, N. R. (2014). Inhibition of amyloid fibril growth and dissolution of amyloid fibrils by curcumin–gold nanoparticles. *Chem. Eur. J.* 20, 6184–6191. doi: 10.1002/chem.201400079

Pannee, J., Törnqvist, U., Westerlund, A., Ingelsson, M., Lannfelt, L., Brinkmalm, G., et al. (2014). The amyloid-β degradation pattern in plasma—a possible tool for clinical trials in Alzheimer's disease. *Neurosci. Lett.* 573, 7–12. doi: 10.1016/j.neulet.2014.04.041

Panza, F., Solfrizzi, V., Seripa, D., Imbimbo, B. P., Lozupone, M., Santamato, A., et al. (2016). Tau-centric targets and drugs in clinical development for the treatment of Alzheimer's disease. *Biomed Res. Int.* 2016:3245935. doi: 10.1155/2016/3245935

Pao, P.-C., Patnaik, D., Watson, L. A., Gao, F., Pan, L., Wang, J., et al. (2020). HDAC1 modulates OGG1-initiated oxidative DNA damage repair in the aging brain and Alzheimer's disease. *Nat. Commun.* 11, 1–17. doi: 10.1038/s41467-020-16361-y

Park, S.-Y., Lee, Y.-H., Seong, A.-R., Lee, J., Jun, W., and Yoon, H.-G. (2013). Selective inhibition of PCAF suppresses microglial-mediated β-amyloid neurotoxicity. *Int. J. Mol. Med.* 32, 469–475. doi: 10.3892/ijmm.2013.1407

Patel, S., Bansoad, A. V., Singh, R., and Khatik, G. (2022). BACE1: A key regulator in Alzheimer's disease progression and current development of its inhibitors. *Curr. Neuropharmacol.* 20, 1174–1193. doi: 10.2174/1570159X19666211201094031

Perluigi, M., Barone, E., Di Domenico, F., and Butterfield, D. (2016). Aberrant protein phosphorylation in Alzheimer disease brain disturbs pro-survival and cell death pathways. *Biochim. Biophys. Acta* 1862, 1871–1882. doi: 10.1016/j.bbadis.2016.07.005

Petit, D., Fernández, S. G., Zoltowska, K. M., Enzlein, T., Ryan, N. S., O'Connor, A., et al. (2022). Aβ profiles generated by Alzheimer's disease causing PSEN1 variants determine the pathogenicity of the mutation and predict age at disease onset. *Mol. Psychiatry* 27, 2821–2832. doi: 10.1038/s41380-022-01518-6

Piedrahita, D., Hernández, I., López-Tobón, A., Fedorov, D., Obara, B., Manjunath, B., et al. (2010). Silencing of CDK5 reduces neurofibrillary tangles in transgenic Alzheimer's mice. *J. Neurosci.* 30, 13966–13976. doi: 10.1523/JNEUROSCI.3637-10.2010

Pini, L., Pievani, M., Bocchetta, M., Altomare, D., Bosco, P., Cavedo, E., et al. (2016). Brain atrophy in Alzheimer's disease and aging. *Ageing Res. Rev.* 30, 25–48. doi: 10.1016/j.arr.2016.01.002

Porsteinsson, A. P., and Antonsdottir, I. M. (2017). An update on the advancements in the treatment of agitation in Alzheimer's disease. *Expert Opin. Pharmacother.* 18, 611–620. doi: 10.1080/14656566.2017.1307340

Potasiewicz, A., Krawczyk, M., Gzielo, K., Popik, P., and Nikiforuk, A. (2020). Positive allosteric modulators of alpha 7 nicotinic acetylcholine receptors enhance procognitive effects of conventional anti-Alzheimer drugs in scopolamine-treated rats. *Behav. Brain Res.* 385:112547. doi: 10.1016/j.bbr.2020.112547

Qian, W., Shi, J., Yin, X., Iqbal, K., Grundke-Iqbal, I., Gong, C.-X., et al. (2010). PP2A regulates tau phosphorylation directly and also indirectly via activating GSK-3β. *J. Alzheimers Dis.* 19, 1221–1229. doi: 10.3233/JAD-2010-1317

Qu, Z.-Q., Zhou, Y., Zeng, Y.-S., Lin, Y.-K., Li, Y., Zhong, Z.-Q., et al. (2012). Protective effects of a Rhodiola crenulata extract and salidroside on hippocampal neurogenesis against streptozotocin-induced neural injury in the rat. *PLoS One.* 7:e29641. doi: 10.1371/journal.pone.0029641

Ramamurthy, E., Welch, G., Cheng, J., Yuan, Y., Gunsalus, L., Bennett, D. A., et al. (2020). Cell type-specific histone acetylation profiling of Alzheimer's Disease subjects and integration with genetics. *bioRxiv [Preprint]* 010330. doi: 10.1101/2020.03.26.010330

Ramesh, M., Gopinath, P., and Govindaraju, T. (2020). Role of post-translational modifications in Alzheimer's disease. *Chembiochem* 21, 1052–1079. doi: 10.1002/cbic.201900573

Raposo, G., and Stahl, P. D. (2019). Extracellular vesicles: A new communication paradigm? *Nat. Rev. Mol. Cell Biol.* 20, 509–510. doi: 10.1038/s41580-019-0158-7

Ravid, T., and Hochstrasser, M. (2008). Diversity of degradation signals in the ubiquitin–proteasome system. *Nat. Rev. Mol. Cell Biol.* 9, 679–689. doi: 10.1038/nrm2468

Reily, C., Stewart, T. J., Renfrow, M. B., and Novak, J. (2019). Glycosylation in health and disease. *Nat. Rev. Nephrol.* 15, 346–366. doi: 10.1038/s41581-019-0129-4

Resh, M. D. (2016). Fatty acylation of proteins: The long and the short of it. *Prog. Lipid Res.* 63, 120–131. doi: 10.1016/j.plipres.2016.05.002

Ridge, P. G., Ebbert, M. T., and Kauwe, J. (2013). Genetics of Alzheimer's disease. *Biomed. Res. Int.* 2013:254954. doi: 10.1155/2013/254954

Rinaldi, P., Polidori, M. C., Metastasio, A., Mariani, E., Mattioli, P., Cherubini, A., et al. (2003). Plasma antioxidants are similarly depleted in mild cognitive impairment and in Alzheimer's disease. *Neurobiol. Aging.* 24, 915–919. doi: 10.1016/S0197-4580(03)00031-9

Robinson, N., and Robinson, A. (2001). Deamidation of human proteins. *Proc. Natl. Acad. Sci. U.S.A.* 98, 12409–12413. doi: 10.1073/pnas.221463198

Roher, A., Lowenson, J., Clarke, S., Wolkow, C., Wang, R., Cotter, R., et al. (1993). Structural alterations in the peptide backbone of beta-amyloid core protein may account for its deposition and stability in Alzheimer's disease. *J. Biol. Chem.* 268, 3072–3083. doi: 10.1016/S0021-9258(18)53661-9

Rouaux, C., Jokic, N., Mbebi, C., Boutillier, S., Loeffler, J. P., and Boutillier, A. L. (2003). Critical loss of CBP/p300 histone acetylase activity by caspase-6 during neurodegeneration. *EMBO J.* 22, 6537–6549. doi: 10.1093/emboj/cdg615

Ruthirakuhan, M., Herrmann, N., Andreazza, A. C., Verhoeff, N. P. L., Gallagher, D., Black, S. E., et al. (2020). Agitation, oxidative stress, and cytokines in Alzheimer disease: Biomarker analyses from a clinical trial with nabilone for agitation. *J. Geriatr. Psychiatry Neurol.* 33, 175–184. doi: 10.1177/0891988719874118

Sacco, F., Perfetto, L., Castagnoli, L., and Cesareni, G. (2012). The human phosphatase interactome: An intricate family portrait. *FEBS Lett.* 586, 2732–2739. doi: 10.1016/j.febslet.2012.05.008

Salloway, S., Farlow, M., McDade, E., Clifford, D. B., Wang, G., Llibre-Guerra, J. J., et al. (2021). A trial of gantenerumab or solanezumab in dominantly inherited Alzheimer's disease. *Nat. Med.* 27, 1187–1196. doi: 10.1038/s41591-021-01369-8

Salloway, S., Honigberg, L. A., Cho, W., Ward, M., Friesenhahn, M., Brunstein, F., et al. (2018). Amyloid positron emission tomography and cerebrospinal fluid results from a crenezumab anti-amyloid-beta antibody double-blind, placebo-controlled, randomized phase II study in mild-to-moderate Alzheimer's disease (BLAZE). *Alzheimers Res. Ther.* 10, 1–13. doi: 10.1186/s13195-018-0424-5

Saman, S., Kim, W., Raya, M., Visnick, Y., Miro, S., Saman, S., et al. (2012). Exosome-associated tau is secreted in tauopathy models and is selectively phosphorylated in cerebrospinal fluid in early Alzheimer disease. *J. Biol. Chem.* 287, 3842–3849. doi: 10.1074/jbc.M111.277061

Santos, A. L., and Lindner, A. B. (2017). Protein posttranslational modifications: Roles in aging and age-related disease. *Oxid. Med. Cell. Longev.* 2017:5716409. doi: 10.1155/2017/5716409

Sathe, G., Albert, M., Darrow, J., Saito, A., Troncoso, J., Pandey, A., et al. (2021). Quantitative proteomic analysis of the frontal cortex in Alzheimer's disease. *J. Neurochem.* 156, 988–1002. doi: 10.1111/jnc.15116

Schedin-Weiss, S., Winblad, B., and Tjernberg, L. O. (2014). The role of protein glycosylation in Alzheimer disease. *FEBS J.* 281, 46–62. doi: 10.1111/febs.12590

Schmidt, M. F., Gan, Z. Y., Komander, D., and Dewson, G. (2021). Ubiquitin signalling in neurodegeneration: Mechanisms and therapeutic opportunities. *Cell Death Differ.* 28, 570–590. doi: 10.1038/s41418-020-00706-7

Schneller, J. L., Lee, C. M., Bao, G., and Venditti, C. P. (2017). Genome editing for inborn errors of metabolism: Advancing towards the clinic. *BMC Med.* 15:43. doi: 10.1186/s12916-017-0798-4

Schumacher-Schuh, A., Bieger, A., Borelli, W. V., Portley, M. K., Awad, P. S., and Bandres-Ciga, S. (2021). Advances in proteomic and metabolomic profiling of neurodegenerative diseases. *Front. Neurol.* 12:792227. doi: 10.3389/fneur.2021.792227

Serenó, L., Coma, M., Rodriguez, M., Sanchez-Ferrer, P., Sánchez, M. B., Gich, I., et al. (2009). A novel GSK-3β inhibitor reduces Alzheimer's pathology and rescues neuronal loss in vivo. *Neurobiol. Dis.* 35, 359–367. doi: 10.1016/j.nbd.2009.05.025

Serrano-Pozo, A., Qian, J., Monsell, S., Betensky, R., and Hyman, B. (2015). APOEε2 is associated with milder clinical and pathological Alzheimer's disease. *Ann. Neurol.* 77, 917–929. doi: 10.1002/ana.24369

Seto, E., and Yoshida, M. (2014). Erasers of histone acetylation: The histone deacetylase enzymes. *Cold Spring Harb. Perspect. Biol.* 6:a018713. doi: 10.1101/cshperspect.a018713

Sevigny, J., Chiao, P., Bussière, T., Weinreb, P. H., Williams, L., Maier, M., et al. (2016). The antibody aducanumab reduces Aβ plaques in Alzheimer's disease. *Nature* 537, 50–56. doi: 10.1038/nature19323

Seymour, T., and Zhang, J. (2021). Porphyromonas gingivalis in the pathogenesis of Alzheimer's disease and its therapeutic target. *J Explor Res. Pharmacol.* 7, 45–53. doi: 10.14218/JERP.2021.00030

Shahbazian, M. D., and Grunstein, M. (2007). Functions of site-specific histone acetylation and deacetylation. *Annu. Rev. Biochem.* 76, 75–100. doi: 10.1146/annurev.biochem.76.052705.162114

Sheline, Y. I., Snider, B. J., Beer, J. C., Seok, D., Fagan, A. M., Suckow, R. F., et al. (2020). Effect of escitalopram dose and treatment duration on CSF Aβ levels

in healthy older adults: A controlled clinical trial. *Neurology* 95, e2658–e2665. doi: 10.1212/WNL.0000000000010725

Shental-Bechor, D., and Levy, Y. (2008). Effect of glycosylation on protein folding: A close look at thermodynamic stabilization. *Proc. Natl. Acad. Sci. U.S.A.* 105, 8256–8261. doi: 10.1073/pnas.0801340105

Shkodina, A. D., Tan, S. C., Hasan, M. M., Abdelgawad, M., Chopra, H., Bilal, M., et al. (2021). Roles of clock genes in the pathogenesis of Parkinson's disease. *Ageing Res. Rev.* 74:101554. doi: 10.1016/j.arr.2021.101554

Singh, S., and Li, S. S.-L. (2012). Epigenetic effects of environmental chemicals bisphenol A and phthalates. *Int. J. Mol. Sci.* 13, 10143–10153. doi: 10.3390/ijms130810143

Snyder, H. M., Carrillo, M. C., Grodstein, F., Henriksen, K., Jeromin, A., Lovestone, S., et al. (2014). Developing novel blood-based biomarkers for Alzheimer's disease. *Alzheimers Dement.* 10, 109–114. doi: 10.1016/j.jalz.2013.10.007

Soares Martins, T., Trindade, D., Vaz, M., Campelo, I., Almeida, M., Trigo, G., et al. (2021). Diagnostic and therapeutic potential of exosomes in Alzheimer's disease. *J. Neurochem.* 156, 162–181. doi: 10.1111/jnc.15112

Soares, H. D., Potter, W. Z., Pickering, E., Kuhn, M., Immermann, F. W., Shera, D. M., et al. (2012). Plasma biomarkers associated with the apolipoprotein E genotype and Alzheimer disease. *Arch. Neurol.* 69, 1310–1317. doi: 10.1001/archneurol.2012.1070

Spiro, R. G. (2002). Protein glycosylation: Nature, distribution, enzymatic formation, and disease implications of glycopeptide bonds. *Glycobiology* 12, 43R–56R. doi: 10.1093/glycob/12.4.43R

Stabler, S. M., Ostrowski, L. L., Janicki, S. M., and Monteiro, M. J. (1999). A myristoylated calcium-binding protein that preferentially interacts with the Alzheimer's disease presenilin 2 protein. *J. Cell Biol.* 145, 1277–1292. doi: 10.1083/jcb.145.6.1277

Steiner, H., Fluhrer, R., and Haass, C. (2008). Intramembrane proteolysis by γ-secretase. *J. Biol. Chem.* 283, 29627–29631. doi: 10.1074/jbc.R800010200

Stoothoff, W. H., and Johnson, G. V. (2005). Tau phosphorylation: Physiological and pathological consequences. *Biochim. Biophys. Acta.* 1739, 280–297. doi: 10.1016/j.bbadis.2004.06.017

Struhl, K. (1998). Histone acetylation and transcriptional regulatory mechanisms. *Genes Dev.* 12, 599–606. doi: 10.1101/gad.12.5.599

Su, R., Han, Z.-Y., Fan, J.-P., and Zhang, Y.-L. (2010). A possible role of myristoylated alanine-rich C kinase substrate in endocytic pathway of Alzheimer's disease. *Neurosci. Bull.* 26, 338–344. doi: 10.1007/s12264-010-0131-0

Suárez-Calvet, M., Kleinberger, G., Araque Caballero, M. Á, Brendel, M., Rominger, A., Alcolea, D., et al. (2016). sTREM 2 cerebrospinal fluid levels are a potential biomarker for microglia activity in early-stage Alzheimer's disease and associate with neuronal injury markers. *EMBO Mol. Med.* 8, 466–476. doi: 10.15252/emmm.201506123

Sultan, A., Nesslany, F., Violet, M., Bégard, S., Loyens, A., Talahari, S., et al. (2011). Nuclear tau, a key player in neuronal DNA protection. *J. Biol. Chem.* 286, 4566–4575. doi: 10.1074/jbc.M110.199976

Sun, J., Carlson-Stevermer, J., Das, U., Shen, M., Delenclos, M., Snead, A. M., et al. (2019). CRISPR/Cas9 editing of APP C-terminus attenuates β-cleavage and promotes α-cleavage. *Nat. Commun.* 10, 1–11. doi: 10.1038/s41467-018-07971-8

Sun, L., Zhou, R., Yang, G., and Shi, Y. (2017). Analysis of 138 pathogenic mutations in presenilin-1 on the in vitro production of Aβ42 and Aβ40 peptides by γ-secretase. *Proc. Natl. Acad. Sci. U.S.A.* 114, E476–E485. doi: 10.1073/pnas.1618657114

Suprun, E. V. (2019). Protein post-translational modifications–A challenge for bioelectrochemistry. *Trends Anal. Chem.* 116, 44–60. doi: 10.1016/j.trac.2019.04.019

Surgucheva, I., Sharov, V. S., and Surguchov, A. (2012). γ-Synuclein: Seeding of α-synuclein aggregation and transmission between cells. *Biochemistry* 51, 4743–4754. doi: 10.1021/bi300478w

Szabo-Reed, A. N., Vidoni, E., Binder, E. F., Burns, J., Cullum, C. M., Gahan, W. P., et al. (2019). Rationale and methods for a multicenter clinical trial assessing exercise and intensive vascular risk reduction in preventing dementia (rrAD Study). *Contemp. Clin. Trials* 79, 44–54. doi: 10.1016/j.cct.2019.02.007

Tampi, R. R., Forester, B. P., and Agronin, M. (2021). Aducanumab: Evidence from clinical trial data and controversies. *Drugs Context* 10, 2021–2027. doi: 10.7573/dic.2021-7-3

Tao, C. C., Hsu, W. L., Ma, Y. L., Cheng, S. J., and Lee, E. H. (2017). Epigenetic regulation of HDAC1 SUMOylation as an endogenous neuroprotection against A β toxicity in a mouse model of Alzheimer's disease. *Cell Death Differ.* 24, 597–614. doi: 10.1038/cdd.2016.161

Tate, E. W., Kalesh, K. A., Lanyon-Hogg, T., Storck, E. M., and Thinon, E. (2015). Global profiling of protein lipidation using chemical proteomic technologies. *Curr. Opin. Chem. Biol.* 24, 48–57. doi: 10.1016/j.cbpa.2014.10.016

Thiel, G., Lietz, M., and Hohl, M. (2004). How mammalian transcriptional repressors work. *Eur. J. Biochem.* 271, 2855–2862. doi: 10.1111/j.1432-1033.2004.04174.x

Thinon, E., Serwa, R. A., Broncel, M., Brannigan, J. A., Brassat, U., Wright, M. H., et al. (2014). Global profiling of co-and post-translationally N-myristoylated proteomes in human cells. *Nat. Commun.* 5, 1–13. doi: 10.1038/ncomms5919

Tönnies, E., and Trushina, E. (2017). Oxidative stress, synaptic dysfunction, and Alzheimer's disease. *J. Alzheimers Dis.* 57, 1105–1121. doi: 10.3233/JAD-161088

Tsou, Y. H., Zhang, X. Q., Zhu, H., Syed, S., and Xu, X. (2017). Drug delivery to the brain across the blood–brain barrier using nanomaterials. *Small* 13:1701921. doi: 10.1002/smll.201701921

Uddin, M. S., Mamun, A. A., Rahman, M. M., Jeandet, P., Alexiou, A., Behl, T., et al. (2021). Natural products for neurodegeneration: Regulating neurotrophic signals. *Oxid. Med. Cell. Longev.* 2021:8820406. doi: 10.1155/2021/8820406

Undurraga, J., Sim, K., Tondo, L., Gorodischer, A., Azua, E., Tay, K. H., et al. (2019). Lithium treatment for unipolar major depressive disorder: Systematic review. *J. Psychopharmacol.* 33, 167–176. doi: 10.1177/0269881118822161

van Rheenen, J., Mulugeta Achame, E., Janssen, H., Calafat, J., and Jalink, K. (2005). PIP2 signaling in lipid domains: A critical re-evaluation. *EMBO J.* 24, 1664–1673. doi: 10.1038/sj.emboj.7600655

Varki, A. (2017). Biological roles of glycans. *Glycobiology* 27, 3–49. doi: 10.1093/glycob/cww086

Vassar, R., Kovacs, D. M., Yan, R., and Wong, P. C. (2009). The β-secretase enzyme BACE in health and Alzheimer's disease: Regulation, cell biology, function, and therapeutic potential. *J. Neurosci.* 29, 12787–12794. doi: 10.1523/JNEUROSCI.3657-09.2009

Vellas, B., Coley, N., Ousset, P.-J., Berrut, G., Dartigues, J.-F., Dubois, B., et al. (2012). Long-term use of standardised Ginkgo biloba extract for the prevention of Alzheimer's disease (GuidAge): A randomised placebo-controlled trial. *Lancet Neurol.* 11, 851–859. doi: 10.1016/S1474-4422(12)70206-5

Venkatesh, S., and Workman, J. L. (2015). Histone exchange, chromatin structure and the regulation of transcription. *Nat. Rev. Mol. Cell Biol.* 16, 178–189. doi: 10.1038/nrm3941

Verkhratsky, A., Zorec, R., Rodríguez, J. J., and Parpura, V. (2016). Astroglia dynamics in ageing and Alzheimer's disease. *Curr. Opin. Pharmacol.* 26, 74–79. doi: 10.1016/j.coph.2015.09.011

Vetrivel, K. S., Meckler, X., Chen, Y., Nguyen, P. D., Seidah, N. G., Vassar, R., et al. (2009). Alzheimer disease Aβ production in the absence of S-palmitoylation-dependent targeting of BACE1 to lipid rafts. *J. Biol. Chem.* 284, 3793–3803. doi: 10.1074/jbc.M808920200

Villarreal, S., Zhao, F., Hyde, L. A., Holder, D., Forest, T., Sondey, M., et al. (2017). Chronic verubecestat treatment suppresses amyloid accumulation in advanced aged Tg2576-AβPP swe mice without inducing microhemorrhage. *J. Alzheimers Dis.* 59, 1393–1413. doi: 10.3233/JAD-170056

Volmar, C.-H., and Wahlestedt, C. (2015). Histone deacetylases (HDACs) and brain function. *Neuroepigenetics* 1, 20–27. doi: 10.1016/j.nepig.2014.10.002

Wakabayashi, T., and De Strooper, B. J. P. (2008). Presenilins: Members of the γ-secretase quartets, but part-time soloists too. *Physiology (Bethesda)* 23, 194–204. doi: 10.1152/physiol.00009.2008

Wakutani, Y., Watanabe, K., Adachi, Y., Wada-Isoe, K., Urakami, K., Ninomiya, H., et al. (2004). Novel amyloid precursor protein gene missense mutation (D678N) in probable familial Alzheimer's disease. *J. Neurol. Neurosurg. Psychiatry* 75, 1039–1042. doi: 10.1136/jnnp.2003.010611

Walia, V., Kaushik, D., Mittal, V., Kumar, K., Verma, R., Parashar, J., et al. (2021). Delineation of neuroprotective effects and possible benefits of antioxidantstherapy for the treatment of Alzheimer's diseases by targeting mitochondrial-derived reactive oxygen species: Bench to bedside. *Mol. Neurobiol.* 59, 657–680. doi: 10.1007/s12035-021-02617-1

Wang, J. Z., Xia, Y. Y., Grundke-Iqbal, I., and Iqbal, K. (2013). Abnormal hyperphosphorylation of tau: Sites, regulation, and molecular mechanism of neurofibrillary degeneration. *J. Alzheimers Dis.* 33, S123–S139. doi: 10.3233/JAD-2012-129031

Wang, R., Ying, Z., Zhao, J., Zhang, Y., Wang, R., Lu, H., et al. (2012). Lys203 and Lys382 are essential for the proteasomal degradation of BACE1. *Curr. Alzheimer Res.* 9, 606–615. doi: 10.2174/156720512800618026

Wang, T., Kuang, W., Chen, W., Xu, W., Zhang, L., Li, Y., et al. (2020). A phase II randomized trial of sodium oligomannate in Alzheimer's dementia. *Alzheimers Res. Ther.* 12, 1–10. doi: 10.1186/s13195-020-00678-3

Wang, W.-Y., Tan, M.-S., Yu, J.-T., and Tan, L. (2015). Role of pro-inflammatory cytokines released from microglia in Alzheimer's disease. *Ann. Transl. Med.* 3:136.

Wang, Z., Yu, K., Tan, H., Wu, Z., Cho, J.-H., Han, X., et al. (2020). 27-Plex tandem mass tag mass spectrometry for profiling brain proteome in Alzheimer's disease. *Anal. Chem.* 92, 7162–7170. doi: 10.1021/acs.analchem.0c00655

Watson, L. S., Hamlett, E. D., Stone, T. D., and Sims-Robinson, C. (2019). Neuronally derived extracellular vesicles: An emerging tool for understanding Alzheimer's disease. *Mol. Neurodegener.* 14, 1–9. doi: 10.1186/s13024-019-0317-5

Weeraratna, A. T., Kalehua, A., DeLeon, I., Bertak, D., Maher, G., Wade, M. S., et al. (2007). Alterations in immunological and neurological gene expression patterns in Alzheimer's disease tissues. *Exp. Cell Res.* 313, 450–461. doi: 10.1016/j.yexcr.2006.10.028

Wellington, H., Paterson, R. W., Portelius, E., Törnqvist, U., Magdalinou, N., Fox, N. C., et al. (2016). Increased CSF neurogranin concentration is specific to Alzheimer disease. *Neurology* 86, 829–835. doi: 10.1212/WNL.0000000000002423

Wessels, A. M., Tariot, P. N., Zimmer, J. A., Selzler, K. J., Bragg, S. M., Andersen, S. W., et al. (2020). Efficacy and safety of lanabecestat for treatment of early and mild Alzheimer disease: The AMARANTH and DAYBREAK-ALZ randomized clinical trials. *JAMA Neurol.* 77, 199–209. doi: 10.1001/jamaneurol.2019.3988

Williamson, R. L., Laulagnier, K., Miranda, A. M., Fernandez, M. A., Wolfe, M. S., Sadoul, R., et al. (2017). Disruption of amyloid precursor protein ubiquitination selectively increases amyloid β (Aβ) 40 levels via presenilin 2-mediated cleavage. *J. Biol. Chem.* 292, 19873–19889. doi: 10.1074/jbc.M117.818138

Wright, M. H., Heal, W. P., Mann, D. J., and Tate, E. W. (2010). Protein myristoylation in health and disease. *J. Chem. Biol.* 3, 19–35. doi: 10.1007/s12154-009-0032-8

Wu, C.-H. (2017). The association between the use of zolpidem and the risk of Alzheimer's disease among older people. *J. Am. Geriatr. Soc.* 65, 2488–2495. doi: 10.1111/jgs.15018

Xia, D., Watanabe, H., Wu, B., Lee, S. H., Li, Y., Tsvetkov, E., et al. (2015). Presenilin-1 knockin mice reveal loss-of-function mechanism for familial Alzheimer's disease. *Neuron* 85, 967–981. doi: 10.1016/j.neuron.2015.02.010

Xiang, Z., Haroutunian, V., Ho, L., Purohit, D., and Pasinetti, G. M. (2006). Microglia activation in the brain as inflammatory biomarker of Alzheimer's disease neuropathology and clinical dementia. *Dis. Markers* 22, 95–102. doi: 10.1155/2006/276239

Xie, L., Zhu, Q., and Lu, J. (2022). Can we use ginkgo biloba extract to treat Alzheimer's disease? Lessons from preclinical and clinical studies. *Cells* 11:479. doi: 10.3390/cells11030479

Xu, K., Dai, X.-L., Huang, H.-C., and Jiang, Z.-F. (2011). Targeting HDACs: A promising therapy for Alzheimer's disease. *Oxid. Med. Cell. Longev.* 2011:143269. doi: 10.1155/2011/143269

Xu, S., Wilf, R., Menon, T., Panikker, P., Sarthi, J., and Elefant, F. (2014). Epigenetic control of learning and memory in Drosophila by Tip60 HAT action. *Genetics* 198, 1571–1586. doi: 10.1534/genetics.114.171660

Xu, T., Li, L., Liu, Y. C., Cao, W., Chen, J. S., Hu, S., et al. (2020). CRISPR/Cas9-related technologies in liver diseases: From feasibility to future diversity. *Int. J. Biol. Sci.* 16:2283. doi: 10.7150/ijbs.33481

Xu, X.-H., Huang, Y., Wang, G., and Chen, S.-D. (2012). Metabolomics: A novel approach to identify potential diagnostic biomarkers and pathogenesis in Alzheimer's disease. *Neurosci. Bull.* 28, 641–648. doi: 10.1007/s12264-012-1272-0

Yamini, P., Ray, R., and Chopra, K. J. I. (2018). Vitamin D_3 attenuates cognitive deficits and neuroinflammatory responses in ICV-STZ induced sporadic Alzheimer's disease. *Inflammopharmacology* 26, 39–55. doi: 10.1007/s10787-017-0372-x

Yan, M. H., Wang, X., and Zhu, X. (2013). Mitochondrial defects and oxidative stress in Alzheimer disease and Parkinson disease. *Free Radic. Biol. Med.* 62, 90–101. doi: 10.1016/j.freeradbiomed.2012.11.014

Yang, C.-C., Chiu, M.-J., Chen, T.-F., Chang, H.-L., Liu, B.-H., and Yang, S.-Y. (2018). Assay of plasma phosphorylated tau protein (threonine 181) and total tau protein in early-stage Alzheimer's disease. *J. Alzheimers Dis.* 61, 1323–1332. doi: 10.3233/JAD-170810

Yang, L., Liu, Y., Wang, Y., Li, J., and Liu, N. J. C. (2021). Azeliragon ameliorates Alzheimer's disease via the Janus tyrosine kinase and signal transducer and activator of transcription signaling pathway. *Clinics* 76:e2348. doi: 10.6061/clinics/2021/e2348

Yiannopoulou, K. G., and Papageorgiou, S. G. (2020). Current and future treatments in Alzheimer disease: An update. *J. Cent. Nerv. Syst. Dis.* 12:1179573520907397. doi: 10.1177/1179573520907397

Yuzwa, S. A., Yadav, A. K., Skorobogatko, Y., Clark, T., Vosseller, K., and Vocadlo, D. J. (2011). Mapping O-GlcNAc modification sites on tau and generation of a site-specific O-GlcNAc tau antibody. *Amino Acids.* 40, 857–868. doi: 10.1007/s00726-010-0705-1

Zarini-Gakiye, E., Amini, J., Sanadgol, N., Vaezi, G., and Parivar, K. (2020). Recent updates in the Alzheimer's disease etiopathology and possible treatment approaches: A narrative review of current clinical trials. *Curr. Mol. Pharmacol.* 13, 273–294. doi: 10.2174/1874467213666200422090135

Zetterberg, H., Wilson, D., Andreasson, U., Minthon, L., Blennow, K., Randall, J., et al. (2013). Plasma tau levels in Alzheimer's disease. *Alzheimers Res. Ther.* 5, 1–3. doi: 10.1186/alzrt163

Zhang, F., Phiel, C. J., Spece, L., Gurvich, N., and Klein, P. S. (2003). Inhibitory phosphorylation of glycogen synthase kinase-3 (GSK-3) in response to lithium: Evidence for autoregulation of GSK-3. *J. Biol. Chem.* 278, 33067–33077. doi: 10.1074/jbc.M212635200

Zhang, L., Yu, H., Sun, Y., Lin, X., Chen, B., Tan, C., et al. (2007). Protective effects of salidroside on hydrogen peroxide-induced apoptosis in SH-SY5Y human neuroblastoma cells. *Eur. J. Pharmacol.* 564, 18–25. doi: 10.1016/j.ejphar.2007.01.089

Zhang, M., Wang, S., Mao, L., Leak, R. K., Shi, Y., Zhang, W., et al. (2014). Omega-3 fatty acids protect the brain against ischemic injury by activating Nrf2 and upregulating heme oxygenase 1. *J. Neurosci.* 34, 1903–1915. doi: 10.1523/JNEUROSCI.4043-13.2014

Zhang, S., Lei, C., Liu, P., Zhang, M., Tao, W., Liu, H., et al. (2015). Association between variant amyloid deposits and motor deficits in FAD-associated presenilin-1 mutations: A systematic review. *Neurosci. Biobehav. Rev.* 56, 180–192. doi: 10.1016/j.neubiorev.2015.07.003

Zhang, Y., Chen, X., Zhao, Y., Ponnusamy, M., and Liu, Y. (2017). The role of ubiquitin proteasomal system and autophagy-lysosome pathway in Alzheimer's disease. *Nat. Rev. Neurosci.* 28, 861–868. doi: 10.1515/revneuro-2017-0013

Zhang, Y.-Q., and Sarge, K. D. (2008). Sumoylation of amyloid precursor protein negatively regulates Aβ aggregate levels. *Biochem. Biophys. Res. Commun.* 374, 673–678. doi: 10.1016/j.bbrc.2008.07.109

Zhao, J., Liu, X., Xia, W., Zhang, Y., and Wang, C. (2020). Targeting amyloidogenic processing of APP in Alzheimer's disease. *Front. Mol. Neurosci.* 13:137. doi: 10.3389/fnmol.2020.00137

Zheng, N., Wang, N., and Jia, J.-M. (2020). Therapeutic benefit of aripiprazole-olanzapine combination in the treatment of senile Alzheimer's disease complicated by mental disorders. *Trop. J. Pharm. Res.* 19, 441–446. doi: 10.4314/tjpr.v19i2.29

Zhou, F., Yan, X.-D., Wang, C., He, Y.-X., Li, Y.-Y., Zhang, J., et al. (2020). Suvorexant ameliorates cognitive impairments and pathology in APP/PS1 transgenic mice. *Neurobiol. Aging* 91, 66–75. doi: 10.1016/j.neurobiolaging.2020.02.020

Zhou, Y., Shi, J., Chu, D., Hu, W., Guan, Z., Gong, C.-X., et al. (2018). Relevance of phosphorylation and truncation of tau to the etiopathogenesis of Alzheimer's disease. *Front. Aging Neurosci.* 10:27. doi: 10.3389/fnagi.2018.00027

Zhou, Y., Zhu, F., Liu, Y., Zheng, M., Wang, Y., Zhang, D., et al. (2020). Blood-brain barrier–penetrating siRNA nanomedicine for Alzheimer's disease therapy. *Sci. Adv.* 6:eabc7031. doi: 10.1126/sciadv.abc7031

Zhu, X., Rottkamp, C. A., Boux, H., Takeda, A., Perry, G., and Smith, M. A. (2000). Activation of p38 kinase links tau phosphorylation, oxidative stress, and cell cycle-related events in Alzheimer disease. *J. Neuropathol. Exp. Neurol.* 59, 880–888. doi: 10.1093/jnen/59.10.880

frontiers | Frontiers in Aging Neuroscience

TYPE Original Research
PUBLISHED 10 October 2022
DOI 10.3389/fnagi.2022.937486

OPEN ACCESS

EDITED BY
Asma Perveen,
Glocal University, India

REVIEWED BY
Ben Nephew,
Worcester Polytechnic Institute, United States
Stephanie D'Souza,
The University of Auckland, New Zealand

*CORRESPONDENCE
Yongping Liu
lypfree@hotmail.com
Fang Han
fyhanfang@wfmc.edu.cn

†These authors have contributed equally to this work and share first authorship

SPECIALTY SECTION
This article was submitted to Alzheimer's Disease and Related Dementias, a section of the journal Frontiers in Aging Neuroscience

RECEIVED 06 May 2022
ACCEPTED 02 September 2022
PUBLISHED 10 October 2022

CITATION
Li X, Feng X, Sun X, Hou N, Han F and Liu Y (2022) Global, regional, and national burden of Alzheimer's disease and other dementias, 1990–2019. *Front. Aging Neurosci.* 14:937486. doi: 10.3389/fnagi.2022.937486

Global, regional, and national burden of Alzheimer's disease and other dementias, 1990–2019

Xue Li[1,2,3†], Xiaojin Feng[1,3†], Xiaodong Sun[1,3], Ningning Hou[1,3], Fang Han[2*] and Yongping Liu[1,3*]

[1]Department of Endocrinology and Metabolism, Affiliated Hospital of Weifang Medical University, Weifang, China, [2]Department of Pathology, Affiliated Hospital of Weifang Medical University, Weifang, China, [3]Department of Clinical Research Center, Affiliated Hospital of Weifang Medical University, Weifang, China

Background: With the increase in the aging population worldwide, Alzheimer's disease has become a rapidly increasing public health concern. Monitoring the dementia disease burden will support health development strategies by providing scientific data.

Methods: Based on the data obtained from the 2019 Global Burden of Disease (GBD) database, the numbers and age-standardized rates (ASRs) of incidence, prevalence, death, and disability-adjusted life-years (DALYs) of Alzheimer's disease and other dementias from 1990 to 2019 were analyzed. Calculated estimated annual percentage changes (EAPCs) and Joinpoint regression analyses were performed to evaluate the trends during this period. We also evaluated the correlations between the epidemiology and the sociodemographic index (SDI), an indicator to evaluate the level of social development in a country or region considering the education rate, economic situation, and total fertility rate.

Results: From 1990 to 2019, the incidence and prevalence of Alzheimer's disease and other dementias increased by 147.95 and 160.84%, respectively. The ASR of incidence, prevalence, death, and DALYs in both men and women consistently increased over the study period. All the ASRs in women were consistently higher than those in men, but the increases were more pronounced in men. In addition, the ASRs of incidence, prevalence, and DALYs were positively correlated with the SDI. Moreover, the proportion of patients over 70 years old with dementia was also positively correlated with the SDI level. Smoking was a major risk factor for the disease burden of dementia in men, while obesity was the major risk factor for women.

Conclusion: From 1990 to 2019, the Alzheimer's disease burden increased worldwide. This trend was more serious in high-SDI areas, especially among elderly populations in high-SDI areas, who should receive additional attention. Policy-makers should take steps to reverse this situation. Notably, women were at a higher risk for the disease, but the risk in men showed a faster increase. We should give attention to the aging population, attach importance

to interventions targeting dementia risk factors, and formulate action plans to address the increasing incidence of dementia.

KEYWORDS

Alzheimer's disease and other dementias, Global Burden of Disease, estimated annual percentage change, risk factors, age-standardized rate (ASR)

Introduction

Dementia is a syndrome, with the most common type being Alzheimer's disease (Oh and Rabins, 2019). Clinically, Alzheimer's disease is mainly characterized by comprehensive dementia, including memory disorder, cognitive disorder, executive dysfunction, and personality and behavior changes, and is accompanied by mental disorder symptoms in most patients (Lyketsos et al., 2011). Although these symptoms can be temporarily relieved by detailed care and medication, there are no specific measures to prevent or cure Alzheimer's disease (Srivastava et al., 2021). Dementia mainly occurs in older age groups, and the incidence and prevalence rates increase with increasing age; this trend is more common in low- and middle-income countries and regions (Gao and Liu, 2021). It has become an increasingly serious global public health problem, imposing serious economic and disease burdens on societies and families (GBD 2016 Dementia Collaborators, 2019).

It has been reported that the global number of people with dementia has increased to 43.8 million in 2016, an increase of 117% compared with 20.3 million in 1990 (GBD 2016 Dementia Collaborators, 2019). It is estimated that, by 2050, there will be 152 million people with Alzheimer's disease and other dementias (GBD 2019 Dementia Forecasting Collaborators, 2022). Given that the onset is closely related to age, the disease burden is expected to increase with the aging population and increased life expectancy. In addition to age, a recent study in the Lancet Commission has reported other risk factors for dementia, including hypertension, obesity, diabetes, physical inactivity, hearing loss, smoking, depression, low level of education, and a low socialization frequency (Livingston et al., 2017). With progressive studies, excessive alcohol intake, brain damage, and air pollution were also added to the list of risk factors for Alzheimer's disease and dementia by 2020 (Livingston et al., 2020). Although no effective measures exist to prevent or cure the onset of dementia, growing evidence has demonstrated that more than a third of dementia cases could be prevented or delayed by managing controllable risk factors (Gauthier et al., 2016; Livingston et al., 2017). Monitoring the risk factors and the epidemiological trends of Alzheimer's disease and dementia over time is critical for the global prevention of dementia (GBD 2016 Dementia Collaborators, 2019). According to the data from 1990 to 2016 in the GBD database, the most recently published study in Lancet Neurology demonstrated a growing challenge to healthcare systems worldwide (GBD 2016 Dementia Collaborators, 2019). However, the temporal trends of the following 3 years (from 2017 to 2019) were absent. In the present study, we tracked the epidemiology trends of the past three decades from 1990 to 2019 based on the data in GBD 2019, hoping to potentially inform efforts toward preventing dementia.

The Global Burden of Disease, Injury, and Risk Factors Study (GBD) 2019 leveraged available data from the literature, medical institution records, and publicly available databases and used Bayesian regression models to perform a systematic and scientific analysis of the epidemiological data of 204 countries and regions; analyses were performed for both genders, and the GBD 2019 covered 369 diseases, with corresponding age-standardized rates of incidence, prevalence, death, and DALYs (GBD 2019 Diseases Injuries Collaborators, 2020). DALYs refer to the number of healthy years of life lost from the development of morbidity to death and are the most representative and widely used indicators of disease burden (Murray et al., 2012). The GBD 2019 also included 87 common disease risks, contributing to the understanding of dementia as a complex disease (GBD 2019 Risk Factors Collaborators, 2020).

We analyzed the changing trends of Alzheimer's disease and other dementias using data from the GBD 2019; described the global distribution characteristics of dementia by gender, age, country, and region; and comprehensively analyzed the risks of dementia in different countries and regions. We hope that this study will aid in the development of targeted policies and control of dementia to improve people's health and guide the rational allocation of medical resources.

Materials and methods

Data sources

The specific data analyzed in the current study were obtained from the most recently updated online Global Health Data Exchange (GHDx) Query Tool (http://ghdx.healthdata.org/gbd-results-tool) on 20 March 2020. The detailed methods followed those of the GBD 2019 (GBD 2017 DALYs HALE Collaborators, 2018; GBD 2017 Disease Injury Incidence Prevalence Collaborators, 2018; GBD 2017 Mortality Collaborators, 2018). The GBD 2019 analysis of risk factors followed the general framework of comparative risk assessment

TABLE 1 The number of incidence cases and ASIR of Alzheimer's disease and other dementias in 1990 and 2019 and its EAPC.

Characteristics	1990		2019		1990–2019
	Incidence cases (*10^6) (95% UI)	ASIR (per 100,000) (95% UI)	Incidence cases (*10^6) (95% UI)	ASIR (per 100,000) (95% UI)	EAPC of ASIR (95% CI)
Global	2.92 (2.49–3.37)	93.58 (80.12–106.7)	7.24 (6.22–8.23)	94.99 (81.59–107.86)	0.06 (0.03 to 0.08)
Gender					
Males	1.01 (0.86–1.17)	81.03 (68.55–93)	2.69 (2.27–3.09)	83.67 (71.06–95.65)	0.13 (0.1 to 0.16)
Females	1.91 (1.63–2.2)	101.64 (87.34–115.71)	4.55 (3.93–5.16)	103.45 (89.24–117.15)	0.06 (0.04 to 0.08)
Sociodemographic index					
Low	0.11 (0.1–0.13)	78.7 (67.02–90.5)	0.27 (0.24–0.31)	76.97 (66.01–87.9)	−0.07 (−0.1 to −0.05)
Low-middle	0.3 (0.25–0.34)	77.31 (65.89–88.63)	0.82 (0.7–0.94)	77.07 (65.7–88.14)	−0.03 (−0.06 to −0.01)
Middle	0.61 (0.52–0.71)	88.38 (74.76–101.4)	1.9 (1.62–2.18)	93.29 (79.52–106.76)	0.11 (0.08 to 0.15)
High-middle	0.84 (0.71–0.99)	97.55 (82.44–111.71)	2.01 (1.71–2.31)	101.68 (86.58–116.12)	0.13 (0.11 to 0.16)
High	1.05 (0.9–1.21)	99.64 (86.19–113.09)	2.23 (1.93–2.51)	100.57 (87.24–113.37)	0.11 (0.08 to 0.14)
21 GBD regions					
Central Asia	0.04 (0.03–0.04)	101.63 (86–116.8)	0.05 (0.04–0.06)	102.74 (87.44–117.42)	0.05 (0.02 to 0.08)
Central Europe	0.13 (0.11–0.16)	104.04 (87.55–119.69)	0.24 (0.2–0.28)	106.31 (89.8–121.85)	0.09 (0.08 to 0.1)
Eastern Europe	0.23 (0.19–0.28)	98.28 (81.88–113.72)	0.36 (0.3–0.42)	101.93 (85.52–116.99)	0.17 (0.13 to 0.2)
Australasia	0.02 (0.02–0.02)	96.01 (82.52–109.28)	0.05 (0.04–0.06)	93.84 (80.46–106.76)	−0.06 (−0.07 to −0.04)
High-income Asia Pacific	0.17 (0.14–0.2)	96.86 (83.48–110.97)	0.63 (0.54–0.71)	108.9 (93.99–123.75)	0.48 (0.45 to 0.52)
High-income North America	0.42 (0.35–0.48)	111.1 (94.6–126.89)	0.74 (0.66–0.82)	105.77 (93.77–116.93)	−0.04 (−0.09 to 0)
Southern Latin America	0.04 (0.03–0.04)	92.71 (78.34–106.93)	0.08 (0.07–0.09)	95.18 (80.96–109.17)	0.1 (0.09 to 0.12)
Western Europe	0.57 (0.49–0.65)	93.49 (81.02–105.5)	1.01 (0.86–1.16)	91.52 (78.13–104.43)	−0.05 (−0.07 to −0.03)
Andean Latin America	0.01 (0.01–0.02)	80.97 (68.97–93.44)	0.04 (0.04–0.05)	83.48 (71.56–95.52)	0.11 (0.08 to 0.13)
Caribbean	0.02 (0.01–0.02)	77.69 (66.39–89.43)	0.04 (0.04–0.05)	78.42 (67.22–89.79)	0.03 (0 to 0.05)
Central Latin America	0.05 (0.05–0.06)	83.83 (71.35–96.9)	0.18 (0.16–0.21)	82.9 (70.84–95.18)	0 (−0.03 to 0.03)
Tropical Latin America	0.07 (0.06–0.08)	102.3 (88.03–116.99)	0.24 (0.21–0.27)	104.09 (90.49–118.13)	0.09 (0.07 to 0.1)
North Africa and Middle East	0.13 (0.11–0.15)	109.25 (92.75–125.03)	0.36 (0.31–0.41)	110.17 (93.94–125.62)	0.04 (0.02 to 0.06)
South Asia	0.22 (0.19–0.25)	64.17 (54.61–73.81)	0.68 (0.58–0.78)	63.63 (54.2–72.95)	−0.04 (−0.1 to 0.01)
East Asia	0.53 (0.45–0.62)	90.36 (76.22–104.02)	1.86 (1.57–2.15)	103.32 (87.6–118.29)	0.33 (0.27 to 0.39)
Oceania	0 (0–0)	88.33 (74.28–101.85)	0 (0–0)	86.26 (73.29–98.98)	−0.09 (−0.12 to −0.06)
Southeast Asia	0.15 (0.13–0.17)	84.62 (72.1–97.18)	0.4 (0.35–0.46)	84.8 (72.56–96.84)	0.02 (−0.02 to 0.06)
Central Sub-Saharan Africa	0.01 (0.01–0.01)	96.41 (83.03–110.18)	0.03 (0.03–0.04)	98.35 (85.22–112.11)	0.08 (0.07 to 0.09)
Eastern Sub-Saharan Africa	0.04 (0.03–0.05)	85.81 (73.42–98.23)	0.09 (0.08–0.11)	85.08 (73.42–96.76)	−0.02 (−0.05 to 0.02)
Southern Sub-Saharan Africa	0.02 (0.02–0.02)	90.15 (77.17–103.33)	0.04 (0.03–0.04)	89.95 (77.28–102.68)	−0.01 (−0.06 to 0.04)
Western Sub-Saharan Africa	0.04 (0.04–0.05)	75.34 (64.05–86.53)	0.09 (0.08–0.11)	73.47 (62.61–83.94)	−0.11 (−0.18 to −0.03)

ASIR, age-standardized incidence rate; EAPC, estimated annual percent change; SDI, sociodemographic index.

(CRA), including the inclusion of risk-outcome pairs, relative risk estimates, estimation of exposure levels and distributions, determination of counterfactual levels of exposure, calculation of population attribution scores and attribution burdens, and estimation of the mediating role of different risk factors through other risk factors (GBD 2019 Risk Factors Collaborators, 2020). The detailed methods refer to previous studies (GBD 2019 Risk Factors Collaborators, 2020). We analyzed the trends of incident cases, prevalent cases, deaths, and DALYs due to Alzheimer's disease and other dementias from 1990 to 2019 at the global, regional, and state levels. Differences among sexes and age ranges were also assessed. Age-standardized rates (ASRs) were used to prevent confounding due to age in the analysis to ensure consistency among most rates.

The sociodemographic index (SDI), which ranges from 0 to 1, is a comprehensive indicator and is calculated considering the education rate, economic situation, and total fertility rate of a country or region (HUMANOSPHERE, 2016). The larger the value of the SDI, the higher the level of social development. All 204 countries and regions were separated into five SDI

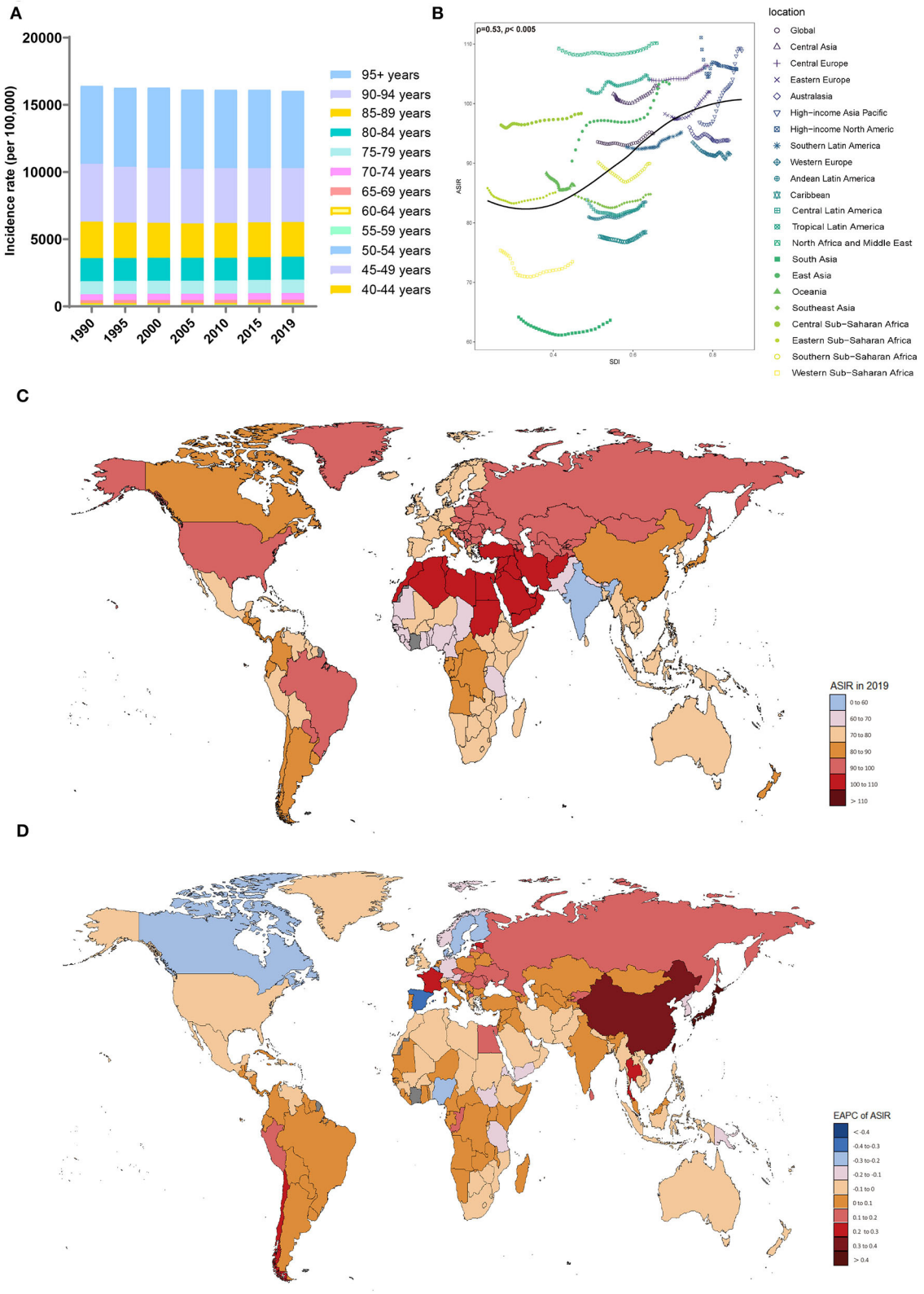

FIGURE 1
Distribution of the incidence of Alzheimer's disease and other dementias in 204 countries and territories from 1990 to 2019 by age group and SDI region. **(A)** Incidence rate in each age group. **(B)** Correlations between the ASIRs of Alzheimer's disease and other dementias

(Continued)

FIGURE 1 (Continued)
and SDI regions in 2019. Associations were calculated with Pearson correlation analysis. **(C)** The ASIRs of 204 countries and territories. **(D)** EAPCs in the ASIRs in 204 countries and territories. SDI, sociodemographic index; ASIR, age-standardized incidence rate; EAPC, estimated annual percent change.

groups: the high-SDI group (> 0.81), medium-high-SDI group (0.70–0.81), medium-SDI group (0.61–0.70), medium-low-SDI group (0.46–0.61), and low-SDI group (<0.46). Based on the geographic location, all the countries were also divided into 21 regions for analysis in the current study. This study was conducted using data obtained from publicly available databases, and hence no ethical approval was required.

Statistical analysis

We described the numbers [with the associated 95% uncertainty intervals (UIs)] and the trends of incident cases, prevalent cases, deaths, and DALYs, and their corresponding ASRs (and the associated 95% UIs) for dementia by sex, age, year, SDI subregion, GBD regions, and 204 countries and regions. Since there were few cases of dementia in people under the age of 40 years, they were not included in this research, and only cases in people over 40 years of age were analyzed.

The time trends of ASRs in a specific time period are represented by the estimated annual percentage change (EAPC) (Ding et al., 2022). In short, we used the $y = \alpha + \beta x + \epsilon$ regression model for these calculations, where y is ln (ASR), x is the time variable, and ε is the error term. The natural logarithm of the ASR was assumed to be linear with time; therefore, $EAPC = 100 \times [\exp(\beta) - 1]$ (Ding et al., 2022). We also used linear models to calculate 95% confidence intervals (95% CIs) for the EAPCs. If both the EAPC and its 95% CI lower bound were greater than 0, the ASR was considered to show an increasing trend. Conversely, if both the EAPC and its 95% CI upper limit were less than 0, the ASR was considered to show a decreasing trend.

Joinpoint regression analysis, performed by fitting different time periods using the simplest logarithmic model, was used to describe the changing trend over a specific time period. It allows for a more detailed assessment of different interval-specific disease variability characteristics on a global time scale. The Joinpoint regression model was mainly implemented by comparing the annual percent change (APC) and the average annual percent change (AAPC) with 0 to evaluate whether the trends of the disease rates in different segments were statistically significant. Joinpoint version 4.9.0.1 software, developed by the National Cancer Institute, was used for the Joinpoint regression analysis. All the other analyses and visualizations were carried out with GraphPad Prism 8 software and R software (version 4.1.2). A P-value < 0.05 was considered statistically significant.

Results

Incidence trends from 1990 to 2019

Globally, the incidence of Alzheimer's disease and other dementias increased by 147.95% from 1990 to 2019, with 2.92 million cases (95% UI: 2.49 to 3.37) in 1990 and 7.24 million cases (95% UI, 6.22 to 8.23) in 2019 (Table 1). Regarding sex, the age-standardized incidence rate (ASIR, per 100,000 population) of dementia increased in both men and women over this period (EAPC, men: 0.13; 95% CI, 0.1 to 0.16; women: 0.06; 95% CI, 0.04 to 0.08) (Table 1, Supplement Figure 1A). The overall ASIR (per 100,000 population) in men increased sharply. It is worth noting that the incidence rate of dementia increased with age (Figure 1A). From 1990 to 2019, the incidence rate in the 70–74 age group was the fastest growing over time (Supplement Figure 1B).

The ASIRs of dementia were positively related to SDI levels ($\rho = 0.53$, $p < 0.005$) (Figure 1B), with the ASIRs (per 100,000 population) in the high-middle-SDI (ASIR = 101.68; 95% UI, 86.58 to 116.12) and high-SDI (ASIR = 100.57; 95% UI, 87.24 to 113.37) areas being much higher than those in other SDI areas in 2019 (Table 1, Supplement Figure 1C). The ASIRs (per 100,000 population) for dementia increased most in the high-middle-SDI regions (EAPC, 0.13; 95% CI, 0.11 to 0.16), while in areas with a low-SDI (EAPC, −0.07; 95% CI, −0.1 to −0.05) and low-middle-SDI (EAPC, −0.03; 95% CI, −0.06 to −0.01), decreasing trends were observed. In 2019, the proportion of female ASIRs in all SDI regions and GBD subregions was higher than that in men (Supplement Figure 1D). In areas with a higher SDI, the incidence of dementia tended to be higher in those over 70 years old (Supplement Figure 1E).

In the 21 regions based on geographic location, the highest ASIRs (per 100,000 population) of dementia were in North Africa and the Middle East (ASIR = 110.17; 95% UI, 93.94 to 125.62), high-income Asia-Pacific (ASIR = 108.9; 95% UI, 93.99 to 123.75), and Central Europe (ASIR = 106.31; 95% UI, 89.8 to 121.85) in 2019; the lowest ASIRs were noticed in South Asia (ASIR = 63.63; 95% UI, 54.2 to 72.95) and Western Sub-Saharan Africa (ASIR = 73.47; 95% UI, 62.61 to 83.94) (Table 1). From 1990 to 2019, the ASIR (per 100,000 population) of dementia increased the most in high-income Asia-Pacific (EAPC, 0.48; 95% CI, 0.45 to 0.52), while the largest decrease occurred in Western Sub-Saharan Africa (EAPC, −0.11; 95% CI, −0.18 to −0.03). The ASIRs in the other territories have remained relatively stable.

TABLE 2 The number of prevalence cases and ASPR of Alzheimer's disease and other dementias in 1990 and 2019 and its EAPC.

Characteristics	1990		2019		1990–2019
	Prevalence cases (*10^6) (95% UI)	ASPR (per 100,000) (95% UI)	Prevalence cases (*10^6) (95% UI)	ASPR (per 100,000) (95% UI)	EAPC of ASPR (95% CI)
Global	19.79 (16.93–22.79)	645.89 (552.86–743.62)	51.62 (44.28–59.02)	682.48 (585.2–782.73)	0.2 (0.18 to 0.21)
Gender					
Males	6.77 (5.71–7.83)	547.5 (463.19–631.56)	18.7 (15.78–21.51)	585.87 (497.37–672.86)	0.26 (0.24 to 0.28)
Females	13.02 (11.17–14.96)	703.9 (605.24–809.19)	32.92 (28.43–37.72)	748.15 (646.36–856.85)	0.21 (0.2 to 0.23)
Sociodemographic index					
Low	0.75 (0.64–0.87)	515.21 (440.9–594.89)	1.83 (1.56–2.1)	514.75 (440.15–591.04)	0.01 (0 to 0.03)
Low-middle	1.96 (1.68–2.26)	513.81 (439.5–593.94)	5.64 (4.8–6.5)	530.64 (453.38–611.28)	0.09 (0.08 to 0.1)
Middle	4.06 (3.45–4.7)	589.56 (504.16–680.86)	13.37 (11.32–15.46)	666.73 (565.41–768.83)	0.32 (0.28 to 0.36)
High-middle	5.75 (4.85–6.66)	682.34 (577.51–789.53)	14.56 (12.35–16.87)	739.18 (626.68–855.07)	0.26 (0.24 to 0.28)
High	7.26 (6.22–8.34)	692.75 (598.34–792.76)	16.2 (14.05–18.36)	721.43 (627.54–817.7)	0.23 (0.2 to 0.26)
21 GBD regions					
Central Asia	0.26 (0.22–0.31)	699.37 (589.17–811.44)	0.34 (0.29–0.4)	716.26 (605.71–834.99)	0.1 (0.08 to 0.13)
Central Europe	0.92 (0.76–1.08)	735.33 (615.6–856.54)	1.74 (1.45–2.03)	761.23 (636.83–884.61)	0.14 (0.13 to 0.14)
Eastern Europe	1.58 (1.31–1.87)	683.38 (568.49–801.74)	2.52 (2.11–2.97)	717.09 (600.77–837.07)	0.23 (0.19 to 0.26)
Australasia	0.15 (0.13–0.17)	681.73 (584.78–782.18)	0.38 (0.32–0.44)	674.23 (574.91–778.88)	−0.02 (−0.03 to −0.01)
High-income Asia Pacific	1.11 (0.96–1.29)	649.53 (556.92–750.35)	4.58 (3.88–5.31)	773.2 (662.42–891.86)	0.69 (0.64 to 0.73)
High-income North America	2.98 (2.52–3.45)	795.59 (675.14–916.53)	5.44 (4.85–5.97)	773.57 (690.32–849.66)	0.06 (0 to 0.12)
Southern Latin America	0.25 (0.21–0.3)	637.38 (535.38–739.47)	0.58 (0.49–0.68)	670.68 (567.9–776.55)	0.19 (0.18 to 0.2)
Western Europe	3.89 (3.36–4.43)	646.9 (562.24–731.98)	7.32 (6.23–8.48)	651.29 (557.74–752.35)	0.04 (0.02 to 0.05)
Andean Latin America	0.09 (0.08–0.1)	520.49 (448.14–597.87)	0.29 (0.25–0.34)	558.72 (481.3–642.17)	0.25 (0.23 to 0.26)
Caribbean	0.12 (0.1–0.14)	514.03 (442.79–590.87)	0.28 (0.24–0.32)	530.93 (457.42–607.2)	0.11 (0.1 to 0.12)
Central Latin America	0.36 (0.31–0.41)	541.69 (464.48–626.82)	1.21 (1.04–1.38)	546.85 (471.02–628.34)	0.08 (0.06 to 0.11)
Tropical Latin America	0.49 (0.42–0.56)	714.71 (617.47–818.28)	1.74 (1.5–1.98)	767.53 (663.42–876.09)	0.34 (0.29 to 0.38)
North Africa and Middle East	0.87 (0.74–1.01)	754.7 (640.49–870.78)	2.49 (2.12–2.86)	777.63 (660.8–895.96)	0.12 (0.11 to 0.13)
South Asia	1.45 (1.24–1.68)	421.73 (360.05–485.43)	4.64 (3.93–5.34)	428.42 (365.02–493.98)	0.04 (0 to 0.09)
East Asia	3.47 (2.9–4.04)	609.05 (515.11–707.65)	13.57 (11.39–15.79)	781.43 (659.97–904.1)	0.65 (0.56 to 0.73)
Oceania	0.01 (0.01–0.01)	581.21 (492–676.1)	0.02 (0.02–0.03)	575.09 (485.96–666.95)	−0.05 (−0.07 to −0.03)
Southeast Asia	1.02 (0.87–1.18)	566.26 (483.98–651.08)	2.79 (2.39–3.2)	590.55 (505.03–677.25)	0.17 (0.14 to 0.2)
Central Sub-Saharan Africa	0.08 (0.07–0.1)	665.37 (567.54–766.03)	0.22 (0.19–0.25)	695.87 (596.01–796.94)	0.17 (0.16 to 0.18)
Eastern Sub-Saharan Africa	0.26 (0.23–0.31)	570.52 (489.37–655.73)	0.62 (0.53–0.71)	574.66 (495.93–657.82)	0.04 (0.02 to 0.07)
Southern Sub-Saharan Africa	0.13 (0.11–0.15)	601.78 (515.22–692.95)	0.26 (0.22–0.3)	607.44 (520.21–699.81)	0.03 (−0.02 to 0.09)
Western Sub-Saharan Africa	0.29 (0.25–0.34)	481.44 (411.98–554.82)	0.61 (0.52–0.69)	469.82 (402.13–539.35)	−0.1 (−0.19 to −0.02)

ASPR, age-standardized prevalence rate; EAPC, estimated annual percent change; SDI, sociodemographic index.

At the country level, Turkey, Bahrain, and Iran showed the highest ASIRs (per 100,000 population) among the 204 countries and regions, while the lowest were in India, Pakistan, and Nepal (Supplement Table 1, Figure 1C). Japan

and China showed the fastest increases in ASIRs (per 100,000 population) over this period (EAPC, 0.58, 95% CI, 0.53 to 0.62 for Japan; EAPC, 0.33, 95% CI, 0.27 to 0.4 for China) (Figure 1D). In most countries and regions, the ASIRs (per 100,000 population) remained relatively stable and even showed significant downward trends, including in Luxembourg (EAPC, −0.42; 95% CI, −0.52 to −0.33), Spain (EAPC, −0.31; 95% CI, −0.37 to −0.26), and Belgium (EAPC, −0.28; 95% CI, −0.3 to −0.25).

Prevalence trends from 1990 to 2019

Globally, in 2019, the number of Alzheimer's disease and other dementia patients was 160.84% higher than that observed in 1990, which was 51.62 million (95% UI, 44.28 to 59.02 million) (Table 2). The ASPR (per 100,000 population) was 682.48 (95% UI, 585.2 to 782.73) in 2019, indicating an upward trend (EAPC, 0.2; 95% CI, 0.18 to 0.21).

The ASPRs (per 100,000 population) in all of the SDI regions showed an upward trend, with the highest in the high-middle-SDI (739.18, 95% UI, 626.68 to 855.07) region, while ASPRs in the middle-SDI region showed the fastest increase (EAPC, 0.32, 95% CI, 0.28 to 0.36) (Table 2, Supplement Figure 2C). Compared with men, women had a higher ASPR (per 100,000 population) (Table 2, Supplement Figures 2A,D). However, there was a larger upward trend in the male ASPR (per 100,000 population) (EAPC, 0.26; 95% CI, 0.24 to 0.28). The prevalence rate increased with age (Figure 2A). From 1990 to 2019, the prevalence rate in the 80–84 age group was the fastest growing over time (Supplement Figure 2B). Notably, younger patients were mainly concentrated in lower SDI regions (Supplement Figure 2E).

The region with the highest ASPR (per 100,000 population) in 2019 was East Asia (781.43, 95% UI, 659.97 to 904.1), and the region with the lowest was South Asia (428.42, 95% UI, 365.02–493.98). In most territories, particularly high-income Asia-Pacific (EAPC, 0.69; 95% CI, 0.64 to 0.73), the ASPR (per 100,000 population) showed upward trends. Only Australia (EAPC, −0.02; 95% CI, −0.03 to −0.01), Oceania (EAPC, −0.05; 95% CI, −0.07 to −0.03), and Western Sub-Saharan Africa (EAPC, −0.1; 95% CI, −0.19 to −0.02) showed a slight downward trend. The ASPRs (per 100,000 population) were also positively related to the SDI values among the 21 regions in 2019 ($\rho = 0.56$, $p < 0.005$) (Figure 2B).

In 2019, the highest ASPRs (per 100,000 population) were noticed in Turkey, Bahrain, and Kuwait, while the lowest ASPRs (per 100,000 population) were observed in India, Nigeria, and Pakistan (Supplement Table 2, Figure 2C). The ASPRs (per 100,000 population) in Taiwan, China (EAPC, 0.78; 95% CI, 0.64 to 0.92), Japan (EAPC, 0.77; 95% CI, 0.71 to 0.83), and China (EAPC, 0.66; 95% CI, 0.57 to 0.75) showed the fastest upward trend (Figure 2D). The ASPRs (per 100,000 population) in Luxembourg (EAPC, −0.43; 95% CI, −0.54 to −0.31), Nigeria (EAPC, −0.34; 95% CI, −0.48 to −0.19), and Spain (EAPC, −0.32; 95% CI, −0.38 to −0.26) showed a significant downward trend.

Death trends from 1990 to 2019

Global deaths due to Alzheimer's disease and other dementias increased from 0.56 million (95% UI, 0.14 to 1.55) in 1990 to 1.62 million (95% UI, 0.41 to 4.21) in 2019, nearly tripling in 30 years (Table 3). The age-standardized death rate (ASDR) (per 100,000 population) also increased (EAPC, 0.13, 95% CI, 0.1 to 0.15). From 1990 to 2019, the ASDRs (per 100,000 population) increased in both men and women (EAPC, men: 0.2; 95% CI, 0.18 to 0.23; women: 0.12; 95% CI, 0.09 to 0.15) (Table 3, Supplement Figure 3A). In 2019, the overall ASDR proportions (per 100,000 population) in women in each SDI region and GBD region were higher than those in men (Supplement Figure 3D). Across the age groups, the death rate increased with age (Figure 3A). From 1990 to 2019, death cases in > 95 age group showed the fastest growth over time (Supplement Figure 3B).

In 2019, the ASDRs (per 100,000 population) were highest in the middle-SDI (ASDR = 23.21; 95% UI, 5.69 to 60.43) and low-SDI (ASDR = 23.03; 95% UI, 5.64 to 62.49) regions (Table 3, Figure 3B). The low-SDI regions had the largest increase in the ASDR (per 100,000 population) (EAPC, 0.4; 95% CI, 0.36 to 0.43). There was no obvious relationship between the SDI and the ASDR (per 100,000 population) values in each region (Supplement Figure 3C). Supplement Figure 5 shows the joinpoint regression analysis of the ASDRs (per 100,000 population) for each SDI region from 1990 to 2019. The global ASDR (per 100,000 population) increased significantly from 1990 to 2009 and then decreased significantly after 2010. Overall, the ASDR (per 100,000 population) in the low-SDI regions remained stable from 1990 to 1996 and increased sharply from 1996 to 2019. The high-SDI regions experienced a significant increase in the ASDR (per 100,000 population) from 1990 to 1995 and from 2000 to 2011 and a sharp decline from 1995 to 2000 and from 2015 to 2019; the overall increase in the ASDR (per 100,000 population) was modest (EAPC, 0.1; 95% CI, 0.056 to 0.139). The lower the SDI, the higher the proportion of younger people who died due to dementia (Supplement Figure 3E).

The regions with the highest ASDRs (per 100,000 population) of dementia in 2019 were high-income Asia-Pacific (27; 95% UI, 7.46 to 65.44), Central Sub-Saharan Africa (26.57; 95% UI, 6.67 to 71.45), and Eastern Sub-Saharan Africa (26.25; 95% UI, 6.52 to 69.47), while the lowest ASDRs were in South Asia (19.17; 95% UI, 4.62 to 52.06), the Caribbean (20.75; 95% UI, 5.26 to 51.95) and high-income North America (20.87;

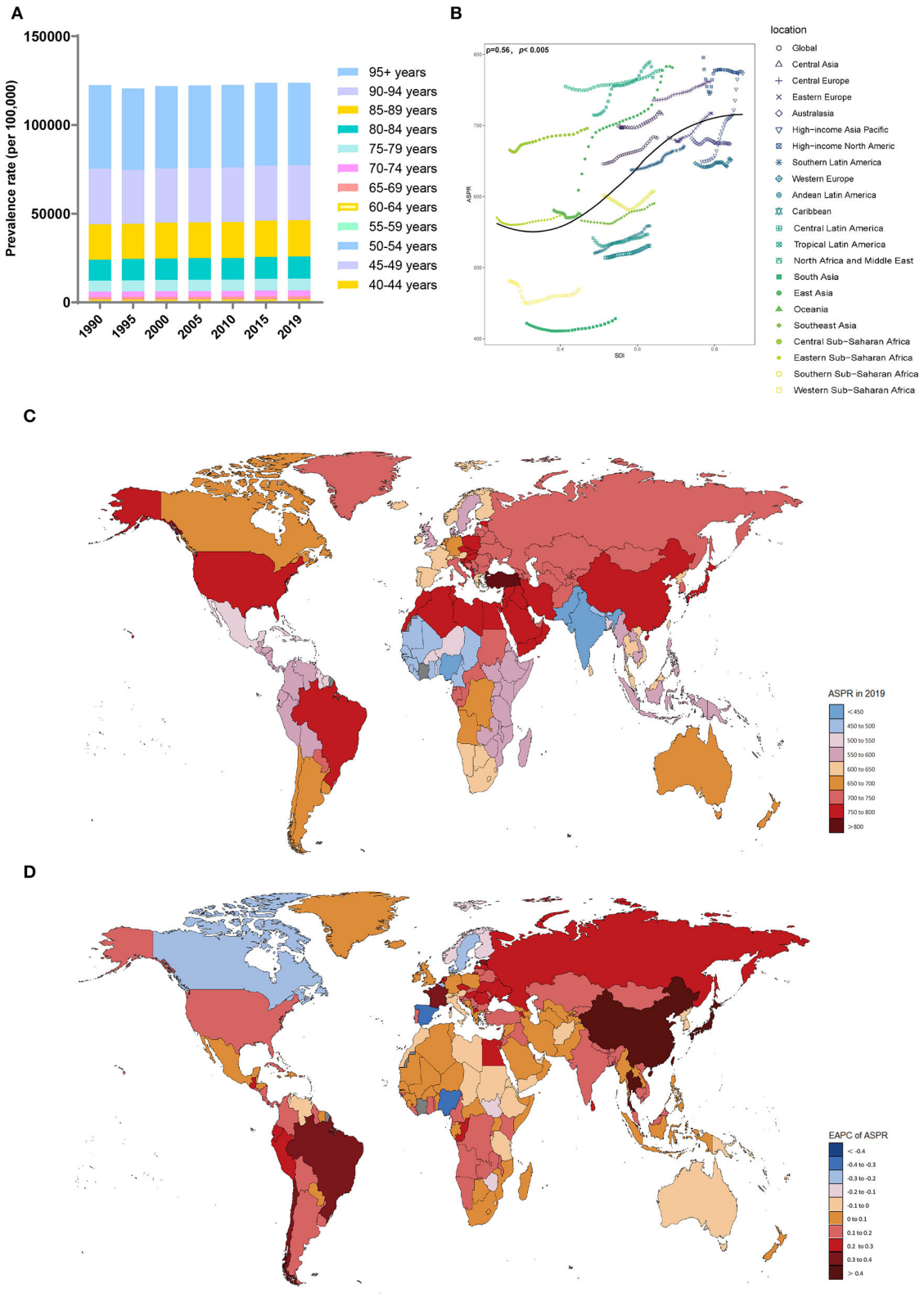

FIGURE 2
Distribution of the prevalence of Alzheimer's disease and other dementias in 204 countries and territories from 1990 to 2019 by age group and SDI region. **(A)** Prevalence rate in each age group; **(B)** Correlations between the ASPRs of Alzheimer's disease and other dementias and SDI regions in 2019; associations were calculated with Pearson correlation analysis; **(C)** The ASPRs in 204 countries and territories; **(D)** EAPCs in the ASPRs in 204 countries and territories. SDI, sociodemographic index; ASPR, age-standardized prevalence rate; EAPC, estimated annual percent change.

TABLE 3 The number of deaths and ASDR of Alzheimer's disease and other dementias in 1990 and 2019 and its EAPC.

Characteristics	1990		2019		1990–2019
	Death cases (*10^6) (95% UI)	ASDR (per 100,000) (95% UI)	Death cases (*10^6) (95% UI)	ASDR (per 100,000) (95% UI)	EAPC of ASDR from 1990 to 2019 (95% CI)
Global	0.56 (0.14–1.55)	22.24 (5.5–59.98)	1.62 (0.41–4.21)	22.92 (5.83–59.2)	0.13 (0.1 to 0.15)
Gender					
Males	0.18 (0.04–0.51)	19.71 (4.7–54.97)	0.56 (0.14–1.51)	20.71 (5.03–55.21)	0.2 (0.18 to 0.23)
Females	0.38 (0.09–1.04)	23.49 (5.86–62.54)	1.06 (0.27–2.71)	24.19 (6.24–61.53)	0.12 (0.09 to 0.15)
Sociodemographic index					
Low	0.02 (0–0.06)	20.9 (4.93–58.1)	0.06 (0.02–0.17)	23.03 (5.64–62.49)	0.4 (0.36 to 0.43)
Low-middle	0.05 (0.01–0.15)	20.12 (4.77–55.72)	0.19 (0.05–0.5)	21.61 (5.22–56.36)	0.26 (0.23 to 0.3)
Middle	0.12 (0.03–0.33)	23.02 (5.52–63.87)	0.39 (0.09–1.03)	23.21 (5.69–60.43)	0.09 (0.06 to 0.12)
High-middle	0.15 (0.04–0.42)	22.53 (5.54–60.52)	0.42 (0.1–1.12)	22.8 (5.68–60.14)	0.09 (0.03 to 0.16)
High	0.22 (0.05–0.58)	21.96 (5.49–57.5)	0.56 (0.15–1.39)	22.66 (5.89–56.63)	0.1 (0.06 to 0.14)
21 GBD regions					
Central Asia	0.01 (0–0.02)	21.61 (5.35–59.48)	0.01 (0–0.02)	23.45 (5.72–64.46)	0.26 (0.22 to 0.31)
Central Europe	0.02 (0.01–0.07)	23.43 (5.7–64.73)	0.05 (0.01–0.13)	23.02 (5.54–59.38)	−0.1 (−0.12 to −0.08)
Eastern Europe	0.04 (0.01–0.11)	20.29 (4.82–55.98)	0.07 (0.02–0.2)	21.55 (5.25–57.33)	0.2 (0.16 to 0.24)
Australasia	0 (0–0.01)	22.57 (5.6–59.73)	0.01 (0–0.03)	22.08 (5.71–56.53)	−0.09 (−0.11 to −0.07)
High-income Asia Pacific	0.03 (0.01–0.09)	21.86 (5.4–58.45)	0.18 (0.05–0.44)	27 (7.46–65.44)	0.96 (0.81 to 1.12)
High-income North America	0.08 (0.02–0.21)	21.38 (5.41–56.38)	0.16 (0.04–0.4)	20.87 (5.34–52.13)	−0.26 (−0.35 to −0.17)
Southern Latin America	0.01 (0–0.02)	20.86 (5.05–56.22)	0.02 (0–0.05)	21.03 (5.13–56.08)	0.08 (0.06 to 0.11)
Western Europe	0.12 (0.03–0.32)	22.27 (5.52–57.2)	0.26 (0.07–0.68)	21.31 (5.37–54.62)	−0.17 (−0.2 to −0.14)
Andean Latin America	0 (0–0.01)	21.48 (5.26–58.33)	0.01 (0–0.03)	21.76 (5.35–55.53)	0.08 (0.05 to 0.1)
Caribbean	0 (0–0.01)	20.59 (5.04–55.72)	0.01 (0–0.03)	20.75 (5.26–51.95)	0.05 (0.04 to 0.07)
Central Latin America	0.01 (0–0.04)	23.44 (5.76–63.72)	0.05 (0.01–0.13)	23.84 (6.04–60.61)	0.02 (0 to 0.05)
Tropical Latin America	0.01 (0–0.04)	26.64 (6.57–71.11)	0.06 (0.01–0.14)	25.57 (6.51–66.21)	−0.08 (−0.11 to −0.05)
North Africa and Middle East	0.02 (0.01–0.07)	26.12 (6.35–72.64)	0.07 (0.02–0.19)	25.52 (6.34–67.06)	−0.06 (−0.09 to −0.02)
South Asia	0.04 (0.01–0.11)	16.79 (3.83–48.06)	0.16 (0.04–0.44)	19.17 (4.62–52.06)	0.44 (0.35 to 0.53)
East Asia	0.1 (0.02–0.27)	23.3 (5.39–63.68)	0.33 (0.08–0.89)	23.19 (5.63–61.19)	0.14 (0.06 to 0.22)
Oceania	0 (0–0)	22.17 (5.12–60.7)	0 (0–0)	21.52 (5.08–58.96)	−0.14 (−0.17 to −0.11)
Southeast Asia	0.03 (0.01–0.09)	22.83 (5.48–62.35)	0.09 (0.02–0.24)	23.62 (5.72–60.72)	0.12 (0.1 to 0.14)
Central Sub-Saharan Africa	0 (0–0.01)	23.66 (5.51–67.36)	0.01 (0–0.02)	26.57 (6.67–71.45)	0.43 (0.4 to 0.45)
Eastern Sub-Saharan Africa	0.01 (0–0.02)	22.95 (5.4–62.79)	0.02 (0.01–0.06)	26.25 (6.52–69.47)	0.54 (0.5 to 0.58)
Southern Sub-Saharan Africa	0 (0–0.01)	21.95 (5.17–59.26)	0.01 (0–0.02)	22.87 (5.49–62.53)	0.12 (0.07 to 0.17)
Western Sub-Saharan Africa	0.01 (0–0.03)	22.9 (5.5–65.94)	0.03 (0.01–0.07)	25.63 (6.31–68.48)	0.51 (0.44 to 0.58)

ASDR, age-standardized death rate; EAPC, estimated annual percent change; SDI, sociodemographic index.

95% UI, 5.34 to 52.13) (Table 3). The ASDRs (per 100,000 population) of dementia increased the most in high-income Asia-Pacific (EAPC, 0.96; 95% CI, 0.81 to 1.12), high-income North America (EAPC, −0.26; 95% CI, −0.35 to −0.17),

and Western Europe (EAPC, −0.17; 95% CI, −0.2 to −0.14) decreased the most.

The countries with the highest ASDRs (per 100,000 population) of dementia in 2019 were Kiribati and Afghanistan, while the countries with the lowest ASDRs (per 100,000 population) were Bangladesh, India, and Luxembourg (Supplement Table 3, Figure 3C). The countries with the largest increase in the ASDRs (per 100,000 population) of dementia were Eritrea (EAPC, 1.37,; 95% CI, 1.19 to 1.55) and Rwanda (EAPC, 1.14; 95% CI, 0.99 to 1.28) (Figure 3D). Most countries, notably Germany (EAPC, −0.94, 95% CI, −1.08 to −0.81), Guam (EAPC, −0.71, 95% CI, −0.82 to −0.61), and the Philippines (EAPC, −0.7, 95% CI, −0.89 to −0.51), showed a downward trend in the ASDRs (per 100,000 population).

DALYs trends from 1990 to 2019

Between 1990 and 2019, the number of DALYs due to Alzheimer's disease and other forms of dementia worldwide increased from 9.66 million (95% UI, 4.23 to 21.37) to 25.28 million (95% UI, 11.2 to 54.56) (Table 4). The ASR also increased (EAPC, 0.15; 95% CI, 0.13 to 0.16). In 2019, the burden of disease attributed to dementia was consistently higher in women than in men. However, the increase was larger in men (EAPC, men: 0.21; 95% CI, 0.2 to 0.23; women: 0.15; 95% CI, 0.13 to 0.17) (Table 4, Supplement Figure 4A). Among the age groups, the DALYs rate increased with age (Figure 4A). From 1990 to 2019, the number of DALYs in the 80–84 age group showed the fastest growth over time (Supplement Figure 4B).

From 1990 to 2019, the ASR of DALYs (per 100,000 population) due to dementia trended upward in all SDI regions, especially in the low-SDI regions (EAPC, 0.28; 95% CI, 0.26 to 0.3) (Table 4, Supplement Figure 4C). In 2019, the DALY ASR (per 100,000 population) was highest in the high-middle-SDI regions (ASR of DALYs = 348.46; 95% UI, 157.71 to 754.37). In 2019, the proportion of the ASR of DALYs in women was higher than that in men in all SDI and GBD territories (Supplement Figure 4D). Patients >70 years of age accounted for a considerable percentage of DALYs due to dementia, and the proportion increased with increasing SDI (Supplement Figure 4E).

In 2019, the GBD region with the highest ASR of DALYs (per 100,000 population) due to dementia was tropical Latin America (ASR of DALYs = 390.88; 95% UI, 172.01 to 855.99), while the region with the lowest ASR of DALYs was South Asia (ASR of DALYs = 262.09; 95% UI, 105.55 to 617.38) (Table 4). The ASR of DALYs due to dementia increased in most regions from 1990 to 2019, with the largest increase in high-income Asia-Pacific (EAPC, 0.81; 95% CI, 0.7 to 0.92). The ASR of DALYs declined in high-income North America (EAPC, −0.22; 95% CI, −0.27 to −0.17). The ASRs of DALYs in each region in 2019 were positively related to the SDI ($\rho = 0.12$, $p < 0.005$) (Figure 4B).

In 2019, the highest ASR of DALYs (per 100,000 population) was observed in Kiribati, Afghanistan, and Oman (Supplement Table 4, Figure 4C). In contrast, the countries with the lowest ASR of DALYs (per 100,000 population) were India and Bangladesh. Since 1990, the ASR of DALYs for Eritrea (EAPC, 0.94, 95% CI: 0.83 to 1.05) and Japan (EAPC, 0.93, 95% CI: 0.81 to 1.05) increased significantly (Figure 4D). In contrast, Spain (EAPC, −0.63, 95% CI: −0.77 to −0.48), the Philippines (EAPC, −0.6, 95% CI: −0.77 to −0.44), and Germany (EAPC, −0.58, 95% CI: −0.66 to −0.5) showed clear downward trends.

Risk factors

Based on GBD2019, high fasting blood glucose, high body mass index [BMI], and smoking were the major risk factors for dementia. The ASDR and DALYs (per 100,000 population) caused by smoking were the highest, at 2.91 (95% UI, 0.64 to 8.06) and 51.30 (95% UI, 20.50 to 116.23), respectively (Supplement Table 5).

In the high-middle-SDI group, risk factors had the highest impact on the dementia burden; the ASDR (per 100,000 population) was 7.49 (95% UI, 1.63 to 22.15), and the ASR of DALYs (per 100,000 population) was 122.65 (95% UI, 48.42 to 302.74) (Supplement Table 5). This was followed by the high-SDI group, with an ASDR (per 100,000 population) of 7.56 (95% UI, 1.69 to 21.41) and ASR of DALYs (per 100,000 population) of 120.88 (95% UI, 49.78 to 282.72). Risk factors had the least impact on the disease burden in the low-SDI regions, with a corresponding ASDR and ASR of DALYs (per 100,000 population) of 4.71 (95% UI, 0.96 to 14.78) and 68.65 (95% UI, 22.57 to 183.31), respectively. Smoking contributed the most to the disease burden in areas with the high-SDI group (Figure 5A). For the low-SDI region, the ASDR and ASR of DALYs (per 100,000 population) attributable to high fasting plasma glucose were the highest. The burden of disease attributable to smoking increased gradually with increasing SDI.

Men were more affected by risk factors than women, with an ASDR of 8.14 (95% UI, 1.91 to 23.50) and ASR of DALYs (per 100,000 population) of 128.80 (95% UI, 51.81 to 303.90) (Supplement Table 5). Men are more susceptible to behavioral risk factors, such as smoking, while women are more susceptible to metabolic risk factors, such as a high BMI (Figure 5B).

Discussion

Globally, the incidence (147.95%), prevalence (160.84%), and number of deaths (189.29%) due to dementia increased dramatically over the study period. Globally, the incidence is predicted to be 152.8 million in 2050 (GBD 2019 Dementia Forecasting Collaborators, 2022). Correspondingly, the global ASIR and ASPR (per 100,000 population) showed consistently

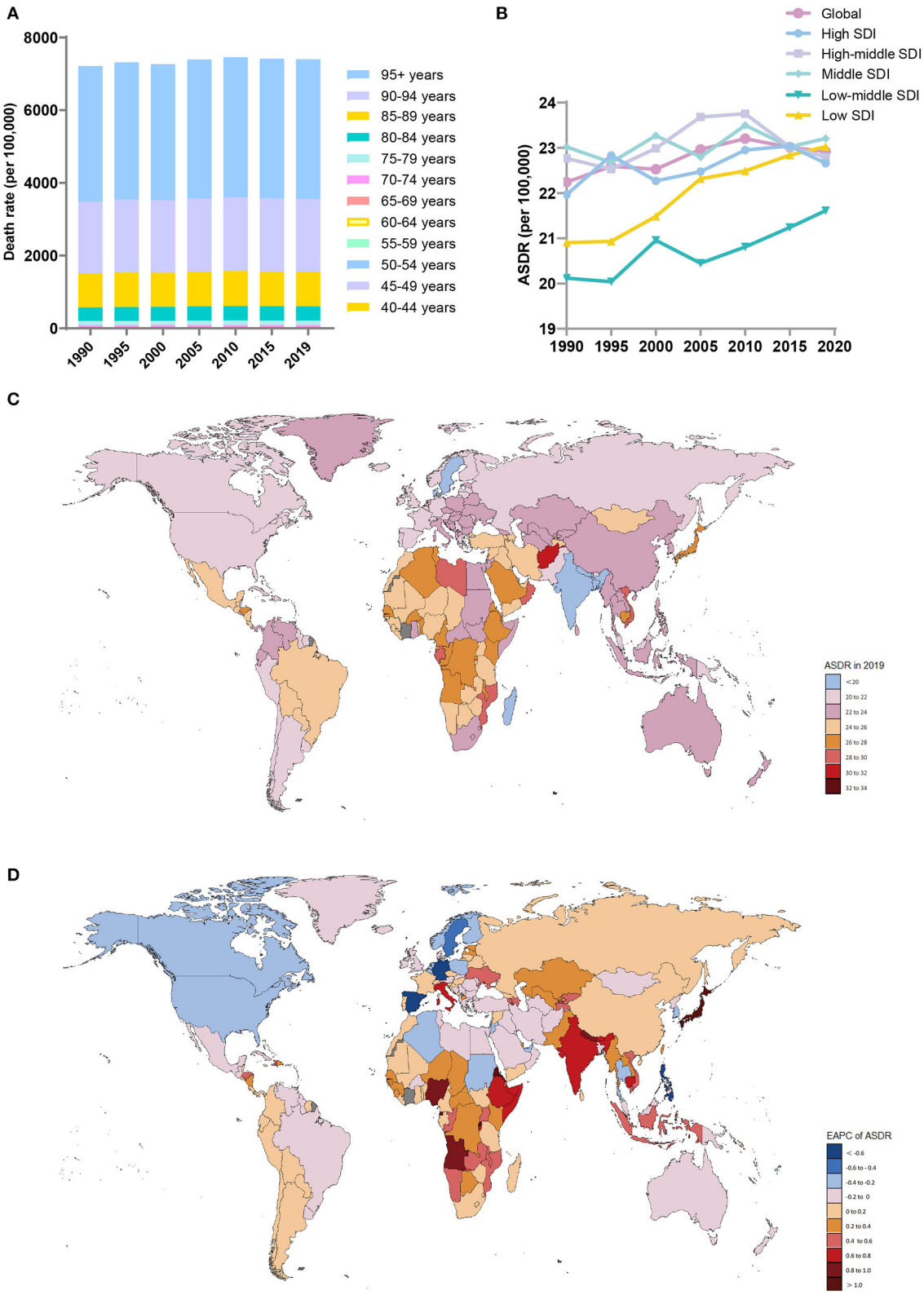

FIGURE 3
Distribution of deaths due to Alzheimer's disease and other dementias in 204 countries and territories from 1990 to 2019 by age group and SDI region. **(A)** Death rate in each age group; **(B)** Trends of the ASDRs in the SDI region; **(C)** ASDRs in 204 countries and territories; **(D)** EAPCs of the ASDRs in 204 countries and territories. SDI, sociodemographic index; ASDR, age-standardized death rate; EAPC, estimated annual percent change.

TABLE 4 The DALYs cases and ASR of DALYs of Alzheimer's disease and other dementias in 1990 and 2019 and its EAPC.

Characteristics	1990		2019		1990–2019
	DALYs (*10^6) (95% UI)	ASR of DALYs (per 100,000) (95% UI)	DALYs (*10^6) (95% UI)	ASR of DALYs (per 100,000) (95% UI)	EAPC of ASR of DALYs (95% CI)
Global	9.66 (4.23–21.37)	326.71 (143.33–731.03)	25.28 (11.2–54.56)	338.64 (151.02–731.27)	0.15 (0.13 to 0.16)
Gender					
Males	3.39 (1.45–7.83)	289.24 (123.24–660.87)	9.37 (4.02–21.1)	304.47 (130.97–679.76)	0.21 (0.2 to 0.23)
Females	6.27 (2.77–13.77)	347.87 (154.52–765.02)	15.9 (7.16–33.81)	361.2 (162.8–767.72)	0.15 (0.13 to 0.17)
Sociodemographic index					
Low	0.39 (0.16–0.91)	295.19 (121.35–694.71)	1.04 (0.43–2.45)	315.76 (129.02–742.9)	0.28 (0.26 to 0.3)
Low-middle	1.01 (0.43–2.41)	287.22 (118.6–672.6)	3.07 (1.28–7.06)	304.76 (126.52–702.3)	0.2 (0.18 to 0.23)
Middle	2.2 (0.92–5.13)	335.33 (139.18–770.43)	6.69 (2.84–15.09)	346.11 (148.62–770.18)	0.14 (0.12 to 0.16)
High-middle	2.71 (1.19–5.92)	335.16 (148.39–736.45)	6.81 (3.08–14.82)	348.46 (157.71–754.37)	0.18 (0.13 to 0.22)
High	3.35 (1.53–7.31)	324.07 (147.34–705.64)	7.66 (3.56–15.74)	332.4 (155–688.29)	0.11 (0.08 to 0.13)
21 GBD regions					
Central Asia	0.12 (0.06–0.27)	326.32 (149.38–721.24)	0.16 (0.07–0.35)	345.47 (155.28–775.08)	0.19 (0.16 to 0.21)
Central Europe	0.42 (0.19–0.94)	349.87 (156.52–778.96)	0.79 (0.37–1.69)	348.75 (160.87–734.47)	−0.04 (−0.05 to −0.02)
Eastern Europe	0.68 (0.31–1.51)	305.52 (140.31–679.46)	1.14 (0.53–2.49)	324.8 (149.89–705.23)	0.23 (0.21 to 0.25)
Australasia	0.07 (0.03–0.15)	326.93 (147.01–726.32)	0.18 (0.08–0.39)	319.88 (146.31–681.98)	−0.09 (−0.11 to −0.07)
High-income Asia Pacific	0.54 (0.24–1.18)	322.6 (143.99–710.51)	2.37 (1.1–4.85)	385.38 (179.3–791.75)	0.81 (0.7 to 0.92)
High-income North America	1.24 (0.59–2.63)	330.78 (158–700.92)	2.27 (1.1–4.7)	317.66 (154.02–653.15)	−0.22 (−0.27 to −0.17)
Southern Latin America	0.12 (0.05–0.26)	304.44 (137–674.68)	0.27 (0.12–0.59)	311.86 (142.12–674.17)	0.13 (0.11 to 0.14)
Western Europe	1.85 (0.84–4.05)	317.02 (141.51–693.85)	3.58 (1.64–7.58)	309.71 (141.53–663.69)	−0.08 (−0.1 to −0.06)
Andean Latin America	0.05 (0.02–0.12)	306.69 (127.33–718.29)	0.16 (0.07–0.36)	312.67 (133.67–691.68)	0.09 (0.08 to 0.11)
Caribbean	0.07 (0.03–0.15)	295.98 (122.92–684.98)	0.16 (0.07–0.34)	299.45 (126.93–661.71)	0.06 (0.05 to 0.07)
Central Latin America	0.21 (0.09–0.49)	329.17 (133.63–765.75)	0.73 (0.3–1.63)	333.23 (136.24–747.25)	0.03 (0.01 to 0.04)
Tropical Latin America	0.24 (0.1–0.55)	384.41 (163.84–871.32)	0.87 (0.38–1.91)	390.88 (172.01–855.99)	0.11 (0.08 to 0.15)
North Africa and Middle East	0.44 (0.19–0.98)	391.32 (170.34–883.07)	1.21 (0.53–2.67)	386.96 (171.95–848.51)	−0.03 (−0.04 to −0.01)
South Asia	0.73 (0.3–1.73)	238.2 (96.13–575.6)	2.62 (1.06–6.23)	262.09 (105.55–617.38)	0.32 (0.25 to 0.39)
East Asia	1.91 (0.79–4.46)	347.44 (143.95–798.77)	6.2 (2.78–13.58)	366.61 (164.75–789.1)	0.25 (0.21 to 0.3)
Oceania	0.01 (0–0.01)	332.94 (136.7–765.18)	0.01 (0.01–0.03)	318.77 (133.77–726.91)	−0.18 (−0.21 to −0.15)
Southeast Asia	0.57 (0.23–1.32)	333.58 (136.46–764.32)	1.55 (0.63–3.43)	342.18 (141.51–765.11)	0.09 (0.07 to 0.1)
Central Sub-Saharan Africa	0.04 (0.02–0.09)	347.02 (149.92–796.7)	0.11 (0.05–0.26)	380.57 (165.07–857.23)	0.35 (0.33 to 0.37)
Eastern Sub-Saharan Africa	0.14 (0.06–0.31)	323.31 (135.15–746.55)	0.35 (0.15–0.82)	356 (144.97–829.93)	0.4 (0.37 to 0.43)
Southern Sub-Saharan Africa	0.06 (0.03–0.15)	313.71 (135.09–712.18)	0.13 (0.06–0.3)	323.81 (138.29–740.97)	0.1 (0.06 to 0.13)
Western Sub-Saharan Africa	0.17 (0.07–0.42)	309.39 (124–769.07)	0.4 (0.16–0.93)	333.53 (129.48–774.76)	0.35 (0.3 to 0.4)

DALYs, disability-adjusted life-years; ASR, age-standardized rate; EAPC, estimated annual percent change; SDI, sociodemographic index.

increasing patterns over the 30-year study period. It is predicted that by 2050, the proportion of the population over the age of 60 years will increase by 22%, and they will experience the fastest population increase (Kanasi et al., 2016). Population growth and

an aging population are causing an increase in the prevalence of the disease, and future medical costs for Alzheimer's disease and other dementias will continue to rise.

Dementia is an age-related disease, and its incidence has increased significantly worldwide with increasing life expectancy (Power et al., 2019). Our analysis supports this observation that the disease burden caused by dementia mainly affects elderly individuals. The incidence, prevalence, death, and DALYs of dementia increase with age. Moreover, the most significant increase in incidence, prevalence, death, and DALYs rates over time was observed in the 70+ age group. However, due to their shortened life expectancy, people over 90 years of age do not lose many life-years due to premature death and disability. During this period, the global DALY value and the ASR increased by 161.7 and 3.65%, respectively. The 2010 World Report on Alzheimer's Disease mentioned that the social cost of dementia was as high as those of tumors, heart disease, and stroke (Alzheimer's Disease International, 2010). According to the World Health Organization (WHO), dementia has become the seventh leading cause of death worldwide (Alzheimer's Association, 2022). Generally, the global burden of dementia has increased over time, and this trend will continue in the future with the aging population.

The ASIRs, ASPRs, ASDRs, and DALYs (per 100,000 population) were consistently higher in women than in men during this period among all the SDI regions. This finding suggests that the disease burden in women is higher than in men. The differences in the prevalence pattern between sexes may be due to reproductive capacity, hormone levels, genetic susceptibility, and mental status (Ngo et al., 2014). Women are more likely to develop structural and functional disorders of the nervous system (Ardekani et al., 2016), and they are two times as likely to suffer from psychological problems, such as depression, than men (Eid et al., 2019). All these conditions are risk factors for Alzheimer's disease. In addition, female brains are inherently more prone to Alzheimer's disease, which is influenced by sex hormones (Zhu et al., 2021). Moreover, women have a longer life expectancy than men (Tower, 2017), thus accounting for a considerable proportion of the aging population. Therefore, the prevention and treatment of dementia and interventions targeting female patients should be strengthened. Interestingly, the EAPCs in the ASIR, ASPR, ASDR, and DALYs (per 100,000 population) were larger in men than in women, suggesting that the disease burden in men is increasing at a faster rate than in women. Higher rates of smoking and drinking in men may explain this phenomenon (Wu et al., 2017).

Except for the ASIRs (per 100,000 population) in the low- and low-middle-SDI regions, the ASIRs, ASPRs, and DALYs (per 100,000 population) have gradually increased since 1995. In the low-SDI regions, the ASDR and ASR of DALYs (per 100,000 population) showed the largest increase. This phenomenon indicates that dementia is not an issue restricted to relatively low-income countries. In most areas, the disease burden of dementia remains significant. We found that the incidence, prevalence, and ASR of DALYs were positively related to the SDI, but the disease burden in young adults was negatively related to the SDI. This may be caused by the higher life expectancy in high-SDI regions and a greater degree of population aging over time (Kontis et al., 2017). However, high-SDI regions have better medical services and higher budgets for the care of people with dementia. Detecting dementia-related risk factors at an early stage greatly reduces the risk of death and the disease burden in people with dementia. In addition, high-SDI regions place greater emphasis on investing in educational attainment and social wellbeing, which can help improve physical, mental, and cognitive health and thus control the risk factors for the disease at an earlier stage (Gao and Liu, 2021). The decline in the ASIRs and ASPRs (per 100,000 population people) in some low-SDI regions may be related to the lower life expectancy of citizens in low-income countries (Chetty et al., 2016). Differences in the economic levels, policies, and cultures among countries may also be potential reasons. However, it is difficult to propose a uniform explanation for these results.

There has been no effective therapy to reverse dementia thus far, and drug treatment has substantial limitations (Gitlin et al., 2012). An effective strategy is to address the relative risk factors to prevent the development of the condition. Studies have shown that with increasing sustenance levels and quality of life, the incidence of metabolic diseases (high systolic blood pressure, high BMI, and diabetes) increases significantly (Charlot et al., 2021). The rapid development in the social economy has intensified the social competition and life pressure experienced by the people; this stress is often accompanied by harmful living habits (smoking, excessive alcohol consumption, and lack of physical activity). Our data showed that regions with higher SDIs were more affected by these risk factors than regions with low SDIs. In other words, high-income countries and regions have a higher risk of obesity, social stress, and lack of physical activity, and thus a higher risk of dementia. There has also been a decline in the incidence of dementia in some European countries. This may be due to effective interventions targeting cardiovascular, metabolic, cognitive, behavioral, and other factors related to dementia in recent years (Solomon et al., 2014). In 2019, the WHO formed a panel to reduce dementia risk, highlighting interventions that may help reduce the incidence of dementia (GBD 2019 Dementia Forecasting Collaborators, 2022). Relevant departments should improve medical services for dementia patients as soon as possible and raise public awareness. Early screening for risk factors and early diagnosis and treatment of associated diseases should be implemented. The government should integrate various resources and facilities in the region to promote improvement in the elderly care service system and the elderly healthcare system.

With the spread of COVID-19 in the last 3 years, some studies have found an increased risk of Alzheimer's

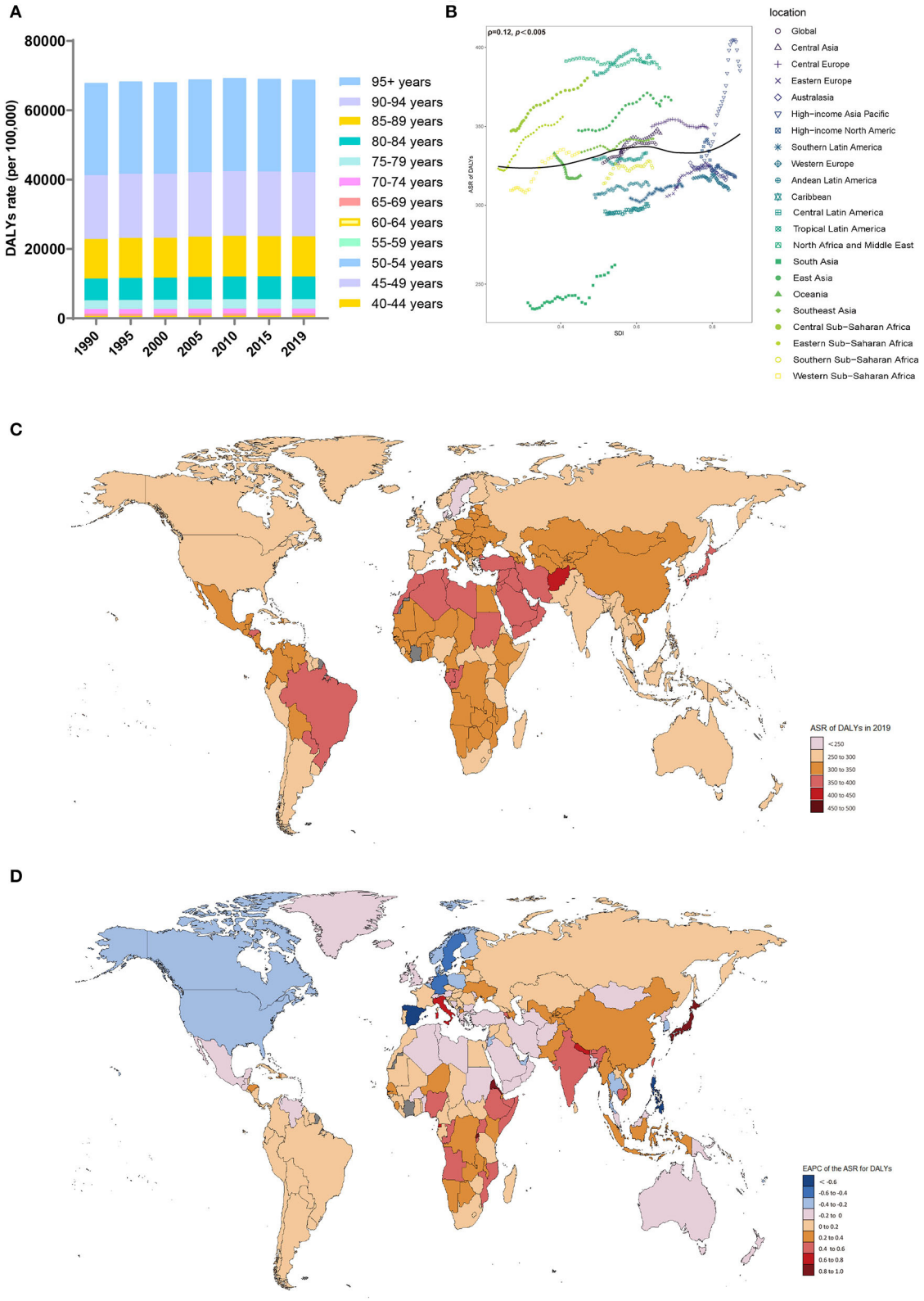

FIGURE 4
Distribution of DALYs due to Alzheimer's disease and other dementias in 204 countries and territories from 1990 to 2019 by age group and SDI region. **(A)** DALYs rate in each age group; **(B)** Correlations between the ASR of DALYs due to Alzheimer's disease and other dementias and SDI regions in 2019; associations were calculated with Pearson correlation analysis; **(C)** ASR of DALYs of 204 countries and territories; **(D)** EAPCs in the ASR of DALYs in 204 countries and territories. DALYs, disability-adjusted life-years; SDI, sociodemographic index; ASR, age-standardized rate; EAPC, estimated annual percent change.

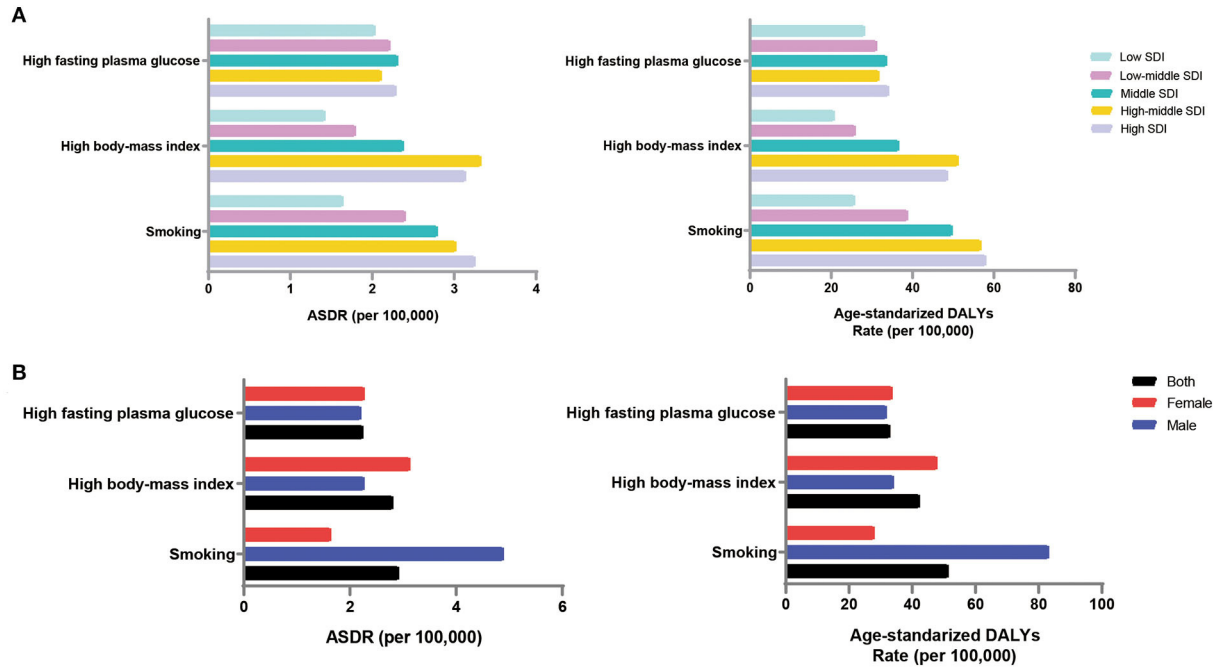

FIGURE 5
Impact of risk factors on the disease burden of Alzheimer's disease by SDI region and gender, 2019. **(A)** Contribution of three risk factors for death and DALYs in different SDI regions; **(B)** Contribution of three risk factors to death and DALYs in both sexes. ASDR, age-standardized death rate; DALYs, disability-adjusted life-years; SDI, sociodemographic index.

disease in COVID-19 patients (Xia et al., 2021). Studies have shown that patients with severe SARS-CoV-2 infection exhibit cognitive decline and may eventually develop AD. This may be due to the viral involvement of the central nervous system directly, combined with the long-term accumulation of pro-inflammatory cytokines, which induces or accelerates the neurodegenerative process; patients are at a higher risk of subsequently developing AD (Heneka et al., 2013; Siu et al., 2019). Delirium is a common symptom of SARS-CoV-2 infection in patients with AD and is associated with a high short-term mortality rate (Poloni et al., 2020). Patients with AD are associated with increased permeability of the blood–brain barrier, which may facilitate the passage of SARS-CoV-2 across the blood–brain barrier (Mok et al., 2020). The virus may also enter the brainstem from the olfactory nerve, which may be responsible for the patient's respiratory failure (Netland et al., 2008). Once infected, patients with dementia are at increased risk of intracranial inflammation and increased mortality (Mok et al., 2020). However, it is unclear whether AD is a long-term complication of COVID-19, and further studies are needed to explain the contribution of COVID-19 to AD.

Conventional limitations have been reported in previous articles (Wang et al., 2021), and the limitations of this article are mainly as follows. To date, 12 risk factors connected with dementia have been reported (Livingston et al., 2020). However, GBD 2019 showed that only metabolic and behavioral factors were associated with dementia, but did not provide data on other risk factors. Second, dementia was not further classified by subtype; for example, dementia can be classified as vascular dementia or dementia with Lewy bodies. They differ in their disease burden and common risk factors, but the GBD 2019 currently has no data stratified by pathological subtype. In addition, the diagnostic criteria, biomarkers, medical records, and insurance codes for dementia globally have been updated over time, and there might be heterogeneity during the past three decades (GBD 2019 Diseases Injuries Collaborators, 2020; GBD 2019 Risk Factors Collaborators, 2020). The fallacies of the disease burden between our analysis and the real world are inevitable. Therefore, the results of our analysis need to be interpreted with caution, and further investigations are needed to perform.

Conclusion

In conclusion, this study illustrates the global epidemiological trends of dementia from 1990 to 2019. Dementia has become a global public health problem as the population ages. The risk of developing dementia is proportional to age. The disease burden remains high in most countries and territories, while

female and elderly individuals should be the focus of attention. More effective prevention and treatment measures are needed to reduce the disease burden caused by dementia.

Data availability statement

The original contributions presented in the study are included in the article/Supplementary material, further inquiries can be directed to the corresponding author/s.

Author contributions

XL and YL conceived and designed the study. XS and NH supervised the study. FH and XF performed the statistical analysis. XL drafted the manuscript. All authors contributed to the acquisition, analysis, interpretation of the data, revised the report, and approved the final version before submission.

Funding

The present study was funded by the National Natural Science Foundation of China (Grant No. 82000755) and the Natural Science Foundation of Shandong Province (Grant No. ZR2020QH086).

Conflict of interest

The authors declare that the research was conducted in the absence of any commercial or financial relationships that could be construed as a potential conflict of interest.

Publisher's note

All claims expressed in this article are solely those of the authors and do not necessarily represent those of their affiliated organizations, or those of the publisher, the editors and the reviewers. Any product that may be evaluated in this article, or claim that may be made by its manufacturer, is not guaranteed or endorsed by the publisher.

Supplementary material

The Supplementary Material for this article can be found online at: https://www.frontiersin.org/articles/10.3389/fnagi.2022.937486/full#supplementary-material

References

Alzheimer's Association (2022). 2022 Alzheimer's disease facts and figures. *Alzheimer's Dementia* 18, 700–789. doi: 10.1002/alz.12638

Alzheimer's Disease International (2010). World Alzheimer Report 2010: The Global Economic Impact of Dementia. Available online at: https://www.alz.co.uk/research/world-report-2010 (accessed April 30, 2022).

Ardekani, B. A., Convit, A., and Bachman, A. H. (2016). Analysis of the MIRIAD data shows sex differences in hippocampal atrophy progression. *J. Alzheimer's Dis.* 50, 847–857. doi: 10.3233/JAD-150780

Charlot, A., Hutt, F., Sabatier, E., and Zoll, J. (2021). Beneficial effects of early time-restricted feeding on metabolic diseases: importance of aligning food habits with the circadian clock. *Nutrients* 13. doi: 10.3390/nu13051405

Chetty, R., Stepner, M., Abraham, S., Lin, S., Scuderi, B., Turner, N., et al. (2016). The association between income and life expectancy in the United States, 2001-2014. *JAMA* 315, 1750–1766. doi: 10.1001/jama.2016.4226

Ding, Q., Liu, S., Yao, Y., Liu, H., Cai, T., and Han, L. (2022). Global, regional, and national burden of ischemic stroke, 1990-2019. *Neurology* 98, e279–e290. doi: 10.1212/WNL.0000000000013115

Eid, R. S., Gobinath, A. R., and Galea, L. (2019). Sex differences in depression: Insights from clinical and preclinical studies. *Prog. Neurobiol.* 176, 86–102. doi: 10.1016/j.pneurobio.2019.01.006

Gao, Y., and Liu, X. (2021). Secular trends in the incidence of and mortality due to Alzheimer's disease and other forms of dementia in China From 1990 to 2019: An age-period-cohort study and joinpoint analysis. *Front. Aging Neurosci.* 13, 709156. doi: 10.3389/fnagi.2021.709156

Gauthier, S., Albert, M., Fox, N., Goedert, M., Kivipelto, M., Mestre-Ferrandiz, J., et al. (2016). Why has therapy development for dementia failed in the last two decades. *Alzheimers Dement* 12, 60–64. doi: 10.1016/j.jalz.2015.12.003

GBD 2016 Dementia Collaborators. (2019). Global, regional, and national burden of Alzheimer's disease and other dementias, 1990-2016: a systematic analysis for the Global Burden of Disease Study 2016. *Lancet Neurol* 18, 88–106. doi: 10.1016/S1474-4422(18)30403-4

GBD 2017 DALYs and HALE Collaborators (2018). Global, regional, and national disability-adjusted life-years (DALYs) for 359 diseases and injuries and healthy life expectancy (HALE) for 195 countries and territories, 1990-2017: a systematic analysis for the Global Burden of Disease Study 2017. *Lancet* 392, 1859–1922. doi: 10.1016/S0140-6736(18)32335-3

GBD 2017 Disease and Injury Incidence and Prevalence Collaborators (2018). Global, regional, and national incidence, prevalence, and years lived with disability for 354 diseases and injuries for 195 countries and territories, 1990-2017: a systematic analysis for the Global Burden of Disease Study 2017. *Lancet* 392, 1789–1858. doi: 10.1016/S0140-6736(18)32279-7

GBD 2017 Mortality Collaborators (2018). Global, regional, and national age-sex-specific mortality and life expectancy, 1950-2017: a systematic analysis for the Global Burden of Disease Study 2017. *Lancet* 392, 1684–1735. doi: 10.1016/S0140-6736(18)31891-9

GBD 2019 Dementia Forecasting Collaborators (2022). Estimation of the global prevalence of dementia in 2019 and forecasted prevalence in 2050: an analysis for the Global Burden of Disease Study 2019. *Lancet Public Health* 7, e105–e125. doi: 10.1016/S2468-2667(21)00249-8

GBD 2019 Diseases and Injuries Collaborators (2020). Global burden of 369 diseases and injuries in 204 countries and territories, 1990-2019: a systematic analysis for the Global Burden of Disease Study 2019. *Lancet* 396, 1204–1222. doi: 10.1016/S0140-6736(20)30925-9

GBD 2019 Risk Factors Collaborators (2020). Global burden of 87 risk factors in 204 countries and territories, 1990-2019: a systematic analysis for the Global Burden of Disease Study 2019. *Lancet* 396, 1223–1249. doi: 10.1016/S0140-6736(20)30752-2

Gitlin, L. N., Kales, H. C., and Lyketsos, C. G. (2012). Nonpharmacologic management of behavioral symptoms in dementia. *JAMA* 308, 2020–2029. doi: 10.1001/jama.2012.36918

Heneka, M. T., Kummer, M. P., Stutz, A., Delekate, A., Schwartz, S., Vieira-Saecker, A., et al. (2013). NLRP3 is activated in Alzheimer's disease and contributes to pathology in APP/PS1 mice. *Nature* 493, 674–678. doi: 10.1038/nature11729

HUMANOSPHERE (2016). A new way to measure progress in global health. https://www.humanosphere.org/global-health/2016/10/a-new-way-to-measure-progress-global-health/ (accessed April 30, 2022).

Kanasi, E., Ayilavarapu, S., and Jones, J. (2016). The aging population: demographics and the biology of aging. *Periodontol.* 72, 13–18. doi: 10.1111/prd.12126

Kontis, V., Bennett, J. E., Mathers, C. D., Li, G., Foreman, K., and Ezzati, M. (2017). Future life expectancy in 35 industrialised countries: projections with a Bayesian model ensemble. *Lancet* 389, 1323–1335. doi: 10.1016/S0140-6736(16)32381-9

Livingston, G., Huntley, J., Sommerlad, A., Ames, D., Ballard, C., Banerjee, S., et al. (2020). Dementia prevention, intervention, and care: 2020 report of the Lancet Commission. *Lancet* 396, 413–446. doi: 10.1016/S0140-6736(20)30367-6

Livingston, G., Sommerlad, A., Orgeta, V., Costafreda, S. G., Huntley, J., Ames, D., et al. (2017). Dementia prevention, intervention, and care. *Lancet* 390, 2673–2734. doi: 10.1016/S0140-6736(17)31363-6

Lyketsos, C. G., Carrillo, M. C., Ryan, J. M., Khachaturian, A. S., Trzepacz, P., Amatniek, J., et al. (2011). Neuropsychiatric symptoms in Alzheimer's disease. *Alzheimer's Dement.* 7, 532–539. doi: 10.1016/j.jalz.2011.05.2410

Mok, V., Pendlebury, S., Wong, A., Alladi, S., Au, L., Bath, P. M., et al. (2020). Tackling challenges in care of Alzheimer's disease and other dementias amid the COVID-19 pandemic, now and in the future. *Alzheimers Dement.* 16, 1571–1581. doi: 10.1002/alz.12143

Murray, C. J., Vos, T., Lozano, R., Naghavi, M., Flaxman, A. D., Michaud, C., et al. (2012). Disability-adjusted life years (DALYs) for 291 diseases and injuries in 21 regions, 1990-2010: a systematic analysis for the Global Burden of Disease Study 2010. *Lancet* 380, 2197–2223. doi: 10.1016/S0140-6736(12)61689-4

Netland, J., Meyerholz, D. K., Moore, S., Cassell, M., and Perlman, S. (2008). Severe acute respiratory syndrome coronavirus infection causes neuronal death in the absence of encephalitis in mice transgenic for human ACE2. *J. Virol.* 82, 7264–7275. doi: 10.1128/JVI.00737-08

Ngo, S. T., Steyn, F. J., and McCombe, P. A. (2014). Gender differences in autoimmune disease. *Front. Neuroendocrinol.* 35, 347–369. doi: 10.1016/j.yfrne.2014.04.004

Oh, E. S., and Rabins, P. V. (2019). Dementia. *Ann. Intern. Med.* 171, ITC33–ITC48. doi: 10.7326/AITC201909030

Poloni, T. E., Carlos, A. F., Cairati, M., Cutaia, C., Medici, V., Marelli, E., et al. (2020). Prevalence and prognostic value of Delirium as the initial presentation of COVID-19 in the elderly with dementia: An Italian retrospective study. *EClinicalMedicine* 26, 100490. doi: 10.1016/j.eclinm.2020.100490

Power, R., Prado-Cabrero, A., Mulcahy, R., Howard, A., and Nolan, J. M. (2019). The role of nutrition for the aging population: implications for cognition and Alzheimer's disease. *Annu. Rev. Food Sci. Technol.* 10, 619–639. doi: 10.1146/annurev-food-030216-030125

Siu, K. L., Yuen, K. S., Castaño-Rodriguez, C., Ye, Z. W., Yeung, M. L., Fung, S. Y., et al. (2019). Severe acute respiratory syndrome coronavirus ORF3a protein activates the NLRP3 inflammasome by promoting TRAF3-dependent ubiquitination of ASC. *FASEB J.* 33, 8865–8877. doi: 10.1096/fj.201802418R

Solomon, A., Mangialasche, F., Richard, E., Andrieu, S., Bennett, D. A., Breteler, M., et al. (2014). Advances in the prevention of Alzheimer's disease and dementia. *J. Intern. Med.* 275, 229–250. doi: 10.1111/joim.12178

Srivastava, S., Ahmad, R., and Khare, S. K. (2021). Alzheimer's disease and its treatment by different approaches: A review. *Eur. J. Med. Chem.* 216, 113320. doi: 10.1016/j.ejmech.2021.113320

Tower, J. (2017). Sex-specific gene expression and life span regulation. *Trends Endocrinol. Metabol.* 28, 735–747. doi: 10.1016/j.tem.2017.07.002

Wang, W., Hu, M., Liu, H., Zhang, X., Li, H., Zhou, F., et al. (2021). Global Burden of Disease Study 2019 suggests that metabolic risk factors are the leading drivers of the burden of ischemic heart disease. *Cell Metab.* 33, 1943–1956.e2. doi: 10.1016/j.cmet.2021.08.005

Wu, Y. T., Beiser, A. S., Breteler, M., Fratiglioni, L., Helmer, C., Hendrie, H. C., et al. (2017). The changing prevalence and incidence of dementia over time - current evidence. *Nat. Rev. Neurol.* 13, 327–339. doi: 10.1038/nrneurol.2017.63

Xia, X., Wang, Y., and Zheng, J. (2021). COVID-19 and Alzheimer's disease: how one crisis worsens the other. *Transl. Neurodegener.* 10, 15. doi: 10.1186/s40035-021-00237-2

Zhu, D., Montagne, A., and Zhao, Z. (2021). Alzheimer's pathogenic mechanisms and underlying sex difference. *Cell. Mol. Life Sci.* 78, 4907–4920. doi: 10.1007/s00018-021-03830-w

frontiers | Frontiers in Aging Neuroscience

TYPE Original Research
PUBLISHED 08 November 2022
DOI 10.3389/fnagi.2022.987244

OPEN ACCESS

EDITED BY
Asma Perveen,
Glocal University, India

REVIEWED BY
Fiorenzo Conti,
Marche Polytechnic University, Italy
Volkmar Lessmann,
University Hospital Magdeburg, Germany

*CORRESPONDENCE
Zaohuo Cheng
zaohuocheng@sina.com

SPECIALTY SECTION
This article was submitted to Alzheimer's Disease and Related Dementias, a section of the journal Frontiers in Aging Neuroscience

RECEIVED 06 July 2022
ACCEPTED 12 October 2022
PUBLISHED 08 November 2022

CITATION
Qian F, Liu J, Yang H, Zhu H, Wang Z, Wu Y and Cheng Z (2022) Association of plasma brain-derived neurotrophic factor with Alzheimer's disease and its influencing factors in Chinese elderly population.
Front. Aging Neurosci. 14:987244.
doi: 10.3389/fnagi.2022.987244

Association of plasma brain-derived neurotrophic factor with Alzheimer's disease and its influencing factors in Chinese elderly population

Fuqiang Qian[1], Jian Liu[2], Hongyu Yang[3], Haohao Zhu[1], Zhiqiang Wang[1], Yue Wu[1] and Zaohuo Cheng[1]*

[1]The Affiliated Wuxi Mental Health Center of Jiangnan University, Wuxi Central Rehabilitation Hospital, Wuxi, China, [2]Hangzhou Seventh People's Hospital, Hangzhou, China, [3]Shanghai Mental Health Center, Shanghai, China

Objective: To explore the association of plasma brain-derived neurotrophic factor (BDNF) levels with Alzheimer's disease and its influencing factors.

Materials and methods: A total of 1,615 participants were included in the present study. Among all subjects, 660 were cognitive normal controls (CNCs), 571 were mild cognitive impairment (MCI) patients, and 384 were dementia with Alzheimer's type (DAT) patients. BDNF in blood samples collected from these subjects was analyzed via the Luminex assay. Additionally, DNA extraction and APOE4 genotyping were performed on leukocytes using a blood genotyping DNA extraction kit. All data were processed with SPSS 20.0 software. Analysis of variance (ANOVA) or analysis of covariance (ANCOVA) was used to compare differences among groups on plasma BDNF. Pearson and Spearman correlation analysis examined the correlation between BDNF and cognitive impairment, and linear regression analysis examined the comprehensive effects of diagnosis, gender, age, education, and sample source on BDNF.

Results: BDNF levels in DAT patients were higher than those in CNC and MCI patients ($P < 0.01$). BDNF levels were significantly correlated with CDR, MMSE, and clinical diagnosis ($P < 0.001$). Age, education, occupation, and sample source had significant effects on BDNF differences among the CNC, MCI, and DAT groups ($P < 0.001$). BDNF first decreased and then increased with cognitive impairment in the ApoE4-negative group ($P < 0.05$).

Conclusion: Plasma BDNF levels decreased in the MCI stage and increased in the dementia stage and were affected by age, education, occupation, and sample source. Unless the effects of sample heterogeneity and methodological differences can be excluded, plasma BDNF is difficult to become a biomarker for the early screening and diagnosis of AD.

KEYWORDS

Alzheimer's disease, biomarker, BDNF, influencing factors, elderly population

Introduction

With the growth and longevity of the elderly population, Alzheimer's disease (AD) has become a global human health problem. The Seventh China National Census reported that there were 264 million elderly people over 60 years old in China in 2020. By a prevalence of 4%, it is estimated that there will be more than 10 million AD patients in 2020, 20 million in 2035, and 40 million in 2060 (Cheng, 2020; Zhao and Li, 2020). AD is a chronic progressive and irreversible neurodegenerative disease (Alzheimer Association, 2017; Knopman et al., 2021). When AD progresses to the dementia stage, there are no disease-modifying drugs to prevent or reverse the disease process (Yiannopoulou and Papageorgiou, 2020). Therefore, early diagnosis and intervention of AD is particularly important. Many researchers are committed to looking for early diagnosis markers of AD, and brain-derived neurotrophic factor (BDNF) is one of the targets (Cheng et al., 2018; Rehiman et al., 2020).

Brain-derived neurotrophic factor plays an important role in brain development, neuroplasticity, and neuronal survival and its effects on neuronal transmission in the hippocampus, cerebral cortex, and basal forebrain are associated with learning and memory processes in the mature brain (Popova and Naumenko, 2019). Growing evidence indicates that changes in cerebral BDNF levels and the BDNF-TrkB signaling pathway may be involved in the etiopathogenesis of AD and that serum and brain BDNF levels are correlated. This evidence suggests that blood BDNF could be used as a biomarker for AD diagnosis, prognosis, and treatment monitoring (Ng et al., 2019; Marta et al., 2020; Mori et al., 2021).

Several recent meta-analyses analyzed the association between BDNF and AD cognitive impairment and found that the results are inconsistent or even contradictory, and higher, lower, or similar levels of circulating BDNF have all been reported in AD or MCI patients compared to healthy controls (Qin et al., 2017; Ng et al., 2019; Xie et al., 2020; Ma et al., 2022). For example, Kim et al. (2017) showed that blood BDNF levels seem to be increased in early AD and decreased in AD patients with low MMSE scores (Kim et al., 2017). Ng et al. (2019) reported that blood BDNF did not change in the MCI stage and only decreased in the late stage of AD. Not only are the conclusions of the difference in BDNF between AD patients and normal controls inconsistent, but there are also great differences in BDNF levels among different studies. Some studies reported that BDNF levels were very low (<5 pg/ml) (Nascimento et al., 2014; Wang et al., 2015), while others reported that BDNF levels were very high (>50 ng/ml) (Liu et al., 2015; Zhang et al., 2019).

These contradictory results may be related to sample heterogeneity (age, gender, education, condition, comorbidity, and medication) and methodological differences (cognitive rating tools and diagnostic criteria, sample type, blood processing, storage duration, etc.) (Balietti et al., 2018); for instance, blood BDNF decreased with age or weight in elderly individuals (Glud et al., 2019), increased in the early AD stage and decreased in the late stage (Laske et al., 2006). It is very important to study and control the influence of these factors on the association between BDNF levels and cognitive impairment, and it is more important to consider the possible influence of various factors in the interpretation of results. This study investigated the association of plasma BDNF levels with cognitive impairment and its influencing factors.

Materials and methods

Participants

This study recruited adult and elderly volunteers over 50 years old from communities and mental health hospitals in four cities with different levels (Shanghai, Hangzhou, Wuxi, Jiangyi). The unified training, containing the purpose, content, and methods, was organized to ensure the comparability of the procedures. All subjects received clinical interviews and examinations, relevant cognitive evaluations, necessary laboratory or imaging examinations, and overnight fasting venous blood was collected. Based on interviews, assessments and examinations, 1,615 valid samples were obtained after excluding serious physical, neurological and mental disorders that may cause cognitive impairment (including uncontrolled hypertension, diabetes, Parkinson's disease, cerebrovascular disease, hypothyroidism, schizophrenia, depression, etc.), including 230 persons in Shanghai, 248 in Hangzhou, 937 in Wuxi, and 200 in Jiangyi. According to the NINCDS-ADRDA criteria (McKhann et al., 1984) for dementia with Alzheimer's type (DAT), DSM-5 criteria (American Psychiatric Association, 2013) for neurocognitive impairment and Petersen criteria (Petersen et al., 1999) for mild cognitive impairment (MCI), 1,615 participants were clinically diagnosed into three groups: 660 cognitive normal controls (CNCs), 571 MCI patients and 384 DAT patients, of which 218 DAT patients were from outpatients and inpatients in mental health hospitals, and other DAT patients and CNC and MCI subjects were from community volunteers. Sample sources and basic information are shown in **Table 1**.

This study was approved by the ethics committee of Wuxi Mental Health Center, the ethics committee of Shanghai Mental Health Center and the ethics committee of Hangzhou Seventh People's Hospital. According to the Declaration of Helsinki, all subjects or their caregivers were informed of the procedure and signed informed consent was obtained before participating in the study.

TABLE 1 Sample source and basic data.

		Total sample	Wuxi	Jiangyi	Hangzhou	Shanghai	χ^2 or F	*P*
Gender (male/female)		678/937	432/505	86/114	87/161	73/157	21.380	<0.001
Age (years)		70.09 ± 9.33	67.89 ± 7.83	67.46 ± 8.16	77.98 ± 9.40	78.53 ± 7.03	189.968	<0.001
Education (years)		7.96 ± 4.07	9.41 ± 3.12	7.61 ± 2.71	5.58 ± 4.57	4.88 ± 4.89	140.581	<0.001
Diagnosis (HC/MCI/DAT)		660/571/384	476/281/180	33/139/28	50/49/149	101/102/27	341.868	<0.001
CDR-GS (score)		0.61 ± 0.70	0.55 ± 0.68	0.60 ± 0.63	0.99 ± 0.84	0.44 ± 0.54	32.576	<0.001
BDNF (pg/mL)	Mean ± SD	10555.7 ± 12135.1	10373.5 ± 9646.3	3632.0 ± 5605.6	24976.2 ± 16152.4	1769.4 ± 2026.5	267.081	<0.001
	Ln(X + 1)	8.55 ± 1.40	8.82 ± 1.05	7.51 ± 1.29	9.79 ± 1.17	7.01 ± 0.97	338.724	<0.001

Clinical interview and examination

Clinical interviews and examinations included four primary sections. (A) Social demographic data: name, gender, age, nationality, marriage, education, occupation, family structure, economic status, smoking and drinking habits, outdoor activities, etc.; (B) Medical history and mental examination: memory and cognitive impairment, mental status examination, family history, past medical history and individual medication; (C) physical examination: general examination, such as heart rate, blood pressure, height, weight, vision, hearing, hair color, and facial plaques, etc., emphasis on neurological examination, such as sensory symmetry, motor function, muscle strength, muscle tone, language function, gait and balance, tremor. (D) Necessary auxiliary examination: ECG, EEG, brain CT, blood biochemistry tests, etc. Only the corresponding author (ZC) could obtain the details of each parameter of the patients. The cognitive test interviewers were only responsible for the scale assessment.

Psychological and neurocognitive assessment

Assessments involved three important aspects: subjective cognitive impairment screening, objective cognitive impairment assessment, and related mental rating. Subjective cognitive impairment of elderly volunteers in the community was screened using Brief Elderly Cognitive Screening Questionnaire Screening (BECSI) (Wu et al., 2016), with a total score of more than four points indicating subjective cognitive impairment. Overall objective cognitive impairments were assessed by the Clinical Dementia Rating (CDR) (Academy of Cognitive Disorder of China, 2018), Alzheimer's Dementia Assessment Scale-cognitive subscale (ADAS-cog) (Wang et al., 2000), and/or Mini Mental State Examination (MMSE) (Li et al., 1988). The cognitive function level of each subject was determined by the cutoff score of each scale (CDR: 0 points for normal cognition, 0.5 for mild cognitive impairment, ≥1 for severe cognitive impairment; ADAS-cog: 0–9 for normal cognition, 10–15 for mild cognitive impairment, ≥ 16 points for severe cognitive impairment, or MMSE: 28–30 for normal cognition, 20–27 for mild cognitive impairment, <20 for severe cognitive impairment). Other related mental ratings included the Activity of Daily Living Scale (ADL) (Lawton and Brody, 1969), Hachinski Ischemic Scale (HIS) (Fan, 1990) and Hamilton Depression Scale (HAMD) (Zhao and Zheng, 1992).

Plasma brain-derived neurotrophic factor assays and APOE genotyping

Blood samples were collected in anticoagulant tubes with 2% EDTA in the morning after an overnight fast. Blood samples were centrifuged at 3,000 rpm (1,000 × *g*) for 30 min at 4°C. Plasma and leukocytes were collected in plastic vials and stored at −80°C for further analyses. Only the corresponding author (ZC) could obtain the details of each parameter of the patients. The blood lab analysis staff was blinded to other results, since the patients were represented by numbers.

Luminex assays

Protein detection was entrusted to Nanjing University of Technology (laboratory certificated Millipore Shanghai Trading Co., Ltd., based on Milliplex technology). The Luminex kit (Milliplex Catalog ID. HNDG3MAG-36K-04. Neu) were obtained from Millipore (Billerica, MA, USA), and assays were performed according to the manufacturer's instructions to determine the plasma levels of multiple proteins, including BDNF (pg/mL). Properly diluted plasma samples were incubated with the antibody-coupled microspheres and then with biotinylated detection antibody before the addition of streptavidin-phycoerythrin. The captured bead complexes were measured with a FLEXMAP 3D system (Luminex Corporation, Austin, TX, USA) using the following instrument settings (events/bead, 50; sample size, 50 μL; discriminator gate, 8,000–15,000). The raw data (mean fluorescence intensity) were collected and further processed to calculate the protein concentration. Before statistical analysis, we examined the performance of each assay using quality checks (QC). Median fluorescent intensity (MFI) was measured using xPONENT 5.1 (Luminex Corporation) and exported into Milliplex Analyst

5.1 (VigeneTech, Carlisle, MA, USA) for estimation of protein concentrations using a five-parameter logistic fit. Briefly, all analysts that passed QC checks based on the following four criteria (standard curve linearity, intra-assay coefficient of variation, interassay coefficient of variation for reference sample, and percentage of missing data) were taken forward for further analysis.

DNA extraction and *APOE4* genotyping

DNA extraction and *APOE4* genotyping were performed by Wuxi Biowing Applied Biotechnology Co., Ltd. DNA was extracted from leukocytes using a blood genotyping DNA extraction kit (Tiangen Biotech, Beijing, China), and the *APOE4* genotype was analyzed using polymerase chain reaction restriction fragment length polymorphism (PCR-RFLP). According to the methods reported by Hixson and Vernier (1990), *APOE4* gene primers were designed and synthesized, and PCR amplification, enzyme digestion, and *APOE4* genotyping were performed. The three alleles were grouped into six genotypes, which were *APOE4* negative (E2/E2, E3/E3, E2/E3) and *APOE4* positive (E2/E4, E3/E4, E4/E4).

Data processing and statistical analysis

All data were processed with SPSS 20.0 software. Logarithmic transformation [Ln(x + 1)] of BDNF data was performed to approximate a normal distribution. Pearson's chi-square test was used to compare differences among groups on gender, marriage, family, occupation, and *APOE4 genotypes*. The F test was used to compare differences among groups for age, years of education, blood pressure, body mass index, psychological test scores and biochemical test results. Analysis of variance (ANOVA) or analysis of covariance (ANCOVA) was used to compare differences among groups on plasma BDNF. Pearson and Spearman correlation analysis examined the correlation between BDNF and cognitive impairment, and linear regression analysis examined the comprehensive effects of diagnosis, gender, age, education, and sample source on BDNF.

Results

Comparison of demographic, clinical and laboratory data among the three groups

The differences in the demographic, clinical and laboratory data among the CNC, MCI, and DAT groups are shown in Table 2. There were significant differences among the three groups in demographic data, such as sex, age, education, marital status, family type, and previous occupation ($P < 0.01$). There were no significant differences in body mass index (BMI), systolic blood pressure (SBP) or diastolic blood pressure (DBP) among the groups ($P > 0.05$). There were no significant differences among the three groups in biochemical indexes such as fasting blood glucose (FBG), triglycerides, thyroid stimulating hormone (TSH), free T4, folic acid and vitamin B12 ($P > 0.05$), but there was a significant difference in laboratory indexes such as *APOE* genotype, total protein, albumin, total cholesterol, high density lipoprotein (HDL), low density lipoprotein (LDL), free T3 and BDNF ($P < 0.05$). There were significant differences in cognitive evaluation scores such as ADAS-cog, MMSE, CDR-GS, and ADL ($P < 0.001$).

Relationship between plasma brain-derived neurotrophic factor and cognitive function

The subjects were divided into four groups (CNC, MCI, mild dementia, and moderate-severe dementia) according to the CDR, MMSE or clinical diagnosis. The plasma BDNF differences among groups were compared by ANCOVA (age and education as covariates), and the correlation between BDNF and cognitive function was calculated by Pearson and Spearman correlation analysis. The results are shown in Table 3 and Figure 1. There was a significant difference in BDNF among the four groups ($P < 0.01$). BDNF levels in dementia patients were higher than those in CNC and MCI patients ($P < 0.01$), and there was no significant difference in BDNF between the CNC and MCI groups. BDNF levels were significantly correlated with CDR, MMSE, and clinical diagnosis ($P < 0.001$). BDNF was positively correlated with CDR scores and clinical diagnosis, and negatively correlated with MMSE score.

Factors influencing the association of brain-derived neurotrophic factor with cognitive impairment

The results of ANCOVA and ANOVA are shown in Table 4. Age, education, occupation and sample source had significant effects on BDNF differences among the CNC, MCI, and DAT groups ($P < 0.001$), and sex and APOE4 had no significant effect on BDNF differences among the groups ($P > 0.05$). The trend of the BDNF expression was the same in different genders with significant difference ($P = 0.000$), which decreased in MCI and increased in DAT. BDNF first decreased and then increased significantly with the aggravation of cognitive impairment in groups aged 51–64 and 65–74 ($P < 0.05$), and BDNF increased gradually with cognitive impairment in the group over 75 years old ($P < 0.05$). BDNF increased gradually with cognitive impairment in the group with 0–6 years of education ($P < 0.05$), and there was no significant change in BDNF with cognitive impairment

TABLE 2 Demographic, clinical and laboratory data and cognitive scores of the three groups.

	Total sample (n = 1615)	CNC (n = 660)	MCI (n = 571)	DAT (n = 384)	χ^2 or F-value	P-value
Gender (Male/Female)	678/937	306/354	229/342	143/241	9.574	0.008
Age (years)	70.09 ± 9.33	68.21 ± 8.26	69.91 ± 8.74	77.00 ± 9.19	130.867	<0.001
Education (years)	7.96 ± 4.07	9.49 ± 3.59	7.44 ± 3.73	6.11 ± 4.37	101.896	<0.001
Marriage (in marriage/other)	1383/232	598/62	490/81	255/129	21.967	<0.001
Family (Big family/Couple/Others)	568/864/183	243/385/32	218/315/38	107/164/113	131.930	<0.001
Occupation (Physical/Technical/Intellectual)	197/1072/346	43/416/201	134/363/74	20/293/71	116.592	<0.001
BMI (kg/m^2)	23.85 ± 3.11	23.74 ± 2.92	24.07 ± 3.29	23.51 ± 3.25	1.848	0.156
SBP (mm/Hg)	136.25 ± 16.76	135.87 ± 16.47	135.91 ± 16.40	139.76 ± 19.45	2.233	0.108
DBP (mm/Hg)	82.23 ± 9.45	82.78 ± 9.28	81.52 ± 9.44	82.29 ± 10.28	1.955	0.142
APOE4 (Positive/Negative)	176/795	80/387	59/330	37/78	17.899	<0.001
Total protein (g/L)	75.27 ± 4.91	75.68 ± 4.93	74.98 ± 4.72	74.31 ± 5.41	4.292	0.014
Albumin (g/L)	46.20 ± 2.96	46.60 ± 2.82	45.95 ± 2.99	45.06 ± 3.18	13.236	<0.001
FBG (mmol/L)	6.14 ± 1.62	6.11 ± 1.62	6.16 ± 1.68	6.21 ± 1.42	0.212	0.809
Triglyceride (mmol/L)	1.66 ± 1.31	1.66 ± 1.08	1.63 ± 1.30	1.81 ± 2.19	0.737	0.473
Total cholesterol (mmol/L)	5.12 ± 1.02	5.17 ± 0.97	5.15 ± 1.09	4.81 ± 0.90	4.981	0.007
HDL (mmol/L)	1.23 ± 0.36	1.19 ± 0.31	1.29 ± 0.41	1.22 ± 0.33	8.533	<0.001
LDL (mmol/L)	2.95 ± 0.74	3.02 ± 0.74	2.93 ± 0.75	2.64 ± 0.65	10.307	<0.001
TSH (mIU/L)	2.33 ± 2.08	2.24 ± 1.65	2.36 ± 1.82	2.75 ± 4.54	1.862	0.156
FreeT3 (pmol/L)	4.77 ± 1.55	4.98 ± 1.39	4.42 ± 1.33	4.92 ± 2.83	13.707	<0.001
FreeT4 (pmol/L)	15.67 ± 3.84	15.87 ± 3.72	15.46 ± 3.97	15.32 ± 4.01	1.408	0.245
Folic acid (nmol/L)	44.63 ± 77.24	50.25 ± 90.47	37.20 ± 53.83	41.11 ± 69.30	2.839	0.059
Vitamin B12 (pmol/L)	350.01 ± 198.01	356.73 ± 202.76	345.94 ± 189.65	327.82 ± 201.96	0.902	0.406
CDR-GS (score)	0.61 ± 0.70	0.18 ± 0.28	0.50 ± 0.22	1.50 ± 0.86	573.035	<0.001
ADAS-cog (score)	9.38 ± 6.22 (n = 996)	6.16 ± 2.56 (n = 508)	11.48 ± 5.26 (n = 419)	20.25 ± 11.05 (n = 69)	326.625	<0.001
MMSE (score)	19.46 ± 8.88 (n = 859)	27.40 ± 3.35 (n = 210)	23.33 ± 4.29 (n = 318)	10.72 ± 7.01 (n = 331)	754.315	<0.001
ADL (score)	18.48 ± 13.04 (n = 1308)	13.67 ± 5.74 (n = 557)	14.85 ± 6.68 (n = 468)	33.95 ± 18.48 (n = 283)	417.864	<0.001
BDNF (pg/mL) Mean ± SD	10555.7 ± 12135.1	10101.6 ± 11748.3	8556.3 ± 10255.5	14309.1 ± 14356.8	27.452	<0.001
BDNF (pg/mL) Ln(X + 1)	8.55 ± 1.40	8.50 ± 1.41	8.32 ± 1.39	8.98 ± 1.29	27.302	<0.001

TABLE 3 Association between BDNF and cognitive function.

	CNC	MCI	Mild dementia	Moderate-severe dementia	ANCOVA Bonferroni test	Pearson correlation	Spearman correlation
CDR group	8.35 ± 1.39 (n = 486)	8.53 ± 1.40 (n = 778)	8.85 ± 1.28 (n = 164)	8.89 ± 1.38 (n = 187)	F = 17.783, P = 0.000 CNC = MCI < Mild = severe	r = 0.124 $P \leq$ 0.001	r_s = 0.124 $P \leq$ 0.001
MMSE group	8.14 ± 1.70 (n = 236)	8.01 ± 1.57 (n = 269)	8.57 ± 1.46 (n = 182)	8.86 ± 1.45 (n = 172)	F = 12.632, P = 0.000 MCI = CNC < Mild = severe	r = −0.183 $P \leq$ 0.001	r_s = 0.183 $P \leq$ 0.001
Clinical diagnosis	8.50 ± 1.41 (n = 660)	8.32 ± 1.39 (n = 571)	9.08 ± 1.19 (n = 198)	8.88 ± 1.38 (n = 186)	F = 26.667, P = 0.000 MCI = CNC < Mild = severe		r_s = 0.117 $P \leq$ 0.001

in the other two groups ($P > 0.05$). BDNF first decreased and then increased significantly with cognitive impairment in physical and technical occupation ($P < 0.05$), and BDNF increased gradually with cognitive impairment in intellectual occupation ($P > 0.05$). BDNF increased gradually with cognitive impairment in the Shanghai group ($P = 0.010$), and there was no significant change in cognitive impairment in other districts ($P > 0.05$). BDNF in the male and female groups first decreased and then increased significantly with cognitive impairment ($P < 0.001$). BDNF first decreased and then increased with cognitive impairment in the ApoE4-negative group ($P < 0.05$), and there was no significant change in

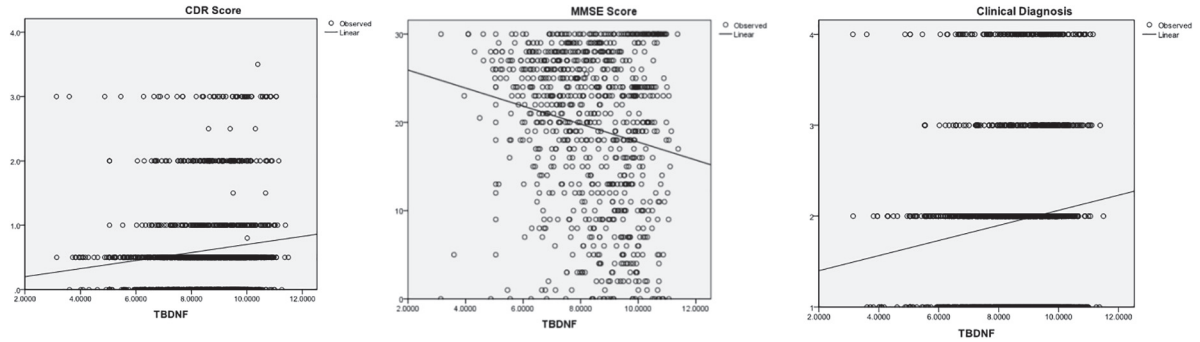

FIGURE 1
The correlations between Brain-Derived Neurotrophic Factor (BNDF) and Clinical Dementia Rating (CDR), Mini Mental State Examination (MMSE), and clinical diagnosis.

BDNF with cognitive impairment in the ApoE4-positive group ($P > 0.05$).

The combined effects of related factors on brain-derived neurotrophic factor

The combined effect of diagnosis, gender, age, education, and sample source on plasma BDNF was examined by ANCOVA and linear regression analysis, and detailed results are shown in **Table 5**. The effects of diagnosis, age and education on plasma BDNF were statistically significant ($P < 0.01$), but the gender effect was not statistically significant ($P = 0.149$), and only 5.1% of the variation could be explained. After adding the sample source, only the sample source and gender effects were statistically significant ($P < 0.05$), the effects of diagnosis, age and education were not statistically significant ($P > 0.05$), and the explained variation reached 37.9%. Linear regression analysis showed that the four factors could explain 3.0% of BDNF variation, of which the effects of diagnosis, age, and education were statistically significant ($P = 0.000$). Adding the sample source explained 38.0% of the BDNF variation; only the effects of sample source and sex were statistically significant ($P < 0.01$), and the effects of diagnosis, age and education were not statistically significant ($P > 0.05$).

Discussion

Growing evidence indicates that BDNF is associated with the pathophysiology of AD. However, the association of BDNF levels in the brain or peripheral blood with cognitive impairment in AD is quite complex and influenced by many factors, such as sample heterogeneity and methodological differences (Kim et al., 2017; Qin et al., 2017; Balietti et al., 2018; Ng et al., 2019; Marta et al., 2020; Xie et al., 2020; Girotra et al., 2022). In the present study, the association of plasma BDNF with AD cognitive impairment and influencing factors was investigated in depth based on a large sample of elderly people in the community. It was preliminarily found that plasma BDNF concentrations were related to AD cognitive impairment but not a simple linear relationship. Since there were significant difference between CNC, MCI, and DAT cohorts regarding age, sex, education, and social status, the factors influencing the association between plasma BDNF and cognitive impairment were analyzed separately. The alterations in the plasma BDNF levels of AD depended on the stages or severity of AD and were affected by factors such as age, education or sample source. The main findings of this study are briefly analyzed and discussed as follows.

Many studies have found alterations in blood BDNF levels in patients with AD and MCI, but the results are inconsistent or even contradictory. Most studies observed a decrease in blood BDNF levels (Borba et al., 2016; Siuda et al., 2017; Zhang et al., 2019; Tang et al., 2020), a few reported an increase in BDNF concentrations (Lee et al., 2015; Ng et al., 2021), and other studies reported no significant change in BDNF levels (O'Bryant et al., 2011; Wang et al., 2015). Xie et al. (2020) meta-analysis showed that peripheral blood BDNF decreased gradually with the aggravation of cognitive impairment. Ng et al. (2019) meta-analysis showed that peripheral BDNF levels decreased in patients with AD and could only be detected at the late stage of the dementia spectrum. Qin et al. (2017) suggested that AD or MCI is accompanied by reduced peripheral blood BDNF levels, supporting an association between the decreasing levels of BDNF and the progression of AD.

In this study, BDNF levels in dementia patients were higher than those in MCI patients and cognitively normal elderly individuals in the total sample and most subsamples. Compared with normal elderly individuals, there were no significant BDNF alterations (higher or lower) in MCI patients in the total sample and most subsamples. From the change trend, BDNF showed three change patterns with cognitive impairment: (1) BDNF

TABLE 4 Factors influencing the association between plasma BDNF and cognitive impairment.

Relevant factors		CNC(A)	MCI(B)	DAT(C)	ANCOVA	ANOVA	LSD test
Gender	Male	8.44 ± 1.34 (n = 306)	8.28 ± 1.38 (n = 229)	8.98 ± 1.25 (n = 143)	Group: F = 26.998 $P \leq 0.001$ Gender: F = 1.182 P = 0.277	F = 12.905 $P \leq 0.001$	C > A = B
	Female	8.55 ± 1.46 (n = 354)	8.35 ± 1.41 (n = 342)	8.98 ± 1.31 (n = 241)		F = 14.411 $P \leq 0.001$	C > A = B
	ANOVA	F = 1.089 P = 0.297	F = 0.427 P = 0.514	F = 0.000 P = 0.995			
Age	51–64 years	8.76 ± 1.28 (n = 255)	8.45 ± 1.35 (n = 186)	8.92 ± 1.21 (n = 47)	Group: F = 37.030 $P \leq 0.001$ Age: F = 26.844 P = 0.001	F = 4.019 P = 0.019	C = A > B
	65–74 years	8.68 ± 1.29 (n = 255)	8.29 ± 1.38 (n = 200)	9.03 ± 1.16 (n = 95)		F = 11.513 $P \leq 0.001$	C > A > B
	>75 years	7.75 ± 1.55 (n = 150)	8.23 ± 1.45 (n = 185)	8.98 ± 1.35 (n = 242)		F = 36.034 $P \leq 0.001$	C > B > A
	ANOVA	F = 30.269 P = 0.000	F = 1.247 P = 0.288	F = 0.129 P = 0.879			
Education	0–6 years	8.09 ± 1.54 (n = 136)	8.12 ± 1.47 (n = 276)	9.05 ± 1.23 (n = 247)	Group: F = 30.665 $P \leq 0.001$ Education: F = 10.703 P = 0.001	F = 34.906 $P \leq 0.001$	C > A = B
	7–9 years	8.62 ± 1.33 (n = 277)	8.46 ± 1.31 (n = 207)	8.87 ± 1.32 (n = 75)		F = 2.765 P = 0.064	C = A = B
	>10 years	8.58 ± 1.38 (n = 247)	8.63 ± 1.23 (n = 88)	8.84 ± 1.45 (n = 50)		F = 0.894 P = 0.410	C = A = B
	ANOVA	F = 7.539 P = 0.001	F = 6.135 P = 0.002	F = 1.047 P = 0.352			
Occupation	Physical	8.32 ± 1.24 (n = 37)	7.81 ± 1.41 (n = 110)	8.74 ± 1.37 (n = 15)	Group: F = 26.556 $P \leq 0.001$ Occupation: F = 22.376 $P \leq 0.001$	F = 4.243 P = 0.016	C > B, A = B
	Technical	8.88 ± 1.23 (n = 352)	8.80 ± 1.22 (n = 298)	9.39 ± 1.09 (n = 218)		F = 17.803 $P \leq 0.001$	C > A = B
	Intellectual	8.75 ± 1.30 (n = 170)	8.98 ± 1.10 (n = 61)	9.17 ± 1.21 (n = 53)		F = 2.648 P = 0.073	C > A, A = B
	ANOVA	F = 3.530 P = 0.030	F = 28.161 P = 0.000	F = 2.859 P = 0.059			
Sample sources	Wuxi	8.79 ± 1.10 (n = 476)	8.87 ± 1.03 (n = 281)	8.84 ± 0.96 (n = 180)	Group: F = 0.405 P = 0.667 Source: F = 896.678 $P \leq 0.001$	F = 0.523 P = 0.593	A = B = C
	Jiangyi	7.42 ± 1.13 (n = 33)	7.56 ± 1.34 (n = 139)	7.33 ± 1.21 (n = 28)		F = 0.486 P = 0.616	A = B = C
	Hangzhou	9.80 ± 1.75 (n = 50)	9.91 ± 0.60 (n = 49)	9.75 ± 1.09 (n = 149)		F = 0.324 P = 0.723	A = B = C
	Shanghai	6.82 ± 0.94 (n = 101)	7.09 ± 0.99 (n = 102)	7.41 ± 0.90 (n = 27)		F = 4.278 P = 0.010	C > A = B
	ANOVA	F = 115.003 P = 0.000	F = 125.701 P = 0.000	F = 74.665 P = 0.000			
APOE4	Negative	8.74 ± 1.15 (n = 387)	8.43 ± 1.25 (n = 330)	8.90 ± 1.04 (n = 78)	Group: F = 9.318 $P \leq 0.001$ APOE: F = 40.063 P = 0.802	F = 8.434 $P \leq 0.001$	C = A > B
	Positive	8.63 ± 1.27 (n = 80)	8.49 ± 1.39 (n = 59)	8.91 ± 0.93 (n = 37)		F = 1.231 P = 0.295	C = A = B
		F = 0.535 P = 0.465	F = 0.130 P = 0.719	F = 0.001 P = 0.971			

TABLE 5 The comprehensive effects of diagnosis, gender, age, education and sample source on brain-derived neurotrophic factor.

Related factors	ANCOVA			Linear regression			
	χ^2	*F*	*P*	B	β	*t*	*P*
Diagnosis	71.948	38.858	<0.001	0.308	0.173	6.446	<0.001
Gender	3.864	2.087	0.149	0.11	0.039	1.536	0.125
Age	38.854	20.984	<0.001	−0.172	−0.100	−3.817	<0.001
Education	14.019	7.572	0.006	0.167	0.095	3.504	<0.001
	$R^2 = 0.053$, Adjust $R^2 = 0.051$			$R^2 = 0.033$, Adjust $R^2 = 0.030$			
Diagnosis	0.32	0.265	0.767	0.021	0.012	0.533	0.594
Gender	9.503	7.853	0.005	0.16	0.056	2.791	0.005
Age	0.033	0.027	0.869	−0.009	−0.005	−0.252	0.801
Education	0.009	0.008	0.93	0.002	0.001	0.041	0.967
Sample sources	1033.37	853.958	<0.001	0.970	0.615	30.135	<0.001
	$R^2 = 0.382$, Adjust $R^2 = 0.379$			$R^2 = 0.382$, Adjust $R^2 = 0.380$			

decreased in the MCI stage and increased in the dementia stage. This pattern was observed in the total sample (clinical diagnosis and MMSE group) and subsamples (men and women, 51–64 years old and 65–74 years old group, physical and technical occupation, 7–9 years education group, and *APOE4* negative and positive group); (2) BDNF increased gradually with cognitive impairment. This pattern was found in the CDR group, over 75 years old group, 0–6 years and more than 10 years of education group, intellectual occupation, and Shanghai sample; (3) Although the unified training has ensured the consistency of research methods, etc., the trend of BDNF values may be different due to regional differences. Therefore, after analyzing the trends in different centers, this study uses the overall trend to conduct a comparative study. As a result, BDNF increased in the MCI stage and decreased in the dementia stage. This pattern was found in Wuxi, Jiangyi, and Hangzhou samples. The three change patterns are supported by research evidence; for example, Woolley et al. (2012) and Forlenza et al. (2015) supported the pattern with BDNF decreasing early and subsequently increasing; Sonali et al. (2013) and Lee et al. (2015) studies supported the gradually increasing BDNF pattern. The results of Laske et al. (2006), Angelucci et al. (2010), and Faria et al. (2014) support the model in which BDNF first increases and then decreases.

These discrepancies might be explained by the heterogeneity of AD samples (Balietti et al., 2018) and BDNF compensatory mechanisms (Laske et al., 2006). BDNF plays an important role in the pathogenesis of AD (Song et al., 2015); with the progression of AD, brain-derived BDNF gradually decreases, and BDNF alterations in peripheral blood may be more complicated. In the early stage of MCI, peripheral blood BDNF can supplement BDNF deficiency in the brain through the blood–brain barrier (Pan et al., 1998; Klein et al., 2011), and peripheral blood BDNF may decrease slightly. In the late stage of MCI or early stage of dementia, the continuous decrease in BDNF may stimulate the compensatory mechanism (increased platelet-derived BDNF synthesis and release) (Fujimura et al., 2002), resulting in increased plasma BDNF levels, and in the late stage of dementia, compensatory failure will reduce blood BDNF levels.

A large number of studies suggest that blood BDNF could be used as a biomarker for AD diagnosis, prognosis, and treatment monitoring, but the survey results of blood BDNF levels in AD patients are very inconsistent (Bathina and Das, 2015; Song et al., 2015; Marta et al., 2020; Xie et al., 2020; Mori et al., 2021). There were not only differences in demographic data (such as sex, age and education) and disease status (stage, severity, medication or comorbidity) among different studies but also differences in demographic data between the AD group and the control group in the same study. The heterogeneity of these samples may be an important reason for the inconsistency of research results (Balietti et al., 2018).

Many studies have found that there are differences in blood BDNF levels by sex (women higher than men), age (decrease with age), plasma/serum (serum higher than plasma), disease stage (increase in the early stage and decrease in the late stage), cognitive impairment severity, depressive symptoms, medication and other factors that also affect blood BDNF levels (Lommatzsch et al., 2005; Laske et al., 2006; Fukumoto et al., 2010). In line with these findings, the present study found that plasma BDNF levels were affected by age, education, occupation and sample source, and BDNF differences among clinical diagnosis groups remained after excluding the influence of each covariate.

In addition, demographic variables such as gender, age and education and clinical variables such as AD severity, disease stage and medication cannot only affect blood BDNF alone but also comprehensively affect BDNF through interactive or synergistic mechanisms. This study further examined the comprehensive impact of multiple factors on BDNF by ANCOVA and linear regression analysis. Four-factor analysis found that diagnosis, age and education had a significant impact on BDNF, which could explain only 3–5% of the variance. When the sample source variable was introduced, only the sample source and gender had significant effects on BDNF, and the explained variance reached 38%. It is worth noting that in this study, the sample source is not a simple variable. It includes not only demographic differences such as gender, age, education and occupation but also AD stage and severity, concomitant diseases and medication, blood sample processing and storage duration. These findings remind us that to make BDNF a biomarker of complex diseases such as AD, we must establish standardized detection methods and cut off values of BDNF according to the weight of each influencing factor.

Data availability statement

The dataset generated during and analyzed during the current study are available from the corresponding author on reasonable request.

Ethics statement

The studies involving human participants were reviewed and approved by the Wuxi Mental Health Center. The patients/participants provided their written informed consent to participate in this study.

Author contributions

ZC designed the study, analyzed the data, and revised the manuscript. FQ and HY collected and drafted the manuscript. JL, HZ, and YW participated in the design of the study, data management, and analysis. ZW contributed to data collection management. All authors contributed to the article and approved the submitted version.

Funding

This study was supported by the Social Development Key Projects in Jiangsu Province (BE2015615), National Natural Science Foundation of China (No. 82104244), Wuxi Municipal Health Commission (Q202101), Wuxi Taihu Talent Project (Nos. WXTTP2020008 and WXTTP2021), and Wuxi Medical Development Discipline Project (No. FZXK2021012).

Conflict of interest

The authors declare that the research was conducted in the absence of any commercial or financial relationships that could be construed as a potential conflict of interest.

Publisher's note

References

Academy of Cognitive Disorder of China (2018). The clinical dementia rating (simplified Chinese). *Chin. J. Geriat.* 37, 367–371.

Alzheimer Association (2017). *Alzheimer's disease facts and figures*. Chicago, IL: Alzheimer Association.

American Psychiatric Association (2013). *Diagnostic and statical manual of mental disorder, DSM-V*. Washington, DC: American Psychiatric Association. doi: 10.1176/appi.books.9780890425596

Angelucci, F., Spalletta, G., di Iulio, F., Ciaramella, A., Salani, F., Varsi, A. E., et al. (2010). Alzheimer's disease (AD) and mild cognitive impairment (MCI) patients are characterized by increased BDNF Serum levels. *Curr. Alzheimer Res.* 7, 15–20. doi: 10.2174/156720510790274473

Balietti, M., Giuli, C., and Conti, F. (2018). Peripheral blood brain-derived neurotrophic factor as a biomarker of Alzheimer's disease: Are there methodological biases? *Mol. Neurobiol.* 55, 6661–6672. doi: 10.1007/s12035-017-0866-y

Bathina, S., and Das, U. N. (2015). Brain-derived neurotrophic factor and its clinical implications. *Arch. Med. Sci.* 11, 1164–1178. doi: 10.5114/aoms.2015.56342

Borba, E. M., Duarte, J. A., Bristot, G., Scotton, E., Camozzato, A. L., and Chaves, M. L. F. (2016). Brain-derived neurotrophic factor serum levels and hippocampal volume in mild cognitive impairment and dementia due to Alzheimer disease. *Dement. Geriatr. Cogn. Disord. Extra* 6, 559–567. doi: 10.1159/000450601

Cheng, Z. (2020). Discussion on related matter of Alzheimers disease. *J. Clin. Res.* 37, 806–807.

Cheng, Z., Yin, J., Yuan, H., Jin, C., Zhang, F., Wang, Z., et al. (2018). Blood-Derived plasma protein biomarkers for Alzheimer's disease in Han Chinese. *Front. Aging Neurosci.* 10:414. doi: 10.3389/fnagi.2018.00414

Fan, B. (1990). Hachinski ischemic scale (HIS). *Shanghai Arch. Psychiatry*, A1, 54–55.

Faria, M. C., Goncalves, G. S., Rocha, N. P., Moraes, E. N., Bicalho, M. A., Gualberto Cintra, M. T., et al. (2014). Increased plasma levels of BDNF and inflammatory markers in Alzheimer's disease. *J. Psychiatr. Res.* 53, 166–172. doi: 10.1016/j.jpsychires.2014.01.019

Forlenza, O. V., Miranda, A. S., Barbosa, I. G., Talib, L. L., Diniz, B. S., Gattaz, W. F., et al. (2015). Decreased neurotrophic support is associated with cognitive decline in non-demented subjects. *J. Alzheimers Dis.* 46, 423–429.

Fujimura, H., Altar, C. A., Chen, R. Y., Nakamura, T., Nakahashi, T., Kambayashi, J., et al. (2002). Brain-derived neurotrophic factor is stored in human platelets and released by agonist stimulation. *Thromb. Haemost.* 87, 728–734. doi: 10.1055/s-0037-1613072

Fukumoto, N., Fujii, T., Combarros, O., Kamboh, M. I., Tsai, S.-J., Matsushita, S., et al. (2010). Sexually dimorphic effect of the val66met polymorphism of BDNF on susceptibility to Alzheimer's disease: New data and meta-analysis. *Am. J. Med. Genet. Part B Neuropsychiatr. Genet.* 153B, 235–242. doi: 10.1002/ajmg.b.30986

Girotra, P., Behl, T., Sehgal, A., Singh, S., and Bungau, S. (2022). Investigation of the molecular role of brain-derived neurotrophic factor in Alzheimer's disease. *J. Mol. Neurosci.* 72, 173–186. doi: 10.1007/s12031-021-01824-8

Glud, M., Christiansen, T., Larsen, L. H., Richelsen, B., and Bruun, J. M. (2019). Changes in circulating BDNF in relation to sex, diet, and exercise: A 12-week randomized controlled study in overweight and obese participants. *J. Obes.* 2019:4537274. doi: 10.1155/2019/4537274

Hixson, J. E., and Vernier, D. T. (1990). Restriction isotyping of human apolipoprotein E by gene amplification and cleavage with HhaI. *J. Lipid Res.* 31, 545–548. doi: 10.1016/S0022-2275(20)43176-1

Kim, B. Y., Lee, S. H., Graham, P. L., Angelucci, F., Lucia, A., Pareja-Galeano, H., et al. (2017). Peripheral brain-derived neurotrophic factor levels in Alzheimer's disease and mild cognitive impairment: A comprehensive systematic review and meta-analysis. *Mol. Neurobiol.* 54, 7297–7311. doi: 10.1007/s12035-016-0192-9

Klein, A. B., Williamson, R., Santini, M. A., Clemmensen, C., Ettrup, A., Rios, M., et al. (2011). Blood BDNF concentrations reflect brain-tissue BDNF levels across species. *Int. J. Neuropsychopharmacol.* 14, 347–353. doi: 10.1017/S1461145710000738

Knopman, D. S., Amieva, H., Petersen, R. C., Chételat, G., Holtzman, D. M., and Hyman, B. T. (2021). Alzheimer disease. *Nat. Rev. Dis. Primers* 7:34. doi: 10.1038/s41572-021-00269-y

Laske, C., Stransky, E., Leyhe, T., Eschweiler, G. W., Wittorf, A., Richartz, E., et al. (2006). Stage-dependent BDNF serum concentrations in Alzheimer's disease. *J. Neural Transm.* 113, 1217–1224. doi: 10.1007/s00702-005-0397-y

Lawton, M. P., and Brody, E. M. (1969). Assessment of older people: Self-maintaining and instrumental activities of daily living. *Gerontologist* 9, 179–186. doi: 10.1093/geront/9.3_Part_1.179

Lee, S. J., Baek, J.-H., and Kim, Y.-H. (2015). Brain-derived Neurotrophic factor is associated with cognitive impairment in elderly korean individuals. *Clin. Psychopharmacol. Neurosci.* 13, 283–287. doi: 10.9758/cpn.2015.13.3.283

Li, G., Shen, Y. C., Chen, C. H., Li, S. R., Zhao, W. Y., Liu, M., et al. (1988). Preliminary application of MMSE in the aged of urban population in Beijing. *Chin. Ment. Health J.* 2, 66–67.

Liu, Y. H., Jiao, S. S., Wang, Y. R., Bu, X. L., Yao, X. Q., Xiang, Y., et al. (2015). Associations between ApoEε4 carrier status and serum BDNF Levels—New insights into the molecular mechanism of ApoEε4 actions in Alzheimer's disease. *Mol. Neurobiol.* 51, 1271–1277. doi: 10.1007/s12035-014-8804-8

Lommatzsch, M., Zingler, D., Schuhbaeck, K., Schloetcke, K., Zingler, C., Schuff-Werner, P., et al. (2005). The impact of age, weight and gender on BDNF levels in human platelets and plasma. *Neurobiol. Aging* 26, 115–123. doi: 10.1016/j.neurobiolaging.2004.03.002

Ma, C., Lin, M., Gao, J., Xu, S., Huang, L., Zhu, J., et al. (2022). The impact of physical activity on blood inflammatory cytokines and neuroprotective factors in individuals with mild cognitive impairment: A systematic review and meta-analysis of randomized-controlled trials. *Aging Clin. Exp. Res.* 34, 1471–1484. doi: 10.1007/s40520-021-02069-6

Marta, B., Cinzia, G., Tiziana, C., Paolo, F., and Fiorenzo, C. (2020). Is blood brain-derived neurotrophic factor a useful biomarker to monitor mild cognitive impairment patients? *Rejuvenation Res.* 23, 411–419. doi: 10.1089/rej.2020.2307

McKhann, G., Drachman, D., Folstein, M., Katzman, R., Price, D., and Stadlan, E. M. (1984). Clinical diagnosis of Alzheimer's disease: Report of the NINCDS-ADRDA work group under the auspices of department of health and human services task force on Alzheimer's disease. *Neurology* 34, 939–944. doi: 10.1212/WNL.34.7.939

Mori, Y., Tsuji, M., Oguchi, T., Kasuga, K., Kimura, A., Futamura, A., et al. (2021). Serum BDNF as a potential biomarker of Alzheimer's disease: Verification through assessment of serum, cerebrospinal fluid, and medial temporal lobe atrophy. *Front. Neurol.* 12:653267. doi: 10.3389/fneur.2021.653267

Nascimento, C. M. C., Pereira, J. R., de Andrade, L. P., Garuffi, M., Talib, L. L., Forlenza, O. V., et al. (2014). Physical exercise in MCI elderly promotes reduction of pro-inflammatory cytokines and improvements on cognition and BDNF peripheral levels. *Curr. Alzheimer Res.* 11, 799–805. doi: 10.2174/1567205011081409101228 49

Ng, T. K. S., Coughlan, C., Heyn, P. C., Tagawa, A., Carollo, J. J., Kua, E. H., et al. (2021). Increased plasma brain-derived neurotrophic factor (BDNF) as a potential biomarker for and compensatory mechanism in mild cognitive impairment: A case-control study. *Aging* 13, 22666–22689. doi: 10.18632/aging.203598

Ng, T. K. S., Ho, C. S. H., Tam, W. W. S., Kua, E. H., and Ho, R. C. M. (2019). Decreased serum brain-derived neurotrophic factor (BDNF) levels in patients with Alzheimer's disease (AD): A systematic review and meta-analysis. *Int. J. Mol. Sci.* 20:257. doi: 10.3390/ijms20020257

O'Bryant, S. E., Hobson, V. L., Hall, J. R., Barber, R. C., Zhang, S., Johnson, L., et al. (2011). Serum brain-derived neurotrophic factor levels are specifically associated with memory performance among Alzheimer's disease cases. *Dement. Geriatr. Cogn. Disord.* 31, 31–36. doi: 10.1159/000321980

Pan, W., Banks, W. A., Fasold, M. B., Bluth, J., and Kastin, A. J. (1998). Transport of brain-derived neurotrophic factor across the blood-brain barrier. *Neuropharmacology* 37, 1553–1561. doi: 10.1016/S0028-3908(98)00141-5

Petersen, R. C., Smith, G. E., Waring, S. C., Ivnik, R. J., Tangalos, E. G., and Kokmen, E. (1999). Mild cognitive impairment–Clinical characterization and outcome. *Arch. Neurol.* 56, 303–308. doi: 10.1001/archneur.56.3.303

Popova, N. K., and Naumenko, V. S. (2019). Neuronal and behavioral plasticity: The role of serotonin and BDNF systems tandem. *Exp. Opin. Ther. Tar.* 23, 227–239. doi: 10.1080/14728222.2019.1572747

Qin, X. Y., Cao, C., Cawley, N. X., Liu, T. T., Yuan, J., Loh, Y. P., et al. (2017). Decreased peripheral brain-derived neurotrophic factor levels in Alzheimer's disease: A meta-analysis study (N=7277). *Mol. Psychiatry* 22, 312–320. doi: 10.1038/mp.2016.62

Rehiman, S. H., Lim, S. M., Neoh, C. F., Majeed, A. B. A., Chin, A.-V., Tan, M. P., et al. (2020). Proteomics as a reliable approach for discovery of blood-based Alzheimer's disease biomarkers: A systematic review and meta-analysis. *Ageing Res. Rev.* 60:101066. doi: 10.1016/j.arr.2020.101066

Siuda, J., Patalong-Ogiewa, M., Zmuda, W., Targosz-Gajniak, M., Niewiadomska, E., Matuszek, I., et al. (2017). Cognitive impairment and BDNF serum levels. *Neurol. Neurochir. Pol.* 51, 24–32. doi: 10.1016/j.pjnns.2016.10.001

Sonali, N., Tripathi, M., Sagar, R., and Vivekanandhan, S. (2013). Val66Met polymorphism and BDNF levels in Alzheimer's disease patients in North Indian population. *Int. J. Neurosci.* 123, 409–416. doi: 10.3109/00207454.2012.762515

Song, J.-H., Yu, J.-T., and Tan, L. (2015). Brain-derived neurotrophic factor in Alzheimer's disease: Risk, mechanisms, and therapy. *Mol. Neurobiol.* 52, 1477–1493. doi: 10.1007/s12035-014-8958-4

Tang, T., Zhao, Y., and Yang, X. R. (2020). Correlations between the serum levels of Irisin, FNDC5, BDNF and cognitive function in patients with Alzheimer's disease. *J. Trop. Med.* 20, 825–828.

Wang, H. B. M. U., Shu, L., Si, T., Tian, C., and Zhang, H. (2000). Validity and reliability of the Chinese version of the Alzheimer's disease assessment scale. *Inst. Ment. Health* 8, 89–93.

Wang, S., Zheng, W. N., Chu, H. S., Sheng, X. N., Sun, W. L., Wang, B. B., et al. (2015). Change and its significance of serum levels of brain-derived neurotrophic factor in patients with Alzheimer disease. *J. Brain Nerv. Dis.* 3, 176–179.

Woolley, J. D., Strobl, E. V., Shelly, W. B., Karydas, A. M., Ketelle, R. N. R., Wolkowitz, O. M., et al. (2012). BDNF serum concentrations show no relationship with diagnostic group or medication status in neurodegenerative disease. *Curr. Alzheimer Res.* 9, 815–821. doi: 10.2174/156720501208240 55395

Wu, Y., Xu, W. W., Cheng, Z. H., Wu, B., Li, T., and Zhou, X. Q. (2016). Brief Elderly cognitive screening inventory: Development, reliability and validity. *Chin. J. Gerontol.* 36, 1211–1213.

Xie, B., Zhou, H., Liu, W., Yu, W., Liu, Z., Jiang, L., et al. (2020). Evaluation of the diagnostic value of peripheral BDNF levels for Alzheimer's disease and mild cognitive impairment: Results of a meta-analysis. *Int. J. Neurosci.* 130, 218–230. doi: 10.1080/00207454.2019.1667794

Yiannopoulou, K. G., and Papageorgiou, S. G. (2020). Current and future treatments in Alzheimer disease: An update. *J. Cent. Nerv. Syst. Dis.* 12:1179573520907397.

Zhang, C., Guo, W., Yang, Y., Qin, D., and Liao, X. (2019). Changes in serum brain-derived neurotrophic factor levels in patients with Alzheimer's disease. *Chin. J. Geriatr.* 38, 151–154.

Zhao, JP, and Zheng, YP (1992). Reliability and validity of Hamilton depression scale assessed in 329 Chinese depression patients. *Chin. Ment. Health J.* 5, 214–216.

Zhao, X., and Li, X. (2020). The prevalence of Alzheimer's disease in the Chinese Han population: A meta-analysis. *Neurol. Res.* 42, 291–298. doi: 10.1080/01616412.2020.1716467

Frontiers in
Aging Neuroscience

Explores the mechanisms of central nervous system aging and age-related neural disease

The third most-cited journal in the field of geriatrics and gerontology, with a focus on understanding the mechanistic processes associated with central nervous system aging.

Discover the latest Research Topics

See more →

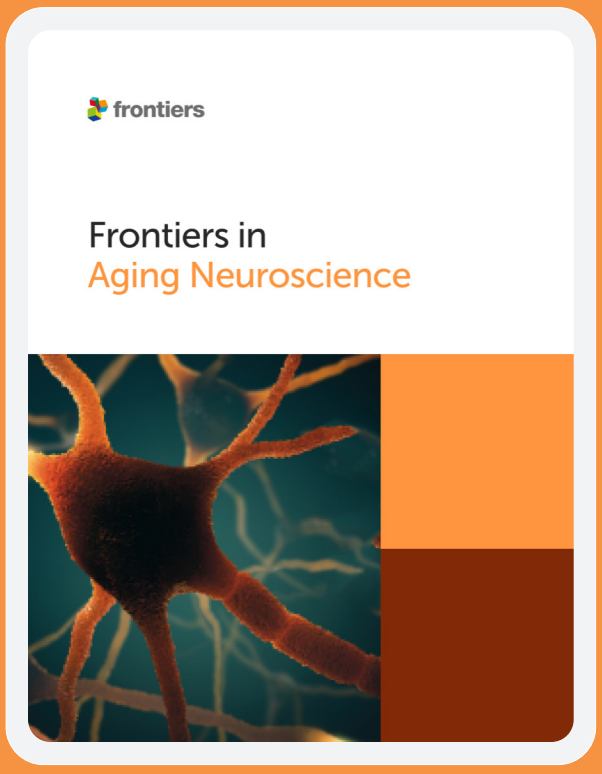

Frontiers

Avenue du Tribunal-Fédéral 34
1005 Lausanne, Switzerland
frontiersin.org

Contact us

+41 (0)21 510 17 00
frontiersin.org/about/contact